



HAL
open science

Rhodium and iron catalyzed transformations via C-H, N-H and P-H activation

Yumeng Yuan

► **To cite this version:**

Yumeng Yuan. Rhodium and iron catalyzed transformations via C-H, N-H and P-H activation. Catalysis. Université de Rennes; Fujian Normal University (Fuzhou, Chine), 2023. English. NNT : 2023URENS139 . tel-04853906

HAL Id: tel-04853906

<https://theses.hal.science/tel-04853906v1>

Submitted on 23 Dec 2024

HAL is a multi-disciplinary open access archive for the deposit and dissemination of scientific research documents, whether they are published or not. The documents may come from teaching and research institutions in France or abroad, or from public or private research centers.

L'archive ouverte pluridisciplinaire **HAL**, est destinée au dépôt et à la diffusion de documents scientifiques de niveau recherche, publiés ou non, émanant des établissements d'enseignement et de recherche français ou étrangers, des laboratoires publics ou privés.

THESE DE DOCTORAT DE

L'UNIVERSITE DE RENNES

ECOLE DOCTORALE N° 638

Science de la Matière, des Molécules et Matériaux

Spécialité : *Chimie moléculaire et macromoléculaire*

Par

Yumeng YUAN

**Rhodium and iron catalyzed transformations
via C-H, N-H and P-H activation**

Thèse présentée et soutenue à Rennes, le 22 décembre 2023

Unité de recherche : Institut des Sciences Chimiques de Rennes, UMR 6226

Thèse N° :

Rapporteurs avant soutenance :

Audrey Auffrant Directrice de Recherche CNRS – Ecole Polytechnique Palaiseau

Jérôme Hannedouche Directeur de Recherche – Université Paris Saclay

Composition du Jury :

Président :

Examineurs : Audrey Auffrant Directrice de Recherche CNRS – Ecole Polytechnique Palaiseau, France

Jérôme Hannedouche Directeur de Recherche – Université Paris Saclay, France

Jeanne Crassous Directrice de Recherche CNRS – Université de Rennes, France

Dir. de thèse : Christophe Darcel Professeur – Université de Rennes, France

Co-dir. de thèse : Qiufeng Huang Professeur – Fujian Normal University, Chine

Résumé de la thèse en français

Ces travaux de thèse ont été réalisés en co-direction entre la Fujian Normal University, Chine et l'Université de Rennes. La première partie a été réalisée à la Fujian Normal University sous la direction du professeur Qiufeng Huang entre septembre 2020 et octobre 2021, puis la seconde dans l'UMR 6226 CNRS – Université de Rennes « *Institut des Sciences Chimiques de Rennes* » dans l'équipe « *Organométalliques : Matériaux et Catalyse* » sous la direction du professeur Christophe Darcel entre novembre 2021 et Novembre 2023.

Les objectifs principaux de ce travail de thèse ont été de développer (i) de nouveaux systèmes catalytiques à base de rhodium pour réaliser des annulations à partir d'activations de liaisons C-H et formation de liaisons C-N, et (ii) de nouvelles transformations catalysées par le fer pour former des liaisons C-P.

Ces dernières décennies, la fonctionnalisation sélective et contrôlée de liaisons C-H inertes afin de construire des liaisons carbone-carbone, carbone-azote et carbone-phosphore a connu une percée et un essor considérables en synthèse moléculaire et a permis un accès rapide, en minimisant les nombres d'étapes, à des molécules d'intérêt de haute valeur ajoutée, avec des applications notamment dans les domaines de la pharmacie, de l'agro-alimentaire, des polymères, de la cosmétique ou des matériaux moléculaires. Pour construire efficacement de telles liaisons C-C, des méthodologies sont basées sur les couplages croisés catalysés au palladium impliquant des partenaires organométalliques tels que RLi, RMgX and RZnX, des dérivés acides boroniques ou d'étain et des halogénures arylés ou d'alkyle. De telles transformations sont également possibles avec des catalyseurs à base de métaux non nobles tels que le fer, le manganèse, le cobalt ou le nickel. Cependant, ces méthodologies produisent toujours des déchets métalliques voire toxiques tels que ceux dérivés de l'étain. En terme d'économie d'atomes et de procédés éco-durables, une stratégie de fonctionnalisation directe de liaisons C-H est souhaitée car elle permettrait entre autre de minimiser la quantité de déchets produits. (Schéma 1)

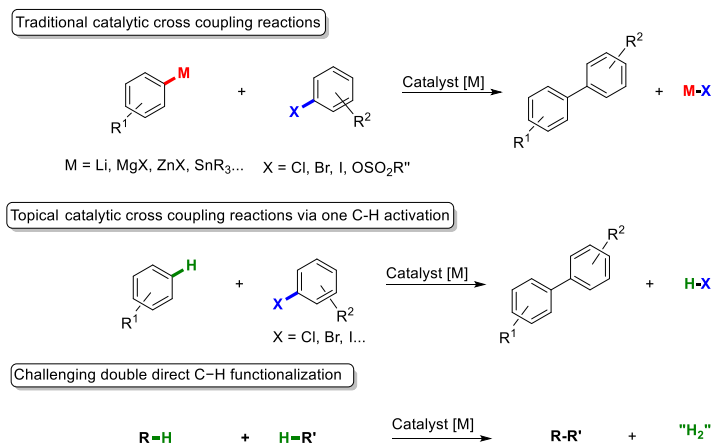
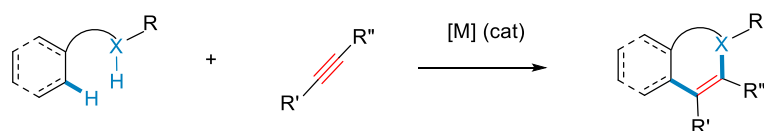


Schéma 1. Fonctionnalisations métallo-catalysées.

En utilisant ce concept de fonctionnalisation C-H utilisé en cascade, des systèmes catalytiques efficaces dérivés de métaux de transition précieux tels que le rhodium, le palladium, l'iridium ou le ruthénium ont permis de réaliser des méthodologies de construction rapides et efficaces de molécules hétérocycliques complexes impliquant la formation de liaisons C-C, C-N et C-P via des réactions de couplage croisé directes. En particulier, durant ces dix dernières années, l'activation-fonctionnalisation de liaisons C-H catalysées par le ruthénium et le rhodium impliquant l'insertion d'un motif alcène ou alcyne a permis d'accéder en une étape à d'importants motifs biologiques. (Schéma 2)



Scheme 2. Principe de l'activation de liaisons C-H suivie de l'insertion d'un motif alcyne par la construction de motifs hétérocycliques via une réaction de cyclisation.

En général, ces méthodologies impliquent des étapes d'oxydation/réduction dans le cycle catalytique de la transformation. Pour les réaliser efficacement, il est souvent nécessaire d'utiliser des quantités stœchiométriques d'oxydants tels que des sels d'argent ou de cuivre pour régénérer l'espèce catalytique active. Afin de réduire l'impact environnemental de ces sels, une méthode élégante pour promouvoir ces couplages C-H oxydants est de les réaliser en absence d'oxydants chimiques *via* des électrocatalyses métal-catalysées. Ainsi de telles méthodologies peuvent être imaginées pour préparer des composés tels que les pyrrolo[3,2,1-*de*] phénanthridines et les azépino[3,2,1-*hi*]indoles. De façon similaire, la construction de motifs benzo[*b*]phosphole peut être imaginés considérant des déconnexions similaires à partir d'oxydes de phosphine et d'alcynes internes. (Schéma 3)

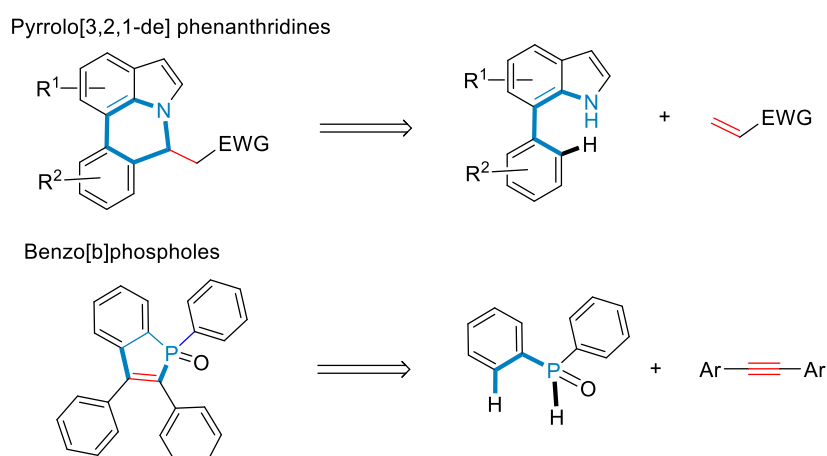


Schéma 3. Analogies pour la préparation de dérivés pyrrolo[3,2,1-*de*]phénanthridines et benzo[*b*]phosphole par des séquences activation C-H /cyclisation.

Ce document de thèse est divisé en neuf chapitres, répartis en deux parties.

En se basant sur une analyse de la bibliographie révélant que les catalyseurs à base de fer n'ont jamais été utilisés seuls pour réaliser des réactions oxyphosphination of de liaisons C=C ou C≡C, la **première partie** de ce document a été dédié au travail de thèse réalisé à Rennes traitant de l'utilisation de la lumière bleue pour réaliser des réactions de phosphinylation d'alcènes et d'alcynes. Elle est composée de 4 chapitres.

Après une introduction générale, le **premier chapitre** décrit, sous la forme d'une étude bibliographique, l'état de l'art sur les réactions de phosphination, phosphinylation et phosphorylation d'alcènes, d'alcynes et d'allènes catalysées par des métaux de transition abondants tels que le manganèse, le fer, le cobalt, le nickel ou le cuivre. (Schéma 4)

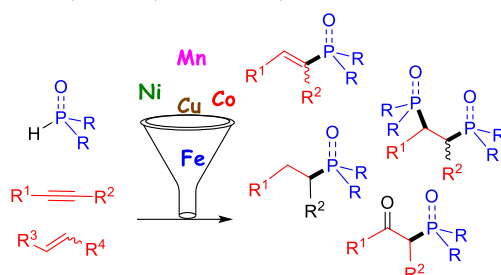


Schéma 4. Réactions de phosphination, phosphinylation et phosphorylation d'alcènes, d'alcynes et d'allènes catalysées par des métaux de transition abondants.

Le second **chapitre 2** décrit l'oxyphosphination d'alcènes activés par des oxydes de phosphine secondaires en présence de catalyseurs à base de sels de fer sous irradiation par de la lumière bleue, permettant de produire efficacement une grande variété d'oxydes de β-cétophosphine fonctionnalisés. En effet, en utilisant des LEDs bleues (2 * 24 W, $h\nu = 450-460$ nm), dans des conditions aérobies, des dérivés substitués de styrène ont été utilisés pour réaliser les réactions oxo-phosphinylation en présence de 10 mol% de Fe(OTf)₂ dans le 1,4-dioxane température ambiante. Les oxydes de β-cétophosphine correspondants sont obtenus avec des rendements entre modérés et bons. Cependant la réaction avec la 4-vinylpyridine et le 4-trifluorométhylstyrène conduit simplement au produit d'hydrophosphination résultant de l'addition anti-Markonikov. (Schéma 5)

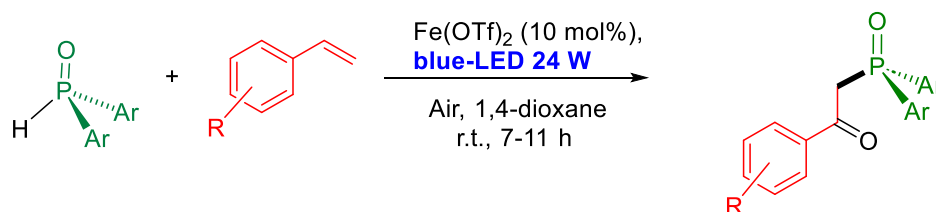


Schéma 5. Synthèse de oxydes de β-cétophosphine par oxo-phosphinylation de styrènes.

Il faut souligner que des études mécanistiques ont révélé le caractère radicalaire de la transformation et que l'association lumière bleue et sels de fer à l'air permettait de générer un radical phosphinoyl qui peut ensuite réagir avec les alcènes activés. (Schéma 6).

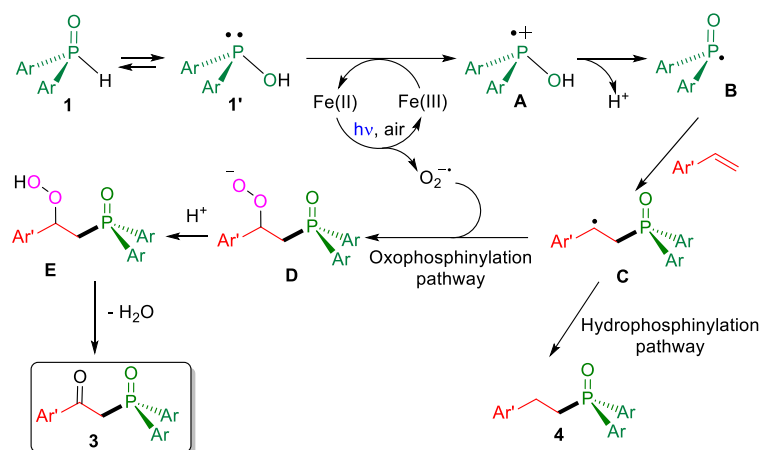


Schéma 6. Mécanisme proposé pour la préparation d'oxydes de β -cétophosphine.

Dans le **chapitre 3**, nous avons développé une nouvelle méthodologie pour la synthèse d'oxydes de benzo[*b*]phosphole par réaction d'oxydes de phosphine secondaires avec des alcynes internes promue par irradiation sous lumière bleue en présence de catalyseur au fer via des fonctionnalisations oxydantes de liaisons C-H/P-H intermoléculaire/intramoléculaires. Ainsi en utilisant 10 mol% de $\text{Fe}(\text{NO}_3)_3$ en présence de 2 éq. de TBHP comme oxydant dans le méthanol, les oxydes de phosphine secondaires réagissent avec les alcynes internes activés pour conduire aux d'oxydes de benzo[*b*]phosphole correspondants avec des rendements modérés. (Schéma 7)

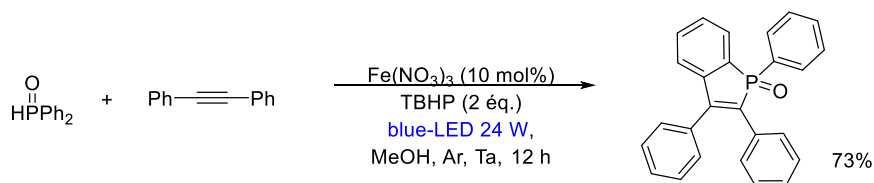


Schéma 7. Synthèse d'oxyde de benzo[*b*]phosphole.

Par une optimisation fine, notamment de la nature du catalyseur et du solvant (10 mol% de $\text{Fe}(\text{OTf})_2$ en présence de 2 éq. de TBHP comme oxydant dans l'acide acétique utilisé comme solvant), des dérivés de type 9-phenyltribenzo[*b,e,g*]phosphindole 9-oxide ont pu être préparés via une réaction tandem intermoléculaire-intramoléculaire de cyclisation impliquant des liaisons C-P et C-C. (Schéma 8)

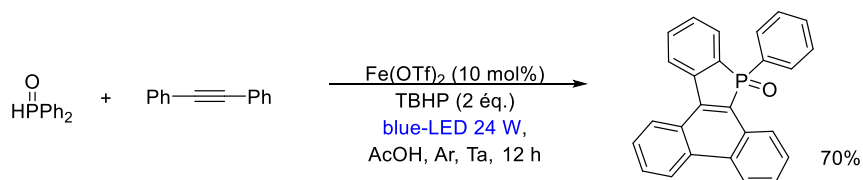


Schéma 8. Synthèse de 9-phenyltribenzo[*b,e,g*]phosphindole 9-oxide.

Le **chapitre 4** regroupe toutes les données expérimentales et caractérisations des composés obtenus and les chapitres 2 et 3.

La **seconde partie** de ce document est consacrée aux travaux de thèse réalisés à Fujian, Chine dédiés à l'accès de dérivés 1,7-fused indoles par catalyse au rhodium. Elle est divisée en cinq chapitres.

Le **chapitre 5** fait l'état de l'art en choisissant des exemples représentatifs de la fonctionnalisation sélective des liaisons C-H du noyau indole sur les positions C2 et C3 (abondamment décrits) *versus* les positions C4, C5, C6 et C7. (Figure 1) Ces exemples choisis démontrent que certaines méthodologies sont efficaces en particulier pour accéder à des indoles de 1,2 fused, 2,3 fused, 3,4 fused, 6,7 fused et 1,7 fused.

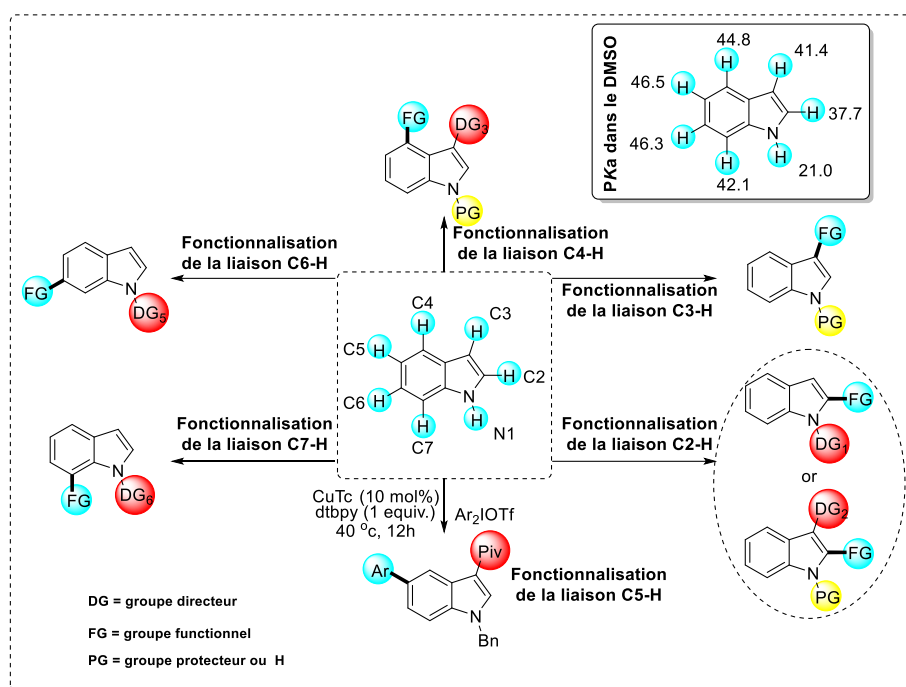
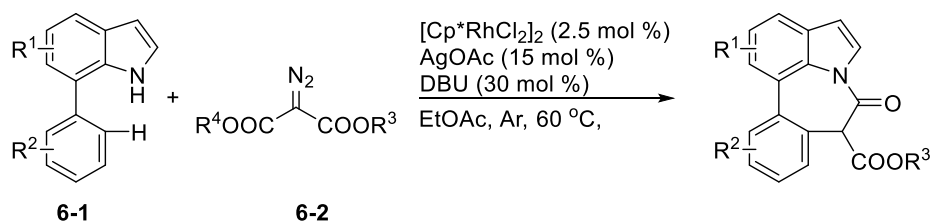


Figure 1. Régio-sélectivités dans les réactions d'activation/fonctionnalisation d'indoles catalysées par des métaux de transition

Dans le **Chapitre 6**, une méthode très efficace est décrite pour l'accès à des composés à sept chaînons de type azépino[3,2,1-*hi*]indoles via une activation/fonctionnalisation de liaison C-H catalysée au rhodium enchainé à une réaction intramoléculaire d'amidation catalysée par le DBU de 7-arylindoles avec des diazomalones. Il a été ainsi développé une méthodologie utilisant 2.5-5 mol% de [Cp**RhCl*]₂ comme catalyseur et des sels d'argent comme oxydants pour la préparation de 1,7 fused indoles à six ou sept chaînons. Il est notamment décrit l'amidation intramoléculaire des 7-phénylindoles avec des diazomalones, l'oléfination/addition aza-Michael des 7-phenyl-1*H*-indoles avec des alcènes et l'annulation des 7-phénylindoles avec des alcynes. La préparation d'azépino[3,2,1-*hi*]indoles a été réalisée par réaction de 7-phényl-1*H*-indoles avec des diazomalones en utilisant 2.5 mol% de [Cp**RhCl*]₂ associé à une quantité catalytique d'AgOAc (15 mol%) et de DBU (30 mol%) à 60 °C. (Schéma 9)



Scheme 9. Synthèse d'azépino[3,2,1-*hi*]indoles à 7 chaînons via une catalyse au rhodium.

Le **Chapitre 7** décrit un processus tandem activation C-H / addition aza-Michael pour la synthèse de dérivés pyrrolo[3,2,1-*de*]phénanthridines à partir de 7-phénylindoles et d'oléfines en utilisant 2.5 mol% de $[\text{Cp}^*\text{RhCl}_2]_2$, 2 éq. d'AgOAc et 10 éq. de Me_4NOAc dans l'acétonitrile sous argon à 80 °C pendant 24 h. Cette transformation tolère une grande variété de groupements fonctionnels et de nombreux dérivés pyrrolo[3,2,1-*de*]phénanthridines ont été obtenus avec de bons voire très bons rendements. (Schéma 10)

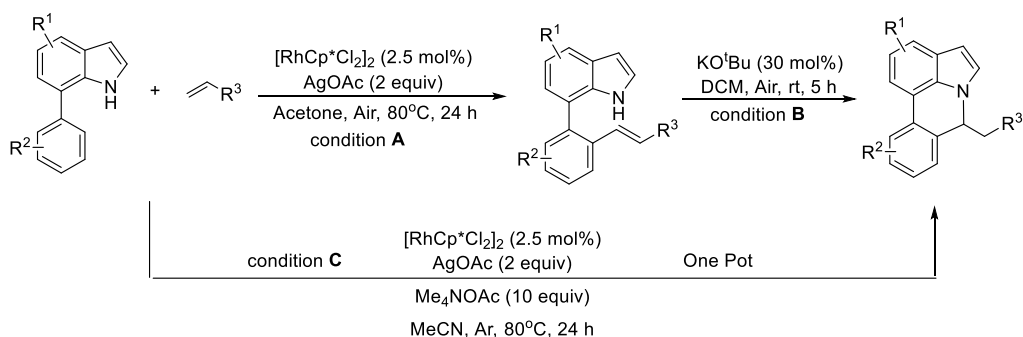


Schéma 10. Synthèse de pyrrolo[3,2,1-*de*]phénanthridines.

Dans le **Chapitre 8**, une méthodologie basée sur une réaction d'électrocatalyse au rhodium impliquant l'annulation oxydante [5+2] de liaisons C-H et N-H d'alcynes et de 7-arylindoles, a permis la préparation de dérivés à sept chaînons de type azépino[3,2,1-*hi*]indoles. Cette transformation se fait sans addition d'oxydant chimique, l'électricité jouant ce rôle. Cette transformation peut être réalisée à l'échelle du gramme en utilisant un procédé en flux. (Schéma 11)

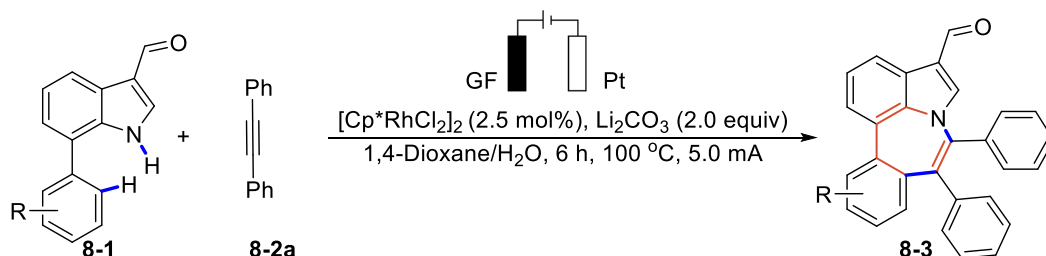


Schéma 11. Préparation de dérivés à sept chaînons de type azépino[3,2,1-*hi*]indoles.

Le **chapitre 9** regroupe toutes les données expérimentales et caractérisations des composés obtenus and les chapitres 6, 7 et 8.

Titre : Transformations catalysées par le rhodium et le fer via des activations C-H, N-H et P-H.

Listes des publications

1- Yumeng Yuan, Qiufeng Huang, Christophe Darcel, *Chem. Eur. J.* **2023**, e202302358.

2- Yumeng Yuan, Jinlan Zhu, Zhongyuan Yang, Shao-Fei Ni, Qiufeng Huang, Lutz Ackermann, *CCS Chem.* **2022**, 4, 1858-1870.

3- Yumeng Yuan, Guoshuai Pan, Xiaofeng Zhang, Qiufeng Huang, *Org. Chem. Front.* **2020**, 7, 53-63.

4- Yumeng Yuan, Guoshuai Pan, Xiaofeng Zhang, Buhong Li, Shengchang Xiang, Qiufeng Huang, *J. Org. Chem.* **2019**, 84, 14701-14711.

Acknowledgement

I had the most wonderful years during my three years PhD. As a joint PhD student, I finished my first year in "College of Chemistry and Materials Science-Fujian Normal University" since 2020, after that I worked in the team of "Organometallics: Materials and Catalysis (OMC)-Université de Rennes from 2021-2023. I would like to thank the important people around me who have contributed to my small achievements and progress.

It's hard to describe in words the appreciation I have for my two supervisors: *Prof.* Qiufeng Huang (China) and *Prof.* Christophe Darcel (France). I would like to thank them first, for *Prof.* Qiufeng Huang to accept me as his student from 2013, teaching and helping me since I was a teenager. I was lucky to become his first PhD student in 2020, and he encouraged me to study with *Prof.* Christophe Darcel in France to gain more knowledge and skills. During the two years study in Rennes, I got a lot of inspiration and help from *Prof.* Christophe Darcel, he is kind and gentle, and even though he is very busy at work, he would always take the time to discuss my projects and patiently explain my problems to me. What impressed me most was when we went to the congress in Nantes together, and his encouraging look at me always cheered me up. I've always considered myself most fortunate to have them as my mentors and also friends. Next, I would like to thank *Prof.* Pierre H. Dixneuf for explaining a lot interesting French customs and cultures to me, thank him for the advices on research during our chats.

Additionally, I would like to thank *Dr.* Christian Bruneau, *Dr.* Cédric Fischmeister, *Dr.* Rafael Gramage-Doria, *Prof.* Henri Doucet, *Prof.* Jean-François Soulé for their kind help.

I also wish to thank my jury members: *Dr.* Audrey Auffrant, *Dr.* Jérôme Hannedouche and *Dr.* Jeanne Crassous for estimating my thesis. Also, I would like to thank *Dr.* Jeanne Crassous and *Dr.* François Carreaux for being my CSI members and for their valuable advices on my topic.

I am also here to thank Mr. Philippe Jéhan, Fabian Lambert and Jérôme Ollivier for the

help in mass analysis, and Ms. Marie Dallon for the contribution to X-ray analysis for my PhD thesis.

During the two-years work in OMC group, I meet nice colleagues and worked in a good atmosphere. I would like to thank the friends I met here. Firstly, I will thank my friend of ten years, *Dr. Jiajun Wu* for introducing my supervisor *Prof. Christophe Darcel* to me, gave me an idea to start a new work experience working with this gentleman. Secondly, thank you to my best friend *Dr. Naba Abuhafez*. To me, she is a rose in the desert that blossoms the most beautifully even in the midst of harsh conditions, she has been my constant companion for the past two years and has brightened up my life with her optimism, passion, cheerfulness and kindness. After I would like to thank *Dr. Marie Peng* for organizing a team drink of many relaxed Friday evenings, and a lot of thank to *Dr. Lucie Cailler*, *Ms. Camille Chenal*, *Ms. Armelle Erussard*, *Ms. Meriem Hadj Rabia*, *Ms. Vanessa Delahaye*, *Ms. Oumaima Gatri*, *Dr. Tony Cousin* and *Mr. Loris Geminiani* for the culture and languages communications. I really enjoyed to work here also with the Chinese friends *Zilong Li*, *Dr. Linhao Liu*, and *Qingxin Zhang* as my colleagues and also as my good friend, they brought a lot of joys to my life and cooked also good dishes.

Furthermore, I would like to thank my parents, *Mr. Alban Schmoll* and my best friends in China: *Dr. Hao Zhang*, *Ms. Yinhua You*, *Ms. Yalin Zhan*, *Mr. Wei Quan* and *Mr. Chenbo Gao* for their support and love.

In the end, I would like to thank China Scholarship Council (CSC) for supporting my study in Rennes so that many wonderful things have happened in my life.

Table of Content

General introduction	1
-----------------------------------	---

Part 1- Blue light driven iron-catalyzed phosphinylation of alkenes and alkynes

PhD work done in Rennes, France

Chapter 1.

Earth abundant transition metal catalyzed phosphination of alkenes and alkynes.

Introduction.....	7
1.1 Hydrophosphination of alkynes and alkynes	9
1.1.1. Manganese-catalyzed hydrophosphination of alkenes.....	9
1.1.2. Iron-catalyzed hydrophosphination of alkenes and alkyne.....	10
1.1.2.1. Hydrophosphination of alkenes.....	10
1.1.2.2. Hydrophosphination of alkynes.....	12
1.1.3. Cobalt-catalyzed hydrophosphination of alkenes and alkynes.....	15
1.1.3.1. Hydrophosphination of alkynes.....	15
1.1.3.2. Hydrophosphination of alkenes.....	16
1.1.4. Nickel-catalyzed hydrophosphination of alkenes and alkynes.....	18
1.1.4.1. Hydrophosphination of alkenes.....	18
1.1.4.2. Hydrophosphination of alkynes.....	21
1.1.5. Copper-catalyzed hydrophosphination of alkenes and alkynes.....	24
1.1.5.1. Hydrophosphination of alkenes.....	24
1.1.5.2. Hydrophosphination of alkynes.....	27
1.2. Oxyphosphorylation	29
1.2.1. Copper-co-catalyzed oxyphosphination of alkenes and alkynes.....	30
1.2.2. Copper- catalyzed oxyphosphination of alkenes and alkynes.....	32
1.2.3. Manganese-catalyzed oxyphosphination of alkenes and alkynes.....	33
1.3. Light driven Hydrophosphination	34
1.4. References	37

Chapter 2.

Blue-light driven iron-catalyzed oxy-phosphinylation of activated alkenes for β -ketophosphine oxide synthesis

2.1. Introduction	42
2.2. Results and Discussion	44
2.3. Conclusion	51
2.4. References	52

Chapter 3.

Blue-light driven iron-catalyzed oxidative C-H/P-H functionalization for the synthesis of benzo[b]phosphole oxides – Preliminary results

3.1. Introduction	56
3.2. Results and discussion	62
3.3. Mechanism discussion	53
3.4. First conclusion and short-term perspectives	64
3.5. References	64

Chapter 4.

Experimental details and characterization datas

4.1. General Remarks.....	67
4.2. Supporting Information of Chapter 2	68
4.2.1. General procedure for blue-light driven iron-catalyzed C–P cross-coupling of styrenes with secondary phosphine oxides.....	68
4.2.2. Characterization data of products 3a- 4c	69
4.2.3. Mechanistic studies.....	77
4.3. Supporting Information of Chapter 3	81
4.3.1. General procedure for the one pot synthesis of 1,2,3-triphenylphosphindole 1-oxide 3-3a	81
4.3.2. Characterization data of products 3-(3a, 3b)	82
4.3.3. General procedure for the one pot synthesis of 9-phenyltribenzo[<i>b,e,g</i>]phosphindole 9-oxides 3-4a	82
4.3.4. Characterization data of products 3-4a	83
4.3.5. X-Ray crystallographic analysis.....	83
4.4. References.....	85

Part 2 - Rhodium Catalyzed Accesses to 1,7-fused Indoles

PhD work done in Fujian, China

Chapter 5.

Transition metal catalyzed selective transformation of indoles. C2-C3 versus C4, C5, C6 and C7 C-H functionalization. Towards efficient methodologies to fused indoles

5.1. Introduction.....	86
5.2. Transition-Metal-Catalyzed C–H Functionalization of Indole framework.....	88
5.2.1. Functionalization at C2 position.....	89
5.2.1.1. Via arylation reactions.....	89
5.2.1.2. Via alkenylation reaction.....	92
5.2.1.3. Via alkylation reaction.....	94
5.2.1.4. Via acylation reaction.....	96
5.2.1.5. Via amidation reaction.....	97
5.2.2. Functionalization at C3.....	98
5.2.2.1. Via arylation reactions.....	98
5.2.2.2. Via alkenylation reaction.....	101
5.2.2.3. Via alkylation reactions.....	102
5.2.2.4. Acylation.....	104
5.2.3. Functionalization at C4.....	106
5.2.4. Functionalization at C5.....	109
5.2.5. Functionalization at C6.....	110
5.2.6. Functionalization at C7.....	111
5.2.7. Annulation from functionalized indoles.....	113
5.3. <i>NH</i> -indole-directed, transition metal catalyzed C-H bond activations.....	116
5.3.1 Approaches of <i>NH</i> -indole-directed, transition metal catalyzed C-H bond activations.....	116
5.4. Conclusions and perspectives of the second part.....	119
5.5. References.....	120

Chapter 6.

Synthesis of seven-membered azepino[3,2,1-*hi*]indoles via rhodium-catalyzed regioselectively C-H activation/1,8-diazabicyclo-[5.4.0]undec-7-ene-catalyzed intramolecular amidation of 7-phenylindoles in one pot

6.1. Introduction	124
6.2. Result and discussion.....	126
6.3. References.....	134

Chapter 7.

One pot synthesis of pyrrolo[3,2,1-*de*]phenanthridines from 7-phenylindoles via tandem C-H olefination/aza-Michael addition

7.1. Introduction.....	136
7.2. Results and discussion.....	139
7.3. Conclusions.....	145
7.4. References.....	146

Chapter 8.

Scalable rhodaelectro-catalyzed expedient access to seven-membered Azepino[3,2,1-*hi*]indoles via [5+2] C-H/N-H annulation

8.1. Introduction.....	148
8.2. Results and discussion.....	150
8.3. Conclusion.....	160
8.4. References.....	160

Chapter 9.

Experimental details and characterization data

9.1. General method.....	164
9.1.1. Characterization data of 7-phenyl-1 <i>H</i> -indoles 6-(1a-1y)	164
9.2. Supporting information of Chapter 6	171
9.2.1. General procedure for the synthesis of azepino[3,2,1- <i>hi</i>]indoles 6-(4a-4x) ...	171
9.2.2. Procedure for synthesis of isopropyl 4-oxo-4,5 dihydrobenzo[4,5]azepino[3,2,1- <i>hi</i>]indole-5-carboxylate 6-4y	181
9.2.3. Competition experiments between 6-1j and 6-1t	182
9.2.4. Experiments for intermolecular kinetic isotope effects.....	182
9.2.5. Procedure for synthesis of benzo[4,5]azepino[3,2,1- <i>hi</i>]indol-4(5 <i>H</i>)-one 6-5a	182
9.2.6. Procedure for synthesis of (<i>E</i>)-methyl 1-(3-ethoxy-3-oxoprop-1-en-1-yl)-4-oxo-4,5-dihydrobenzo[4,5]azepino[3,2,1- <i>hi</i>]indole-5-carboxylate 6-6a	183
9.2.7. Gram-scale experiment of 6-4a	184
9.2.8. Single crystal X-ray structure determination.	184
9.3. Supporting information of Chapter 7	198
9.3.1. General procedure for the <i>ortho</i> C-H olefination reaction (condition A)	198
9.3.2. General procedure for the aza-Michael reaction (condition B)	206
9.3.3. General procedure for the one pot synthesis of pyrrolo[3,2,1- <i>de</i>]phenanthridines (condition C).....	207
9.3.4. Optimization of the C-H olefination of 7-phenyl-1 <i>H</i> -indole 1a with ethyl acrylate 7-2a	215
9.3.5. Optimization of the intramolecular aza-Michael addition of (<i>E</i>)-ethyl 3-(2-(1 <i>H</i> -indol-7-yl)phenyl)acrylate 7-3a	216
9.3.6. Single crystal X-ray structure determination.	216
9.4. Supporting information of Chapter 8	219

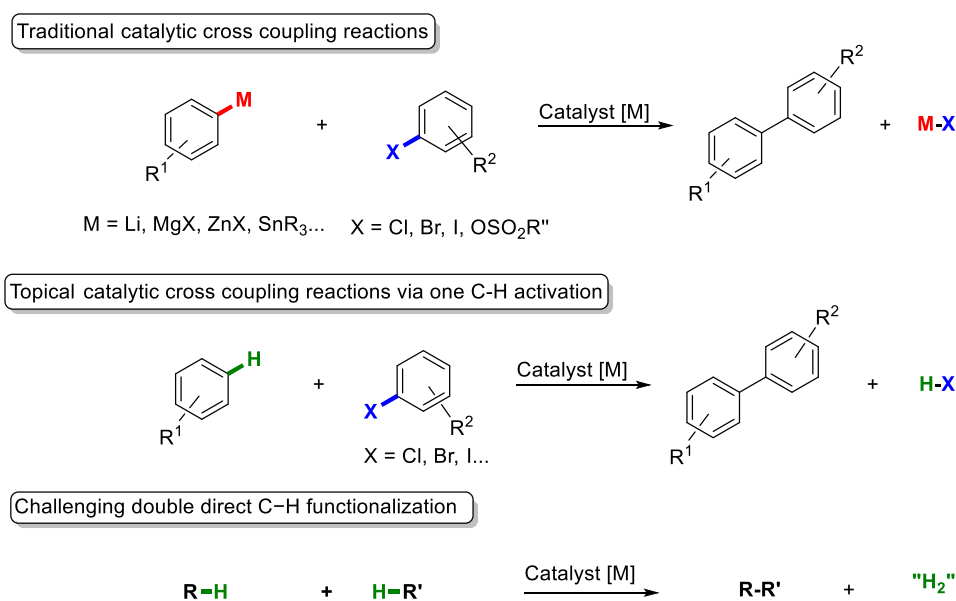
9.4.1. General remarks.....	219
9.4.2. Procedure for synthesis of 7-phenyl-1 <i>H</i> -indole-3-carbaldehydes 8-1	219
9.4.3. Characterization data of materials 8-(1a-1r)	220
9.4.4. Procedure for synthesis of 4,5-diphenylbenzo[4,5]azepino[3,2,1- <i>hi</i>]indole-1-carbaldehydes 8-3	227
9.4.5. Characterization data of products 8-(3aa-3bn')	229
9.4.6. Results of the synthesis of 8-3bo	243
9.4.7. Characterization data of synthetic transformation products 8-4aa	245
9.4.8. Mechanistic studies.....	245
9.4.9. X-Ray crystallographic analysis.....	251
9.4.10. Cyclic voltammetry studies.....	258
9.4.11. XPS studies.....	280
9.4.12. Computational details.....	261
9.5. References.....	277
General conclusions and perspective.....	278
Conclusions générales et perspectives.....	283

General Introduction

General Introduction

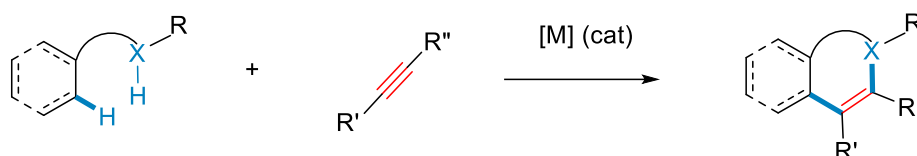
C-C, C-N, C-P bond formation via iron and rhodium catalyzed sustainable C-H and P-H bond activation and functionalization

During the last decades, the selective and controlled C–H functionalization producing selectively carbon-carbon, carbon-nitrogen and carbon-phosphorus bond have brought a breakthrough in synthetic methodologies for a faster access to high value molecules which have applications in the fields of pharmacy, food processing, polymers, organophosphorus ligand, cosmetic or molecular materials.^[1] To achieve efficient C-C bond formation, synthetic chemists used traditional palladium cross-coupling reactions involving organometallic coupling partners (such as RLi, RMgX and RZnX), boronic acid or tin derivatives or pre-functionalized alkyl halides.^[2] Such transformations were also catalyzed by non-noble metals such as manganese, iron, or nickel based catalysts.^[3] However, these methods always produced wastes (and notably metallic ones or toxic ones with tin). In terms of atom economy and sustainability, the direct and widely applicable C–H functionalization strategy would bring significant benefits, notably generating less wastes. Additionally, using earth abundant metals, significant progresses were made.^[4] (Scheme 1)



Scheme 1. Metal-catalyzed functionalizations.

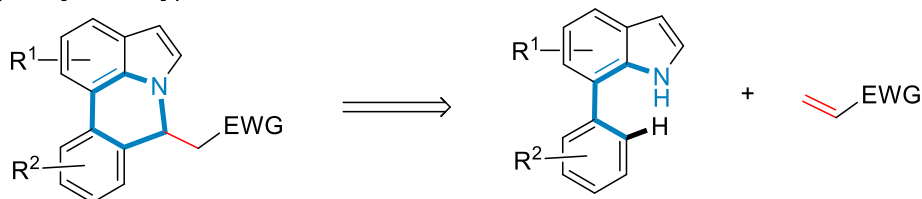
In the other hand, in recent years, significant catalytic systems derived from rare precious metals such as Rh, Pd, Ir, and Au, provided efficient approaches for the rapid construction of heterocyclic molecules, as they permitted the building of C-C, C-N and C-P bonds via direct cross-coupling reactions. Notably, in the last decade, interesting Ru- and Rh-catalyzed C-H activation/annulation via alkene or alkene insertion tandem processes permitted to access in one step in biological important scaffolds.^[5,6] (Scheme 2)



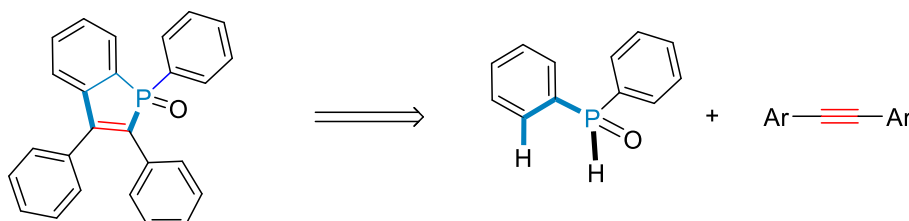
Scheme 2. Principle of transition metal catalyzed C–H bond activation and alkyne annulation reactions for heterocyclic scaffold formation.

Usually, these methodologies involved oxidation/reduction steps in the transition metal catalytic cycles. To promote them efficiently, stoichiometric amounts of chemical oxidants, based on Cu^[7] and Ag^[8] salts were required for the regeneration of the active high valent catalyst. In order to reduce the environmental impact of such metal oxides and to lower process costs, an elegant alternative to perform such oxidative C–H coupling reactions can be to conduct them in the absence of exogenous oxidants *via* transition metal electrocatalysis. Pyrrolo[3,2,1-*de*] phenanthridines and azepino[3,2,1-*hi*]indoles can be efficiently prepared using such methodologies (see below).

Pyrrolo[3,2,1-*de*] phenanthridines



Benzo[*b*]phospholes



Scheme 3. Analogy for the preparation of pyrrolo[3,2,1-*de*] phenanthridines and benzo[*b*]phosphole *via* transition metal catalyzed C-H activation/annulation.

In a similar way, the construction of benzo[*b*]phosphole derivatives can be done using similar disconnections starting from phosphine oxides and internal alkynes. (Scheme 3) In the area of C-P bond formation, during the last decade, among the numerous transition metals used, significant numbers of examples described iron based catalyzed formation of C-P bond via hydrophosphination of alkenes and alkynes.^[9-16] By contrast, no example of oxyphosphination reaction performed by a sole iron catalyst was described, and only few reports mentioned the use of copper/iron as co-catalysts.^[17-19] It was then interesting to develop such iron-catalyzed C-P bond formation, mainly for the preparation of benzo[*b*]phosphole derivatives. Indeed, despite the considerable progress made in these reactions, the high reaction costs due to the use of precious metals cannot be ignored. Therefore, the quest for cheaper, earth-abundant, non-toxic catalysts for hetero-atom insertion processes is of continuing importance. As iron is one of the most abundant metals on the earth and is also economically and environmentally friendly, it can be an interesting substitute to perform C-heteroatom bond formation and thus prepare heterocyclic compounds.

My doctoral research work was made in Fujian Normal University (from September 2020 to October 2021) and in the Université de Rennes (From November 2021 and November 2023). My PhD research in Rennes was dedicated to iron catalyzed C-P bond formation. Another part in China was the rhodium catalyzed annulation of C-H and C-N bond.

The manuscript includes nine chapters.

Based on the observations that sole iron catalyst has been never described to perform oxyphosphination of unsaturated C-C bonds, the **first part** of this manuscript will be dedicated to the work performed in Rennes, France on blue light driven iron-catalyzed phosphinylation of alkenes and alkynes. It will be divided in four chapters.

The **Chapter 1** will give a general introduction on phosphination, phosphinylation and phosphorylation of alkenes and alkynes by using earth abundant transition metal catalysts such as Mn, Fe, Co, Ni and Cu.

The **Chapter 2** will describe the oxyphosphination of activated alkenes with secondary phosphine oxides, using iron salt as the catalyst and driven by blue LED irradiation, leading efficiently to a variety of functionalized β -ketophosphine oxides.

In **Chapter 3** will report the preliminary results obtained on blue light driven iron salt-catalyzed synthesis of benzo[*b*]phosphole oxides by reaction of secondary phosphine oxides with internal alkynes via intermolecular/intramolecular oxidative C-H/P-H functionalization.

The **Chapter 4** will collect the experimental details and characterization data of Chapters 2 and 3, including general procedures, NMR spectroscopy and X-ray crystallographic analysis.

The **second part** of this manuscript will be devoted to the work performed in Fujian, China on Rhodium catalyzed accesses to 1,7-fused indoles. It will be divided in five chapters.

The **Chapter 5** will give representative examples of the selective transition metal catalyzed C2-C3 versus C4, C5, C6 and C7 C-H functionalization of indoles, thus highlighting efficient methodologies to access to challenging 1,2 fused, 2,3 fused, 3,4 fused, 6,7 fused and 1,7 fused indoles.

In **Chapter 6**, we will describe a straightforward route to efficiently prepare seven-membered azepino[3,2,1-*hi*]indoles through a rhodium-catalyzed regioselective C-H activation followed by a DBU-catalyzed intramolecular amidation of 7-arylindoles with diazomalonates.

The **Chapter 7** will present an C-H olefination/aza-Michael addition tandem process for the synthesis of pyrrolo[3,2,1-*de*]phenanthridines from 7-phenylindoles and alkenes

using a $[\text{Cp}^*\text{RhCl}_2]_2/\text{AgOAc}/\text{Me}_4\text{NOAc}$ catalytic system. This synthesis tolerates a relatively wide range of functional groups, and a variety of pyrrolo[3,2,1-de]phenanthridines are obtained in good to excellent yields.

In **Chapter 8**, a rhodaelectro-catalyzed [5+2] N–H/C–H oxidative annulation of alkynes by 7-arylindoles, enabling the synthesis of seven-membered azepino[3,2,1-*hi*]indoles using electricity as the sole oxidant will be presented. Noticeably, the reaction can be scaled up to gram-scale by flow-electrocatalysis. Two key rhodium(III) intermediates were isolated and fully characterized. Cyclovoltammetric analysis, XPS studies and DFT calculations are suggestive of a rhodium(III-IV-II-III) manifold.

The **Chapter 9** combines the experimental descriptions and characterization data of the chapters 6, 7 and 8, including general procedures, NMR spectroscopy, X-ray crystallographic analysis, Cyclic Voltammetry studies, XPS studies and computational details.

References

- [1] For selected leading reviews on transition metal catalyzed C–H activation, see: (a) R. Giri, B.-F. Shi, K. M. Engle, N. Mugel, J.-Q. Yu, *Chem. Soc. Rev.* **2009**, *38*, 3242–3272; (b) O. Baudoin, *Chem. Soc. Rev.* **2011**, *40*, 4902–4911; (c) L. Ackermann, *Chem. Rev.* **2011**, *111*, 1315–1345; (d) P. B. Arockiam, C. Bruneau, P. H. Dixneuf, *Chem. Rev.* **2012**, *112*, 5879–5918; (e) P. Gandeepan, T. Müller, D. Zell, G. Cera, S. Warratz, L. Ackermann, *Chem. Rev.* **2019**, *119*, 2192–2452; (f) W. Ali, G. Prakash, D. Maiti, *Chem. Sci.* **2021**, *12*, 2735–2759 (g) S. Rey, A. Das, N. Chatani, *Chem. Soc. Rev.* **2021**, *431*, 213683; (g) J. H. Docherty, T. M. Lister, G. McArthur, M. T. Findlay, P. Domingo-Legarda, J. Kenyon, S. Choudhary, I. Larrosa, *Chem. Rev.* **2023**, *123*, 12, 7692–7760.
- [2] For representative examples, see: (a) N. Miyaura, A. Suzuki, *Chem. Rev.* **1995**, *95*, 2457–2483; (b) C. C. C. Johansson Seecurn, M. O. Kitching, T. J. Colacot, V. Snieckus, *Angew. Chem. Int. Ed.* **2012**, *51*, 5062–5085; (c) K. C. Nicolaou, P. G. Bulger, D. Sarlah, *Angew. Chem. Int. Ed.* **2005**, *44*, 4442–4489; (d) C. Torborg, M. Beller, *Adv. Synth. Catal.* **2009**, *351*, 3027–3043.
- [3] For selected leading reviews on first row transition metal catalyzed cross-coupling reactions, see: (a) J. R. Carney, B. R. Dillon, S. P. Thomas, *Eur. J. Org. Chem.* **2016**, 3912–3929; (b) S. Rana, J. P. Biswas, S. Paul, A. Paika, D. Maiti, *Chem. Soc. Rev.* **2021**, *50*, 243–472; (c) O. M. Kuzmina, A. K. Steib, A. Moyeux, G. Cahiez, P. Knochel, *Synthesis* **2015**, 1696–1705; (d) C. Darcel, J.-B. Sortais, S. Quintero Duque, *RSC Green Chemistry Series* **2015**, *26*, 67–92; (e) C. Guérinot, J. Cossy, *Acc. Chem. Res.* **2020**, *53*, 1351–1363; (f) O. Planas, C. J. Whiteoak, X. Ribas, in *Non-Noble Metal Catalysis* Ed. R. J. Klein Gebbink, M.-E. Moret, John Wiley & sons, **2019**, pp 297–328.

- [4] For selected leading reviews on first row transition metal catalyzed C-H activation, see: (a) J. Miao, H. Ge, *Eur. J. Org. Chem.* **2015**, 7859–7868; (b) B. Su, Z.-C. Cao, Z.-J. Shi, *Acc. Chem. Res.* **2015**, *48*, 886–896; (c) R. Shang, L. Ilies, E. Nakamura, *Chem. Rev.* **2017**, *117*, 9086–9139; (d) M. Moselage, J. Li, L. Ackermann, *ACS Catal.* **2016**, *6*, 498–525; (e) W. Liu, L. Ackermann, *ACS Catal.* **2016**, *6*, 3743–3752; (f) J. Loup, U. Dhawa, F. Pescioioli, J. Wencel-Delord, L. Ackermann, *Angew. Chem. Int. Ed.* **2019**, *58*, 12803–12818; (g) R. Mei, U. Dhawa, R. C. Samanta, W. Ma, J. Wencel-Delors, L. Ackermann, *ChemSusChem* **2020**, *13*, 3306–3356; (h) T. Aneeja, M. Neetha, C. M. A. Afsina, G. Anilkumar, *Catal. Sci. Technol.* **2021**, *11*, 444–458.
- [5] (a) G. Duarah, P.P. Kaishap, T. Begum, S. Gogoi, *Adv. Synth. Catal.* **2018**, *361*, 654–672; (b) L. Ackermann, *Acc. Chem. Res.* **2014**, *47*, 2, 281–295.
- [6] (a) S. Das, A. Dutta, *Tetrahedron*, **2023**, *146*, 133633; (b) C. Wang, F. Chen, P. Qian, J. Cheng, *Org. Biomol. Chem.* **2021**, *19*, 1705–1721; (c) Y. Yang, K. Li, Y. Cheng, D. Wan, M. Li, J. You, *Chem. Commun.* **2016**, *52*, 2872–2884.
- [7] Selected examples using copper salt as stoichiometric oxidants: (a) Z. Wang, J. Yin, F. Zhou, Y. Liu, J. You, *Angew. Chem. Int. Ed.* **2019**, *58*, 254–258; (b) A. D. Streit, A. J. Zoll, G. L. Hoang, J. A. Ellman, *Org. Lett.* **2020**, *22*, 1217–1221.
- [8] Selected examples using silver salt as stoichiometric oxidants: (a) Bai, D. Xu, T. Ma, C. Zheng, X. Liu, B. Xie, F. Li, X. ACS *Catal.* **2018**, *8*, 4194–4200; (b) X. Kou, K. G. M. Kou, *ACS Catal.* **2020**, *10*, 3103–3109; (c) S. Qian, X. Pu, G. Chang, Y. Huang, Y. Yang, *Org. Lett.* **2020**, *22*, 5309–5313; (d) L. Sun, H. Chen, B. Liu, J. Chang, L. Kong, F. Wang, Y. Lan, X. Li, *Angew. Chem. Int. Ed.* **2021**, *60*, 8391–8395.
- [9] K. J. Gallagher, R. L. Webster, *Chem. Commun.*, **2014**, *50*, 12109–12111.
- [10] A. K. King, A. Buchard, M. F. Mahon, R. L. Webster, *Chem. Eur. J.* **2015**, *21*, 15960 – 15963.
- [11] K. J. Gallagher, M. Espinal-Viguri, M. F. Mahon, R. L. Webster, *Adv. Synth. Catal.* **2016**, *358*, 2460 – 2468.
- [12] M. Espinal-Viguri, A. K. King, J. P. Lowe, M. F. Mahon, R. L. Webster, *ACS Catal.* **2016**, *6*, 7892–7897.
- [13] M. Kamitani, M. Itazaki, C. Tamiya, H. Nakazawa, *J. Am. Chem. Soc.* **2012**, *134*, 11932–11935.
- [14] L. Routaboul, F. Toulgoat, J. Gatignol, J.-F. Lohier, B. Norah, O. Delacroix, C. Alayrac, M. Taillefer, A.-C. Gaumont, *Chem. Eur. J.* **2013**, *19*, 8760 – 8764.
- [15] M. Itazaki, S. Katsube, M. Kamitani, H. Nakazawa, *Chem. Commun.*, **2016**, *52*, 3163–3166.
- [16] A. K. King, K. J. Gallagher, M. F. Mahon, R. L. Webster, *Chem. Eur. J.* **2017**, *23*, 9039 – 9043.
- [17] W. Wei, J. Ji, *Angew. Chem. Int. Ed.* **2011**, *50*, 9097–9099.
- [18] N. Yi, R. Wang, H. Zou, W. He, W. Fu, W. He, *J. Org. Chem.* **2015**, *80*, 5023–5029.
- [19] M. Zhou, M. Chen, Y. Zhou, K. Yang, J. Su, J. Du, Q. Song, *Org. Lett.* **2015**, *17*, 1786–1789.

**Part 1- Blue light driven Iron-catalyzed
phosphinylation of alkenes and alkynes.**

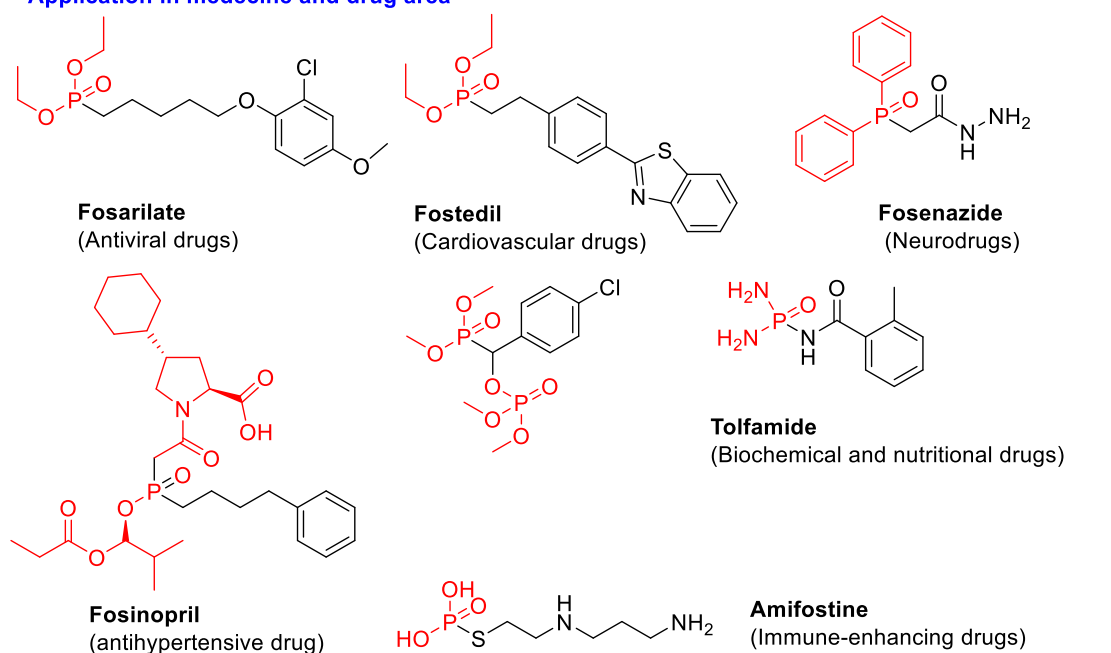
PhD contribution done in Rennes. France

Chapter 1 - Earth abundant transition metal catalyzed phosphination of alkenes and alkynes

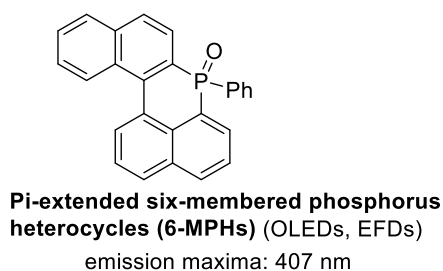
Introduction

Phosphorus-containing derivatives are prevalent in many day life areas including medicine & drug discovery,^[1] material sciences notably for electronic properties,^[2] and agriculture & crop protection.^[3] (Figure 1-1)

Application in medicine and drug area



Application in material science



Application in agriculture and crop protection

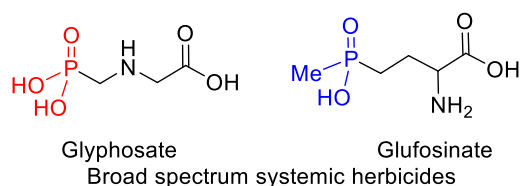
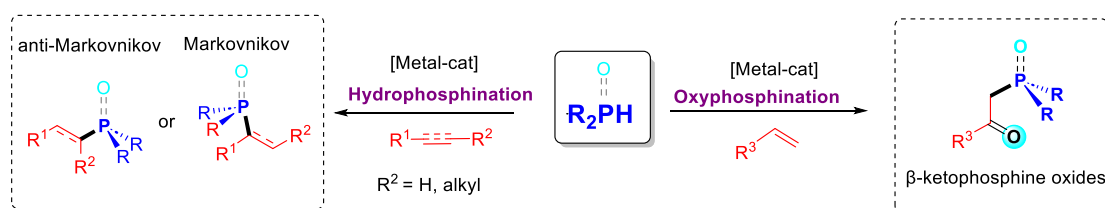


Figure 1-1. Applications of few representative P-containing molecules in medicine & drug area, material sciences and agriculture and crop protection.

Additionally, phosphines are useful partners in molecular synthesis. Indeed, tertiary phosphines have ubiquitous use as ligands for coordination and organometallic chemistry, transition metal homogeneous catalysis,^[4] and for organocatalysis, notably

in an enantioselective way.^[5] Thanks to their huge and various applications, significant progress has been achieved in the development of new for constructing the carbon–phosphorus bonds in addition to classical reaction of organometallic compounds with halophosphines, reaction of metal phosphides with alkyl halides, and reduction of other phosphorus compounds.^[6] Alternatively, catalytic versions of preparation of organophosphorus derivatives via P-C couplings were also performed *via* catalytic Hirao type cross-coupling reactions of organohalides with transition metals^[7] such as palladium,^[8] nickel or copper.^[9]

On the other hand, transition-metal-catalyzed hydrophosphination and oxyphosphination of activated alkene/alkynes are considered as the straightforward methods for the synthesis of organophosphorus compounds, such transformations classically being performed with noble metals such as gold, platinum, palladium or ruthenium.^[10] (Scheme 1-1).



Scheme 1-1. Transition metal-catalyzed hydrophosphination and oxyphosphination strategies.

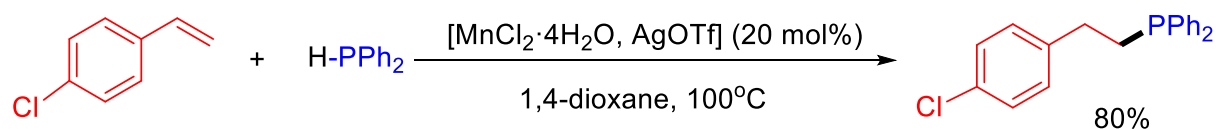
Indeed, in the light of the current crucial concerns about climate changes and the associated green chemistry principles, the substitution of noble transition metals by the more benign first-row transition metals constitutes one of the important current challenges. During the last decade, the evaluation of cheap, environmentally friendly and less toxic metal catalysts based on manganese, iron, cobalt, nickel, and copper was made and exhibited promising activity in hydroelementation transformations.^[11] Thus, this **introduction chapter** will provide a concise overview of the literature in the catalyzed hydrophosphination and oxyphosphination of activated alkenes/alkynes and show the potential of manganese, iron and cobalt, nickel and copper as surrogate transition metal catalysts to the noble ones.

1.1. Hydrophosphination of alkynes and alkenes

Since the first patent in 1958 by Reuter and Orthner dealing hydrophosphination of formaldehyde,^[12] and the first catalytic hydrophosphination of olefins by Pringle,^[13] both transformations being catalyzed by platinum, numerous reports of hydrophosphination were described with or without catalysts, one of the main advantages of the catalyzed versions being better selectivity of the transformations.^[10] This first paragraph will describe hydrophosphinations of alkenes and alkenes by first row transition metals.

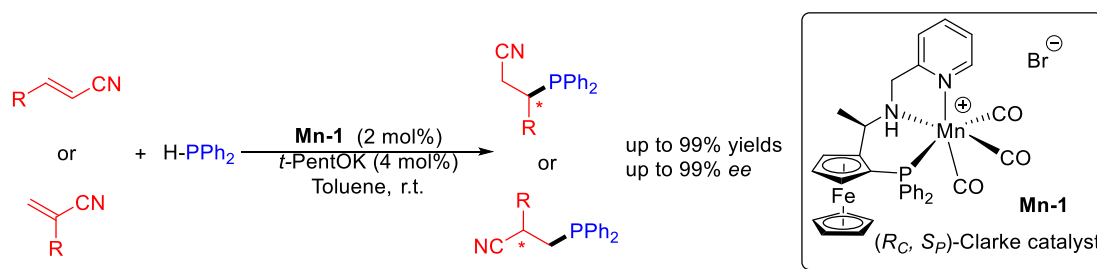
1.1.1. Manganese-catalyzed hydrophosphination of alkenes

The use of manganese-based catalysts for alkene hydrophosphination is rarely mentioned. In 2011, A. Corma and co-workers reported the use of 20 mol% of a pre-formed catalytic species from $\text{MnCl}_2 \cdot 4\text{H}_2\text{O}$ and 2 equiv. of AgOTf for the hydrophosphination of *p*-chlorostyrene leading to 80% of the anti-Markovnikov product.^[14] (Scheme 1-2)



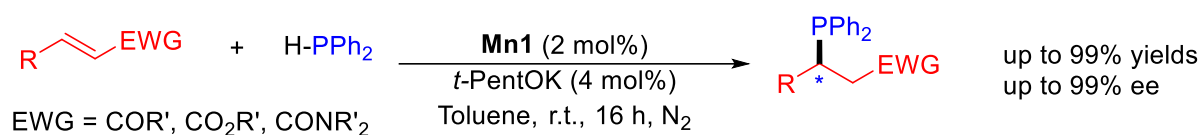
Scheme 1-2. Mn salt catalyzed hydrophosphination of *p*-chlorostyrene.

A decade later, L. Ge, S. R. Harutyunyan and co-workers developed a Mn(I)-catalyzed enantioselective hydrophosphination of internal and terminal α , β -unsaturated nitriles. Using 2 mol% of a well-defined chiral (R_C , S_P)-PNN pincer Mn complex (Clarke catalyst, **Mn1**), 4 mol% of *t*-pen'OK, in toluene at rt, the corresponding chiral phosphines were obtained in high yields (up to 99%) and enantioselectivity (up to 99%).^[15] (Scheme 1-3)



Scheme 1-3. Mn(I)-catalyzed enantioselective hydrophosphination of internal and terminal α , β -unsaturated nitriles.

Using the same complex **Mn-1**, the same group extended the Mn(I)-catalyzed hydrophosphination of secondary phosphines to α,β -unsaturated ketones, esters and carboxamides.^[16] (Scheme 1-4)



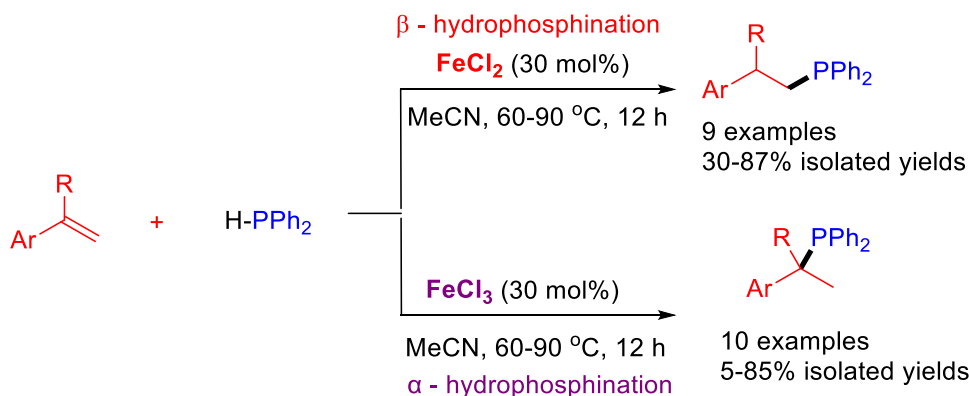
Scheme 1-4. Mn(I)-catalyzed enantioselective hydrophosphination of α,β -unsaturated carbonyl and carboxylic derivatives.

1.1.2. Iron-catalyzed hydrophosphination of alkenes and alkynes

1.1.2.1. Hydrophosphination of alkenes

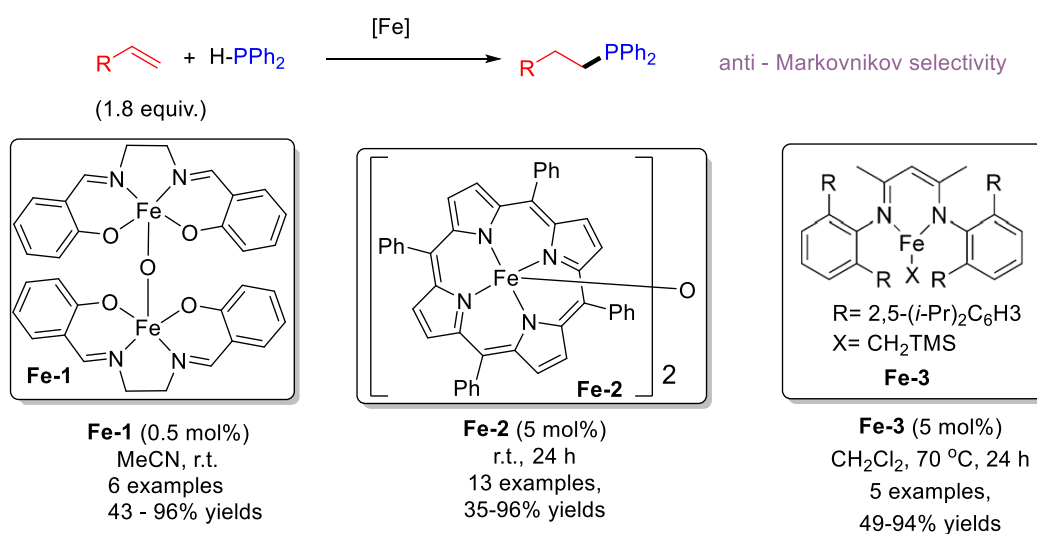
In comparison, iron catalyzed hydrophosphination of alkenes and alkynes were more extensively studied.

In 2013, A.-C. Gaumont, M. Taillefer and co-workers reported the switchable regioselective iron-catalyzed addition of diphenylphosphine to styrene derivatives. By a simple modification of the iron salt used, the regioselectivity of the phosphinylation was inverted. Using 30 mol% of FeCl_3 permitted to access to the α -addition products and performing the reaction with 30 mol% of FeCl_2 led to the β -addition.^[17] The switch of regioselectivity was rationalized by the difference of Lewis acidity between Fe salts, the Fe(III)-salt generating a polarized and intramolecularly stabilized π -complex. (Scheme 1-5)



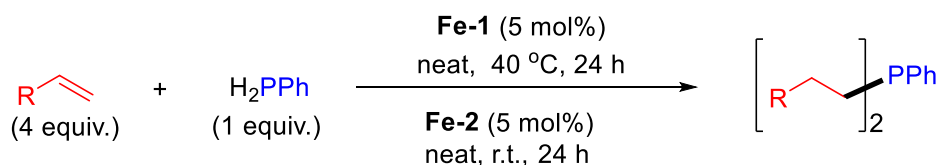
Scheme 1-5. Iron-catalyzed α - or β -addition of diphenylphosphine to styrene derivatives.

One year later, R. L. Webster and co-workers developed a series of well-defined iron catalysts to promote the hydrophosphination of styrene, vinylpyridine and acrylate derivatives. Thus, using 0.5 mol% of the μ -*oxo*-bis(N,N-ethylenebis(salicylideneiminato)iron(III) complex **Fe-1** in acetonitrile at r.t., activated olefins such as styrene, acrylic esters and 2-vinylpyridine led to the corresponding anti-Markovnikov phosphine derivatives in moderate to high yields.^[18] (Scheme 1-6) Using the iron(III) porphyrin complex **Fe-2** as a catalyst (5 mol%), this group also succeeded to perform the same reaction with similar efficiency.^[19] β -diketiminato iron(II) complex **Fe-3** was also a good catalyst for the reaction which should have been conducted at 70 °C. Noticeably, allylbenzene and 1-hexene were less reactive and gave only low amounts of the corresponding phosphines.^[20]



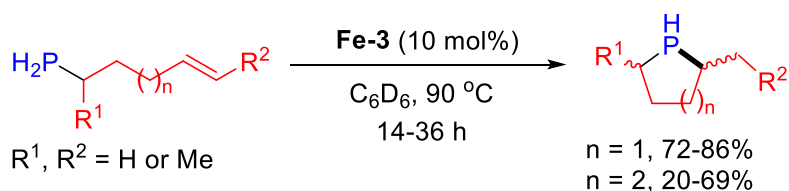
Scheme 1-6. Well defined iron complexes for the catalyzed hydrophosphination of activated alkenes.

Interestingly, R. L. Webster also succeeded to perform double hydrophosphination of activated alkenes such as styrene derivatives with a primary phosphine, phenylphosphine. Thus, using 1.25 mol% of **Fe-1** or 5 mol% of **Fe-2**, in neat conditions, the corresponding tertiary phosphines were obtained in 62-96% yields.^[19] It was shown that the first hydrophosphination step leading to the secondary phosphines (R-CH₂-CH₂)(Ph)PH can be conducted with H₂PPh and styrene at 80°C without any catalyst. (Scheme 1-7)



Scheme 1-7. Iron catalyzed double hydrophosphination of primary phosphine with activated alkenes.

R. L. Webster also reported the first example of intramolecular hydrophosphination of a series of non-activated phosphinoalkenes leading to the 5- and 6-membered cyclophosphines (phospholanes and phosphinanes, respectively). Thus, using 10 mol% of the β -diketiminato Iron(II) complex **Fe-3** at 90 °C for 14-36 h, the cyclophosphines were obtained with yields up to 86%.^[21] (Scheme 1-8)

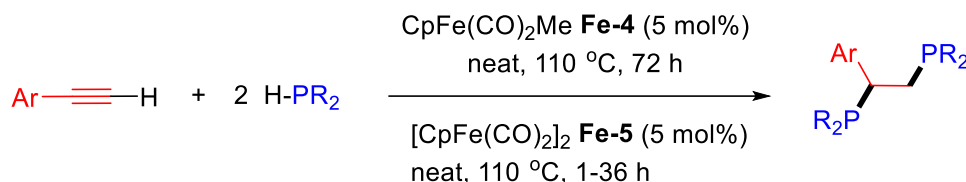


Scheme 1-8. Iron-catalyzed hydrophosphination of non-activated phosphinoalkenes.

1.1.2.2. hydrophosphination of alkynes

Hydrophosphination of alkynes could be also performed at iron. Indeed, H. Nakazawa and co-workers reported the first iron-catalyzed double hydrophosphination of terminal arylalkynes with secondary arylphosphines. This reaction was performed in the presence of 10 mol% of CpFe(CO)₂Me **Fe-4** in the presence of 2 equiv. of secondary phosphines at 110 °C for 72 h. 1,2-bisphosphinoethane derivatives were

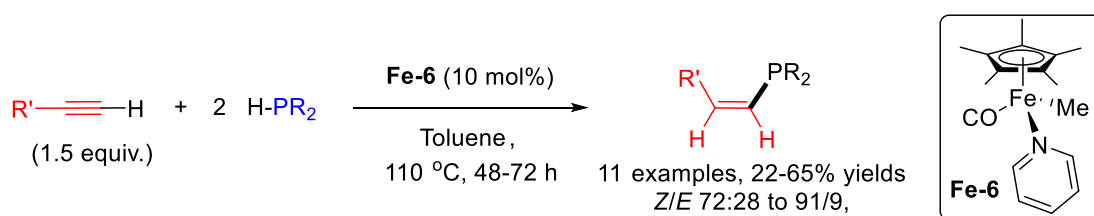
regioselectively obtained in 27-95% yields.^[22] Notably, with *n*-hexyl-, cyclohexyl-, and benzyl-acetylene, dicyclohexylphosphine and di-*tert*-butylphosphine no reaction took place. (Scheme 1-9)



Scheme 1-9. Iron-catalyzed double hydrophosphination of terminal alkynes and secondary arylphosphines.

Similarly, Waterman has shown that [CpFe(CO)₂]₂ (5 mol%, **Fe-5**), also permitted to perform the double hydrophosphination of terminal arylalkynes conducting the reaction with diphenylphosphine at 110 °C, thus leading to the corresponding products were isolated in 66-99% yields. (Scheme 1-9).^[23]

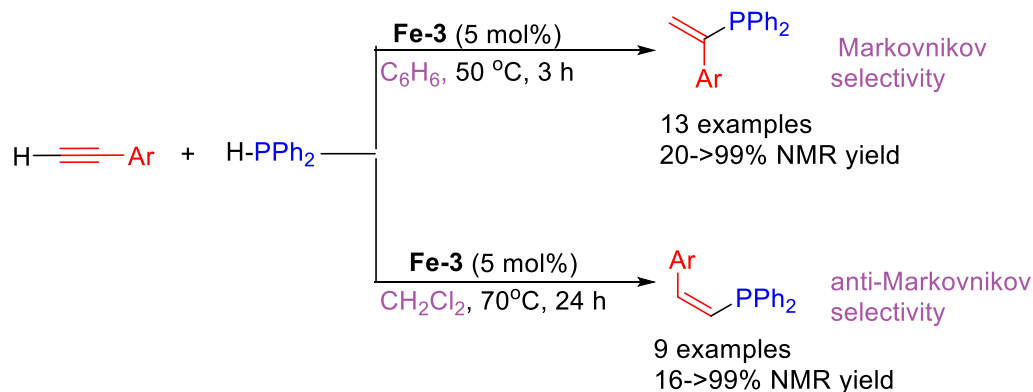
The mono-hydrophosphination of terminal alkynes can be also selectively performed. By reaction with secondary phosphines and terminal arylalkynes, Kamitani's group prepared (*Z*)-vinylphosphines and unsymmetric diphosphines using 10 mol% of Cp*Fe(CO)(py)(Me) **Fe-6** by reaction in toluene at 110 °C.^[24] (Scheme 1-10)



Scheme 1-10. Fe-catalyzed hydrophosphination of terminal arylalkynes with secondary phosphines.

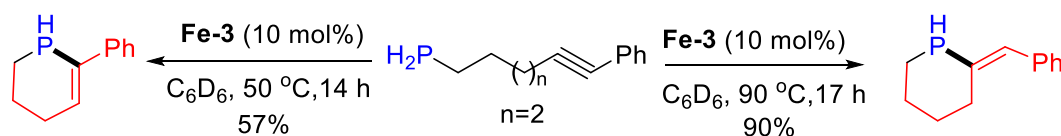
Using the iron(III) porphyrin complex **Fe-3** as a catalyst, R. L. Webster and co-workers described the synthesis of vinyl phosphines from terminal (hetero)aryl alkynes. During their investigations, they highlighted the crucial role of the solvent on the regioselectivity of the reaction. Conducting the reaction in benzene at 50 °C for 3 h led to the formation of Markovnikov products *gem*-vinylphosphines, whereas performing the reaction in dichloromethane at 70 °C for 24 h permitted to obtain (*Z*)-

vinylphosphines anti-Markovnikov products.^[25] Even if not fully rationalized, the authors suggested thanks to preliminary mechanistic studies that the regioselectivities may depend of the oxidation state of the active species [Fe(II) vs Fe(III)]. (Scheme 1-11)



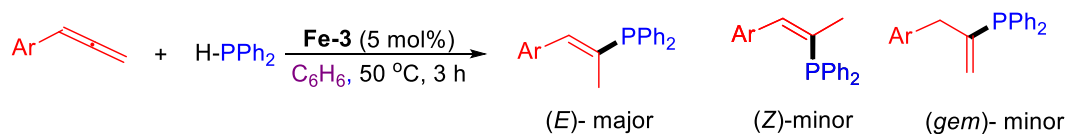
Scheme 1-11. Iron-catalyzed Markovnikov or anti-Markovnikov hydrophosphination of terminal alkynes.

In addition to their work on intramolecular hydrophosphination of a series of non-activated phosphinoalkenes leading to phospholanes and phosphinanes, R. L. Webster also reported two examples of intramolecular hydrophosphination of phosphinoalkynes under similar conditions [10 mol% of **Fe-3** at 50-90 °C for 14-17 h], the cyclophosphines were obtained with yields up to 90%.^[21] (Scheme 1-12)



Scheme 1-12. Iron-catalyzed hydrophosphination of non-activated phosphinoalkynes.

The same group has recently developed an original iron-catalyzed hydrophosphination of allenes. Using 5 mol% of the Fe(II) β -diketiminate pre-catalyst **Fe-3**, they succeeded to promote the reaction of HPPH₂ with aryl- and alkyl-allenes in C₆D₆ at 80 °C for 16 h. Starting from arylallenes, *E*-vinyl products were produced as the major species (e.g., 6:3:1 as *E/gem/Z*).^[26]

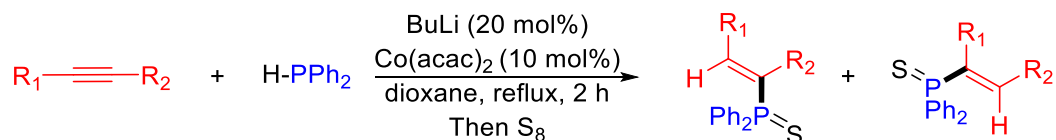


Scheme 1-13. Iron-catalyzed hydrophosphination of allenes.

1.1.3. Cobalt-catalyzed hydrophosphination of alkenes and alkynes

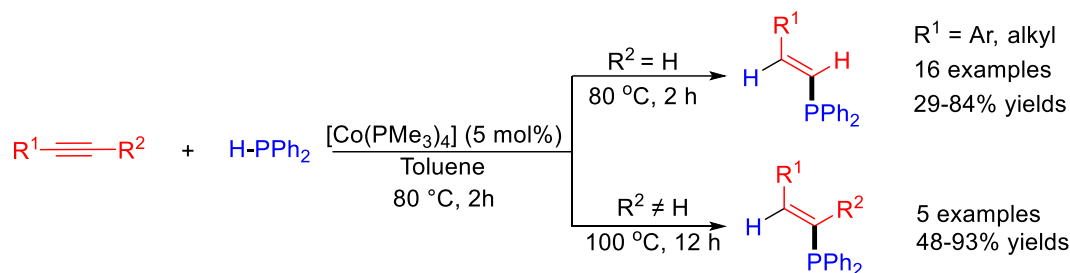
1.1.3.1. Hydrophosphination of alkynes

Group 9 metals have also attracted notable attention for catalyzed hydrophosphination. The first example was reported in 2005 by K. Oshima's group for the Co(II)-catalyzed hydrophosphination of alkynes with diphenylphosphine.^[27] The catalytic active species was generated in situ adding successively 10 mol% of Co(acac)₂, 1,4-dioxane and alkyne to a mixture of 1 equiv. of diphenylphosphine and 20 mol% butyllithium. The mixture was then refluxed for 2 h. After sulfidation with S₈, the corresponding vinyl phosphine sulfide resulting from a *syn*-addition were obtained, the regioselectivity being governed by the steric interactions of the two alkyne substituents. (Scheme 1-14)



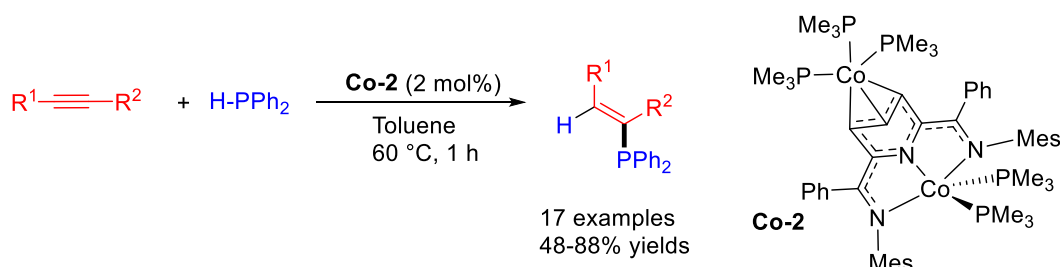
Scheme 1-14. Cobalt-catalyzed *syn* hydrophosphination of alkynes.

In 2018, M. Shanmugam and co-workers reported a Co(0)-catalyzed hydrophosphination of internal and terminal alkynes with diphenylphosphine using 5 mol% of the well-defined cobalt complex Co(PMe₃)₄ **Co-1**, in toluene at 80 °C.^[28] Noticeably, (*E*)-vinylphosphines were obtained efficiently. The proposed active catalytic species CoH(PMe₃)₃(PPh₂) resulted from the oxidative addition of diphenylphosphine to **Co-1** which explained the stereoselectivity observed resulting from the insertion of the C≡C bond in the Co-hydride bond then reductive elimination. (Scheme 1-15)



Scheme 1-15. Cobalt-catalyzed hydrophosphination of alkynes.

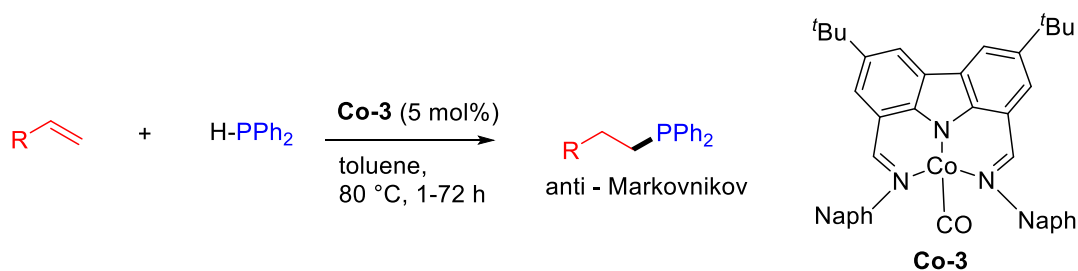
Recently, Rajaraman and Shanmugan reported the use of an original binuclear cobalt complex **Co-2** (2 mol%) for the anti-Markovnikov hydrophosphination of alkynes leading the corresponding (*E*)-vinylphosphines in 48-88% yields.^[29] Similarly, a cobalt hydride phosphide was proposed as a catalytic species. (Scheme 1-16)



Scheme 1-16. Binuclear cobalt complex for the anti-Markovnikov hydrophosphination of alkynes.

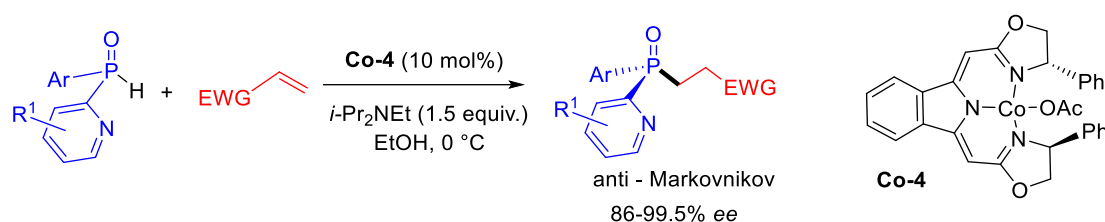
1.1.3.2. Hydrophosphination of alkenes

D. L. Kays and co-workers described Co-catalyzed hydrophosphination of activated alkenes with diphenylphosphane using a cobalt(I) *N,N,N*-pincer complex **Co-3**. The linear phosphine resulting a β -addition in an anti-Markovnikov fashion were selectively obtained with moderate to good yields. It should be underlined that the functional tolerance of the transformation as cyano, esters, lactone, ketone moieties were not altered.^[30]



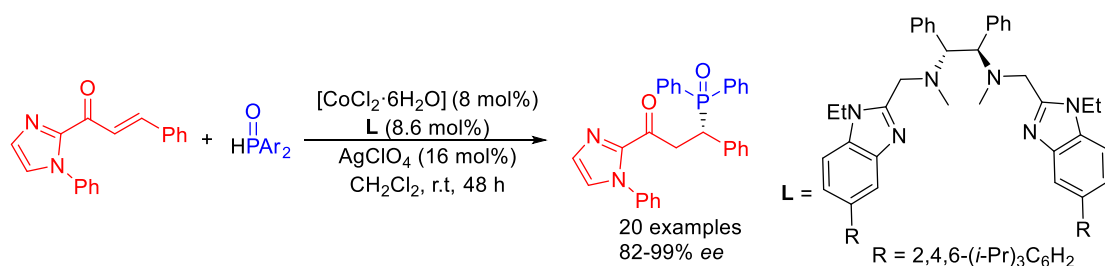
Scheme 1-17. Cobalt(I) pincer complex for catalyzed hydrophosphination of activated alkenes.

In an asymmetric version of hydrophosphination of alkenes, W.-L. Duan et al. reported the use of a chiral NNN-pincer cobalt complex **Co-4** for the preparation of P-chirogenic tertiary phosphine oxides starting from a racemic secondary pyridinyl phosphine oxides and activated alkenes. Using 10 mol% of **Co-4** and 1.5 equiv. of *i*Pr₂NEt in ethanol at 0 °C, a series of enantioenriched tertiary phosphine oxides were prepared with good to excellent yields and 86-99.5% *ee*.^[31] (Scheme 1-18) In this strategy, the presence of the pyridyl group on the phosphorus atom via its coordination to cobalt center permitted to distinguish the two aryl groups thus performing a highly stereoselective transformation.



Scheme 1-18. Cobalt-catalyzed preparation of P-chirogenic tertiary phosphine oxides by hydrophosphination.

D.-Q. Shi, M.-P. Song and co-workers also developed a protocol for the cobalt-catalyzed hydrophosphination of diarylphosphine oxides with electron-deficient alkenes for the synthesis of chiral phosphine oxides. In this case, the directing imidazolyl group was linked to the activated olefins, and using an in situ generated catalyst from 8 mol% of CoCl₂ and 8.6 mol% of N,N,N,N ligand **L** in the presence of 16 mol% of AgClO₄ in dichloromethane at rt for 48 h, the corresponding optically active phosphine oxides were obtained in moderate to excellent yields and 82-99% *ee*.^[32]

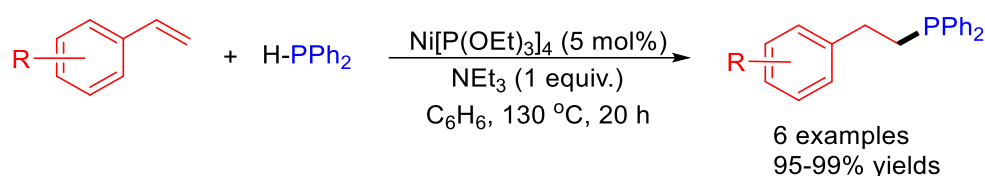


Scheme 1-19. Enantioselective cobalt-catalyzed hydrophosphination of diarylphosphine oxides with electron-deficient alkenes.

1.1.4. Nickel-catalyzed hydrophosphination of alkenes and alkynes

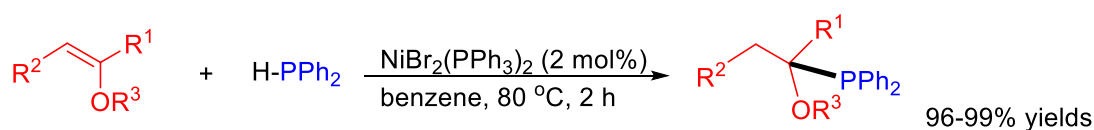
1.1.4.1. Hydrophosphination of alkenes

At nickel, the first report of catalyzed intermolecular hydrophosphination of styrenes was described by I. P. Beletskaya et al. in 2002. Thus, the reaction of secondary phosphines with activated alkenes such as styrene, vinylpyridine, methoxystyrene, and 5-vinyl-2-methylpyridine was carried out using 5 mol% of $\text{Ni}[\text{P}(\text{OEt})_3]_4$ **Ni-1** in the presence of 1 equiv. of NEt_3 in benzene at 130 °C for 20 h. The anti-Markovnikov products were then obtained in high yields.^[33] (Scheme 1-20)



Scheme 1-20. Ni-catalyzed intermolecular hydrophosphination of styrenes.

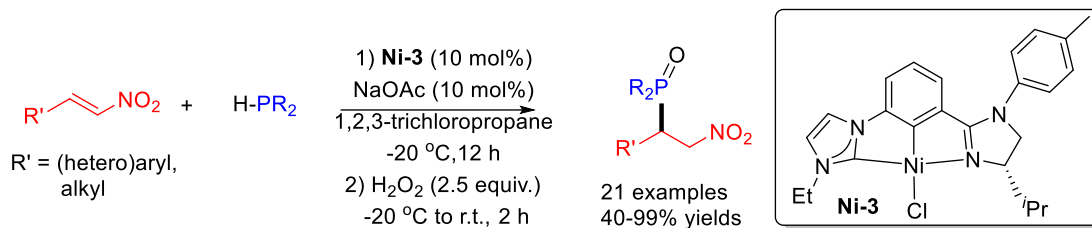
The same group then developed another Ni(II)-catalyzed hydrophosphination of secondary phosphines with alkyl vinyl ethers. In the presence of 2 mol% of $\text{NiBr}_2(\text{PPh}_3)_2$ **Ni-2** as the catalyst in benzene at 90 °C for 2 h, the corresponding Markovnikov products was obtained in high yield and regioselectivity.^[34] (Scheme 1-21)



Scheme 1-21. Ni-catalyzed hydrophosphination of secondary phosphines with alkyl vinyl ethers.

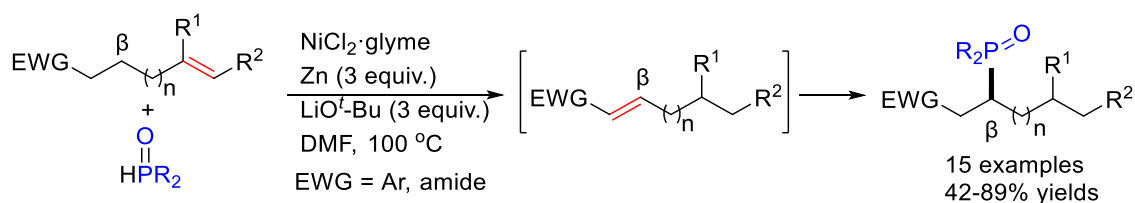
X. Zhu's group reported the use of Ni (II) well-defined complex **Ni-3** for catalyzed hydrophosphination of nitroalkenes with diphenylphosphine and diadamentylphosphine. Using 10 mol% of **Ni-3** and 10 mol% of NaOAc in 1,2,3-trichloropropane at -20 °C for 12 h, the 1,4-addition product was then oxidized for purification and the corresponding phosphine oxides was obtained in good yields.^[35]

Noticeably, even if a chiral complex **Ni-3** was used, no enantioselectivity was described. (Scheme 1-22)



Scheme 1-22. Ni-catalyzed hydrophosphination of nitroalkenes.

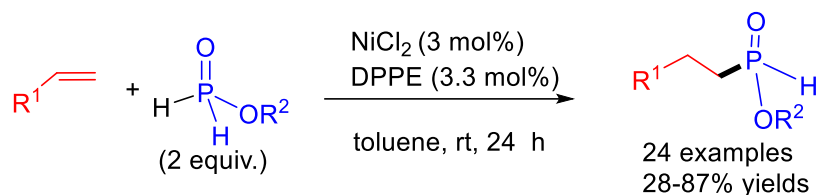
M. J. Koh's group investigated a Ni-catalyzed remote hydrophosphination of secondary phosphines. They have first demonstrated that a catalyst based on 10 mol% of $\text{NiCl}_2 \cdot \text{glyme}$ and 20 mol% of $\text{Ph}_2\text{PH}(\text{O})$ was able to perform C=C bond isomerization up to nine double-bond migrations within terminal and internal olefins when conducting the reaction in the presence of 3 equiv. of zinc in toluene at 60 °C for 12 h.^[36] They then used similar catalytic system [10 mol% of $\text{NiCl}_2 \cdot \text{glyme}$ and equiv. of $\text{Ph}_2\text{PH}(\text{O})$] in the presence of 3 equiv. of zinc and 3 equiv. of $\text{LiO-}t\text{-Bu}$ in DMF at 100 °C for 12 h to perform a tandem one step regiocontrolled “chain-walking isomerization” and hydrophosphination. (Scheme 1-23)



Scheme 1-23. $\text{NiCl}_2 \cdot \text{glyme}$ -catalyzed tandem isomerization-hydrophosphination of remote olefins with secondary phosphines.

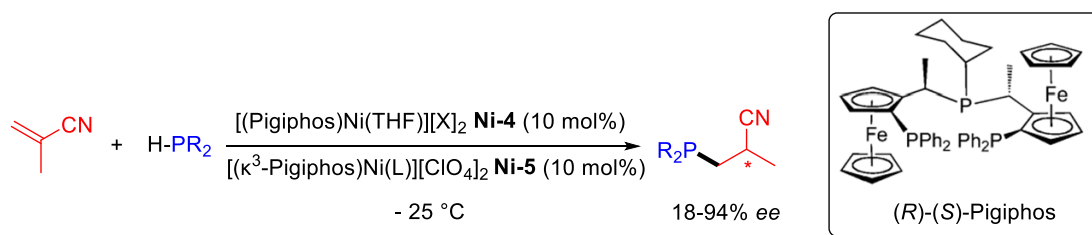
J.-L. Montchamp et al. performed the hydrophosphinylation of alkylphosphinates with olefins catalyzed by 3 mol% of nickel chloride associated to 3.3 mol% of *dppe* in toluene at rt for 24 h. The corresponding *H*-phosphinate derivatives were isolated in moderate to good yields. It should be underlined that the reaction tolerated several functional groups such as esters, ketone, carbamate, TMS, halides, and acetal. Noticeably, by a basic treatment with 2M NaOH permitted to access the corresponding

H-phosphinic acids.^[37] (Scheme 1-24)



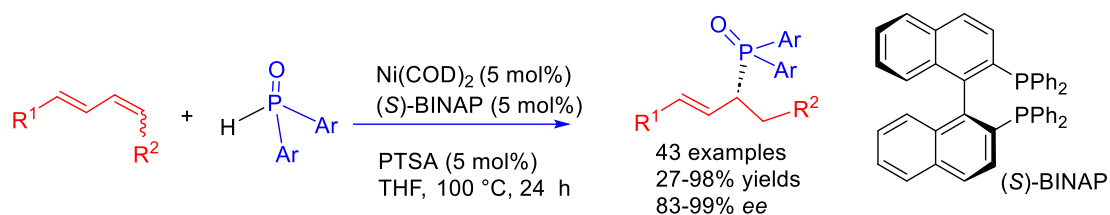
Scheme 1-24. Ni-catalyzed intermolecular hydrophosphinylation of olefins with H-phosphonates.

A. Togni described an enantioselective version of intermolecular Ni-catalyzed hydrophosphination of vinyl nitriles and methacrylonitrile. The transformation was catalyzed 10 mol% of (*R*)-(*S*)-Pigiphos-Nickel(II) based catalysts **Ni-4** and **Ni-5** and chiral 2-cyanopropylphosphines were obtained in good yields and *ee* up to 94%.^[38] (Scheme 1-25)



Scheme 1-25. Enantioselective Ni-catalyzed hydrophosphination of vinyl nitriles and methacrylonitriles.

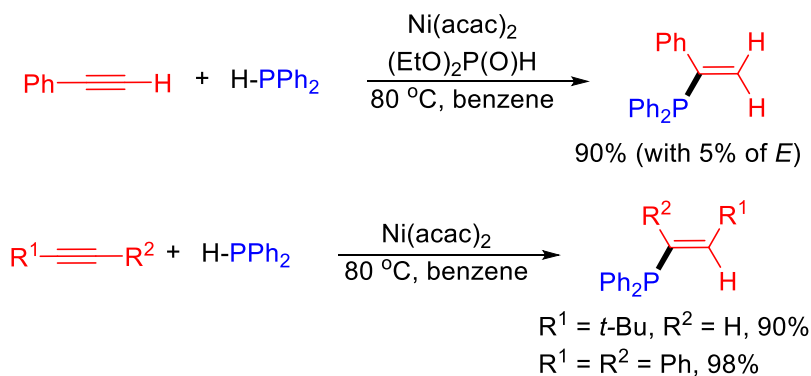
In 2022, Yin et al. developed a Ni-catalyzed regio- and enantio-selective hydrophosphinylation of 1,3-dienes using diarylphosphine oxides with the assistance of a Brønsted acid. By reaction of internal aryl, aryl- and aryl, alkyl-substituted dienes with secondary phosphine oxides in the presence of 5 mol% of Ni(COD)₂ associated to 5 mol% of (*S*)-BINAP and 5 mol% of *p*-toluenesulfonic acid (PTSA), the corresponding tertiary chiral allylic phosphine oxides were obtained with an exclusive 1,2-regioselectivity and with typically >90% *ee* and up to 99%. Noticeably, with unsymmetrically substituted phosphine oxides, even if the regio- and enantioselectivity remained very good, the diastereoselectivity was disappointing.^[39] (Scheme 1-26)



Scheme 1-26. Enantioselective Ni-catalyzed hydrophosphination of dienes.

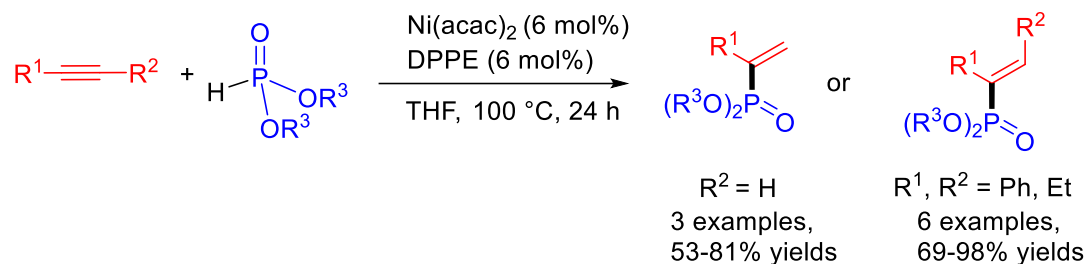
1.1.4.2. Hydrophosphination of alkynes

I. P. Beletskaya and co-workers also described the first Ni-catalyzed hydrophosphination reaction involving alkynes. Using in situ generated catalyst from $\text{Ni}(\text{acac})_2$ and $(\text{EtO})_2\text{P}(\text{O})\text{H}$, the *gem*-alkenylphosphine was obtained in 90% yield, with trace amount of (*E*-) isomer (5%) by reaction in benzene at 80 °C. Noticeably, this reaction using $\text{Pd}(\text{PPh}_3)_4$ catalyst led selectively to the (*Z*)-alkenylphosphine (*E/Z* = 10:90). When starting from *tert*-butyl acetylene or diphenylacetylene using $\text{Ni}(\text{acac})_2$ as the catalyst, (*E*)-diphenyl(2-*tert*-butylvinyl)phosphine and (*E*)-diphenyl(1,2-diphenylvinyl)phosphine, respectively by reaction in benzene at 80 °C. Noticeably, the reaction was not selective with pent-1-yne and hept-1-yne.^[40,41] (Scheme 1-27)



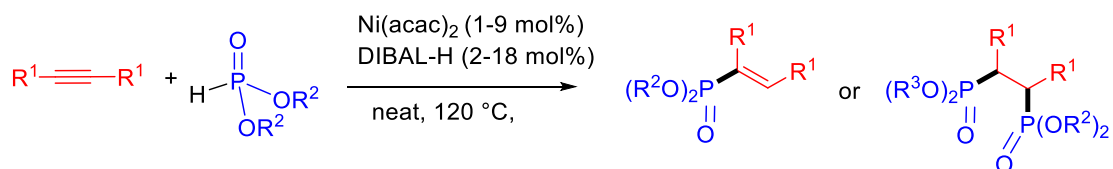
Scheme 1-27. $\text{Ni}(\text{acac})_2$ -catalyzed hydrophosphination reaction of alkynes.

V. P. Ananikov, I. P. Beletskaya et al. extended the reaction to the intermolecular hydrophosphorylation of terminal and internal alkynes with H-phosphonates. Using 6 mol% of catalyst from $\text{Ni}(\text{acac})_2$ and bis(diphenylphosphino)ethane (DPPE) in THF at 100 °C, the addition took place via a Markovnikov stereoselectivity leading to vinyl phosphonates in 53-98% isolated yields.^[42] (Scheme 1-28)



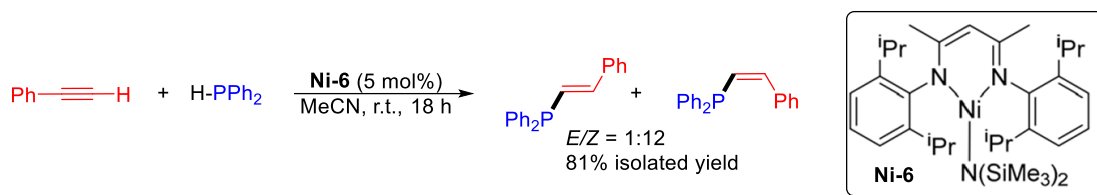
Scheme 1-28. Ni-catalyzed intermolecular hydrophosphorylation of alkynes with H-phosphonates.

Noticeably, using a catalytic system based on Ni(acac)₂ and DIBAL, and working in solvent free conditions, the same group succeeded to control the access to mono- and bis-phosphonates by finely modifying the catalyst loading and the ratio of the starting substrates. Typically, when using 9 mol% of Ni(acac)₂ and 18 mol% of DIBAL, with a ratio alkyne/(RO)₂PH(O) 1:1 for 40 minutes at 120 °C, vinylphosphonates were obtained as the sole product. By contrast, when using 1 mol% of Ni(acac)₂ and 2 mol% of DIBAL, with a ratio alkyne/(RO)₂PH(O) 1:2.5 for 28 h at 120 °C, bisphosphonates were produced.^[43] (Scheme 1-29)



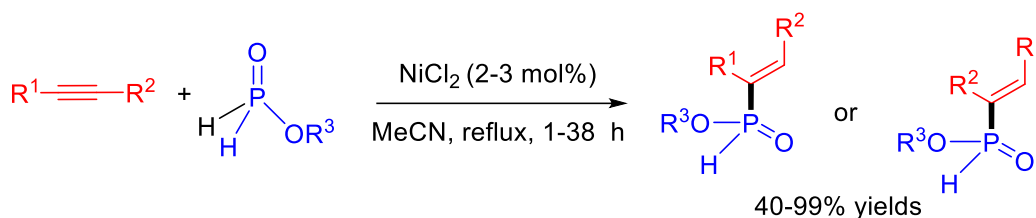
Scheme 1-29. Ni-catalyzed intermolecular hydrophosphorylation of alkynes with H-phosphonates for mono- and bis-phosphonates synthesis.

In 2018, R. L. Webster reported Ni(II)-catalyzed hydrophosphination of alkynes using a Ni(II) β -diketiminato complex. Using 5 mol% of β -diketiminato Ni(II) complex **Ni-6**, the best selectivity was obtained by reaction of diphenylphosphine with acetylene at rt leading to the styryldiphenylphosphine in 81% in a 1:12 *E/Z* ratio. With other terminal alkynes, the yields were moderate and the *E/Z* ratio from 2:1 to 1/1. It should be underlined that this complex was also applied for the hydrophosphination of alkenes with good efficiency. Additionally, this Ni β -diketiminato catalyst, even if efficient, did not exhibit the same levels selectivity compared to the previously reported Fe(II) congener.^[44] (Scheme 1-30)



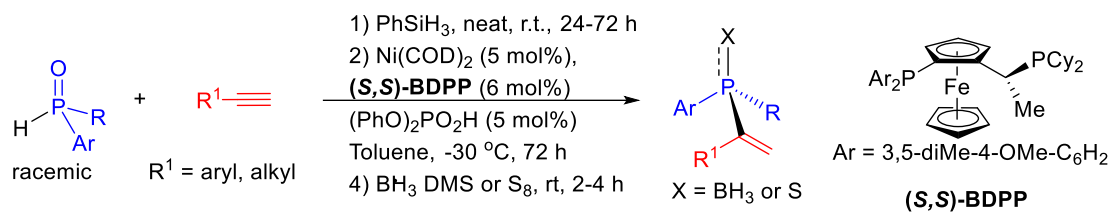
Scheme 1-30. β-diketiminates Ni(II) complex for catalyzed hydrophosphination.

J.-L. Montchamp et al. performed the hydrophosphinylation of alkylphosphinates with alkynes catalyzed by 2-4 mol% of nickel chloride without addition of ligand in refluxing acetonitrile. Alkenyl H-phosphinates were then obtained in 40-99% yields.^[45] (Scheme 1-31)



Scheme 1-31. Ni-catalyzed intermolecular hydrophosphorylation of alkynes with H-phosphonates.

Q.-W. Zhang and co-workers described a Ni-catalyzed asymmetric hydrophosphination of unactivated alkynes with racemic secondary phosphines to produce P-stereogenic tertiary phosphines. After reduction of the secondary phosphine oxides by phenylsilanes at rt, the hydrophosphination with terminal alkynes took place using 5 mol% of Ni(COD)₂, 6 mol% of (*S,S*)-BDPP, 5 mol% of (PhO)₂PO₂H in toluene at -30 °C for 72 h. Finally, a protection step with BH₃·DMS or S₈ led to the corresponding chiral tertiary vinylphosphine borane or sulfide derivatives. Starting from terminal alkynes, 47 examples were described with 42-99 yields, with 61-96% *ee* and branch/linear ratio from 1:1 to >20/1. Starting from internal alkynes, 8 examples were reported with 65-88% yields, 48-94% *ee* and branch/linear ratio from 7:1 to >20/1.^[46] (Scheme 1-32)

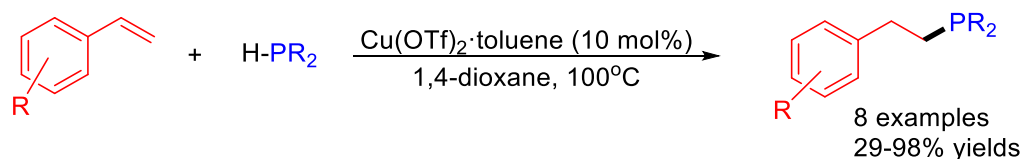


Scheme 1-32. Ni-catalyzed asymmetric hydrophosphination of non-activated alkynes with racemic secondary phosphine oxides.

1.1.5. Copper-catalyzed hydrophosphination of alkenes and alkynes

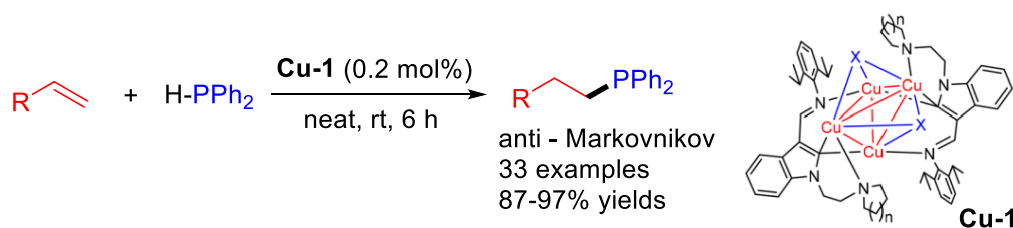
1.1.5.1. Hydrophosphination of alkenes

The first report employing Cu salt used as a catalyst for the hydrophosphination of styrenes was reported by A. Corma and co-workers. Using 10 mol% of Cu(OTf)₂·toluene in 1,4-dioxane at 100 °C for 18-24 h, styrenes reacted with secondary phosphines (PCy₂PH and PPh₂PH) and led to the corresponding tertiary phosphines in good yields via an anti-Markovnikov selectivity.^[14] (Scheme 1-33)



Scheme 1-33. Cu(II)-catalyzed hydrophosphination of styrenes.

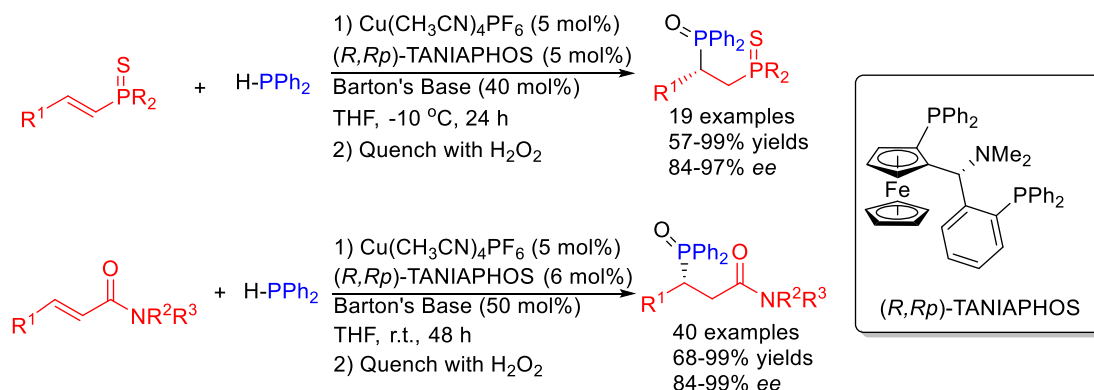
S. Zhou et al. then reported the use of a halide-bridged tetranuclear Cu(I) cluster **Cu-1** bearing pincer-type ligands based on the electron-rich indolyl motif for the hydrophosphination of alkenes. This reaction was then conducted with 0.2 mol% of **Cu-1** in solvent free conditions at rt for 6h, styrene derivatives led to the anti-Markovnikov phosphine derivatives in 87-97% yields. Noticeably, halides, acetate, nitro and pyridyl moieties were tolerated.^[47] (Scheme 1-34)



Scheme 1-34. Cu(I) cluster catalyzed hydrophosphination of styrenes.

B. H. Lipshutz et al. reported an interesting copper-catalyzed hydrophosphinations of styrene compounds with diphenylphosphine conducted in water at room temperature. Using 5 mol% of $\text{Cu}(\text{OAc})_2 \cdot \text{H}_2\text{O}$ in a mixture of a surfactant TPGS-750-M/water, the anti-Markovnikov linear phosphines were obtained in 37-97% (10 examples).^[48]

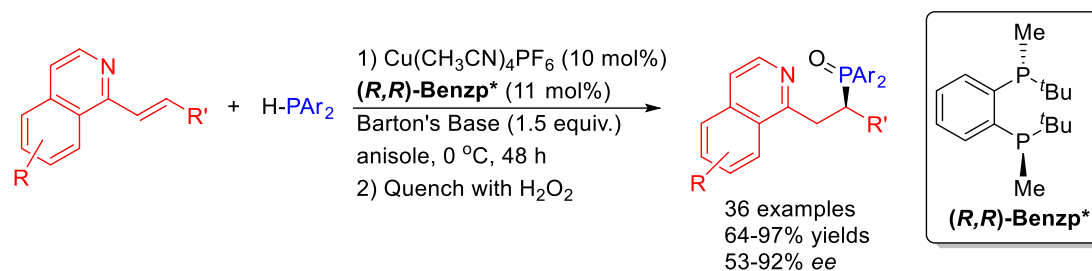
Remarkably, several contributions described enantioselective versions of Cu-hydrophosphination of olefins. In 2020, L. Yin and co-workers described a copper(I)-catalyzed asymmetric hydrophosphorylation of α,β -unsaturated phosphine sulfides affording 1,2-diphosphine derivatives. Thus, using 5 mol% of $\text{Cu}(\text{CH}_3\text{CN})_4\text{PF}_6$ in association with 5 mol% of (*R,Rp*)-TANIAPHOS with 0.4 equiv. of Barton base ($\text{Me}_2\text{N}-\text{C}(=\text{NH})-\text{NH}_2$) in THF at -10°C for 24 h, chiral diphosphines were obtained in 57-99% yields and 84-97% *ee*.^[49] (Scheme 1-35)



Scheme 1-35. Copper-catalyzed asymmetric hydrophosphination of α,β -unsaturated amides and phosphine sulfides.

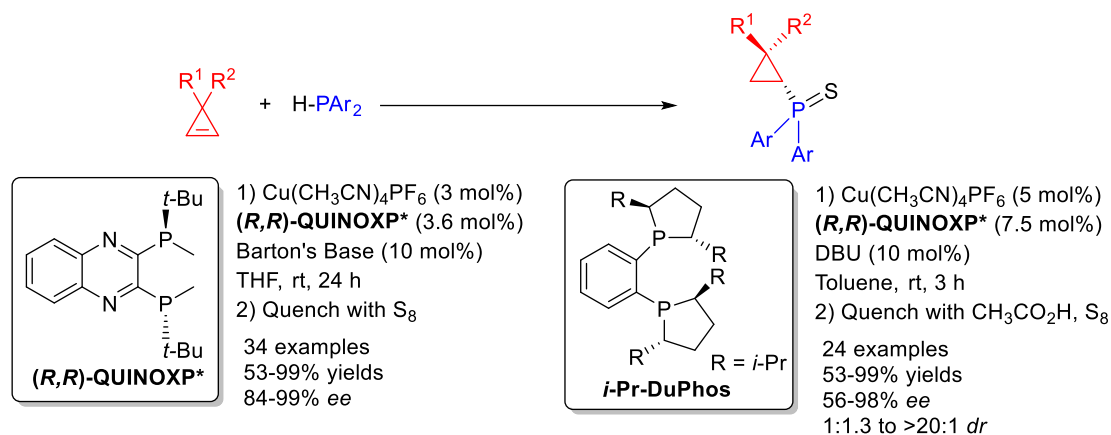
The same authors applied their methodology for the asymmetric hydrophosphination of α,β -unsaturated amides. The corresponding amidophosphine oxides were obtained in 68-99% yields and 84-99% *ee*.^[50] They also applied it for the asymmetric hydrophosphination of α,β -unsaturated amides with racemic secondary phosphines to produce P-stereogenic tertiary phosphines with 5/1 to 16/1 *dr* and 92-96% *ee*. Additionally, the asymmetric hydrophosphination of α,β -unsaturated esters was similarly performed.^[51]

Enantioselective hydrophosphorylation were also performed with alkenyl isoquinolines and diphenylphosphane by Wang's group using a copper chiral diphosphine ligand catalysts. It provides a direct, atomically efficient method to prepare various chiral phosphines with isoquinoline units in good yields and high enantioselectivity. [52] (Scheme 1-36)



Scheme 1-36. Copper-catalyzed asymmetric hydrophosphination of alkenyl isoquinolines and diphenylphosphine.

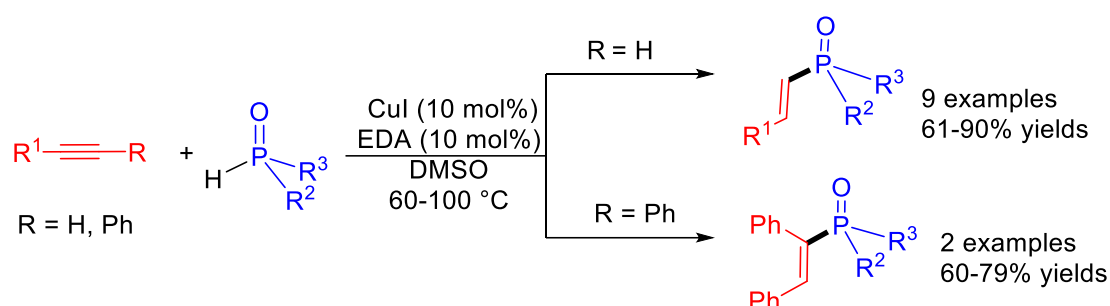
Interestingly, L. Yin reported a copper-catalyzed asymmetric hydrophosphination of 3,3-disubstituted cyclopropenes. Using 3 mol% of $\text{Cu}(\text{CH}_3\text{CN})_4\text{PF}_6$ in association with 3.6 mol% of (*R,R*)-QUINOXP with 10 mol% of Barton base in THF at rt for 24 h. After quenching with S_8 , chiral cyclopropyldiarylphosphine sulfides were obtained in 53-99% yields and 84-99% ee. [53] (Scheme 1-37) V. M. Dong, J. S. Hirschi, S. Nie, et al. described very similar report using 5 mol% of $\text{Cu}(\text{CH}_3\text{CN})_4\text{PF}_6$, 7.5 mol% of Duphos ligand and DBU (1,8-Diazabicyclo [5.4.0]undec-7-ene) as the base and obtained very similar results. [54]



Scheme 1-37. Copper-catalyzed asymmetric hydrophosphination of 3,3-disubstituted cyclopropenes and diarylphosphines.

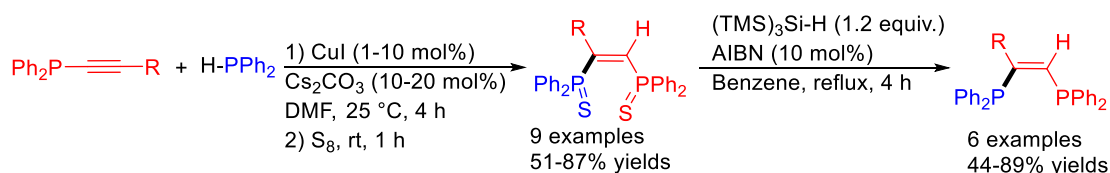
1.1.5.2. Hydrophosphination of alkynes

In 2007, H. Fu and co-workers developed the first example of copper-catalyzed hydrophosphinylation of alkynes with secondary phosphine oxides to synthesize alkenylphosphine oxides. Using a catalytic in situ generated from 10 mol% of CuI and 15 mol% of ethylenediamine (EDA) in DMSO at 60-100 °C for 3-18 h, (*E*)-alkenylphosphine oxides were obtained regioselectively in moderate to good yields. [55] (Scheme 1-38)



Scheme 1-38. Cu-catalyzed hydrophosphinylation of alkynes with secondary phosphine oxides.

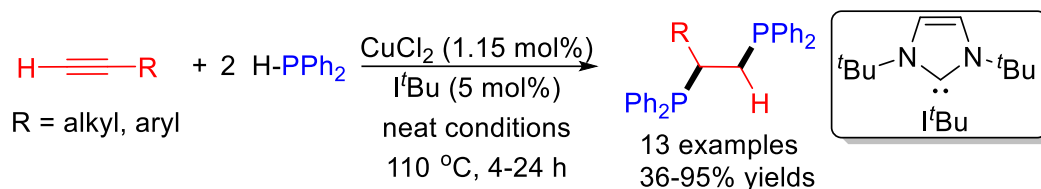
The same year, K. Oshima and co-workers described a copper-catalyzed hydrophosphination of 1-alkynylphosphines with diphenylphosphine. The reaction was performed using CuI as the catalyst (1-10 mol%) assisted by a base (CS_2CO_3 , 10-20 mol%) in DMF at 25 °C, and the (*Z*)-1,2-diphosphino-1-alkenes were purified as disulfide derivatives in 51-87% yields. The desulfidation was performed with tris(trimethylsilyl)silane in presence of 10 mol% of AIBN. [56] (Scheme 1-39)



Scheme 1-39. Copper-catalyzed hydrophosphinylation of alkynes

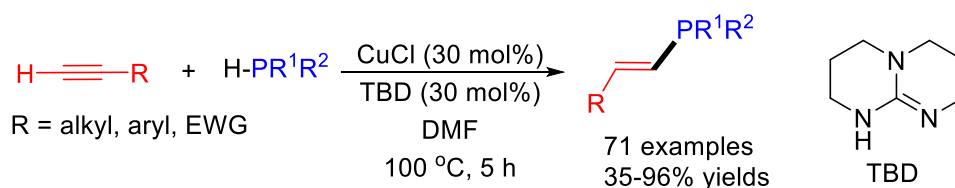
In 2017, C. Cui and co-workers developed a protocol for the Cu-catalyzed selective double hydrophosphination of terminal alkynes with diphenylphosphine to yield 1,2-diphosphinoethanes by using an *in situ* generated active species from 1.15 mol% of CuI and 5 mol% of *t*Bu. The reaction was performed in neat conditions at 110 °C for 4-24

h and led to 1,2-diphosphinoethane derivatives in 36-95% yields. Noticeably, internal alkynes such as diphenylacetylene did not work under such conditions. Additionally, an NHC-Cu(I) phosphide complex was identified as a possible catalytic species.^[57] (Scheme 1-40)



Scheme 1-40. NHC-Cu-catalyzed hydrophosphination of terminal alkynes with diphenylphosphine.

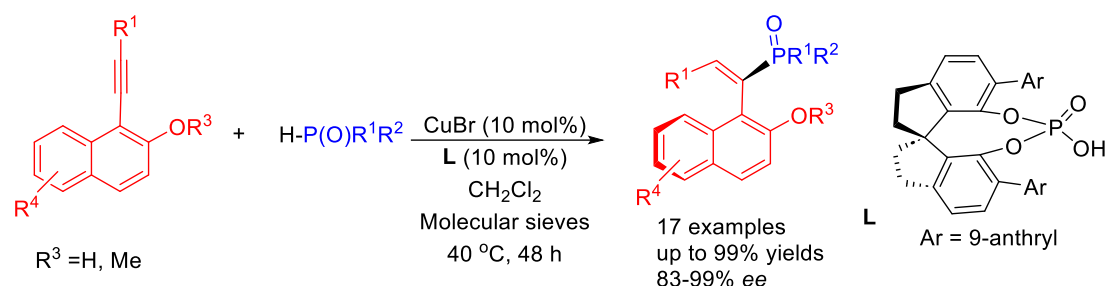
X. Bi, E. Shi, J. Xiao et al. recently described a general copper-catalyzed stereo- and regioselective hydrophosphorylation, hydrophosphinylation and hydrophosphination of terminal alkynes with secondary phosphine oxides, phosphinates and phosphites, respectively. Using 30 mol% of CuCl, 30 mol% of TBD in DMF at 100 °C for 5 h under air, numerous terminal alkynes such as propiolate derivatives, aliphatic alkynes, phosphorylated alkynes, aryl alkynes and multi-functionalized alkynes (derived from estradiol, β -D-glucopyranoside or 2-deoxyuridine) were successfully transformed leading to the corresponding (*E*)-alkenylphosphorus derivatives in 35-96% yields (71 examples). Importantly, numerous functional groups were tolerated: aldehydes, ketones, ester, amide, halides, trifluoromethoxy, nitro, cyano, alcohols, cyclopropyl, etc.^[58] (Scheme 1-41)



Scheme 1-41. General Cu-catalyzed hydrophosphination of terminal alkynes with secondary phosphine oxides, phosphinates and phosphites.

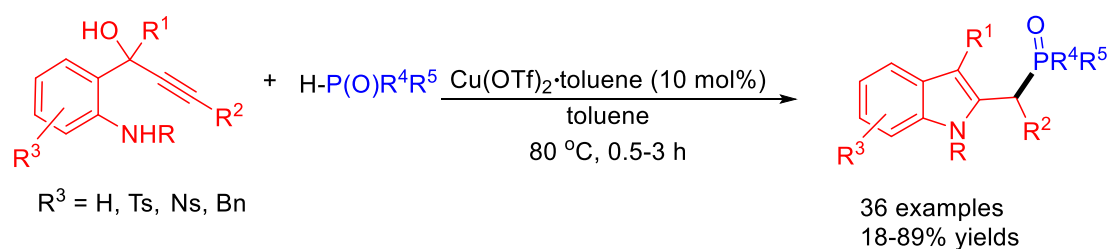
L. Yang, B. Tan, J. Wang, et al. developed an interesting and efficient synthesis of axially chiral styrene-phosphine derivatives via the direct hydrophosphinylation of alkynes with secondary phosphine oxides. Using 10 mol% of CuBr and 10 mol% of

axially chiral 1,1'-spirobiindane-7,7'-diol (SPINOL) bearing 9-anthryl substituents in dichloromethane at 40 °C for 48 h, numerous hydroxynaphthylalkynes reacted with diarylphosphine oxides to produce axially chiral phosphorus-containing alkene derivatives in up to 99 % yield and 83-99 % *ee*.^[59] (Scheme 1-42)



Scheme 1-42. Synthesis of axially chiral styrene-phosphines via the direct hydrophosphinylation of alkynes with secondary phosphine oxides.

This copper catalyzed hydrophosphinylation of alkynes with secondary phosphine oxides was elegantly applied by H.-L. Ni, L. Chen et al. for the preparation of C2-phosphorylmethyl indoles by cascade reaction from 1-(*o*-aminophenyl)prop-2-ynols (via a tandem phosphorylation/intramolecular 5-*exo*-trig cyclization). Indeed, using 10 mol% of $\text{Cu}(\text{OTf})_2$ toluene in toluene at 80 °C, various secondary phosphine oxides led to C2-phosphorylmethyl indoles in 18-89% yields. Noticeably, starting from 1-(*o*-hydroxyphenyl)prop-2-ynol and 1-(*o*-mercaptophenyl)prop-2-ynol, phosphorylated benzofurans and its sulfur analogs can be also prepared.^[60] (Scheme 1-43)



Scheme 1-43. Synthesis of C2-phosphorylmethyl indoles via the hydrophosphinylation of 1-(*o*-aminophenyl)prop-2-ynols with secondary phosphine oxides.

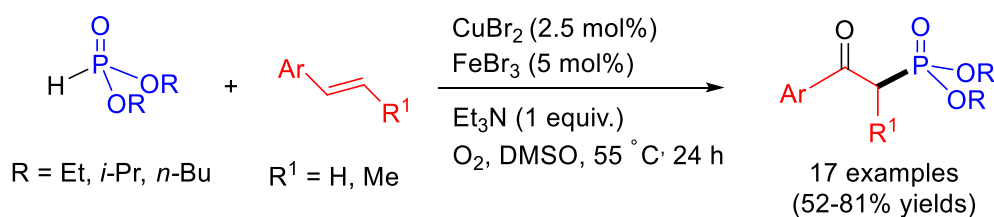
1.2. Oxyphosphorylation

In contrast to the well-developed transition-metal-catalyzed hydrophosphination methods, oxyphosphorylation has been less reported, with only a few representative

examples with copper as the major player, associated with another metal such as Cu/Ag or Cu/Fe, manganese or organocatalysts to obtain β -ketophosphonates, β -ketophosphine oxides and β -ketophosphinates.^[61]

1.2.1. Copper-co-catalyzed oxyphosphination of alkenes and alkynes

The first methodology dealing with catalytic oxidative reactions affording β -ketophosphonates was reported by J.-X. Ji, in 2011, *via* a Cu/Fe-co-catalyzed oxyphosphorylation of styrene derivatives with H-phosphonates. The corresponding β -ketophosphonates were obtained in 52-91% yields using 2.5 mol% of CuBr associated to 5 mol% of FeBr₃ in the presence 1 equiv. of Et₃N under oxygen atmosphere in DMSO at 55 °C.^[62] The reaction can be also performed with 9-vinylcarbazole, but not with aliphatic alkenes. (Scheme 1-44)

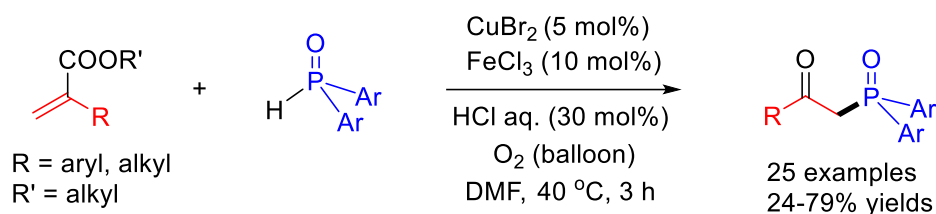


Scheme 1-44. Cu/Fe-co-catalyzed oxyphosphorylation of styrenes with H-phosphonates.

With similar Cu/Fe catalytic system, C. Cai et al. have described β -ketophosphonate preparation using 10 mol% of CuCl, 20 mol% of FeCl₃ in the presence of 1 equiv. of Et₃N and 2 equiv. of di-*tert*-butylperoxide (DTBP) in DMSO at 90 °C for 15 h.^[63] To perform the same transformation, Moghaddam used 10 mol% of copper ferrite nanoparticles (CuFe₂O₄ NPs), in the presence of 1 equiv. of Et₃N and 2 equiv. of DTBP in MeCN at 85 °C under air for 6 h (15 examples, 35-85% yields).^[64]

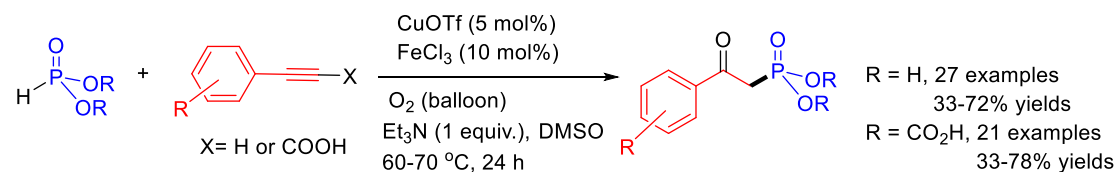
D. Yi and co-workers developed the hydrochloric acid-promoted Cu/Fe-co-catalyzed oxyphosphorylation of secondary phosphine oxides with 2-substituted acrylates. Using 5 mol% of CuBr₂, 10 mol% of FeCl₃, 30 mol% of HCl in DMF at 40 °C for 3 h under an atmosphere of O₂, β -ketophosphine oxides were synthesized in 24-79% yields.

Noticeably, an interesting functional group tolerance was demonstrated (halides, cyano, nitro, hydroxyl).^[65] (Scheme 1-45)



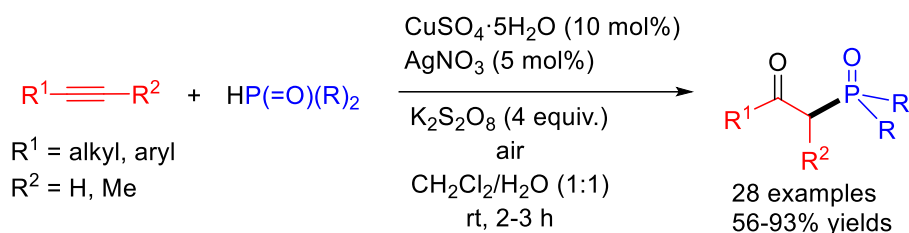
Scheme 1-45. Cu/Fe-co-catalyzed oxyphosphorylation of secondary phosphine oxides with 2-substituted acrylates

With similar Cu/Fe catalytic system, oxyphosphorylation of alkynes and alkynyl carboxylic acids with H-phosphonates can be also performed. Q. Song and co-workers obtained the corresponding β -keto-organophosphorus derivatives using 5 mol% of CuOTf, 10 mol% of FeCl₃, 1 equiv. of NEt₃ in DMF at 60-70 °C for 24 h under an atmosphere of O₂.^[66] (Scheme 1-46) Oxyphosphorylation of arylalkynes can be also performed as shown by W. He and co-workers, using 10 mol% of Cu(acac)₂, 20 mol% of FeCl₃, 1 equiv. of NEt₃ in DMSO at 80 °C for 24 h under an atmosphere of O₂.^[67]



Scheme 1-46. Cu/Fe-co-catalyzed oxyphosphorylation of alkynes or alkynyl carboxylic acids.

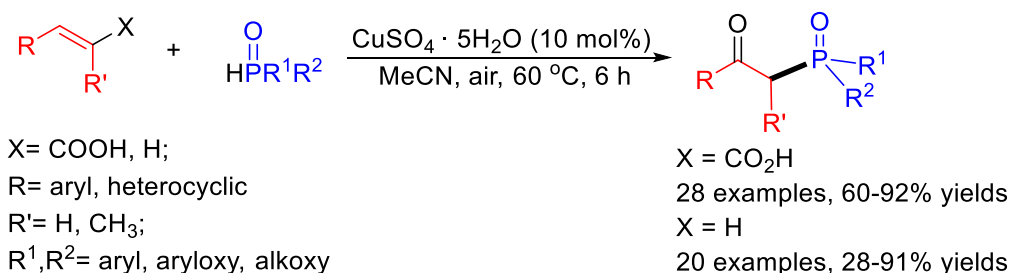
Copper can be also associated to silver to promote such oxyphosphorylation. For example, in 2015, Y.-F. Zhao and co-workers developed an Ag/Cu-co-catalyzed oxyphosphorylation and oxyphosphinylation of alkynes with H-phosphonates and H-phosphinates. A large variety of β -keto-phosphonates and phosphinates were synthesized using 10 mol% of CuSO₄, 5 mol% of AgNO₃ in the presence of 4 equiv. of K₂S₂O₈ in a mixture CH₂Cl₂/water under air.^[68] (Scheme 1-47)



Scheme 1-47. Ag/Cu-co-catalyzed oxyphosphorylation and oxyphosphinylation of alkynes with H-phosponates and H-phosphinates.

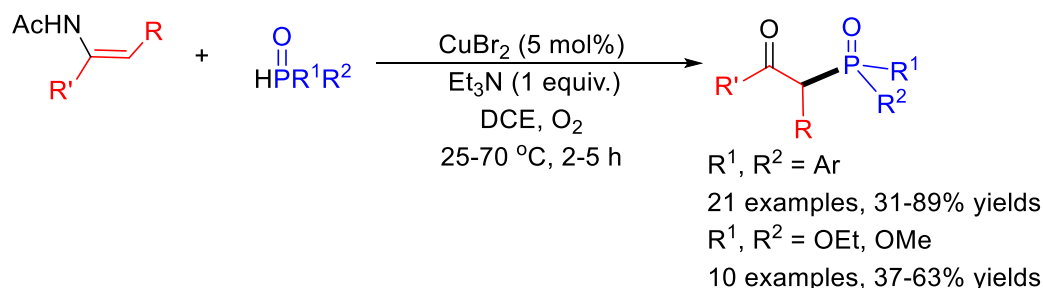
1.2.2. Copper-catalyzed oxyphosphination of alkenes and alkynes

Copper can be also used as the sole catalyst for catalyzed oxyphosphination. X. Chen and co-workers described a Cu-catalyzed oxyphosphorylation, oxophosphinylation and oxyphosphination of α,β -alkenyl acids or alkenes by H-phosponates, H-phosphinates and phosphine oxides to lead to β -keto-phosponates, phosphinates and phosphines, respectively. The reaction was catalyzed by 10 mol% of $\text{CuSO}_4 \cdot 5\text{H}_2\text{O}$, under air in CH_3CN at 60°C .^[69] (Scheme 1-48)



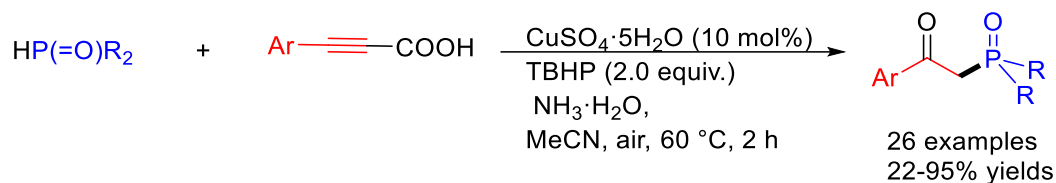
Scheme 1-48. Cu-catalyzed oxyphosphorylation, oxophosphinylation and oxyphosphination of α,β -alkenyl acids or alkenes.

F. Du, W. Wei, et al. then described a copper-catalyzed direct oxyphosphorylation and oxyphosphination of enamides. Using 5 mol% of CuBr_2 , and 1 equiv. of NEt_3 in 1,2-dichloroethane (DCE) under air, β -ketophosphine oxides were obtained by reaction at 25°C for 2 h and β -ketophosponates by reaction at 70°C for 5 h.^[70] (Scheme 1-49)



Scheme 1-49. Cu-catalyzed oxyphosphorylation, and oxyphosphination of enamides.

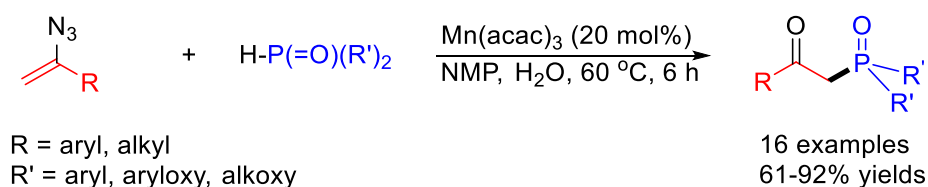
G. Tang and co-workers also performed the preparation of β -ketophosphines through copper-catalyzed tandem phosphination–decarboxylation– oxidation process from alkynyl carboxylic acids with secondary phosphine oxides, using 5 mol% of $\text{CuSO}_4 \cdot 5\text{H}_2\text{O}$, in the presence of 2 equiv. of TBHP and $\text{NH}_3 \cdot \text{H}_2\text{O}$ under air in CH_3CN at 60 °C.^[71] (Scheme 1-50)



Scheme 1-50. Cu-catalyzed oxyphosphorylation of alkynyl acids with secondary phosphine oxides.

1.2.3. Manganese-catalyzed oxyphosphination of alkenes and alkynes

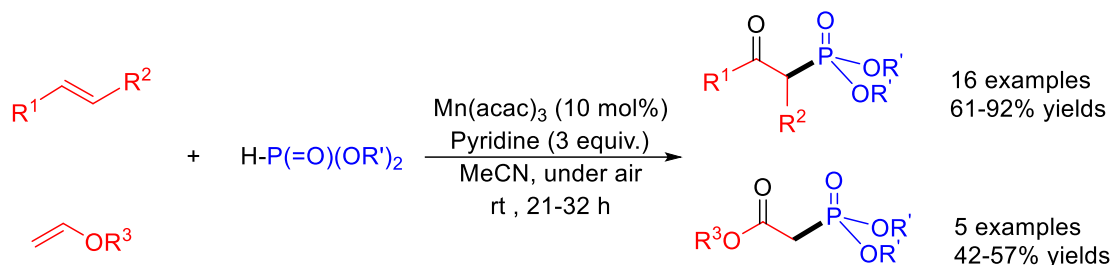
Following the pioneering work of R.-S. Zeng and J.-P. Zou et al. on manganese-mediated oxyphosphorylation of styrenes with H-phosphonates and secondary phosphine oxides,^[72] manganese also became a player in oxophosphination. Nevertheless, up to now, only few contributions dealing with manganese-catalyzed were reported. In 2017, W. Chen and Y. Yu and co-workers prepared β -keto-phosphonates and phosphine oxides starting from vinyl azides and H-phosphonates or secondary phosphine oxides in the presence of 20 mol% of $\text{Mn}(\text{acac})_2$ in NMP at 60 °C for 6 h. The key step of the reaction is the addition of a phosphorus oxide radical to vinyl azides leading to a β -keto-phosphorus imine radical $\text{R}'_2\text{P}(\text{O})\text{-CH}_2\text{-N(=N')}\text{-R}$.^[73] (Scheme 1-51)



Scheme 1-51. Mn(III)-catalyzed preparation of β -keto-phosphonates and phosphine oxides starting from vinyl azides.

One year later, D. Yamamoto, K. Makino et al. reported an aerobic Mn-catalyzed oxyphosphorylation of styrene and vinyl ether derivatives with H-phosphonates.

Conducting the reaction with 10 mol% of $\text{Mn}(\text{acac})_3$ and 3 equiv. of pyridine in acetonitrile under air at rt for 21-32 h, β -Ketophosphonates and 2-diethoxyphoryl)acetate were obtained in 23-82% yields.^[74] (Scheme 1-52)



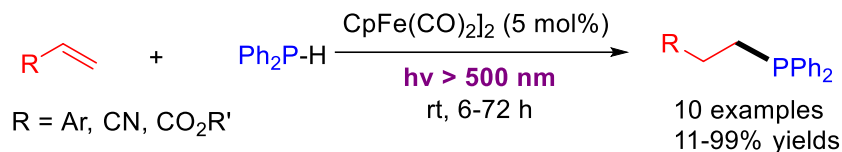
Scheme 1-52. Mn(III)-catalyzed preparation of β -keto-phosphonates and 2-diethoxyphoryl)acetate starting from styrenes and vinyl ethers, respectively.

1.3. Light driven Hydrophosphination

Visible light-promoted transformations are nowadays powerful and efficient tools in molecular synthesis, and their uses has amazingly increased since 15 years.^[75] In this area of research, classical visible light photocatalysis reactions had to involve a photosensitization sequence by a photocatalyst able to perform either redox-, atom transfer-, or energy transfer processes.^[76] Another pathway involves cooperative/dual photocatalysis, combining in a synergic fashion a transition metal catalyst.^[77] Nevertheless, light promoted transition-metal catalyzed transformations without the use of external photo-sensitizer, is another interesting process which involve the direct light to promote the activation of the inner sphere of the catalyst.^[78] In another hand, in terms of more sustainable transformations, the use of visible light to conduct chemical reactions can be considered as good alternative to thermic transformation mainly when conducted at high temperatures. In hydrophosphination reactions area, as shown afore, heating was always required. In recent years, few examples of visible-light-driven, earth abundant metal-catalyzed hydrophosphination have been developed using copper and iron complexes as catalysts.

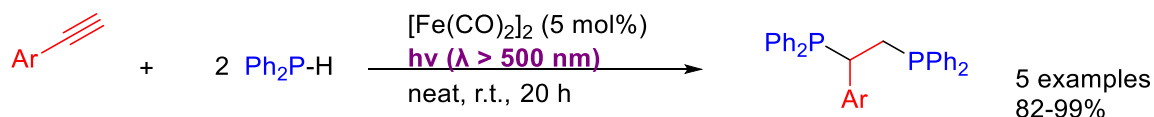
In 2017, Waterman's group reported a visible light promoted Fe-catalyzed hydrophosphination of alkenes with Ph_2PH using 5 mol % in neat conditions at rt under irradiation (commercial LED bulb ($\lambda_{\text{irr}} > 500 \text{ nm}$)). Substituted styrenes,

vinylpyridines, and acrylic esters were hydrophosphinated in moderate to good yields. On contrast, no reaction took place with dialkylphosphines.^[79] (Scheme 1-53)



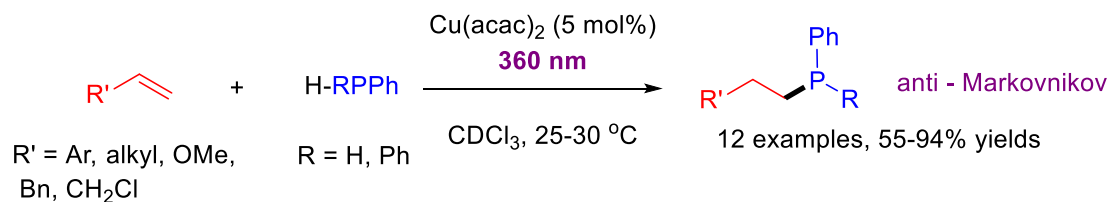
Scheme 1-53. Visible light promoted Fe-catalyzed hydrophosphination of alkenes.

The same group also reported the visible light promoted Fe-catalyzed double hydrophosphination of terminal arylalkynes. The reaction was performed using $[\text{CpFe(CO)}_2]_2$ as the catalyst (5 mol%), in neat conditions at rt for 20 h to generate 1,2-bis(diphenylphosphino)ethane products in 82-99% yields.^[23] (Scheme 1-54) Noticeably, this reaction can be also performed in thermic conditions (100 °C). (see Scheme 1-9)



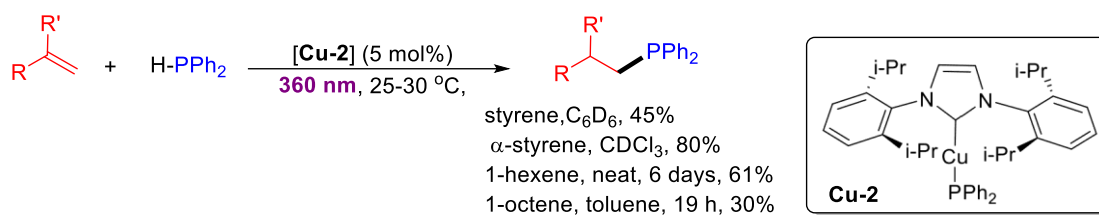
Scheme 1-54. Visible-light-driven-Fe-catalyzed double hydrophosphination of terminal alkynes.

Waterman also investigated such light-promoted hydrophosphination of activated and non-activated alkenes with copper catalysts. They reported the use of $\text{Cu}(\text{acac})_2$ (5 mol%) under low intensity UV-A (360 nm) irradiation for the reaction of both primary and secondary phosphines with styrene and linear alkene derivatives.^[81] (Scheme 1-55) Noticeably, this system was also applied for the hydrophosphination of alkynes. It should be also underlined that the catalytic system was successfully with more sterically encumbered olefins such as α - and β -methylstyrene, or norbornene.



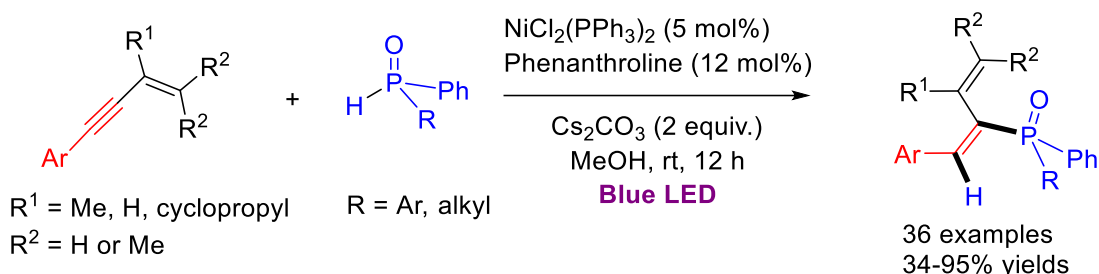
Scheme 1-55. UV-A-driven-Cu-catalyzed hydrophosphination of activated and unactivated alkenes.

Additionally, they described the use of a well-defined NHC-copper **Cu-2** for photocatalyzed hydrophosphination of alkenes. Using 5 mol% of **Cu-2** under irradiation with 360 nm light bulb, hydrophosphination can be performed with moderate to good yield. Additionally, they demonstrated that the hydrophosphination of styrene with diphenylphosphine can be also performed with blue light LED (77% yield) or 23W compact fluorescent lamp (90% yield).^[82] (Scheme 1-56)



Scheme 1-56. Well-defined NHC-Cu-catalyzed photocatalyzed hydrophosphination of alkenes.

Nickel was also studied by H. Hou, S. Zhu, et al. for the stereo- and region-selective *cis*-hydrophosphorylation of the internal alkyne of 1,3-enynes with secondary phosphine oxides. Using 5 mol% of NiCl₂(PPh₃)₂ and 12 mol% of phenanthroline in the presence of 2 equiv. of cesium carbonate in methanol at rt under blue LED irradiation, the internal acetylenic moiety of 1,3-enynes was selectively hydrophosphorylated, and the corresponding phosphinoyl 1,3-butadienes were obtained in 34-95% yields. Thanks to X-ray analysis, the (*E*)-configuration of the internal C=C bond and the (*S*)-*trans*-configuration of the 1,3-diene were confirmed.^[83] (Scheme 1-57)



Scheme 1-57. Ni-catalyzed photocatalyzed hydrophosphination of alkynes.

This introduction chapter demonstrated that the development of new strategies to access to alkenylphosphine (oxides) and β -ketophosphine oxide derivatives are well documented using earth transition metals such as manganese, iron, cobalt, nickel and copper. However, visible light and more especially blue light promoted abundant metal-catalyzed methodologies are far away less reported.

The goals of this thesis research work were to combine visible light promoted catalysis and iron-based catalysts in order to promote hydrophosphination and oxyphosphorylation reactions of alkenes and alkynes with secondary phosphines. Indeed, even if there are significant results on iron catalyzed hydrophosphination of alkynes, to the best of our knowledge, there is no report dealing with such transformation using sole iron as a catalyst. This was the starting point of our research work.

The following 3 chapters will describe those doctoral works performed in Rennes.

The **Chapter 2** will describe blue-light driven iron-catalyzed oxy-phosphinylation of activated alkenes such as styrenes for the synthesis of β -ketophosphine oxide derivatives.

The **Chapter 3** will present the preliminary results on blue-light driven iron-catalyzed oxidative C-H/P-H functionalization for the synthesis of benzo[*b*]phosphole oxides.

The **Chapter 4** will deal with the experimental section of the first part.

1.4. References

- [1] H. Yu, H. Yang, E. Shi, W. Tang, *Med. Drug. Discov.* **2020**, *8*, 100063.
- [2] (a) E. Regulska, C. Romero-Nieto, *Mat. Today Chem.* **2021**, *22*, 100604; (b) T. Baumgartner, R. Réau, *Chem. Rev.* **2006**, *106*, 4681–4727; (c) R. Szucs, P.-A. Bouit, L. Nyuljuszi, M. Hissler, *ChemPhysChem* **2017**, *18*, 2618 – 2630.
- [3] (a) A. T. Woodburn *Pest Manag Sci* **2000**, *56*, 309-312; (b) J. M. Green, *Pest. Manag. Sci.* **2018**, *74*, 1035–1039; (c) C. Zhou, X. Luo, N. Chen, L. Zhang, J. Gao, *J. Agric. Food Chem.* **2020**, *68*, 3344–3353.
- [4] For representative reviews, see: (a) P. W. N. M. van Leeuwen, I. Cano, Z. Freixa, *ChemCatChem* **2020**, *12*, 3982–3994; (b) A. Gallen, A. Riera, X. Verdager, A. Grabulosa, *Catal. Sci. Technol.* **2019**, *9*, 5504–5561; (c) V. V. Grushin, *Chem. Rev.* **2004**, *104*, 1629–1662; (d) T. M. Shaikh, C.-M. Weng, F.-E. Hong, *Coord. Chem. Rev.* **2012**, *256*, 771–803; (e) A. Borner, *Phosphorus*

ligands in asymmetric catalysis, Wiley-VCH, Weinheim, **2008**.

- [5] For representative references, see: (a) C. Xie, A. J. Smaligo, X.-R. Song, O. Kwon, *ACS Cent. Sci.* **2021**, *7*, 536–558; (b) H. Guo, Y. C. Fan, Z. Sun, Y. Wu, O. Kwon, *Chem. Rev.* **2018**, *118*, 10049–10293; (c) A. Voituriez, A. Marinetti, M. Gicquel, *Synlett* **2015**, 142–166; (d) Y. Wei, M. Shi, *Chem. Asian J.* **2014**, *9*, 2720–2734; (e) Y. Xiao, Z. Sun, H. Guo, O. Kwon, *Beilstein J. Org. Chem.* **2014**, *10*, 2089–2121; (f) C. Gomez, J.-F. Betzer, A. Voituriez, A. Marinetti, *ChemCatChem* **2013**, *5*, 1055–1065; (g) M. Benaglia, S. Rossi, *Org. Biomol. Chem.* **2010**, *8*, 3824–3830.
- [6] D. G. Gilheany, C. M. Mitchell, Preparation of Phosphines. In *Organophosphorus Compounds*; Ed. F. R. Hartley, John Wiley and Sons: Chichester, U.K., **1990**; Vol. 1, pp 151–190.
- [7] Representative reviews with transition metals, see: (a) L. Rout, T. Punniyamurthy, *Coord. Chem. Rev.* **2021**, *431*, 213675; (b) R. Henyecz, G. Keglevich, P–C couplings by the Hirao reaction, in *Organophosphorus Chemistry: Novel Developments*, Ed. G. Keglevich, Berlin, Boston: De Gruyter, 2018.
- [8] For representative reviews with palladium and nickel (Hirao type cross-coupling), see: (a) A. L. Schwan, *Chem. Soc. Rev.* **2004**, *33*, 218–224; (b) R. Henyecz, G. Keglevich, *Curr. Org. Synth.*, **2019**, *16*, 523–545; (c) G. Keglevich, R. Henyecz, Z. Musci, *Molecules* **2020**, *25*, 3897.
- [9] For representative reviews with copper, see: (a) H. Zhang, X.-Y. Zhang, D.-Q. Dong, Z.-Li Wang, *RSC Adv.* **2015**, *5*, 52824–52831; (b) C. Alayrac, A.-C. Gaumont, Copper-catalyzed formation of C-P bonds with aryl halides in *Copper-Mediated Cross-Coupling Reactions; 1st edition*, Eds: G. Evano, N. Blanchard, John Wiley & Sons, Inc., **2014**, pp 93–111 |
- [10] For representative reviews on transition metal catalyzed hydrophosphination, see: (a) D. S. Glueck, *Top. Organomet. Chem.* **2010**, *31*, 65–100; (b) V. Koshti, S. Gaikwad, S. H. Chikkali, *Coord. Chem. Rev.* **2014**, *265*, 52–73; (c) C. A. Bange, R. Waterman, *Chem. Eur. J.* **2016**, *22*, 12598–12605; (d) S. A. Pullarkat, *Synthesis*, **2016**, 493–503; (e) D. S. Glueck, *J. Org. Chem.* **2020**, *85*, 14276–14285; (f) J. W. K. Seah, R. H. X. Teo, P.-H. Leung, *Dalton Trans.* **2021**, *50*, 16909–1691; (g) B. T. Novas, R. Waterman, *ChemCatChem* **2022**, *14*, e202200988.
- [11] Representative contributions dealing with earth abundant first row transition metal catalyzed hydroelementation, see: V. Rodriguez-Ruiz, R. Carlino, S. Bezzenine-Lafollee, R. Gil, D. Prim, E. Schulz, J. Hannedouche, *Dalton Trans.* **2015**, *44*, 12029–12059; (b) S. Bezzenine-Lafollee, R. Gil, D. Prim, J. Hannedouche, *Molecules* **2017**, *22*, 1901; (c) M. D. Greenhalgh, A. S. Jones, S. P. Thomas, *ChemCatChem* **2015**, *7*, 190–222; (d) D. Wei, C. Darcel, *Chem. Rev.* **2019**, *119*, 2550–2610; D. Wei, C. Darcel, *J. Org. Chem.* **2020**, *85*, 14298–14306.
- [12] M. Reuter, L. Orthner, Ger. Pat. 1035135 (**1958**); *Chem. Abstr.* **1960**, *54*, 14125a.
- [13] G. Pringle, M. B. Smith, *Chem. Commun.* **1990**, 1701–1702.
- [14] A. Leyva-Pérez, J. A. Vidal-Moya, J. R. Cabrero-Antonino, S. S. Al-Deyab, S. I. Al-Resayes, A. Corma, *J. Organomet. Chem.* **2011**, *696*, 362–367.
- [15] J. M. Pérez, R. Postolache, M. Castiñeira Reis, E. G. Sinnema, D. Vargová, F. de Vries, E. Otten, L. Ge, S. R. Harutyunyan, *J. Am. Chem. Soc.* **2021**, *143*, 20071–20076.
- [16] R. Postolache, J. M. Pérez, M. Castiñeira Reis, L. Ge, E. G. Sinnema, S. R. Harutyunyan, *Org. Lett.* **2023**, *25*, 1611–1615.
- [17] L. Routaboul, F. Toulgoat, J. Gatignol, J.-F. Lohier, B. Norah, O. Delacroix, C. Alayrac, M. Taillefer, A.-C. Gaumont, *Chem. Eur. J.* **2013**, *19*, 8760–8764.
- [18] K. J. Gallagher, R. L. Webster, *Chem. Commun.*, **2014**, *50*, 12109–12111.

- [19] K. J. Gallagher, M. Espinal-Viguri, M. F. Mahon, R. L. Webster, *Adv. Synth. Catal.* **2016**, *358*, 2460–2468.
- [20] A. K. King, A. Buchard, M. F. Mahon, R. L. Webster, *Chem. Eur. J.* **2015**, *21*, 15960–15963.
- [21] M. Espinal-Viguri, A. K. King, J. P. Lowe, M. F. Mahon, R. L. Webster, *ACS Catal.* **2016**, *6*, 7892–7897.
- [22] M. Kamitani, M. Itazaki, C. Tamiya, H. Nakazawa, *J. Am. Chem. Soc.* **2012**, *134*, 11932–11935.
- [23] B. J. Ackley, J. K. Pagano, R. Waterman, *Chem. Commun.* **2018**, *54*, 2774–2776.
- [24] M. Itazaki, S. Katsube, M. Kamitani, H. Nakazawa, *Chem. Commun.* **2016**, *52*, 3163–3166.
- [25] A. K. King, K. J. Gallagher, M. F. Mahon, R. L. Webster, *Chem. Eur. J.* **2017**, *23*, 9039–9043.
- [26] C. R. Wolf, T. G. Lindford-Wodd, M. F. Mahon, R. L. Webster, *Synthesis* **2023**, 927–933.
- [27] H. Ohmiya, H. Yorimitsu, K. Oshima, *Angew. Chem. Int. Ed.* **2005**, *44*, 2368–2370.
- [28] J. Rajpurohit, P. Kumar, P. Shukla, M. Shanmugam, M. Shanmugam, *Organometallics* **2018**, *37*, 2297–2304.
- [29] P. Kumar, A. Sen, G. Rajaraman, M. Shanmugam, *Inorg. Chem. Front.* **2022**, *9*, 2161–2172.
- [30] R. N. Saltiel, A. M. Geer, L. J. Taylor, O. Churchill, E. S. Davies, W. Lewis, A. J. Blake, D. L. Kays, *Adv. Synth. Catal.* **2020**, *362*, 3148–3157.
- [31] Z. Wu, A. Cheng, M. Yuan, Y. Zhao, H. Yang, L. Wei, H. Wang, T. Wang, Z. Zhang, W. Duan, *Angew. Chem. Int. Ed.* **2021**, *60*, 27241–27246.
- [32] X.-H. Yu, L.-Q. Lu, Z.-H. Zhang, D.-Q. Shi, W.-J. Xiao, *Org. Chem. Front.* **2023**, *10*, 133–139.
- [33] M. O. Shulyupin, M. A. Kazankova, I. P. Beletskaya, *Org. Lett.* **2002**, *4*, 761–763.
- [34] M. O. Shulyupin, I. G. Trostyanskaya, M. A. Kazankova, I. P. Beletskaya, *Russ. J. Org. Chem.* **2006**, *42*, 17–22.
- [35] J. Yan, Y.-B. Wang, S. Hou, L. Shi, X. Zhu, X. Hao, M. Song, *Appl. Organomet. Chem.* **2020**, *34*, e5954.
- [36] L. Huang, E. Q. Lim, M. J. Koh, *Chem Catal.* **2022**, *2*, 508–518.
- [37] S. Ortial, H. C. Fisher, J.-L. Montchamp, *J. Org. Chem.* **2013**, *78*, 6599–6608.
- [38] (a) A. D. Sadow, I. Haller, L. Fadini, A. Togni, *J. Am. Chem. Soc.* **2004**, *126*, 14704–14705; (b) A. D. Sadow, A. Togni, *J. Am. Chem. Soc.* **2005**, *127*, 17012–17024.
- [39] J. Long, Y. Li, W. Zhao, G. Yin, *Chem. Sci.* **2022**, *13*, 1390–1397.
- [40] M. A. Kazankova, I. V. Efimova, A. N. Kochetkov, V. V. Afanas'ev, I. P. Beletskaya, P. H. Dixneuf, *Synlett* **2001**, 497–500.
- [41] M. A. Kazankova, I. V. Efimova, A. N. Kochetkov, V. V. Afanas'ev, I. P. Beletskaya, *Russ. J. Org. Chem.* **2002**, *38*, 1465–1474.
- [42] V. P. Ananikov, L. L. Khemchyan, I. P. Beletskaya, Z. A. Starikova, *Adv. Synth. Catal.* **2010**, *352*, 2979–2992.
- [43] L. L. Khemchyan, J. V. Ivanova, S. S. Zalesskiy, V. P. Ananikov, I. P. Beletskaya, Z. A. Starikova, *Adv. Synth. Catal.* **2014**, *356*, 771–780.
- [44] R. L. Webster, *Inorganics* **2018**, *6*, 120.
- [45] P. Ribiere, K. Bravo-Altamirano, M. I. Antczak, J. D. Hawkins, J.-L. Montchamp, *J. Org. Chem.* **2005**, *70*, 4064–4072.
- [46] X. Liu, X. Han, Y. Wu, Y. Sun, L. Gao, Z. Huang, Q. Zhang, *J. Am. Chem. Soc.* **2021**, *143*, 11309–11316.
- [47] Q. Yuan, Z. Huang, W. Wu, D. Hong, S. Zhu, J. Wei, S. Zhou, S. Wang, *Dalton Trans.*, **2022**,

51, 17795–17803.

- [48] N. A. Isley, R. T. Linstadt, E. D. Slack, B. H. Lipshutz, *Dalton Trans.* **2014**, 43, 13196–13200.
- [49] Y. Li, H. Tian, L. Yin, *J. Am. Chem. Soc.* **2020**, 142, 20098–20106.
- [50] W. Yue, J. Xiao, S. Zhang, L. Yin, *Angew. Chem. Int. Ed.* **2020**, 59, 7057–7062.
- [51] Y. Wang, Z.-Q. Wang, L. Yin, *Synthesis* **2023**, 55, 2228–2240.
- [52] Q. Yang, J. Zhou, J. Wang, *Chem. Sci.*, **2023**, 14, 4413–4417.
- [53] S. Zhang, N. Jiang, J.-Z. Xiao, G.-Q. Lin, L. Yin, *Angew. Chem. Int. Ed.* **2023**, 62, e202218798.
- [54] B. S. Daniels, X. Hou, S. A. Corio, L. M. Weissman, V. M. Dong, J. S. Hirschi, S. Nie, Shaozhen, *Angew. Chem. Int. Ed.* **2023**, 62, e202306511.
- [55] M. Niu, H. Fu, Y. Jiang, Y. Zhao, *Chem. Commun.* **2007**, 272–274.
- [56] A. Kondoh, H. Yorimitsu, K. Oshima, *J. Am. Chem. Soc.* **2007**, 129, 4099–4104.
- [57] J. Yuan, L. Zhu, J. Zhang, J. Li, C. Cui, *Organometallics* **2017**, 36, 455–459.
- [58] J. Li, Z. Gao, Y. Guo, H. Liu, P. Zhao, X. Bi, E. Shi, J. Xiao, *RSC Adv.* **2022**, 12, 18889–18896.
- [59] B. Cai, Y. Cui, J. Zhou, Y.-B. Wang, L. Yang, B. Tan, J. Wang, *Angew. Chem. Int. Ed.* **2023**, 62, e202215820.
- [60] X.-Y. Liu, Y.-X. Zou, H.-L. Ni, J. Zhang, H.-B. Dong, L. Chen, *Org. Chem. Front.* **2020**, 7, 980–986.
- [61] A. Bakhtiary, M. R. P. Heravi, A. Hassanpour, I. Amini, E. Vessally, *RSC Adv.* **2021**, 11, 470–483.
- [62] W. Wei, J. Ji, *Angew. Chem. Int. Ed.* **2011**, 50, 9097–9099.
- [63] J. Gu, C. Cai, *Org. Biomol. Chem.* **2017**, 15, 4226–4230.
- [64] F. M. Moghaddam, M. Daneshfar, R. Azaryan, J.-L. Pirat, *Catal. Commun.* **2020**, 141, 106015.
- [65] H. Wang, Q. Fu, Z. Zhang, M. Gao, J. Ji, D. Yi, *Chin. J. Org. Chem.* **2018**, 38, 1977–1984.
- [66] M. Zhou, M. Chen, Y. Zhou, K. Yang, J. Su, J. Du, Q. Song, *Org. Lett.* **2015**, 17, 1786–1789.
- [67] N. Yi, R. Wang, H. Zou, W. He, W. Fu, W. He, *J. Org. Chem.* **2015**, 80, 5023–5029.
- [68] X. Chen, X. Li, X. Chen, L. Qu, J. Chen, K. Sun, Z. Liu, W. Bi, Y. Xia, H. Wua, Y. Zhao, *Chem. Commun.* **2015**, 51, 3846–3849.
- [69] X. Chen, X. Chen, X. Li, C. Qu, L. Qu, W. Bi, K. Sun, Y. Zhao, *Tetrahedron* **2017**, 73, 2439–2446.
- [70] W. Liang, Z. Zhang, D. Yi, Q. Fu, S. Chen, L. Yang, F. Du, J. Ji, W. Wie, *Chin. J. Chem.* **2017**, 35, 1378–1382.
- [71] P. Zhang, L. Zhang, Y. n Gao, J. Xu, H. Fang, G. Tang, Y. Zhao, *Chem. Commun.*, **2015**, 51, 7839–7842.
- [72] (a) G.-Y. Zhang, C.-K. Li, D.-P. Li, R.-S. Zeng, A. Shoberu, J.-P. Zou, *Tetrahedron* **2016**, 72, 2972–2978; (b) P. Zhou, B. Hu, L. Li, K. Rao, J. Yang, F. Yu, *J. Org. Chem.* **2017**, 82, 13268–13276.
- [73] P. Tang, C. Zhang, E. Chen, B. Chen, W. Chen, Y. Yu, *Tetrahedron Lett.* **2017**, 58, 2157–2161.
- [74] D. Yamamoto, H. Ansai, J. Hoshino, K. Makino, *Chem. Pharm. Bull.* **2018**, 66, 873–879.
- [75] For special issues on photochemistry and photoredox catalysis in organic synthesis: a) *Acc. Chem. Res.* **2016**, 49 2059–2060 and 2261–2327; b) *Chem. Rev.* **2016**, 116, 9629–10342.
- [76] For representative reviews on reactions involving photo-catalyst, see: a) C. K. Prier, D. A. Rankic, D. W. C. MacMillan, *Chem. Rev.* **2013**, 113, 5322–5363; b) N. A. Romero, D. A. Nicewicz, *Chem. Rev.* **2016**, 116, 10075–10166; c) M. H. Shaw, J. Twilton, D. W. C.

- MacMillan, *J. Org. Chem.* **2016**, *81*, 6898–6926; d) L. Marzo, S. K. Pagire, O. Reiser, B. König, *Angew. Chem. Int. Ed.* **2018**, *57*, 10034–10072.
- [77] For representative reviews on reactions involving dual/cooperative photo-catalysis, see: a) J. C. Tellis, C. B. Kelly, D. N. Primer, M. Jouffroy, N. R. Patel, G. A. Molander, *Acc. Chem. Res.* **2016**, *49*, 1429–1439; b) K. L. Skubi, T. R. Blum, T. P. Yoon, *Chem. Rev.* **2016**, *116*, 10035–10074; c) X. Lang, J. Zhao, X. Chen, *Chem. Soc. Rev.* **2016**, *45*, 3026–3038.
- [78] For representative reviews, see: a) M. Parasram, V. Gevorgyan, *Chem. Soc. Rev.* **2017**, *46*, 6227–6240; b) W.-M. Cheng, R. Shang, *ACS Catal.* **2020**, *10*, 9170–9196; c) K. P. S. Cheung, S. Sarkar, V. Gevorgyan, *Chem. Rev.* **2022**, *122*, 1543–1625.
- [79] J. K. Pagano, C. A. Bange, S. E. Farmiloe, R. Waterman, *Organometallics* **2017**, *36*, 3891–3895.
- [80] B. J. Ackley, J. K. Pagano, R. Waterman, *Chem. Commun.* **2018**, *54*, 2774–2776.
- [81] S. G. Dannenberg, R. Waterman, *Chem. Commun.* **2020**, *56*, 14219–14222.
- [82] S. G. Dannenberg, D. M. Seth Jr., E. J. Finfer, R. Waterman, *ACS Catal.* **2023**, *13*, 550–562.
- [83] H. Hou, B. Zhou, J. Wang, D. Zhao, D. Sun, X. Chen, Y. Han, C. Yan, Y. Shi, S. Zhu, *Org. Lett.* **2021**, *23*, 2981–2987.

Chapter 2.

Blue-Light Driven Iron-Catalyzed Oxy-phosphinylation of Activated Alkenes for β -Ketophosphine Oxide Synthesis

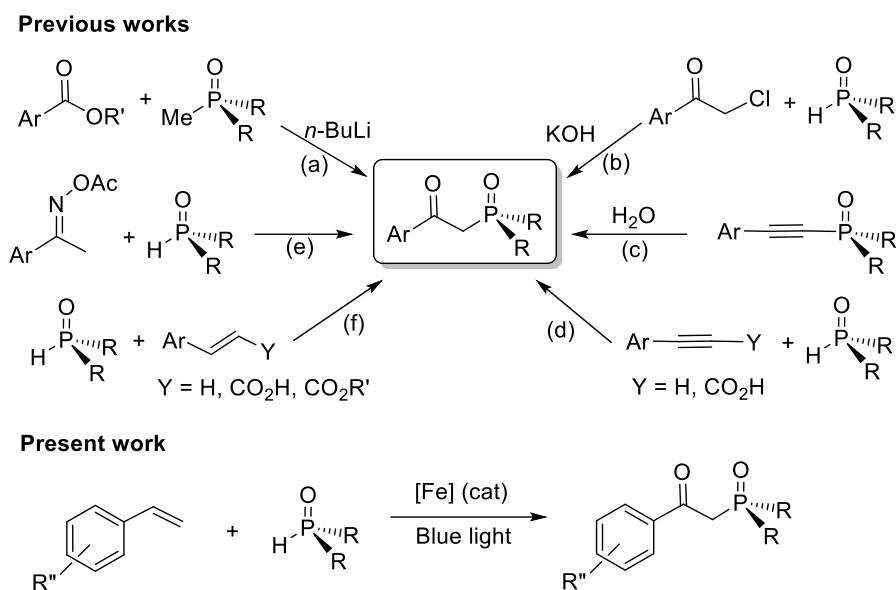
This chapter is adapted from the publication: Yumeng Yuan, Qiufeng Huang, Christophe Darcel, *Chem. Eur. J.* **2023**, e202302358.

Chapter 2 - Blue-Light Driven Iron-Catalyzed Oxy-phosphinylation of Activated Alkenes for β -Ketophosphine Oxide Synthesis

2.1. Introduction

In molecular chemistry, β -keto-organophosphorus derivatives such as β -keto-phosphonates or phosphine oxides are useful intermediates in organic synthesis, notably for the preparation of α,β -unsaturated carbonyl derivatives via classical Horner–Wadsworth–Emmons reactions.^[1] More particularly, β -keto-phosphine oxides are useful intermediates for the preparation of substituted ketones,^[2] and stereoselective molecular synthesis.^[3] Additionally, they can serve of bidentate ligands in coordination chemistry^[4] or be used as extractants in the separation of *f*-elements from acidic solutions in solvent extraction.^[5]

Typical synthesis of β -ketophosphine oxides were conducted via the acylation of alkylphosphine oxides by esters^[6] or by the reaction of chloroacetophenone with secondary phosphine oxides under basic conditions.^[7] (Scheme 1a-b). Another access to β -ketophosphine oxides can be performed by hydration of alkynylorganophosphorus derivatives.^[8] (Scheme 2-1c) Alternative preparations can be done starting from secondary phosphine oxides $R_2HP(=O)$ by reaction with acetylenic derivatives such as terminal alkynes^[9] or arylpropionic acid,^[10] and with aryl ketone *o*-acetyloximes.^[11] (Scheme 2-1(d-e)) Similar reactivity of secondary phosphine oxides $R_2HP(=O)$ was observed with alkenyl derivatives such as non-functionalized alkenes,^[12] or α,β -unsaturated carboxylic compounds.^[13] (Scheme 2-1f) Main of these transformations were performed using copper or silver based catalysts.^[9a-c,10a, 11, 12c, 13a] It should be underlined that few of them are catalyzed by both iron and copper,^[9d-e,12b] and notably, β -ketophosphine oxides can be also prepared from aldehydes via a domino Fe/Cu-catalyzed Knoevenagel reaction.^[14] To the best of our knowledge, only one contribution described the use of iron salt catalyst in phosphinylation of 1,3-diketones using secondary phosphine oxides at 100 °C.^[15]



Scheme 2-1. Previous approaches and present work on β -ketophosphine oxide synthesis.

On the other hand, since the beginning of this millennium, iron has emerged as a useful substitute for noble metals, more particularly in reduction and hydroelementation areas.^[16] Noticeably, iron-catalyzed regioselective hydrophosphination of alkenes and alkynes with secondary diphenylphosphine Ph_2PH led to the corresponding alkyl- and alkenyl- diphenylphosphines, respectively.^[17,18] Interestingly, when using $[\text{CpFe}(\text{CO})_2]_2$ (5 mol%) under visible light irradiation (LED bulb, $h\nu > 500$ nm), the hydrophosphination of styrene, acrylic derivatives and the double hydrophosphination of terminal arylalkynes with Ph_2PH can be performed at 25-28 °C instead of 100 °C without light activation.^[19]

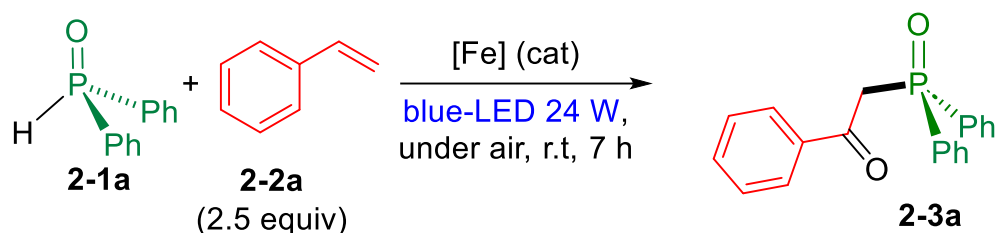
Following our continuous contribution in iron catalyzed transformations,^[20] notably involving hydroelementations such as hydroboration or dehydrogenative borylation,^[21] or via α -alkylation reaction of methyl diarylphosphine oxides,^[22] we report herein the iron-catalyzed oxo-phosphinylation of activated alkenes using secondary phosphine oxides leading to β -ketophosphine oxide derivatives under blue-light irradiation. (Scheme 2-1) To the best of our knowledge, there is no report dealing with such transformation using sole iron as a catalyst.

2.2. Results and Discussion

First of all, in order to evaluate the ability of iron salts to catalyze the oxo-phosphinylation of alkenes to generate β -ketophosphine oxide derivatives, the reaction of styrene **2-2a** with diphenylphosphine oxide **1a** was selected as the benchmark reaction. (Table 2-1)

We thus began our initial work by performing the reaction of diphenylphosphine oxide **1a** with 2.5 equiv. of styrene **2-2a** in the presence of 10 mol% of FeCl₃ in acetonitrile upon blue light irradiation (using two 24-watt LED lamps, 450-460 nm) at room temperature for 7 h. Noticeably, the β -ketophosphine oxide **2-3a** was obtained in 70%. (Entry 1) We then evaluated the effect of the iron salt nature on the reaction. (Entries 2-6) Among the tested salts (10 mol%), FeBr₂ did not exhibited reactivity whereas the other ones led to the desired product with moderate yields (14-37%). Noticeably, whereas Fe(OTf)₃ led to only 37% yield, 77% was obtained when using with Fe(OTf)₂. (Entries 6 vs 8) Decreasing the quantity of Fe(OTf)₂ to 5 mol% had a deleterious effect on the efficiency of the transformation as only 43% of **2-3a** was produced, whereas the increase of the catalytic amount of Fe(OTf)₂ to 15 mol% had no effect. (Entries 7-9) The nature of the light had also a crucial effect on the reaction: with white light (24-watt compact fluorescent lamp), a reduced efficiency was observed (15% yield, entry 10). Control experiments showed that light, iron catalyst and oxygen are all essential to the reaction. (Entries 11-13) Additionally, the nature of the solvent was evaluated. (Entries 14-19) Moderate yields were obtained when the reaction was conducted in THF and methanol, whereas no reaction took place with TFE and CPME The best efficiency was observed in 1,4-dioxane, **2-3a** being obtained in 97% yield.

Table 2-1. Optimization of the light driven iron-catalyzed oxo-phosphinylation of styrene with diphenylphosphine oxide.^{a)}

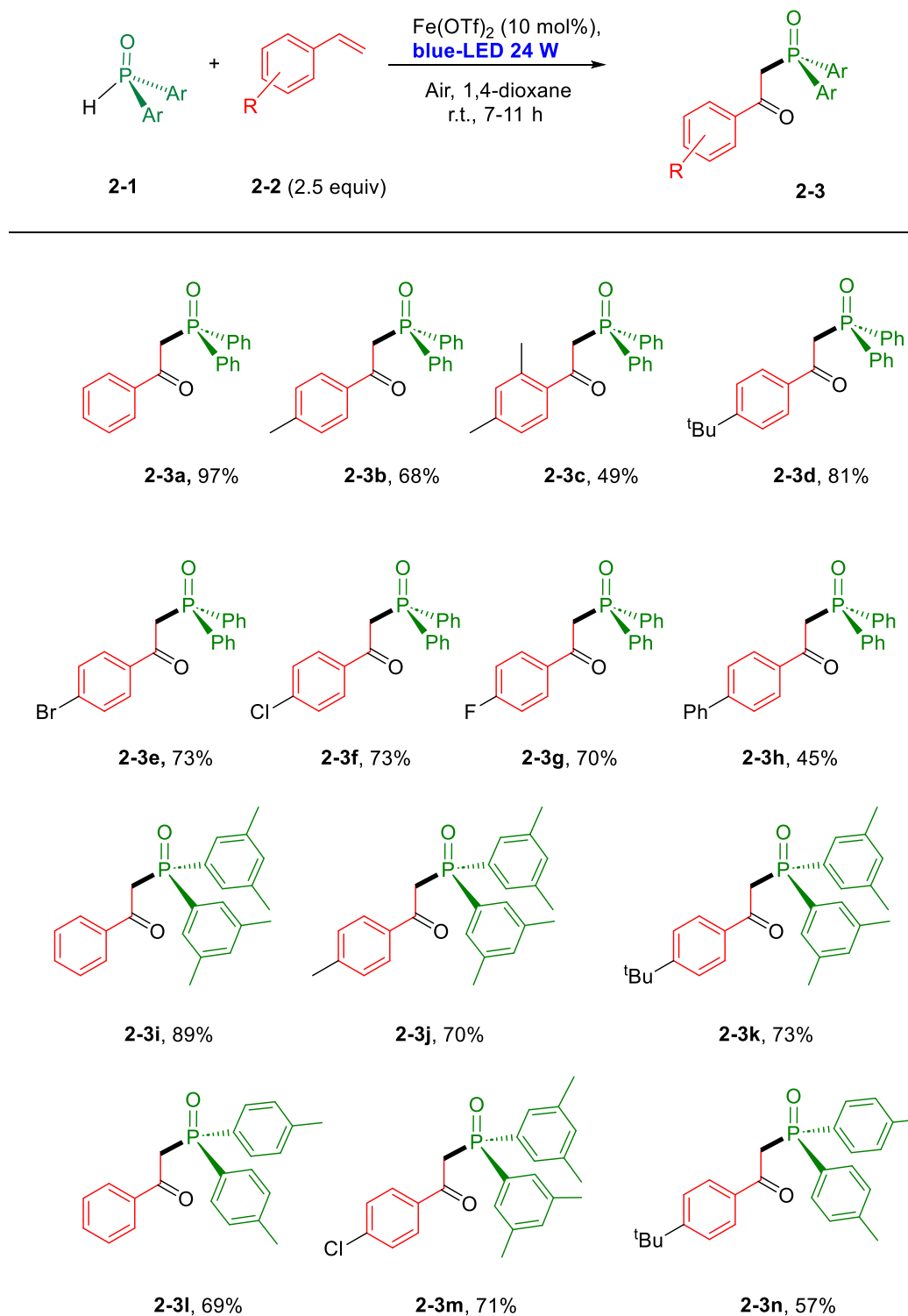


Entry	Cat (10 mol%)	light	Solvent	2-3a Yield(%)
1	FeCl ₃	Blue-LED	CH ₃ CN	70
2	FeBr ₂	Blue-LED	CH ₃ CN	-
3	FeF ₃	Blue-LED	CH ₃ CN	14
4	Fe(OAc) ₂	Blue-LED	CH ₃ CN	33
5	Fe(BF ₄) ₂ ·6H ₂ O	Blue-LED	CH ₃ CN	30
6	Fe(OTf) ₃	Blue-LED	CH ₃ CN	37
7	Fe(OTf) ₂ (5 mol%)	Blue-LED	CH ₃ CN	43
8	Fe(OTf) ₂ (10 mol%)	Blue-LED	CH ₃ CN	77
9	Fe(OTf) ₂ (15 mol%)	Blue-LED	CH ₃ CN	75
10	Fe(OTf) ₂	White	CH ₃ CN	15
11	Fe(OTf) ₂	No light	CH ₃ CN	14
12	none	Blue-LED	CH ₃ CN	7
13 ^[b]	Fe(OTf) ₂	Blue-LED	CH ₃ CN	NR
14	Fe(OTf) ₂	Blue-LED	1,4-dioxane	97
15	Fe(OTf) ₂	Blue-LED	TFE	< 5
16	Fe(OTf) ₂	Blue-LED	1,2-DCE	70
17	Fe(OTf) ₂	Blue-LED	MeOH	23
18	Fe(OTf) ₂	Blue-LED	CPME	NR
19	Fe(OTf) ₂	Blue-LED	THF	47

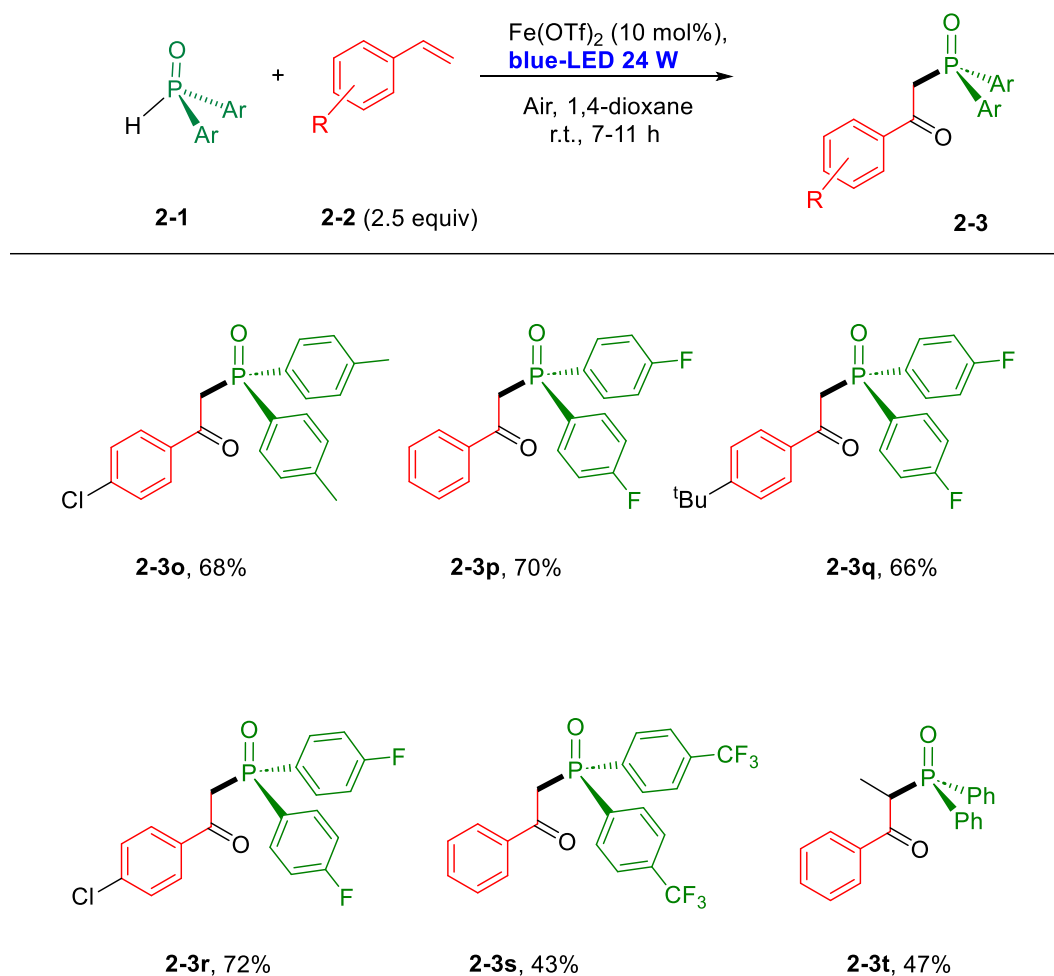
[a] Reaction conditions: **2-1a** (0.2 mmol), **2-2a** (0.5 mmol), $[Fe]$ (10 mol%), solvent (1 mL), 2 blue-LEDs 24 W (450-460 nm), r.t., 10 h under air. Isolated yields. [b] Reaction under argon atmosphere. TFE: 2,2,2-trifluoroethanol; 1,2-DCE: 1,2-dichloroethane; CPME: cyclopropylmethylether.

With these optimized reaction conditions in hands [Fe(OTf)₂ (10 mol%), 2.5 equiv. of alkene, 1 equiv. of secondary phosphine oxide in 1,4-dioxane for 7 h at room temperature under blue light activation (2×24W-blue LED) and air], we then evaluated the substrate scope and limitation of this oxo-phosphinylation of alkenes. (Scheme 2-2) The reaction of diphenylphosphine oxide **1a** was successfully performed with substituted styrenes bearing *para*-electron donating groups such as methyl or *tert*-butyl, leading to the corresponding β -ketophosphine oxides **2-(3b-3d)** in 49-81% yields. Styrenes with *p*-substituted halides such as fluoro, chloro and bromo were also selectively converted in the β -ketophosphine oxides **2-(3e-3g)** in 70-73% yields. The reaction can be also conducted with 4-phenylstyrene, thus leading to **2-3h** in 45% yield. By contrast, when starting from 4-methoxystyrene, no reaction took place. Similarly, using 4-vinylaniline, 4-vinylbenzoic acid or 4-acetoxystyrene, no corresponding product was obtained under such conditions. Diarylphosphine oxides such as bis(*m,m'*-dimethylphenyl)phosphine oxide **2-1b** and bis(*p*-tolyl)-phosphine oxide **2-1c** can be used and the corresponding β -ketophosphine oxides **2-(3i-3k)** were obtained in 70-89% yields and **2-(3l-3o)** in 57-71%, respectively. The transformation can be accomplished with bis(*p*-trifluoromethylphenyl)phosphine oxide **1d** as coupling partner, and the reaction with styrene afforded the corresponding β -ketophosphine oxide **2-3s** in 43% yield. This result showed that the transformation can occurred with *para*-substituted bis-arylphosphine oxide with a strong electron-withdrawing CF₃ group, but in only a moderate efficiency.

The transformation can be also done with internal olefin such as (*E*)-1-phenylpro-1-ene, which reacted smoothly with diphenylphosphine oxide **1a** affording β -ketophosphine oxide **2-3t** in 47% yield. By contrast, no reaction took place with α -methylstyrene. Notably, when performing the reaction with 4-vinylpyridine and 4-trifluoromethylstyrene, no trace of the desired product **2-3** was observed, but the derivatives corresponding to the classical anti-Markonikov hydrophosphinylation derivatives Ar-CH₂-CH₂-PPh₂(=O) **2-(4a-4c)** were obtained in 52-81%.^[17-19] (Scheme S2-1, Chapter 4)



Scheme 2-2. Scope of blue-light driven iron-catalyzed oxophosphinylation of styrene derivatives. $\text{Fe}(\text{OTf})_2$ (10 mol%), alkene (2.5 equiv.), secondary phosphine oxide (1 equiv.), 1,4-dioxane, 7 h at room temperature under blue light activation ($2 \times 24\text{W}$ -blue LED) and air. Isolated yields.



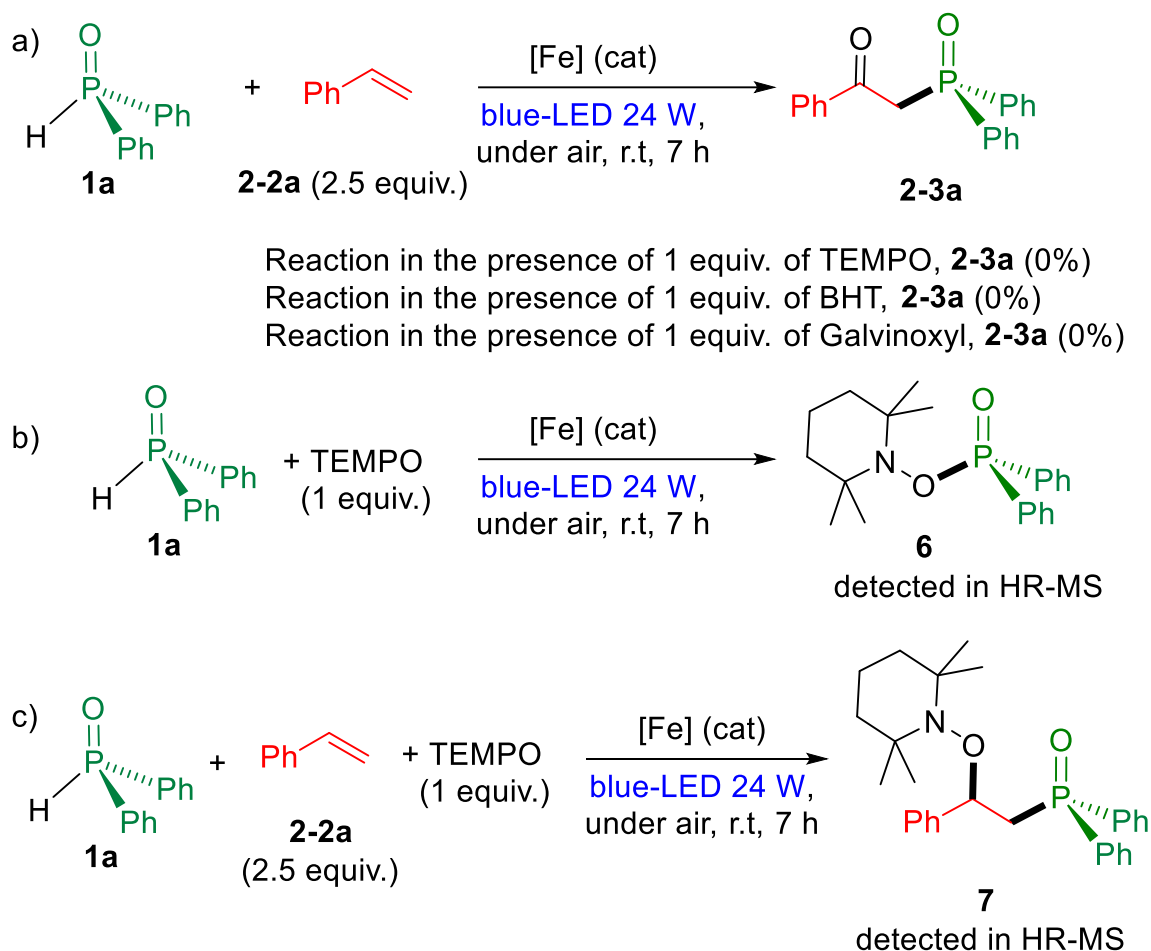
Scheme 2-2 (continued). Scope of blue-light driven iron-catalyzed oxophosphinylation of styrene derivatives. $\text{Fe}(\text{OTf})_2$ (10 mol%), alkene (2.5 equiv.), secondary phosphine oxide (1 equiv.), 1,4-dioxane, 7 h at room temperature under blue light activation ($2 \times 24\text{W}$ -blue LED) and air. Isolated yields.

To demonstrate the synthetic usefulness of this methodology, a gram scale reaction starting from 24.75 mmol (1.00 g) of diphenylphosphine oxide **1a** led to the corresponding product **2-3d** in 70% isolated yield.

We then conducted preliminary mechanistic studies in order to gain insights into this transformation. First, when performing the reaction of styrene, with a 92% deuterium labeled diphenylphosphine oxide $\text{Ph}_2\text{P}(\text{O})\text{D}$, no deuterium incorporation was observed in the obtained β -ketophosphine oxide **2-3a**. In order to check if a radical process was involved, 1 equiv. of TEMPO (2,2,6,6-tetramethyl-1-piperidinyloxy) was added to the reaction mixture (1 equiv. of diphenylphosphine **1a**, 2.5 equiv. of styrene **2-2a**, in the presence of 10 mol% of $\text{Fe}(\text{OTf})_2$ at RT under blue light activation for 7 h). Under

such conditions, no trace of β -ketophosphine oxide **2-3a** was detected. Similarly, when using 1 equiv. of BHT (2,6-di-*tert*-butyl-4-methylphenol) or galvinoxyl as alternative radical scavengers, the formation of **2-3a** was also totally suppressed. (Scheme 2-3a) These experimental evidences support a radical pathway. Additionally, when the reaction was conducted under argon atmosphere and blue light activation, no reaction occurred, thus suggesting that aerobic oxidation should be involved to produce the keto moiety (Table 2-1, entry 13) Interestingly, when performing the reaction of diphenylphosphine oxide **1a** with 1 equiv. of TEMPO under blue light activation and air at ambient temperature for 7 h, the TEMPO adduct **6** was detected in HR-MS with $m/z = 358.1931$, demonstrating that a phosphorus radical **B** was generated thanks to the blue light activation and air. (Scheme 2-3b)

Additionally, when performing the reaction in presence of 2.5 equiv. styrene, even if no trace of **2-3a** was observed, it was detected in HR-MS a signal at $m/z = 462.2651$ corresponding to the formation of the TEMPO adduct **7**, thus demonstrating that the reaction went through the formation of the radical species **C**. (Scheme 2-3c)

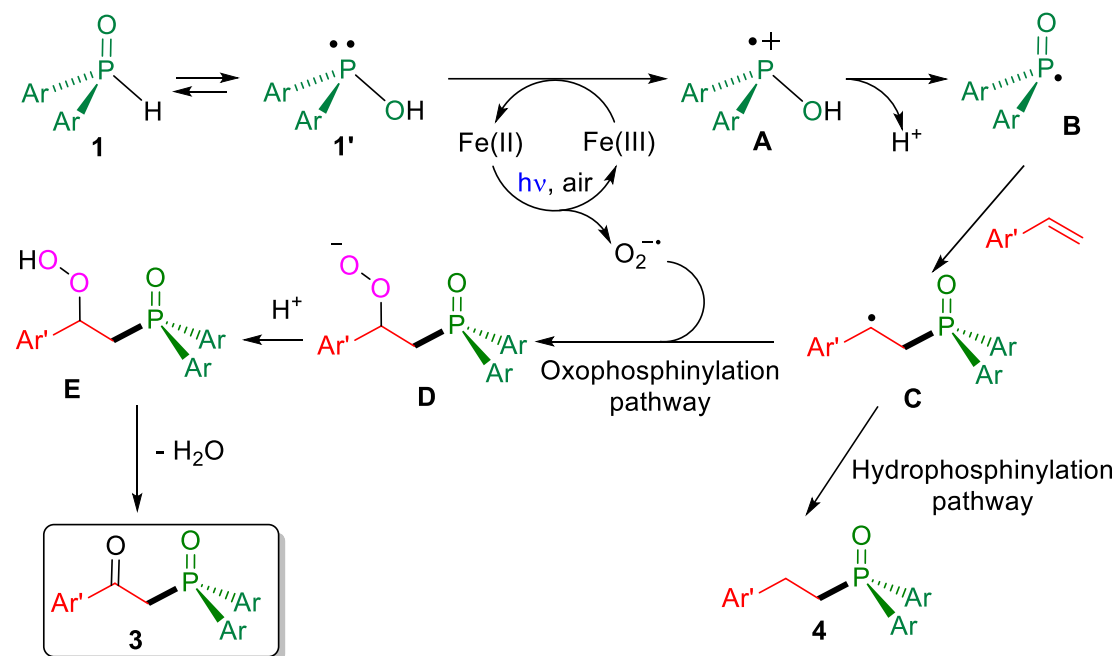


Scheme 2-3. Control experiments.

Furthermore, a light on/off experiment for the reaction of the diphenylphosphine oxide **1a** with 2 equiv. of 4-fluorostyrene in the presence of 10 mol% of $\text{Fe}(\text{OTf})_2$ under the standard reaction conditions in CD_3CN indicated that the reaction almost stopped in the absence of blue light in dark, and restarted as soon as exposed to blue light. (See Chapter 4, Figure S2-1). This result suggested that chain propagation should not be the main reaction pathway, and continuous irradiation of blue light was mandatory for the success of the reaction.

On the basis of the above experimental evidences, a plausible mechanism is described in Scheme 2-4. In an initial step, the secondary phosphine oxide **1** is oxidized to phosphorus radical **B**^[9e-g,12a,13f,23] via a blue light promoted aerobic process catalyzed by iron^[9b,12b,17d] species. This former radical **B** then reacted with activated alkene leading to the corresponding benzyl radical **C** via an anti-Markovnikov radical addition.

Thus, this radical intermediate can be trapped by $O_2^{\cdot -}$ generating the peroxy intermediate **D** which after reaction with proton gave the peroxide phosphine oxide species **E**. A subsequent dehydration furnished the β -ketophosphine oxide **3**.



Scheme 2-4. Proposed reaction mechanism for the oxyphosphinylation of activated alkenes.

2.3. Conclusion

In summary, we have developed a practical protocol for the synthesis of β -ketophosphine oxides starting from secondary diarylphosphine oxides and styrene derivatives catalyzed by $Fe(OTf)_2$ and promoted by blue light activation under air at ambient temperature. Control experiments revealed that a radical process is involved in the mechanism. Thus, a blue light promoted aerobic process catalyzed by iron generated a phosphorus radical from the starting secondary phosphine oxide which then reacted with styrene.

2.4. References

- [1] a) B. E. Maryanoff, A. B. Reitz, *Chem. Rev.* **1989**, *89*, 863-927; b) K. Kobayashi, K. Tanaka III, H. Kogen, *Tetrahedron Lett.* **2018**, *59*, 568-582; c) D. Roman, M. Sauer, C. Beemelmans, *Synthesis* **2021**, 2713-2739.
- [2] For selected examples, see: a) D. J. Fox, D. S. Pedersena, S. Warren, *Org. Biomol. Chem.* **2006**, *4*, 3102-3107; b) D. J. Fox, D. S. Pedersen, S. Warren, *Chem. Commun.* **2004**, 2598-2599.
- [3] J. Clayden, S. Warren, *Angew. Chem., Int. Ed. Engl.* **1996**, *35*, 241-270.
- [4] For selected examples, see: a) B. Guilbert, B. Demerseman, P. H. Dixneuf, C. Meaili, *J. Chem. Soc.* **1989**, 10035-1037; b) P. Braunstein, S. C. Cea, A. Decian, J. Fisher, *Inorg. Chem.* **1992**, *31*, 4203-4206; c) P. Crochet, B. Demerseman, C. Rocaboy, D. Schleyer, *Organometallics* **1996**, *15*, 3048-3061; d) P. Braunstein, *Chem. Rev.* **2006**, *106*, 134-159.
- [5] For selected examples, see: a) L. A. Mitchell, B. J. Holliday, *ACS Macro Lett.* **2016**, *5*, 1100-1103; b) R. Babecki, A. W. G. Platt, J. Fawcett, *J. Chem. Soc., Dalton Trans.* **1992**, 675; c) B. M. Papko in *Separations of f-elements* (Eds.: K. L. Nash, G. R. Choppin), Springer, New York, **1995**, pp. 99-124.
- [6] a) R. S. Torr, S. Warren, *J. Chem. Soc. Pak.* **1979**, *1*, 15-19; b) D. Cavalla, C. Gueguen, A. Nelson, P. O'Brien, M. G. Russell, S. Warren, *Tetrahedron Lett.* **1996**, *37*, 7465-7468.
- [7] A. E. Antoshin, Y. N. Reikhov, K. V. Tugushov, I.V. Rybal'chenko, V. F. Taranchenko, S. A. Lermontov, A. N. Malkova, *Russ. J. Gen. Chem.* **2009**, *79*, 2113-2115.
- [8] a) X. Li, G. Hu, P. Luo, G. Tang, Y. Gao, P. Xu, Y. Zhao, *Adv. Synth. Catal.* **2012**, *354*, 2427-2432; b) J. Yang, X. Sun, K. Yan, H. Sun, S. Sun, X. Jia, F. Zhang, J. Wen, *Adv. Synth. Catal.* **2022**, *364*, 2735-2740.
- [9] Selected examples starting from terminal alkynes, see: a) X. Chen, X. Li, X.-L. Chen, L.-B. Qu, J.-Y. Chen, K. Sun, Z.-D. Liu, W.-Z. Bi, Y. Y.-Y. Xia, H.-T. Wu, Y. Zhao, *Chem. Commun.* **2015**, *51*, 3846-3849; b) M. Zhou, M. Chen, Y. Zhou, K. Yang, J. Su, J. Du, Q. Song, *Org. Lett.* **2015**, *17*, 1786-1789; c) N. Yi, R. Wang, H. Zou, W. He, W. Fe, W. He, *J. Org. Chem.* **2015**, *80*, 5023-5029; d) W.-W. Zhong, Q. Zhang, M.-S. Li, D.-Y. Hu, M. Cheng, F.-T. Du, J.-X. Ji, W. Wei, *Synth. Commun.* **2016**, *46*, 1377-1385; e) P. Peng, Q. Lu, L. Peng, C. Liu, G. Wang, A. Lei, *Chem. Commun.* **2016**, *52*, 12338-12341; f) M.-J. Bu, G.-P. Lu, C. Cai, *Catal. Sci. Technol.* **2016**, *6*, 413-416; g) B. Liu, Q. Song, Z. Liu, Z. Wang, *Adv. Synth. Catal.* **2021**, *363*, 3214-3219; h) W. Zhong, T. Tan, L. Shi, X. Zeng, *Synlett* **2018**, 1379-1384.
- [10] Selected examples starting from arylpropionic acids, see: a) P. Zhang, L. Zhang, Y. Gao, J. Xu, H. Fang, G. Tang, Y. Zhao, *Chem. Commun.* **2015**, *51*, 7839-7842; b) Y.-F. Zeng, D.-H. Tan, W.-X. Lv, Q. Li, H. Wang, *Eur. J. Org. Chem.* **2015**, 4335-4339.
- [11] J. Ke, Y. Tang, H. Yi, Y. Li, Y. Cheng, C. Liu, A. Lei, *Angew. Chem. Int. Ed.* **2015**, *54*, 6604-6607.
- [12] Selected examples starting from α,β -unsaturated carboxylic derivatives, see: a) H.-F. Qian, C.-K. Li, Z.-K. Tao, A. Shoberu, K.-P. Zou *Org. Lett.* **2018**, *18*, 5947-5951; b) Y. Zhou, M. Zhou, M. Chen, J. Su, J. Du, Q. Song, *RSC Adv.* **2015**, *5*, 103977-103981; c) X. Chen, X. Chen, X. Li, C. Qu, L. Qu, W. Ni, K. Sun, Y. Zhao, *Tetrahedron* **2017**, *73*, 2439-2446.
- [13] Selected examples starting from unfunctionalized alkenes f) Y. Shi, R. Chen, K. Guo, F. Meng, S. Cao, C. Gu, Y. Zhu *Tetrahedron Lett.* **2018**, *59*, 2062-2065; g) G. Nan, H. Yue, *Tetrahedron Lett.* **2018**, *59*, 2071-2074.

- [14] M. Zhou, Y. Zhou, Q. Song, *Chem. Eur. J.* **2015**, *21*, 10654-10659.
- [15] Y. Ou, Y. Huang, Y. Liu, Y. Huo, X. Li, Q. Chen, *Adv. Synth. Catal.* **2020**, *362*, 5783-5787.
- [16] For selected reviews and book chapters, see: a) C. Bolm, J. Legros, J. Le Paih, L. Zani, *Chem. Rev.* **2004**, *104*, 6217-6254; b) B. Plietker, *Iron Catalysis in Organic Chemistry: Reactions and Applications*. Wiley-VCH: Weinheim, 2008; c) R. H. Morris, *Chem. Soc. Rev.* **2009**, *38*, 2282-2291; d) C.-L. Sun, B.-J. Li, Z.-J. Shi, *Chem. Rev.* **2010**, *111*, 1293-1314; e) M. Zhang, A. Zhang, *Appl. Organometal. Chem.* **2010**, *24*, 751-757; f) K. Junge, K. Schröder, M. Beller, *Chem. Commun.* **2011**, *47*, 4849-4859; g) B. A. F. Le Bailly, S. P. Thomas, *RSC Adv.* **2011**, *1*, 1435-1445; h) C. Darcel, J.-B. Sortais, Iron-Catalysed Reduction and Hydroelementation Reactions. In *Iron Catalysis II*, E. Bauer, Ed. Springer, Cham, **2015**; Vol. 50, pp 173-216; j) I. Bauer, H.-J. Knölker, *Chem. Rev.* **2015**, *115*, 3170-3387; k) N. Guo, S. F. Zhu, *Chin. J. Org. Chem.* **2015**, *35*, 1383-1398; l) D. S. Mérel, M. L. T. Do, S. Gaillard, P. Dupau, J.-L. Renaud, *Coord. Chem. Rev.* **2015**, *288*, 50-68; m) L. C. Misal Castro, H. Li, J.-B. Sortais, C. Darcel, *Green Chem.* **2015**, *17*, 2283-2303; n) R. Lopes, B. Royo, *Isr. J. Chem.* **2017**, *57*, 1151-1159; o) D. Wei, C. Darcel, *Chem. Rev.* **2019**, *119*, 2550-2610; p) N. S. Shaikh, *ChemistrySelect* **2019**, *4*, 6753-6777; q) D. Wei, C. Netkaew, C. Darcel, *Eur. J. Inorg. Chem.* **2019**, 2471-2487; r) S. Rana, J. Prasad Biswas, S. Paul, A. Paik, D. Maiti, *Chem. Soc. Rev.* **2021**, *50*, 243-472.
- [17] a) L. Routaboul, F. Toulgoat, J. Gatignol, J.-F. Lohier, B. Norah, O. Delacroix, C. Alayrac, M. Taillefer, A.-C. Gaumont, *Chem. Eur. J.* **2013**, *19*, 8760-8764; b) K. J. Gallagher, R. L. Webster, *Chem. Commun.* **2014**, *50*, 12109-12111; c) K. J. Gallagher, M. Espinal-Viguri, M.-F. Mahon, R. L. Webster, *Adv. Synth. Catal.* **2016**, *358*, 2460-2468; d) A. K. King, A. Buchard, M. F. Mahon, R. L. Webster, *Chem. Eur. J.* **2015**, *21*, 15960-15963.
- [18] a) M. Espinal-Viguri, A. K. King, J. P. Lowe, M. F. Mahon, R. L. Webster, *ACS Catal.* **2016**, *6*, 7892-7897; b) M. Kamitani, M. Itazaki, C. Tamiya, H. Nakazawa, *J. Am. Chem. Soc.* **2012**, *134*, 11932-11935; c) M. Itazaki, S. Katsube, M. Kamitani, H. Nakazawa, *Chem. Commun.* **2016**, *52*, 3163-3166; d) A. K. King, K. J. Gallagher, M. F. Mahon, R. L. Webster, *Chem. Eur. J.* **2017**, *23*, 9039-9043.
- [19] a) J. K. Pagano, C. A. Bange, S. E. Farmiloe, R. Waterman, *Organometallics* **2017**, *36*, 3891-3895; b) B. J. Ackley, J. K. Pagano, R. Waterman, *Chem. Commun.* **2018**, *54*, 2774-2776.
- [20] D. Wei, C. Darcel, *J. Org. Chem.* **2020**, *85*, 14298-14306.
- [21] a) J. Zheng, J.-B. Sortais, C. Darcel, *ChemCatChem* **2014**, *6*, 763-766; b) S. Jiang, S. Quintero-Duque, T. Roisnel, V. Dorcet, M. Grellier, E. Sabo-Etienne, C. Darcel, J.-B. Sortais, *Dalton Trans.* **2016**, *45*, 11101-11108; c) T. Dombrey, G. C. Werncke, S. Jiang, M. Grellier, L. Vendier, S. Bontemps, J.-B. Sortais, S. Sabo-Etienne, C. Darcel, *J. Am. Chem. Soc.* **2015**, *137*, 4062-4065.
- [22] J. Wu, S. N. Narayanasamy, C. Darcel, *J. Organomet. Chem.* **2022**, *979*, 122510.
- [23] a) D. Leca, L. Fensterbank, E. Lacôte, M. Malacria, *Chem. Soc. Rev.* **2005**, *34*, 858-865; b) K. Luo, W.-C. Yang, L. Wu, *Asian J. Org. Chem.* **2016**, 350-367; c) W.-J. Yoo, S. Kobayashi, *Green Chem.* **2013**, *15*, 1844-1848.
- [24] S. Feng, J. Li, F. He, T. Li, H. Li, X. Wang, X. Xie, X. She, *Org. Chem. Front.* **2019**, *6*, 946.
- [25] A. W. J. Platten, A. M. Borys, E. Hevia, *ChemCatChem* **2022**, *14*, e202101853.

Chapter 3.

Blue-light driven Iron-catalyzed oxidative C-H/P-H functionalization for the synthesis of benzo[*b*]phosphole oxides – Preliminary results

Chapter 3 - Blue-light driven Iron-catalyzed oxidative C-H/P-H functionalization for the synthesis of benzo[*b*]phosphole oxides – Preliminary results

3.1. Introduction

It was exemplified in the first chapter that regioselective earth-abundant metal catalyzed hydrophosphorylation, hydrophosphinylation and hydrophosphination reactions can be performed with both alkenes and alkynes leading to alkyl- and alkenyl-organophosphorus derivatives. Additionally, the oxyphosphorylation, oxyphosphinylation and oxyphosphination versions are less reported. In the continuation of our work dealing with blue light driven iron-catalyzed phosphination of unsaturated C-C bonds, this chapter will be dedicated to the study of iron-catalyzed reaction of secondary phosphines to alkynes under blue light irradiation.

Indeed, phosphorus-containing heterocycles showed a wide application in organic synthesis, medicinal chemistry, and materials science.^[1-4] Among these compounds, benzo[*b*]phospholes derivatives have attracted significant amount of interest from synthetic chemists in the last few years due to their intrinsic physical and optical properties,^[5-8] which have enabled the development of novel photoelectrochemical materials. (Figure 3-1)

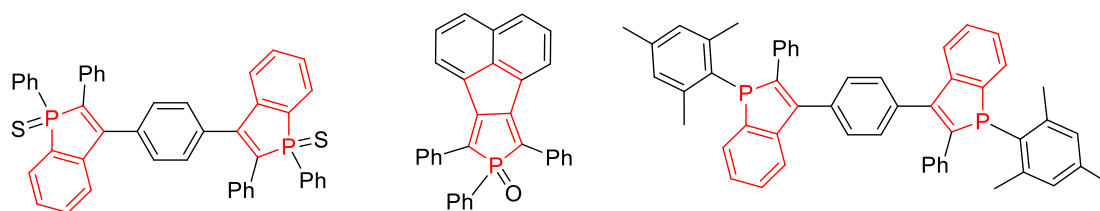
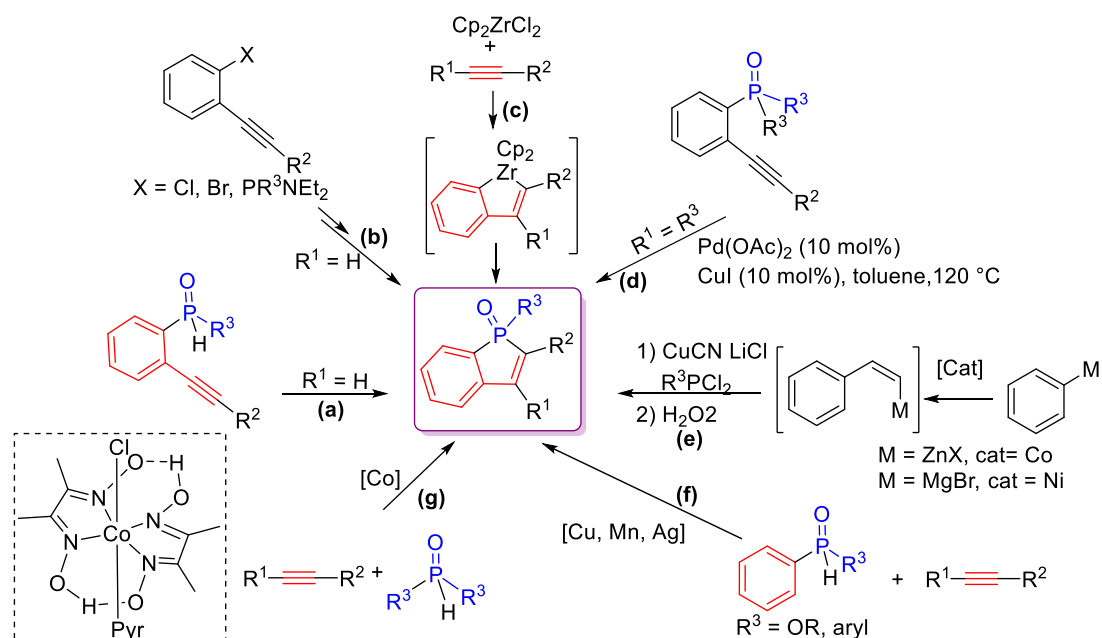


Figure 3-1. Representative examples of benzo[*b*]phosphole photoelectrochemical molecules.

However, most of the conventional preparations of benzo[*b*]phosphine derivatives^[9] were mainly performed starting from alkynes bearing *ortho*-phosphorus substituents involving one intramolecular cyclization step,^[10-15] the main limitation of such

pathways being the preparation of the starting materials. (Scheme 3-1(a-b)) Benzophosphole synthesis can be also done through electrophilic trapping with PhPCl_2 of a zirconaindene species, obtained from Cp_2ZrPh_2 and an alkyne, again for this preparation, only scarce examples were described.^[16] (Scheme 3-1c)

To circumvent such limitation and develop huger scope, transition metal catalysis has shown its advantages for the preparation of benzo[*b*]phosphole oxide derivatives, mainly starting from easier accessible starting materials. Thus, using $\text{Pd}(\text{OAc})_2/\text{CuI}$ cocatalysts (10 mol%), *o*-diarylphosphinophenylalkynes cyclized in refluxing toluene via C–P bond cleavage and arylphosphination of the $\text{C}\equiv\text{C}$ bond.^[17] (Scheme 3-1d)



Scheme 3-1. Traditional methodologies and catalyzed ones for benzo[*b*]phosphine synthesis.

Starting from metallated arenes ($\text{M} = \text{ZnX}$, MgBr), benzo[*b*]phosphole oxides can be obtained via the insertion of the alkyne catalyzed by nickel or cobalt, then electrophilic trapping reaction with R^3PCl_2 , Friedel-Crafts type cyclisation and oxidation.^[18,19] (Scheme 3-1e)

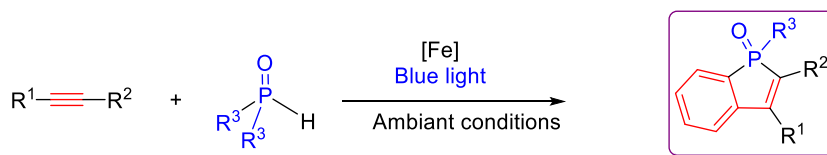
In another hand, during the past decade, transition metal-catalyzed C–H bond functionalization reactions have been extensively studied to afford a wide variety of heterocyclic compounds in a more efficient approach, and the synthesis of P-containing

heterocyclic compounds via such C-H functionalization pathway has demonstrated significant advances in stepwise and atom economy.

Several contributions described catalyzed oxidative C-H/P-H functionalization reactions starting from internal alkynes and secondary phosphine oxides or H-phosphonates using copper salts such as $\text{CuSO}_4 \cdot 5\text{H}_2\text{O}$ with TBHP as the oxidant (2 equiv.),^[20-21] manganese salt such as $\text{Mn}(\text{OAc})_2$ with MnO_2 as the oxidant in the presence of AcONa ,^[22] and silver oxide (Ag_2O , 5 mol%) in the presence of 1 equiv. of $\text{Zn}(\text{NO}_3)_2 \cdot 6\text{H}_2\text{O}$.^[23] (Scheme 3-1f) In 2019, L.-Z. Wu et al. has shown that using a well-defined cobaloxime based catalyst $\text{Co}(\text{dmgH}_2)_2\text{PyCl}$ (15 mol%) in the presence of HCO_2Na in dichloromethane at 60 °C for 20 h under blue LED irradiation, internal alkynes reacted with diarylphosphine oxides to lead to benzo[*b*]phosphole oxides in 43-90% yields (16 examples).^[24] (Scheme 3-1g) Noticeably, with terminal alkynes, (*E*)-alkenylphosphine oxides were obtained.

Remarkably, to the best of our knowledge, no system involving iron catalysts was reported up to now. Furthermore, it should be underlined that in the reported works above, the reactions required significant heating.

Based on these observations, the goal of this chapter research was to develop a blue-light driven iron-controlled oxidative C-H/P-H functionalization method for benzo[*b*]phospholes oxide synthesis using secondary phosphine oxides with alkynes, conducting the reaction at ambient conditions. (Scheme 3-2)



Scheme 3-2. Goal of this chapter research.

3.2. Results and discussion

Our initial efforts focused on the annulation of diphenylphosphine oxide **1a** with diphenylacetylene **3-2a** using several iron salts as the catalysts. Thus, in the presence of 10 mol% $\text{Fe}(\text{NO}_3)_3$, 2 equiv. of *tert*-butylhydroperoxide (TBHP) as the oxidant, 0.2 mmol of **1a** reacted with 0.4 mmol of **3-2a** in acetonitrile upon blue light irradiation

(using two 24-watt LED lamps, 450-460 nm) at room temperature for 12 h, and the corresponding benzo[*b*]phosphole oxide product **3-3a** was obtained in 40% isolated yield. (Table 3-1, entry 1)

Table 3-1. Optimization of the light driven iron-catalyzed annulation of diphenylacetylene **3-2a** with diphenylphosphine oxide **3-1a**.

$$\text{HPPPh}_2 + \text{Ph-C}\equiv\text{C-Ph} \xrightarrow[\text{blue-LED 24 W, Ar, 12 h}]{[\text{Fe}] 10 \text{ mol\%}} \text{3-3a}$$

Entry	[Fe]	Oxidant	light	Solvent	3-3a Yield(%)
1	Fe(NO ₃) ₃	TBHP	Blue-LED	CH ₃ CN	40
2	FeBr ₃	TBHP	Blue-LED	CH ₃ CN	-
3	FeF ₃	TBHP	Blue-LED	CH ₃ CN	6
4	Fe(OTf) ₂	TBHP	Blue-LED	CH ₃ CN	-(a)
5	FeCl ₃	TBHP	Blue-LED	CH ₃ CN	-(b)
6	FeSO ₄	TBHP	Blue-LED	CH ₃ CN	12 ^(c)
7	Fe(NO ₃) ₃	TBHP	Blue-LED	toluene	30
8	Fe(NO ₃) ₃	TBHP	Blue-LED	1,4-dioxane	54
9	Fe(NO ₃) ₃	TBHP	Blue-LED	1-Pentanol	50
10	Fe(NO ₃) ₃	TBHP	Blue-LED	MeOH	73
11	Fe(NO ₃) ₃	TBHP	white	MeOH	53
12	Fe(NO ₃) ₃	TBHP	No light	MeOH	2
13	Fe(NO ₃) ₃	-	Blue-LED	MeOH	-
14	-	TBHP	Blue-LED	MeOH	-
15	-	-	Blue-LED	MeOH	-

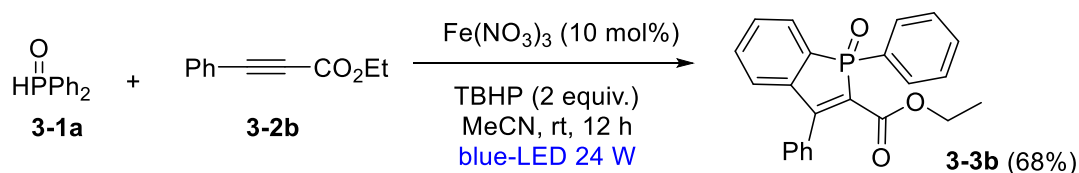
Reaction conditions: **3-1a** (0.2 mmol), **3-2a** (0.4 mmol), catalyst (10 mol%), oxidant (2.0 equiv), solvent (1.0 mL), 2 blue-LEDs 24 W (450-460 nm), r.t., 12 h under argon. Isolated yields after purification by flash chromatography on silica. (a) A by-product was observed in 40% yield and was identified as 9-phenyltribenzo[*b, e, g*]phosphindole 9-oxide **3-4a**. (b) **3-4a** was obtained in 22% yield. (c) > 5% of **3-4a** was observed as a by-product.

Other iron salts such as FeBr₃, FeF₃, FeCl₃, FeSO₄ and Fe(OTf)₂ were then evaluated under similar conditions, but they did not show activity, except with FeF₃ and Fe(SO₄) which permitted to obtain 7% and 14% of **3-3a**, respectively. (Entries 2-6) It should be underlined that the reaction with Fe(OTf)₂ and FeCl₃ led to a by-product was obtained in a in 45 and 22% yields, respectively and was identified as 9-phenyltribenzo-*[b,e,g]*phosphindole 9-oxide **3-4a**.

The nature of the solvent was then evaluated, and among the solvent tested (acetonitrile, 1,4-dioxane, toluene, 1-pentanol), methanol exhibited the best efficiency with 73% of **3-3a** obtained. (Entries 1, 7-9 vs 10)

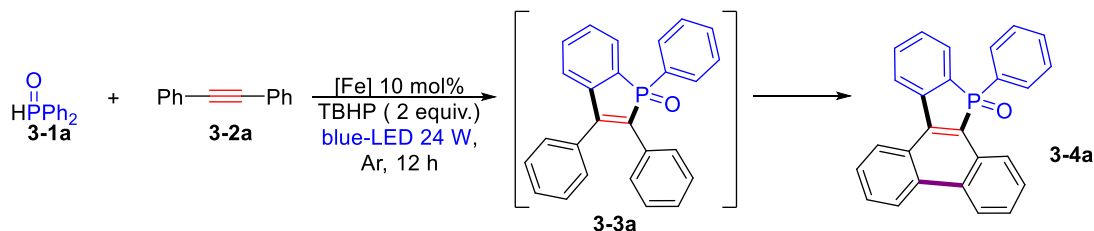
The nature of the light has also a great influence on the efficiency of the transformation. Indeed, switching the irradiation source to white light reduced the yield but did not inhibit the reactivity by contrast with the reaction conducted in dark. (53% vs 73%, Entries 11 vs 10 and 12) Control experiments showed that in the absence of catalyst, and of TBHP oxidant, no reaction took place. (Entries 12-15) Additionally, when the reaction was performed under air instead of under argon, only trace amount of product **3-3a** were detected.

In summary of this optimization, the best efficiency obtained for the reaction of diphenylphosphine oxide **3-1a** with diphenylacetylene **3-2a** was performing the transformation with 10 mol% of Fe(NO₃)₃ as catalyst, 2 equiv. of TBHP (*tert*-Butyl hydroperoxide) as the oxidant under blue light irradiation in CH₃CN at ambient conditions for 12 h which permitted to obtained the expected benzo[*b*]phosphole oxide **3-3a** in 73% yield. We thus started to extend the scope of this transformation performing the reaction of diphenylphosphine oxide **3-1a** with ethyl 3-phenylprop-2-ynoate **3-2b** under optimized conditions, and the ethyl 1,3-diphenylphosphindole-2-carboxylate 1-oxide **3-3b** was obtained in 68% isolated yield. (Scheme 3-3)



Scheme 3-3. Preliminary scope with ethyl 3-phenylprop-2-ynoate.

Of important interest, when evaluating the activity of Fe(OTf)₂, FeCl₃ and Fe(SO₄) for the formation of **3-3a** from **1a** and **3-2a**, (Table 3-1, entries 4-6), no trace of product **3-3a** was obtained, but the 9-phenyltribenzo[*b,e,g*]phosphindole 9-oxide **3-4a** was isolated in >5-40% yields and characterized. **3-4a** seems to result from the intramolecular C-H bond coupling reaction of **3-3a**. (Scheme 3-4)



Scheme 3-4. Iron-catalyzed tandem oxidative C-H/P-H then C-H C-H functionalization leading to 9-phenyltribenzo[*b,e,g*]phosphindole 9-oxide **3-4a**.

Noticeably, crystals suitable for X-ray analysis were grown by diffusion of petroleum ether into a solution of **3-4a** in CH₂Cl₂. The molecular structure of **3-4a** is depicted in Figure 3-2. First of all, it demonstrated the formation of benzo[*b*]phosphindole motif, and additionally, the formation of the C-C bond (herein C13-C14) between the two phenyls located on position C2 and C3 of the benzo[*b*]phosphindole (herein numbering C7 and C20) via two C-H bond activation.

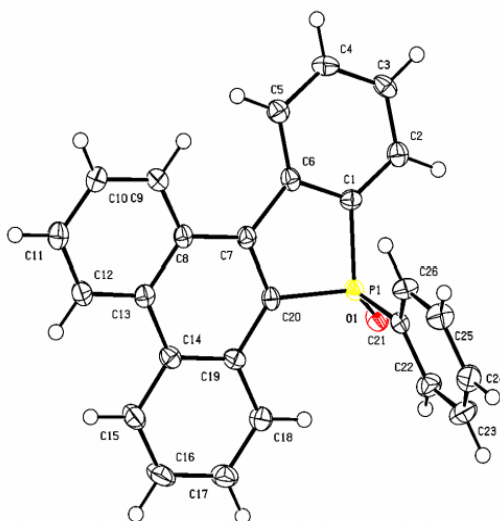


Figure 3-2. Molecular structure of 9-phenyltribenzo[*b,e,g*]phosphindole 9-oxide **3-4a**. Thermal ellipsoids correspond to 50% probability.

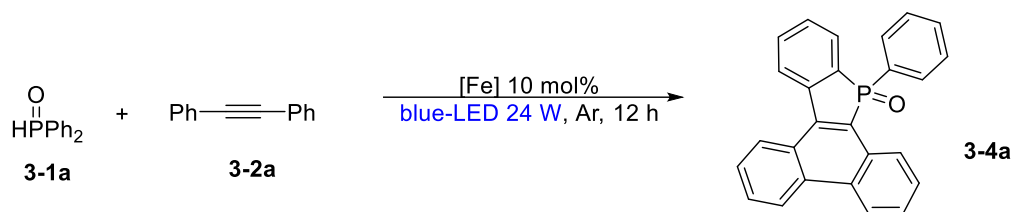
Based on these promising results, we then decided to evaluate the parameters of the reaction in order to switch the chemoselectivity of the reaction of diphenylphosphine oxide **3-1a** with diphenylacetylene **3-2a** towards the formation of 9-phenyltribenzo[*b,e,g*]phosphindole 9-oxide **3-4a**. (Table 3-2)

Among the 3 tested salts, Fe(OTf)₂, FeCl₃ and FeSO₄ (5 mol%), for the reaction of 0.2 mmol of **3-1a** with 0.4 mmol of **3-2a** in the presence of 2 equiv. of TBHP in acetonitrile upon blue light irradiation at room temperature for 12 h, Fe(OTf)₂ exhibited the highest catalytic activity, **3-4a** being obtained in 40% yield. (Table 3-2, entries 1-3) We then evaluated the effect of solvents on the efficiency of the transformation. In non-protonic chlorinated solvents such as dichloromethane and 1,2-dichloroethane (1,2-DCE), the formation of **3-4a** was not favored with a maximum of 22% yield in CH₂Cl₂. (Entries 4 and 5) Conducting the reaction in 1,4-dioxane led to a better efficiency and 54% of **3-4a**. (Entry 6) However, protic solvents such as 2,2,2-trifluoromethanol (TFE) and acetic acid were found to favor the reaction. (Entries 7 and 8) Especially when acetic acid was used as the solvent, the product **3-4a** can be isolated in 70% yield.

Replacing *tert*-Butyl hydroperoxide (TBHP) to other peroxides such as dicumyl peroxide, cumyl hydroperoxide and di-*tert*-butyl peroxide (DTBP) didn't favor the efficiency of the reaction (up to 27% yield, entries 9-11).

In this tandem catalytic process, the nature of the light is also crucial. When activating the reaction with white light (24W bulk lamp) in acetic acid, only trace amount of **3-4a** was detected. Noticeably, in dark, no reaction took place. (Entries 12 and 13)

Table 3-2. Optimization of the light driven iron-catalyzed tandem C-P/C-H and C-H/C-H annulation.



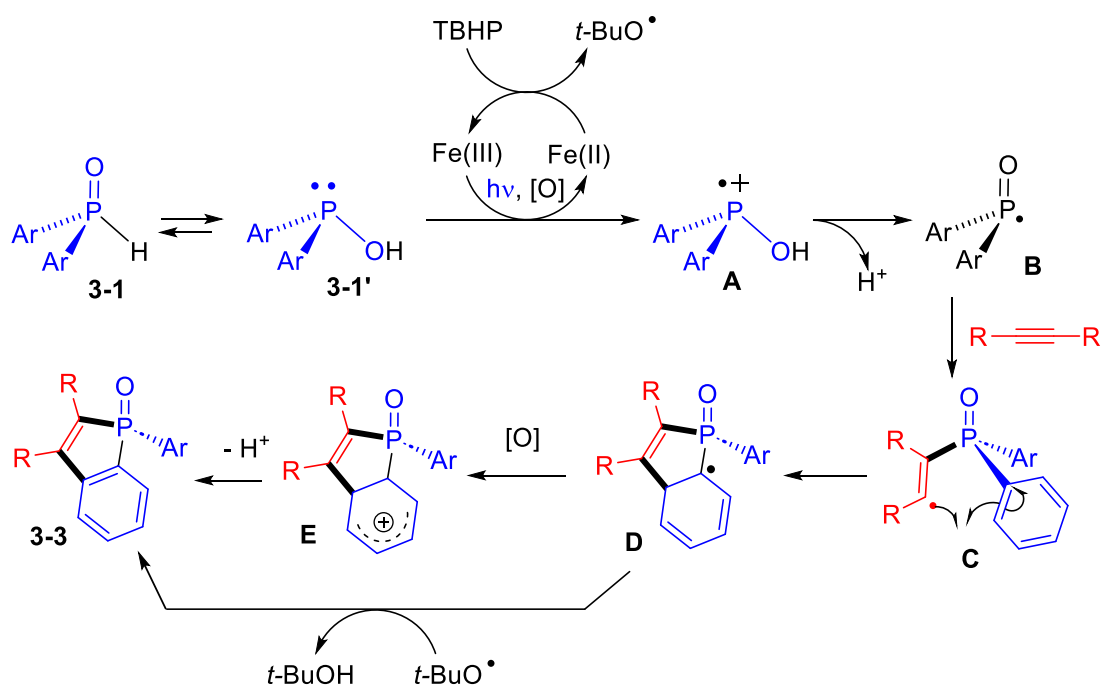
Entry	[Fe](10 mol%)	Oxidant	light	Solvent	3-4a Yield(%)
1	Fe(OTf) ₂	TBHP	Blue-LED	CH ₃ CN	40
2	FeCl ₃	TBHP	Blue-LED	CH ₃ CN	22
3	FeSO ₄	TBHP	Blue-LED	CH ₃ CN	Trace ^(a)
4	Fe(OTf) ₂	TBHP	Blue-LED	CH ₂ Cl ₂	26
5	Fe(OTf) ₂	TBHP	Blue-LED	1,2-DCE	-
6	Fe(OTf) ₂	TBHP	Blue-LED	Dioxane	54
7	Fe(OTf) ₂	TBHP	Blue-LED	TFE	61
8	Fe(OTf) ₂	TBHP	Blue-LED	AcOH	70
9	Fe(OTf) ₂	Dicumyl peroxide	Blue-LED	AcOH	trace
10	Fe(OTf) ₂	Cumyl Hydroperoxide	Blue-LED	AcOH	27
11	Fe(OTf) ₂	DTBP	Blue-LED	AcOH	20
12	Fe(OTf) ₂	TBHP	white	AcOH	trace
13	Fe(OTf) ₂	TBHP	No light	AcOH	-

Reaction conditions: **3-1a** (0.2 mmol), **3-2a** (0.4 mmol), [Fe] (10 mmol%), oxidant (2.0 equiv), solvent (1.0 mL), 2 blue-LEDs 24 W (450-460 nm), r.t., 12 h under Argon. Isolated yields. (a) 12% of **3-3a** was also obtained.

3.3. Mechanism discussion

Even if we have not studied yet in detail the mechanism of these two transformations, based on our previous contribution on iron-catalyzed oxyphosphination of styrenes and on literature reports, we proposed the following mechanism proposals.

For the formation of the benzo[*b*]phosphoindole motif, it was shown that the reaction worked efficiently under blue light irradiation, but also moderately under white light illumination. By contrast, no reaction took place in dark. Thus, in an initial step, the secondary phosphine oxide **3-1** is oxidized by iron Fe(III) salt to phosphinoyl radical **B**^[25] via a blue light promoted oxidative process catalyzed by iron^[26] species. The obtained Fe(II) can be re-oxidized in Fe(III) thanks to TBHP as demonstrated by Barton.^[27] (Scheme 3-5)

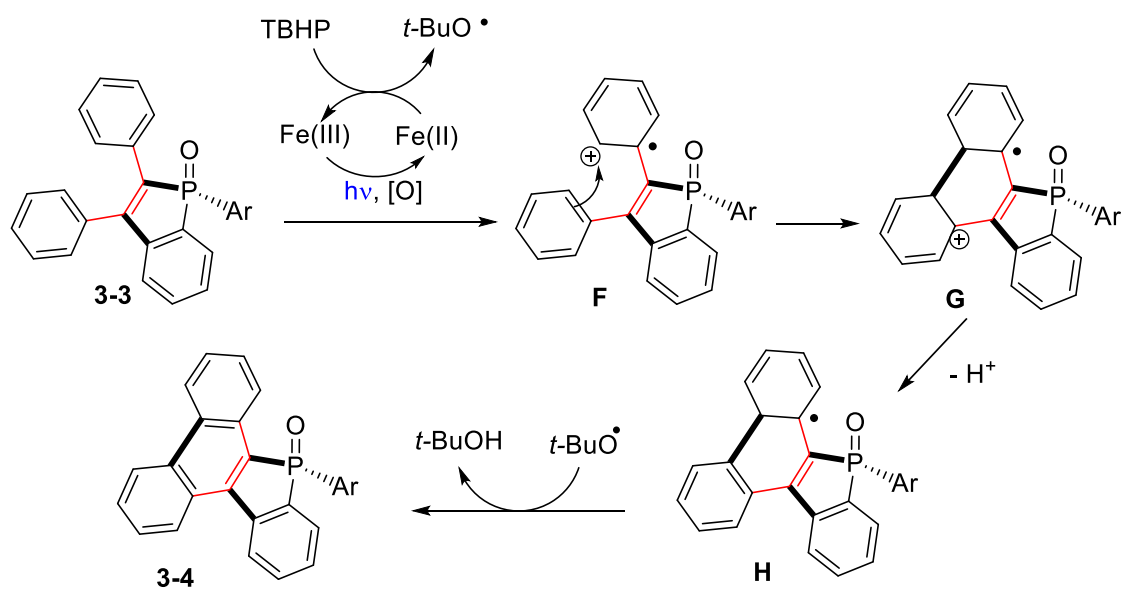


Scheme 3-5. Proposed mechanism for the formation of benzo[*b*]phosphoindole **3-3**.

This radical **B** then reacted with internal alkynes leading to the corresponding alkenyl radical **C** which then attacks the aromatic ring linked to the phosphine oxide moiety to generate the cyclohexadienyl radical **D**. As the reaction was conducted with two equivalents of TBHP, a subsequent oxidation of the radical **D** can lead to Wheland type species **E** which finally gave the expected benzo[*b*]phosphoindole **3-3** by loss of

proton.^[22,28] Alternatively, the generated *t*-BuO[•] radical generated during the formation of the phosphinoyl radical **B**, can abstract one H to lead to **3-3**. As no β-ketophosphine was observed seems to highlight that the intramolecular attack **C** to **D** is a faster step than the intermolecular reaction of **C** with the radical *t*-BuOO[•] which can be produced from Fe(III) and TBHP.^[27]

The Csp²-Csp² bond formation between two aromatic rings was already described at iron using oxidants in dehydrogenative cross-coupling reactions.^[29] Notably, Q. Wang described the FeCl₃-catalyzed intramolecular dehydrogenative cross-coupling of 1,2-diarylethene derivatives in the presence of TBHP leading to phenanthrenes.^[30] Based on these reports, a plausible mechanism is proposed in Scheme 3-6. In a first step, thanks to the combination of Fe salt, TBHP and blue light, a radical cationic species **F** (is generated and underwent an electrophilic attack to another phenyl ring to form a Csp²-Csp² bond. Finally, biaryl moiety is generated after a H[•] abstraction by the *t*-BuO[•] radical.



Scheme 3-6. Proposed mechanism for the formation of 9-phenyltribenzo[*b,e,g*]phosphindole 9-oxide **3-4** from benzo[*b*]phosphindole **3-3**.

In the state, due to the early advancement of the development of this reaction, we have no experimental evidences of both proposed mechanism; except that blue light

irradiation is crucial for the success of the reaction. Several experiments will be conducted to gain information:

- (i) the use of deuterated labeled diphenylphosphine oxide $\text{Ph}_2\text{P}(\text{O})\text{D}$, in order to see if there is incorporated deuterium in **3-3** and **3-4**;
- (ii) the use of radical scavengers [such as TEMPO (2,2,6,6-tetramethyl-1-piperidinyloxy), BHT (2,6-di-*tert*-butyl-4-methylphenol) or galvinoxyl] to confirm the proposed radical pathways in Schemes 3-5 and 3-6;
- (iii) try to isolate TEMPO adducts to identify some mechanism intermediates such as $\text{Ph}_2\text{P}(\text{O})\text{-TEMPO}$;
- (iv) perform light on/off experiment to identify if chain propagation can be involved in the reaction pathway.

3.4. First conclusion and short-term perspectives

In conclusion, we have established the feasibility of a blue-light driven iron catalyzed-controlled preparations of benzo[*b*]phosphole oxides and 9-phenyltribenzo[*b,e,g*]phosphindole 9-oxides by reaction of secondary phosphine oxides and internal alkynes in one pot sequences. $\text{Fe}(\text{NO}_3)_3$ catalyst favors the formation of benzo[*b*]phosphole oxides via intermolecular C-H/P-H annulation, while $\text{Fe}(\text{OTf})_2$ led to the extra intramolecular C-H/C-H annulation in a tandem fashion.

The short term target will be to generalize these two transformation and prepare a variety of benzo[*b*]phosphole oxides and 9-phenyltribenzo[*b,e,g*]phosphindole 9-oxides. Additionally, several experiments have to be done in order to gain insights to support the proposed mechanism.

3.4. References

- [1] F. E. Dayan, *Plants* **2019**, *8*, 341–359.
- [2] S. Demkowicz, J. Rachon, M. Daśkoa, W. Kozak, *RSC Adv.* **2016**, *6*, 7101–7112.
- [3] V. D. Romanenko, V. P. Kukhar, *Chem. Rev.* **2006**, *106*, 3868–3935.
- [4] F. Orsini, G. Sello, M. Sisti, *Curr. Med. Chem.* **2010**, *17*, 264–289.

- [5] Y. Matano, H. Imahori, *Org. Biomol. Chem.* **2009**, *7*, 1258–1271.
- [6] Y. Matano, A. Saito, T. Fukushima, Y. Tokudome, F. Suzuki, D. Sakamaki, H. Kaji, A. Ito, K. Tanaka, H. Imahori, *Angew. Chem. Int. Ed.* **2011**, *50*, 8016–8020.
- [7] Y. Ren, W. H. Kan, M. A. Henderson, P. G. Bomben, C. P. Berlinguette, V. Thangadurai, T. Baumgartner, *J. Am. Chem. Soc.* **2011**, *133*, 17014–17026.
- [8] Y. Ren, T. Baumgartner, *J. Am. Chem. Soc.* **2011**, *133*, 1328–1340.
- [9] For a review on benzo[b]phosphole derivatives, see: B. Wu, N. Yoshikai, *Org. Biomol. Chem.* **2016**, *14*, 5402–5416.
- [10] J. G. Cordaro, D. Stein, H. Grützmaier, *J. Am. Chem. Soc.* **2006**, *128*, 14962–14971.
- [11] H. Tsuji, K. Sato, L. Ilies, Y. Itoh, Y. Sato, E. Nakamura, *Org. Lett.*, **2008**, *10*, 2263–2265.
- [12] T. Sanji, K. Shiraishi, T. Kashiwabara, M. Tanaka, *Org. Lett.*, **2008**, *10*, 2689–2692.
- [13] A. Fukazawa, M. Hara, T. Okamoto, E.-C. Son, C. Xu, K. Tamao, S. Yamaguchi, *Org. Lett.*, **2008**, *10*, 913–916.
- [14] A. Fukazawa, H. Yamada, S. Yamaguchi, *Angew. Chem., Int. Ed.*, **2008**, *47*, 5582–5585.
- [15] T. Sanji, K. Shiraishi, T. Kashiwabara, M. Tanaka, *Chem. Asian J.* **2009**, *4*, 1729–1740
- [16] (a) M. Ogasawara, S. Arae, S. Watanabe, V. Subbarayan, H. Sato, T. Takahashi, *Organometallics* **2013**, *32*, 4997–5000; (b) X. Yan, C. Xi, *Acc. Chem. Res.* **2015**, *48*, 935–946.
- [17] Y. Zhou, Z. Gan, B. Su, J. L. Z. Duan, F. Mathey, *Org. Lett.* **2015**, *17*, 5722–5724.
- [18] B. Wu, M. Santra, N. Yoshikai, *Angew. Chem., Int. Ed.* **2014**, *53*, 7543–7546.
- [19] B. Wu, R. Chopra, N. Yoshikai, *Org. Lett.* **2015**, *17*, 5666–5669.
- [20] P. Zhang, Y. Gao, L. Zhang, Z. Li, Y. Liu, G. Tang, Y. Zhao, *Adv. Synth. Catal.* **2016**, *358*, 138–142.
- [21] One example of synthesis of was reported in this contribution using 20 mol% of Cu(OTf)₂ and 4 equiv. of Mn(OAc)₂: Z. Tao, C. Li, J. Li, A. Shoberu, W. Zhang, J. Zou, *Org. Lett.* **2021**, *23*, 4342–4347.
- [22] O. Berger, J. Montchamp, *J. Org. Chem.* **2019**, *84*, 9239–9256.
- [23] Y. Chen, W. Duan, *J. Am. Chem. Soc.* **2013**, *135*, 16754–16757.
- [24] W. Liu, T. Lei, S. Zhou, X. Yang, J. Li, B. Chen, J. Sivaguru, C. Tung, L. Wu, *J. Am. Chem. Soc.* **2019**, *141*, 13941–13947.
- [25] (a) D. Leca, L. Fensterbank, E. Lacôte, M. Malacria, *Chem. Soc. Rev.* **2005**, *34*, 858–865; (b) W.-J. Yoo, S. Kobayashi, *Green Chem.* **2013**, *15*, 1844–1848; (c) K. Luo, W.-C. Yang, L. Wu, *Asian J. Org. Chem.* **2016**, 350–367; (d) P. Peng, Q. Lu, L. Peng, C. Liu, G. Wang, A. Lei, *Chem. Commun.* **2016**, *52*, 12338–12341; (e) M.-J. Bu, G.-P. Lu, C. Cai, *Catal. Sci. Technol.* **2016**, *6*, 413–416; (f) H.-F. Qian, C.-K. Li, Z.-K. Tao, A. Shoberu, K.-P. Zou *Org. Lett.* **2018**, *18*, 5947–5951; (g) Y. Shi, R. Chen, K. Guo, F. Meng, S. Cao, C. Gu, Y. Zhu *Tetrahedron Lett.* **2018**, *59*, 2062–2065; **2005**, *34*, 858–865; (h) B. Liu, Q. Song, Z. Liu, Z. Wang, *Adv. Synth. Catal.* **2021**, *363*, 3214–3219.
- [26] For representative examples of blue light promoted oxidative process catalyzed by iron involving secondary phosphorus oxide derivatives, see: (a) M. Zhou, M. Chen, Y. Zhou, K. Yang, J. Su, J. Du, Q. Song, *Org. Lett.* **2015**, *17*, 1786–1789; (b) Y. Zhou, M. Zhou, M. Chen, J. Su, J. Du, Q. Song, *RSC Adv.* **2015**, *5*, 103977–103981.
- [27] D. H. R. Barton, V. N. Le Gloahec, H. Patin, F. Launay, *New J. Chem.* **1998**, 559–563.

- [28] For an example of reaction of phosphinoyl radical on alkynes leading to benzo[b]phosphoindole derivatives, see: V. Quint, F. Morlet-Savary, J.-F. Lohier, J. Lalevée, A.-C. Gaumont, S. Lakhdar, *J. Am. Chem. Soc.* **2016**, *138*, 7436–7441.
- [29] For representative examples of iron-catalyzed dehydrogenative cross coupling Csp²-Csp² reactions, see: (a) M. Chandrasekharan, B. Chiranjeevi, K. S. Gupta, B. Sridhar, *J. Org. Chem.* **2011**, *76*, 10229–10235; (b) B. Chiranjeevi, G. Koyyada, S. Prabhus-Reenivasan, V. Kumar, P. Sujitha, C. G. Kumar, B. Sridhar, S. Shaik, M. Chandrasekharam, *RSC Adv.* **2013**, *3*, 16475–16485; (c) E. Gaster, Y. Vainer, A. Regev, S. Narute, K. Sudheendran, A. Werbeloff, H. Shalit, D. Pappo, *Angew. Chem. Int. Ed.* **2015**, *54*, 4198–4202; (d) V. Vershinin, A. Dyadyuk, D. Pappo, *Tetrahedron* **2017**, *73*, 3660–3668; (e) H. Shalit, A. Libman, D. Pappo, *J. Am. Chem. Soc.* **2017**, *139*, 13404–13413; (f) H. Shalit, A. Dyadyuk, D. Pappo, *J. Org. Chem.* **2019**, *84*, 1677–1686. (g) H. Egami, T. Katsuki, *J. Am. Chem. Soc.* **2009**, *131*, 6082–6083; (h) H. Egami, K. Matsumoto, T. Oguma, T. Kunisu, T. Katsuki, *J. Am. Chem. Soc.* **2010**, *132*, 13633–13635. (i) T. Niu, Y. Zhang, *Tetrahedron Lett.* **2010**, *51*, 6847–6851; (j) K. Matsumoto, M. Yoshida, M. Shindo, *Angew. Chem. Int. Ed.* **2016**, *55*, 5272–5276; (k) R. F. Fritsche, G. Theumer, O. Kataeva, H.-J. Knölker, *Angew. Chem. Int. Ed.* **2017**, *56*, 549–553; (l) C. Brütting, R. F. Fritsche, S. K. Kutz, C. Börger, A. W. Schmidt, O. Kataeva, H.-J. Knölker, *Chem. Eur. J.* **2017**, *23*, 458–470.
- [30] K. Wang, M. Lü, A. Yu, X. Zhu, Q. Wang, *J. Org. Chem.* **2009**, *74*, 935–938.

Chapter 4 - Experimental Details and Characterization Data

4.1. General Remarks

All reagents were obtained from commercial sources and used as received. All reactions were carried out with dried glassware using standard Schlenk techniques under an inert atmosphere of dry argon. Technical grade petroleum ether and ethyl acetate were used for column chromatography. Analytical TLC was performed on Merck 60F254 silica gel plates (0.25 mm thickness). Column chromatography was performed on Kieselgel silica gel (mesh size 40-63 μm , 60 \AA).

^1H NMR spectra were recorded in CDCl_3 at ambient temperature on Bruker AVANCE 400 spectrometers at 400 MHz or 500 MHz, using the solvent as the internal standard (CDCl_3 7.26 ppm). ^{13}C NMR spectra were obtained at 101 MHz or 126 MHz, and referenced to the internal solvent signals (CDCl_3 , central peak is 77.00 ppm). ^{31}P NMR spectra were obtained at 162 MHz, and ^{19}F NMR spectra were obtained at 376 MHz in CDCl_3 . Chemical shift (δ) and coupling constants (J) are given in ppm and in Hz respectively. The peak patterns are indicated as follows: (s, singlet; d, doublet; t, triplet; q, quartet; m, multiplet, and br. for broad).

HR-MS spectra were carried out by using a time flight Agilent 6510 [Agilent Technologies Santa Clara (CA), USA] in an electrospray positive ionization mode at the CRMPO (Centre Régional de Mesures Physiques de l'Ouest, ScanMAT, UMS 2001 CNRS – Université de Rennes 1).

The X-ray Analysis were performed at The Centre de Diffractométrie X (CDFX) of the Institut des Sciences Chimiques de Rennes. The detailed crystallographic data and structure refinement parameters for these compounds are summarized in Table S2 contains the supplementary crystallographic data for the molecule 3-4a. These data can be obtained free of charge from The Cambridge Crystallographic Data Centre via www.ccdc.cam.ac.uk/data_request/cif.

UV-Vis spectra were performed using. UV/Vis absorption spectra were recorded with a V-770 spectrophotometer from Jasco company and quartz cuvettes of 1 cm path length.

Chapter 4.

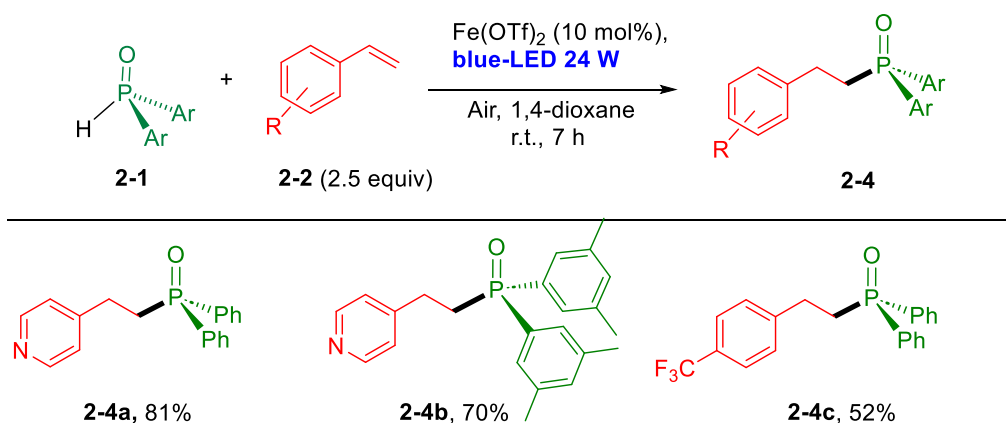
Experimental Details and Characterization Data

4.2. Supporting Information of Chapter 2

4.2.1. General procedure for blue-light driven iron-catalyzed C–P cross-coupling of styrenes with secondary phosphine oxides

In a Schlenk tube under air atmosphere, diphenylphosphine oxide **2-1a** (0.2 mmol), styrene **2-2a** (0.5 mmol), Fe(OTf)₂ (10 mol%), were dissolved in 0.5 mL of 1,4-dioxane and the resulting mixture was stirred at room temperature under blue light irradiation (2 × 24 W; λ = 450-460 nm) for 12 h. Thus, the crude reaction mixture was diluted with EtOAc (5 mL), filtered through a Celite pad, and then washed with 10 mL of CH₂Cl₂. The volatiles were then removed under reduced pressure, and the residue was subjected to silica gel column chromatography [eluting with petroleum ether (PE)/ethyl acetate (EA)] to afford the corresponding products **2-(3a-3t)**. It might be underline that even if in each reaction, the conversion was quite complete, it was observed in GC-MS of the crude mixtures, several unidentified peaks, which explained the moderate isolated yield obtained.

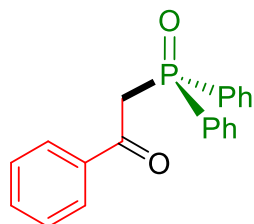
Using the same reactions conditions, with 4-vinylpyridine and 4-trifluoromethylstyrene, no trace of the product **2-3** was observed, but only the derivatives resulting of the classical anti-Markonikov hydrophosphinylation Ar-CH₂-CH₂-PPh₂(=O) **2-(4a-4c)** were obtained. (Scheme S2-1)



Scheme S2-1. Blue-light driven iron-catalyzed hydrophosphinylation of 4-vinylpyridine and 4-trifluoromethylstyrene. Fe(OTf)₂ (10 mol%), alkene (2.5 equiv.), secondary phosphine oxide (1 equiv.), 1,4-dioxane, 7 h at room temperature under blue light activation (2 × 24W-blue LED) and air. Isolated yields.

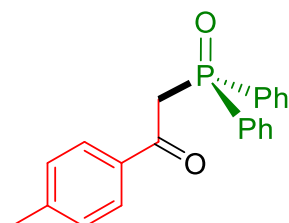
4.2.2. Characterization data of products 2-(3a-4c)

2-(Diphenylphosphoryl)-1-phenylethan-1-one **2-3a**



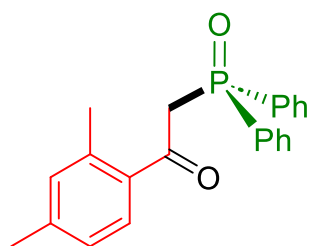
2-3a was obtained as a white solid (62 mg, 97%). ^1H NMR (400 MHz, CDCl_3) δ 8.04 – 7.96 (m, 2H), 7.81 (m, 4H), 7.56 – 7.39 (m, 9H), 4.14 (d, $J = 15.4$ Hz, 2H). $^{13}\text{C}\{^1\text{H}\}$ NMR (101 MHz, CDCl_3) δ 192.8 (d, $J = 5.0$ Hz), 137.0, 133.6, 132.1 (d, $J = 3.0$ Hz), 132.0 (d, $J = 104.0$ Hz), 131.1 (d, $J = 9.8$ Hz), 129.2, 128.6 (d, $J = 12.4$ Hz), 128.5, 43.3 (d, $J = 58.6$ Hz). $^{31}\text{P}\{^1\text{H}\}$ NMR (162 MHz, CDCl_3) δ 27.0. Analytical data in accordance with the literature.^[1]

2-(Diphenylphosphoryl)-1-(*p*-tolyl)ethan-1-one **2-3b**



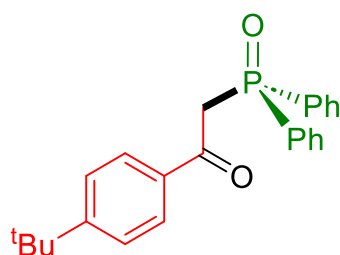
2-3b was obtained as a white solid (45 mg, 68%). ^1H NMR (400 MHz, CDCl_3) δ 7.90 – 7.74 (m, 6H), 7.52 – 7.40 (m, 6H), 7.19 (d, $J = 8.0$ Hz, 2H), 4.10 (d, $J = 15.3$ Hz, 2H), 2.36 (s, 3H). $^{13}\text{C}\{^1\text{H}\}$ NMR (101 MHz, CDCl_3) δ 192.2 (d, $J = 6.0$ Hz), 144.5, 134.5, 132.1 (d, $J = 104.0$ Hz), 132.0 (d, $J = 3.0$ Hz), 131.0 (d, $J = 9.7$ Hz), 129.3, 129.1, 128.6 (d, $J = 13.1$ Hz), 43.1 (d, $J = 58.6$ Hz), 21.6. $^{31}\text{P}\{^1\text{H}\}$ NMR (162 MHz, CDCl_3) δ 26.9. Analytical data in accordance with the literature.^[1]

1-(2,4-Dimethylphenyl)-2-(diphenylphosphoryl)ethan-1-one **2-3c**



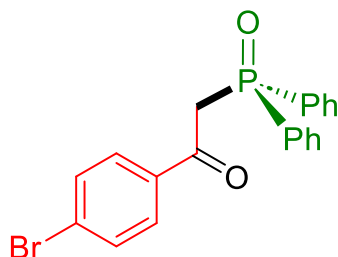
2-3c was obtained as a white solid (34 mg, 49%). ^1H NMR (400 MHz, CDCl_3) δ 7.84 – 7.73 (m, 5H), 7.54 – 7.42 (m, 6H), 7.05 (d, $J = 7.2$ Hz, 1H), 6.96 (s, 1H), 4.10 (d, $J = 15.1$ Hz, 2H), 2.32 (s, 3H), 2.28 (s, 3H). $^{13}\text{C}\{^1\text{H}\}$ NMR (101 MHz, CDCl_3) δ 195.0 (d, $J = 6.1$ Hz), 142.7, 139.5, 134.6, 132.7, 132.3 (d, $J = 104$ Hz), 132.0 (d, $J = 2.8$ Hz), 131.1 (d, $J = 9.8$ Hz), 131.0, 128.5 (d, $J = 12.1$ Hz), 126.4, 41.5 (d, $J = 58.6$ Hz), 21.4, 21.3. $^{31}\text{P}\{^1\text{H}\}$ NMR (162 MHz, CDCl_3) δ 27.1. HRMS (ESI): m/z $[\text{M}+\text{H}]^+$ calculated for $\text{C}_{22}\text{H}_{22}\text{O}_2\text{P}$: 349.1352, found: 349.1353.

1-(4-(*tert*-Butyl)phenyl)-2-(diphenylphosphoryl)ethan-1-one **2-3d**



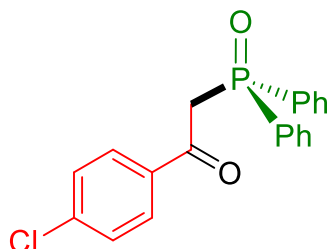
2-3d was obtained as a white solid (61 mg, 81%). ^1H NMR (400 MHz, CDCl_3) δ 7.96 – 7.88 (m, 2H), 7.84 – 7.75 (m, 4H), 7.52 – 7.40 (m, 8H), 4.11 (d, $J = 15.3$ Hz, 2H), 1.30 (s, 9H). $^{13}\text{C}\{^1\text{H}\}$ NMR (101 MHz, CDCl_3) δ 192.2 (d, $J = 6.1$ Hz), 157.3, 134.4, 132.0 (d, $J = 103.6$ Hz), 131.9 (d, $J = 2.8$ Hz), 131.1 (d, $J = 10.1$ Hz), 129.2, 128.5 (d, $J = 12.1$ Hz), 125.4, 43.1 (d, $J = 56.6$ Hz), 35.0, 30.9. $^{31}\text{P}\{^1\text{H}\}$ NMR (162 MHz, CDCl_3) δ 27.1. Analytical data in accordance with the literature.^[2]

1-(4-Bromophenyl)-2-(diphenylphosphoryl)ethan-1-one **2-3e**



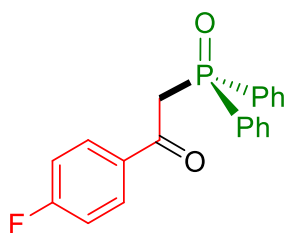
2-3e was obtained as a white solid (58 mg, 73%). ^1H NMR (400 MHz, CDCl_3) δ 7.90 – 7.84 (m, 2H), 7.83 – 7.74 (m, 4H), 7.57 – 7.43 (m, 8H), 4.09 (d, $J = 15.1$ Hz, 2H). $^{13}\text{C}\{^1\text{H}\}$ NMR (101 MHz, CDCl_3) δ 191.8 (d, $J_{\text{C-P}} = 6.1$ Hz), 135.7, 132.2 (d, $J_{\text{C-P}} = 2.8$ Hz), 131.8, 131.7 (d, $J_{\text{C-P}} = 104.0$ Hz), 131.0 (d, $J_{\text{C-P}} = 9.8$ Hz), 130.8, 129.1, 128.7 (d, $J_{\text{C-P}} = 12.3$ Hz), 43.6 (d, $J_{\text{C-P}} = 57.6$ Hz). $^{31}\text{P}\{^1\text{H}\}$ NMR (162 MHz, CDCl_3) δ 26.7. Analytical data in accordance with the literature.^[2]

1-(4-Chlorophenyl)-2-(diphenylphosphoryl)ethan-1-one **2-3f**



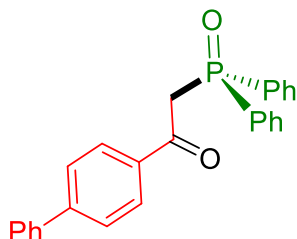
2-3f was obtained as a white solid (52 mg, 73%). ^1H NMR (400 MHz, CDCl_3) δ 8.00 – 7.90 (m, 2H), 7.83 – 7.73 (m, 4H), 7.55 – 7.43 (m, 6H), 7.38 (d, $J = 8.4$ Hz, 2H), 4.10 (d, $J = 15.2$ Hz, 2H). $^{13}\text{C}\{^1\text{H}\}$ NMR (101 MHz, CDCl_3) δ 192.0 (d, $J = 6.1$ Hz), 140.2, 135.3, 132.2 (d, $J = 3.0$ Hz), 131.7 (d, $J = 104.0$ Hz), 131.1 (d, $J = 9.8$ Hz), 130.8, 128.8, 128.7 (d, $J = 12.3$ Hz), 43.6 (d, $J = 56.6$ Hz). $^{31}\text{P}\{^1\text{H}\}$ NMR (162 MHz, CDCl_3) δ 26.9. Analytical data in accordance with the literature.^[2]

2-(Diphenylphosphoryl)-1-(4-fluorophenyl)ethan-1-one **2-3g**



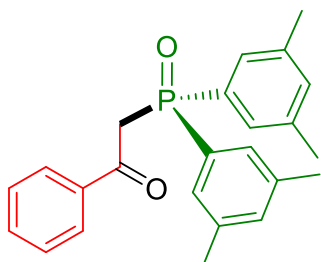
2-3g was obtained as a white solid (47 mg, 70%). ^1H NMR (400 MHz, CDCl_3) δ 8.09 – 7.99 (m, 2H), 7.85 – 7.74 (m, 4H), 7.55 – 7.43 (m, 6H), 7.08 (m, 2H), 4.10 (d, $J = 15.3$ Hz, 2H). $^{13}\text{C}\{^1\text{H}\}$ NMR (101 MHz, CDCl_3) δ 191.2 (d, $J = 6.1$ Hz), 166.0 (d, $J = 257.0$ Hz), 133.4 (d, $J = 2.0$ Hz), 132.2 (d, $J = 2.8$ Hz), 132.1 (d, $J = 9.7$ Hz), 131.8 (d, $J = 104.0$ Hz), 131.0 (d, $J = 9.7$ Hz), 128.6 (d, $J = 12.1$ Hz), 115.6 (d, $J = 22.2$ Hz), 43.6 (d, $J = 57.6$ Hz). $^{31}\text{P}\{^1\text{H}\}$ NMR (162 MHz, CDCl_3) δ 26.8. ^{19}F NMR (376 MHz, CDCl_3) δ -104.1. Analytical data in accordance with the literature.^[3]

1-([1,1'-Biphenyl]-4-yl)-2-(diphenylphosphoryl)ethan-1-one **2-3h**



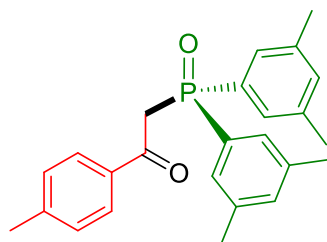
2-3h was obtained as a white solid (35 mg, 45%). ^1H NMR (400 MHz, CDCl_3) δ 8.07 (d, $J = 8.4$ Hz, 2H), 7.90 – 7.77 (m, 4H), 7.65 – 7.58 (m, 4H), 7.55 – 7.51 (m, 2H), 7.49 – 7.44 (m, 5H), 7.43 – 7.36 (m, 2H), 4.18 (d, $J = 15.4$ Hz, 2H). $^{13}\text{C}\{^1\text{H}\}$ NMR (101 MHz, CDCl_3) δ 192.3 (d, $J = 5.5$ Hz), 146.2, 139.8, 135.7, 132.2 (d, $J = 2.8$ Hz), 132.0 (d, $J = 104.2$ Hz), 131.2 (d, $J = 9.8$ Hz), 129.9, 128.9, 128.6 (d, $J = 12.1$ Hz), 128.3, 127.3, 127.2, 43.5 (d, $J = 58.6$ Hz). $^{31}\text{P}\{^1\text{H}\}$ NMR (162 MHz, CDCl_3) δ 27.2. Analytical data in accordance with the literature.^[3]

2-(bis(3,5-Dimethylphenyl)phosphoryl)-1-phenylethan-1-one **2-3i**



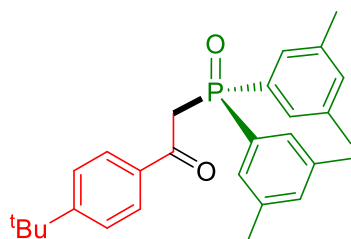
2-3i was obtained as a white solid (67 mg, 89%). ^1H NMR (400 MHz, CDCl_3) δ 8.00 – 7.95 (m, 2H), 7.53 – 7.48 (m, 1H), 7.42 – 7.37 (m, 6H), 7.11 (s, 2H), 4.08 (d, $J = 15.3$ Hz, 2H), 2.31 (s, 12H). $^{13}\text{C}\{^1\text{H}\}$ NMR (101 MHz, CDCl_3) δ 192.9 (d, $J = 5.1$ Hz), 138.3 (d, $J = 13.1$ Hz), 137.1, 133.7 (d, $J = 3.0$ Hz), 133.3, 131.8 (d, $J = 102.6$ Hz), 129.2, 128.6 (d, $J = 9.8$ Hz), 128.3, 43.4 (d, $J = 57.0$ Hz), 21.2. $^{31}\text{P}\{^1\text{H}\}$ NMR (162 MHz, CDCl_3) δ 27.30. Analytical data in accordance with the literature.^[1]

2-(bis(3,5-Dimethylphenyl)phosphoryl)-1-(*p*-tolyl)ethan-1-one **2-3j**



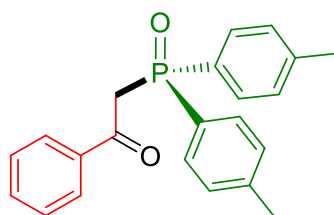
2-3j was obtained as a white solid (55 mg, 70%). ^1H NMR (400 MHz, CDCl_3) δ 7.93 – 7.82 (m, 2H), 7.38 (m, 4H), 7.20 (d, $J = 8.0$ Hz, 2H), 7.12 (s, 2H), 4.06 (d, $J = 15.3$ Hz, 2H), 2.38 (s, 3H), 2.31 (s, 12H). $^{13}\text{C}\{^1\text{H}\}$ NMR (101 MHz, CDCl_3) δ 192.5 (d, $J = 6.1$ Hz), 144.3, 138.2 (d, $J = 13.1$ Hz), 134.7, 133.7 (d, $J = 3.0$ Hz), 131.9 (d, $J = 103.0$ Hz), 129.4, 129.1, 128.6 (d, $J = 9.1$ Hz), 43.3 (d, $J = 57.6$ Hz), 21.6, 21.3. $^{31}\text{P}\{^1\text{H}\}$ NMR (162 MHz, CDCl_3) δ 27.4. HRMS (ESI): m/z $[\text{M}+\text{H}]^+$ calculated for $\text{C}_{25}\text{H}_{29}\text{O}_2\text{P}$: 391.1821, found: 391.1818.

2-(bis(3,5-Dimethylphenyl)phosphoryl)-1-(4-(*tert*-butyl)phenyl)ethan-1-one **2-3k**



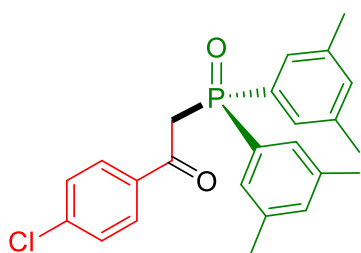
2-3k was obtained as a white solid (63 mg, 73%). ^1H NMR (400 MHz, CDCl_3) δ 7.95 – 7.86 (m, 2H), 7.43 – 7.39 (m, 4H), 7.37 (s, 2H), 7.10 (s, 2H), 4.07 (d, $J = 15.4$ Hz, 2H), 2.31 (s, 12H), 1.31 (s, 9H). $^{13}\text{C}\{^1\text{H}\}$ NMR (101 MHz, CDCl_3) δ 192.5 (d, $J = 6.1$ Hz), 157.1, 138.2 (d, $J = 13.1$ Hz), 134.6, 133.7, 133.0 (d, $J = 103.0$ Hz), 129.2, 128.6 (d, $J = 9.8$ Hz), 125.3, 43.2 (d, $J = 56.6$ Hz), 35.1, 31.0, 21.2. $^{31}\text{P}\{^1\text{H}\}$ NMR (162 MHz, CDCl_3) δ 27.6. HRMS (ESI): m/z $[\text{M}+\text{H}]^+$ calculated for $\text{C}_{28}\text{H}_{34}\text{O}_2\text{P}$: 433.2291, found: 433.2293.

2-(di-*p*-Tolylphosphoryl)-1-phenylethan-1-one **2-3l**



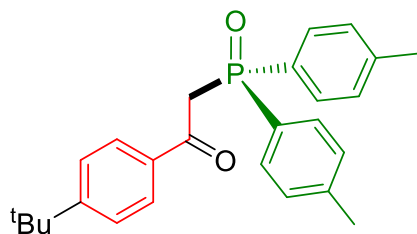
2-3l was obtained as a white solid (48 mg, 69%); white solid. ^1H NMR (400 MHz, CDCl_3) δ 8.04 – 7.89 (m, 2H), 7.67 (m, 4H), 7.55 – 7.50 (m, 1H), 7.40 (m, 2H), 7.24 (m, 4H), 4.10 (d, $J = 15.4$ Hz, 2H), 2.37 (s, 6H). $^{13}\text{C}\{^1\text{H}\}$ NMR (101 MHz, CDCl_3) δ 193.0 (d, $J = 5.1$ Hz), 142.6 (d, $J = 3.0$ Hz), 137.1, 133.4, 131.2 (d, $J = 11.1$ Hz), 129.3 (d, $J = 12.1$ Hz), 129.2, 128.8 (d, $J = 106.0$ Hz), 128.5, 43.6 (d, $J = 56.6$ Hz), 21.5. $^{31}\text{P}\{^1\text{H}\}$ NMR (162 MHz, CDCl_3) δ 27.6. Analytical data in accordance with the literature.^[1]

2-(bis(3,5-Dimethylphenyl)phosphoryl)-1-(4-chlorophenyl)ethan-1-one **2-3m**



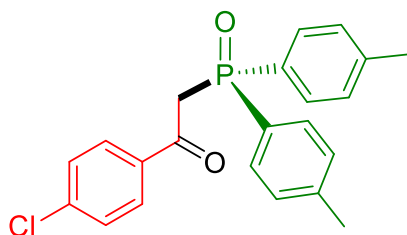
2-3m was obtained as a white solid (58 mg, 71%). ^1H NMR (400 MHz, CDCl_3) δ 7.97 – 7.91 (m, 2H), 7.40 – 7.34 (m, 6H), 7.12 (s, 2H), 4.04 (d, $J = 15.1$ Hz, 2H), 2.31 (s, 12H). $^{13}\text{C}\{^1\text{H}\}$ NMR (101 MHz, CDCl_3) δ 191.7 (d, $J = 6.1$ Hz), 139.9, 138.3 (d, $J = 13.1$ Hz), 135.4, 133.9 (d, $J = 3.0$ Hz), 131.6 (d, $J = 103.0$ Hz), 130.7, 128.6 (d, $J = 10.1$ Hz), 128.4, 43.7 (d, $J = 55.6$ Hz), 21.2. $^{31}\text{P}\{^1\text{H}\}$ NMR (162 MHz, CDCl_3) δ 27.1. HRMS (ESI): m/z $[\text{M}+\text{H}]^+$ calculated for $\text{C}_{24}\text{H}_{25}\text{O}_2\text{ClP}$: 411.1275, found: 411.1272.

1-(4-(*tert*-Butyl)phenyl)-2-(di-*p*-tolylphosphoryl)ethan-1-one **2-3n**



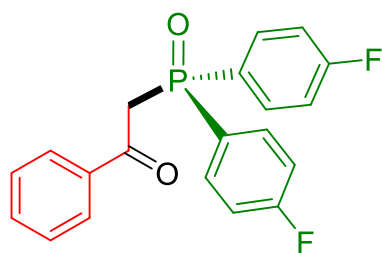
2-3n was obtained as a white solid (46 mg, 57%). ^1H NMR (400 MHz, CDCl_3) δ 7.95 – 7.89 (m, 2H), 7.70 – 7.63 (m, 4H), 7.43 – 7.38 (m, 2H), 7.24 (m, 4H), 4.07 (d, $J = 15.4$ Hz, 2H), 2.36 (s, 6H), 1.30 (s, 9H). $^{13}\text{C}\{^1\text{H}\}$ NMR (101 MHz, CDCl_3) δ 192.5 (d, $J = 6.1$ Hz), 157.2, 142.4 (d, $J = 3.0$ Hz), 134.5, 131.1 (d, $J = 10.1$ Hz), 129.2 (d, $J = 12.7$ Hz), 129.2, 128.9 (d, $J = 106.1$ Hz), 125.4, 43.4 (d, $J = 58.6$ Hz), 35.0, 31.0, 21.5. $^{31}\text{P}\{^1\text{H}\}$ NMR (162 MHz, CDCl_3) δ 27.5. HRMS (ESI): m/z $[\text{M}+\text{H}]^+$ calculated for $\text{C}_{26}\text{H}_{30}\text{O}_2\text{P}$: 405.1978, found: 405.1979.

1-(4-Chlorophenyl)-2-(di-*p*-tolylphosphoryl)ethan-1-one **2-3o**



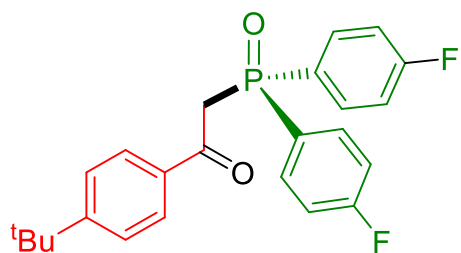
2-3o was obtained as a white solid (52 mg, 68%). ^1H NMR (400 MHz, CDCl_3) δ 7.99 – 7.94 (m, 2H), 7.69 – 7.61 (m, 4H), 7.41 – 7.36 (m, 2H), 7.29 – 7.23 (m, 4H), 4.05 (d, $J = 15.3$ Hz, 2H), 2.38 (s, 6H). $^{13}\text{C}\{^1\text{H}\}$ NMR (101 MHz, CDCl_3) δ 191.9 (d, $J = 5.1$ Hz), 142.8 (d, $J = 3.0$ Hz), 140.1, 135.4, 131.1 (d, $J = 10.1$ Hz), 130.8, 129.4 (d, $J = 13.1$ Hz), 128.8, 128.6 (d, $J = 107.1$ Hz), 43.5 (d, $J = 55.6$ Hz), 21.6. $^{31}\text{P}\{^1\text{H}\}$ NMR (162 MHz, CDCl_3) δ 27.0. HRMS (ESI): m/z $[\text{M}+\text{H}]^+$ calculated for $\text{C}_{22}\text{H}_{21}\text{O}_2\text{ClP}$: 383.0962, found: 383.0961.

2-(bis(4-Fluorophenyl)phosphoryl)-1-phenylethan-1-one **2-3p**



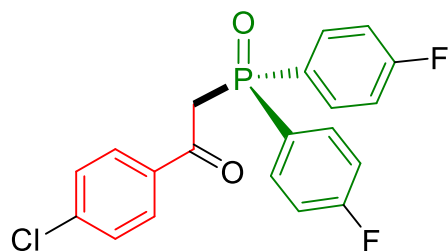
2-3p was obtained as a white solid (50 mg, 70%). ^1H NMR (400 MHz, CDCl_3) δ 7.98 – 7.93 (m, 2H), 7.84 – 7.76 (m, 4H), 7.58 – 7.53 (m, 1H), 7.45 – 7.40 (m, 2H), 7.18 – 7.13 (m, 4H), 4.12 (d, $J = 15.8$ Hz, 2H). $^{13}\text{C}\{^1\text{H}\}$ NMR (101 MHz, CDCl_3) δ 192.8 (d, $J_{\text{C-P}} = 5.7$ Hz), 165.3 (dd, $J_{\text{C-F}} = 254.6$ Hz, $J_{\text{C-P}} = 3.5$ Hz), 136.9, 133.8 (dd, $J_{\text{C-F}} = 2.3$ Hz, $J_{\text{C-P}} = 11.1$ Hz), 133.7, 129.3, 128.7, 127.8 (dd, $J_{\text{C-F}} = 3.3$ Hz, $J_{\text{C-P}} = 107.0$ Hz), 116.2 (dd, $J_{\text{C-P}} = 13.6$ Hz, $J_{\text{C-F}} = 21.5$ Hz), 43.5 (d, $J_{\text{C-P}} = 59.6$ Hz). $^{31}\text{P}\{^1\text{H}\}$ NMR (162 MHz, CDCl_3) δ 25.9. ^{19}F NMR (376 MHz, CDCl_3) δ -105.8. Analytical data in accordance with the literature.^[4]

2-(bis(4-Fluorophenyl)phosphoryl)-1-(4-(*tert*-butyl)phenyl)ethan-1-one **2-3q**



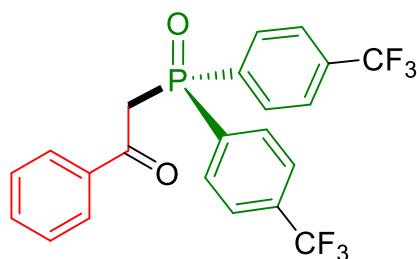
2-3q was obtained as a white solid (54 mg, 66%). ^1H NMR (400 MHz, CDCl_3) δ 7.90 – 7.85 (m, 2H), 7.83 – 7.76 (m, 4H), 7.46 – 7.41 (m, 2H), 7.17 – 7.11 (m, 4H), 4.10 (d, $J = 15.8$ Hz, 2H), 1.31 (s, 9H). $^{13}\text{C}\{^1\text{H}\}$ NMR (101 MHz, CDCl_3) δ 192.2 (d, $J_{\text{C-P}} = 5.1$ Hz), 165.2 (dd, $J_{\text{C-F}} = 254.2$ Hz, $J_{\text{C-P}} = 3.3$ Hz), 157.8, 134.2, 133.8 (dd, $J_{\text{C-F}} = 8.9$ Hz, $J_{\text{C-P}} = 11.4$ Hz), 129.2, 127.8 (dd, $J_{\text{C-F}} = 3.4$ Hz, $J_{\text{C-P}} = 106.8$ Hz), 125.6, 116.1 (dd, $J_{\text{C-P}} = 13.6$ Hz, $J_{\text{C-F}} = 21.5$ Hz), 43.3 (d, $J_{\text{C-P}} = 59.6$ Hz), 35.2, 31.0. $^{31}\text{P}\{^1\text{H}\}$ NMR (162 MHz, CDCl_3) δ 26.1. ^{19}F NMR (376 MHz, CDCl_3) δ -106.0. HRMS (ESI): m/z $[\text{M}+\text{H}]^+$ calculated for $\text{C}_{24}\text{H}_{24}\text{O}_2\text{F}_2\text{P}$: 413.1477, found: 413.1482.

2-(bis(4-Fluorophenyl)phosphoryl)-1-(4-chlorophenyl)ethan-1-one **2-3r**



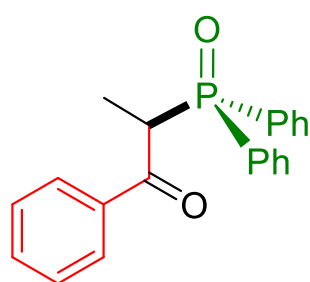
2-3r was obtained as a white solid (56 mg, 72%). ^1H NMR (400 MHz, CDCl_3) δ 7.96 – 7.91 (m, 2H), 7.83 – 7.74 (m, 4H), 7.43 – 7.38 (m, 2H), 7.20 – 7.13 (m, 4H), 4.08 (d, $J = 15.5$ Hz, 2H). $^{13}\text{C}\{^1\text{H}\}$ NMR (101 MHz, CDCl_3) δ 191.4 (d, $J_{\text{C-P}} = 5.6$ Hz), 165.3 (dd, $J_{\text{C-F}} = 254.7$ Hz, $J_{\text{C-P}} = 3.4$ Hz), 140.5, 135.1, 133.7 (dd, $J_{\text{C-F}} = 9.0$ Hz, $J_{\text{C-P}} = 11.7$ Hz), 130.7, 128.9, 127.4 (dd, $J_{\text{C-F}} = 3.4$ Hz, $J_{\text{C-P}} = 107.1$ Hz), 116.2 (dd, $J_{\text{C-P}} = 13.6$ Hz, $J_{\text{C-F}} = 21.5$ Hz), 43.6 (d, $J_{\text{C-P}} = 58.1$ Hz). $^{31}\text{P}\{^1\text{H}\}$ NMR (162 MHz, CDCl_3) δ 25.7. ^{19}F NMR (376 MHz, CDCl_3) δ -105.5. HRMS (ESI): m/z $[\text{M}+\text{H}]^+$ calculated for $\text{C}_{20}\text{H}_{15}\text{O}_2\text{F}_2\text{ClP}$: 391.0461, found: 391.0462.

2-(bis(4-(Trifluoromethyl)phenyl)phosphoryl)-1-phenylethan-1-one **2-3s**



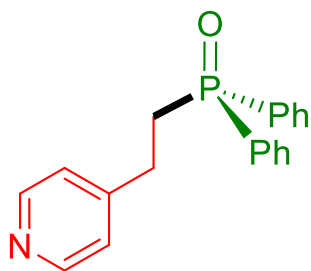
2-3s was obtained as a white solid (39 mg, 43%). ^1H NMR (400 MHz, CDCl_3) δ 8.02 – 7.90 (m, 6H), 7.74 (m, 4H), 7.57 (m, 1H), 7.43 (m, 2H), 4.20 (d, $J = 15.5$ Hz, 2H). $^{13}\text{C}\{^1\text{H}\}$ NMR (101 MHz, CDCl_3) δ 192.1 (d, $J_{\text{C-P}} = 5.7$ Hz), 136.6 (d, $J_{\text{C-P}} = 1.1$ Hz), 135.6 (d, $J_{\text{C-P}} = 101.3$ Hz), 134.3 (dq, $J_{\text{CP}} = 3.0$ Hz, $J_{\text{C-F}} = 33\text{Hz}$), 134.1, 131.7 (d, $J_{\text{C-P}} = 10.1$ Hz), 129.1, 128.7, 125.6 (dq, $J_{\text{C-F}} = 3.0$ Hz, $J_{\text{C-P}} = 12.6$ Hz), 123.3 (q, $J_{\text{C-F}} = 272.8$ Hz), 42.6 (d, $J_{\text{C-P}} = 60.9$ Hz). $^{31}\text{P}\{^1\text{H}\}$ NMR (162 MHz, CDCl_3) δ 25.1. ^{19}F NMR (376 MHz, CDCl_3) δ -63.4. HRMS (ESI): m/z $[\text{M}+\text{H}]^+$ calculated for $\text{C}_{22}\text{H}_{16}\text{O}_2\text{F}_6\text{P}$: 457.0787, found: 457.0792.

2-(Diphenylphosphoryl)-1-phenylpropan-1-one **2-3t**



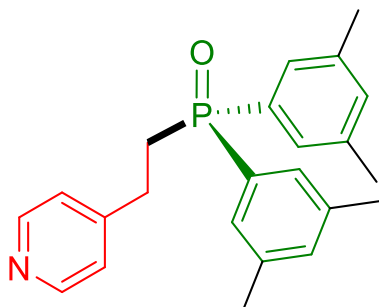
2-3t was obtained as a white solid (31 mg, 47%). ^1H NMR (400 MHz, CDCl_3) δ 7.94 – 7.86 (m, 2H), 7.86 – 7.80 (m, 2H), 7.79 – 7.69 (m, 2H), 7.54 – 7.29 (m, 9H), 4.64 – 4.52 (m, 1H), 1.57 (dd, $J = 16.1, 7.1$ Hz, 3H). $^{13}\text{C}\{^1\text{H}\}$ NMR (101 MHz, CDCl_3) δ 198.1 (d, $J = 2.8$ Hz), 137.1 (d, $J = 1.3$ Hz), 133.1, 132.0 (d, $J = 2.8$ Hz), 131.9-128.4 (m), 45.9 (d, $J = 59.5$ Hz), 13.0 (d, $J = 3.3$ Hz). $^{31}\text{P}\{^1\text{H}\}$ NMR (162 MHz, CDCl_3) δ 31.2.

Diphenyl(2-(pyridin-4-yl)ethyl)phosphine oxide **2-4a**



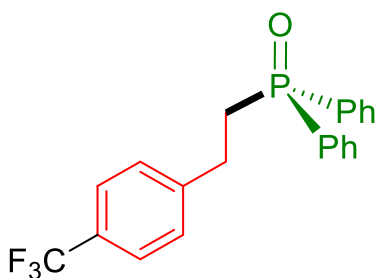
2-4a was obtained as a white solid (38 mg, 81%). ^1H NMR (400 MHz, CDCl_3) δ 8.43 (d, $J = 5.3$ Hz, 2H), 7.79 – 7.69 (m, 4H), 7.55 – 7.41 (m, 6H), 7.06 (d, $J = 5.7$ Hz, 2H), 3.00 – 2.80 (m, 2H), 2.59 – 2.50 (m, 2H). $^{13}\text{C}\{^1\text{H}\}$ NMR (101 MHz, CDCl_3) δ 149.8, 149.8 (d, $J_{\text{C-P}} = 14.7$ Hz), 132.3 (d, $J_{\text{C-P}} = 99.0$ Hz), 131.9 (d, $J_{\text{C-P}} = 2.7$ Hz), 130.7 (d, $J_{\text{C-P}} = 9.4$ Hz), 128.7 (d, $J_{\text{C-P}} = 11.7$ Hz), 123.4, 30.5 (d, $J_{\text{C-P}} = 70.4$ Hz), 26.9 (d, $J_{\text{C-P}} = 2.9$ Hz). $^{31}\text{P}\{^1\text{H}\}$ NMR (162 MHz, CDCl_3) δ 31.0. Analytical data in accordance with the literature.^[5]

bis(3,5-Dimethylphenyl)(2-(pyridin-4-yl)ethyl)phosphine oxide **2-4b**



2-4b was obtained as a white solid (51 mg, 70%). ^1H NMR (400 MHz, CDCl_3) δ 8.46 (m, 2H), 7.34 (m, 4H), 7.14 (s, 2H), 7.09 (m, 2H), 2.95 – 2.87 (m, 2H), 2.56 – 2.47 (m, 2H), 2.33 (s, 12H). $^{13}\text{C}\{^1\text{H}\}$ NMR (101 MHz, CDCl_3) δ 150.2 (d, $J = 14.5$ Hz), 149.8, 138.5 (d, $J = 12.3$ Hz), 133.6 (d, $J = 2.8$ Hz), 132.3 (d, $J = 98.3$ Hz), 128.2 (d, $J = 9.3$ Hz), 123.5, 30.5 (d, $J = 69.9$ Hz), 27.0 (d, $J = 2.7$ Hz), 21.3. $^{31}\text{P}\{^1\text{H}\}$ NMR (162 MHz, CDCl_3) δ 31.3. HRMS (ESI): m/z $[\text{M}+\text{H}]^+$ calculated for $\text{C}_{23}\text{H}_{27}\text{NOP}$: 364.1825, found: 364.1828.

Diphenyl(4-(trifluoromethyl)phenethyl)phosphine oxide **2-4c**

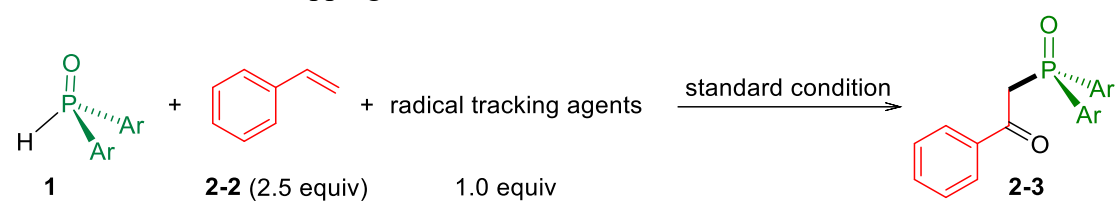


2-4c was obtained as a white solid (31 mg, 52%). ^1H NMR (400 MHz, CDCl_3) δ 7.78 – 7.69 (m, 4H), 7.56 – 7.41 (m, 8H), 7.25 (d, $J = 7.0$ Hz, 2H), 3.02 – 2.96 (m, 2H), 2.60 – 2.51 (m, 2H). $^{13}\text{C}\{^1\text{H}\}$ NMR (101 MHz, CDCl_3) δ 145.2 (d, $J_{\text{C-P}} = 14.4$ Hz), 132.5 (d, $J_{\text{C-P}} = 98.8$ Hz), 131.9 (d, $J_{\text{C-P}} = 2.7$ Hz), 130.7 (d, $J_{\text{C-P}} = 9.4$ Hz), 128.7 (d, $J_{\text{C-P}} = 11.7$ Hz), 128.7 (q, $J_{\text{C-F}} = 32.3$ Hz), 128.4, 125.4 (q, $J_{\text{C-F}} = 3.8$ Hz), 124.1 (q, $J_{\text{C-F}} = 271.9$ Hz), 31.5 (d, $J_{\text{C-P}} = 70.0$ Hz), 27.5 (d, $J_{\text{C-P}} = 3.0$ Hz). $^{31}\text{P}\{^1\text{H}\}$ NMR (162 MHz, CDCl_3) δ 31.0. ^{19}F NMR (376 MHz, CDCl_3) δ -62.5. Analytical data in accordance with the literature.^[5]

4.2.3. Mechanistic Studies

1) Control experiments

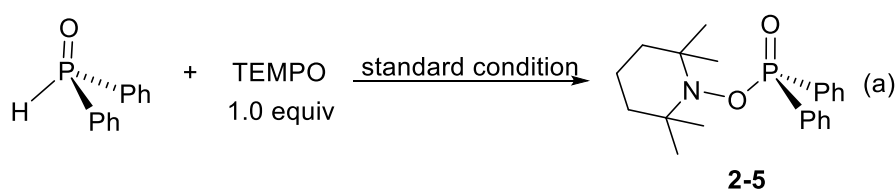
Table S2-1. Radical trapping reactions



Entry	Radical tracking agents	Yield of 2-3 (%)
1	TEMPO	0
2	BHT	0
3	Galvinoxyl	0

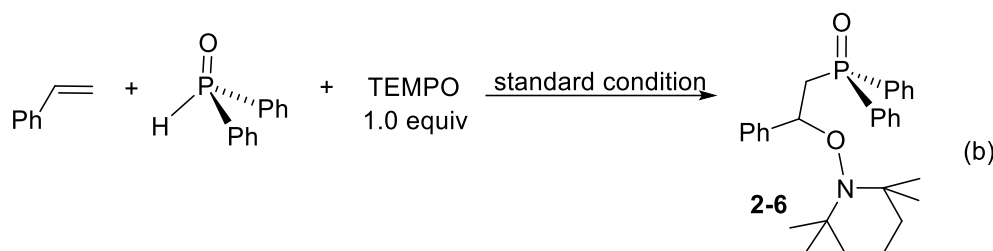
Under air atmosphere, diphenylphosphine oxide **1** (0.2 mmol, 1.0 equiv.), styrene **2-2** (0.5 mmol, 2.5 equiv.), radical tracking agents (0.2 mmol, 1.0 equiv.), $\text{Fe}(\text{OTf})_2$ (10 mol%), in 1,4-dioxane at room temperature under blue light (2 blue-LED 24 W, 450-460 nm) irradiation for 10 h. The mixture was filtered through a celite pad, and analyzed by GC-MS.

2) Radical trapping reactions



Scheme S2-2. Reaction of diphenylphosphine oxide in presence of TEMPO.

Under air atmosphere, diphenylphosphine oxide **1** (0.2 mmol, 1.0 equiv.), TEMPO (0.2 mmol, 1.0 equiv.), Fe(OTf)₂ (10 mol%), in 1,4-dioxane at room temperature under blue light (2 blue-LED 24 W, 450-460 nm) irradiation for 10 h. In the crude mixture, the compound **2-5** was detected and identified by HR-MS (ESI): *m/z* [M+H]⁺ calculated for C₂₁H₂₉NO₂P: 358.1930, found: 358.1931.



Scheme S2-3. Reaction of diphenylphosphine oxide and styrene in presence of TEMPO.

Under air atmosphere, diphenylphosphine oxide **1** (0.2 mmol, 1.0 equiv.), styrene **2-2** (0.5 mmol, 2.5 equiv.), TEMPO (0.2 mmol, 1.0 equiv.), Fe(OTf)₂ (10 mol%), in 1,4-dioxane at room temperature under blue light (2 blue-LED 24 W, 450-460 nm) irradiation for 10 h. In the crude mixture, the compound **2-6** was detected and identified by HR-MS (ESI): *m/z* [M+H]⁺ calculated for C₂₉H₃₇NO₂P: 462.2556, found: 462.2561.

3) Reaction of Ph₂P(O)D with styrene under optimized conditions

Ph₂P(O)D was prepared starting from Ph₂P(O)H in d⁴-MeOD (1.2 mL) at room temperature for 12 hours. After evaporation of the volatiles, Ph₂P(O)D was obtained with 92% of deuterium incorporation in 93% yield.

We then performed, in a Young NMR tube, under air, the reaction of Ph₂P(O)-D (0.2 mmol) with styrene (2 equiv.) in the presence of Fe(OTf)₂ (10 mol%) in 1,4-dioxane under blue light (2 blue-LED 24 W, 450-460 nm) irradiation for 10 h. Thus, the crude reaction mixture was diluted with EtOAc (5 mL), filtered through a Celite pad, and then washed with 10 mL of CH₂Cl₂. The volatiles were then removed under reduced pressure, and the residue was subjected to silica gel column chromatography [eluting with

petroleum ether (PE)/ethyl acetate (EA)] to afford the corresponding product **3a** in 95% isolated yield. Notably no deuterium incorporation was detected.

4) Blue light on/off experiments

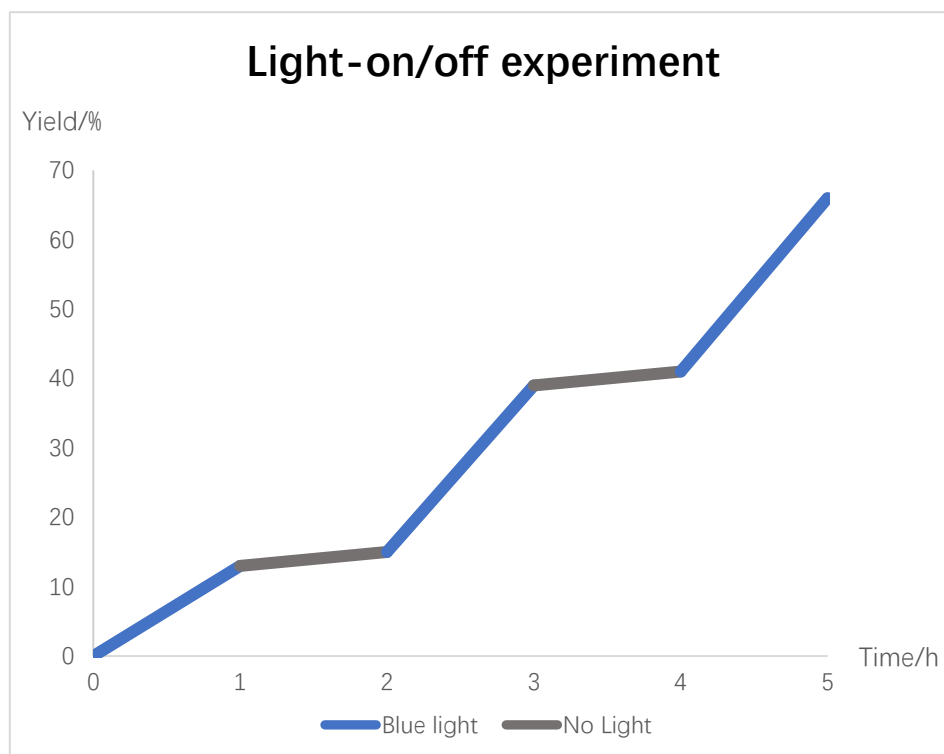


Figure S2-1 – In a young tube under air atmosphere, diphenylphosphine oxide **2-1a** (0.1 mmol), 4-Fluorostyrene (0.2 mmol), Fe(OTf)₂ (10 mmol%), were dissolved in 0.7 mL of acetonitrile-d³, and 1,4-Difluorobenzene (5 mg) was added as the internal standard. The resulting mixture was stirred at room temperature under blue light irradiation (2 × 24 W; λ = 450-460 nm) for 1 h. Then, the crude mixture was analyzed by ¹⁹F NMR to determine the NMR yield of the corresponding product **2-3g**. The Young NMR tube was then placed in dark for 1 h. An NMR was then performed to determine the NMR yield of **2-3g**. Such successive blue light irradiation/dark sequences were performed up to 5 h. The blue line represents the reaction under blue-light LED irradiation and the black line under dark conditions.

5) Copies of UV-Vis spectra

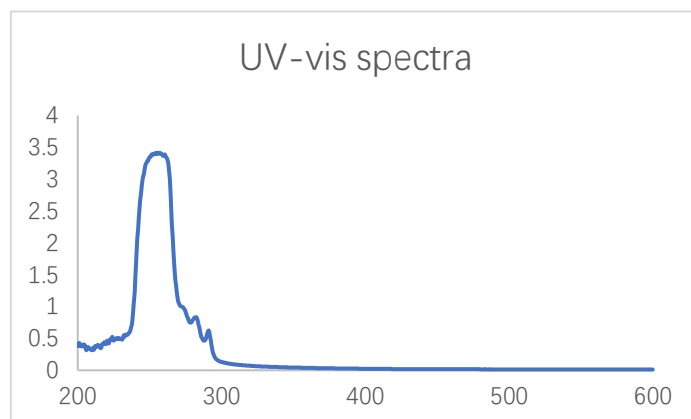


Figure S2-2 - UV-vis spectrum of a mixture of $\text{Ph}_2\text{P}(\text{O})\text{H}$ and styrene in the presence of 10 mol% of $\text{Fe}(\text{OTf})_2$ in 1.4-dioxane, after 10 h of irradiation with 2 blue light LEDs (2×24 W, 450-460 nm).

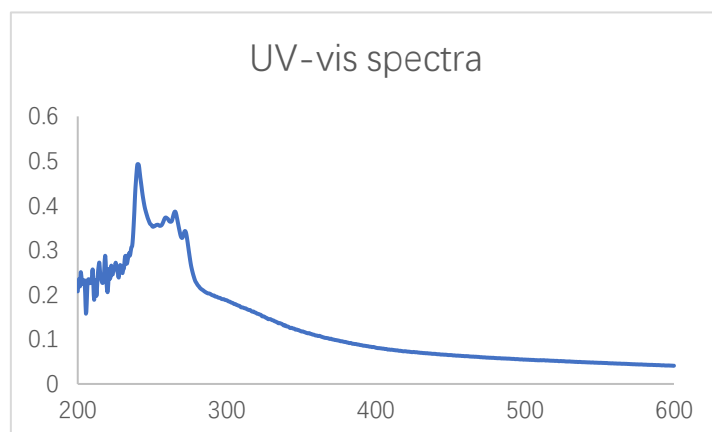


Figure S2-3 - UV-vis spectrum of a mixture of $\text{Ph}_2\text{P}(\text{O})\text{H}$ in the presence of 10 mol% of $\text{Fe}(\text{OTf})_2$ in 1.4-dioxane, after 10 h of irradiation with 2 blue light LEDs (2×24 W, 450-460 nm).

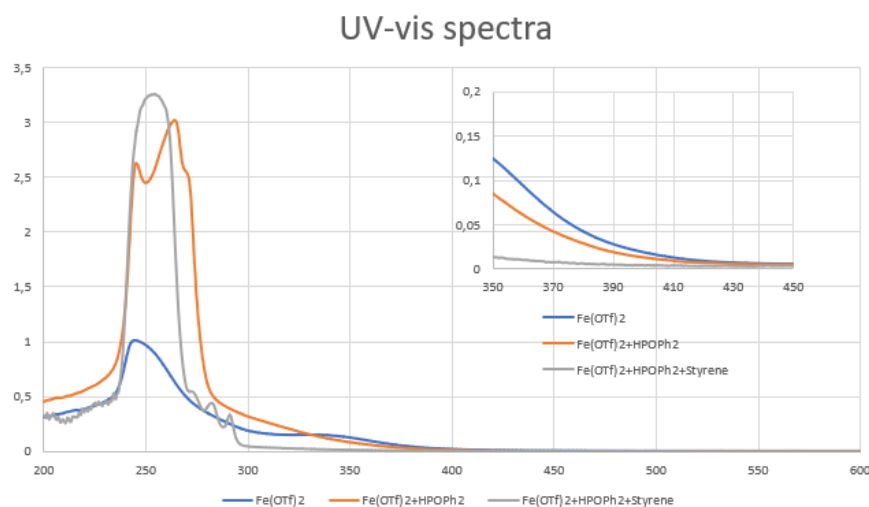


Figure S2-4 - UV-vis spectra of a mixture of Fe(OTf)₂ (blue), Fe(OTf)₂ and Ph₂P(O)H (orange) and Fe(OTf)₂, Ph₂P(O)H and styrene in the presence of 10 mol% in 1,4-dioxane (grey) without blue light irradiation.

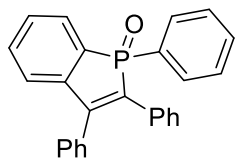
4.3. Supporting Information of Chapter 3

4.3.1. General procedure for the one pot synthesis of 1,2,3-triphenylphosphindole 1-oxide **3-3a** and ethyl 1,3-diphenylphosphindole-2-carboxylate 1-oxide **3-3b**

In a Schlenk tube under argon atmosphere, diphenylphosphine oxide **3-1a** (0.2 mmol), diphenylacetylene **3-2a** (0.4 mmol), Fe(NO₃)₃ (10 mol%), and TBHP (2.0 equiv.), were dissolved in 1.0 mL of MeOH and the resulting mixture was stirred at room temperature under blue light irradiation (2 × 24 W LED; λ = 450-460 nm) for 12 h. Thus, the crude reaction mixture was diluted with EtOAc (5 mL), filtered through a Celite pad which is then washed with 10 mL of CH₂Cl₂. The volatiles were then removed under reduced pressure, and the residue was subjected to silica gel column chromatography [eluting with petroleum ether (PE)/ethyl acetate (EA)] to afford the corresponding product **3-3a**. To obtain **3-3b**, 0.4 mmol of ethyl 3-phenylprop-2-ynoate was used.

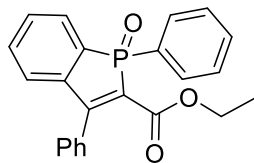
4.3.2. Characterization Data of products 3-3a and 3-3b

1,2,3-Triphenylphosphindole 1-oxide 3-3a



3-3a was obtained as pale yellow solid. (55 mg, 73%). ^1H NMR (400 MHz, CDCl_3) δ 7.84 – 7.70 (m, 3H), 7.54 – 7.39 (m, 8H), 7.38 – 7.33 (m, 2H), 7.28 – 7.21 (m, 3H), 7.15 – 7.08 (m, 3H). $^{13}\text{C}\{^1\text{H}\}$ NMR (101 MHz, CDCl_3) δ 150.0 (d, $J = 21.2$ Hz), 143.7 (d, $J = 27.3$ Hz), 134.2 (d, $J = 96.0$ Hz), 134.1 (d, $J = 15.2$ Hz), 132.9 (d, $J = 2.0$ Hz), 132.6 (d, $J = 14.6$ Hz), 132.0 (d, $J = 110.8$ Hz), 132.1 (d, $J = 3.0$ Hz), 130.9 (d, $J = 10.7$ Hz), 129.9 (d, $J = 100.2$ Hz), 129.4–128.6 (m), 128.2, 127.8, 124.0 (d, $J = 11.1$ Hz). ^{19}C , $^{31}\text{P}\{^1\text{H}\}$ NMR (CDCl_3 , 162 MHz): δ 39.2.^[6a,b]
GC-MS m/z (%): 378 (M^+ , 75), 377 (100), 299 (25), 252 (25), 77 (10).

Ethyl 1,3-diphenylphosphindole-2-carboxylate 1-oxide 3-3b



3-3b was obtained as colorless solid. (51 mg, 68%). ^1H NMR (400 MHz, CDCl_3) δ 7.84 – 7.71 (m, 3H), 7.61 – 7.37 (m, 10H), 7.27 – 7.21 (m, 1H), 4.14 – 3.96 (m, 2H), 0.99 (t, $J = 7.1$ Hz, 3H). $^{13}\text{C}\{^1\text{H}\}$ NMR (101 MHz, CDCl_3) δ 163.8 (d, $J = 18.2$ Hz), 162.5 (d, $J = 12.1$ Hz), 142.3 (d, $J = 25.3$ Hz), 133.4 (d, $J = 2.0$ Hz), 133.0, 132.5 (d, $J = 95$ Hz), 132.3 (d, $J = 2.9$ Hz), 131.7 (d, $J = 10.7$ Hz), 131.1 (d, $J = 11.0$ Hz), 129.8, 129.5 (d, $J = 9.6$ Hz), 129.3, 128.6 (d, $J = 12.9$ Hz), 128.3, 128.0, 126.5 (d, $J = 98.1$ Hz), 126.4 (d, $J = 10.1$ Hz), 60.9, 13.7. $^{31}\text{P}\{^1\text{H}\}$ NMR (162 MHz, CDCl_3) δ 35.7.^[7]

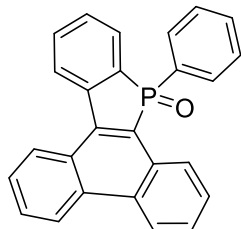
4.3.3. General procedure for the one pot synthesis of 9-phenyltribenzo[*b,e,g*]phosphindole 9-oxide 3-4a

In a Schlenk tube, under argon atmosphere, diphenylphosphine oxide **3-1a** (0.2 mmol), diphenylacetylene **3-2a** (0.4 mmol), $\text{Fe}(\text{OTf})_2$ (10 mol%), TBHP (2.0 equiv.), were dissolved in 1.0 mL of AcOH and the resulting mixture was stirred at room temperature under blue light irradiation (2×24 W LED; $\lambda = 450\text{--}460$ nm) for 12 h. Thus, the crude reaction mixture was diluted with EtOAc (5 mL), filtered through a Celite pad which was then washed with 10 mL of CH_2Cl_2 . The volatiles were then removed under reduced pressure, and the residue was subjected to silica gel column chromatography

[eluting with petroleum ether (PE)/ethyl acetate (EA)] to afford the corresponding product **3-4a**.

4.3.4 Characterization Data of the product 3-4a

9-Phenyltribenzo[*b,e,g*]phosphindole 9-oxide **3-4a**



3-4a was obtained as white solid. (52 mg, 70%) ^1H NMR (400 MHz, CDCl_3) δ 9.02 (dd, $J = 7.8, 1.8$ Hz, 1H), 8.85 (dd, $J = 7.6, 1.9$ Hz, 1H), 8.70 (d, $J = 8.5$ Hz, 1H), 8.56 (dd, $J = 8.0, 3.5$ Hz, 1H), 8.34 (d, $J = 8.0$ Hz, 1H), 7.90 – 7.74 (m, 5H), 7.73 – 7.64 (m, 2H), 7.61 – 7.56 (m, 1H), 7.50 – 7.44 (m, 2H), 7.41 – 7.35 (m, 2H). $^{13}\text{C}\{^1\text{H}\}$ NMR (101 MHz, CDCl_3) δ 142.5 (d, $J = 23.2$ Hz), 139.5 (d, $J = 20.2$ Hz), 134.7 (d, $J = 106.1$ Hz), 134.0 (d, $J = 2.0$ Hz), 133.1 (d, $J = 2.0$ Hz), 132.1 (d, $J = 3.0$ Hz), 131.1 (d, $J = 11.1$ Hz), 130.9 (d, $J = 102.8$ Hz), 130.7, 130.1 (d, $J = 103.3$ Hz), 130.1 (d, $J = 10.1$ Hz), 129.3 (d, $J = 9.1$ Hz), 128.9 (d, $J = 11.1$ Hz), 128.8 (d, $J = 12.1$ Hz), 128.6, 128.1, 128.0 (d, $J = 12.1$ Hz), 127.8, 127.4, 127.5 (d, $J = 5.1$ Hz), 125.8, 125.6 (d, $J = 11.1$ Hz), 124.1, 123.0 (d, $J = 1.0$ Hz). $^{31}\text{P}\{^1\text{H}\}$ NMR (162 MHz, CDCl_3) δ 33.9. [22]

4.3.5. X-ray crystallographic analysis

The detailed crystallographic data and structure refinement parameters for this compound is summarized in **Table S3-1**. CCDC **2302243** contains the supplementary crystallographic data.

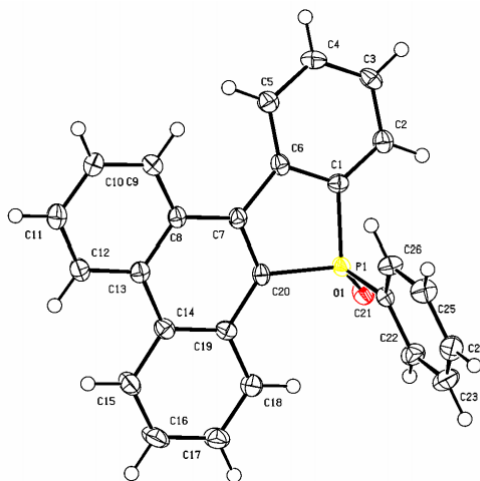


Table S3-1. 3-4a (CCDC 2302243)

Identification code	YY524
Empirical formula	C ₂₆ H ₁₇ OP
Formula weight	376.36
Temperature/K	150 (2)
Crystal system	monoclinic
Space group	P2 ₁ /n
a/Å	17.649 (3)
b/Å	12.912 (2)
c/Å	8.0563 (12)
α/°	90
β/°	91.600 (7)
γ/°	90
Volume/Å ³	1835.2 (5)
Z	4
ρ _{calc} /cm ³	1.362
μ/mm ⁻¹	0.164
F(000)	784
Radiation	Mo-Kalpha (λ = 0.71073)
2θ range for data collection/°	3.155 to 27.510
Index ranges	-20 ≤ h ≤ 22, -16 ≤ k ≤ 16, -10 ≤ l ≤ 10
Reflections collected	3648
Independent reflections	9885 [R _{int} = 0.0404, R _{sigma} = 0.0370]
Data/restraints/parameters	3958/2/254
Goodness-of-fit on F ²	1.052
Final R indexes [I ≥ 2σ (I)]	R ₁ = 0.0402, wR ₂ = 0.0840
Final R indexes [all data]	R ₁ = 0.0455, wR ₂ = 0.0863
Largest diff. peak/hole / e Å ⁻³	0.266/-0.239

4.4. References

- [1] Y. Ou, Y. Huang, Y. Liu, Y. Huo, Y. Gao, X. Li, Q. Chen, *Adv. Synth. Catal.* **2020**, *362*, 5783-5787.
- [2] B. Liu, Q. Song, Z. Liu, Z. Wang, *Adv. Synth. Catal.* **2021**, *363*, 3214-3219.
- [3] Y. Zeng, D. Tan, W. Lv, Q. Li, H. Wang, *Eur. J. Org. Chem.* **2015**, 4335-4339.
- [4] S. Feng, J. Li, F. He, T. Li, H. Li, X. Wang, X. Xie, X. She, *Org. Chem. Front.* **2019**, *6*, 946.
- [5] A. W. J. Platten, A. M. Borys, E. Hevia, *ChemCatChem* **2022**, *14*, e202101853.
- [6] (a) Y. Chen, W. Duan, *J. Am. Chem. Soc.* **2013**, *135*, 16754-16757; (b) V. Quint, F. Morlet-Savary, J.-F. Lohier, J. Lalevée, A.-C. Gaumont, S. Lakhdar, *J. Am. Chem. Soc.* **2016**, *138*, 7436-7441. c) Y. Unoh, K. Hirano, T. Satoh, M. Miura, *Angew. Chem. Int. Ed.* **2013**, *52*, 12975-12979.
- [7] K. Nishimura, S. Xu, Y. Nishii, K. Hirano, *Org. Lett.* **2023**, *25*, 1503-1508.

Part 2 - Rhodium Catalyzed Accesses to 1,7-fused Indoles

PhD contribution done in Fujian, China

Chapter 5 – Transition metal catalyzed selective transformation of indoles. C2-C3 versus C4, C5, C6 and C7 C-H functionalization. Towards efficient methodologies to fused indoles

5.1. Introduction

Fused tetracyclic ring systems containing indole units are the constituents of a variety of natural products and pharmaceutical compounds. In particular, indole-annulated tetracyclic compounds and their derivatives containing six-membered ring or seven-membered ring are among the most important compounds present in various natural products and biologically active compounds such as Hippadine, Erythrivarine B, Nodulisporic acid A, and Tivantinib (Figure 5-1).^[1-13] Therefore, it is of great significance for the construction of indole-annulated six-membered ring and seven-membered ring skeletons.

There were several described accesses to such indole-based skeletons performed by modification of the indole skeleton for example starting from 7-bromoindole derivatives,^[11] or by functionalization of indoles bearing N-directed group.^[12] Another strategy was to build the indole skeleton from 1,2,3,4-tetrahydroquinoline derivatives.^[13]

On another hand, catalyzed intramolecular annulations involving C-H activations can be view as an elegant methodology which permits to shortcut the length of the synthesis of such azapolycyclic derivatives. Indeed, during the two last decades, transition metal catalyzed methodologies, in particular cross-coupling reactions and C-H bond activation/functionalization have made amazing breakthroughs in the synthesis of polycyclic containing indole molecules, notably in terms of atom- and step-economy, lower cost, and lower waste amounts. Therefore, transition metal-catalyzed C-H bond activation/functionalization of compounds bearing an indole motif has become one of the most direct and rapid methods to construct various indole derivatives and has been studied by many groups and made amazing progress. Transition metal-catalyzed C-H

bond functionalization of indole compounds can be accomplished by two main approaches:

1. The regioselective transition-metal-catalyzed C–H activation/functionalization of the indole framework,
2. The *NH*-indole-directed, transition metal catalyzed C-H bond activation/functionalization.

In this introduction, we will exemplify these two approaches.

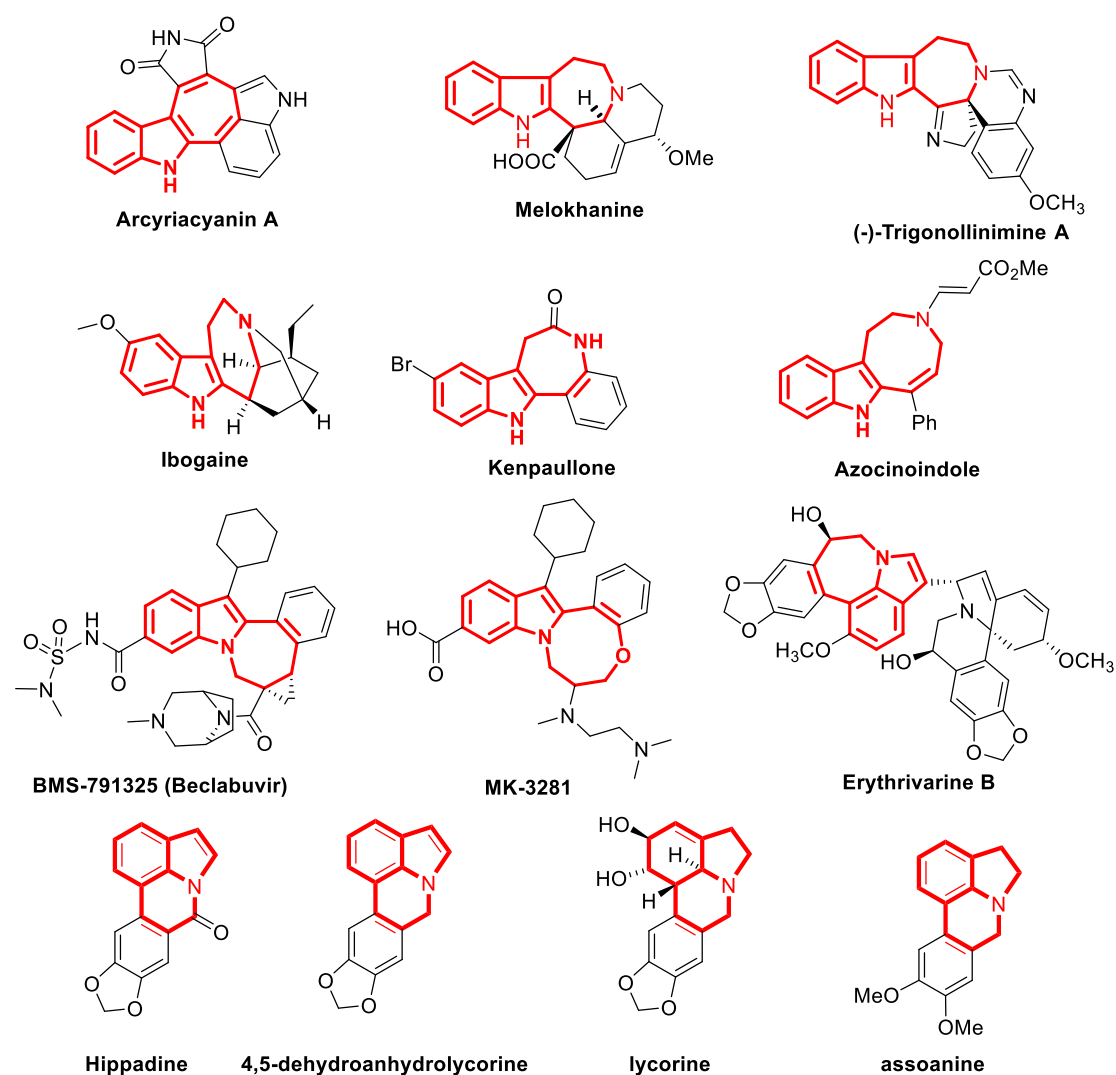


Figure 5-1. Drugs or active molecules bearing indole-annulated six-membered ring and seven-membered ring skeletons.

5.2. Transition-Metal-Catalyzed C–H Functionalization of Indole Framework

With the presence of six C-H bonds in indoles, the indole core can be functionalized on C2 to C3 (pyrrole core) and C4 to C7 (benzene core) positions, notably via transition metal-catalyzed selective C-H activation/functionalization methodologies. Due to the inherent reactivity of the pyrrole ring, C2 and C3 are the most electron-rich carbon centers on the indole structure. (Figure 5-2)

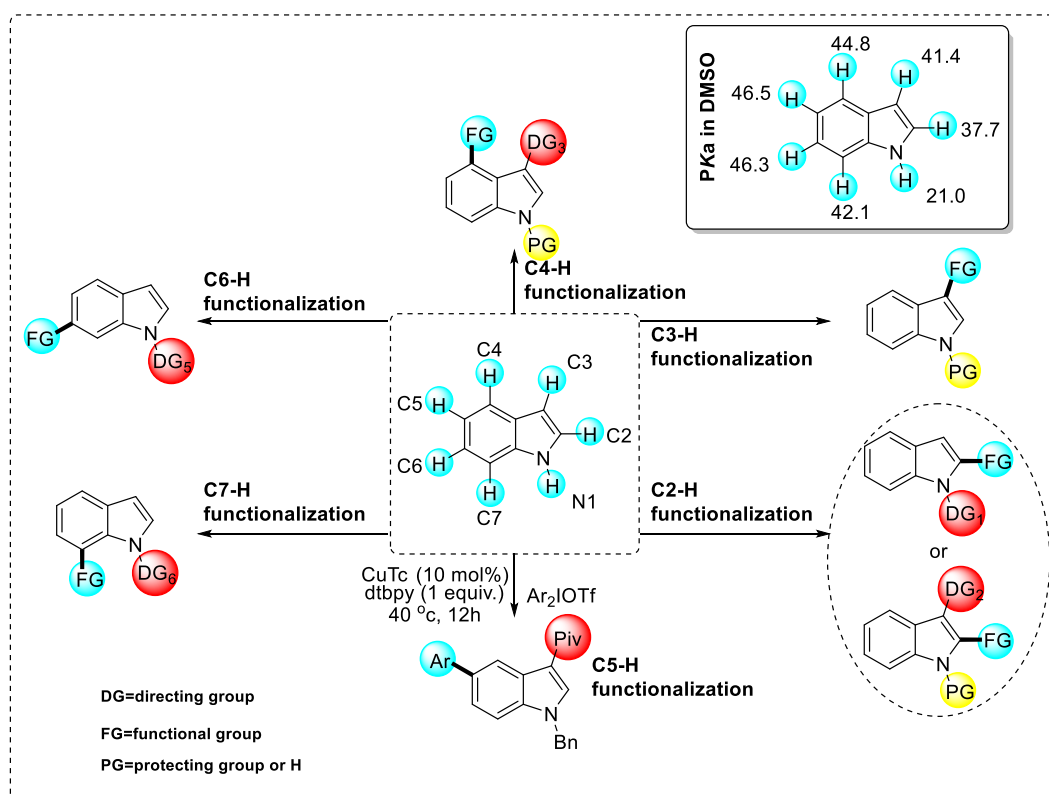


Figure 5-2. Regio-selectivity in transition metal catalyzed C-H bond activation of indoles.

Therefore, early developments were mainly focused on C2 and C3 functionalization such as arylation, alkenylation, alkylation, acylation and amidation during recent decades. More recently, advances were made for the functionalization of the more challenging C4 to C7 (benzene core) positions. Noticeably, the N-H function being reactive, in such transformation, it should be either protected or functionalized in order to serve as directing group.

This first paragraph will then describe representative examples of elegant functionalization of each carbon position of indole.

5.2.1. Functionalization at C2 position

Due to their inherent reactivity, the C–H functionalization of the indole framework mostly takes place at the C3 position *via* an aromatic electrophilic substitution pathway. Nevertheless, thanks to transition metal catalyzed C-H activation *via* direct C2 metalation, the C2 position can be activated.

5.2.1.1. Via arylation reactions

The main challenge of the transition metal catalyzed arylation is the selective arylation of the C2 and C3 position without protection of the N-H bond, usually more reactive in cross coupling reactions. (Figure 5-3)

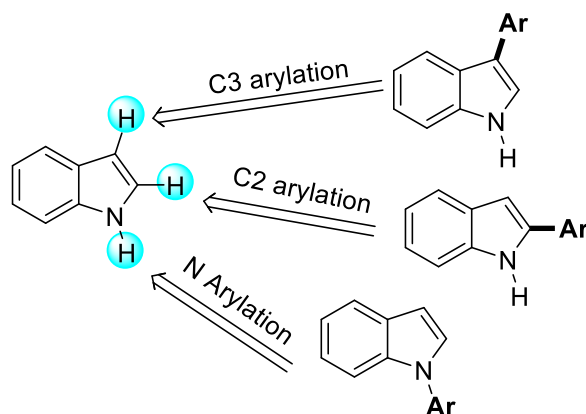
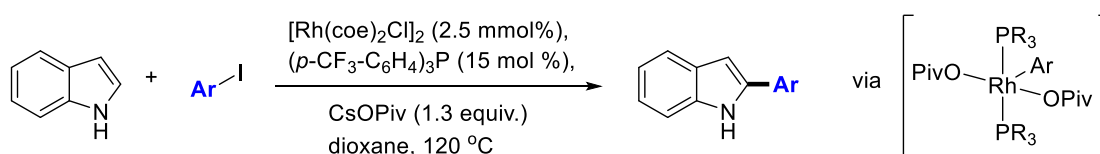


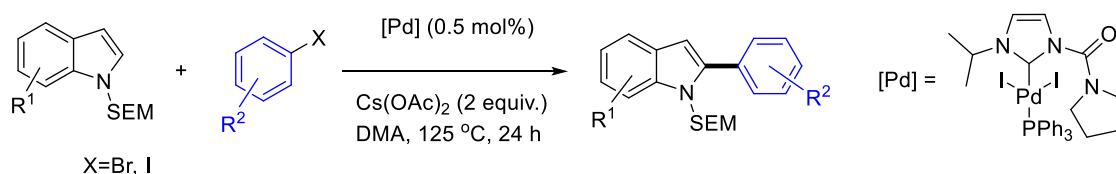
Figure 5-3. Regio-selectivity NH vs C2-H vs C3-H arylations of indoles.

In 2005, Sames and co-workers described the direct C2-arylation using aryl iodides of unprotected indole *via* a $[\text{Rh}(\text{coe})_2\text{Cl}]_2$ (coe=*cis*-cyclooctene) catalyzed cross coupling reaction in the presence of 1.4 equiv. of CsOPiv.^[14] The selectivity was rationalized by a greater electrophilicity of the Ar-Rh(III) fragment. (Scheme 5-1)



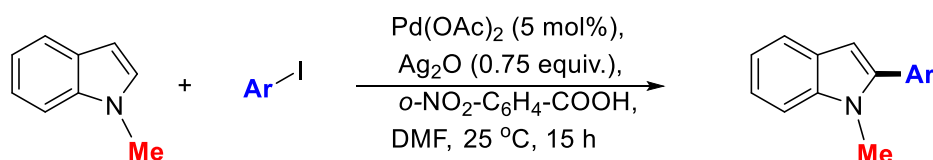
Scheme 5-1. Direct C2-arylation of NH-free indoles and aryl iodides.

Another protocol was developed by the Sames group for C-2 arylation, exploiting SEM [2-(trimethylsilyl)ethoxymethyl] protected indoles.^[15] With palladium catalyst, it is necessary to protect the N-H function with SEM protecting group as in its absence, no reaction was observed. Thus, using a palladium complex containing an imidazolyl carbene ligand, the cross coupling of the SEM protected indoles with aryl iodides in the presence of 2 equiv. of cesium acetate in DMA at 125 °C led exclusively to the C2-arylated indoles with good yields. (Scheme 5-2)



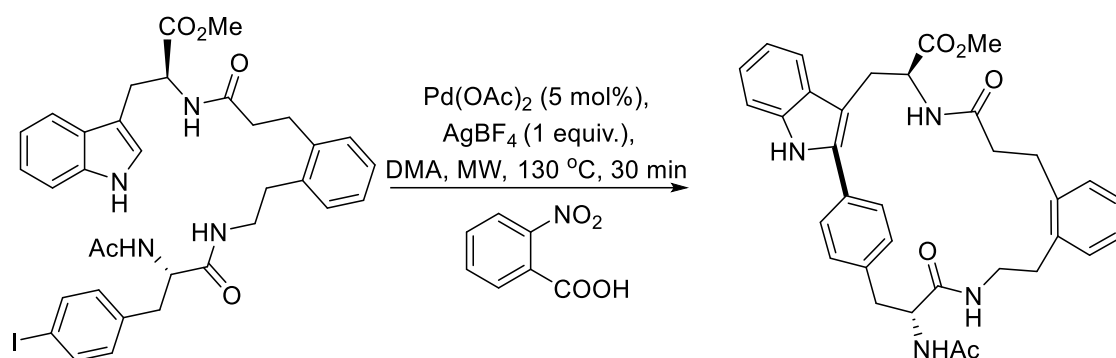
Scheme 5-2. Direct C2-arylation of NH-protected indoles and aryl iodides.

Thus, using palladium catalysts, several contributions were reported using protected indoles. In 2008, Larrosa's group has developed the C2-arylation of N-methylindoles, using a ligand free palladium catalyzed methodology with 5 mol% of Pd(OAc)₂ catalyst in the presence of silver oxide and *p*-nitrobenzoic acid at room temperature.^[16] (Scheme 5-3)



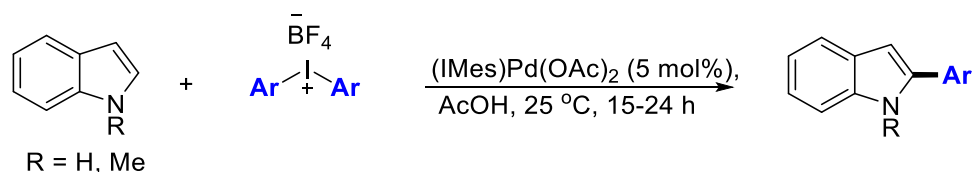
Scheme 5-3. Palladium-catalyzed arylation of *N*-methylindoles.

Based on these results, James et al. applied this palladium-catalyzed C–H activation reaction to the construction of indole-aryl bridged macrocycles through intramolecular reaction of one side chain of tryptophan with the side chain of a phenylalanine derivative.^[17] Noticeably, in these specific examples, no protection of the NH moiety was required and the C–H arylation proceeded exclusively at the C2 position of the indole backbone. (Scheme 5-4)



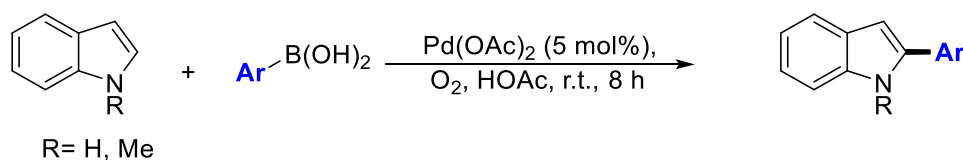
Scheme 5-4. Palladium-catalyzed C2-arylation of indole motif in a macrocyclisation reaction.

Using diaryliodonium salt ($[\text{Ph-I-Ph}]\text{BF}_4$) as the electrophilic partner (1-3 equiv.), M. S. Sanford and co-workers developed the arylation of *N*-methylindoles and noticeably unprotected indoles in the presence of 5 mol % of $(\text{IMes})\text{Pd}(\text{OAc})_2$ and AcOH as the solvent at room temperature for 15-24 h. The authors suggested a plausible mechanism involving a reaction which took place through the Pd(II)/(IV) species.^[18] (Scheme 5-5)



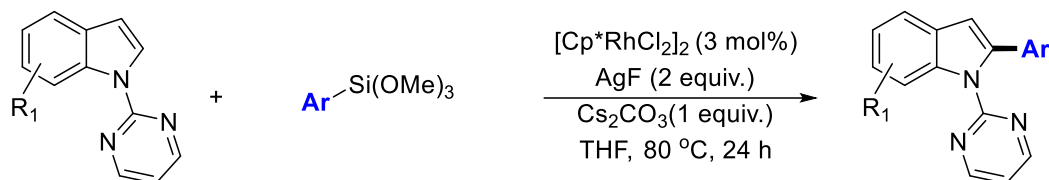
Scheme 5-5. Palladium(II)-catalyzed arylation of indoles using diaryliodonium salts.

Aryl boronic acids can be also used as coupling partners as demonstrated by Z. Shi's group who described a direct construction of indole-aryl C-C bonds by a Pd(II)-catalyzed oxidative arylation of indole with arylboronic acids in the presence of 5 mol% of $\text{Pd}(\text{OAc})_2$, under an oxygen atmosphere in acetic acid at room temperature.^[19] (Scheme 5-6)



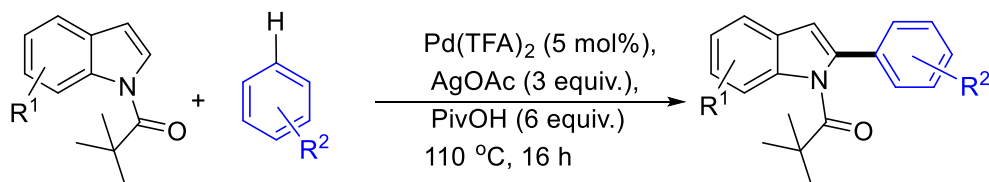
Scheme 5-6. Palladium(II)-catalyzed arylation of indoles using aryl boronic acid partners.

Similarly, T-P. Loh and co-workers used organosilanes as coupling partners *via* a rhodium(III)-catalyzed C–H bond activation/arylation. Using 3 mol% of $[\text{Cp}^*\text{RhCl}_2]_2$ in the presence of 2 equiv. of silver fluoride and 1 equiv. of cesium carbonate at 80 °C for 24 h, thanks to N-(2-pyrimidyl) directing group, exclusive C2-arylation was observed.^[20] (Scheme 5-7)



Scheme 5-7. Rhodium-catalyzed arylation of indoles using organosilane partners.

In 2007, Fagnou and co-workers did a breakthrough in arylation of N-acyl-indole *via* a Pd-catalyzed oxidative cross coupling reaction using arenes as coupling partners. Indeed, they performed the reaction using 5 mol% of $\text{Pd}(\text{TFA})_2$ in the presence of 3 equiv. of AgOAc as the oxidant. Noticeably, the C2/C3 selectivity is dramatically dependent of the additives: AgOAc favored C2-H activation of indoles, whereas $\text{Cu}(\text{OAc})_2$ favored the C3-H activation.^[21] (Scheme 5-8)

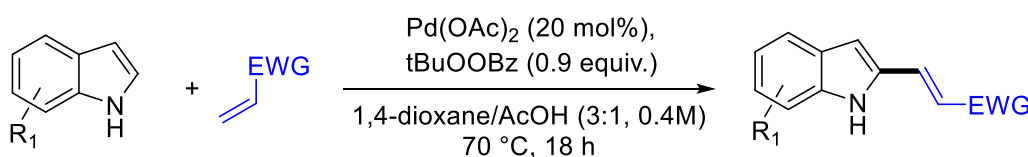


Scheme 5-8. Palladium catalyzed C2-arylation via C-H activation.

5.2.1.2. Via alkenylation reaction

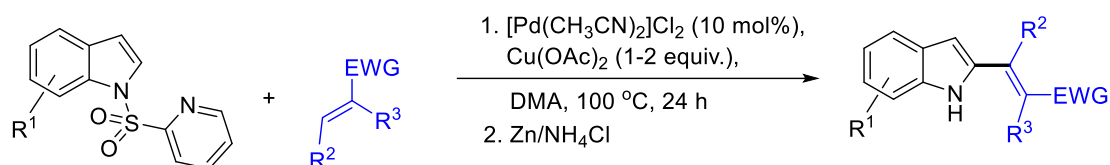
In a pioneering report in 2005, Ricci et al. reported that C2 alkenylation can be observed when performing the reaction of *N*-pyridylmethylindole with methyl acrylate in the presence of 10 mol% PdCl_2 , 2 equiv. of $\text{Cu}(\text{OAc})_2$, in MeCN at 60 °C for 14 h. Noticeably, the pyridylmethyl directing group is crucial for the selectivity of the transformation: indeed, when starting from *N*-benzylindole, under similar conditions, exclusive C3-alkenylation reaction was observed.^[22]

The same year, Gaunt has shown that the nature of the solvent can have also a great influence on the regioselectivity of the alkenylation of unprotected indole starting from alkenes such as acrylic derivatives. Using 20 mol% of Pd(OAc)₂, 0.9 equiv. of *t*-BuOOBz in a mixture 1,4-dioxane/acetic acid at 70 °C for 18 h, the C2-alkenylated indoles were obtained in moderate yields. By contrast, when conducting the reaction in DMSO/DMF in the presence of 10 mol% of Pd(OAc)₂ and 1.8 equiv. of Cu(OAc)₂, C3-alkenylated indoles were obtained in good yields.^[23] (Scheme 5-9)



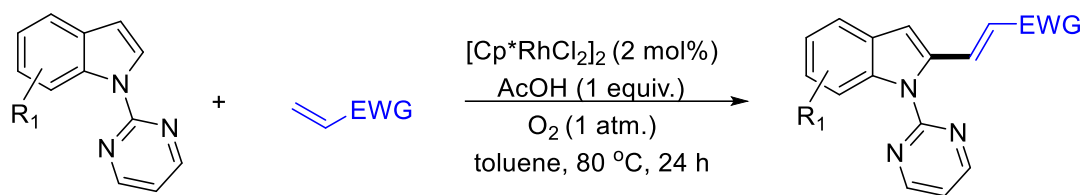
Scheme 5-9. Palladium catalyzed C2-alkenylation of unprotected indoles.

Thanks to a 2-pyridylsulfonyl directing group, Carretero and co-workers described a Pd-catalyzed C-H activation of N-(2-pyridylsulfonyl)-indoles and the coupling with activated olefins. Thus, using 10 mol% of Pd(CH₃CN)₂Cl₂ in the presence of 1-2 equiv. of Cu(OAc)₂·H₂O as an oxidant in DMA at 110 °C for 24 h, the C2-alkenylated derivatives were obtained in moderate to good yields. The reductive removal of the directing group was simply achieved by the use of Zn/NH₄Cl.^[24] (Scheme 5-10)



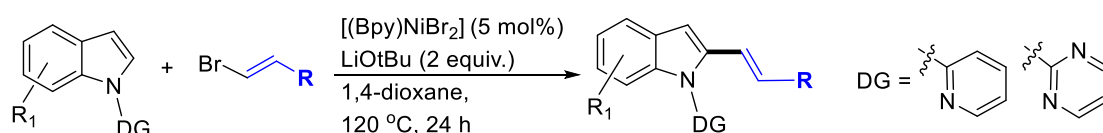
Scheme 5-10. 2-Pyridylsulfonyl directing group for palladium catalyzed C2 alkenylation.

In the goal to use greener oxidant, H. Huang and co-workers have developed a rhodium(III)-catalyzed direct selective C-2 alkenylation reaction of indoles with alkenes using oxygen as the sole oxidant. Similarly to Loh (Scheme 7), they performed the reaction of N-(2-pyrimidyl)indoles in the presence of 3 mol% of [Cp**Rh*Cl₂]₂, 1 equiv. of acetic acid in toluene at 80 °C for 24 h under 1 atm. of O₂, exclusive C2-arylation was observed.^[25] (Scheme 5-11)



Scheme 5-11. Rhodium-catalyzed alkenylation of N-(2-pyrimidyl)indoles.

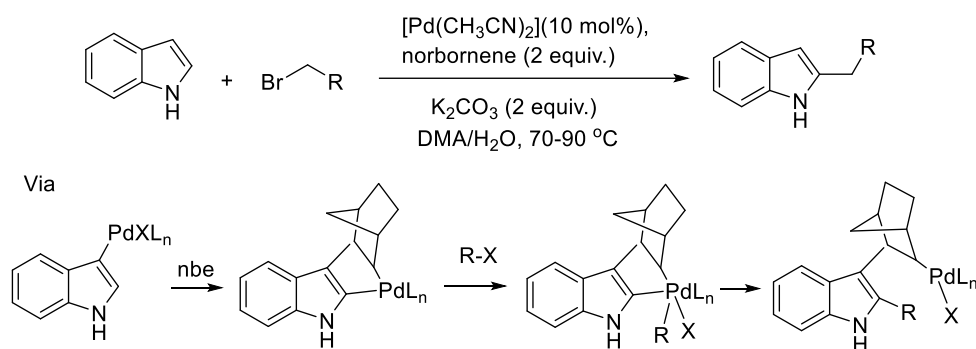
Punji et al. succeeded to perform a general nickel-catalyzed the C2-alkenylation of indoles bearing a N-(2-pyridinyl) or N-(2-pyrimidinyl) directing groups with alkenyl bromides using 5 mol% of (bpy)NiBr₂ in the presence of 2 equiv. of LiO^tBu in 1,4-dioxane at 120 °C for 24 h. Noticeably, many alkenyl bromides were tolerated, such as aromatic and heteroaromatics, α - and β -substituted as well as exo- and endo-cyclic alkenyl functionality.^[26] (Scheme 5-12)



Scheme 5-12. Nickel catalyzed C2-cross coupling of indoles bearing N-directing groups.

5.2.1.3. Via alkylation reaction

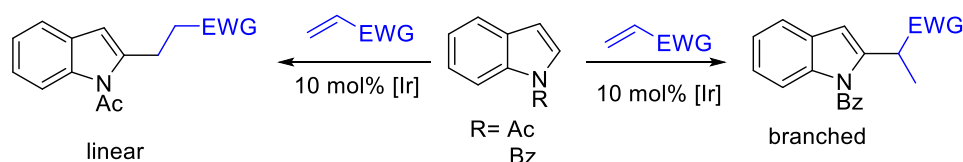
In order to perform selectively C2-alkylation of unprotected indoles, Bach and co-workers developed the first protocol of Pd-catalyzed, cascade C-H activation sequence mediated by norbornene coupling reaction of alkyl bromides and indoles. Using 10 mol% of PdCl₂(MeCN)₂ in the presence of 2 equiv. of norbornene (nbe) and 2 equiv. of K₂CO₃ in a mixture DMA/water at 70-90 °C, 2-alkylindoles were obtained in moderate to good yields.^[27] As the direct palladation of indole with a Pd(II) complex should occur preferentially at the C3 of indole, in order to rationalize the selectivity observed and the crucial role of norbornene, the obtained 3-palladated indole then inserted norbornene and underwent a second intramolecular C-H activation at the C2 to form an indole-fused palladacycle. The oxidative addition of RX led to a Pd(IV) species which after reductive elimination, installed the alkyl group at the C2 position. A final beta-elimination of norbornene. (Scheme 5-13)



Scheme 5-13. Palladium-catalyzed C2-alkylation of unprotected indoles thanks to norbornene mediation.

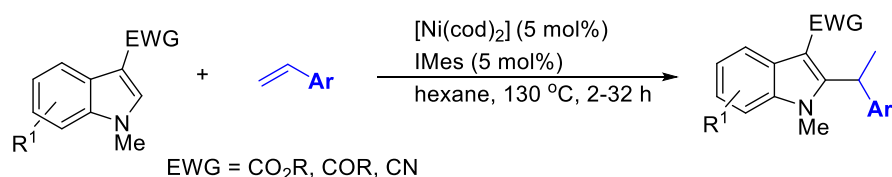
Shibata and co-workers reported an iridium-catalyst coupling reaction of indoles and terminal activated olefins to perform either linear or branched alkylindoles, the regioselectivity of product depending on the directing group on the N of the indole moiety. Using 10 mol% of $[\text{Ir}(\text{cod})_2]\text{BF}_4$ with 10 mol% of ligand [*S*-DM-SEGPHOS or rac-BINAP], unprotected indole led to no reaction. After a screening of the protecting groups, it was shown that the acetyl group favored the formation of linear 2-alkylindoles, and the benzoyl one favored led to the formation of branched 2-alkylindoles.^[28]

(Scheme 5-14)



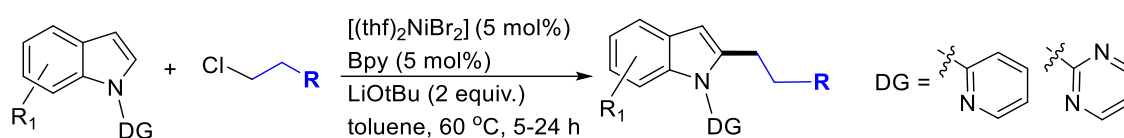
Scheme 5-14. Protecting group dependence for the regioselectivity of iridium-catalyzed C2-alkylation.

At nickel, even if using only N-methyl C3-substituted indole derivatives, Hiyama and co-workers demonstrated that the heteroarylation of vinylarenes was also possible. Indeed, using an *in-situ* generated catalyst (5 mol%) from $\text{Ni}(\text{cod})_2$ and IMes NHC ligand in hexane at 130 °C for 7-31 h, branched-chain 2-alkylindoles were obtained selectively.^[29] (Scheme 5-15)



Scheme 5-15. Nickel catalyzed cross coupling of N-methyl C3-substituted indoles.

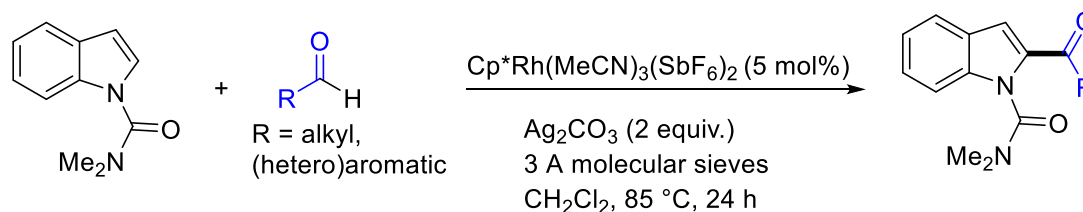
Using similar conditions to alkenylation (Scheme 12), [5 mol% of $(\text{thf})_2\text{NiBr}_2$, 5 mol% of Bpy, 2 equiv. of LiO^tBu , toluene, 60 °C, 5-24 h], Punji et al. succeeded to promote the cross coupling of unactivated primary and secondary alkyl chlorides with *N*-(2-pyridinyl) or *N*-(2-pyrimidinyl)indoles, with an exclusive C2-selectivity.^[30] (Scheme 5-16)



Scheme 5-16. Nickel catalyzed C2-cross coupling of indoles bearing N-directing groups.

5.2.1.4. Via acylation reaction

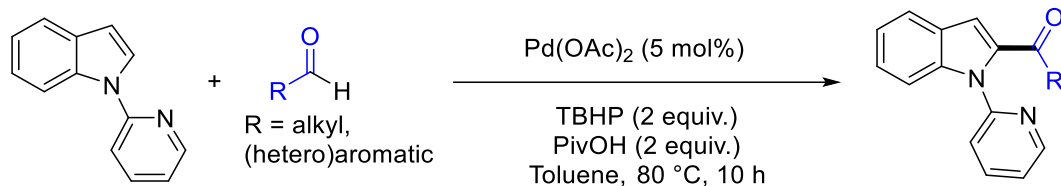
The classical route to 2-acylindoles is the condensation of acyl electrophiles with 2-lithioindole reagents, which should be prepared regio-selectively. In the area of cross-coupling reactions, Li and co-workers described a rhodium-catalyzed oxidative C2-acylation of *N,N*-dimethylcarbamoylindoles with both (hetero)aromatic and alkyl aldehydes via C–H bond activation. Using 5 mol% of $\text{Cp}^*\text{Rh}(\text{MeCN})_3(\text{SbF}_6)_2$ in the presence of 2 equiv. of silver carbonate in dichloromethane at 85 °C for 24 h, selective C2-acylation was performed in moderate to good yields.^[31] (Scheme 5-17)



Scheme 5-17. Rhodium-catalyzed C2-acylation of *N,N*-dimethylcarbamoylindoles.

Similarly, Li et al. described a palladium-catalyzed oxidative C2-acylation of *N*-(2-pyridinyl)indoles by reaction with both (hetero)aromatic and alkyl aldehydes. Indeed, using 10 mol% of $\text{Pd}(\text{OAc})_2$ in the presence of 2 equiv. of TBHP (*tert*-butyl hydroperoxide) as the oxidant and 2 equiv. of pivalic acid in toluene at 80 °C, they

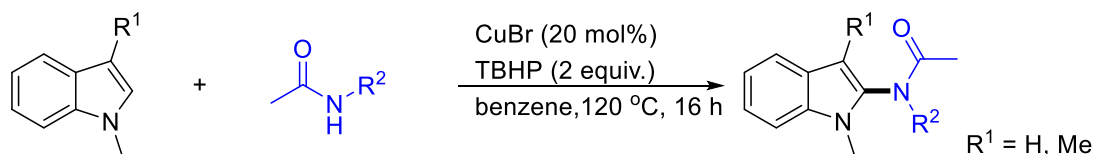
succeeded to obtain numerous 2-aryloindoles thanks to the 2-pyridynyl directing group.^[32]



Scheme 18. Palladium-catalyzed C2-arylation of *N*-(2-pyridynyl)indoles.

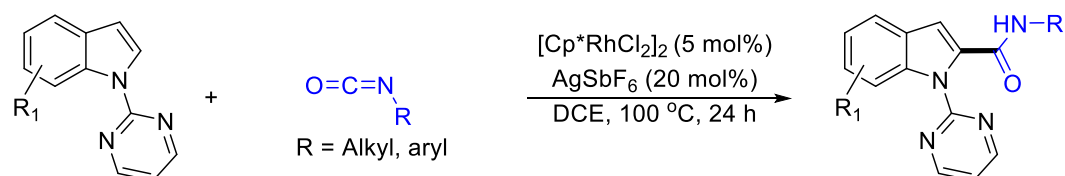
5.2.1.5. Via amidation reaction

Li and co-workers developed a direct access for amidation of indoles via a Cu(I)-catalyzed cross-dehydrogenative coupling reaction of *N*-methylindoles and secondary amides, using 20 mol% of CuBr in the presence of 2 equivalents of TBHP (*tert*-butyl hydroperoxide) as the oxidant in benzene at 120 °C for 16 h. Noticeably, when starting with *N*-methylindoles which did not bear a methyl substituent at C3 position, the C2-amidation was still observed.^[33] (Scheme 5-19)



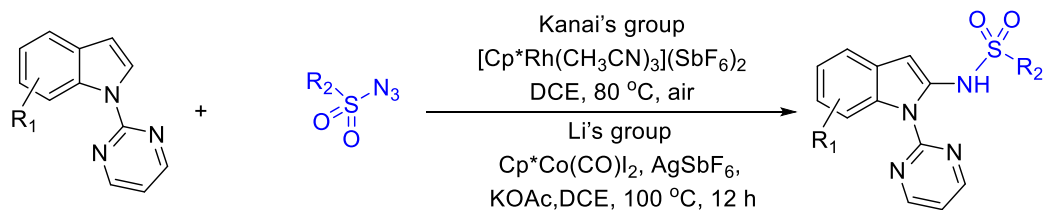
Scheme 5-19. Cu-catalyzed cross-dehydrogenative coupling reaction of *N*-methylindoles and secondary amides.

C2-amidation of indoles can be also perform using isocyanate partners as demonstrated by Kim et al. in rhodium catalysis. Indeed, using 5 mol% of $[\text{Cp}^*\text{RhCl}_2]_2$ and 20 mol% of AgSbF_6 in 1,2-dichloroethane at 100 °C for 24 h, selective C2-amidation of *N*-(2-pyrimidinyl)indoles was performed in moderate to good yields.^[34] (Scheme 5-20)



Scheme 5-20. Rh-catalyzed C2-amidation of *N*-(2-pyrimidinyl)indoles by isocyanates.

The direct access to the class of sulfonyl amides is also a challenging task and can also be performed by the direct directed C-2 selective C-H amidation of indoles using sulfonyl azides. The cobalt- and rhodium-catalyzed versions have been reported by Y. M. Kanai's group and Li's group, respectively. Thus, the catalyzed coupling of sulfonyl azides and *N*-(2-pyrimidinyl)indoles led to the introduction of amide groups at the C-2 position.^[35] (Scheme 5-21)



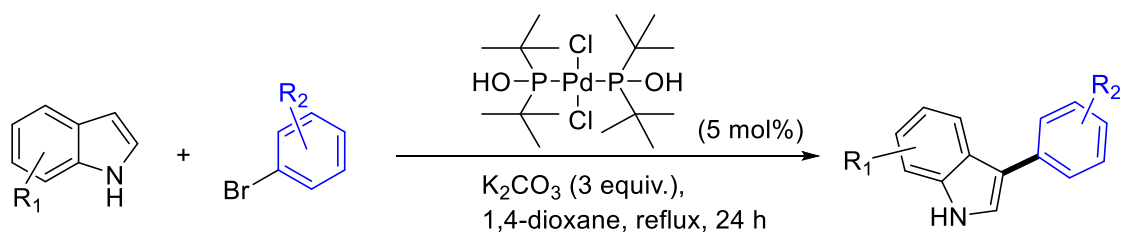
Scheme 5-21. Rhodium- and cobalt-catalyzed C2-amidation of *N*-(2-pyrimidinyl)indoles using sulfonyl azides.

5.2.2. Functionalization at C3

In indole reactivity, one of the most classic reactions involves the electrophilic functionalization at the electron-rich C3 position, the nitrogen activating specifically this position. The major advances in indole chemistry is the transition-metal-catalyzed C–H functionalizations at C3 position via cross coupling transformations. In this paragraph, representative examples of transition metal catalyzed functionalization of the C3 carbon of indole will be discussed.

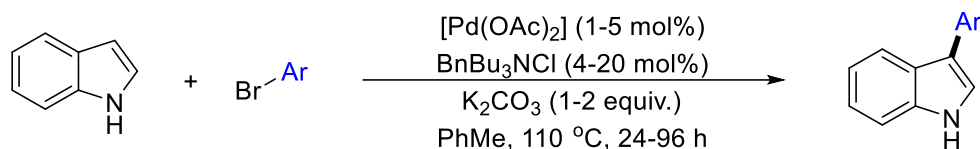
5.2.2.1. Via arylation reactions

R. He and co-workers have described an efficient palladium-catalyzed protocol for the direct C3 arylation of NH-free indoles with bromoarenes as coupling partners. The arylation reaction proceeded in the presence of 5 mol% of palladium phosphinous acid complex and 2 equiv. of K_2CO_3 in refluxing 1,4-dioxane for 24 h and led to the corresponding C3-arylindoles in moderate to good yields.^[36] (Scheme 5-22)



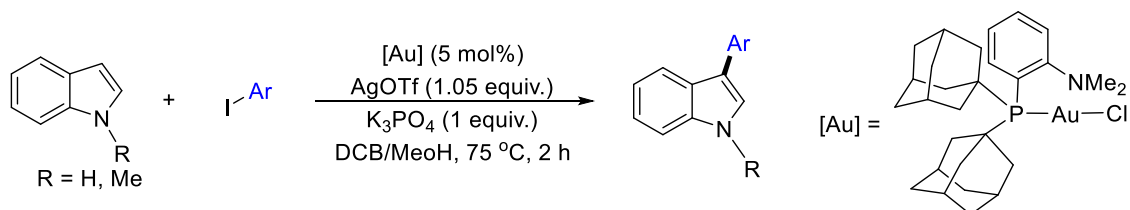
Scheme 5-22. Pd-catalyzed C3-arylation of indoles.

Bellina, Rossi et al. have developed another protocol for palladium-catalyzed direct C3 arylation of NH-free indoles using any types of aryl bromides. Performing the reaction in refluxing toluene in the presence of 1-2 equiv. of K_2CO_3 , 1-5 mol% of $Pd(OAc)_2$ and 4-20 mol% of benzyl(tributyl)ammonium chloride, the arylation took place specifically at the C-3 position with good efficiency.^[37] (Scheme 5-23)



Scheme 5-23. Palladium catalyzed C3-arylation of indoles.

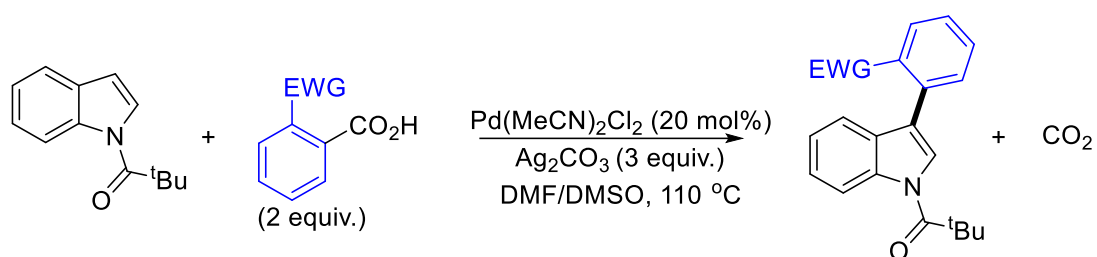
D. Bourissou et al. developed an original gold version of the cross coupling of aryl iodide with indoles leading to C3-arylindoles.^[38] Indeed conducting the reaction with 5 mol% of (Medalpos)AuCl complex, 1.05 equiv. of $AgSbF_6$, 1 equiv. of K_3PO_4 , in *o*-DCB/MeOH (50 : 1) at 75 °C for 2 h, 3-arylindoles were obtained in good to excellent yields.^[38] (Scheme 5-24)



Scheme 5-24. Gold-catalyzed C3-arylation of indoles with aryl iodides.

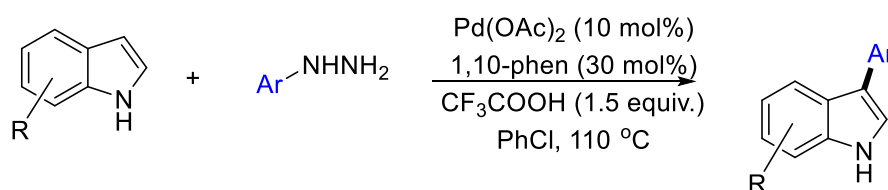
Larrosa and co-workers developed a palladium-catalyzed arylation of *N*-pivaloylindoles using carboxylic acids as cross-coupling partners. Noticeably, using 20 mol% of $Pd(MeCN)_2Cl_2$, 3 equiv. of silver carbonate in the presence of 2 equiv. of

carboxylic acids in a mixture DMF/DMSO at 110 °C for 16 h, C3-arylated indoles were obtained in moderate to good yields. The main limitation of the reaction is the use of electron-deficient ortho-substituted benzoic acids. It was suggested that the double role of silver salt was (i) to oxidize Pd(0) to Pd(II) able to perform the electrophilic palladation of indole [C3-Pd-X] and (ii) to generate *in situ*, via a decarboxylation, an Ar-Ag species able to transmetalate the [C3-Pd-X] species and after reductive elimination generating the arylated compound.^[39] (Scheme 5-25)



Scheme 5-25. Pd/Ag promoted C3-cross coupling of indoles with carboxylic acids.

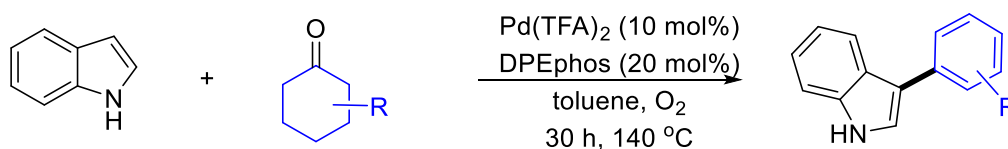
Similarly, starting from arylhydrazines, B. Chen and co-workers have developed a palladium-catalyzed direct denitrogenative C3-arylation of NH-free indoles with arylhydrazines using air as the oxidant. Indeed, using 10 mol% of Pd(OAc)₂, 30 mol% of 1,10-phenanthroline, in the presence of 1.5 equiv. of trifluoroacetic acid at 110 °C in chlorobenzene for 12 h, the C3-arylated derivatives were in moderate to good yields.^[40] (Scheme 5-26)



Scheme 5-26. Pd-catalyzed C3-cross coupling of indoles with carboxylic acids.

G.-J. Deng and co-workers reported an amazing palladium-catalyzed direct arylation which could be done using indoles and cyclohexanones as the coupling partners. Indeed, using 20 mol% of DPEphos [(bis{2-diphenylphosphino}phenyl)ether] and 10 mol% of Pd(TFA)₂ in toluene under atmosphere of oxygen at 140 °C for 30 h, 3-arylindoles were selectively obtained from various cyclohexanones. Such transformation can be

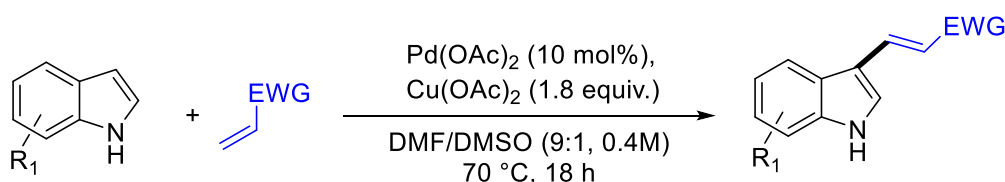
explained first by the formation of 3-(cyclohex-1-yl)indole by reaction of cyclohexanone with indole (in the absence of Pd(TFA)₂), and then by a the palladium-catalyzed dehydrogenation–tautomerization reactions, favored by the presence of oxygen as an efficient hydrogen acceptor.^[41] (Scheme 5-27)



Scheme 5-27. Palladium-catalyzed direct arylation with indoles and cyclohexanones.

5.2.2.2. Via alkenylation reaction

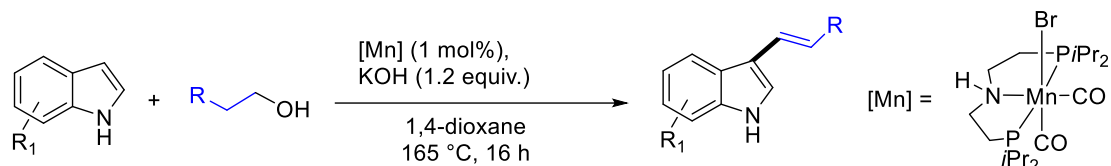
As already mentioned in Scheme 5-9, Gaunt has shown that the nature of the solvent can have also a great influence on the regioselectivity of the alkenylation of unprotected indole starting from alkenes such as acrylic derivatives. When conducting the reaction in DMSO/DMF in the presence of 10 mol% of Pd(OAc)₂ and 1.8 equiv. of Cu(OAc)₂, C3-alkenylated indoles were obtained in good yields.^[23] (Scheme 5-28)



Scheme 5-28. Palladium catalyzed C3-alkenylation of unprotected indoles

Y.-Q. Wang reported similar results with N-free and N-methylindoles using 10 mol% of Pd(OAc)₂, 8 equiv. of TFA in DMSO at 60 °C for 1.5-48 h under oxygen atmosphere.^[42]

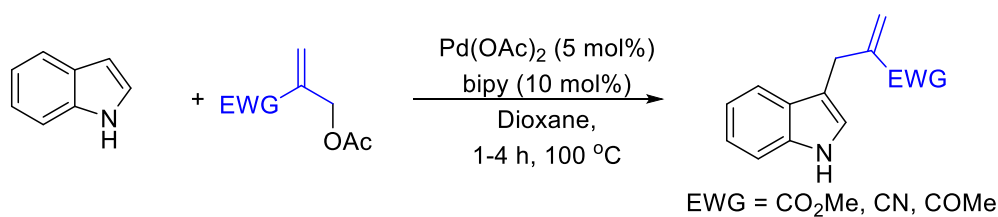
Recently, M. Zhao et al. reported a C3-alkenylation of indoles via a manganese-catalyzed dehydrogenation methodology from 2-arylethanols. Indeed, using of 1 mol% of Macho pincer manganese complex as the catalyst in the presence of 1.2 equiv. of KOH in 1,4-dioxane at 165 °C for 16 h, 3-alkenylindoles were obtained in moderate yields. Noticeably, when starting from primary and secondary benzylalcohols, C3-alkylated indoles were also selectively formed.^[43] (Scheme 5-29)



Scheme 5-29. Manganese catalyzed C3-alkenylation of unprotected indoles using 2-arylethanol.

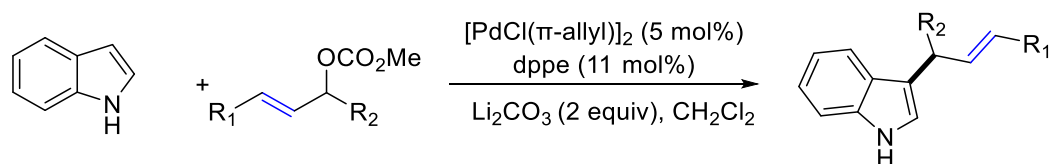
5.2.2.3. Via alkylation reactions

S. Ma and S. Yu investigated the palladium-catalyzed alkenylation of NH-free indoles with 2-acetoxymethyl substituted electron-deficient alkenes. Using 5 mol% of Pd(OAc)₂ and 10 mol% of bipyridine in 1,4-dioxane at 80 °C for 2-3 h, 2-acetoxymethyl acrylic acid methyl ester led selectively to 3-allylindoles were obtained in moderate yields.^[44] (Scheme 5-30)



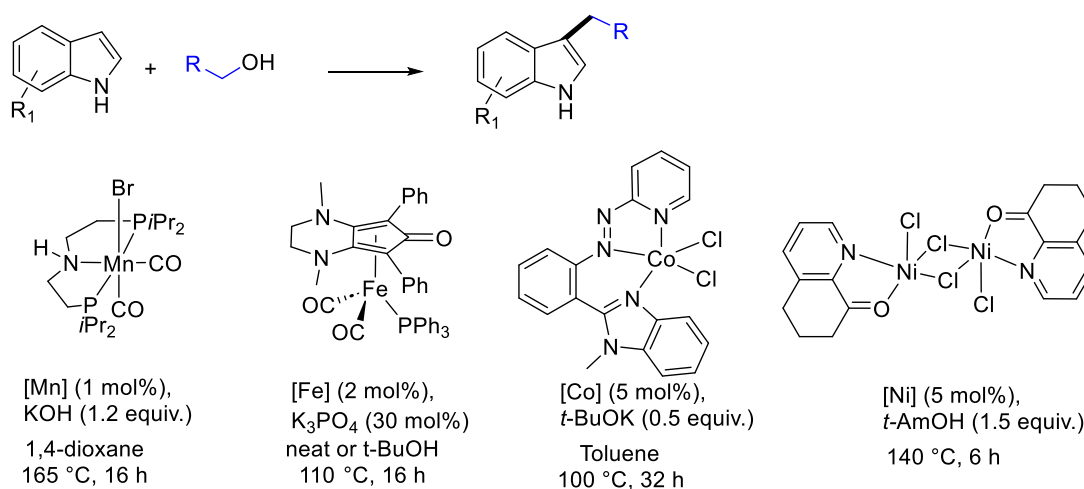
Scheme 5-30. Palladium-catalyzed C3-allylation of indoles.

Similarly, using allylic carbonates as coupling partners, M. Bandini, A. Umani-Ronchi et al. described a Pd-catalyzed alkylation of indoles providing C3-allylindoles in excellent yields. Indeed, using 5 mol% of Pd(Cl(π-allyl))₂ and 11 mol% of dppe as catalyst, in the presence of 2 equiv. of Li₂CO₃ in CH₂Cl₂, C3-allyl derivatives were obtained in good yields. Noticeably, working in THF in the presence of K₂CO₃ or Cs₂CO₃ promoted the N-allylation.^[45] (Scheme 5-31)



Scheme 5-31. Palladium-catalyzed C3-allylation of indoles.

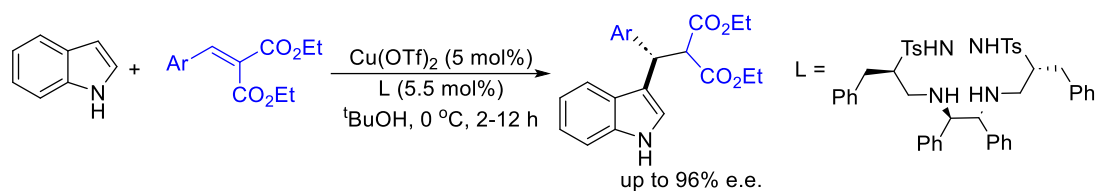
C3-Alkenylation of indoles can be also performed starting from benzyl alcohols as already mentioned in Scheme 28 with manganese macho type complexes.^[43] Similarly, L. Jin reported a nickel-catalyzed C3-alkylation of indoles with primary and secondary alcohols via a borrowing hydrogen strategy.^[46] Using 5 mol% of a binuclear nickel complex ligated by tetrahydroquinolin-8-one ligand, 1.5 equiv. of *t*-Am-OK at 150 °C for 12 h, various benzyl and aliphatic alcohols were evaluated and led to the selective C3 alkylation in moderate to good yields. (Scheme 5-32)



Scheme 5-32. Earth-abundant transition metal catalyzed C3-alkylation of unprotected indoles using benzyl and aliphatic alcohols.

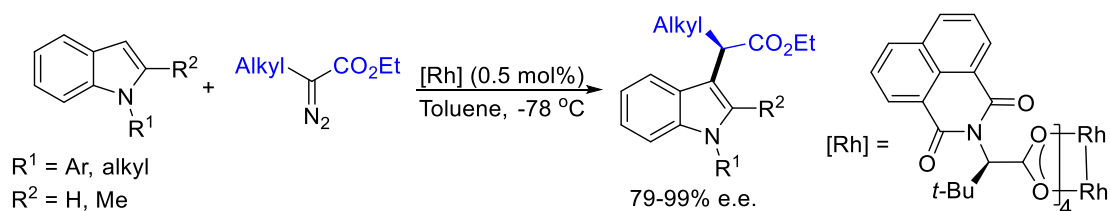
Similarly, Samata reported a cobalt version of such C3-alkylation of indoles with alcohols via a borrowing hydrogen strategy using an azo-benzimidazole containing cobalt complex (5 mol%) with 0.5 equiv. of *t*-BuOK in toluene at 100 °C for 32 h.^[47] Renaud also reported the use of the Knölker type iron catalyst for such transformation.^[48]

C3-Alkylation of indoles can be also performed in an enantioselective fashion, as illustrated in the two following examples. Wan and co-workers developed an efficient Friedel-Crafts alkylation of arylidene malonates promoted by a catalytic system based on 5 mol% Cu(OTf)₂ and 5.5 mol% of a chiral bis-sulfonamide diamine ligand. C3-alkylated indoles were obtained in good yields and with e.e. up to 96%.^[49] (Scheme 5-33)



Scheme 5-33. Copper-catalyzed Friedel-Crafts C3-alkylation of indoles with arylidene malonates.

Another example of C3-enantioselective C-H functionalization of indoles was described by J.-H. Li's group using rhodium catalysts. Indeed, with 0.5 mol% of the $\text{Rh}_2(\text{SNTTL})_4$ catalyst, diazoesters can react with indoles at C3 position to provide α -alkyl- α -indolylacetates in good yields and up to 99% e.e.^[50] (Scheme 5-34)

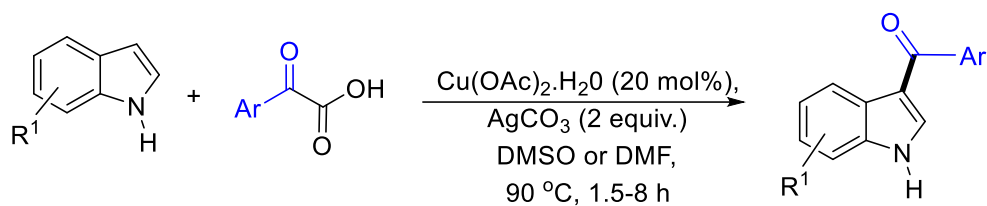


Scheme 5-34. Rhodium-catalyzed C3-alkylation of indoles with diazoesters.

5.2.2.4. Acylation

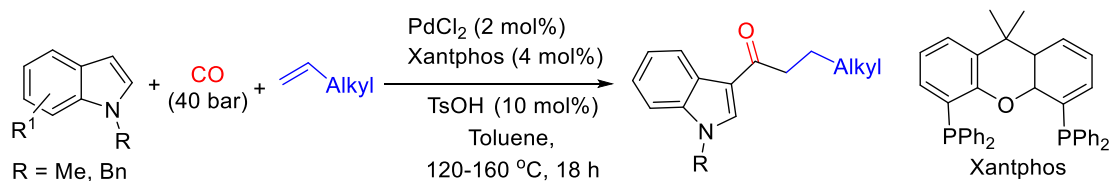
The most classic methods for the preparation of 3-acylindoles are Friedel–Crafts reaction, Vilsmeier–Haack reaction, and the reaction of indole with acyl chlorides. Nevertheless, in recent years, their synthesis received attention, mainly through transition metal catalysis.

In 2014, Z. Zhang developed a Cu-catalyzed decarboxylative C3-acylation of NH-free indoles using α -oxocarboxylic acids as acylating agents.^[51] Using 20 mol% of $\text{Cu}(\text{OAc})_2 \cdot \text{H}_2\text{O}$ in the presence of 2 equiv. of Ag_2CO_3 in DMSO or DMF at 90 °C, for 1.5–8 h, under air, the corresponding 3-aryl-indoles were obtained in moderate to good yields. (Scheme 5-35)



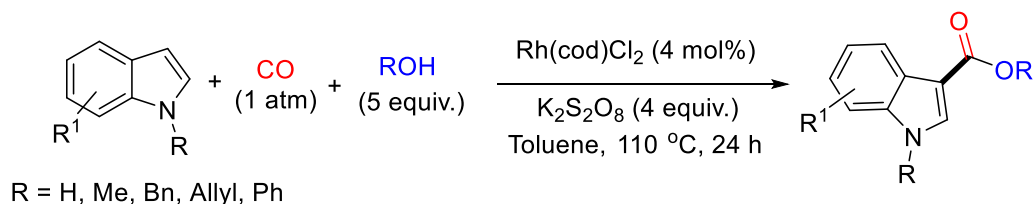
Scheme 5-35. Cu-catalyzed decarboxylative C3-acylation of indoles using α -oxocarboxylic acids.

Another methodology to introduce a CO functionality at C3 of indole is the transition catalyzed carbonylative transformation. M. Beller et al. have shown that the selective C3-acylation of N-protected indoles can be performed via a palladium-catalyzed carbonylation in presence of olefins. Indeed, using 2 mol% of PdCl₂, 4 mol% of Xantphos, 10 mol% of *p*-TsOH under 40 bar of CO in toluene at 120-160 °C for 18 h, selective C3 vs C2 acylation were performed with N-methyl- and N-benzyl-indoles (C3:C2 from 20:1 to 50/1).^[52] (Scheme 5-36)



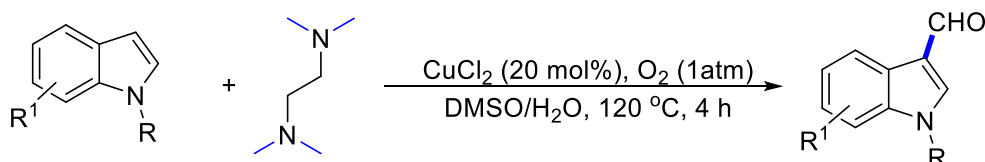
Scheme 5-36. Palladium-catalyzed carbonylation of indoles in presence of olefins.

F. Li and co-workers described a Rh-catalyzed direct carbonylation of indoles in the presence of alcohols to form selectively indole-3-carboxylates. Under 1 atm of CO, with of [Rh(cod)Cl₂]₂ as the catalyst (4 mol%), K₂S₂O₈ as the oxidant (4 equiv.) and an appropriate aliphatic alcohol (5 equiv.), indoles led to indole-3-carboxylates in good to excellent yields.^[53] (Scheme 5-37)



Scheme 5-37. Rh-catalyzed direct carbonylation of indoles with aliphatic alcohols.

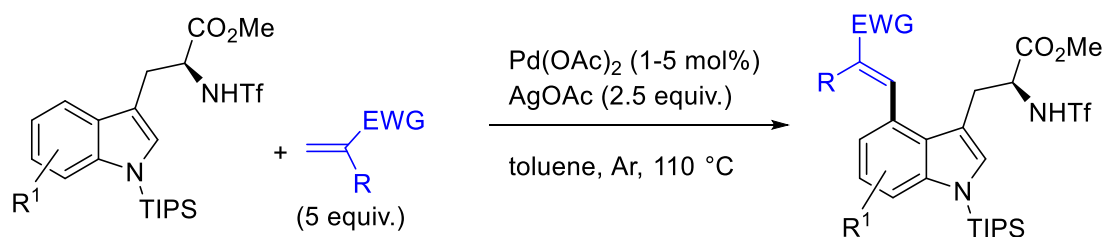
J. Cheng co-workers developed an original copper-catalyzed formylation reaction of N-protected indoles using TMEDA (tetramethylethylenediamine) as C1 source. Indeed, working under oxygen atmosphere, N-protected indoles reacted with TMEDA in the presence of 20 mol% of CuCl₂ in a mixture DMSO/water at 120 °C for 4 h. The corresponding 3-formylindoles were obtained in moderate to excellent yields with a good functional group tolerance.^[54] (Scheme 5-38)



Scheme 5-38. Copper catalyzed C3-formylation of N-protected indoles with TMEDA.

5.2.3. Functionalization at C4

Due to the higher reactivity of the C3 position, the C4 position of indoles has been accessed almost exclusively through the blocking of the C3 position. This would then make the C4 position the next most electron-rich carbon center on the indole structure. Y. Jia and co-workers described the first Pd-catalyzed method for the direct olefination at the C4 position of the indole moiety of tryptophan derivatives. The reaction was carried out with 1-5 nmol% of Pd(OAc)₂ in the presence of 2.5 equiv. of AgOAc in toluene at 110 °C. Notably, the N position was protected with a TIPS group.^[55] (Scheme 5-39)

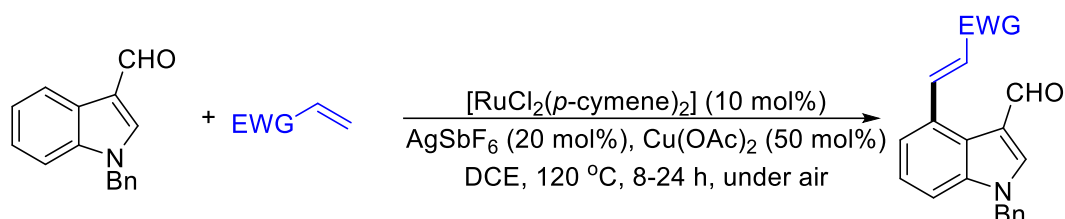


Scheme 5-39. Pd-catalyzed direct olefination at the C4 position of tryptophan derivatives.

V. Lanke and K. R. Prabhu described a ruthenium-catalyzed alkenylation of indoles by employing a formyl as directing group, in order to perform the reaction at the C4

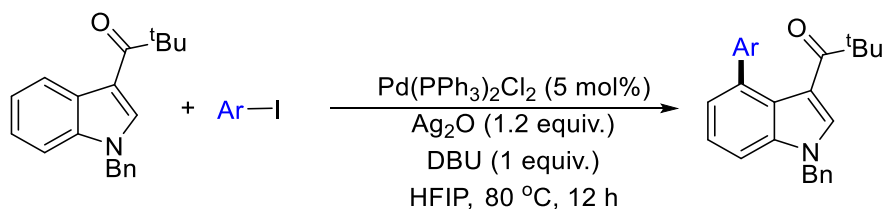
position. Notably, the indoles have also to be protected at the N position. The reaction took place using 10 mol% of $[\text{RuCl}_2(p\text{-cymene})_2]$, 20 mol% of AgSbF_6 , 50 mol% of $\text{Cu}(\text{OAc})_2$ in 1,2-dichloroethane at 120 °C for 8-24 h under air. ^[56]

Similarly, 3-thioether and 3-ester functionalized N-protected indoles can be alkylated when using $[\text{Cp}^*\text{RhCl}_2]_2/\text{AgSbF}_6$ based catalyst in the presence of 1 equiv. of $\text{Cu}(\text{OAc})_2$.^[57,58] (Scheme 5-40)



Scheme 5-40. Ru-catalyzed direct olefination at the C4 position of N-benzyl-3-formylindoles.

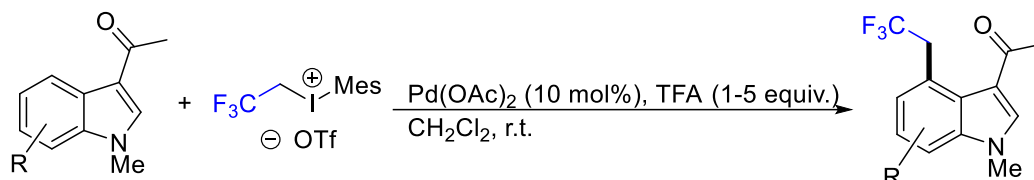
Arylation can be also performed at the position C4 as demonstrated by Z. Shi's group *via* a direct Pd-catalyzed selective C4- arylation of N-benzy-3-pivaloyl-indoles by aryl iodides. In the presence of 5 mol% of $\text{Pd}(\text{PPh}_3)_2\text{Cl}_2$ as the catalyst, 1.2 equiv. of Ag_2O as the oxidant and 1 equiv. of DBU in hexafluoroisopropanol (HFIP) at 80 °C for 12 h, the 4-arylated products were obtaining moderate to high yields.^[59] (Scheme 5-41) Noticeably, the pivaloyl group at C3 position can be removed by a TsOH/glycol treatment. Yu and co-workers reported similar functionalization using palladium catalyst for the C4-arylation of N-tosyl-3-formylindole.^[60]



Scheme 5-41. Pd-catalyzed direct arylation at the C4 position of N-benzy-3-pivaloyl-indoles.

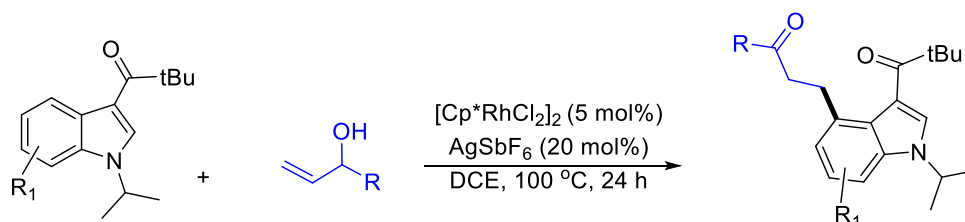
Alkylation can be also done at the position C4 as reported by Z. Shi's group for the C4-fluoroalkylation of N-methyl-3-acetyl-indoles with iodonium triflate salts through

palladium-catalyzed C–H activation with 10 mol% of Pd(OAc)₂ in the presence of 1-5 equiv. of TFA at rt.^[61] (Scheme 5-42) Moderate to good yields and good functional group tolerance were observed with ketones as directing groups at C3 and poor yields with aldehydes.



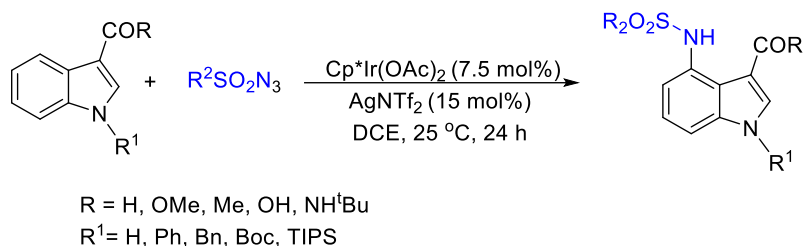
Scheme 5-42. Palladium- catalyzed C4- fluoroalkylation of N-methyl-3-acetyl-indoles.

J. T. Yu described in 2020 a rhodium(III)-catalyzed C4-alkylation of N-isopropyl-3-pivaloyl-indoles with allylic alcohols. With 5 mol% of [Cp**RhCl*]₂, 20 mol% of AgSbF₆, 30 mol% of Cu(OAc)₂ in DCE at 40 °C for 48 h, the corresponding β-indolyl ketones were obtained in moderate to good yields.^[62] (Scheme 5-43) Using similar conditions [3 mol% of [Cp**RhCl*]₂, 50 mol% of Cu(OAc)₂ in THF at 50 °C] T. Punniyamurthy also obtained corresponding β-indolyl ketones, but starting from 1-substituted cyclopropanols.^[63]



Scheme 5-43. Rhodium- catalyzed C4-alkylation of N-isopropyl-3-pivaloyl-indoles.

In another hand, J. You's group described a direct regioselective C4-amidation of N-protected indoles bearing a carbonyl or carboxyl group in C3 position using sulfonyl azides as coupling partners. With 7.5 mol% of Cp**Ir*(OAc)₂ as the catalyst, 15 mol% of AgNTf₂ as the oxidant in DCE at 25 °C, a variety of C4 -amidated indoles were prepared.^[64] (Scheme 5-44)

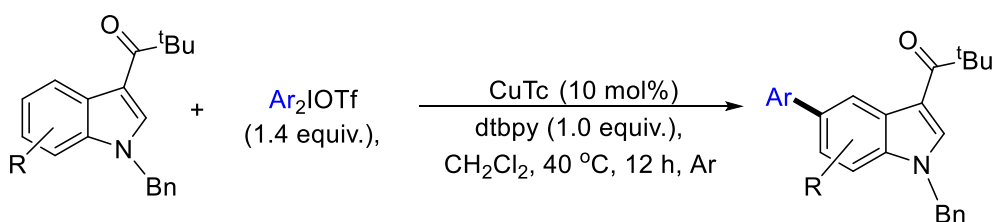


Scheme 5-44. Ir-catalyzed C4-amidation of N-protected indoles bearing a carbonyl or carboxyl group in C3 position.

5.2.4. Functionalization at C5

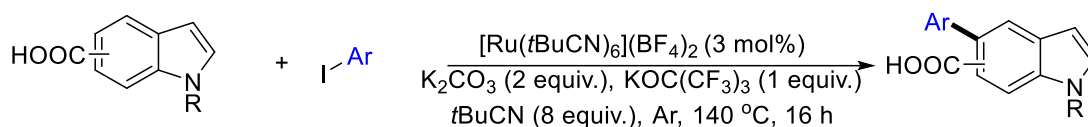
The C5 position of indoles lies remotely from a possible directing group, which makes the remote C5–H functionalization of indole one of the most sparing observed scenarios. In this context, there have been incredibly limited reports showing conditions allowing for C5 selectivity.

Z. Shi's group described a direct Cu-catalyzed C5-arylation of N-benzyl-3-pivaloyl-indoles and diaryliodonium triflate salts Ar_2IOTf using 10 mol% of CuTc (copper(I) thiophene-2-carboxylate) in association with 1 equiv. of dtbpy (2,6-di-*tert*-butylpyridine) as the catalyst in CH_2Cl_2 at 40 °C for 12 h, in oxidant free conditions, thus leading to the corresponding products in moderate to high yields.^[65] (Scheme 5-45)



Scheme 5-45. Cu-catalyzed C5-arylation of N-benzyl-3-pivaloyl- indoles.

In a work dealing with ruthenium-catalyzed arylation of benzoic acids, 4-, 5-, 6-, and 7-indole carboxylic acids, Larrosa et al. demonstrated that the reaction took place exclusively at the carboxylic acid ortho position(s), without any side-arylation by-products at either C2 or C3 positions. Noticeably, they succeeded to perform C-5 arylation starting from N-methyl 4- and 6-indole carboxylic acids.^[66] (Scheme 5-46)

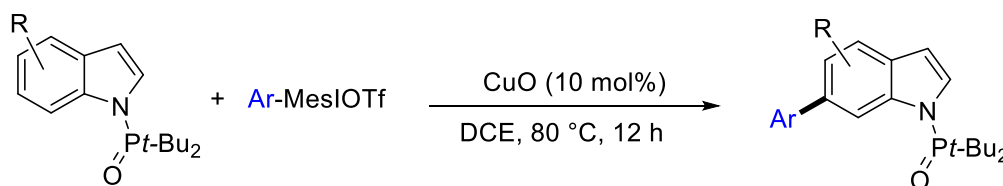


4- and 6-indole carboxylic acids

Scheme 5-46. Ruthenium-catalyzed C5-arylation of benzoic acids, 4- and 6-indole carboxylic acids.

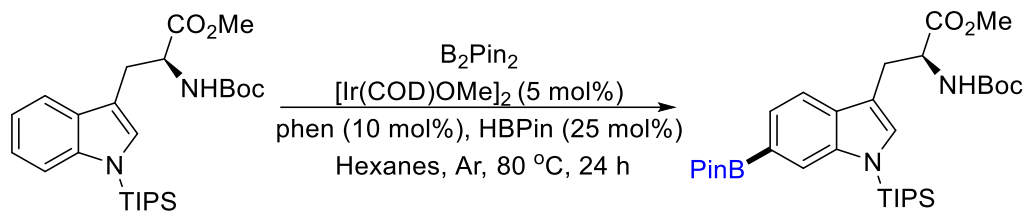
5.2.5. Functionalization at C6

Transition metal-regioselective C6 functionalization is also a challenging target and scarcely reported. In 2009, Gaunt's group has reported an example of C6-arylation of indoline with diaryliodonium salt using copper catalyst.^[67] Based on such pioneering work, Shi developed a copper catalyzed C6 selective arylation of N-(P(O)*t*Bu₂) indoles with diaryliodonium triflates, just using 10 mol% of CuO in DCE at 80 °C for 12h.^[68] (Scheme 5-47) The selectivity was explained by the coordination of the copper intermediate [Cu-Ar] to the oxygen of the N-*t*Bu₂PO which was then transferred to the C6 position of indole *via* a Heck-type four-membered-ring transition state.



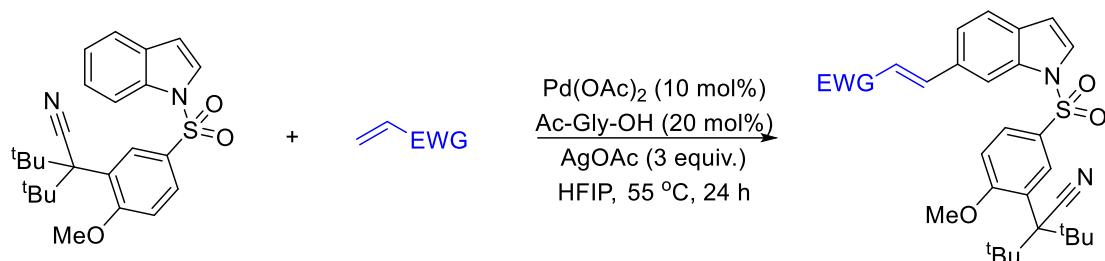
Scheme 5-47. Copper-catalyzed C6-arylation of N-(P(O)*t*Bu₂) indoles.

Baran and co-workers reported the remote C6-selective C–H borylation of tryptophan derivatives utilizing iridium chemistry. In this reaction, a N-TIPS group was employed as the directing group to control the reaction selectivity for the synthesis of C6-functionalized indoles. Using 5 mol% of [Ir(COD)OMe]₂, 10 mol% of 1,10-phenanthroline, 25 mol% of HBpin in the presence of 4 equiv. of B₂Pin₂ in hexanes at 80 °C for 24 h, C6/C5-Bpin coupling products were obtained in a ratio 8:1. The reaction was extended to N-TIPS-3-substituted indoles with ratios C6/C5-Bpin coupling products from 6:1 to 14:1.^[69] (Scheme 5-48)



Scheme 5-48. Iridium C6-selective C–H borylation.

In his continuous work to develop methodologies for the *meta*-selective C–H functionalization using U-shaped nitrile-containing template, J.-Q. Yu has developed Pd(II)-catalyzed C6-olefination, and arylation of indolines. Using 10 mol% of Pd(OAc)₂, 20 mol% of N-acetylglycine (Ac-Gly-OH), 3 equiv. of AgOAc in hexafluoroisopropanol at 55 °C for 24 h, olefination can be selectively performed at C6 position. Notably, when performing the reaction with various arylboronic acid pinacol esters, C5-arylated indolines were obtained, with a slight modification of the conditions adding 2.5 equiv. of CsF and 3 equiv. of NBu₄PF₆ and conducting the reaction at 100 °C for 36 h.^[70] (Scheme 5-49)

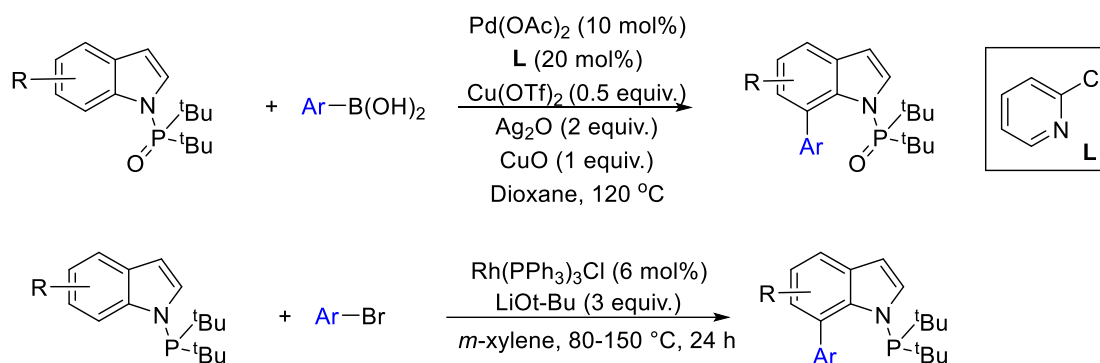


Scheme 5-49. Pd(II)-catalyzed C5-olefination and arylation, of indolines using a U-Shaped Template.

5.2.6. Functionalization at C7

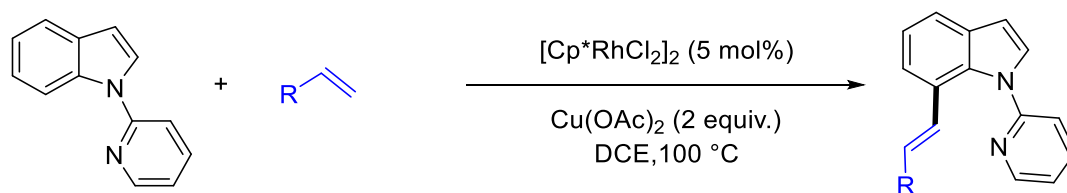
In comparison to C5 and C6 functionalization, there were more reports dealing with the C7 one. Z. Shi and co-workers described a methodology involving the N-TBPO (N-P(O)^tBu₂) directing group to favor the C7-arylation. Thus, they performed a Pd-catalyzed C7-arylation *via* a coupling of indoles with arylboronic acids. In the presence of 10 mol% of Pd(OAc)₂, 20 mol% of 2-chloropyridine, 0.5 equiv. of Cu(OAc)₂, 2 equiv. of Ag₂O, 1 equiv. of CuO in 1,4-dioxane at 120 °C, the C7-arylated compounds were

obtained in moderate yields.^[71] In a similar fashion, starting from *N*-*P*^tBu₂ indoles, arylation took place on the C7 position when performing the reaction using the Wilkinson catalyst, RhCl(PPh₃)₃ (6 mol%) in the presence of 3 equiv. of LiO^t-Bu in *m*-xylene at 80-150 °C.^[72] (Scheme 5-50)



Scheme 5-50. Pd- and Rh-catalyzed C7-arylation of indoles

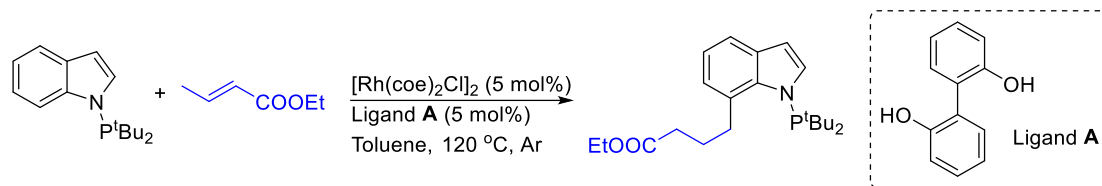
Alkenylation at C7 position can be also performed. T.-P. Loh has shown that using 4.5-10 mol% of [Cp^{*}RhCl₂]₂, 2 equiv. of Cu(OAc)₂ in DCE at 100 °C, *N*-(2-pyridinyl) indoles can be alkenylated using activated olefins.^[73] (Scheme 5-51) Similar reactions were also performed with *N*-CONMe₂ indoles at palladium [10 mol% of Pd(OAc)₂, 1,4-benzoquinone (2 equiv.), PTSA (1 equiv.) in AcOH at 40°C],^[74] or ruthenium [Ru(OAc)₂-*p*-cymene (10 mol%), AgSbF₆ (20 mol%), Cu(OAc)₂ (2 equiv.) in TFE at 40 °C].^[75]



Scheme 5-51. Rh-catalyzed C7-alkenylation of indoles.

In 2018, A. Borah and Z. Shi have also shown that C7-alkylation of *N*-*P*^tBu₂ indoles can be promoted in a similar way using a rhodium-catalyzed hydroarylation of activated olefins, using 5 mol% of [Rh(coe)₂Cl]₂, 5 mol% of 2,2'-biphenol in toluene at 120 °C.^[76] Interestingly, this catalytic system can be applied to remote terminal hydroarylation

of activated olefins through long-range deconjugative isomerization of the C=C bond.
(Scheme 5-52)

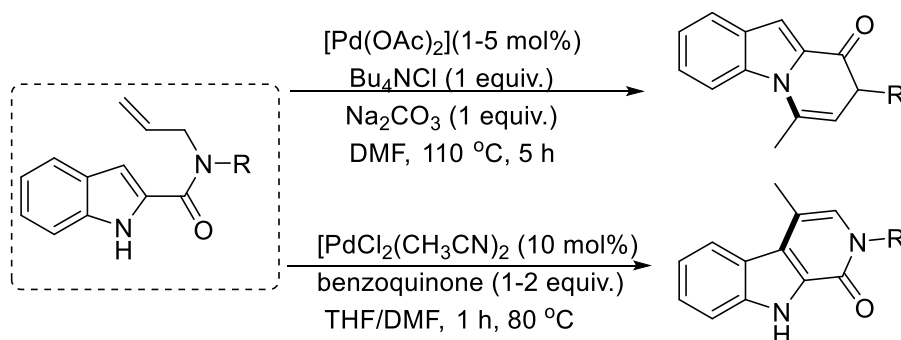


Scheme 5-52. Rhodium catalyzed C7-hydroarylation.

5.2.7. Annulation from functionalized indoles

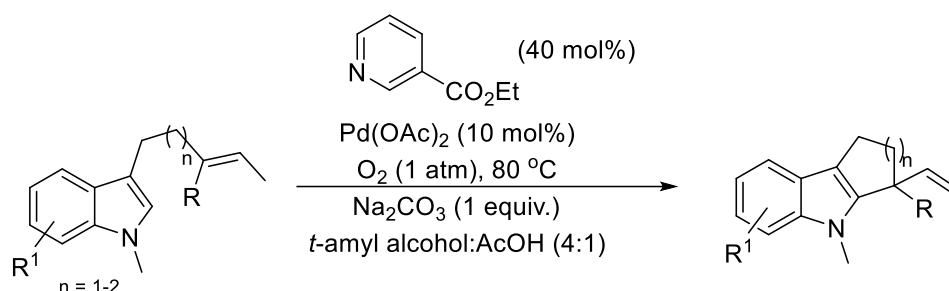
With the development of selective transition metal-catalyzed indole functionalization, in particular on C4, C5 C6 and C7 positions, various functionalized indoles were synthesized with potential for further cyclization. A few representative examples of cyclization are described hereafter.

Numerous examples of intramolecular annulation involving C2 or C3-functionalized indoles were reported. With a functional group in the C2 position, for example, Brogginì and co-workers have performed the intramolecular annulation of indole-2-carboxamides. Depending of the reaction conditions, they obtained different selectivities: using 1.5 mol% of Pd(OAc)₂ in the presence of 1 equiv. of Bu₄NCl and 1 equiv. of Na₂CO₃ in DMF at 110 °C, the annulation took place on the nitrogen of the indole ring affording pyrazino[1,2-*α*]indoles in moderate yields. By contrast with 10 mol% of PdCl₂(MeCN)₂ and 1-2 equiv. of benzoquinone in THF/THF at 80 °C, *β*-carbolines were obtained with yields up to 98%.^[77] (Scheme 5-53)



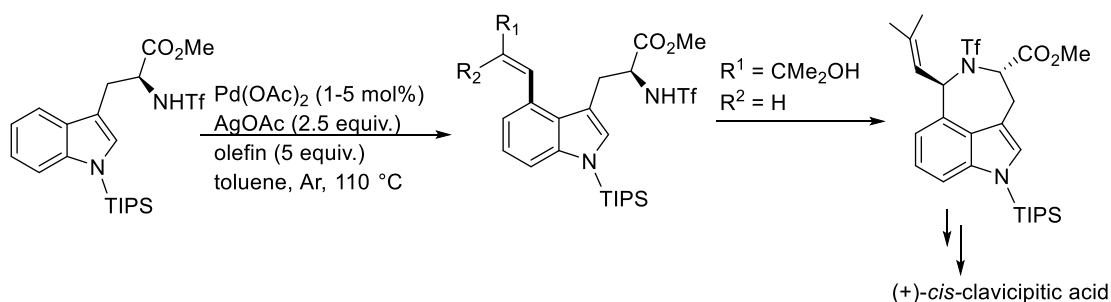
Scheme 5-53. Selectivity in Pd-catalyzed annulation indole-2-carboxamides.

With functional groups such as remoted alkenyl groups at the C3 position, for example, Stoltz and co-workers described an early example of intramolecular indole annulation leading to annulated tri- and tetracyclic indoles. Indeed, conducting the reaction of *N*-methyl-3-alkenylindoles with 10 mol% of Pd(OAc)₂ in the presence of 40 mol% of ethyl nicotinate and 1 equiv. of Na₂CO₃ in *tert*-amylalcohol at 80 °C, under an oxygen atmosphere, both 5- and 6-membered fused rings were obtained in moderate to good yields, the annulation taking place at C2 position. [78] (Scheme 5-54)



Scheme 5-54. Pd-catalyzed annulation of *N*-methyl-3-alkenylindoles

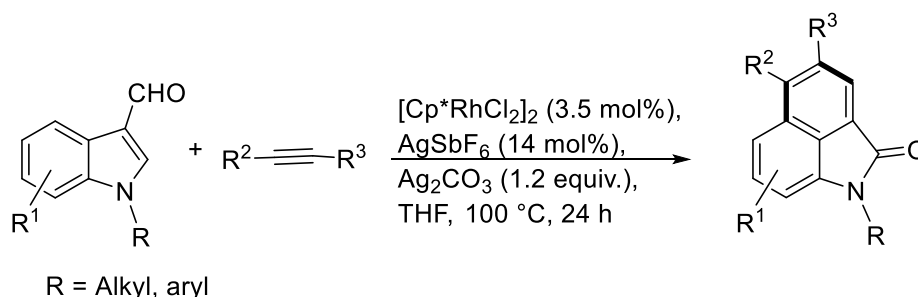
With functional groups at the C4 position, Y. Jia et al. developed a Pd-catalyzed direct C4-alkenylation of *N*-TIPS-tryptophan derivatives leading to the corresponding C4-alkenyl derivatives using 1-5 mol% of Pd(OAc)₂ in the presence of 2.5 equiv. of AgOAc in toluene at 110 °C. Noticeably when performing the reaction with 2-methyl-3-buten-2-ol, an additional intramolecular annulation took place thus leading to a precursor of clavicipitic acid. [79] (Scheme 5-55)



Scheme 5-55. Pd-catalyzed C4-alkylation/annulation for clavicipitic acid preparation.

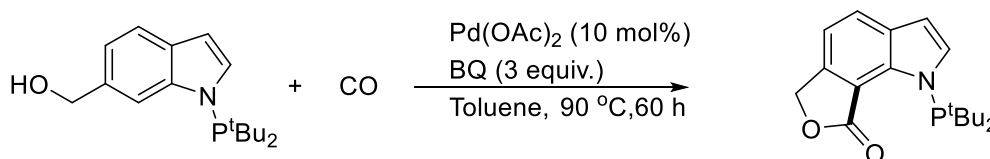
Another representative example was described by J. You et al. Benzo-fused oxindoles, were obtained *via* a rhodium-catalyzed reaction of 3-formyl- and 3-keto-indoles with alkynes, using 3.5 mol% of [Cp**Rh*Cl₂]₂, 14 mol% of AgSbF₆, 1.2 equiv. of Ag₂CO₃,

in THF at 100 °C. The new fused aromatic ring resulted from the sequential C4-fontionalization, cyclization and aromatization.^[80] (Scheme 5-56)



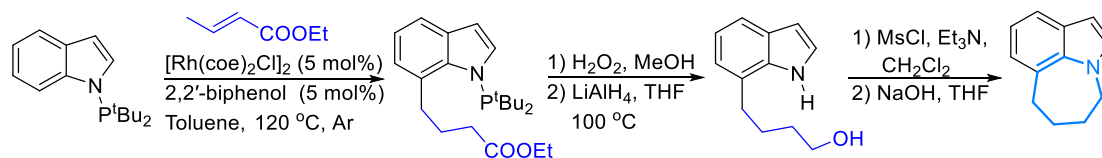
Scheme 5-56. Rh-catalyzed of 3-formyl- and 3-keto-indoles with alkynes for benzo-fused oxindole synthesis.

With functional groups such as alcohol group at the C6 position, for example, Z. Shi and co-workers reported a C7-selective lactonization of *N*-P^tBu₂-6-hydroxymethyl-indoles, using 10 mol% of Pd(OAc)₂, 3 equiv. of benzoquinone in toluene at 90 °C under pressure of CO.^[81] (Scheme 5-57)



Scheme 5-57. Pd-catalyzed C7-lactonization of *N*-PtBu₂-6-hydroxymethyl-indoles.

In 2018, In their contribution dealing with C7-alkenylation of *N*-P^tBu₂ indoles via rhodium-catalyzed hydroarylation of activated olefins, Z. Shi's group also mentioned an example of synthesis of an indole-annulated seven-membered ring compound by intramolecular 1,7-annulated multi-step reaction.^[76] (Scheme 5-58)



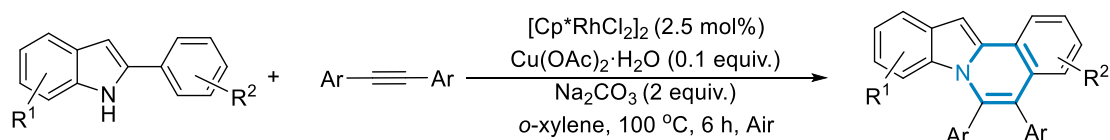
Scheme 5-58. Synthesis of an indole-annulated seven-membered ring compound.

5.3. *NH*-indole-directed, transition metal catalyzed C-H bond activations

The former examples illustrated that the C–H activation is achieved regioselectively either *via* a reactive metal center or through a chelation assistance thanks to a directing group. These methodologies usually required the protection of the N atom or its transformation to a directing group. Thus, the strategy using the unprotected *NH*-indole as the intrinsic directing group turned out to be a good alternative for the rapid and efficient construction of diverse indole-fused heterocyclic scaffolds which then can avoid the installation and removal of directing groups. Therefore, transition metal catalyzed C-H functionalization/intramolecular cyclization cascade reactions have become in the recent years one of the most reliable tools for the efficient preparation of fused tetracyclic indoles. In the past decade, few strategies of *NH*-indole-directed oxidative annulations of 2-arylindoles with different coupling partners, such as alkynes, halides, alkenes, carbon monoxide, were developed to build indole-containing fused tetracyclic skeletons.

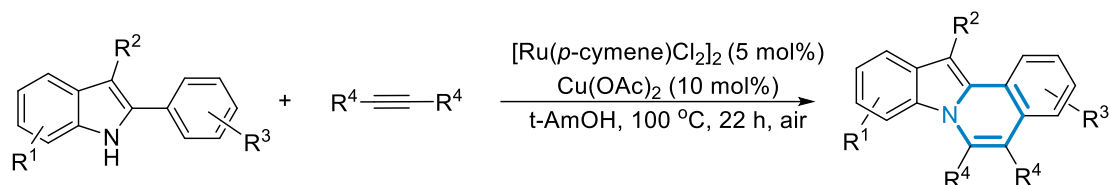
5.3.1 Approaches of *NH*-indole-directed, transition metal catalyzed C-H bond activations

In 2010, T. Satoh, and M. Miura reported the synthesis of indolo[2,1-*a*]isoquinoline derivatives which has been achieved by the rhodium-catalyzed aerobic oxidative coupling/cyclization of 2-phenylindoles with alkynes. Indeed, using 2.5 mol% of [Cp**RhCl*₂]₂, 10 mol% of Cu(OAc)₂·H₂O, 2 equiv. of Na₂CO₃, in *o*-xylene at 100 °C.^[82a] (Scheme 5-59) Using 2.5 mol% of [Cp**RhCl*₂]₂, 1 equiv. of *n*-Bu₄OAc, in xylene at 80 °C under air, Q. Huang described similar results.^[82b] (Scheme 5-59)



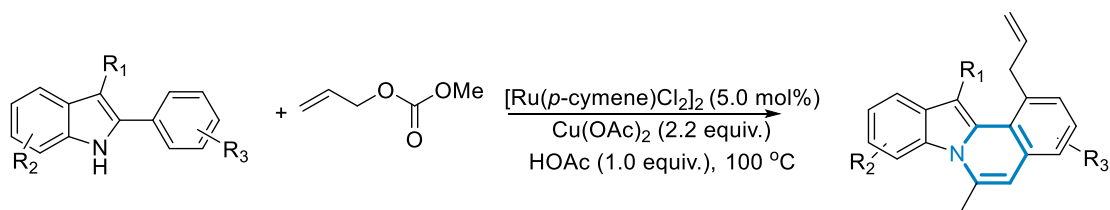
Scheme 5-59. Rhodium-catalyzed oxidative annulation/ cyclization reaction.

In 2012, Ackermann's group has reported the first ruthenium-catalyzed version of such oxidative C–H/N–H bond annulation of 2-arylimidoles and alkynes using 5 mol% of $[\text{Ru}(p\text{-cymene})\text{Cl}_2]$ and 10 mol% of $\text{Cu}(\text{OAc})_2 \cdot \text{H}_2\text{O}$ in *t*-AmOH at 100 °C under ambient air as the sacrificial oxidant to produce pyrrolo[2,1-*a*]isoquinolines.^[83] (Scheme 5-60)



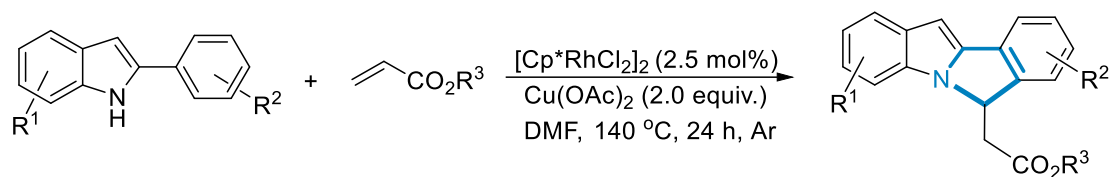
Scheme 5-60. Ruthenium-Copper co-catalyzed oxidative C–H/N–H annulation.

Oxidative C–H/N–H annulation can be also performed with olefins. In 2017, Y.-Q. Xia and L. Dong reported a facile one-pot process synthesizing indolo[2,1-*a*]isoquinoline based derivatives via a Ru-catalyzed tandem C–H allylation and oxidative annulation of 2-phenylimidoles with allyl methyl carbonate, using 5 mol% of $[\text{Ru}(p\text{-cymene})\text{Cl}_2]$ and 2.2 equiv. of $\text{Cu}(\text{OAc})_2 \cdot \text{H}_2\text{O}$ in acetic acid at 100 °C. The pathway of this reaction first produced a diallylated intermediate via the *o,o*-diallylation of the C2-aromatic substituent, and then one of the allyl groups underwent intramolecular cyclization to generate indolo[2,1-*a*]isoquinoline skeletons.^[84] (Scheme 5-61)



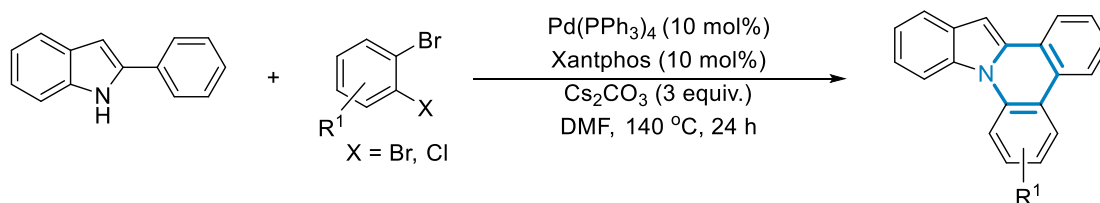
Scheme 5-61. Ru-catalyzed tandem C–H allylation and oxidative annulation of 2-phenylimidoles with allyl carbonates.

In 2017, Q. Huang's group has developed an efficient and straightforward methodology for the preparation of biologically useful 6*H*-isoindolo[2,1-*a*]indoles from 2- or 7-phenyl-NH-indoles and activated alkenes, using 2.5 mol% of $[\text{Cp}^*\text{RhCl}_2]_2$, 2 equiv. of $\text{Cu}(\text{OAc})_2$ in DMF at 140 °C under air.^[85] (Scheme 5-62)



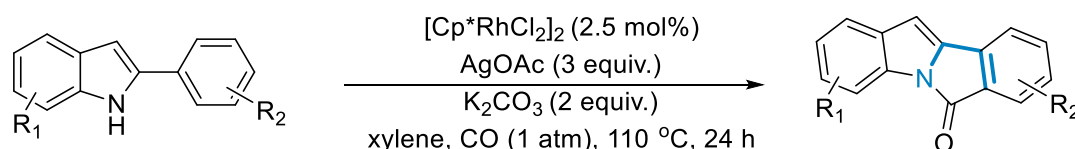
Scheme 5-62. Rh-catalyzed oxidative annulation of 2-phenyl-NH-indoles with alkenes.

Oxidative C–H/N–H annulation can be also performed with 1,2- dihaloarenes. Indeed, J. You and co-workers reported a palladium-catalyzed tandem N–H/C–H arylation starting from 2-aryl-indoles and 1,2- dihaloarenes using 10 mol% of Pd(PPh₃)₄, 10 mol% of Xantphos, 3 equiv. of Cs₂CO₃ in DMF at 140 °C. Two examples of N-heterocycle-fused phenanthridines were obtained in 75-82% yields.^[86] (Scheme 5-63)



Scheme 5-63. Pd-catalyzed tandem N–H/C–H arylation of 2-aryl-N-heteroarenes with 1,2-dihaloarenes.

Oxidative C–H/N–H annulation can be also performed under CO pressure. In 2016, Q. Huang's group reported an efficient Rhodium-catalyzed cyclocarbonylation of 2-arylindoles with carbon monoxide via N–H bond cleavage and subsequent C–H bond cleavage to prepare 6*H*-isoindolo[2,1-*a*]indol-6-ones. Conducting the reaction with 2.5 mol% of [Cp*RhCl₂]₂, 3 equiv. of AgOAc, 2 equiv. of K₂CO₃ in xylene at 110 °C under 1 atm of CO.^[87] (Scheme 5-64)



Scheme 5-64. Rh-catalyzed cyclocarbonylation of 2-arylindoles with carbon monoxide.

5.4. Conclusions and perspectives of the second part

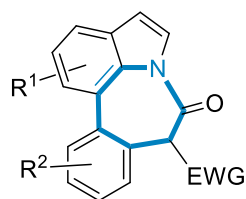
This introductory chapter, thanks to selected examples, demonstrated the highly versatile chemistry of indoles *via* transition-metal catalyzed C–H functionalization developed over few past decades. Taking advantage of the inherent reactivity of the pyrrole ring and thanks to the use of directing groups, the selective C–H functionalization at C2 and C3-positions of indoles were widely reported. Nevertheless, in this area, the challenges are still associated to the development of efficient methodologies to enable selective C–H functionalization at C4–C7 positions, which can be performed via transition metal C–H activation/functionalization, with or without directing groups.

Noticeably, it was also shown that the access to the 1,7 fused indoles can be built through *NH*-indole-directed, transition metal catalyzed C–H bond activations, such development of simple and efficient new strategies to construct such scaffolds being still in high demand and of great significance.

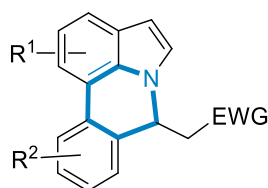
Inspired by those previous works and in the line of the work already developed in the group of Q. Huang in Fujian Normal University, the second part of my PhD project is devoted to the development of new protocols to access 1,7 fused tetracyclic indoles. To build such 1,7 fused tetracyclic indole motifs, it was chosen to start from 7-aryl-1*H*-indole derivatives and perform annulation reactions with different coupling partners, such as diazo compounds, alkynes and alkenes through Rh-catalyzed oxidative annulations strategies.

Thus, the following 3 chapters will describe those works.

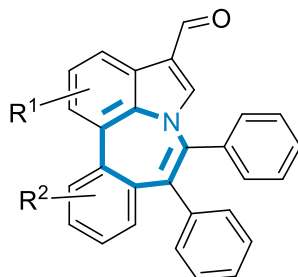
The **Chapter 6** will be devoted to the synthesis of seven-membered via rhodium-azepino[3,2,1-*hi*]indoles catalyzed regioselective C–H activation/1,8-diazabicyclo-[5.4.0]undec-7-ene-catalyzed intramolecular amidation of 7-phenylindoles in one pot.



The **Chapter 7** will be dedicated to the one pot synthesis of pyrrolo[3,2,1-*de*]phenanthridines from 7-phenylindoles via tandem C–H olefination/aza-Michael addition.



The **Chapter 8** will developed an alternative access to seven-membered azepino[3,2,1-*hi*]indoles via [5+2] C-H/N-H annulation via scalable rhodaelectro-catalyzed transformation.



5.5. References

- [1] G. Mayer, G. Wille, M. Brenner, K. Zeitler, W. Steglich, *Synthesis* **2011**, 330-336.
- [2] G.-G. Cheng, D. Li, B. Hou, X.-N. Li, L. Liu, Y.-Y. Chen, P.-K. Lunga, A. Khan, Y.-P. Liu, Z.-L. Zuo, X.-D. Luo, *J. Nat. Prod.* **2016**, *79*, 2158–2166.
- [3] T. Buyck, Q. Wang, J. Zhu, *Angew. Chem. Int. Ed.* **2013**, *52*, 12714–12718.
- [4] B. González, N. Veiga, G. Hernández, G. Seoane, I. Carrera, *J. Nat. Prod.* **2023**, *86*, 1500–1511.
- [5] Y. Hu, Y. Yang, P. Tan, Y. Zhang, M. Han, J. Yu, X. Zhang, Z. Jia, D. Wang, K. Yao, H. Pang, Z. Hu, Y. Li, T. Ma, K. Liu, S. Ding *Nature* **2023**, *617*, 792–797.
- [6] L. Zhang, Y. Wang, Z.-J. Yao, S. Wang, Z.-X. Yu, *J. Am. Chem. Soc.* **2015**, *137*, 13290–13300.
- [7] J.-L. Wang, C.-X. Zhuo, *Synlett* **2022**, 599-608.
- [8] F. Narjes, B. Crescenzi, M. Ferrara, J. Habermann, S. Colarusso, M. del Roario Rico Ferreira, I. Stansfield, A. C. Mackay, I. Conte, C. Ercolani, S. Zaramella, M.-C. Palumbi, P. Meuleman, G. Leroux-Roels, C. Giuliano, F. Fiore, S. Di Marco, P. Baiocco, U. Koch, G. Migliaccio, S. Altamura, R. Laufer, R. De Francesco, M. Rowley, *J. Med. Chem.* **2011**, *54*, 289–301.
- [9] B.-J. Zhang, M.-F. Bao, C.-X. Zeng, X.-H. Zhong, L. Ni, Y. Zeng, X.-H. Cai, *Org. Lett.* **2014**, *16*, 6400–6403.

- [10] (a) P. Mugabo, A. Philander, I. Raji, D. Dietrich, I. Green, *J. Ethnopharmacol.* **2014**, *158*, 123-131; (b) S. Ghosal, Y. Kumar, D. K. Chakrabarti, J. Lal, S. K. Singh, *Phytochemistry* **1986**, *25*, 1097–1102; (c) Q. Yuan, X. Zhang, W. Wei, J. Zhao, Y. Wu, S. Zhao, L. Zhu, P. Wang, J. Hao, *Pharmacol. Res.* **2022**, *175*, 105985; (d) S.-L. Ding, Y. Ji, Y. Su, R. Li, P. Gu, *J. Org. Chem.* **2019**, *84*, 2012–2021.
- [11] For representative examples, see: (a) A. P. Dobbs, K. Jones, K. T. Veal, *Tetrahedron Lett.* **1997**, *38*, 5379-5382; (b) O. Tsuge, T. Hatta, H. A. Tsuchiyama, *Chem. Lett.* **1998**, *27*, 155-156.
- [12] For a representative example, see: A. J. Borah, Z. Shi, *Z. J. Am. Chem. Soc.* **2018**, *140*, 6062-6066.
- [13] For few representative examples, see: (a) P. J. Llabres-Campaner, R. Ballesteros-Garrido, R. Ballesteros, B. Abarca, *Tetrahedron* **2017**, *73*, 5552-5561; (b) P. J. Llabres-Campaner, R. Ballesteros-Garrido, R. Ballesteros, B. Abarca, *J. Org. Chem.* **2018**, *83*, 521-526; (c) Z. Shi, C. Zhang, S. Li, D. Pan, S. Ding, Y. Cui, N. Jiao, *Angew. Chem. Int. Ed.* **2009**, *48*, 4572-4576.
- [14] X. Wang, B. S. Lane, D. Sames, *J. Am. Chem. Soc.* **2005**, *127*, 4996–4997.
- [15] B. B. Toure, B. S. Lane, D. Sames, *Org. Lett.* **2006**, *8*, 1979–1982.
- [16] N. Lebrasseur, I. Larrosa, *J. Am. Chem. Soc.* **2008**, *130*, 2926–2927.
- [17] H. Dong, C. Limberakis, S. Liras, D. Price, K. James, *Chem. Commun.* **2012**, *48*, 11644–11646.
- [18] N. R. Deprez, D. Kalyani, A. Krause, M. S. Sanford, *J. Am. Chem. Soc.* **2006**, *128*, 4972–4973.
- [19] S.-D. Yang, C.-L. Sun, Z. Fang, B.-J. Li, Y.-Z. Li, Z.-J. Shi, *Angew. Chem.* **2008**, *120*, 1495–1498.
- [20] M.-Z. Lu, P. Lu, Y.-H. Xu, T.-P. Loh, *Org. Lett.* **2014**, *16*, 2614–2617.
- [21] D. R. Stuart, E. Villemure, K. Fagnou, *J. Am. Chem. Soc.* **2007**, *129*, 12072–12073.
- [22] E. Capito, J. M. Brown, A. Ricci, *Chem. Commun.* **2005**, 1854-1856.
- [23] N. P. Grimster, C. Gaunlett, C. R. A. Godfrey, M. J. Gaunt, *Angew. Chem. Int. Ed.* **2005**, *44*, 3125–3129.
- [24] A. Garcia-Rubia, R. G. Arrayas, J. C. Carretero, *Angew. Chem.* **2009**, *121*, 6633–6637.
- [25] L. Yang, G. Zhang, H. Huang, *Adv. Synth. Catal.* **2014**, *356*, 1509 – 1515.
- [26] R. A. Jagtap, C. P. Vinod, B. Punji, *ACS Catal.* **2019**, *9*, 431-441.
- [27] L. Jiao, T. Bach, *J. Am. Chem. Soc.* **2011**, *133*, 12990–12993.
- [28] S. Pan, N. Ryu, T. Shibata, *J. Am. Chem. Soc.* **2012**, *134*, 17474–17477.
- [29] Y. Nakao, N. Kashiwara, K. S. Kanyiva, T. Hiyama, *Angew. Chem.* **2010**, *122*, 4553–4556.
- [30] D. Pandey, S. Ankade, A. Ali, C. Vinod, B. Punji, *Chem. Sci.* **2019**, *10*, 9493-9500.
- [31] B. Zhou, Y. Yang, Y. Li, *Chem. Commun.* **2012**, *48*, 5163–5165.
- [32] X.-B. Yan, Y.-W. Shen, D.-Q. Chen, P. Gao, Y.-X. Li, X.-R. Song, X.-Y. Liu, Y.-M. Liang, *Tetrahedron* **2014**, *70*, 7490–7495.
- [33] Q. Shuai, G. Deng, Z. Chua, D. S. Bohle, C. J. Li, *Adv. Synth. Catal.* **2010**, *352*, 632–636.
- [34] T. Jeong, S. Han, N. K. Mishra, S. Sharma, S.-Y. Lee, J. S. Oh, J. H. Kwak, Y. H. Jung, I. S. Kim, *J. Org. Chem.* **2015**, *80*, 7243–7250.
- [35] a) B. Sun, T. Yoshino, S. Matsunaga, M. Kanai, *Adv. Synth. Catal.* **2014**, *356*, 1491–1495. b) J. Shi, B. Zhou, Y. Yang, Y. Li, *Org. Biomol. Chem.* **2012**, *10*, 8953–8955.
- [36] Z. Zhang, Z. Hu, Z. Yu, P. Lei, H. Chi, Y. Wang, R. He, *Tetrahedron Lett.* **2007**, *48*, 2415–2419.
- [37] F. Bellina, F. Benelli, R. Rossi, *J. Org. Chem.* **2008**, *73*, 5529–5535.

- [38] J. Rodriguez, A. Zeineddine, E. D. Sosa Carrizo, K. Miqueu, N. Saffon-Merceron, A Amgoune, D. Bourissou, *Chem. Sci.* **2019**, *10*, 7183–7192.
- [39] J. Cornella, P. Lu, I. Larrosa, *Org. Lett.* **2009**, *11*, 5506–5509.
- [40] Y. Chen, S. Guo, K. Li, J. Qu, H. Yuan, Q. Hua, B. Chen, *Adv. Synth. Catal.* **2013**, *355*, 711–715.
- [41] S. Chen, Y. Liao, F. Zhao, H. Qi, S. Liu, G. J. Deng, *Org. Lett.* **2014**, *16*, 1618–1621.
- [42] W.-L. Chen, Y.-R. Gao, S. Mao, Y.-L. Zhang, Y.-F. Wang, Y.-Qiang Wang, *Org. Lett.* **2012**, *14*, 5920–5923.
- [43] M. Zhao, X. Li, X. Zhang, Z. Shao, *Chem. Asian J.* **2022**, *17*, e20220048
- [44] S. Ma, S. Yu, *Tetrahedron Lett.* **2004**, *45*, 8419–8422.
- [45] M. Bandini, A. Melloni, A. Umami-Ronchi, *Org. Lett.* **2004**, *6*, 3199–3203.
- [46] M. Hu, Y. Jiang, N. Sun, B. Hu, Z. Shen, X. Hu, L. Jin, *New J. Chem.* **2021**, *45*, 10057–10062.
- [47] Kamal, M. Khatua, S. Rani, B. Goswami, S. Samata, *J. Org. Chem.* **2023**, *88*, 5827–5843.
- [48] C. Seck, M. D. Mbaye, S. Gaillard, J.-L. Renaud, *Adv. Synth. Catal.* **2018**, *360*, 4640–4645.
- [49] J. Wu, D. Wang, F. Wu, B. Wan, *J. Org. Chem.* **2013**, *78*, 5611–5617.
- [50] A. De Angelis, V. W. Shurtleff, O. Dmitrenko, J. M. Fox, *J. Am. Chem. Soc.* **2011**, *133*, 1650–1653.
- [51] C. Wang, S. Wang, H. Li, J. Yan, H. Chi, X. Chen, Z. Zhang, *Org. Biomol. Chem.*, **2014**, *12*, 1721–1724.
- [52] J. Liu, Z. Wie, H. Jiao, R. Jackstell, M. Beller, *ACS Cent. Sci.* **2018**, *4*, 30–38.
- [53] R. Lang, J. Wu, L. Shi, C. Xia, F. Li, *Chem. Commun.* **2011**, *47*, 12553–12555.
- [54] J. Chen, B. Liu, D. Liu, S. Liu, J. Cheng, *Adv. Synth. Catal.* **2012**, *354*, 2438–2442.
- [55] Q. Liu, Q. Li, Y. Ma, Y. Jia, *Org. Lett.* **2013**, *15*, 4528–4531.
- [56] V. Lanke, K. R. Prabhu, *Org. Lett.* **2013**, *15*, 6262–6265.
- [57] Q. Wu, P. Gao, Y. Yuan, *Asian J. Org. Chem.* **2021**, *10*, 749–752.
- [58] C. N. Kona, Y. Nishii, M. Miura, *Org. Lett.* **2018**, *20*, 4898–4901.
- [59] Y. Yang, P. Gao, Y. Zhao, Z. Shi, *Angew. Chem., Int. Ed.* **2017**, *56*, 3966–3971.
- [60] X.-H. Liu, H. Park, J.-H. Hu, Y. Hu, Q.-L. Zhang, B.-L. Wang, B. Sun, K.-S. Yeung, F.-L. Zhang, J.-Q. Yu, *J. Am. Chem. Soc.* **2017**, *139*, 888–896.
- [61] A. J. Borah, Z. Shi, *Chem. Commun.* **2017**, *53*, 3945–3948.
- [62] C. Pan, G. Huang, Y. Shan, Y. Li, J.-T. Yu, *Org. Biomol. Chem.* **2020**, *18*, 3038–3042.
- [63] T. Paul, S. Basak, T. Punniyamurthy, *Org. Lett.* **2022**, *24*, 6000–6005.
- [64] S. Chen, B. Feng, X. Zheng, J. Yin, S. Yang, J. You, *Org. Lett.* **2017**, *19*, 2502–2505.
- [65] (a) Y. Yang, P. Gao, Y. Zhao, Z. Shi, *Angew. Chem., Int. Ed.* **2017**, *56*, 3966–3971; (b) T. Wang, L. Zhou, Y. Yang, X. Zhang, Z. Shi, Y.-D. Wu, *Org. Lett.* **2018**, *20*, 6502–6505.
- [66] M. Simonetti, D. M. Cannas, A. Panigrahi, S. Kujawa, M. Kryjewski, P. Xie, I. Larrosa, *Chem. Eur. J.* **2017**, *23*, 549–543.
- [67] R. J. Phipps, M. J. Gaunt, *Science* **2009**, *323*, 1593–1597.
- [68] Y. Yang, R. Li, Y. Zhao, D. Zhao, Z. Shi, *J. Am. Chem. Soc.* **2016**, *138*, 8734–8737.
- [69] Y. Feng, D. Holte, J. Zoller, S. Umemiya, L. R. Simke, P. S. Baran, *J. Am. Chem. Soc.* **2015**, *137*, 10160–10163
- [70] G. Yang, P. Lindovska, D. Zhu, J. Kim, P. Wang, R.-Y. Tang, M. Movassaghi, J.-Q. Yu, *J. Am. Chem. Soc.* **2014**, *136*, 10807–10813.
- [71] Y. Yang, X. Qiu, Y. Zhao, Y. Mu, Z. Shi, *J. Am. Chem. Soc.* **2016**, *138*, 495–498.

- [72] X. Qiu, H. Deng, Y. Zhao, Z. Shi, *Sci. Adv.* **2018**, *4*, eaau6468.
- [73] X.-F Yang, X.-H. Hu, C. Feng, T.-P. Loh, *Chem. Commun.* **2015**, *51*, 2532-2535.
- [74] C. Naidu, K. Nishi, M. Miura, *Org. Lett.* **2021**, *23*, 6252–6256.
- [75] I. Choi, A. M. Messinis, L. Ackermann, *Angew. Chem. Int. Ed.* **2020**, *59*, 12534-12540.
- [76] A. J. Borah, Z. Shi, *Z. J. Am. Chem. Soc.* **2018**, *140*, 6062–6066.
- [77] G. Abbiati, E. M. Beccalli, G. Broggini, C. Zoni, *J. Org. Chem.* **2003**, *68*, 7625–7628.
- [78] E. M. Ferreira, B. M. Stoltz, *J. Am. Chem. Soc.* **2003**, *125*, 9578–9579.
- [79] Q. Liu, Q. Li, Y. Ma, Y. Jia, *Org. Lett.* **2013**, *15*, 4526–4531.
- [80] X. Liu, G. Li, F. Song, J. You, *Nature Commun.* **2014**, *5*, 5030.
- [81] B. Dong, J. Qian, M. Ji, Z.-J. Wang, M. Wang, D. Wang, C. Yuan, Y. Han, Y. Zhao, Z. Shi, *Sci. Adv.* **2020**, *6*, eabd1378.
- [82] (a) K. Morimoto, K. Hirano, T. Satoh, M. Miura, *Org. Lett.*, **2010**, *12*, 2068–2071; (b) W. Zhuang, J. Zhang, Y. Zheng, Q. Huang, *Molecules* **2021**, *26*, 5329.
- [83] L. Ackermann, L. Wang, A. V. Lygin, *Chem. Sci.*, **2012**, *3*, 177–180.
- [84] Y. Xia, L. Dong, *Org. Lett.* **2017**, *19*, 2258–2261.
- [85] (a) Q. Huang, Q. Han, S. Fu, Z. Yao, L. Su, X. Zhang, S. Lin, S. Xiang, *J. Org. Chem.* **2016**, *81*, 12135–12142; (b) Q. Han, X. Guo, Z. Tang, L. Su, Z. Yao, X. Zhang, S. Lin, S. Xiang, Q. Huang, *Adv. Synth. Catal.* **2018**, *360*, 972–984.
- [86] L. Yan, D. Zhao, J. Lan, Y. Cheng, Q. Guo, X. Li, N. Wu, J. You, *Org. Biomol. Chem.*, **2013**, *11*, 7966–7977.
- [87] Q. Huang, Q. Han, S. Fu, Z. Yao, L. Su, X. Zhang, S. Lin, S. Xiang, *J. Org. Chem.* **2016**, *81*, 12135–12142.

Chapter 6.

Synthesis of Seven-membered Azepino[3,2,1-*hi*]indoles via Rhodium-Catalyzed Regioselectively C-H Activation/DBU-Catalyzed Intramolecular Amidation of 7-Phenylindoles in One Pot

This chapter is adapted from the publication: Yumeng Yuan, Guoshuai Pan, Xiaofeng Zhang, Buhong Li, Shengchang Xiang and Qiufeng Huang, *J. Org. Chem.* **2019**, *84*, 14701-14711.

Chapter 6 - Synthesis of Seven-membered Azepino[3,2,1-*hi*]indoles via Rhodium-Catalyzed Regioselectively C-H Activation/DBU-Catalyzed Intramolecular Amidation of 7-Phenylindoles in One Pot

6.1. Introduction

Transition-metal-catalyzed C-H bond activation is a versatile synthetic tool for the construction of carbon-carbon bonds and carbon-heteroatom bonds.^[1] In particular, transition-metal-catalyzed C-H activation/cyclization is a powerful and distinct method for the synthesis of cyclic and heterocyclic compounds.^[2] In this context, recent years have witnessed a lot of efficient methods for the synthesis of five-membered or six-membered cyclic compounds.^[3] However, one pot C-H activation/cyclization strategies leading to seven-membered rings have rarely been developed due to entropic factors and transannular interactions.^[4] Azepino[3,2,1-*hi*]indoles and their derivatives are important classes of fused tricyclic compounds containing a seven-membered ring that are found in a wide range of natural products and biological active compounds (Figure 6-1). For example, erythrivarine B was isolated from the flower of *Erythrina Variegata*,^[5] and extracts from the roots of stemonaceae plants were found to contain a class of polycyclic alkaloids which are structurally characterized by the presence of a azepino[3,2,1-*hi*]indole nucleus as show in stenine,^[6] stemona-lactam,^[7] tuberostemonol,^[8] dehydrostenine^[9] and tridehydrotuberostemonine.^[10] These alkaloids exhibit a wide variety of biological activities, such as antitussive activity, insecticidal activity, anti-inflammatory and so on.^[11] The structural diversity associated with biological activities of azepino[3,2,1-*hi*]indoles have attracted the attention of the synthetic community.^[12] However, the synthesis of azepino[3,2,1-*hi*]indoles usually requires multistep approaches, and the development of novel strategies for efficient and straightforward construction of azepino[3,2,1-*hi*]indoles still remains a great challenge. Indole nuclei are ubiquitous structural motifs. Recently, our group and other laboratories have demonstrated that *NH*-indole was explored as an intrinsic directing

group which is present in the final product.^[13] Herein, we report a regioselective Cp*Rh(III)-catalyzed C-H activation/base-catalyzed intramolecular amidation of 7-phenylindoles with diazomalonates to give the corresponding azepino[3,2,1-*hi*]indoles in good to excellent yields (Scheme 6-1). This catalytic method offers opportunities for the synthesis of azepino[3,2,1-*hi*]indoles derivatives' synthesis.

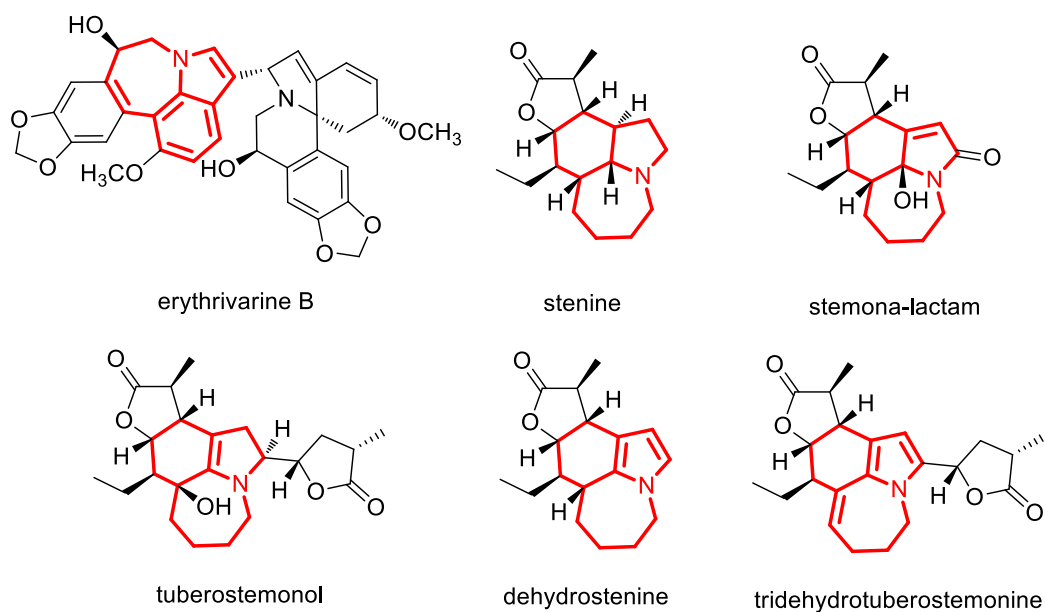
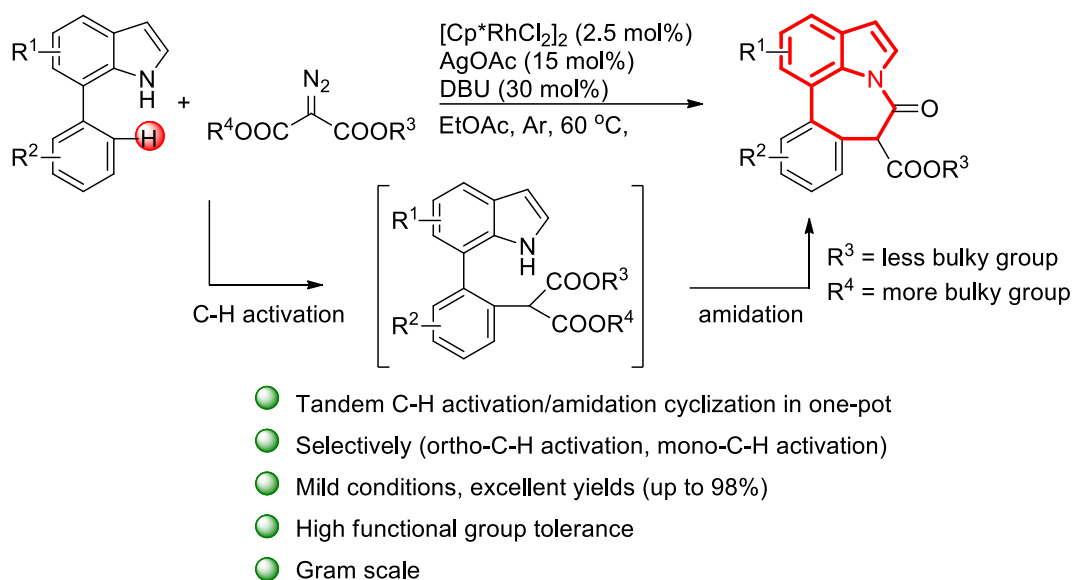


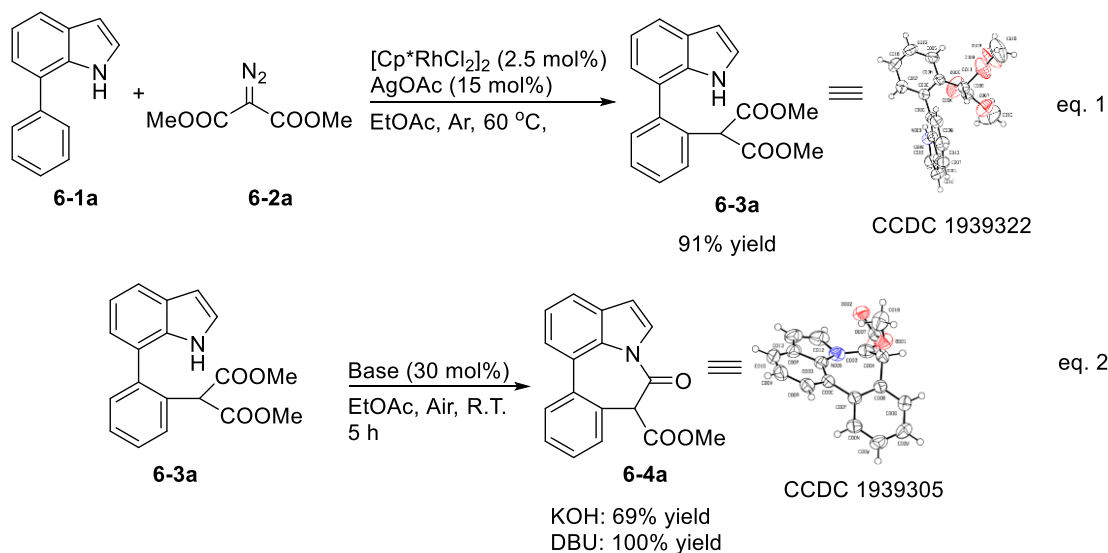
Figure 6-1. Natural products bearing azepino[3,2,1-*hi*]indole core



Scheme 6-1. Synthesis of Azepino[3,2,1-*hi*]indoles via Tandem C-H Activation/Amidation in One Pot

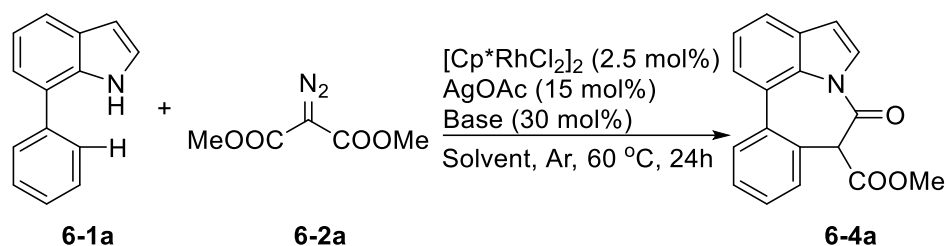
6.2. Result and discussion

To begin, the experiments were performed with 7-phenyl-1*H*-indole (**6-1a**, 1 equiv) and dimethyl diazomalonate (**6-2a**, 1.5 equiv) in the presence of [Cp**RhCl*₂]₂ (2.5 mol %) and AgOAc (15 mol %) at 60 °C for 24 h, and the desired mono-substituted product **6-3a** was obtained selectively in 91% yield (Scheme 6-2, eq. 1). No disubstituted product^[13b-c] or C3-substituted product^[14] was found in the reaction mixture. The structure of **6-3a** was confirmed by X-ray crystallography (Table S6-1). Treating **6-3a** with 30 mol % KOH in EtOAc resulted in intramolecular amidation to provide 7-membered ring **6-4a** in 69% yield.



Scheme 6-2. Rhodium-Catalyzed ortho C-H Coupling of 7-Arylindoles with Diazo Compounds (eq. 1); Base-Catalyzed Intramolecular Amidation Cyclization (eq. 2).

Changing the base to DBU afforded **6-4a** in quantitative yield (Scheme 6-2, eq. 2). The structure of **6-4a** was also confirmed by X-ray crystallography (Table S6-2). Encouraged by the above results, the tandem C-H activation/amidation of 7-phenyl-1*H*-indole with dimethyl diazomalonate leading to azepino[3,2,1-*hi*]indole **6-4a** in one pot was surveyed (Table 6-1). It is found that KOH was incompatible with the [Cp**RhCl*₂]₂/AgOAc catalyst system; almost no annulated product was formed, and the starting material **6-1a** was recovered totally (Table 6-1, entry 1).

Table 6-1. Optimization of the Reaction Conditions^a

Entry	base	Solvent	6-3a Yield(%) ^[b]
1	KOH	EtOAc	trace
2	DBU	EtOAc	94
3	Et ₃ N	EtOAc	0
4	KO ^t Bu	EtOAc	trace
5	DMAP	EtOAc	trace
6	LiOH	EtOAc	0
7	piperidine	EtOAc	trace
8	Me ₄ NOAc	EtOAc	22
9	ⁿ Bu ₄ NOAc	EtOAc	30
10	DBU	xylene	91
11	DBU	CH ₃ CN	trace
12	DBU	1,4-dioxane	47
13	DBU	DCM	79
14	DBU	DCE	trace
15	DBU	MeOH	0

^aReaction conditions: **6-1a** (0.3 mmol), **6-2a** (0.45 mmol), $[\text{Cp}^*\text{RhCl}_2]_2$ (2.5 mol%), AgOAc (15 mol%), base (30 mol%), solvent (2 mL), argon atmosphere, 60°C, 24 h. ^bisolated yield on the basis of the amount of **6-1a** used.

We reasoned that strong base KOH had an adverse impact on Rhodium-catalyzed *NH*-indole directed C-H activation cycle. To our delight, by changing the base from KOH to DBU, the yield of the desired product was significantly improved to 94% (Table 6-

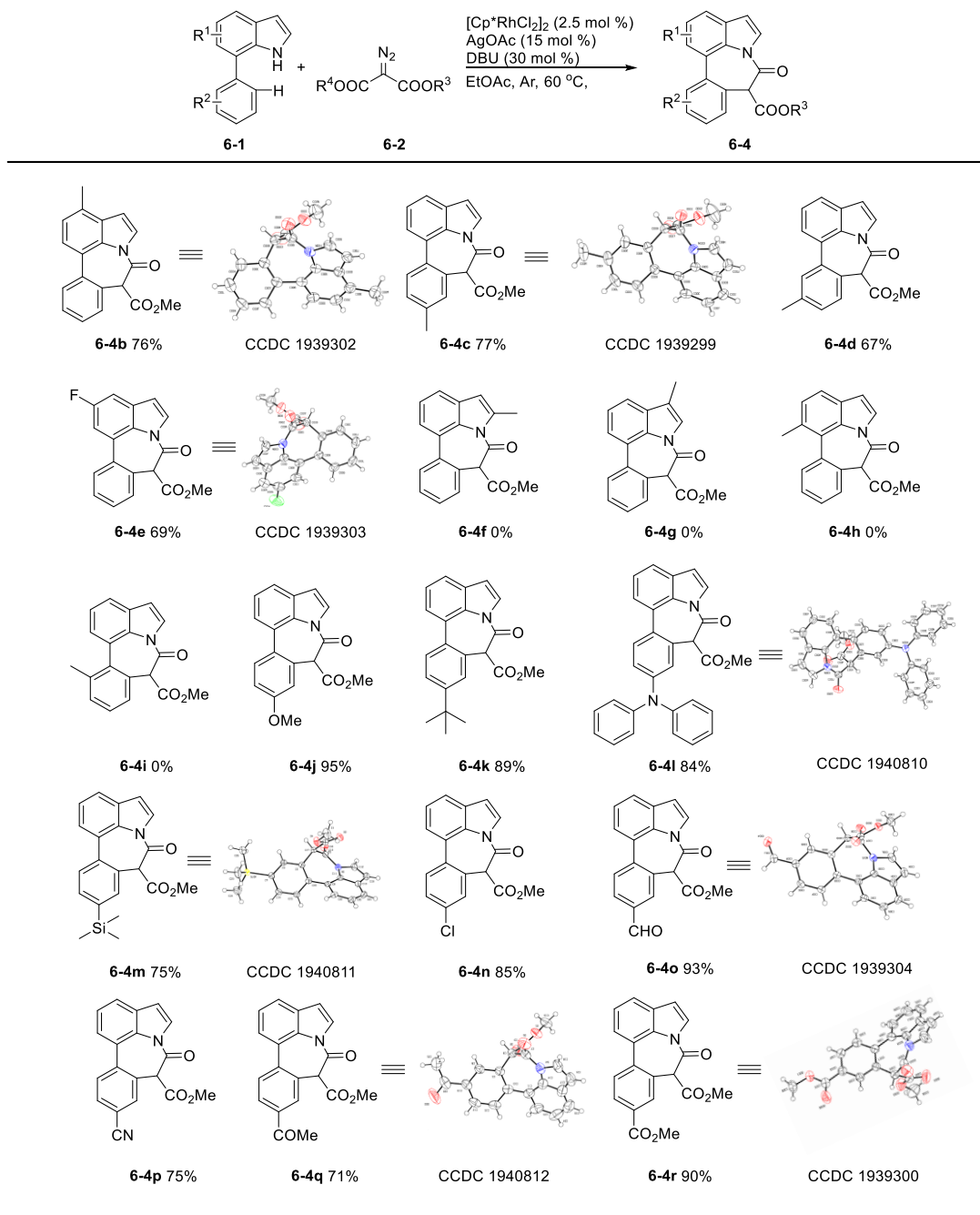
1, entry 2). Other bases such as Et₃N, KO^tBu, DMAP, LiOH, piperidine, Me₄NOAc and ⁿBu₄NOAc gave unsatisfactory results (Table 6-1, entries 3-9). The effect of the solvent on the formation of **6-4a** was also briefly investigated. In xylene, the reaction proceeded as smoothly as in EtOAc (Table 6-1, entry 10). However, the use of other solvents such as CH₃CN, 1,4-dioxane, DCM and MeOH resulted in significant decreases of the yields (Table 6-1, entries 11-15).

Under the optimal catalytic reaction conditions, the generality of the Rh(III)-catalyzed tandem C-H activation/cyclization was examined (Table 6-2). The reaction is found to be very sensitive with respect to the positions of substituents. Substituents at the 4 or 5-positions of the indole ring or the 3 or 4-positions of the benzene ring favored the reaction, affording the desired products in good to excellent yields (Table 6-2. **6-(4b-4e)**), while substituents on other positions led to complete reaction shutdown **6-(4f-4i)**. Notably, a wide range of functional groups, including F, OMe, NPh₂, SiMe₃, Cl, CN, CHO, COMe, CO₂Me, CF₃, NO₂ were all well tolerated **6-(4e, 4j, 4l-4t)**, providing the corresponding products in 56-95% yields. The diverse groups in the products can serve as a handle for further transformation. Only 18% yield of the desired product was detected when an OH group was present, which is probably a result of the chelating ability of the OH group with Rh metal (see **6-4w**). It is worth mentioned that 7-naphthylindole and 1,4-diindolylbenzene both coupled smoothly with **6-2a** to afford the annulated products. The resulting structures **6-4u** and **6-4v** may be useful as valuable intermediate for preparing optoelectronic materials. In order to determine if the electronic nature of the substituent affected the reaction, an intermolecular competition experiment was conducted with an equimolar mixture of 7-(4-methoxyphenyl)-1*H*-indole and 7-(4-nitrophenyl)-1*H*-indole. A ratio of 3:1 was obtained between **6-4j** and **6-4t** after 12 h, which suggests that electron-rich substrates are favorable to the reaction (Scheme 6-3, eq. 1). An intermolecular competition reaction between 7-phenyl-1*H*-indole **6-1a** and its deuterated derivative (**6-1a**)-**D5** gave a KIE value of 2.5, indicating that the C-H bond cleavage might be involved in the rate-determining step (Scheme 6-3, eq. 2). Next, various diazo compounds were examined under the standard conditions.

It is found that the steric effects of the substituents on the diazomalonates play an important role in the cyclization step. Changing the methyl group to ethyl group afforded a lower yield (**6-4x**, 55%). Diisopropyl 2-diazomalonate was found to couple with **6-1a** to afford the mono-substituted product **6-3y** in quantitative yield; and the amidation cyclization of **6-3y** can not happen in one pot. However, treating **6-3y** with 30 mol% KOH in DCM delivered cyclization product **6-4y** in 50% yield. Interestingly, when the unsymmetrical diazomalonate *n*-butyl methyl 2-diazomalonate was employed, the amidation occurred at the more bulky group and reserved the less bulky group in the final product **6-4a**.

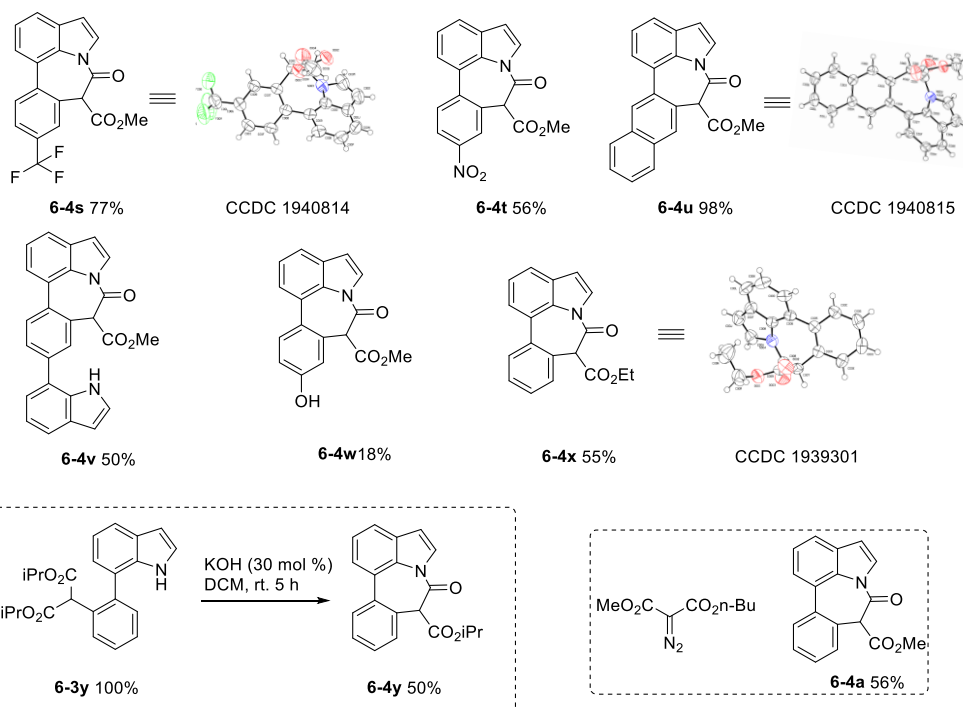
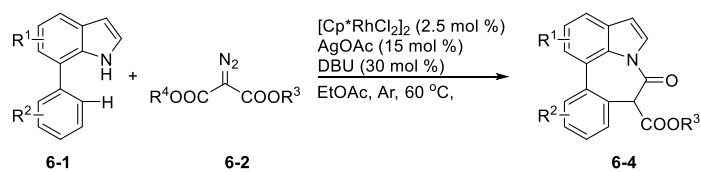
In order to demonstrate the practical application of the methodology, the reaction of **6-1a** and **6-2a** was carried out on a gram scale, which provided an 89% yield of **6-4a** (1.55 g, Scheme 6-4, eq. 1). Demethoxycarbonylation of **6-4a** through a saponification and decarboxylation sequence gave benzo[4,5]azepino[3,2,1-*hi*]indol-4(5*H*)-one **6-5a** in 60% yield (Scheme 6-4, eq. 2).^[15] Finally, **6-4a** can be efficiently alkenylated at the 3-position with acrylate affording **6-6a** in 80% yield by a Pd(OAc)₂-catalyzed Fujiwara-Moritani reaction (Scheme 6-4, eq. 3).^[16]

Table 6-2. Substrate Scope^a

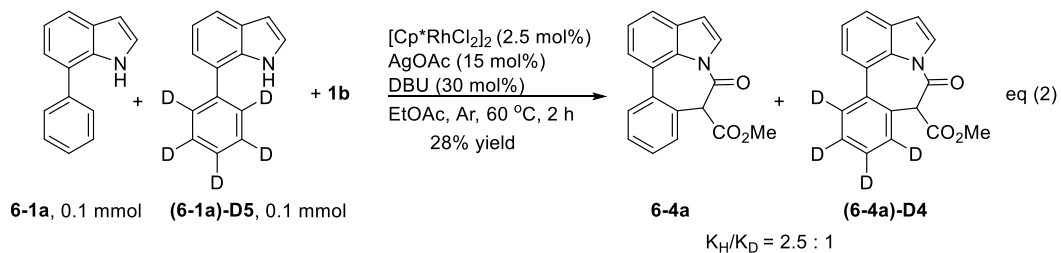
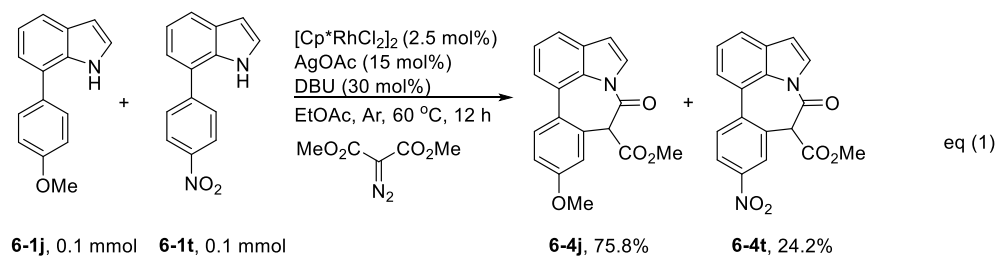


^aReaction conditions: **6-1** (0.3 mmol), **6-2** (0.45 mmol), [Cp*RhCl₂]₂ (2.5 mol%), AgOAc (15 mol%), DBU (30 mol%), EtOAc (2 mL), argon atmosphere, 60 °C, 24 h; isolated yield.

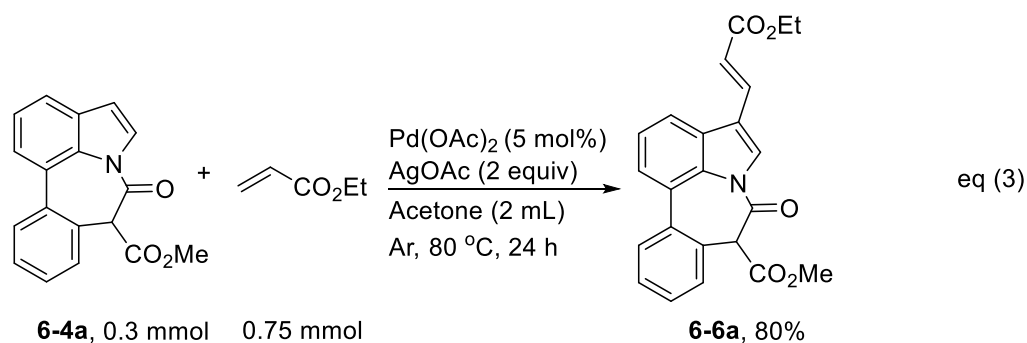
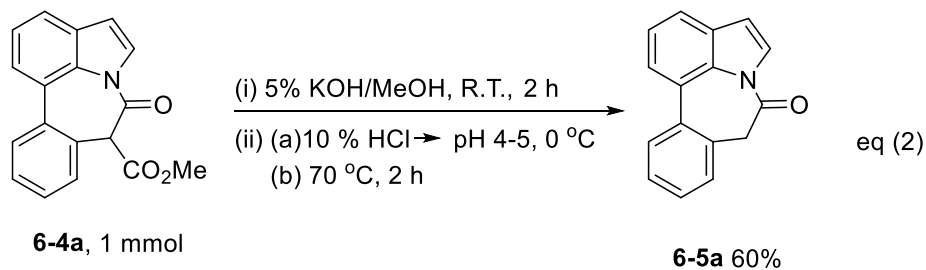
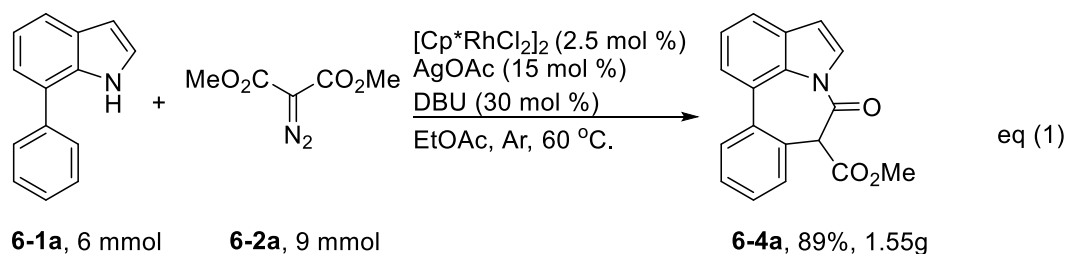
Table 6-2. Substrate Scope (continued)^a



Reaction conditions: **6-1** (0.3 mmol), **6-2** (0.45 mmol), $[\text{Cp}^*\text{RhCl}_2]_2$ (2.5 mol%), AgOAc (15 mol%), DBU (30 mol%), EtOAc (2 mL), argon atmosphere, 60 °C, 24 h; isolated yield.

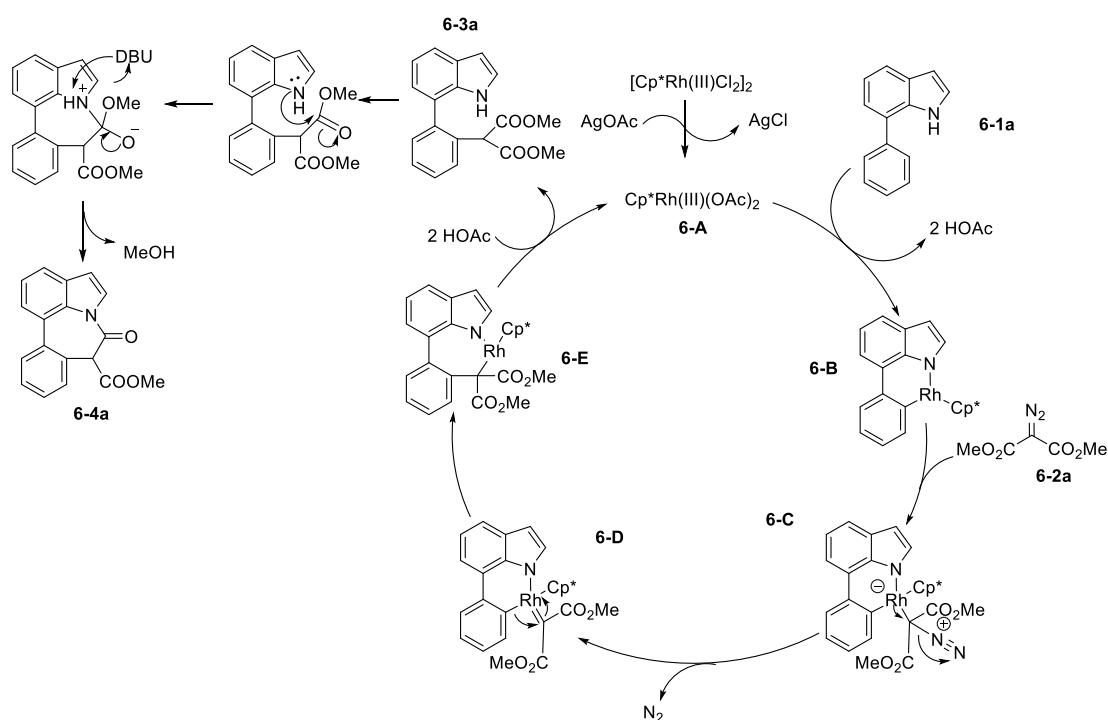


Scheme 6-3. Competition Experiment



Scheme 6-4. Synthetic Transformations

In fact, several attempts to recrystallize or in situ characterize the key intermediates from the reaction of 7-phenyl-1H-indole with equimolar $[\text{Cp}^*\text{RhCl}_2]_2$ were problematic. However, based on our group's previous research of NH-indole-directed C-H bond functionalization,^[13a-b] a possible mechanism for the present reaction is depicted briefly in Scheme 6-5. First, the active Rh(III) species **6-A** is generated with the assistance of AgOAc, which undergoes N-H bond cleavage and C-H bond cleavage to give six-membered rhodacycle **6-B**. Then rhodacycle **6-B** decomposes the diazo compound **6-2a** to generate metal carbene species **6-D**; **6-D** undergoes migratory insertion to produce seven-membered rhodacycle **6-E**. At this point, **6-E** is protonated to afford the coupling product **6-3a** and regenerate the active Rh(III) catalyst **6-A**. Finally, **6-3a** can be converted into the seven-membered product **6-4a** via intramolecular amidation in the presence of DBU catalyst.



Scheme 6-5. Proposed Reaction Mechanism

In conclusion, we have developed a significant advancement to catalytic C-H activation/cyclization. This protocol enables unprecedented general access to the seven-

membered azepino[3,2,1-*hi*]indoles. The tandem rhodium-catalyzed C-H coupling of 7-phenylindoles with diazo compounds and DBU-catalyzed intramolecular amidation proceeds in one pot under mild reaction conditions. The reactions have a broad range of substrates giving a variety of functionalized products in high yields. A wide range of functional groups, including F, OMe, NPh₂, SiMe₃, Cl, CN, CHO, COMe, CO₂Me, CF₃, NO₂ were all well tolerated. Further applications of this C-H activation/cyclization in the synthesis of related targets are in progress.

6.3. References

- [1] (a) J. C. K. Chu, T. Rovis, *Angew. Chem. Int. Ed.* **2017**, *56*, 2. (b) Y.-P. Li, Z.-Q. Li, S.-F. Zhu, *Tetrahedron Lett.* **2018**, *59*, 2307. (c) R. R. Karimov, J. F. Hartwig, *Angew. Chem. Int. Ed.* **2018**, *57*, 4234. (d) X. Qi, Y. Li, R. Bai, Y. Lan, *Acc. Chem. Res.* **2017**, *50*, 2799. (e) Y. Yang, J. Lan, J. You, *Chem. Rev.* **2017**, *117*, 8787. (f) Y. Xia, D. Qiu, Wang, *J. Chem. Rev.* **2017**, *117*, 13810. (g) P. Gandeepan, T. Müller, D. Zell, G. Cera, S. Warratz, L. Ackermann, *Chem. Rev.* **2019**, *119*, 2192. (h) S. Rej, N. Chatani, *Angew. Chem. Int. Ed.* **2019**, *58*, 8304. (i) Z. Chen, B. Wang, J. Zhang, W. Yu, Z. Liu, Y. Zhang, *Org. Chem. Front.* **2015**, *2*, 1107. (j) C. Liu, J. Yuan, M. Gao, S. Tang, W. Li, R. Shi, A. Lei, *Chem. Rev.* **2015**, *115*, 12138.
- [2] (a) N. K. Mishra, J. Park, H. Oh, S. H. Han, I. S. Kim, *Tetrahedron* **2018**, *74*, 6769. (b) X. Liu, Y. Huang, X. Meng, L. Li, D. Wang, Y. Chen, D. Tang, B. Chen, *Synlett* **2019**, *30*, 1026. (c) O. Baudoin, *Acc. Chem. Res.* **2017**, *50*, 1114. (d) F. Rafiee, *Appl. Organometal. Chem.* **2017**, *31*, 1. (e) S. Agasti, A. Dey, D. Maiti, *Chem. Commun.* **2017**, *53*, 6544. (f) G. Duarah, P. P. Kaishap, T. Begun, S. Gogoi, *Adv. Synth. Catal.* **2019**, *361*, 654. (g) S. Prakash, R. Kuppusamy, C.-H. Cheng, *ChemCatChem* **2018**, *10*, 683. (h) Y. Xiang, C. Wang, Q. Ding, Y. Peng, *Adv. Synth. Catal.* **2019**, *361*, 919. (i) X.-X. Guo, D.-W. Gu, Z. Wu, W. Zhang, *Chem. Rev.* **2015**, *115*, 1622. (j) J. R. Hummel, J. A. Boerth, J. A. Ellman, *Chem. Rev.* **2017**, *117*, 9163.
- [3] (a) W.-B. Zhang, X.-T. Yang, J.-B. Ma, Z.-M. Su, S.-L. Shi, *J. Am. Chem. Soc.* **2019**, *141*, 5628. (b) Y.-X. Wang, S.-L. Qi, Y.-X. Luan, X.-W. Han, S. Wang, H. Chen, M. Ye, *J. Am. Chem. Soc.* **2018**, *140*, 5360. (c) Y. Li, J. Li, X. Wu, Y. Zhou, H. Liu, *J. Org. Chem.* **2017**, *82*, 8984. (d) M. Sen, R. Mandal, A. Das, D. Kalsi, B. Sundararaju, *Chem. Eur. J.* **2017**, *23*, 17454. (e) J. Tang, S. Li, Z. Liu, Y. Zhao, Z. She, V. D. Kadam, G. Gao, J. Lan, J. You, *Org. Lett.* **2017**, *19*, 604. (f) X. Chen, S. Yang, H. Li, B. Wang, G. Song, *ACS Catal.* **2017**, *7*, 2392. (g) K. Alam, S. W. Hong, K. H. Oh, J. K. Park, *Angew. Chem. Int. Ed.* **2017**, *56*, 13387. (h) M. Li, F. Y. Kwong, *Angew. Chem. Int. Ed.* **2018**, *57*, 6512. (i) X. Li, J. Pan, H. Wu, N. Jiao, *Chem. Sci.* **2017**, *8*, 6266. (j) L. Kong, X. Han, X. Li, *Chem. Commun.* **2019**, *55*, 7339.
- [4] (a) F. Ling, Z. Xie, J. Chen, C. Ai, H. Shen, Z. Wang, X. Yi, W. Zhong, *Adv. Synth. Catal.* **2019**, *361*, 3094. (b) T. Zhou, B. Li, B. Wang, *Chem. Commun.* **2016**, *52*, 14117. (c) Q. Li, B. Li, B. Wang, *Chem. Commun.* **2018**, *54*, 9147. (d) P. Bai, X.-F. Huang, G.-D. Xu, Z.-Z. Huang, *Org. Lett.* **2016**, *18*, 3058.
- [5] B.-J. Zhang, M.-F. Bao, C.-X. Zeng, X.-H. Zhong, L. Ni, Y. Zeng, X.-H. Cai, *Org. Lett.* **2014**, *16*, 6400.
- [6] (a) H. Harada, H. Irie, N. Masaki, K. Osaki, S. Uyeo, *Chem. Commun.* **1967**, *3*, 460. (b) D.-H. Lai, Z.-D. Yang, W.-W. Xue, J. Sheng, Y. Shi, X.-J. Yao, *Fitoterapia* **2013**, *89*, 257.
- [7] Y. Hitotsuyanagi, H. Fukaya, E. Takeda, S. Matsuda, Y. Saishu, S. Zhu, K. Komatsu, K. Takeya, *Tetrahedron* **2013**, *69*, 6297.
- [8] W.-H. Lin, Y. Ye, R.-S. Xu, *J. Nat. Prod.*, **1992**, *55*, 571.
- [9] J.-L. Dong, Z.-D. Yang, S.-Y. Zhou, H.-T. Yu, X.-J. Yao, H.-Y. Xue, Z.-M. Shu, *Phytochem. Lett.* **2017**, *19*, 259.
- [10] L.-G. Lin, H. P.-H. Leung, J.-Y. Zhu, C.-P. Tang, C.-Q. Ke, J. A. Rudd, G. Lin, Y. Ye, *Tetrahedron* **2008**, *64*, 10155.

- [11] (a) P. K. Mandal, D. Limbrick, D. R. Coleman, G. A. Dyer, Z. Ren, J. S. Birtwistle, C. Xiong, X. Chen, J. M. Briggs, J. S. MuMurray, *J. Med. Chem.* **2009**, *52*, 2429. (b) H. Greger, *Planta Med.* **2006**, *72*, 99. (c) H.-S. Chung, P.-M. Hon, G. Lin, P. P.-H. But, H. Dong, *Planta Med.* **2003**, *69*, 914. (d) K.-H. Jung, Y.-S. Kil, J. Jung, S. Park, D. Shim, K. Lee, E.-K. Seo, H. Bae, *Phytomedicine* **2016**, *23*, 79. (e) Y. Gao, J. Wang, C.-F. Zhang, X.-H. Xu, M. Zhang, L.-Y. Kong, *Tetrahedron* **2014**, *70*, 967. (f) H. Greger, *Phytochem. Rev.* **2019**, *18*, 463.
- [12] (a) S. P. Cooper, K. I. Booker-Milburn, *Angew.Chem. Int. Ed.* **2015**, *54*, 6496. (b) P. Hu, Y. Zhang, B. Liu, X. Li, *Org. Chem. Front.* **2018**, *5*, 3263. (c) J. Barluenga, M. Fananás-Mastral, F. Aznar, *Chem. Eur. J.* **2008**, *14*, 7508. (d) J. Chen, Y. Xie, J. Chen, H. Zhang, *Tetrahedron* **2015**, *71*, 3747. (e) J. Chen, J. Chen, Y. Xie, H. Zhang, *Angew.Chem.Int. Ed.* **2012**, *51*, 1024. (f) P. Wipf, S. R. Spencer, *J. Am. Chem. Soc.* **2005**, *127*, 225. (g) K. J. Frankowski, J. E. Golden, Y. Zeng, Y. Lei, J. Aubé, *J. Am. Chem. Soc.* **2008**, *130*, 6018. (h) A. Padwa, J. D. Ginn, *J. Org. Chem.* **2005**, *70*, 5197. (i) R. W. Bates, S. Sridhar, *J. Org. Chem.* **2011**, *76*, 5026. (j) J. H. Rigby, S. Laurent, A. Cavezza, Heeg, M. J. *J. Org. Chem.* **1998**, *63*, 5587. (k) J. D. Ginn, A. Padwa, *Org. Lett.* **2002**, *4*, 1515. (l) Q. Wang, A. Padwa, *Org. Lett.* **2006**, *8*, 601. (m) J. Zhang, Y.-Q. Wang, X.-W. Wang, W.-D. Z. Li, *J. Org. Chem.* **2013**, *78*, 6154. (n) R. L. Connelly, J. P. Knowles, *Org. Lett.* **2019**, *21*, 18.
- [13] (a) Q. Huang, Q. Han, S. Fu, Z. Yao, L. Su, X. Zhang, S. Lin, S. Xiang, *J. Org. Chem.* **2016**, *81*, 12135. (b) Q. Han, X. Guo, Z. Tang, L. Su, Z. Yao, X. Zhang, S. Lin, S. Xiang, Q. Huang, *Adv. Synth. Catal.* **2018**, *360*, 972. (c) X. Guo, Q. Han, Z. Tang, L. Su, X. Zhang, S. Lin, Q. Huang, *Tetrahedron Lett.* **2018**, *59*, 1568. (d) K. Morimoto, K. Hirao, T. Satoh, M. Miura, *Org. Lett.* **2010**, *12*, 2068. (e) L. Ackermann, L. Wang, A. V. Lygin, *Chem. Sci.* **2012**, *3*, 177.
- [14] I. E. Tsyshchuk, D. V. Vorobyeva, A. S. Peregodov, S. N. Osipov, *Eur. J. Org. Chem.* **2014**, *2014*, 2480. (b) M. Delgado-Rebollo, A. Prieto, P. J. Pérez, *ChemCatChem* **2014**, *6*, 2047. (c) J. M. Fraile, K. L. Jeune, J. A. Mayoral, N. Ravasio, F. Zaccheria, *Org. Biomol. Chem.* **2013**, *11*, 4327. (d) M. B. Johansen, M. A. Kerr, *Org. Lett.* **2010**, *12*, 4956.
- [15] A. Rouchaud, J.-C. Brackman, *Eur. J. Org. Chem.* **2009**, *2009*, 2666.
- [16] C. Jia, W. Lu, T. Kitamura, Y. Fujiwara, *Org. Lett.* **1999**, *1*, 2097.

Chapter 7.

One pot synthesis of pyrrolo[3,2,1-*de*]phenanthridines from 7-phenylindoles via tandem C-H olefination/aza-Michael addition

This chapter is adapted from the publication: Yumeng Yuan, Guoshuai Pan, Xiaofeng Zhang, Qiufeng Huang, *Org. Chem. Front.* **2020**, 7, 53-63.

Chapter 7 - One pot synthesis of pyrrolo[3,2,1-*de*]phenanthridines from 7-phenylindoles via tandem C-H olefination/aza-Michael addition

7.1. Introduction

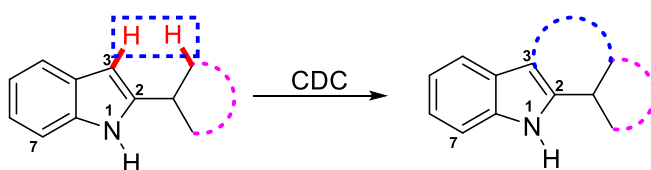
The indole skeleton is unarguably one of the most important structural moieties in innumerable natural and unnatural compounds.^[1] In particular, fused tetracyclic ring systems containing indole units attracted the synthetic chemists due to their prevalent occurrence in many biologically active molecules.^[2] As the synthesis of these fused tetracyclic indoles usually requires multistep procedures,^[3] efficient, simple and divergent production of these molecules remains an important challenge facing synthetic organic chemists.

In recent years, the transition-metal-catalyzed cross-dehydrogenative-coupling (CDC) has emerged as an attractive and ideal strategy to synthesize complex heterocyclic molecules, as it permits the building of C-C bonds by directly connecting two C-H bonds. The benefits of CDC include atom and step economy, lower cost and less waste.^[4] CDC tools were realized for the preparation of 2,3-fused (Scheme 7-1a) or 1,2-fused tetracyclic indoles (Scheme 7-1b). For examples, the CDC reaction of 2-arylindoles with alkynes, alkenes, ketenes, diazo compounds and carbon monoxide leading to indolo[2,1-*a*]isoquinolines,^[5] indole-indolones,^[6] benzo[*a*]carbazoles,^[7] 5*H*-benzo[*a*]carbazol-5-ones^[8] and 6*H*-isoindolo[2,1-*a*]indol-6-ones^[9] have been developed. The synthesis of indolo[3,2-*c*]coumarins,^[10] indolo[3,2-*c*]quinolinones^[11] and indole[3,2-*c*]pyrones^[12] via intramolecular CDC reaction were also uncovered. Greaney and co-workers disclosed a palladium-catalyzed intramolecular CDC reaction between aromatic ring and indolyl moiety producing a set of indole-containing seven- and eight-membered rings.^[13] Inspired by those advances and as part of our continued interest in the *NH*-indole-directed C-H functionalization,^[9, 14] we

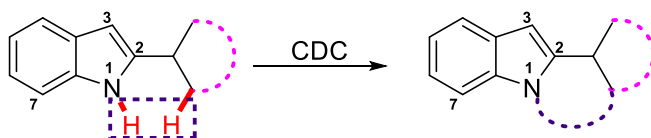
herein present a protocol for the rhodium-catalyzed C-H alkenylation and subsequent intramolecular aza-Michael reaction of 7-arylindoles with alkenes leading to diverse biologically important pyrrolo[3,2,1-*de*]phenanthridines (Figure 7-1).^[15] To the best of our knowledge, the synthesis of such attractive 1,7-fused tetracyclic indoles via CDC reaction has yet to be described (Scheme 7-1c).

previous work:

a) The synthesis of 2,3-fused tetracyclic indoles via CDC reaction

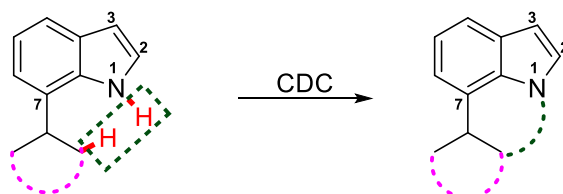


b) The synthesis of 1,2-fused tetracyclic indoles via CDC reaction



this work:

c) The synthesis of 1,7-fused tetracyclic indoles via CDC reaction



Scheme 7-1. Approaches of CDC reactions: synthesis of fused tetracyclic indoles

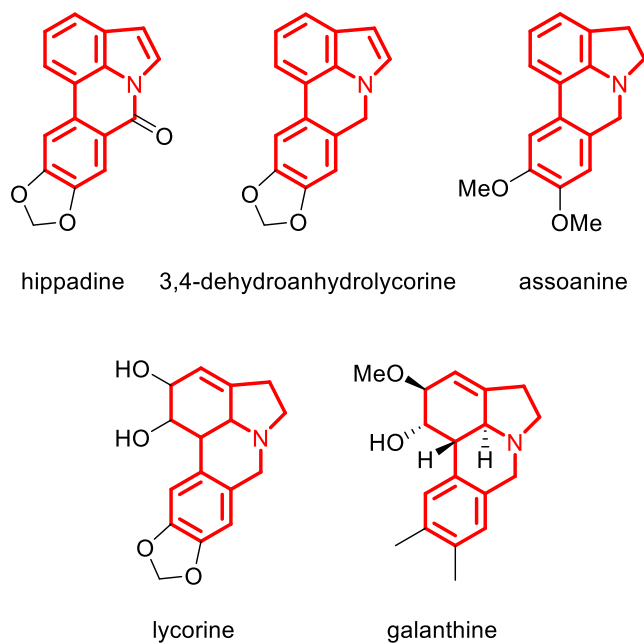
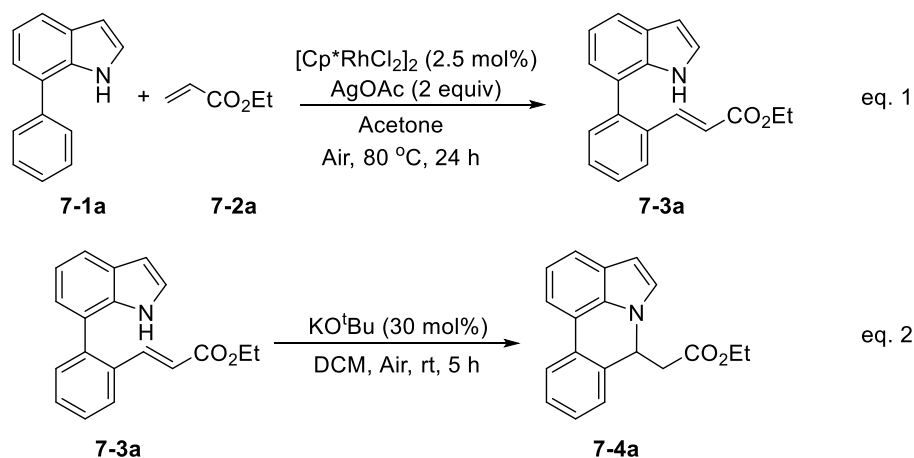
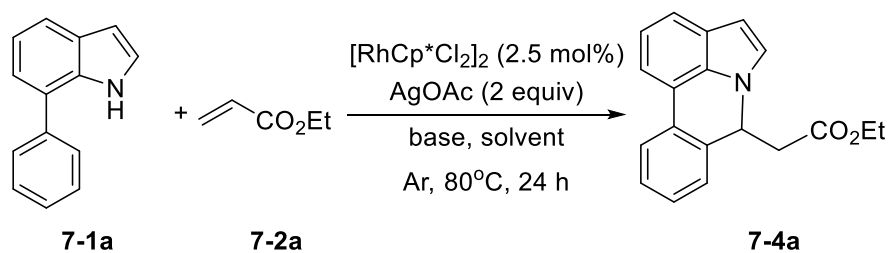


Figure 7-1. Some biologically active pyrrolo[3,2,1-*de*]phenanthridine derivatives



Scheme 7-2. Rhodium-catalyzed ortho C-H olefination of 7-arylindoles (eq. 1); KO^tBu-catalyzed intramolecular aza-Michael addition (eq. 2).

Table 7-1. Optimization of Reaction Conditions of one-pot synthesis of 7*H*-pyrrolo[3,2,1-*de*]phenanthridinea



Entry	base	Solvent	7-4a Yield(%) ^[b]
-------	------	---------	------------------------------

1	KO ^t Bu	acetone	trace
2	DBU (2 equiv.)	acetone	trace
3	DMAP (2 equiv.)	acetone	trace
4	KOH (2 equiv.)	acetone	trace
5	KPF ₆ (2 equiv.)	acetone	trace
6	ⁿ Bu ₄ NOAc (2 equiv.)	acetone	35
7	Me ₄ NOAc (2 equiv.)	acetone	28
8	ⁿ Bu ₄ NOAc (10 equiv.)	acetone	30
9	Me ₄ NOAc (10 equiv.)	acetone	58
10 ^c	other acetate salts (10 equiv.)	acetone	0
11	Me ₄ NOAc (10 equiv.)	xylene	trace
12	Me ₄ NOAc (10 equiv.)	DCE	trace
13	Me ₄ NOAc (10 equiv.)	DCM	trace
14	Me ₄ NOAc (10 equiv.)	1,4-dioxane	trace
15	Me ₄ NOAc (10 equiv.)	EtOAc	trace
16	Me₄NOAc (10 equiv.)	MeCN	99 (97)
17	Me ₄ NOAc (5 equiv.)	MeCN	88

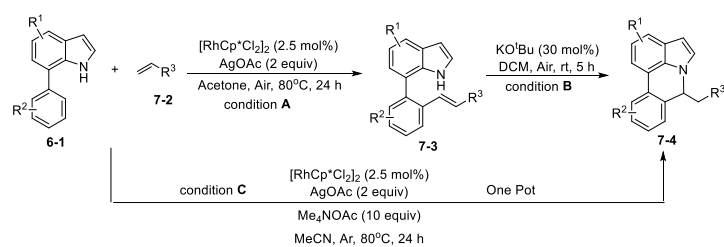
^a Conditions: **7-1a** (0.3 mmol), **7-2a** (0.75mmol), [Cp*⁺RhCl₂]₂ (2.5 mol%), AgOAc (2 equiv.), base, solvent (2 mL), 80 °C, 24 h. ^b ¹H NMR Yield on the basis of the amount of **1a** used, Number in parenthesis is isolated yield. ^c Other acetate salts = KOAc, NaOAc, CsOAc, LiOAc.

7.2. Results and Discussion

Our initial studies involved the intermolecular Fujiwara-Moritani of 7-phenyl-1*H*-indol (**7-1a**) with ethyl acrylate (**7-2a**) employing the conditions of [Cp*⁺RhCl₂]₂ (2.5 mol%) and AgOAc (2 equiv.) in ethyl acetate (EtOAc) at 100 °C. This leads to the generation of mono *ortho*-alkenylated product **7-3a** in 35% (Table 2-S1, entry 1 in Chapter 9) with complete *E*-stereoselectivity. None di-alkenylated or C3-alkenylated product was found in the reaction mixture. We were delighted to find that changing the solvent from EtOAc to acetone could

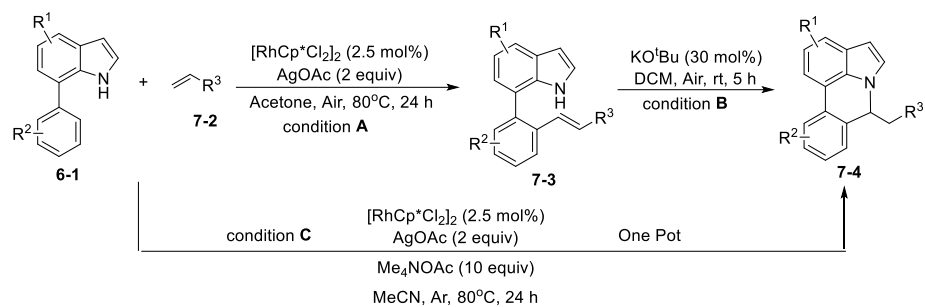
lead to dramatically increase of the yield of **7-3a** to 84% (Table S7-1, entry 2 in Chapter 9). The optimum reaction temperature is 80 °C, thus affording near quantitative yield (Table S7-1, entry 8 in Chapter 9). Notably, this transformation can also be performed in an air atmosphere; the isolated yield of **7-3a** is 97% (Scheme 7-2, eq. 1). Treating **7-3a** with 30 mol% KO^tBu in dichloromethane (DCM) resulted in intramolecular aza-Michael reaction. The aza-Michael product 7*H*-pyrrolo[3,2,1-*de*]phenanthridine **7-4a** is obtained in quantitative yield in pure form directly after workup without the need for column chromatography (Scheme 7-2, eq. 2). Replacing KO^tBu with other bases such as KOH, DMAP, Et₃N, KOAc, NaOAc, CsOAc, LiOAc and so on failed to furnish the desired products, and starting material **7-3a** was recovered (Table S7-2 in Chapter 9). Encouraged by the above results, one-pot synthesis of 7*H*-pyrrolo[3,2,1-*de*]phenanthridine **7-4a** by combining intermolecular C-H olefination and intramolecular aza-Michael addition of 7-phenyl-1*H*-indole (**7-1a**) with ethyl acrylate (**7-2a**) was surveyed (Table 7-1). KO^tBu had a detrimental effect on [Cp**Rh*Cl₂]₂/AgOAc catalyst system, the starting material **7-1a** was recovered totally (Table 7-1, entry 1). Other bases such as DBU, DMAP, KOH and KPF₆ also gave unsatisfactory results (entries 2-5). Interestingly, employing quaternary ammonium salts such as ⁿBu₄NOAc and Me₄NOAc in acetone at 80 °C for 24 h, the desired product **7-4a** can be obtained in 35% and 28% yield, respectively (entries 6-7). When the amount of Me₄NOAc was increased from 2 equiv. to 10 equiv., the yield of **7-4a** improved to 58% NMR yield (entry 9). No significant change in the yield of **7-4a** was observed on using 10 equiv. of ⁿBu₄NOAc (entry 8). When 10 equiv. of other acetate salt such as KOAc, NaOAc, CsOAc, LiOAc was employed, the reaction was stop after olefination and intramolecular aza-Michael addition

Table 7-2. Substrates scope^a



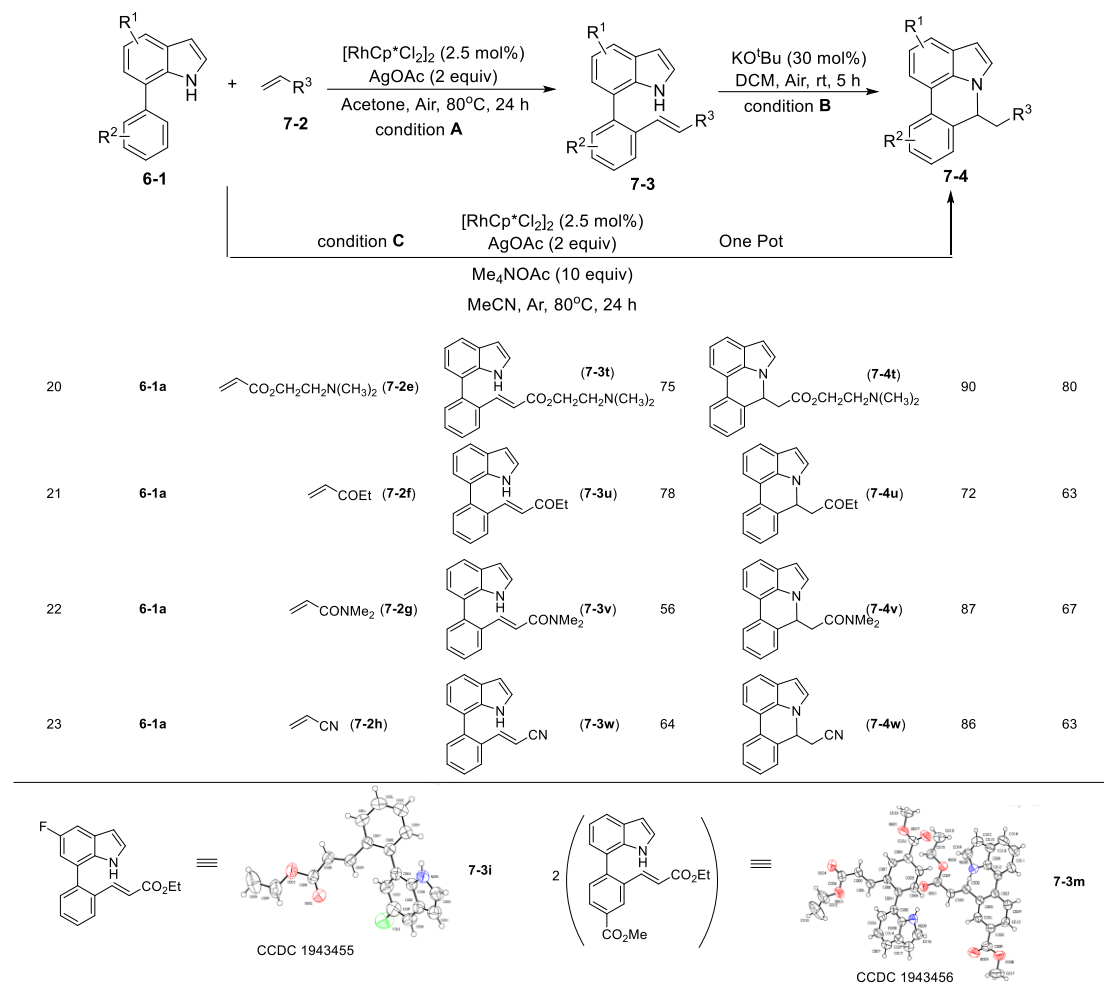
entry	7-aryl-1 <i>H</i> -indole 6-1	alkene 7-2	product 7-3	yield of 7-3 (%) ^b	product 7-4	yield of 7-4 (%) ^b	
						Condition B	Condition C
1				97		100	99
2		7-2a		75		93	80
3		7-2a		78		92	76
4		7-2a		79		90	80
5		7-2a		30		87	45
6		7-2a		NR			
7		7-2a		16			
8		7-2a		13			
9		7-2a		88		93	82
10		7-2a		73		93	80
11		7-2a		73		92	72

Continued **Table 7-2**



12		(6-1l)	7-2a		(7-3l)	64		(7-4l)	91	90
13		(6-1m)	7-2a		(7-3m)	80		(7-4m)	72	77
14		(6-1n)	7-2a		(7-3n)	77		(7-4n)	95	74
15		(6-1o)	7-2a		(7-3o)	79		(7-4o)	93	81
16		(6-1p)	7-2a		(7-3p)	87		(7-4p)	91	89
17	6-1a		(7-2b)		(7-3q)	92		(7-4q)	90	93
18	6-1a		(7-2c)		(7-3r)	78		(7-4r)	88	97
19	6-1a		(7-2d)		(7-3s)	81		(7-4s)	89	73

Continued **Table 7-2**



^a Conditions **A**: **6-1a** (0.3 mmol), **7-2a** (0.75mmol), [Cp**Rh*Cl₂]₂ (2.5 mol%), AgOAc (2 equiv.), acetone (2 mL), 80 °C, air, 24 h; Conditions **B**: **7-3a** (0.2 mmol), KO^tBu (30 mmol%), DCM (2 mL), rt, air, 5 h; Conditions **C**: **6-1a** (0.3 mmol), **7-2a** (0.75 mmol), [Cp**Rh*Cl₂]₂ (2.5 mol%), AgOAc (2 equiv.), Me₄NOAc (10 equiv.), MeCN (2 mL), 80 °C, 24 h. Isolated yields reported.

product **7-4a** was not formed totally. After an extensive screen of solvents, we found that the use of CH₃CN gave the best result in 99% yield of **7-4a** after 24 h (entry 15, 97% isolated yield). MeOH as the solvent gave **7-3a** selectively, and other solvent such as EtOH, DCE, DCM, 1,4-dioxane, EtOAc led to complete reaction shutdown. Finally, a decrease in the loading of Me₄NOAc (5 equiv.) resulted in a lower yield of **7-4a** (88%, Table 7-1, entry 17)

With optimized reaction conditions in hand, we then investigated the scope and generality of the present processes (Table 7-2). With the conditions **7-A**, a broad range of 7-phenylindoles could be transformed to the *ortho*-mono-alkenylated products with up to 97% yield. Many functional groups, such as fluoro (**7-3i**), cyano (**7-3j**), nitro (**7-3k**), chloro (**7-3l**, **7-3o**), ester (**7-3m**), methoxy (**7-3n**) and naphthyl (**7-3p**) were well tolerated. The positions of substituent play an important role in the reaction efficiency and regioselectivity. 7-phenyl-1*H*-indoles with the substituents on 4,5-positions of the indole ring or *meta*, *para*-positions of the benzene ring, were delivered easily to *ortho*-alkenylated 7-phenyl-1*H*-indoles in excellent yields **7-(3b-3d, 3i-3n)**. However, reaction of 3-methyl-7-phenyl-1*H*-indole **6-1e** with **7-2a** provided the corresponding product **7-3e** in low yield (30%), while 2-methyl-7-phenyl-1*H*-indole **1f** led to complete reaction shutdown. When 6-methyl-7-phenyl-1*H*-indole (**6-1g**) or 7-(*o*-tolyl)-1*H*-indole (**6-1h**) was employed, a low yield of the 3-alkenylated 7-phenyl-1*H*-indole was formed selectively (**7-3g**, 16%; **7-3h**, 13%). No *ortho*-alkenylated product was formed. On the other hand, the experiment results showed that the electronic properties of the substituents had no discernible effect on the reaction efficiency. As expected, other acrylates such as 2-methoxyethyl acrylate (**7-2b**), *tert*-butyl acrylate (**7-2c**), *n*-butyl acrylate (**7-2d**) and 2-(dimethylamino)ethyl acrylate (**7-2e**) were all smoothly reacted with **6-1a** to afford the desired products **7-(3q-3t)** in good yields. Further, ethyl vinyl ketone (**7-2f**), *N,N*-dimethylacrylamide (**7-2g**) or acrylonitrile (**7-2h**) also efficiently reacted with **6-1a** yielding *ortho*-alkenylated products **7-(3u-3w)** in 78%, 56% and 64% yields, respectively. However, methyl methacrylate is less reactive than ethyl acrylate **7-2a** in this system. Almost no desired product **7-3** was obtained.

Next, we turned our attention to the synthesis of annulated product 7*H*-pyrrolo[3,2,1-*de*]phenanthridines. To our delight, with the condition **B**, KO^tBu-catalyzed intramolecular aza-Michael reaction proceeded quite well to give the desired products **7-4** in high yield. The reaction seems to be insensitive to the electronic and steric effects of substituents. With condition **C**, a great variety of

7-phenyl-1*H*-indoles can be converted into the corresponding 7*H*-pyrrolo[3,2,1-*de*]phenanthridines through a one-pot C-H olefination/aza-Michael addition sequence. The yield of product mainly depends on the efficiency of C-H olefination step. It is worth noting that the first equilibrium reaction (C-H olefination) will be shifted to the right, according to the Le Châtelier's principle, as intermediate **7-3** undergoes aza-Michael reaction efficiently. Consequently, the yield of one-pot reaction is higher than overall yield of two-steps procedure. For example, 3-methyl-7-phenyl-1*H*-indole **6-1e** provided the product **7-4e** in a synthetically useful yield via one-pot procedure (45%). On the contrary, the two-steps route to **7-4e** was hampered by low yielding step and provided **7-4e** in only 29% overall yield. In addition, when compound **7-4a** is resubjected to the reaction condition **B** and **C**, no reaction occurred, and compound **7-4a** were recovered. This result likely indicates that the intramolecular aza-Michael addition is irreversibly.

7.3. Conclusions

In conclusion, we have successfully developed [Cp**RhCl*₂]₂/AgOAc-catalyzed regioselectively *ortho* C-H olefination of 7-phenylindoles and KO^tBu-catalyzed intramolecular aza-Michael addition leading to pyrrolo[3,2,1-*de*]phenanthridines. More importantly, the tandem C-H olefination/aza-Michael addition can be proceeded in one-pot under mild reaction conditions using [Cp**RhCl*₂]₂/AgOAc/Me₄NOAc catalytic system. A relatively wide range of functional groups are tolerated, and a variety of pyrrolo[3,2,1-*de*]phenanthridines are obtained in good to excellent yields. The developed efficient and straightforward synthesis of pyrrolo[3,2,1-*de*]phenanthridines will be useful for the establishment of compound libraries for drug discovery.

7.4. References

- [1] (a) E. Stempel, T. Gaich, *Acc. Chem. Res.*, **2016**, *49*, 2390-2402; (b) N. Chadha, O. Silakari, *Eur. J. Med. Chem.*, **2017**, *134*, 159-184; (c) T. V. Sravanthi, S. L. Manju, *Eur. J. Pharm. Sci.*, **2016**, *91*, 1-10; (d) M.-Z. Zhang, Q. Chen, G.-F. Yang, *Eur. J. Med. Chem.*, **2015**, *89*, 421-441; (e) A. J. Kochanowska-Karamyan, M. T. Hamann, *Chem. Rev.*, **2010**, *110*, 4489-4497; (f) W. Zi, Z. Zuo, D. Ma, *Acc. Chem. Res.*, **2015**, *48*, 702-711; (g) R. Dalpozzo, *Chem. Soc. Rev.*, **2015**, *44*, 742-778; (h) S. Lancianesi, A. Palmieri, M. Petrini, *Chem. Rev.*, **2014**, *114*, 7108-7149.
- [2] (a) T. Föster, S. López-Tosco, S. Ziegler, A. P. Antonchick, H. Waldmann, *ChemBioChem*, **2017**, *18*, 1098-1108; (b) W. Yu, L. Tong, B. Hu, B. Zhong, J. Hao, T. Ji, S. Zan, C. A. Coburn, O. Selyutin, L. Chen, L. Rokosz, S. Agrawal, R. Liu, S. Curry, R. McMonagle, P. Ingravallo, E. Asante-Appiah, S. Chen, J. A. Kozlowski, *J. Med. Chem.*, **2016**, *59*, 10228-10243; (c) N. Yadav, T. Khanam, A. Shukla, N. Rai, K. Hajela, R. Ramachandran, *Org. Biomol. Chem.*, **2015**, *13*, 5475-5487; (d) S. Li, A. N. O. Lowell, S. A. Newmister, F. Yu, R. M. Williams, D. H. Sherman, *Nat. Chem. Bio.*, **2017**, *13*, 467-470; (e) V. Psarra, M. A. Fousteris, L. Hennig, M. Bantzi, A. Giannis, S. S. Nikolaropoulos, *Tetrahedron*, **2016**, *72*, 2376-2385; (f) E. Yamuna, R. A. Kumar, M. Zeller, K. J. R. Prasad, *Eur. J. Med. Chem.*, **2012**, *47*, 228-238.
- [3] (a) A. Suárez, M. Gohain, M. A. Fernández-Rodríguez, R. Sanz, *J. Org. Chem.*, **2015**, *80*, 70421-10430; (b) S.-L. Ding, Y. Ji, Y. Su, R. Li, P. Gu, *J. Org. Chem.*, **2019**, *84*, 2012-2021; (c) M. Taguchi, Y. Tokimizu, S. Qishi, N. Fujii, H. Ohno, *Org. Lett.*, **2015**, *17*, 6250-6253; (d) C. C. Forneris, Y.-P. Wang, G. Mamaliga, T. P. Willumstad, R. L. Danheiser, *Org. Lett.*, **2018**, *20*, 6318-6322; (e) C. Adouama, M. E. Budén, W. D. Guerra, M. Puiatti, B. Joseph, S. M. Barolo, R. A. Rossi, M. Médebielle, *Org. Lett.*, **2019**, *21*, 320-324; (f) A. M. Kulkarni, K. Srinivas, M. V. Deshpande, C. V. Ramana, *Org. Chem. Front.*, **2016**, *3*, 43; (g) J.-Q. Chen, Y. Mi, Z.-F. Shi, X.-P. Cao, *Org. Biomol. Chem.*, **2018**, *16*, 3801; (h) Y. Wang, F. Xie, B. Lin, M. Chen, Y. Liu, *Chem. Eur. J.*, **2018**, *24*, 14302-14315; (i) J. Park, S.-Y. Kim, J.-E. Kim, C.-G. Cho, *Org. Lett.*, **2014**, *16*, 178-181; (j) P. Pérez-Galán, H. Waldmann, K. Kumar, *Tetrahedron*, **2016**, *72*, 3647-3652.
- [4] (a) B. V. Varun, J. Dhineshkumar, K. R. Bettadapur, Y. Siddaraju, K. Alagiri, K. R. Prabhu, *Tetrahedron Lett.*, **2017**, *58*, 803-824; (b) Y. Yang, J. Lan, J. You, *Chem. Rev.*, **2017**, *117*, 8787-8863; (c) H. Kim, S. Chang, *ACS Catal.*, **2016**, *6*, 2341-2351; (d) M. K. Lakshman, P. K. Vuram, *Chem. Sci.*, **2017**, *8*, 5845-5888; (e) C. Liu, J. Yuan, M. Gao, S. Tang, W. Li, R. Shi, A. Lei, *Chem. Rev.*, **2015**, *115*, 12138-12204; (f) W. Ma, P. Gandeepan, J. Li, L. Ackermann, *Org. Chem. Front.*, **2017**, *4*, 1435-1467; (g) M. C. Henry, M. A. B. Mostafa, A. Sutherland, *Synthesis*, **2017**, *49*, 4586-4598; (h) L. Zheng, R. Hua, *Chem. Rec.*, **2018**, *18*, 556-569.
- [5] (a) K. Morimoto, K. Hirano, T. Satoh, M. Miura, *Org. Lett.*, **2010**, *12*, 2068-2071; (b) L. Ackermann, L. Wang, A. V. Lygin, *Chem. Sci.*, **2012**, *3*, 177; (c) Y.-Q. Xia, L. Dong, *Org. Lett.*, **2017**, *19*, 2258-2261.
- [6] X. Wang, Z. Li, S. Cao, H. Rao, *Adv. Synth. Catal.*, **2016**, *358*, 2059-2065.
- [7] (a) S.-S. Li, Y.-Q. Xia, F.-Z. Hu, C.-F. Liu, F. Su, L. Dong, *Chem. Asian J.*, **2016**, *11*, 3165-3168; (b) Q. Li, B. Li, B. Wang, *Chem. Commun.*, **2018**, *54*, 9147-9150; (c) B. Li, B.

- Zhang, X. Zhang, X. Fan, *Chem. Commun.*, **2017**, 53, 1297-1300; (d) Z. Zhang, K. Liu, X. Chen, S.-J. Su, Y. Deng, W. Zeng, *RSC Adv.*, **2017**, 7, 30554-30558.
- [8] X. Yang, Y. Li, L. Kong, X. Li, *Org. Lett.*, **2018**, 20, 1957-1960.
- [9] Q. Huang, Q. Han, S. Fu, Z. Yao, L. Su, X. Zhang, S. Lin, S. Xiang, *J. Org. Chem.*, **2016**, 81, 12135-12142.
- [10] (a) A. Dey, M. S. Ali, S. Jana, S. Samanta, A. Hajra, *Tetrahedron Lett.*, **2017**, 58, 313-316; (b) D. Ding, G. Zhu, X. Jiang, *Angew.Chem. Int. Ed.*, **2018**, 57, 9028-9032; (c) C. Cheng, W.-W.Chen, B. Xu, M.-H.Xu, *Org. Chem. Front.*, **2016**, 3, 1111-1115; (d) J. Wu, J. Lan, S. Guo, J. You, *Org. Lett.*, **2014**, 16, 5862-5865.
- [11] (a) L. Kong, Z. Zheng, R. Tang, M. Wang, Y. Sun, Y. Li, *Org. Lett.*, **2018**, 20, 5696-5699; (b) T.-Y.Zhang, C. Liu, C. Chen, J.-X.Liu, H.-Y.Xiang, W. Jiang, T.-M.Ding, S.-Y. Zhang, *Org. Lett.*, **2018**, 20, 220-223.
- [12] C. Cheng, W.-W.Chen, B. Xu, M.-H.Xu, *J. Org. Chem.*, **2016**, 81, 11501-11507.
- [13] D. G. Pintori, M. F. Greaney, *J. Am. Chem. Soc.*, **2011**, 133, 1209-1211.
- [14] (a) Q. Huang, Q. Song, J. Cai, X. Zhan, S. Lin, *Adv. Synth. Catal.*, **2013**, 355, 1512-1516; (b) Q. Han, S. Fu, X. Zhang, S. Lin, Q. Huang, *Tetrahedron Lett.*, **2016**, 57, 4165-4169; (c) X. Guo, Q. Han, Z. Tang, L. Su, X. Zhang, X. Zhang, S. Lin, Q. Huang, *Tetrahedron Lett.*, **2018**, 59, 1568-1572; (d) Q. Han, X. Guo, Z. Tang, L. Su, Z. Yao, X. Zhang, S. Lin, S. Xiang, Q. Huang, *Adv. Synth. Catal.*, **2018**, 360, 972-984.
- [15] (a) Y. Miki, H. Umemoto, M. Dohshita, H. Hamamoto, *Tetrahedron Lett.*, **2012**, 53, 1924-1927; (b) K. Suzuki, H. Iwasaki, R. Domasu, N. Hitotsuyanagi, Y. Wakizaka, M. Tominaga, N. Kojima, M. Ozeki, M. Yamashita, *Tetrahedron*, **2015**, 71, 5513-5519; (c) A. Emir, C. Emir, B. Bozkurt, M. A. Onur, J. Bastida, N. U. Somer, *Phytochem. Lett.*, **2016**, 17, 167-172; (d) A. Monaco, B. R. Szulc, Z. X. Rao, M. Barniol-Xicotá, M. Sehalia, B. M. A. Borges, S. T. Hilton, *Chem. Eur. J.*, **2017**, 23, 4750-4755; (e) S.-L. Ding, Y. Ji, Y. Su, R. Li, P. Gu, *J. Org. Chem.*, 2019, **84**, 2012-2021; (f) R. Rocaboy, D. Dailler, O. Baudoin, *Org. Lett.*, **2018**, 20, 772-775; (g) W. L. Yu, T. Nunns, J. Richardson, K. I. Booker-Milburn, *Org. Lett.*, **2018**, 20, 1272-1274; (h) S. Z. Tasker, A. E. Cowfer, P. J. Hergenrother, *Org. Lett.*, **2018**, 20, 5894-5898; (i) M. H. Wahl, C. Jandl, T. Bach, *Org. Lett.*, **2018**, 20, 7674-7678; (j) J. Wang, J. Li, X. Shen, C. Dong, J. Lin, K. Wei, *Org. Chem. Front.*, **2017**, 4, 1149; (k) U. V. Mentzel, D. Tanner, J. E. Tøneder, *J. Org. Chem.*, **2006**, 71, 5807-5810; (l) H. S. Kim, M. G. Banwell, A. C. Willis, *J. Org. Chem.*, **2013**, 78, 5103-5109; (m) M. D. Ganton, M. A. Kerr, *Org. Lett.*, **2005**, 7, 4777-4779; (n) C. G. Hartung, A. Fecher, B. Chapell, V. Snieckus, *Org. Lett.*, 2003, **5**, 1899-1902; (o) C. Tsukano, N. Muto, I. Enkhtaivan, Y. Takemoto, *Chem. Asian J.*, **2014**, 9, 2628-2634.
- [16] S. Caccchi, G. Fabrizi, A. Goggiamani, A. Lazzetti, *Tetrahedron*, **2015**, 71, 9346-9356.

Chapter 8.

Scalable Rhodaelectro-Catalyzed Expedient Access to Seven-membered Azepino[3,2,1-*hi*]indoles via [5+2] C-H/N-H Annulation

This chapter is adapted from the publication: Yumeng Yuan, Jinlan Zhu, Zhongyuan Yang, Shao-Fei Ni, Qiufeng Huang, Lutz Ackermann,
CCS Chem. **2022**, *4*, 1858-1870.

Chapter 8 - Scalable Rhodaelectro-Catalyzed Expedient Access to Seven-membered Azepino[3,2,1-*hi*]indoles via [5+2] C-H/N-H Annulation

8.1. Introduction

The synthesis of nitrogen-containing heterocycles, which are considered to be privileged scaffolds in medicinal and material chemistry, is of key relevance for molecular synthesis, crop protection and drug discovery.^[1-5] Among various available methods, transition-metal-catalyzed C–H/N–H oxidative annulation is an ideal approach for the rapid construction of nitrogen-containing heterocycles.^[6-8] In this context, past decades have witnessed the emergence of efficient synthesis of five^[9-17] or six-membered^[18-26] nitrogen-containing heterocyclic compounds. In sharp contrast, transition-metal-catalyzed C–H/N–H oxidative annulations leading to seven-membered rings still remain a challenge.^[27-29] Thus far, transition-metal-catalyzed C–H/N–H oxidative annulations have been dominated by stoichiometric chemical oxidants, such as hypervalent iodine(III) reagents as well as copper(II)^[30-32] and silver(I)^[33-38] salts for the regeneration of the active high valent active catalyst. The merger of transition-metal catalysis and electrocatalysis has recently emerged as a powerful platform for unlocking new synthetic methodologies.^[39-46] Furthermore, oxidative C–H coupling reaction, which can proceed under exogenous-oxidant-free conditions by metal-electrocatalysis, has expedited with major contributions by Xu^[47-49], Mei^[50-59], Lei^[60-67], and Ackermann^[68-89], among others^[90-95]. Within our program on the metal-electrochemical C-H activation, we herein present the first example of electrooxidative [5+2] C-H/N-H annulation for the efficient synthesis of seven-membered azepino[3,2,1-*hi*]indoles. Salient features of our findings include (1) exogenous-oxidant-free C–H activations, (2) scalability through flow electrooxidation, (3) isolation of two key rhodium(III) intermediates, (4) X-ray Photo-electronic Spectroscopy (XPS) studies, and (5) DFT calculations providing key mechanistic insights. (Figure 8-1)

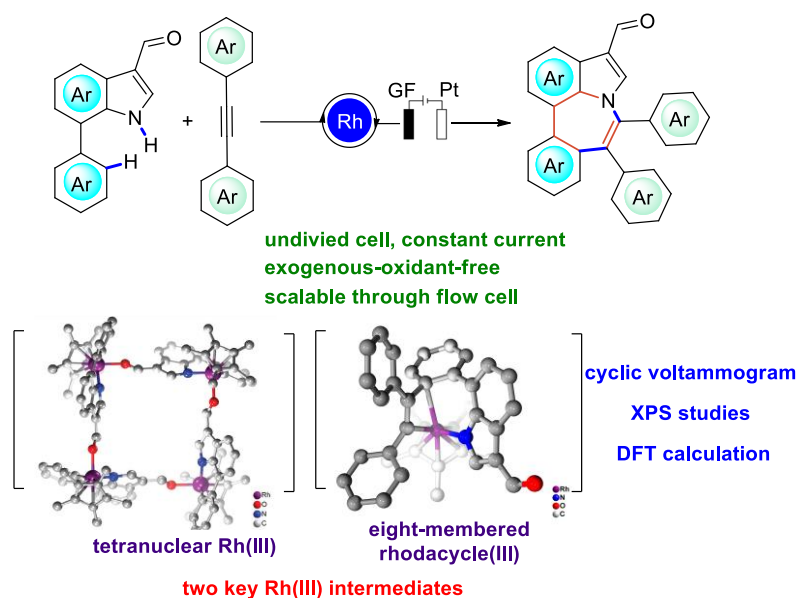
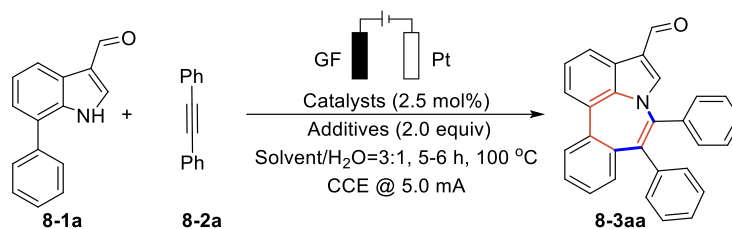


Figure 8-1.

8.2. Results and Discussion

Our research was initially performed by exploring the reaction conditions of metalla-electrochemical [5+2] C–H/N–H annulation using 7-phenyl-1*H*-indole-3-carbaldehyde **8-1a** and diphenylacetylene **8-2a** in a facile undivided cell set-up equipped with a graphite felt (GF) anode and a platinum (Pt) cathode (Table 8-1). After considerable experimentation, we observed that the desired product **8-3aa** was obtained with the use of [Cp**RhCl*₂]₂ (2.5 mol%) with Li₂CO₃ (2.0 equiv.) as the optimal combination. Amongst various solvents, the desired product **8-3aa** was obtained in 1,4-dioxane with 86% yield (entries 1-5). Replacing Li₂CO₃ with other additives, such as NaOPiv, K₃PO₄, ^{*n*}Bu₄NPF₆, K₂CO₃ and Na₂CO₃, resulted in a sharp decrease in yield (entries 6-10). Increasing or decreasing the amount of Li₂CO₃ also reduced the yield (entries 11-12). Control experiments verified the crucial role of Li₂CO₃, rhodium catalysts and electricity (entries 13-15). Three other typical transition metals were also explored, but no target products were obtained (entries 16-18). The present rhodium-catalyzed [5 + 2] C–H/N–H annulation can also precede with Ag₂CO₃ as the terminal oxidant instead of electricity, delivering a comparable yield (84%, entry 19).

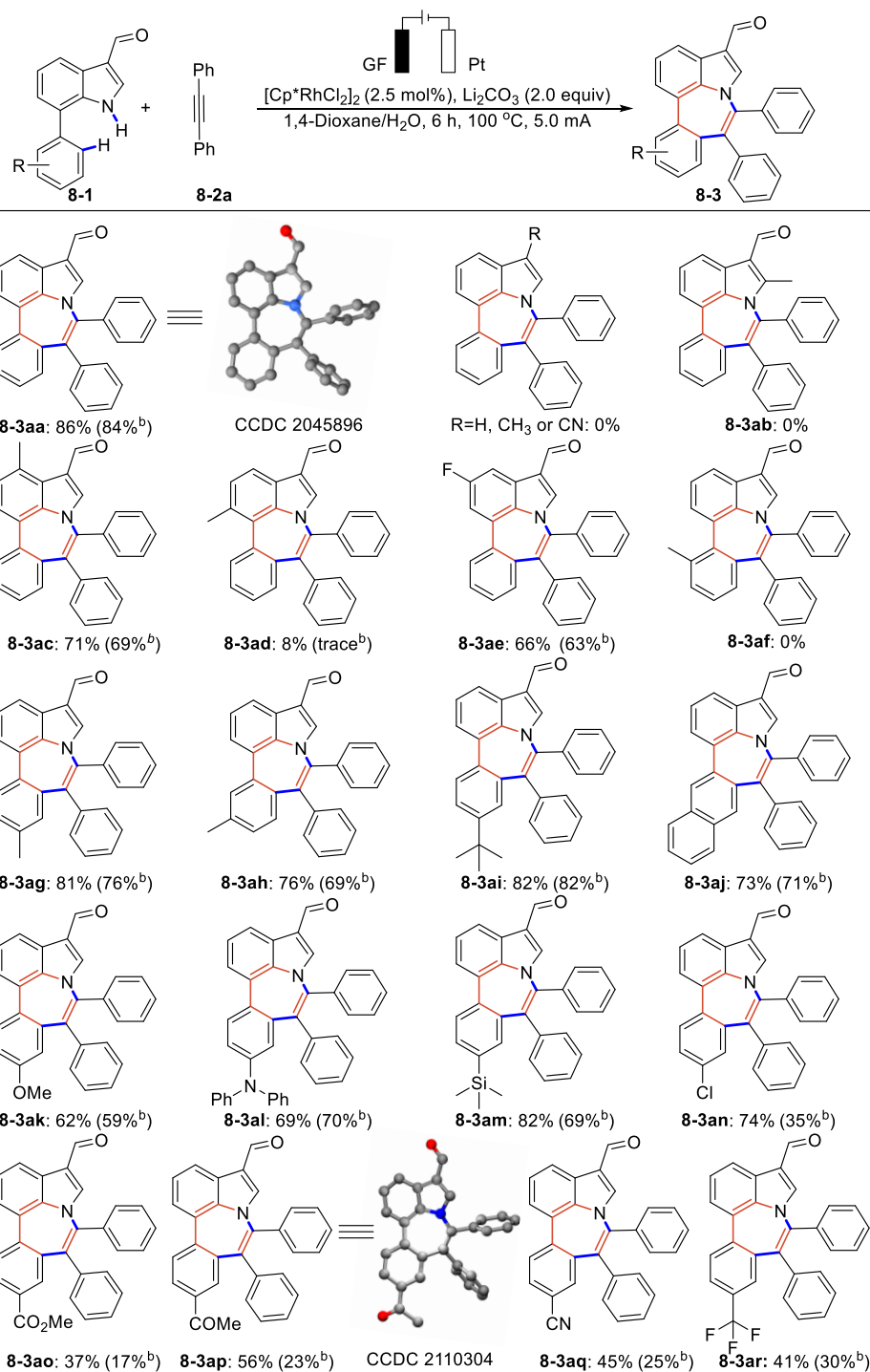
Table 8-1. Optimization of the rhodaelectro-catalyzed [5 + 2] C-H/N-H cyclization reaction.^[a]



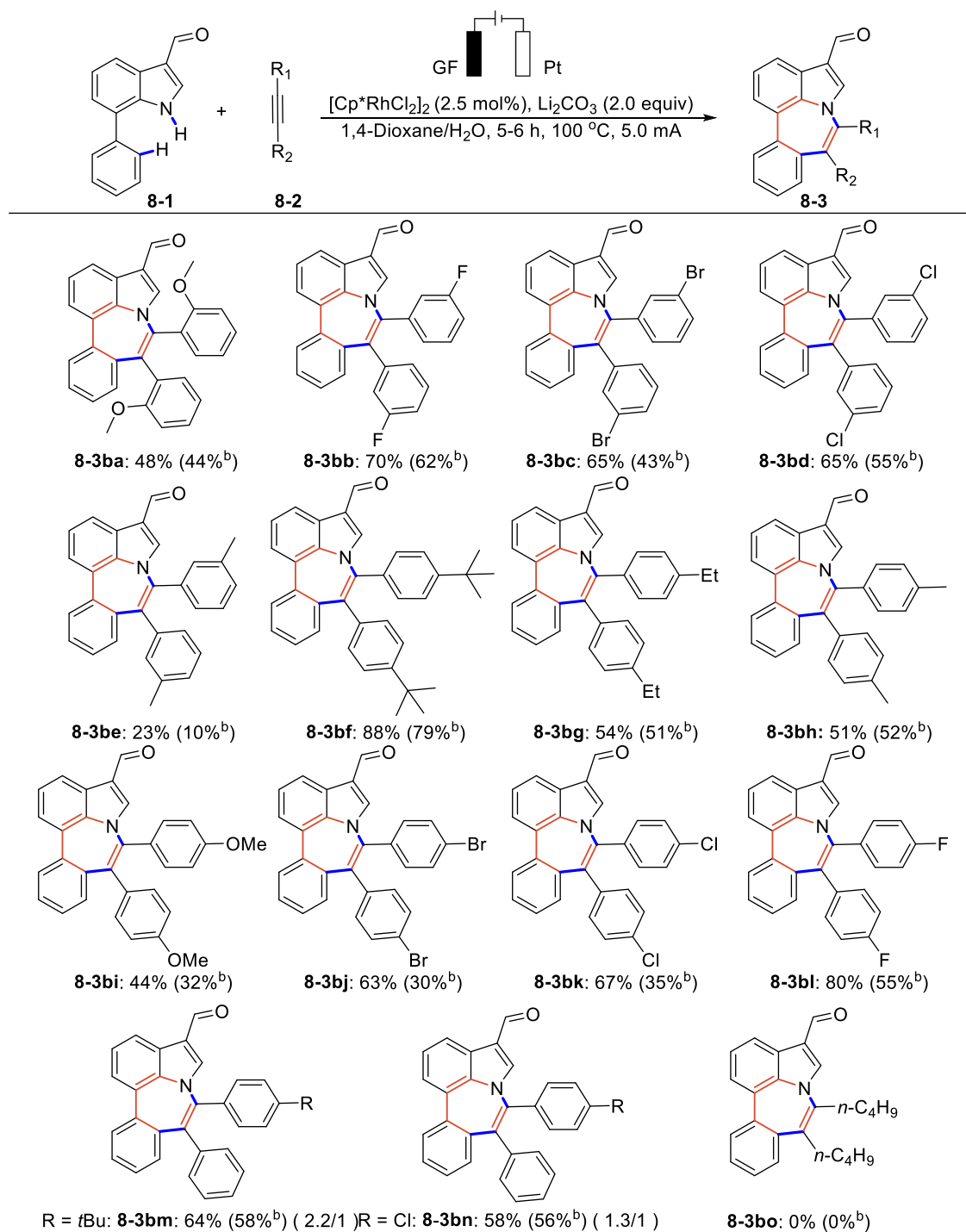
Entry	Catalyst	Additive	Solvent	Yield [%] ^[b]
1	[Cp*RhCl ₂] ₂	Li ₂ CO ₃	MeCN	21
2	[Cp*RhCl ₂] ₂	Li ₂ CO ₃	<i>t</i> -AmOH	0
3	[Cp*RhCl ₂] ₂	Li ₂ CO ₃	THF	0
4	[Cp*RhCl ₂] ₂	Li ₂ CO ₃	DMF	0
5	[Cp*RhCl ₂] ₂	Li ₂ CO ₃	1,4-dioxane	86
6	[Cp*RhCl ₂] ₂	NaOPiv	1,4-dioxane	45
7	[Cp*RhCl ₂] ₂	ⁿ Bu ₄ NPF ₆	1,4-dioxane	trace
8	[Cp*RhCl ₂] ₂	K ₃ PO ₄	1,4-dioxane	30
9	[Cp*RhCl ₂] ₂	K ₂ CO ₃	1,4-dioxane	15
10	[Cp*RhCl ₂] ₂	Na ₂ CO ₃	1,4-dioxane	40
11	[Cp*RhCl ₂] ₂	Li ₂ CO ₃	1,4-dioxane	69 ^[c]
12	[Cp*RhCl ₂] ₂	Li ₂ CO ₃	1,4-dioxane	73 ^[d]
13	[Cp*RhCl ₂] ₂	-	1,4-dioxane	NR
14	-	Li ₂ CO ₃	1,4-dioxane	NR
15	[Cp*RhCl ₂] ₂	Li ₂ CO ₃	1,4-dioxane	trace ^[e]
16	Pd(OAc) ₂	Li ₂ CO ₃	1,4-dioxane	NR
17	[Cp*IrCl ₂] ₂	Li ₂ CO ₃	1,4-dioxane	NR
18	[Ru(<i>p</i> -cymene) ₂ Cl ₂] ₂	Li ₂ CO ₃	1,4-dioxane	NR
19	[Cp*RhCl ₂] ₂	Ag ₂ CO ₃	<i>t</i> -AmOH	84 ^[e]

^a Reaction conditions: Undivided cell, **8-1a** (0.2 mmol), **8-2a** (0.4 mmol), catalyst (2.5 mmol%), additive (2.0 equiv), solvent (4.0 mL), 100 °C, 5 h, constant current = 5 mA, graphite felt (GF) anode, platinum (Pt) cathode. ^b Yields of isolated product **8-3aa**. ^c Li₂CO₃ (1.0 equiv). ^d Li₂CO₃ (3.0 equiv). ^e No electricity.

Having determined the optimal reaction conditions, the scope of the electrooxidative rhodium-catalyzed C–H/N–H annulation reaction was first examined with a set of 7-phenyl-1*H*-indole-3-carbaldehyde **8-1** (Scheme 8-1). The reaction is found to be very sensitive in relation to the substituents at the 3-position of the indole ring.



Scheme 8-1. Scope of the Rhodaelectro-catalyzed C–H/N–H annulation by indoles **8-1**.



^a Reaction Condition: Undivided cell, **8-1a** (0.2 mmol), **8-2a** (0.4 mmol), [Cp*RhCl₂]₂ (2.5 mmol%), Li₂CO₃ (2.0 equiv.), 1,4-Dioxane/H₂O = 3:1 (4.0 mL), 100 °C, 5 h, constant current = 5 mA, graphite felt (GF) anode, platinum (Pt) cathode.

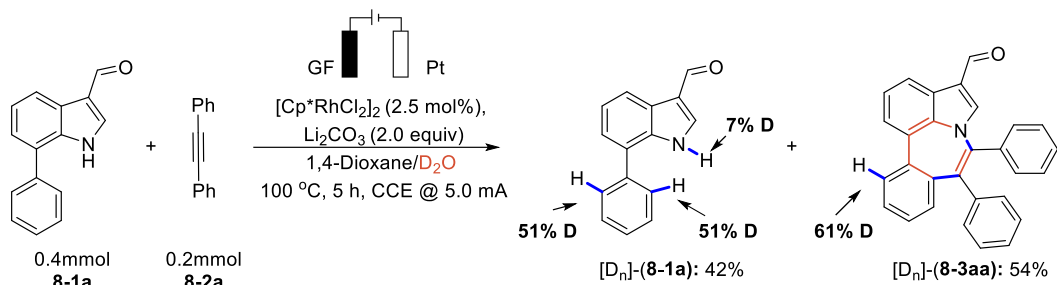
^b Reaction condition: **8-1a** (0.2 mmol), **8-2a** (0.4 mmol), [Cp*RhCl₂]₂ (2.5 mmol%), Ag₂CO₃ (2.0 equiv.), *t*-AmOH, 12 h, 100 °C.

Scheme 8-2. Scope of the Rhodoelectro-catalyzed C-H/N-H annulation by diphenylacetylenes **8-2**.

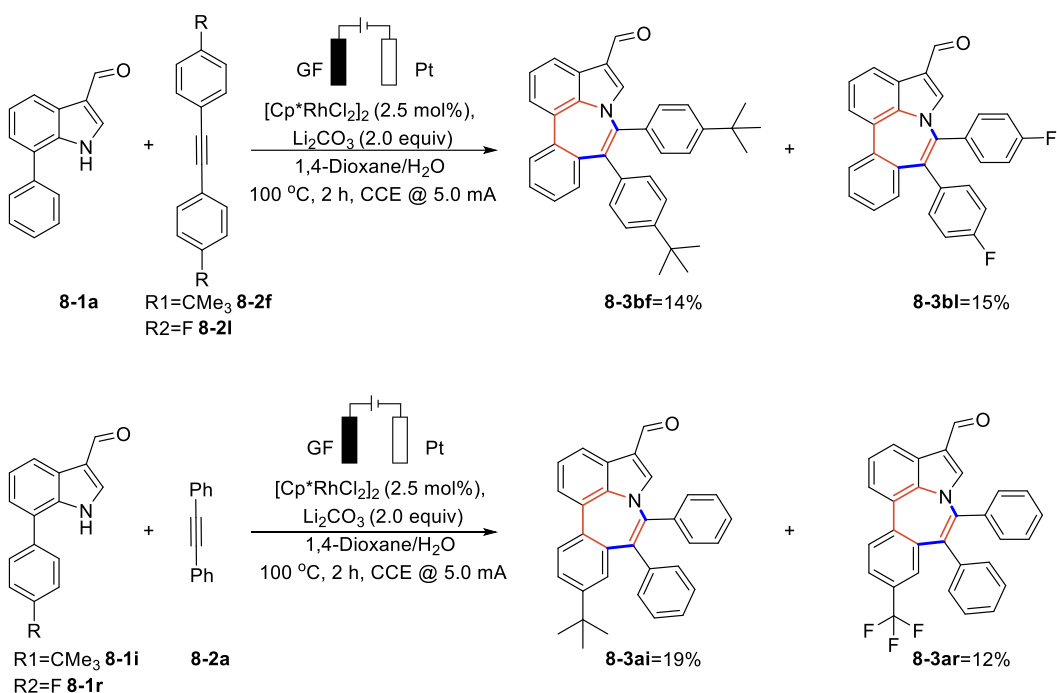
With the formyl group at the 3-position favored the reaction, delivering the required product in an excellent yield **8-3aa**, while other substitution patterns at C-3 proved less suitable, and the starting material **8-1** was recovered. It was also found that the position of substituents played a dominant role as to the catalyst's efficiency. Substrates **8-1** with substituents at the heteroaromatic motif or the benzene moiety provided high to excellent yields of the desired products **8-(3ac, 3ae, 3ag, 3ai-3ar)**. The electrocatalysis was however sluggish, when the 6-position of the indole ring was replaced by a methyl group **8-3ad**. Substituents at the 2-position of the indole ring or the benzene ring disabled the reaction **8-(3ab, 3af)**, and the starting material was recovered. The electrochemical annulation was amenable to functional groups, such as F, CF₃, Cl, OMe, NPh₂, SiMe₃, CO₂Me, COMe, and CN. It is noteworthy that electrolytic protocol generally provided a superior performance to the conventional reoxidation strategy ([Cp*RhCl₂]₂/Ag₂CO₃) in term of yields.

The scope of the rhodaelectro-catalyzed [5 + 2] C–H/N–H cyclization was next explored with decorated diphenylacetylenes **8-2** (Scheme 8-2). *Ortho*, *meta*, or *para*-substituted diphenylacetylenes bearing various functional groups, such as methoxy, fluoro, bromo and chloro, were all compatible with the standard conditions, affording the corresponding products. When an unsymmetrical internal alkyne was employed, the formation of two possible regioisomers was observed. The reaction of 4-octyne was unsuccessful and failed to generate the desired product **8-3bo** with all the starting material **8-1a** remaining.

a) H/D exchange experiments



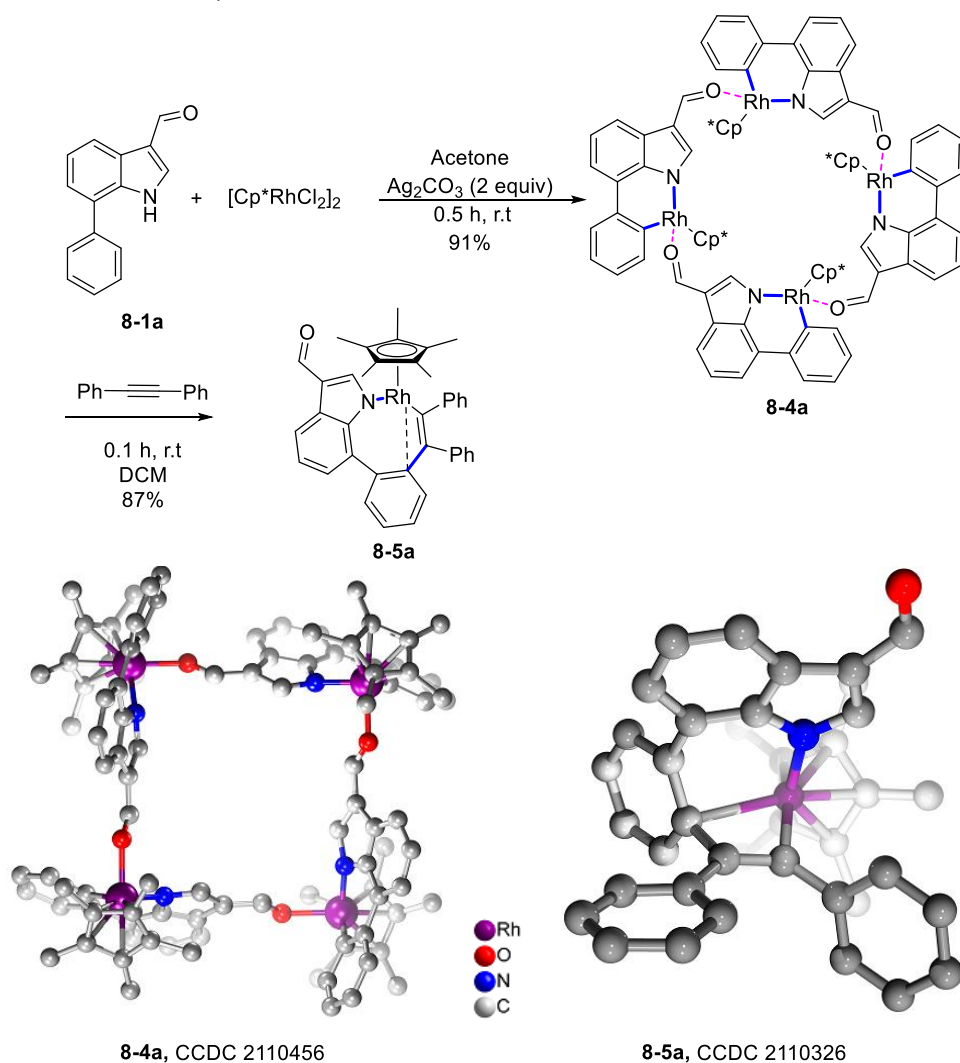
b) competition reactions



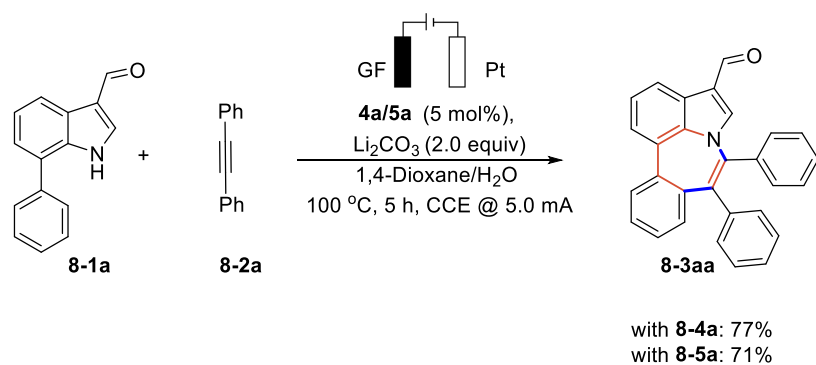
Scheme 8-3. Summary of key mechanistic experiments.

Deuterium-labeling and competition experiments were conducted to cast light on the reaction mechanism. First, H/D exchange experiment using D_2O as the isotopically labeled solvent showed that deuterium incorporation was observed both in product **8-3aa** and the recovered substrate **8-1a** (Scheme 8-3a). These findings are suggestive of the C–H cleavage being reversible. Intermolecular competition experiments using electron-rich and electron-poor 7-phenyl-1H-indole **8-1i** and **8-1r** indicated that electronic effects of the substituent on the 7-phenyl-1H-indole played an important role. In contrast, no significant electronic effect on the reaction efficiency was observed between electron-rich and electron-deficient alkynes **8-2f** and **8-2l** (Scheme 8-3b).

a) Synthesis of rhodium complexes **8-4a** and **8-5a**



b) Catalytic reactivity of **8-4a** and **8-5a**



Scheme 8-4. Preparation and electrolysis studies of Rh complexes

Due to the essential role of metallacyclic intermediates in the rhodium-catalyzed C–H activations, we have conducted extensive experiments to isolate the crucial rhodium

complexes. Notably, a tetrameric six-membered cyclometalated rhodium(III) complex **8-4a** via *NH*-directed C–H activation was obtained in 91% yield upon treatment of **8-1a** with [Cp*RhCl₂]₂ and Ag₂CO₃. We reasoned that formal group was beneficial to achieve relative stable six-membered cyclometalated rhodium(III) intermediate **8-4a** enabled by weak coordination of carbonyl oxygen with rhodium. While attempts to recrystallize or in-situ HRMS analysis of intermediates of stoichiometric reaction of 7-phenyl-*1H*-indole with [Cp*RhCl₂]₂ have failed. Mixing **8-4a** with 2 equiv of diphenylacetylene **8-2a** in CH₂Cl₂ at room temperature for 0.1 h allowed for the isolation of the eight-membered cyclometalated rhodium(III) complex **8-5a** in 87% yield. The connectivities of metallacycles **8-4a** and **8-5a** were unambiguously verified by X-ray crystallography. The electrooxidative [5+2] annulation in the presence of **8-4a** and **8-5a** as the catalyst in place of [Cp*RhCl₂]₂ under the standard conditions gave **8-3aa** in 77% and 71% yield, respectively, indicating that **8-4a** and **8-5a** are both competent in the present catalytic cycle. Furthermore, the rhodium(III) complex **8-5a** remained intact even when it is was heated at 130 °C for an extended period of time under N₂ atmosphere (Figure S8-4 in Chapter 9), which suggested that two-electron reductive elimination from **8-5a** affording rhodium(I) complex may be slow, and kinetically and thermodynamically unfavorable. Cyclic voltammogram of **8-5a** showed the first irreversible oxidation peak at E_{pa} = 0.349 V (versus Fc/Fc⁺, 100 mV/s), which was assigned to the oxidation of rhodium(III) species to Rh(IV) (Figure 8-1).

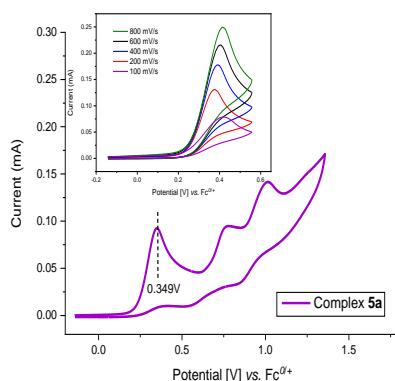


Figure 8-1. Cyclic voltammetry studies. Full scan of **5a** at 100 mV/s. Inset: Narrow scan of **8-5a** in variable scan rates. Reaction condition: **8-5a** (2.5 mM) and *n*Bu₄NPF₆ (0.1 M), MeCN, r.t

The XPS was employed to investigate the rhodium valent state. For intermediate **8-5a**, the peak of Rh 3d_{5/2} locates at 308.48 eV.⁹⁶ After 650 CV cycles across a potential range of 0 to 0.5 V vs Ag/AgNO₃, this peak slightly shifts toward lower binding energy (308.13 eV), suggesting a decrease in rhodium valent state, most likely Rh(II) species deriving from reductive elimination of Rh(IV) intermediate. After electrolyzed under standard reaction condition (Table 8-1, entry 5), the peak of Rh 3d_{5/2} shifts toward higher binding energy (308.93 eV), which is similar with Cp*RhCO₃ or [Cp*RhCl₂]₂, indicating that low valent state rhodium(II) is oxidized back to Rh(III) (Figure 8-2).

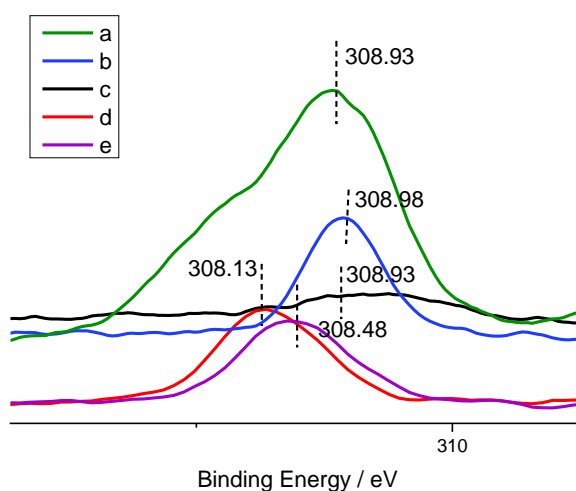


Figure 8-2. Rh 3d_{5/2} XPS spectra showing: a) Cp*RhCO₃ (green line); b) [Cp*RhCl₂]₂ (blue line); c) Electrolysis of 5a at the current of 5 mA for 6 h (black line); d) After 650 CV cycles across a potential range of 0 to 0.5 V of 8-5a (red line); e) 8-5a (purple line).

These findings provided strong support for an oxidation-induced reductive elimination within a rhodium(III/IV) regime.⁹⁷⁻⁹⁹ The oxidation-induced reductive elimination mechanism was further confirmed by DFT calculations (see Supporting Information for details). The transition state of the direct reductive elimination of rhodium(III) intermediate **8-5a** was located as **TS(A-B)** (Figure 8-3), which has a Gibbs free energy barrier of 32.3 Kcal/mol, unreasonable under the current experimental conditions. However, an oxidatively-induced reductive elimination mechanism, whose transition state was located as **TS(A'-B')**, required only an energy barrier of 6.7 Kcal/mol.

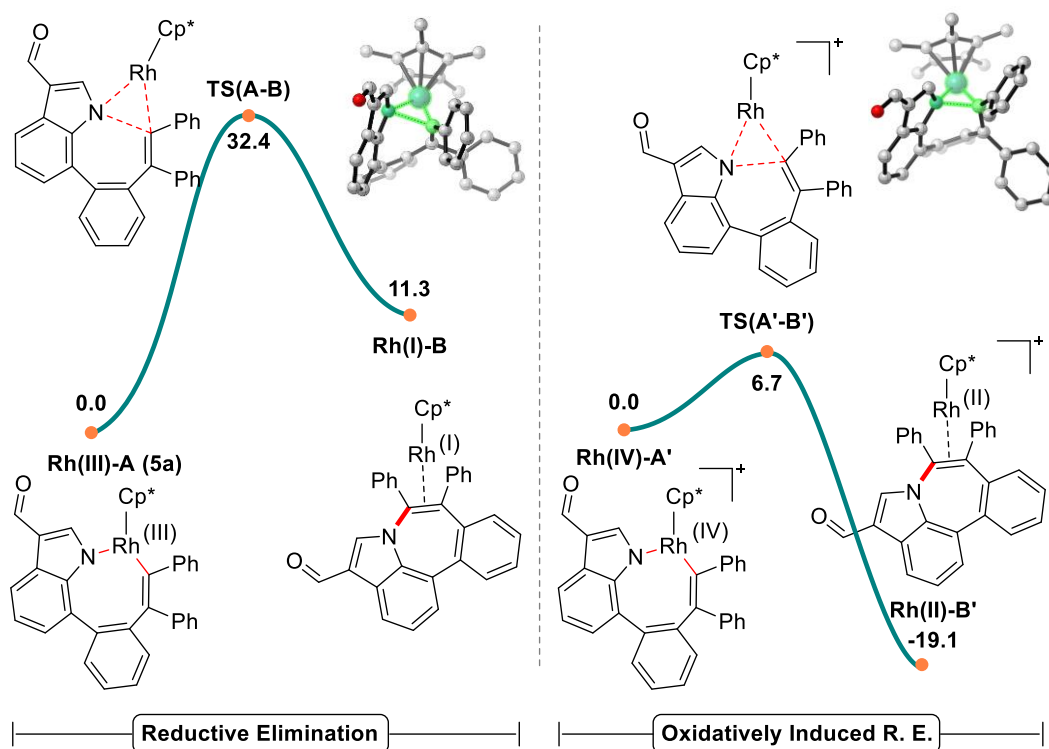
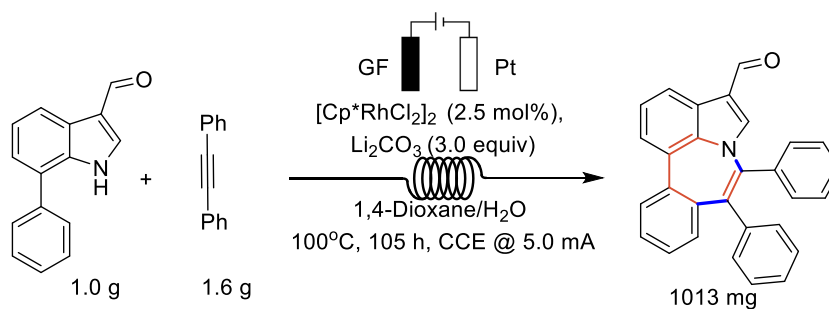
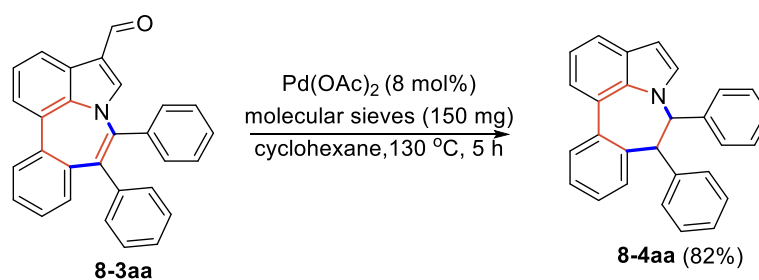


Figure 8-3. DFT calculated Gibbs free energy profile in kcal/mol comparing the direct reductive elimination and oxidatively induced reductive elimination pathways at the ω B97X-D/6-311++G(d,p), LANL2DZ(Rh)+SMD(1,4-dioxane)// ω B97X-D/6-31G(d), LANL2DZ(Rh) level of theory.

a) Gram-scale with a simple flow cell:

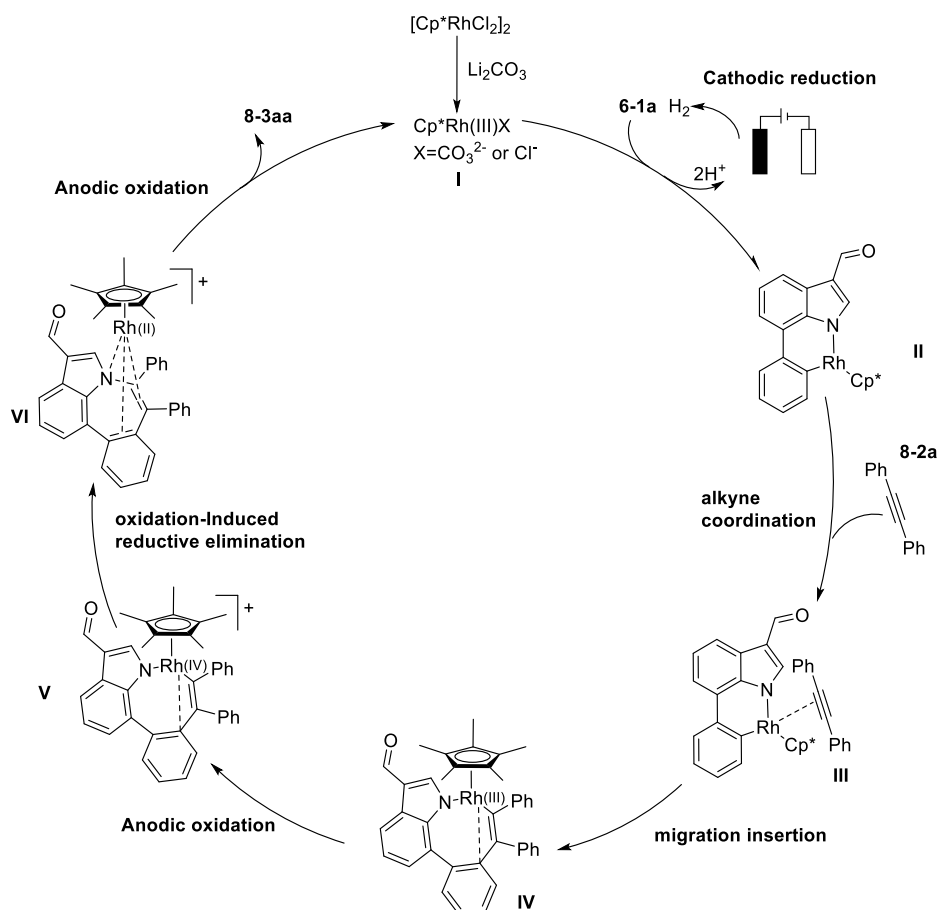


b) Synthetic Transformation



Scheme 8-5. Summary of gram-scale reaction and transformation of **8-3aa**.

To demonstrate the practical application of the rhodaelectro-catalyzed [5 + 2] C–H/N–H cyclization, the gram-scale reaction was carried out within a simple flow-cell device, yielding 1.013 g of the desired product **8-3aa** (Scheme 8-5a). A reduction driven by Pd(OAc)₂ transformed **8-3aa** into the deformylation product **8-4aa** with high yield (82% yield, Scheme 8-5b).



Scheme 8-6. Proposed catalytic cycle.

Based on the detailed mechanistic studies, the catalytic cycle is proposed as depicted in Scheme 8-6. First, the active rhodium(III) species **I** undergoes N–H bond cleavage and subsequent C–H bond cleavage to give six-membered rhoda(III)cycle **II**. Then, alkyne coordination and migratory insertion provide eight-membered rhoda(III)cycle **IV**. DFT calculations indicate that the migratory insertion process is fast with a free energy barrier of 12.1 kcal/mol (Figure S8-12 in Chapter 9). Subsequently, anodic oxidation-induced reductive elimination of **IV** by a rhodium (III-IV-II) manifold gives intermediate **VI**. Further anodic oxidation of **VI** regenerates the active rhodium(III)

catalyst **I** and the final product **8-3aa**. Molecular hydrogen was generated as a byproduct at the cathode.

8.3. Conclusion

In conclusion, we have developed a rhodaelectro-catalyzed oxidative annulation of 7-phenylindoles with alkynes using electricity as the sole oxidant in an undivided cell. A variety of highly functionalized seven-membered azepino[3,2,1-*hi*]indoles were obtained in good to excellent yield. Significantly, this electrolytic reaction can be conducted in flow with gram scale. Two key rhodium intermediates, including a six-membered cyclometalated rhodium(III) complex via *NH*-directed C-H activation and an eight-membered metallacyclic rhodium(III) species via alkyne insertion, were isolated and fully characterized. Detailed mechanistic studies were carried out to cast light on the mechanism. Cyclovoltammetric analysis, XPS studies and DFT calculations provided strong support for a rhodium(III-IV-II-III) manifold.

8.4. References

- [1] S. Dongbang, D. N. Confair, J. A. Ellman, *Acc. Chem. Res.* **2021**, *54*, 1766-1778.
- [2] X. X. Guo, D. W. Gu, Z. Wu, W. Zhang, *Chem. Rev.* **2015**, *115*, 1622-1651.
- [3] Y. Jiang, K. Xu, C. Zeng, *Chem. Rev.* **2018**, *118*, 4485-4540.
- [4] B. Nie, W. Wu, Y. Zhang, H. Jiang, J. Zhang, *Org. Chem. Front.* **2020**, *7*, 3067-3099.
- [5] K. Sun, H. Shan, G. P. Lu, C. Cai, M. Beller, *Angew. Chem.Int. Ed.* **2021**, *60*, 25188-25202.
- [6] V. P. Boyarskiy, D. S. Ryabukhin, N. A. Bokach, A. V. Vasilyev, *Chem. Rev.* **2016**, *116*, 5894-986.
- [7] P. Gandeepan, T. Muller, D. Zell, G. Cera, S. Warratz, L. Ackermann, *Chem. Rev.* **2019**, *119*, 2192-2452.
- [8] H. Wang, X. Gao, Z. Lv, T. Abdelilah, A. Lei, *Chem. Rev.* **2019**, *119*, 6769-6787.
- [9] W. Chen, D. Seidel, *Org. Lett.* **2021**, *23*, 3729-3734.
- [10] Q. Huang, Q. Han, S. Fu, Z. Yao, L. Su, *J. Org. Chem.* **2016**, *81*, 12135-12142.
- [11] A. Liu, Q. Han, X. Zhang, B. Li, Q. Huang, *Org. Lett.* **2019**, *21*, 6839-6843.
- [12] S. Pradhan, S. Roy, S. Banerjee, P. B. De, T. Punniyamurthy, *J. Org. Chem.* **2020**, *85*, 5741-5749.
- [13] B. Ramesh, M. Tamizmani, M. Jeganmohan, *J. Org. Chem.* **2019**, *84*, 4058-4071.
- [14] S. C. Sau, R. Mei, J. Struwe, L. Ackermann, *ChemSusChem.* **2019**, *12*, 3023-3027.
- [15] H. Shen, T. Liu, D. Cheng, X. Yi, Z. Wang, L. Liu, D. Song, F. Ling, W. Zhong, *J. Org. Chem.* **2020**, *85*, 13735-13746.
- [16] C. Tian, U. Dhawa, A. Scheremetjew, L. Ackermann, *ACS Catal.* **2019**, *9*, 7690-7696.
- [17] X. Zhou, H. Xu, Q. Yang, H. Chen, S. Wang, H. Zhao, *Chem. Commun.* **2019**, *55*, 8603-8606.

- [18] K. Ghosh, Y. Nishii, M. Miura, *ACS Catal.* **2019**, *9*, 11455-11460.
- [19] M. G. Huang, S. Shi, M. Li, Y. J. Liu, M. H. Zeng, *Org. Lett.* **2021**, *23*, 7094-7099.
- [20] S. Li, L. Liu, R. Wang, Y. Yang, J. Li, J. Wei, *Org. Lett.* **2020**, *22*, 7470-7474.
- [21] R. Mei, X. Fang, L. He, J. Sun, L. Zou, W. Ma, L. Ackermann, *Chem. Commun.* **2020**, *56*, 1393-1396.
- [22] J. Mo, T. Muller, J. C. A. Oliveira, S. Demeshko, F. Meyer, L. Ackermann, *Angew. Chem. Int. Ed.* **2019**, *58*, 12874-12878.
- [23] A. Obata, A. Sasagawa, K. Yamazaki, Y. Ano, N. Chatani, *Chem. Sci.* **2019**, *10*, 3242-3248.
- [24] X. Tan, X. Hou, T. Rogge, L. Ackermann, *Angew. Chem. Int. Ed.* **2021**, *60*, 4619-4624.
- [25] Y. Xu, C. Yu, X. Zhang, X. Fan, *J. Org. Chem.* **2021**, *86*, 5805-5819.
- [26] Y. Yuan, G. Pan, X. Zhang, Q. Huang, *Org. Chem. Front.* **2020**, *7*, 53-63.
- [27] T. Li, Z. Yang, Z. Song, R. Chauvin, Cui, X. *Org. Lett.* **2020**, *22*, 4078-4082.
- [28] K. Selvaraj, S. Debnath, K. C. K. Swamy, *Org. Lett.* **2019**, *21*, 5447-5451.
- [29] X. Song, Q. Zhou, J. Zhao, Y. Jiang, X. Zhang, X. Zhang, X. Fan, *Org. Lett.* **2020**, *22*, 9506-9512.
- [30] V. D. Kadam, B. Feng, X. Chen, W. Liang, F. Zhou, Y. Liu, G. Gao, J. You, *Org. Lett.* **2018**, *20*, 7071-7075.
- [31] A. D. Streit, A. J. Zoll, G. L. Hoang, J. Ellman, A. *Org. Lett.* **2020**, *22*, 1217-1221.
- [32] Z. Wang, J. Yin, F. Zhou, Y. Liu, J. You, *Angew. Chem. Int. Ed.* **2019**, *58*, 254-258.
- [33] (a) D. Bai, T. Xu, C. Ma, X. Zheng, B. Liu, F. Xie, X. Li, *ACS Catal.* **2018**, *8*, 4194-4200.
- [34] X. Kou, K. G. M. Kou, *ACS Catal.* **2020**, *10*, 3103-3109.
- [35] S. Qian, X. Pu, G. Chang, Y. Huang, Y. Yang, *Org. Lett.* **2020**, *22*, 5309-5313.
- [36] L. Sun, H. Chen, B. Liu, C. J. hang, L. Kong, F. Wang, Y. Lan, X. Li, *Angew. Chem. Int. Ed.* **2021**, *60*, 8391-8395.
- [37] R. S. Thombal, Y. R. Lee, *Org. Lett.* **2020**, *22*, 3397-3401.
- [38] J. M. Villar, J. Suarez, J. A. Varela, C. Saa, *Org. Lett.* **2017**, *19*, 1702-1705.
- [39] L. Ackermann, *Acc. Chem. Res.* **2020**, *53*, 84-104.
- [40] K. J. Jiao, Y. K. Xing, Q. L. Yang, H. Qiu, T. S. Mei, *Acc. Chem. Res.* **2020**, *53*, 300-310.
- [41] C. Ma, P. Fang, Z.-R. Liu, S.-S. Xu, K. Xu, X. Cheng, A. Lei, H.-C. Xu, C. Zeng, T.-S. Mei, *Sci. Bull.* **2021**, *66*, 2412-2429.
- [42] L. F. T. Novaes, J. Liu, Y. Shen, L. Lu, J. M. Meinhardt, S. Lin, *Chem. Soc. Rev.* **2021**, *50*, 7941-8002.
- [43] Y. Qiu, C. Zhu, M. Stangier, J. Struwe, L. Ackermann, *CCS Chemistry* **2021**, *3*, 1529-1552.
- [44] C. Kingston, M. D. Palkowitz, Y. Takahira, J. C. Vantourout, B. K. Peters, Y. Kawamata, P. S. Baran, *Acc Chem Res* **2020**, *53*, 72-83.
- [45] Y. Yuan, A. Lei, *Acc Chem Res* **2019**, *52*, 3309-3324.
- [46] N. Sauermann, T. H. Meyer, Y. Qiu, L. Ackermann, *ACS Catalysis* **2018**, *8*, 7086-7103.
- [47] C. Y. Cai, Z. J. Wu, J. Y. Liu, M. Chen, J. Song, H. C. Xu, *Nat. Commun.* **2021**, *12*, 3745.
- [48] Z. J. Wu, F. Su, W. Lin, J. Song, T. B. Wen, H. J. Zhang, H. C. Xu, *Angew. Chem. Int. Ed.* **2019**, *58*, 16770-16774.
- [49] F. Xu, Y.-J. Li, C. Huang, H.-C. Xu, *ACS Catal.* **2018**, *5*, 3820-3824.
- [50] Y. G. Chen, B. Shuai, X. T. Xu, Y. Q. Li, Q. L. Yang, H. Qiu, K. Zhang, P. Fang, T. S. Mei, *J. Am. Chem. Soc.* **2019**, *141*, 3395-3399.

- [51] P. S. Gao, X. J. Weng, Z. H. Wang, C. Zheng, B. Sun, Z. H. Chen, S. L. You, T. S. Mei, *Angew. Chem. Int. Ed.* **2020**, *59*, 15254-15259.
- [52] D. Liu, Z. R. Liu, C. Ma, K. J. Jiao, B. Sun, L. Wei, J. Lefranc, S. Herbert, T. S. Mei, *Angew. Chem. Int. Ed.* **2021**, *60*, 9444-9449.
- [53] D. Liu, H. X. Ma, P. Fang, T. S. Mei, *Angew. Chem. Int. Ed.* **2019**, *58*, 5033-5037.
- [54] H. Qiu, B. Shuai, Y. Z. Wang, D. Liu, Y. G. Chen, P. S. Gao, H. Ma, X. S. Chen, T. S. Mei, *J. Am. Chem. Soc.* **2020**, *142*, 9872-9878.
- [55] Y. K. Xing, X. R. Chen, Q. L. Yang, S. Q. Zhang, H. M. Guo, X. Hong, T. S. Mei, *Nat. Commun.* **2021**, *12*, 930.
- [56] Q. L. Yang, H. W. Jia, Y. Liu, Y. K. Xing, R. C. Ma, M. M. Wang, G. R. Qu, T. S. Mei, H. M. Guo, *Org. Lett.* **2021**, *23*, 1209-1215.
- [57] Q. L. Yang, X. Y. Wang, T. L. Wang, X. Yang, D. Liu, X. Tong, X. Y. Wu, T. S. Mei, *Org. Lett.* **2019**, *21*, 2645-2649.
- [58] Q. L. Yang, Y. K. Xing, X. Y. Wang, H. X. Ma, X. J. Weng, X. Yang, H. M. Guo, T. S. Mei, *J. Am. Chem. Soc.* **2019**, *141*, 18970-18976.
- [59] X. Yang, Q. L. Yang, X. Y. Wang, H. H. Xu, T. S. Mei, Y. Huang, P. Fang, *J. Org. Chem.* **2020**, *85*, 3497-3507.
- [60] Y. Cao, Y. Yuan, Y. Lin, X. Jiang, Y. Weng, T. Wang, F. Bu, L. Zeng, A. Lei, *Green Chem.* **2020**, *22*, 1548-1552.
- [61] Z. Duan, L. Zhang, W. Zhang, L. Lu, L. Zeng, R. Shi, A. Lei, *ACS Catal.* **2020**, *10*, 3828-3831.
- [62] X. Gao, P. Wang, L. Zeng, S. Tang, A. Lei, *J. Am. Chem. Soc.* **2018**, *140*, 4195-4199.
- [63] L. Niu, C. Jiang, Y. Liang, D. Liu, F. Bu, R. Shi, H. Chen, A. D. Chowdhury, A. Lei, *J. Am. Chem. Soc.* **2020**, *142*, 17693-17702.
- [64] S. Tang, D. Wang, Y. Liu, L. Zeng, A. Lei, *Nat. Commun.* **2018**, *9*, 798.
- [65] S. Wang, Q. Xue, Z. Guan, Y. Ye, A. Lei, *ACS Catal.* **2021**, *11*, 4295-4300.
- [66] Y. Wu, L. Zeng, H. Li, Y. Cao, J. Hu, M. Xu, R. Shi, H. Yi, A. Lei, *J. Am. Chem. Soc.* **2021**, *143*, 12460-12466.
- [67] Y. Yuan, Y. Zheng, B. Xu, J. Liao, F. Bu, S. Wang, J.-G. Hu, A. Lei, *ACS Catal.* **2020**, *10*, 6676-6681.
- [68] N. W. J. Ang, J. C. A. Oliveira, L. Ackermann, *Angew. Chem. Int. Ed.* **2020**, *59*, 12842-12847.
- [69] X. R. Chen, S. Q. Zhang, T. H. Meyer, C. H. Yang, Q. H. Zhang, J. R. Liu, H. J. Xu, F. H. Cao, L. Ackermann, *Chem. Sci.* **2020**, *11*, 5790-5796.
- [70] U. Dhawa, C. Li, W. Tian, L. Ackermann, *ACS Catal.* **2020**, *10*, 6457-6462.
- [71] U. Dhawa, C. Tian, T. Wdowik, J. C. A. Oliveira, J. Hao, L. Ackermann, *Angew. Chem. Int. Ed.* **2020**, *59*, 13451-13457.
- [72] U. Dhawa, T. Wdowik, X. Hou, B. Yuan, J. C. A. Oliveira, L. Ackermann, *Chem. Sci.* **2021**, *12*, 14182-14188.
- [73] W. J. Kong, Z. Shen, L. H. Finger, L. Ackermann, *Angew. Chem. Int. Ed.* **2020**, *59*, 5551-5556.
- [74] L. Massignan, X. Tan, T. H. Meyer, R. Kuniyil, A. M. Messinis, L. Ackermann, *Angew. Chem. Int. Ed.* **2020**, *59*, 3184-3189.
- [75] L. Massignan, C. Zhu, X. Hou, J. C. A. Oliveira, A. Salamé, L. Ackermann, *ACS Catal.* **2021**, *11*, 11639-11649.
- [76] T. H. Meyer, J. C. A. Oliveira, D. Ghorai, L. Ackermann, *Angew. Chem. Int. Ed.* **2020**, *59*, 10955-10960.

- [77] T. H. Meyer, R. C. Samanta, D A. el Vecchio, L. Ackermann, *Chem. Sci.* **2020**, *12*, 2890-2897.
- [78] R. C. Samanta, J. Struwe, L. Ackermann, *Angew. Chem. Int. Ed.* **2020**, *59*, 14154-14159.
- [79] Z. Shen, I. Maksso, R. Kuniyil, T. Rogge, L. Ackermann, *Chem. Commun.* **2021**, *57*, 3668-3671.
- [80] M. Stangier, A. M. Messinis, J. C. A. Oliveira, H. Yu, L. Ackermann, *Nat. Commun.* **2021**, *12*, 4736.
- [81] X. Tan, L. Massignan, X. Hou, J. Frey, J. C. A. Oliveira, M. N. Hussain, L. Ackermann, *Angew. Chem. Int. Ed.* **2021**, *60*, 13264-13270.
- [82] C. Tian, U. Dhawa, A. Scheremetjew, L. Ackermann, *ACS Catal.* **2019**, *9*, 7690-7696.
- [83] Y. Wang, J. C. A. Oliveira, Z. Lin, L. Ackermann, *Angew. Chem. Int. Ed.* **2021**, *60*, 6419-6424.
- [84] L. Yang, R. Steinbock, A. Scheremetjew, R. Kuniyil, L. H. Finger, A. M. Messinis, *Angew. Chem. Int. Ed.* **2020**, *59*, 11130-11135.
- [85] S. K. Zhang, J. Struwe, L. Hu, L. Ackermann, *Angew. Chem. Int. Ed.* **2020**, *59*, 3178-3183.
- [86] S.-K. Zhang, A. Del Vecchio, R. Kuniyil, A. M. Messinis, Z. Lin, L. Ackermann, *Chem.* **2021**, *7*, 1379-1392.
- [87] Y. Zhang, J. Struwe, L. Ackermann, *Angew. Chem. Int. Ed.* **2020**, *59*, 15076-15080.
- [88] C. Zhu, N. W. J. Ang, T. H. Meyer, Y. Qiu, L. Ackermann, *ACS Cent. Sci.* **2021**, *7*, 415-431.
- [89] N. Sauermann, T. H. Meyer, C. Tian, L. Ackermann, *J. Am. Chem. Soc.* **2017**, *139*, 18452-18455.
- [90] Q. Lin, S. Luo, *Org. Chem. Front.* **2020**, *7*, 2997-3000.
- [91] Z. Xu, Y. Li, G. Mo, Y. Zheng, S. Zeng, P. H. Sun, Z. Ruan, *Org. Lett.* **2020**, *22*, 4016-4020.
- [92] X. Ye, C. Wang, S. Zhang, J. Wei, C. Shan, L. Wojtas, Y. Xie, X. Shi, *ACS Catal.* **2020**, *10*, 11693-11699.
- [93] Z. Zeng, J. F. Goebel, X. Liu, L. J. Gooßen, *ACS Catal.* **2021**, *11*, 6626-6632.
- [94] C. Zhu, A. P. Kale, H. Yue, M. Rueping, *JACS Au* **2021**, *1*, 1057-1065.
- [95] M. Zhu, M. Alami, S. Messaoudi, *Chem. Commun.* **2020**, *56*, 4464-4467.
- [96] A. V. Naumkin, A. Kraut-Vass, S. W. Gaarenstroom, C. J. Powell, National Institute of Standards and Technology (NIST) X-ray Photoelectron Spectroscopy Database, NIST Standard Reference Database 20, Version 4.1.
- [97] W. J. Kong, L. H. Finger, A. M. Messinis, R. Kuniyil, J. C. A. Oliveira, L. Ackermann, *J. Am. Chem. Soc.* **2019**, *141*, 17198-17206.
- [98] Z.-J. Wu, F. Su, W. Lin, J. Song, T.-B. Wen, H.-J. Zhang, H.-C. Xu, *Angew. Chem. Int. Ed.* **2019**, *58*, 16770-16774.
- [99] L. Li, W. W. Brennessel, W. D. Jones, *J. Am. Chem. Soc.* **2008**, *130*, 12414-12419.

Chapter 9.

Experimental Details and Characterization Data

Chapter 9 - Experimental Details and Characterization Data

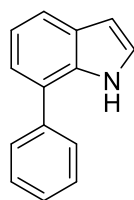
9.1. General Method

Diazo compounds **6-2** were prepared according to the reported procedures, and the compounds' spectra data are in agreement with the reports.^[3] ¹H NMR spectra were recorded at 400 MHz and ¹³C NMR spectra at 100 MHz, respectively. ¹H chemical shifts (δ) were referenced to TMS, and ¹³C NMR chemical shifts (δ) were referenced to internal solvent resonance. ESI-HRMS spectra were recorded by using a Q-TOF mass spectrometer. Data collection and structural analysis of crystal were collected on an Agilent Technologies SuperNova Single Crystal Diffractometer equipped with graphite monochromatic Cu/Mo K α radiation ($\lambda = 1.54184 \text{ \AA}$). The crystal was kept at 293 (10) K during data collection. Using Olex2^[4], the structure was solved with the Superflip structure solution program using Charge Flipping and refined with the ShelXL refinement package using Least Squares minimisation. The hydrogen atoms on the ligands were placed in idealized positions and refined using a riding model.

9.1.1 Preparation and characterization data of the starting 7-Phenyl-1*H*-indole derivatives **6-(1a-1w)**

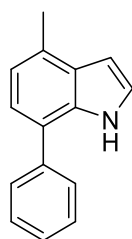
7-Phenyl-1*H*-indoles **6-1** were synthesized from 7-bromo-1*H*-indoles and Phenylboronic acid via Suzuki coupling.^[1] **6-1a**, **6-1c**, **6-1f**, **6-(1h-j)**, **6-1p**, **6-(1s-u)** are known compounds, ¹H NMR data of the isolated products were in agreement with the literature reports.^[2] **6-1b**, **6-(1d-e)**, **6-1g**, **6-(1k-o)**, **6-1q**, **6-(1v-w)** are new compounds. They were characterized by ¹H NMR, ¹³C NMR and HRMS.

7-Phenyl-1*H*-indole **6-1a**



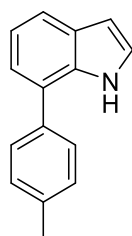
6-1a was obtained as colorless solid. ^1H NMR (400 MHz, CDCl_3) δ 8.43 (s, 1H), 7.69 – 7.64 (m, 3H), 7.55 – 7.50 (m, 2H), 7.47 (t, $J = 7.4$ Hz, 1H), 7.26 – 7.20 (m, 3H), 6.64 (dd, $J = 3.2, 2.1$ Hz, 1H).

4-Methyl-7-phenyl-1*H*-indole **6-1b**



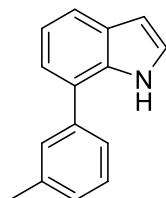
6-1b was obtained as colorless solid. ^1H NMR (400 MHz, CDCl_3) δ 8.45 (s, 1H), 7.64 (dt, $J = 7.7, 1.5$ Hz, 2H), 7.54 – 7.49 (m, 2H), 7.42 – 7.38 (m, 1H), 7.23 (dd, $J = 3.2, 2.5$ Hz, 1H), 7.16 (d, $J = 7.3$ Hz, 1H), 7.03 (dd, $J = 7.5, 1.0$ Hz, 1H), 6.66 (dd, $J = 3.2, 2.1$ Hz, 1H), 2.63 (s, 3H). $^{13}\text{C}\{^1\text{H}\}$ NMR (100 MHz, CDCl_3) δ 139.4, 133.3, 129.6, 129.1, 128.2, 128.0, 127.1, 123.7, 123.3, 122.0, 120.5, 101.6, 18.7. HRMS (ESI) m/z : $[\text{M}+\text{H}]^+$ Calcd for $\text{C}_{15}\text{H}_{14}\text{N}$, 208.1121; found, 208.1117.

7-(*p*-Tolyl)-1*H*-indole **6-1c**



6-1c was obtained as colorless solid. ^1H NMR (400 MHz, CDCl_3) δ 8.45 (s, 1H), 7.71 – 7.57 (m, 3H), 7.44 – 7.20 (m, 5H), 6.68 (s, 1H), 2.49 (s, 3H).

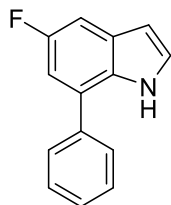
7-(*m*-Tolyl)-1*H*-indole **6-1d**



6-1d was obtained as colorless solid. ^1H NMR (400 MHz, CDCl_3) δ 8.43 (s, 1H), 7.68 – 7.63 (m, 1H), 7.48 – 7.44 (m, 2H), 7.41 (td, $J = 7.2, 1.4$ Hz, 1H), 7.25 – 7.19 (m, 4H), 6.64 (dd, $J = 3.2, 2.1$ Hz, 1H), 2.46 (s, 3H). $^{13}\text{C}\{^1\text{H}\}$ NMR (100 MHz, CDCl_3) δ 139.2,

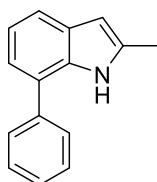
138.8, 133.7, 129.0, 128.9, 128.2, 128.1, 125.7, 125.2, 124.2, 121.8, 120.2, 119.9, 103.0, 21.6. HRMS (ESI) m/z : $[M+H]^+$ Calcd for $C_{15}H_{14}N$, 208.1121; found, 208.1119.

5-Fluoro-7-phenyl-1*H*-indole **6-1e**



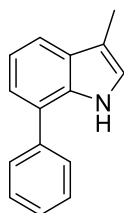
6-1e was obtained as colorless solid. 1H NMR (400 MHz, $CDCl_3$) δ 8.37 (s, 1H), 7.65 – 7.61 (m, 2H), 7.56 – 7.51 (m, 2H), 7.47 – 7.42 (m, 1H), 7.31 (dd, $J = 9.3, 2.3$ Hz, 1H), 7.25 (t, $J = 2.9$ Hz, 1H), 7.02 (dd, $J = 10.0, 2.4$ Hz, 1H), 6.60 (dd, $J = 3.1, 2.1$ Hz, 1H). $^{13}C\{^1H\}$ NMR (100 MHz, $CDCl_3$) δ 158.2 (d, $J = 234.5$ Hz), 138.1, 130.2, 129.2, 128.5 (d, $J = 10.5$ Hz), 128.1, 127.9, 126.3 (d, $J = 9.4$ Hz), 125.9, 110.1 (d, $J = 26.6$ Hz), 104.6 (d, $J = 23.4$ Hz), 103.2 (d, $J = 4.8$ Hz). ^{19}F NMR (376 MHz, $CDCl_3$) δ -124.7 (t, $J = 9.3$ Hz). HRMS (ESI) m/z : $[M+H]^+$ Calcd for $C_{14}H_{11}FN$, 212.0870; found, 212.0865.

2-Methyl-7-phenyl-1*H*-indole **6-1f**



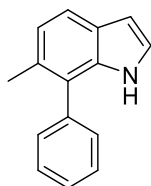
6-1f was obtained as colorless solid. 1H NMR (400 MHz, $CDCl_3$) δ 8.12 (s, 1H), 7.67 – 7.63 (m, 2H), 7.55 – 7.50 (m, 3H), 7.43 – 7.38 (m, 1H), 7.19 – 7.13 (m, 2H), 6.33 – 6.27 (m, 1H), 2.45 (s, 3H).

3-Methyl-7-phenyl-1*H*-indole **6-1g**



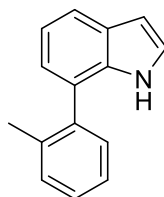
6-1g was obtained as colorless solid. 1H NMR (400 MHz, $CDCl_3$) δ 8.16 (s, 1H), 7.73 – 7.64 (m, 2H), 7.64 – 7.59 (m, 1H), 7.57 – 7.49 (m, 2H), 7.44 – 7.39 (m, 1H), 7.27 – 7.24 (m, 2H), 7.00 (dd, $J = 2.3, 1.2$ Hz, 1H), 2.40 (s, 3H). $^{13}C\{^1H\}$ NMR (100 MHz, $CDCl_3$) δ 139.3, 134.0, 129.1, 128.6, 128.2, 127.3, 125.4, 121.8, 119.6, 118.1, 112.1, 9.8. HRMS (ESI) m/z : $[M+H]^+$ Calcd for $C_{15}H_{14}N$, 208.1121; found, 208.1116.

6-Methyl-7-phenyl-1*H*-indole **6-1h**



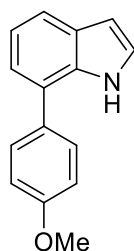
6-1h was obtained as colorless solid. ^1H NMR (400 MHz, CDCl_3) δ 7.87 (s, 1H), 7.56 – 7.49 (m, 3H), 7.45 – 7.40 (m, 3H), 7.12 – 7.05 (m, 2H), 6.55 (dd, $J = 3.2, 2.1$ Hz, 1H), 2.31 (s, 3H).

7-(*o*-Tolyl)-1*H*-indole **6-1i**



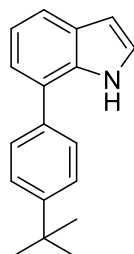
6-1i was obtained as colorless solid. ^1H NMR (400 MHz, CDCl_3) δ 7.95 (s, 1H), 7.68 (dt, $J = 8.0, 0.9$ Hz, 1H), 7.40 – 7.30 (m, 4H), 7.24 – 7.18 (m, 2H), 7.10 (dd, $J = 7.2, 1.1$ Hz, 1H), 6.64 (dd, $J = 3.2, 2.1$ Hz, 1H), 2.21 (s, 3H).

7-(4-Methoxyphenyl)-1*H*-indole **6-1j**



6-1j was obtained as colorless solid. ^1H NMR (400 MHz, CDCl_3) δ 8.40 (s, 1H), 7.65 – 7.55 (m, 3H), 7.23 – 7.18 (m, 3H), 7.08 – 7.02 (m, 2H), 6.66 – 6.59 (m, 1H), 3.89 (s, 3H).

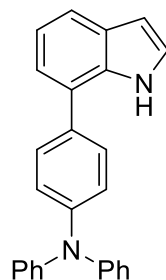
7-(4-(*Tert*-butyl)phenyl)-1*H*-indole **6-1k**



6-1k was obtained as colorless solid. ^1H NMR (400 MHz, CDCl_3) δ 8.45 (s, 1H), 7.65 (ddd, $J = 6.8, 2.1, 0.7$ Hz, 1H), 7.62 – 7.58 (m, 2H), 7.57 – 7.53 (m, 2H), 7.25 – 7.20 (m, 3H), 6.64 (dd, $J = 3.2, 2.1$ Hz, 1H), 1.42 (s, 9H). $^{13}\text{C}\{^1\text{H}\}$ NMR (100 MHz, CDCl_3)

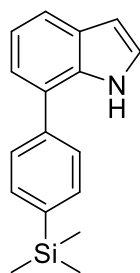
δ 150.3, 136.3, 133.8, 128.2, 127.9, 126.0, 125.5, 124.2, 121.8, 120.3, 119.8, 103.0, 34.6, 31.4. HRMS (ESI) m/z : $[M+H]^+$ Calcd for $C_{18}H_{20}N$, 250.1590; found, 250.1584.

4-(1*H*-Indol-7-yl)-*N,N*-diphenylaniline **6-1l**



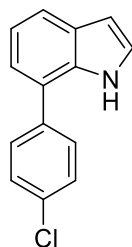
6-1l was obtained as colorless solid. 1H NMR (400 MHz, $CDCl_3$) δ 8.47 (s, 1H), 7.63 (dd, $J = 6.4, 2.2$ Hz, 1H), 7.55 – 7.48 (m, 2H), 7.33 – 7.27 (m, 4H), 7.24 – 7.16 (m, 8H), 7.13 (dt, $J = 8.7, 1.8$ Hz, 1H), 7.09 – 7.04 (m, 2H), 6.63 (dd, $J = 3.2, 2.1$ Hz, 1H). $^{13}C\{^1H\}$ NMR (100 MHz, $CDCl_3$) δ 147.6, 147.2, 133.7, 133.1, 129.3, 129.2, 128.9, 128.2, 127.3, 125.2, 124.5, 124.3, 124.2, 124.0, 123.1, 122.8, 121.6, 120.3, 119.7, 103.1. HRMS (ESI) m/z : $[M+H]^+$ Calcd for $C_{26}H_{21}N_2$, 361.1699; found, 361.1689.

7-(4-(Trimethylsilyl)phenyl)-1*H*-indole **6-1m**



6-1m was obtained as colorless solid. 1H NMR (400 MHz, $CDCl_3$) δ 8.45 (s, 1H), 7.71 – 7.63 (m, 5H), 7.26 – 7.20 (m, 3H), 6.64 (dd, $J = 3.2, 2.1$ Hz, 1H), 0.35 (t, 9H). $^{13}C\{^1H\}$ NMR (100 MHz, $CDCl_3$) δ 139.6, 139.5, 134.1, 133.7, 128.2, 127.5, 125.5, 124.3, 121.8, 120.3, 120.1, 103.0, -1.1. HRMS (ESI) m/z : $[M+H]^+$ Calcd for $C_{17}H_{20}NSi$, 266.1360; found, 266.1352.

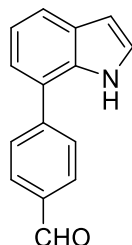
7-(4-Chlorophenyl)-1*H*-indole **6-1n**



6-1n was obtained as colorless solid. 1H NMR (400 MHz, $CDCl_3$) δ 8.34 (s, 1H), 7.67 (ddd, $J = 7.3, 1.9, 0.7$ Hz, 1H), 7.60 – 7.56 (m, 2H), 7.51 – 7.47 (m, 2H), 7.24 – 7.18 (m, 3H), 6.64 (dd, $J = 3.2, 2.0$ Hz, 1H). $^{13}C\{^1H\}$ NMR (100 MHz, $CDCl_3$) δ 137.7,

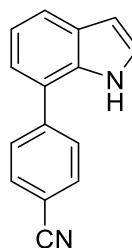
133.5, 133.3, 129.5, 129.3, 128.4, 124.5, 124.3, 121.9, 120.4, 120.3, 103.2. HRMS (ESI) m/z : $[M+H]^+$ Calcd for $C_{14}H_{11}ClN$, 228.0575; found, 228.0569.

4-(1*H*-Indol-7-yl)benzaldehyde **6-1o**



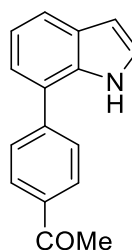
6-1o was obtained as colorless solid. 1H NMR (400 MHz, $CDCl_3$) δ 10.06 (s, 1H), 8.51 (s, 1H), 8.03 – 8.00 (m, 2H), 7.84 – 7.81 (m, 2H), 7.71 (ddd, $J = 7.2, 1.8, 0.7$ Hz, 1H), 7.29 – 7.21 (m, 3H), 6.66 (dd, $J = 3.2, 2.0$ Hz, 1H). $^{13}C\{^1H\}$ NMR (100 MHz, $CDCl_3$) δ 191.8, 145.7, 135.2, 133.4, 130.6, 128.7, 128.6, 124.7, 124.1, 122.2, 121.2, 120.4, 103.3. HRMS (ESI) m/z : $[M+H]^+$ Calcd for $C_{15}H_{12}NO$, 222.0913; found, 222.0908.

4-(1*H*-Indol-7-yl)benzonitrile **6-1p**



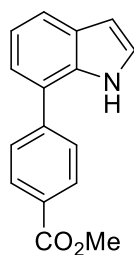
6-1p was obtained as colorless solid. 1H NMR (400 MHz, $CDCl_3$) δ 8.43 (s, 1H), 7.81 – 7.75 (m, 4H), 7.73 – 7.68 (m, 1H), 7.28 – 7.19 (m, 4H), 6.66 (dd, $J = 3.2, 2.0$ Hz, 1H).

1-(4-(1*H*-Indol-7-yl)phenyl)ethan-1-one **6-1q**



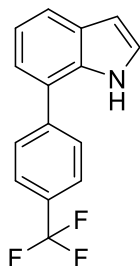
6-1q was obtained as colorless solid. 1H NMR (400 MHz, $CDCl_3$) δ 8.56 (s, 1H), 8.11 – 8.06 (m, 2H), 7.77 – 7.73 (m, 2H), 7.70 (dd, $J = 7.0, 1.7$ Hz, 1H), 7.28 – 7.21 (m, 3H), 6.66 (dd, $J = 3.1, 2.1$ Hz, 1H), 2.65 (s, 3H). $^{13}C\{^1H\}$ NMR (100 MHz, $CDCl_3$) δ 197.8, 144.3, 135.8, 129.2, 128.5, 128.3, 124.7, 124.3, 122.0, 121.0, 120.3, 104.9, 103.2, 26.6. HRMS (ESI) m/z : $[M+H]^+$ Calcd for $C_{16}H_{14}NO$, 236.1070; found, 236.1064.

Methyl 4-(1*H*-indol-7-yl)benzoate **6-1r**



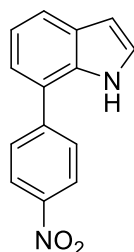
6-1r was obtained as colorless solid. ^1H NMR (400 MHz, CDCl_3) δ 8.50 (s, 1H), 8.17 (d, $J = 8.2$ Hz, 2H), 7.72 (d, $J = 8.2$ Hz, 2H), 7.69 (dd, $J = 7.0, 2.0$ Hz, 1H), 7.27 – 7.21 (m, 3H), 6.65 (dd, $J = 3.2, 2.1$ Hz, 1H), 3.96 (s, 3H). $^{13}\text{C}\{^1\text{H}\}$ NMR (100 MHz, CDCl_3) δ 166.9, 144.0, 133.4, 130.4, 128.9, 128.5, 128.1, 124.6, 124.4, 122.0, 120.9, 120.3, 103.2, 52.2. HRMS (ESI) m/z : $[\text{M}+\text{H}]^+$ Calcd for $\text{C}_{16}\text{H}_{14}\text{NO}_2$, 252.1019; found, 252.1012.

7-(4-(Trifluoromethyl)phenyl)-1*H*-indole **6-1s**



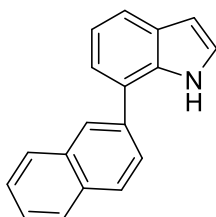
6-1s was obtained as colorless solid. ^1H NMR (400 MHz, CDCl_3) δ 8.37 (s, 1H), 7.80 – 7.75 (m, 4H), 7.72 – 7.68 (m, 1H), 7.26 – 7.22 (m, 3H), 6.66 (dd, $J = 3.2, 2.0$ Hz, 1H).

7-(4-Nitrophenyl)-1*H*-indole **6-1t**



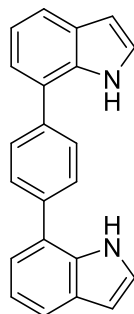
6-1t was obtained as colorless solid. ^1H NMR (400 MHz, CDCl_3) δ 8.43 (s, 1H), 8.39 – 8.35 (m, 2H), 7.85 – 7.80 (m, 2H), 7.75 – 7.71 (m, 1H), 7.32 – 7.20 (m, 3H), 6.67 (dd, $J = 3.2, 2.0$ Hz, 1H).

7-(Naphthalen-2-yl)-1*H*-indole **6-1u**



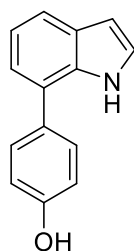
6-1u was obtained as colorless solid. ^1H NMR (400 MHz, CDCl_3) δ 8.50 (s, 1H), 8.11 (s, 1H), 8.00 (d, $J = 8.4$ Hz, 1H), 7.95 – 7.90 (m, 2H), 7.78 (dd, $J = 8.4, 1.7$ Hz, 1H), 7.70 (d, $J = 7.8$ Hz, 1H), 7.59 – 7.51 (m, 2H), 7.35 (d, $J = 7.1$ Hz, 1H), 7.30 – 7.23 (m, 2H), 6.67 (m, 1H).

1,4-Di(1*H*-indol-7-yl)benzene **6-1v**



6-1v was obtained as colorless solid. ^1H NMR (400 MHz, CDCl_3) δ 8.51 (s, 2H), 7.80 (s, 4H), 7.69 (d, $J = 7.2$ Hz, 2H), 7.31 – 7.23 (m, 6H), 6.67– 6.65 (m, 2H). $^{13}\text{C}\{^1\text{H}\}$ NMR (100 MHz, CDCl_3) δ 138.4, 133.7, 128.9, 128.4, 127.7, 125.1, 124.4, 121.9, 120.4, 120.3, 103.2. HRMS (ESI) m/z : $[\text{M}+\text{H}]^+$ Calcd for $\text{C}_{22}\text{H}_{17}\text{N}_2$, 309.1386; found, 309.1379.

4-(1*H*-Indol-7-yl)phenol **6-1w**



6-1w was obtained as colorless solid. ^1H NMR (400 MHz, CDCl_3) δ 8.39 (s, 1H), 7.64 (d, $J = 7.0$ Hz, 1H), 7.52 (d, $J = 8.4$ Hz, 2H), 7.27 – 7.17 (m, 3H), 6.97 (d, $J = 8.4$ Hz, 2H), 6.67 – 6.59 (m, 1H), 5.09 (s, 1H). $^{13}\text{C}\{^1\text{H}\}$ NMR (100 MHz, CDCl_3) δ 154.9, 133.8, 131.8, 129.5, 128.2, 125.2, 124.3, 121.7, 120.3, 119.6, 116.0, 103.0. HRMS (ESI) m/z : $[\text{M}+\text{H}]^+$ Calcd for $\text{C}_{14}\text{H}_{12}\text{NO}$, 210.0913; found, 210.0908.

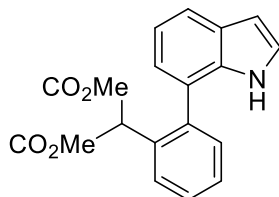
9.2. Supporting information of Chapter 6

9.2.1. General procedure for the synthesis of azepino[3,2,1-*hi*]indoles **6-(4a-4x)**

Under argon atmosphere, 7-aryl-1*H*-indoles **6-1** (0.3 mmol), diazo compounds **6-2** (0.45 mmol, 1.5 equiv.), $[\text{Cp}^*\text{RhCl}_2]_2$ (4.7 mg, 0.0075 mmol, 2.5 mol%), AgOAc (7.5 mg, 0.045 mmol, 15 mol%), DBU (13.5 μL , 0.09 mmol, 30 mmol%) and EtOAc (2 mL) were placed in a 25 mL seal tube. The mixture was heated in oil bath at 60 $^\circ\text{C}$ for 24 h

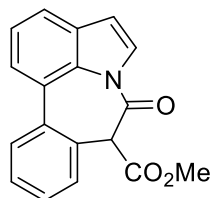
and then cooled to room temperature. The crude reaction mixture was diluted with EtOAc to 5 mL, filtered through a celite pad, and then washed with 10 mL EtOAc. The volatiles were removed under reduced pressure, and the residue was subjected to silica gel column chromatography [eluting with petroleum ether/ethyl acetate] to afford the corresponding product.

Dimethyl 2-(2-(1*H*-indol-7-yl)phenyl)malonate **6-3a**



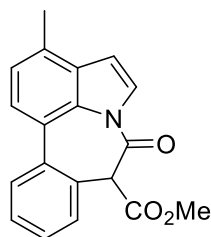
6-3a was obtained as colorless solid. (88 mg, 91%) mp 151-152 °C; Purification (Petroleum ether/ethyl acetate = 10/1). ¹H NMR (400 MHz, CDCl₃) δ 8.22 (s, 1H), 7.68 (dt, *J* = 8.0, 1.0 Hz, 1H), 7.67 – 7.63 (m, 1H), 7.51 – 7.38 (m, 3H), 7.20 (dd, *J* = 8.0, 7.2 Hz, 1H), 7.14 (dd, *J* = 3.2, 2.4 Hz, 1H), 7.06 (dd, *J* = 7.2, 1.2 Hz, 1H), 6.60 (dd, *J* = 3.2, 2.1 Hz, 1H), 4.72 (s, 1H), 3.68 (s, 3H), 3.63 (s, 3H). ¹³C{¹H} NMR (100 MHz, CDCl₃) δ 169.7, 168.9, 138.9, 134.6, 131.7, 130.6, 129.4, 128.5, 128.3, 127.8, 124.6, 123.3, 122.8, 120.4, 119.9, 102.8, 53.8, 52.8. HRMS (ESI) *m/z*: [M+Na]⁺ Calcd for C₁₉H₁₇NO₄Na, 346.1050; found, 346.1051. It was crystallized from cyclohexane/dichloromethane.

Methyl 4-oxo-4,5-dihydrobenzo[4,5]azepino[3,2,1-*hi*]indole-5-carboxylate **6-4a**



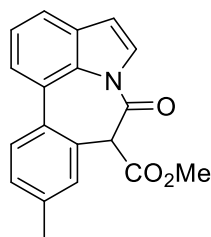
6-4a was obtained as colorless solid. (82 mg, 94%) mp 128-129 °C; Purification (Petroleum ether/ethyl acetate = 10/1). ¹H NMR (400 MHz, CDCl₃) δ 7.88 (d, *J* = 3.7 Hz, 1H), 7.75 – 7.72 (m, 2H), 7.66 (dd, *J* = 7.7, 1.0 Hz, 1H), 7.56 – 7.47 (m, 3H), 7.41 (t, *J* = 7.7 Hz, 1H), 6.77 (d, *J* = 3.7 Hz, 1H), 5.07 (s, 1H), 3.26 (s, 3H). ¹³C{¹H} NMR (100 MHz, CDCl₃) δ 167.3, 165.1, 135.6, 131.8, 131.6, 131.5, 129.6, 129.5, 129.0, 128.6, 127.1, 125.6, 124.2, 123.5, 121.6, 109.8, 62.1, 52.6. HRMS (ESI) *m/z*: [M+Na]⁺ Calcd for C₁₈H₁₃NO₃Na, 314.0788; found, 314.0788. It was crystallized from cyclohexane/dichloromethane.

Methyl 12-methyl-4-oxo-4,5-dihydrobenzo[4,5]azepino[3,2,1-*hi*]indole-5-carboxylate
6-4b



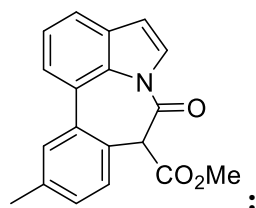
6-4b was obtained as colorless solid. (70 mg, 76%) mp 172-173 °C; Purification (Petroleum ether/ethyl acetate = 10/1). ¹H NMR (400 MHz, CDCl₃) δ 7.87 (d, *J* = 3.8 Hz, 1H), 7.71 (d, *J* = 7.6 Hz, 1H), 7.63 (d, *J* = 7.8 Hz, 1H), 7.53 – 7.43 (m, 3H), 7.21 (dd, *J* = 7.8, 0.9 Hz, 1H), 6.81 (d, *J* = 3.8 Hz, 1H), 5.07 (s, 1H), 3.27 (s, 3H), 2.60 (s, 3H). ¹³C{¹H} NMR (100 MHz, CDCl₃) δ 167.5, 165.0, 135.7, 131.6, 131.5, 131.44, 131.41, 131.1, 129.2, 128.9, 128.3, 126.4, 125.0, 123.5, 123.2, 108.1, 62.1, 52.6, 18.4. HRMS (ESI) *m/z*: [M+Na]⁺ Calcd for C₁₉H₁₅NO₃Na, 328.0944; found, 328.0944. It was crystallized from cyclohexane/dichloromethane.

Methyl 7-methyl-4-oxo-4,5-dihydrobenzo[4,5]azepino[3,2,1-*hi*]indole-5-carboxylate
6-4c



6-4c was obtained as colorless solid. (71 mg, 77%) mp 164-165 °C; Purification (Petroleum ether/ethyl acetate = 10/1). ¹H NMR (400 MHz, CDCl₃) δ 7.86 (d, *J* = 3.7 Hz, 1H), 7.70 (d, *J* = 7.7 Hz, 1H), 7.63 (d, *J* = 7.7 Hz, 2H), 7.41 – 7.28 (m, 3H), 6.76 (d, *J* = 3.7 Hz, 1H), 5.01 (s, 1H), 3.25 (s, 3H), 2.45 (s, 3H). ¹³C{¹H} NMR (100 MHz, CDCl₃) δ 167.4, 165.1, 138.7, 132.8, 132.1, 131.7, 131.5, 129.9, 129.4, 127.1, 125.6, 124.2, 123.3, 121.2, 109.7, 62.1, 52.6, 21.0. HRMS (ESI) *m/z*: [M+Na]⁺ Calcd for C₁₉H₁₅NO₃Na, 328.0944; found, 328.0944. It was crystallized from cyclohexane/dichloromethane.

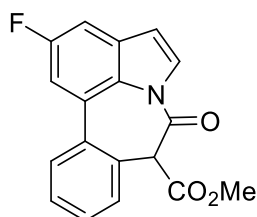
Methyl 8-methyl-4-oxo-4,5-dihydrobenzo[4,5]azepino[3,2,1-*hi*]indole-5-carboxylate
6-4d



6-4d was obtained as colorless solid. (61 mg, 67%) white solid, mp 127-128 °C; Purification (Petroleum ether/ethyl acetate = 10/1). ¹H NMR (400 MHz, CDCl₃) δ 7.87

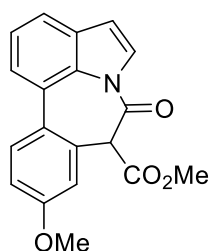
(d, $J = 3.7$ Hz, 1H), 7.72 (dd, $J = 7.7, 1.0$ Hz, 1H), 7.64 (dd, $J = 7.7, 1.0$ Hz, 1H), 7.55 – 7.53 (m, 1H), 7.39 (dd, $J = 15.7, 7.8$ Hz, 2H), 7.29 (d, $J = 7.7$ Hz, 1H), 6.76 (d, $J = 3.7$ Hz, 1H), 5.03 (s, 1H), 3.25 (s, 3H), 2.46 (s, 3H). $^{13}\text{C}\{^1\text{H}\}$ NMR (100 MHz, CDCl_3) δ 167.5, 165.3, 139.0, 135.4, 131.8, 131.7, 131.4, 130.2, 129.5, 127.1, 126.9, 125.7, 124.2, 123.4, 121.5, 109.7, 61.7, 52.6, 21.3. HRMS (ESI) m/z : $[\text{M}+\text{Na}]^+$ Calcd for $\text{C}_{19}\text{H}_{15}\text{NO}_3\text{Na}$, 328.0944; found, 328.0943.

Methyl 11-fluoro-4-oxo-4,5-dihydrobenzo[4,5]azepino[3,2,1-*hi*]indole-5-carboxylate
6-4e



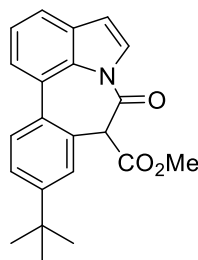
6-4e was obtained as colorless solid. (64 mg, 69%) mp 140-141 °C; Purification (Petroleum ether/ethyl acetate = 10/1). ^1H NMR (400 MHz, CDCl_3) δ 7.90 (d, $J = 3.7$ Hz, 1H), 7.70 (dd, $J = 7.3, 1.7$ Hz, 1H), 7.57 – 7.43 (m, 4H), 7.33 (dd, $J = 8.1, 2.4$ Hz, 1H), 6.73 (d, $J = 3.7$ Hz, 1H), 5.07 (s, 1H), 3.30 (s, 3H). $^{13}\text{C}\{^1\text{H}\}$ NMR (100 MHz, CDCl_3) δ 167.1, 164.6, 159.8 (d, $^1J_{\text{C-F}} = 240.8$ Hz), 134.6, 132.9 (d, $^2J_{\text{C-F}} = 10.5$ Hz), 131.7, 129.5 (d, $^3J_{\text{C-F}} = 4.6$ Hz), 129.2 (d, $^3J_{\text{C-F}} = 4.3$ Hz), 128.8, 128.1, 126.8 (d, $^2J_{\text{C-F}} = 9.2$ Hz), 110.7, 110.5, 109.6 (d, $^3J_{\text{C-F}} = 4.0$ Hz), 107.6, 107.4, 62.0, 52.8. ^{19}F NMR (376 MHz, CDCl_3) δ -118.9 (t, $J = 9.0$ Hz, 1F). HRMS (ESI) m/z : $[\text{M}+\text{Na}]^+$ Calcd for $\text{C}_{18}\text{H}_{12}\text{FNO}_3\text{Na}$, 332.0693; found, 332.0693. It was crystallized from cyclohexane/dichloromethane.

Methyl 7-methoxy-4-oxo-4,5-dihydrobenzo[4,5]azepino[3,2,1-*hi*]indole-5-carboxylate
6-4j



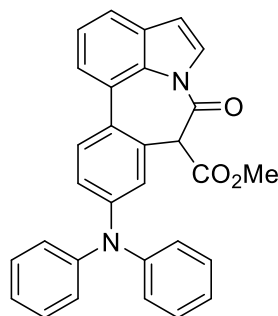
6-4j was obtained as colorless solid. (92 mg, 95%) mp 125-126 °C; Purification (Petroleum ether/ethyl acetate = 4/1). ^1H NMR (400 MHz, CDCl_3) δ 7.86 (d, $J = 3.7$ Hz, 1H), 7.67 – 7.63 (m, 2H), 7.60 (dd, $J = 7.7, 1.0$ Hz, 1H), 7.37 (t, $J = 7.7$ Hz, 1H), 7.07 (dd, $J = 8.7, 2.7$ Hz, 1H), 7.01 (d, $J = 2.7$ Hz, 1H), 6.76 (d, $J = 3.7$ Hz, 1H), 5.00 (s, 1H), 3.89 (s, 3H), 3.26 (s, 3H). $^{13}\text{C}\{^1\text{H}\}$ NMR (100 MHz, CDCl_3) δ 167.2, 164.8, 159.9, 131.7, 131.3, 130.8, 130.7, 128.2, 127.0, 125.4, 124.2, 123.0, 120.8, 116.2, 115.1, 109.8, 62.1, 55.5, 52.6. HRMS (ESI) m/z : $[\text{M}+\text{Na}]^+$ Calcd for $\text{C}_{19}\text{H}_{15}\text{NO}_4\text{Na}$, 344.0893; found, 344.0893.

Methyl 7-(*tert*-butyl)-4-oxo-4,5-dihydrobenzo[4,5]azepino[3,2,1-*hi*]indole-5-carboxylate **6-4k**



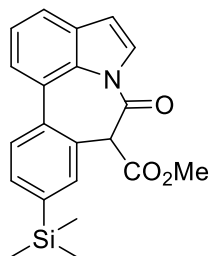
6-4k was obtained as colorless solid. (93 mg, 89%) mp 167-168 °C; Purification (Petroleum ether/ethyl acetate = 10/1). ¹H NMR (400 MHz, CDCl₃) δ 7.87 (d, *J* = 3.7 Hz, 1H), 7.71 (dd, *J* = 7.7, 1.0 Hz, 1H), 7.67 (d, *J* = 8.2 Hz, 1H), 7.63 (dd, *J* = 7.7, 1.0 Hz, 1H), 7.55 (dd, *J* = 8.2, 2.0 Hz, 1H), 7.45 (d, *J* = 2.0 Hz, 1H), 7.39 (t, *J* = 7.7 Hz, 1H), 6.76 (d, *J* = 3.7 Hz, 1H), 5.07 (s, 1H), 3.26 (s, 3H), 1.39 (s, 9H). ¹³C{¹H} NMR (100 MHz, CDCl₃) δ 167.5, 165.2, 151.9, 132.8, 131.7, 131.6, 129.2, 129.2, 128.4, 127.0, 126.3, 125.6, 124.2, 123.2, 121.2, 109.7, 62.5, 52.6, 34.7, 31.3. HRMS (ESI) *m/z*: [M+H]⁺ Calcd for C₂₂H₂₂NO₃, 348.1594; found, 348.1589.

Methyl 7-(diphenylamino)-4-oxo-4,5-dihydrobenzo[4,5]azepino[3,2,1-*hi*]indole-5-carboxylate **6-4l**



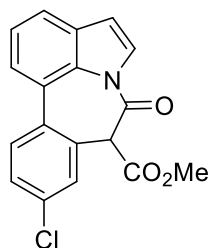
6-4l was obtained as colorless solid. (116 mg, 84%) mp 198-199 °C; Purification (Petroleum ether/ethyl acetate = 10/1). ¹H NMR (400 MHz, CDCl₃) δ 7.85 (d, *J* = 3.7 Hz, 1H), 7.65 (d, *J* = 7.7 Hz, 1H), 7.60 (dd, *J* = 7.7, 1.0 Hz, 1H), 7.56 (d, *J* = 8.6 Hz, 1H), 7.37 (t, *J* = 7.7 Hz, 1H), 7.31 (td, *J* = 8.5, 7.2 Hz, 4H), 7.21 – 7.15 (m, 5H), 7.13 – 7.07 (m, 3H), 6.75 (d, *J* = 3.7 Hz, 1H), 4.84 (s, 1H), 3.26 (s, 3H). ¹³C{¹H} NMR (100 MHz, CDCl₃) δ 167.3, 164.9, 148.4, 147.1, 131.7, 131.3, 130.4, 130.3, 129.5, 128.7, 127.0, 125.5, 125.2, 124.3, 124.2, 123.8, 123.0, 122.6, 120.8, 109.8, 62.1, 52.6. HRMS (ESI) *m/z*: [M+H]⁺ Calcd for C₃₀H₂₃N₂O₃, 459.1698; found, 459.1698. It was crystallized from cyclohexane/dichloromethane.

Methyl 4-oxo-7-(trimethylsilyl)-4,5-dihydrobenzo[4,5]azepino[3,2,1-*hi*]indole-5-carboxylate **6-4m**



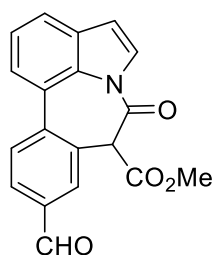
6-4m was obtained as colorless solid. (82 mg, 75%) mp 153-154 °C; Purification (Petroleum ether/ethyl acetate = 8/1). ^1H NMR (400 MHz, CDCl_3) δ 7.88 (d, $J = 3.7$ Hz, 1H), 7.76 – 7.71 (m, 2H), 7.69 – 7.64 (m, 2H), 7.59 (d, $J = 0.8$ Hz, 1H), 7.41 (t, $J = 7.7$ Hz, 1H), 6.77 (d, $J = 3.7$ Hz, 1H), 5.12 (s, 1H), 3.26 (s, 3H), 0.35 (t, 9H). $^{13}\text{C}\{^1\text{H}\}$ NMR (100 MHz, CDCl_3) δ 167.4, 165.2, 141.4, 136.5, 135.9, 133.9, 131.8, 131.6, 128.8, 128.6, 127.1, 125.7, 124.2, 123.4, 121.6, 109.7, 62.3, 52.6, -1.2. HRMS (ESI) m/z : $[\text{M}+\text{Na}]^+$ Calcd for $\text{C}_{21}\text{H}_{21}\text{NO}_3\text{SiNa}$, 386.1183; found, 386.1183. It was crystallized from cyclohexane/dichloromethane.

Methyl 7-chloro-4-oxo-4,5-dihydrobenzo[4,5]azepino[3,2,1-*hi*]indole-5-carboxylate **6-4n**



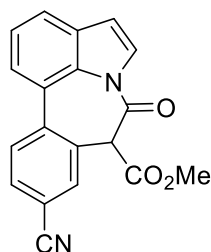
6-4n was obtained as colorless solid. (83 mg, 85%) mp 165-166 °C; Purification (Petroleum ether/ethyl acetate = 10/1). ^1H NMR (400 MHz, CDCl_3) δ 7.87 (d, $J = 3.7$ Hz, 1H), 7.70– 7.64 (m, 3H), 7.54 – 7.46 (m, 2H), 7.40 (t, $J = 7.7$ Hz, 1H), 6.77 (d, $J = 3.7$ Hz, 1H), 5.00 (s, 1H), 3.27 (s, 3H). $^{13}\text{C}\{^1\text{H}\}$ NMR (100 MHz, CDCl_3) δ 166.7, 164.4, 134.5, 134.2, 131.9, 131.4, 131.2, 130.9, 130.7, 129.1, 127.2, 124.5, 124.3, 123.4, 121.9, 109.9, 61.5, 52.8. HRMS (ESI) m/z : $[\text{M}+\text{Na}]^+$ Calcd for $\text{C}_{18}\text{H}_{12}\text{ClNO}_3\text{Na}$, 348.0398; found, 348.0398.

Methyl 7-formyl-4-oxo-4,5-dihydrobenzo[4,5]azepino[3,2,1-*hi*]indole-5-carboxylate **6-4o**



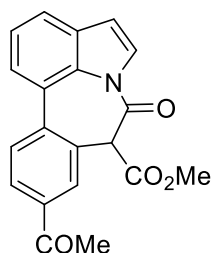
6-4o was obtained as colorless solid. (89 mg, 93%) mp 222-223 °C; Purification (Petroleum ether/ethyl acetate = 3/1). ¹H NMR (400 MHz, CDCl₃) δ 10.11 (s, 1H), 8.04 – 7.99 (m, 2H), 7.92 – 7.88 (m, 2H), 7.77 (dt, *J* = 7.8, 0.6 Hz, 1H), 7.73 (dd, *J* = 7.7, 1.0 Hz, 1H), 7.45 (t, *J* = 7.7 Hz, 1H), 6.80 (d, *J* = 3.7 Hz, 1H), 5.19 (s, 1H), 3.27 (s, 3H). ¹³C{¹H} NMR (100 MHz, CDCl₃) δ 191.1, 166.7, 164.3, 141.5, 135.9, 133.1, 132.1, 131.7, 130.4, 130.3, 129.6, 127.4, 124.4, 124.1, 122.9, 109.9, 61.8, 52.9. HRMS (ESI) *m/z*: [M+Na]⁺ Calcd for C₁₉H₁₃NO₄Na, 342.0737; found, 342.0731. It was crystallized from cyclohexane/dichloromethane.

Methyl 7-cyano-4-oxo-4,5-dihydrobenzo[4,5]azepino[3,2,1-*hi*]indole-5-carboxylate **6-4p**



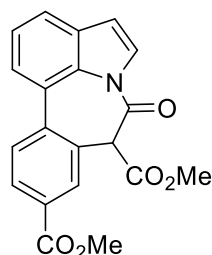
6-4p was obtained as colorless solid. (71 mg, 75%) mp 160-161 °C; Purification (Petroleum ether/ethyl acetate = 4/1). ¹H NMR (400 MHz, CDCl₃) δ 7.89 (d, *J* = 3.7 Hz, 1H), 7.85 (d, *J* = 8.5 Hz, 1H), 7.82 – 7.78 (m, 2H), 7.76 – 7.71 (m, 2H), 7.45 (t, *J* = 7.7 Hz, 1H), 6.80 (d, *J* = 3.7 Hz, 1H), 5.09 (s, 1H), 3.28 (s, 3H). ¹³C{¹H} NMR (100 MHz, CDCl₃) δ 166.3, 164.0, 140.3, 135.0, 132.2, 132.2, 131.7, 130.6, 130.3, 127.4, 124.54, 124.51, 124.0, 123.2, 118.0, 112.3, 110.0, 61.4, 53.0. HRMS (ESI) *m/z*: [M+Na]⁺ Calcd for C₁₉H₁₂N₂O₃Na, 339.0740; found, 339.0740.

Methyl 7-acetyl-4-oxo-4,5-dihydrobenzo[4,5]azepino[3,2,1-*hi*]indole-5-carboxylate **6-4q**



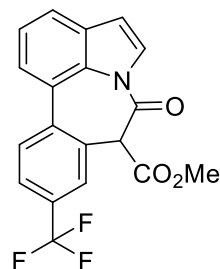
6-4q was obtained as colorless solid. (71 mg, 71%) mp 149-150 °C; Purification (Petroleum ether/ethyl acetate = 3/1). ¹H NMR (400 MHz, CDCl₃) δ 8.11 – 8.06 (m, 2H), 7.88 (d, *J* = 3.7 Hz, 1H), 7.84 – 7.81 (m, 1H), 7.75 (dd, *J* = 7.7, 0.9 Hz, 1H), 7.71 (dd, *J* = 7.7, 0.9 Hz, 1H), 7.43 (tt, *J* = 7.7, 0.6 Hz, 1H), 6.78 (dd, *J* = 3.7 Hz, 1H), 5.17 (s, 1H), 3.26 (s, 3H), 2.68 (t, *J* = 0.6 Hz, 3H). ¹³C{¹H} NMR (100 MHz, CDCl₃) δ 197.0, 166.9, 164.6, 140.2, 136.7, 132.0, 131.7, 131.7, 129.9, 129.9, 128.7, 127.3, 124.6, 124.4, 124.0, 122.7, 109.9, 77.1, 62.0, 52.8, 26.8. HRMS (ESI) *m/z*: [M+Na]⁺ Calcd for C₂₀H₁₅NO₄Na, 356.0893; found, 356.0888. It was crystallized from cyclohexane/dichloromethane.

Dimethyl 4-oxo-4,5-dihydrobenzo[4,5]azepino[3,2,1-*hi*]indole-5,7-dicarboxylate **6-4r**



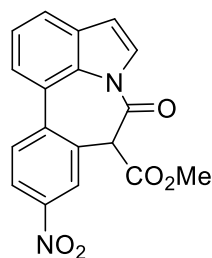
6-4r was obtained as colorless solid. (94 mg, 90%) mp 170-171 °C; Purification (Petroleum ether/ethyl acetate = 4/1). ¹H NMR (400 MHz, CDCl₃) δ 8.18 – 8.13 (m, 2H), 7.88 (d, *J* = 3.7 Hz, 1H), 7.79 (d, *J* = 8.1 Hz, 1H), 7.74 (dd, *J* = 7.7, 0.9 Hz, 1H), 7.68 (dd, *J* = 7.7, 0.9 Hz, 1H), 7.41 (td, *J* = 7.7, 0.7 Hz, 1H), 6.77 (dd, *J* = 3.7, 0.7 Hz, 1H), 5.16 (s, 1H), 3.96 (d, *J* = 0.7 Hz, 3H), 3.24 (s, 3H). ¹³C{¹H} NMR (100 MHz, CDCl₃) δ 166.8, 166.2, 164.5, 139.9, 132.8, 131.9, 131.6, 129.9, 129.8, 129.6, 129.6, 127.2, 124.5, 124.3, 123.9, 122.5, 109.7, 61.8, 52.7, 52.3. HRMS (ESI) *m/z*: [M+Na]⁺ Calcd for C₂₀H₁₅NO₅Na, 372.0842; found, 372.0842. It was crystallized from cyclohexane/dichloromethane.

Methyl 4-oxo-7-(trifluoromethyl)-4,5-dihydrobenzo[4,5]azepino[3,2,1-*hi*]indole-5-carboxylate **6-4s**



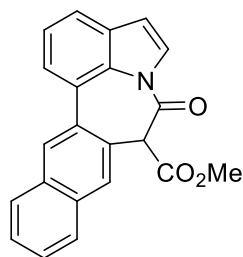
6-4s was obtained as colorless solid. (83 mg, 77%) mp 149-151 °C; Purification (Petroleum ether/ethyl acetate = 10/1). ¹H NMR (400 MHz, CDCl₃) δ 7.89 (d, *J* = 3.7 Hz, 1H), 7.86 (d, *J* = 8.1 Hz, 1H), 7.79 – 7.70 (m, 4H), 7.44 (t, *J* = 7.7 Hz, 1H), 6.79 (d, *J* = 3.7 Hz, 1H), 5.13 (s, 1H), 3.27 (s, 3H). ¹³C{¹H} NMR (100 MHz, CDCl₃) δ 166.6, 164.3, 139.2, 132.0, 131.7, 130.5 (q, *J* = 33.0 Hz), 130.3, 130.0, 128.4 (q, *J* = 3.0 Hz), 127.3, 126.5 (q, *J* = 271 Hz), 125.7 (q, *J* = 4.0 Hz), 124.4, 124.3, 123.9, 122.6, 109.9, 61.8, 52.8. ¹⁹F NMR (376 MHz, CDCl₃) δ -62.4 (s, 3F). HRMS (ESI) *m/z*: [M+Na]⁺ Calcd for C₁₉H₁₂F₃NO₃Na, 382.0661; found, 382.0661. It was crystallized from cyclohexane/dichloromethane.

Methyl 7-nitro-4-oxo-4,5-dihydrobenzo[4,5]azepino[3,2,1-*hi*]indole-5-carboxylate **6-4t**



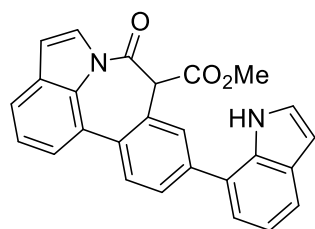
6-4t was obtained as yellow solid. (57 mg, 56%) mp 177-178 °C; Purification (Petroleum ether/ethyl acetate = 5/1). ¹H NMR (400 MHz, CDCl₃) δ 8.40 (d, *J* = 2.4 Hz, 1H), 8.35 (dd, *J* = 8.6, 2.4 Hz, 1H), 7.92 – 7.87 (m, 2H), 7.76 (d, *J* = 7.7 Hz, 2H), 7.46 (dd, *J* = 8.0, 7.5 Hz, 1H), 6.81 (d, *J* = 3.7 Hz, 1H), 5.20 (s, 1H), 3.28 (s, 3H). ¹³C{¹H} NMR (100 MHz, CDCl₃) δ 166.2, 163.8, 147.3, 142.1, 132.2, 131.6, 130.6, 130.5, 127.5, 126.6, 124.6, 124.3, 123.7, 123.6, 123.4, 110.0, 61.5, 53.0. HRMS (ESI) *m/z*: [M+Na]⁺ Calcd for C₁₈H₁₂N₂O₅Na, 359.0638; found, 359.0637.

Methyl 4-oxo-4,5-dihydronaphtho[2',3':4,5]azepino[3,2,1-*hi*]indole-5-carboxylate **6-4u**



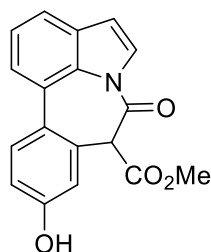
6-4u was obtained as colorless solid. (101 mg, 98%) mp 169-170 °C; Purification (Petroleum ether/ethyl acetate = 10/1). ¹H NMR (400 MHz, CDCl₃) δ 8.17 (s, 1H), 8.01 – 7.85 (m, 5H), 7.67 (dd, *J* = 7.7, 1.0 Hz, 1H), 7.59 – 7.52 (m, 2H), 7.44 (t, *J* = 7.7 Hz, 1H), 6.78 (d, *J* = 3.7 Hz, 1H), 5.25 (s, 1H), 3.27 (s, 3H). ¹³C{¹H} NMR (100 MHz, CDCl₃) δ 167.5, 165.2, 133.3, 133.2, 132.8, 132.1, 131.9, 130.7, 129.2, 128.14, 128.07, 127.5, 127.14, 127.12, 126.9, 126.0, 124.4, 123.5, 121.5, 109.8, 62.4, 52.7. HRMS (ESI) *m/z*: [M+Na]⁺ Calcd for C₂₂H₁₅NO₃Na, 364.0944; found, 364.0944. It was crystallized from cyclohexane/dichloromethane.

Methyl 7-(1*H*-indol-7-yl)-4-oxo-4,5-dihydrobenzo[4,5]azepino[3,2,1-*hi*]indole-5-carboxylate **6-4v**



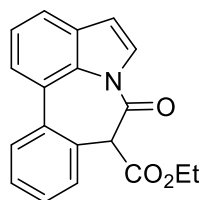
6-4v was obtained as colorless solid. (61mg, 50%) mp 208-209 °C; Purification (Petroleum ether/ethyl acetate = 4/1). ¹H NMR (400 MHz, CDCl₃) δ 8.55 (s, 1H), 7.90 (d, *J* = 3.8 Hz, 1H), 7.87 (d, *J* = 8.1 Hz, 1H), 7.81 – 7.75 (m, 3H), 7.69 (dq, *J* = 7.7, 1.3 Hz, 2H), 7.45 (t, *J* = 7.7 Hz, 1H), 7.31 – 7.22 (m, 3H), 6.80 (d, *J* = 3.7 Hz, 1H), 6.66 (dd, *J* = 3.2, 2.0 Hz, 1H), 5.14 (s, 1H), 3.29 (s, 3H). ¹³C{¹H} NMR (100 MHz, CDCl₃) δ 167.2, 164.9, 139.8, 134.6, 133.6, 131.9, 131.6, 131.1, 130.3, 130.3, 128.8, 128.5, 127.2, 125.3, 124.6, 124.4, 124.0, 123.5, 122.0, 121.7, 120.6, 120.4, 109.9, 103.2, 62.1, 52.8. HRMS (ESI) *m/z*: [M+Na]⁺ Calcd for C₂₆H₁₈N₂O₃Na, 429.1210; found, 429.1202.

Methyl 7-hydroxy-4-oxo-4,5-dihydrobenzo[4,5]azepino[3,2,1-*hi*]indole-5-carboxylate
6-4w



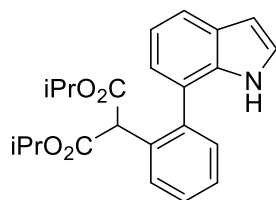
6-4w was obtained as colorless solid. (17 mg, 18%) mp 124-125 °C; Purification (Petroleum ether/ethyl acetate = 2/1). ¹H NMR (400 MHz, CDCl₃) δ 7.86 (d, *J* = 3.7 Hz, 1H), 7.65 (dd, *J* = 7.8, 1.0 Hz, 1H), 7.63 – 7.58 (m, 2H), 7.38 (t, *J* = 7.7 Hz, 1H), 6.99 (dd, *J* = 8.5, 2.6 Hz, 1H), 6.94 (d, *J* = 2.6 Hz, 1H), 6.76 (d, *J* = 3.7 Hz, 1H), 5.84 (s, 1H), 4.96 (s, 1H), 3.28 (s, 3H). ¹³C{¹H} NMR (100 MHz, CDCl₃) δ 167.3, 165.0, 156.4, 131.7, 131.3, 131.1, 130.8, 128.2, 127.0, 125.5, 124.3, 123.1, 120.9, 118.0, 116.6, 110.0, 61.8, 52.8. HRMS (ESI) *m/z*: [M+Na]⁺ Calcd for C₁₈H₁₃NO₄Na, 330.0737; found, 330.0731.

Ethyl 4-oxo-4,5-dihydrobenzo[4,5]azepino[3,2,1-*hi*]indole-5-carboxylate **6-4x**



6-4x was obtained as colorless solid. (51 mg, 55%) mp 119-120 °C; Purification (Petroleum ether/ethyl acetate = 10/1). ¹H NMR (400 MHz, CDCl₃) δ 7.88 (d, *J* = 3.7 Hz, 1H), 7.75 – 7.71 (m, 2H), 7.65 (dd, *J* = 7.7, 1.1 Hz, 1H), 7.55 – 7.46 (m, 3H), 7.40 (t, *J* = 7.7 Hz, 1H), 6.77 (d, *J* = 3.7 Hz, 1H), 5.05 (s, 1H), 3.82 – 3.74 (m, 1H), 3.72 – 3.64 (m, 1H), 0.60 (t, *J* = 7.1 Hz, 3H). ¹³C{¹H} NMR (100 MHz, CDCl₃) δ 166.7, 165.3, 135.6, 131.9, 131.7, 131.6, 129.9, 129.5, 129.0, 128.6, 127.2, 125.9, 124.2, 123.6, 121.5, 109.6, 62.3, 61.7, 13.4. HRMS (ESI) *m/z*: [M+Na]⁺ Calcd for C₁₉H₁₅NO₃Na, 328.0944; found, 328.0944. It was crystallized from cyclohexane/dichloromethane.

Diisopropyl 2-(2-(1*H*-indol-7-yl)phenyl)malonate **6-3y**

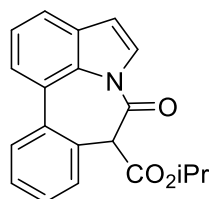


6-3y was obtained as colorless solid. (114 mg, 100%) mp 84-85 °C; Purification (Petroleum ether/ethyl acetate = 10/1). ¹H NMR (400 MHz, CDCl₃) δ 8.37 (s, 1H), 7.72 – 7.65 (m, 2H), 7.50 (td, *J* = 7.5, 1.8 Hz, 1H), 7.45 (td, *J* = 7.4, 1.5 Hz, 1H), 7.42 – 7.38 (m, 1H), 7.21 (dd, *J* = 8.0, 7.2 Hz, 1H), 7.17 (dd, *J* = 3.2, 2.5 Hz, 1H), 7.08 (dd, *J* = 7.2, 1.1 Hz, 1H), 6.62 (dd, *J* = 3.2, 2.0 Hz, 1H), 5.07 – 4.94 (m, 2H), 4.62 (s, 1H), 1.24 (dd, *J* = 6.3, 4.3 Hz, 6H), 1.18 (d, *J* = 6.3 Hz, 3H), 1.11 (d, *J* = 6.3 Hz, 3H). ¹³C{¹H} NMR (100 MHz, CDCl₃) δ 169.0, 167.8, 139.0, 134.6, 132.2, 130.7, 129.4, 128.3, 127.8, 124.5, 123.7, 123.0, 120.2, 119.9, 102.7, 69.6, 69.2, 54.7, 21.5. HRMS (ESI) *m/z*: [M+Na]⁺ Calcd for C₂₃H₂₅NO₄Na, 402.1676; found, 402.1676.

9.2.2. Procedure for Synthesis of Isopropyl 4-oxo-4,5-dihydrobenzo[4,5]azepino[3,2,1-*hi*]indole-5-carboxylate **6-4y**

Compound **6-3y** (0.3 mmol) and KOH (0.09 mmol, 30 mol%) were added in an oven-dried sealing tube, then CH₂Cl₂ was added. The reaction mixture was stirred at room temperature for 2 h and then filtered through a plug of silica and washed with EtOAc. The filtrate was concentrated under vacuum and purified by flash column chromatography (petroleum ether/EtOAc = 2/1) to give product **6-4y** as a white solid.

Isopropyl 4-oxo-4,5-dihydrobenzo[4,5]azepino[3,2,1-*hi*]indole-5-carboxylate **6-4y**



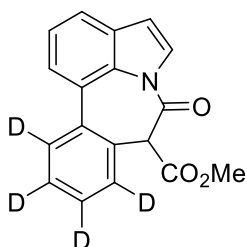
6-4y was obtained as colorless solid. (48 mg, 50%) mp 135-136 °C; Purification (Petroleum ether/ethyl acetate = 10/1). ¹H NMR (400 MHz, CDCl₃) δ 7.87 (d, *J* = 3.2 Hz, 1H), 7.76 – 7.69 (m, 2H), 7.64 (d, *J* = 7.4 Hz, 1H), 7.55 – 7.45 (m, 3H), 7.39 (td, *J* = 7.7, 2.2 Hz, 1H), 6.76 (t, *J* = 3.1 Hz, 1H), 5.02 (s, 1H), 4.59 – 4.49 (m, 1H), 0.87 (dd, *J* = 6.1, 2.2 Hz, 3H), 0.43 (dd, *J* = 6.1, 2.2 Hz, 3H). ¹³C{¹H} NMR (100 MHz, CDCl₃) δ 166.2, 165.5, 135.6, 132.0, 131.7, 131.7, 130.2, 129.5, 128.9, 128.6, 127.3, 126.0, 124.2, 123.6, 121.4, 109.5, 105.0, 69.6, 62.5, 21.1, 20.6. HRMS (ESI) *m/z*: [M+Na]⁺ Calcd for C₂₀H₁₇NO₃Na, 342.1101; found, 342.1110.

9.2.3. Competition experiments between 6-1j and 6-1t

The reaction of 7-(4-methoxyphenyl)-1*H*-indole **6-1j** (22.3 mg, 0.1 mmol), 7-(nitrophenyl)-1*H*-indole **6-1t** (23.8 mg, 0.1 mmol) was run following the general procedure. After 12 h, the reaction mixture was subjected to silica gel column chromatography [eluting with petroleum ether/ethyl acetate=10:1] to provide the product including **6-4j** (24.3 mg, 76% yield) and **6-4t** (8.1 mg, 24% yield).

9.2.4. Experiments for intermolecular kinetic isotope effects

The reaction of 7-phenyl-1*H*-indole **6-1a** (19.3 mg, 0.1 mmol), D5-7-phenyl-1*H*-indole (**6-1a**)-D5 (19.8 mg, 0.1 mmol) was run for 2 h following the general procedure. After the reaction the crude reaction mixture was subjected to silica gel column chromatography [eluting with petroleum ether/ethyl acetate=10:1] to provide the product including **6-4a** and (**6-4a**)-D4 (16.8 mg, ~28% yield). This mixture was analyzed by ¹H NMR to give the relative ration of two isomers.

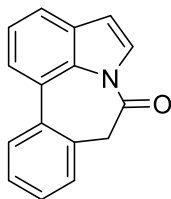


(6-4a)-D4: ¹H NMR (400 MHz, CDCl₃) δ 7.88 (d, J = 3.7 Hz, 1H), 7.73 (d, J = 7.8 Hz, 1H), 7.66 (d, J = 7.8 Hz, 1H), 7.41 (td, J = 7.8, 0.5 Hz, 1H), 6.77 (d, J = 3.7 Hz, 1H), 5.08 (s, 1H), 3.26 (s, 3H).

9.2.5. Procedure for Synthesis of Benzo[4,5]azepino[3,2,1-*hi*]indol-4(5*H*)-one 6-5a

Compound **6-4a** (291.4 mg, 1 mmol) was dissolved in aqueous KOH (5%, 10 mL), and the mixture was stirred at 20 °C for 2 h. HCl (10%) was then added dropwise at 0 °C until pH 2.5 was reached. The resulting mixture was heated at 70 °C for 2 h, basified with NH₄OH (1 mL) and extracted with CH₂Cl₂ (30 mL). The combined organic layers were filtered, and the solvents were evaporated in vacuum to yield an oily residue that was purified by flash-chromatograph on silica gel [PE/EA (10:1-20:1)]. This afforded benzo[4,5]azepino[3,2,1-*hi*]indol-4(5*H*)-one **6-5a** 140 mg, 0.61 mmol, 60% yield.

Benzo[4,5]azepino[3,2,1-*hi*]indol-4(5*H*)-one **6-5a**

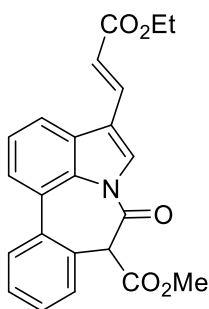


6-5a was obtained as white oil. (140 mg, 60%) Purification (Petroleum ether/ethyl acetate = 15/1). ^1H NMR (400 MHz, CDCl_3) δ 7.83 (d, $J = 3.7$ Hz, 1H), 7.76 (dd, 1H), 7.70 – 7.66 (m, 2H), 7.47 – 7.41 (m, 4H), 6.73 (d, $J = 3.8$ Hz, 1H), 3.93 (s, 2H). $^{13}\text{C}\{^1\text{H}\}$ NMR (100 MHz, CDCl_3) δ 168.0, 135.9, 132.7, 132.1, 130.3, 130.1, 128.9, 128.5, 128.0, 126.3, 126.2, 123.9, 123.5, 121.3, 109.0, 45.5. HRMS (ESI) m/z : $[\text{M}+\text{H}]^+$ Calcd for $\text{C}_{16}\text{H}_{12}\text{NO}$, 234.0913; found, 234.0926.

9.2.6. Procedure for Synthesis of (*E*)-Methyl 1-(3-ethoxy-3-oxoprop-1-en-1-yl)-4-oxo-4,5-dihydrobenzo[4,5]azepino[3,2,1-*hi*]indole-5-carboxylate **6-6a**

Under argon atmosphere, **6-4a** (0.3 mmol), ethyl acrylate (0.36 mmol, 1.2 equiv.), $\text{Pd}(\text{OAc})_2$ (3.4 mg, 0.015 mmol, 5 mol%), AgOAc (100 mg, 0.6 mmol, 2 equiv.), and acetone (2 mL) were placed in a 25 mL seal tube. The reaction solution was degassed twice and refilled with Ar. The mixture was heated in an oil bath at 80 °C for 24 h and then cooled to room temperature. The crude reaction mixture was diluted with EtOAc to 5 mL, filtered through a celite pad, and then washed with 10 mL EtOAc. The volatiles were removed under reduced pressure, and the residue was subjected to silica gel column chromatography [eluting with petroleum ether/ethyl acetate = 4/1] to afford (*E*)-methyl 1-(3-ethoxy-3-oxoprop-1-en-1-yl)-4-oxo-4,5-dihydrobenzo[4,5]azepino[3,2,1-*hi*]indole-5-carboxylate **6a** (93.46 mg, 0.24 mmol) in 80% yield.

(*E*)-1-(3-Ethoxy-3-oxoprop-1-en-1-yl)-4-oxo-4,5-dihydrobenzo[4,5]azepino[3,2,1-*hi*]indole-5-carboxylate **6-6a**



6-6a was obtained as white oil. (94 mg, 80%) Purification (Petroleum ether/ethyl acetate = 4/1). ^1H NMR (400 MHz, CDCl_3) δ 8.12 (s, 1H), 7.92 (dd, $J = 7.9, 0.9$ Hz, 1H), 7.85

(dd, $J = 16.2$ Hz, 1H), 7.78 (d, $J = 7.7$ Hz, 1H), 7.72 (d, $J = 7.4$ Hz, 1H), 7.56 – 7.47 (m, 4H), 6.60 (d, $J = 16.2$ Hz, 1H), 5.09 (s, 1H), 4.30 (q, $J = 7.1$ Hz, 2H), 3.26 (s, 3H), 1.36 (t, $J = 7.1$ Hz, 3H). $^{13}\text{C}\{^1\text{H}\}$ NMR (100 MHz, CDCl_3) δ 167.0, 164.6, 135.4, 135.3, 132.5, 131.6, 129.8, 129.3, 129.2, 129.2, 128.9, 128.9, 126.0, 124.9, 124.5, 120.8, 119.1, 118.9, 61.8, 60.6, 52.8, 14.3. HRMS (ESI) m/z : $[\text{M}+\text{Na}]^+$ Calcd for $\text{C}_{23}\text{H}_{19}\text{NO}_5\text{Na}$, 412.1155; found, 412.1148.

9.2.7. Gram-Scale Experiment of 6-4a

Under argon atmosphere, 7-phenyl-1*H*-indoles **6-1a** (6 mmol), dimethyl 2-diazomalonate **6-2a** (9 mmol, 1.5 equiv.), $[\text{Cp}^*\text{RhCl}_2]_2$ (94 mg, 0.15 mmol, 2.5 mol%), AgOAc (150 mg, 0.9 mmol, 15 mol%), DBU (270 μL , 1.8 mmol, 30 mmol%) and EtOAc (35 mL) were placed in a 100 mL seal tube. The mixture was heated in oil bath at 60 °C for 24 h and then cooled to room temperature. The crude reaction mixture was diluted with EtOAc to 50 mL, filtered through a celite pad, and then washed with 20 mL EtOAc. The volatiles were removed under reduced pressure, and the residue was subjected to silica gel column chromatography [eluting with petroleum ether/ethyl acetate] to afford the corresponding product **6-4a** (1.55 g, 89% yield).

9.2.8. Single Crystal X-ray Structure Determination.

The detailed crystallographic data and structure refinement parameters for these compounds are summarized in **Table 6-(S1-S13)**. CCDC 1939299-305, 1939322, 1940810-812 and 1940814-815 contain the supplementary crystallographic data for this paper. These data can be obtained free of charge from The Cambridge Crystallographic Data Centre via www.ccdc.cam.ac.uk/data_request/cif.

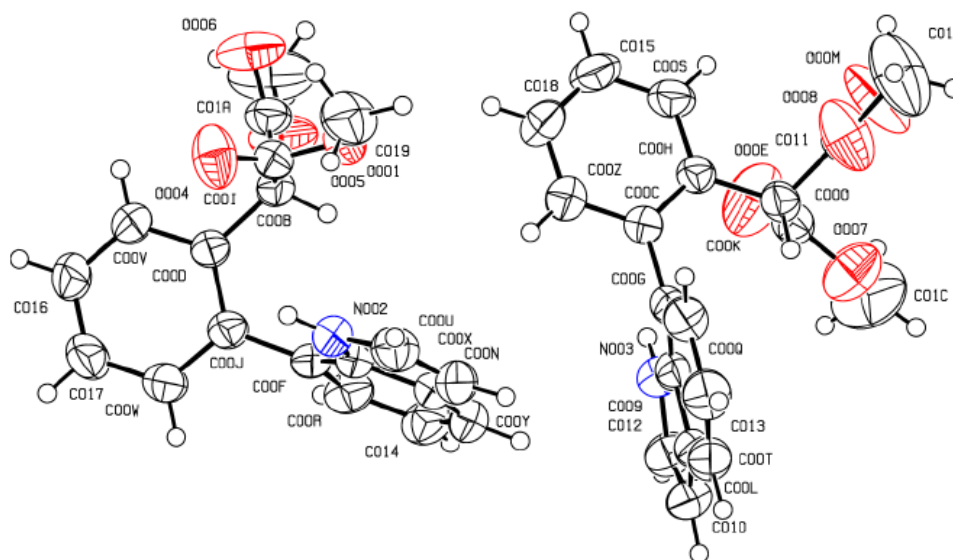


Table S6-1. 6-3a (CCDC 1939322)

Identification code	Y-II-162
Empirical formula	2(C ₁₉ H ₁₇ NO ₄)
Formula weight	646.68
Temperature/K	294.41(10)
Crystal system	monoclinic
Space group	P2 ₁ /n
a/Å	13.9277(3)
b/Å	14.1983(3)
c/Å	18.4795(4)
α/°	90
β/°	110.551(3)
γ/°	90
Volume/Å ³	3421.75(14)
Z	64
ρ _{calc} /cm ³	1.336
μ/mm ⁻¹	1.062
F(000)	1408.0
Radiation	CuKα (λ = 1.54184)
2θ range for data collection/°	6.908 to 145.378
Index ranges	-15 ≤ h ≤ 17, -17 ≤ k ≤ 12, -22 ≤ l ≤ 22
Reflections collected	13598
Independent reflections	6607 [R _{int} = 0.0173, R _{sigma} = 0.0190]
Data/restraints/parameters	6607/0/438
Goodness-of-fit on F ²	1.020
Final R indexes [I > 2σ (I)]	R ₁ = 0.0438, wR ₂ = 0.1201
Final R indexes [all data]	R ₁ = 0.0526, wR ₂ = 0.1297
Largest diff. peak/hole / e Å ⁻³	0.26/-0.25

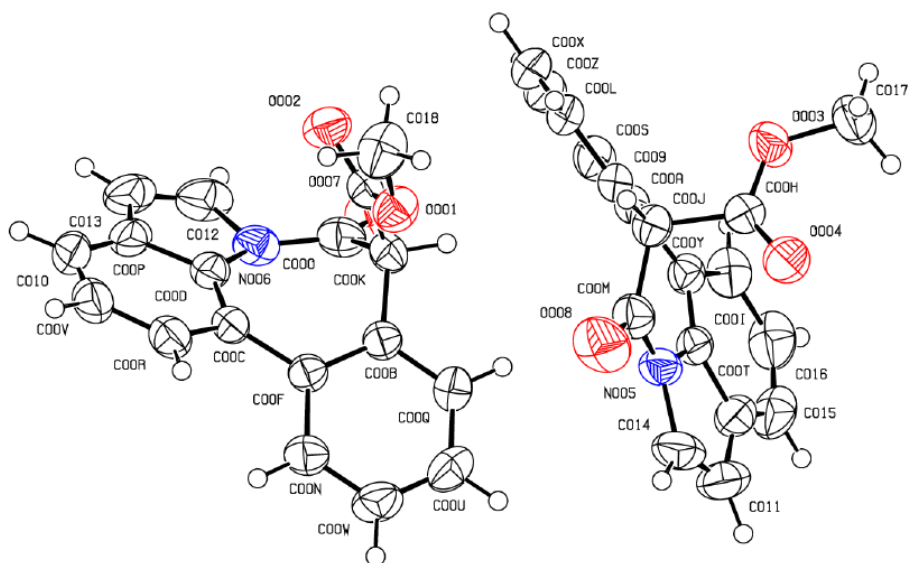


Table S6-2. 6-4a (CCDC 1939305)

Identification code	Y2-032
Empirical formula	2(C ₁₈ H ₁₃ NO ₃)
Formula weight	582.59
Temperature/K	294.31(15)
Crystal system	monoclinic
Space group	P2 ₁ /n
a/Å	15.3481(6)
b/Å	8.6768(4)
c/Å	21.2841(8)
α/°	90
β/°	93.940(4)
γ/°	90
Volume/Å ³	2827.8(2)
Z	4
ρ _{calc} /cm ³	1.368
μ/mm ⁻¹	0.767
F(000)	1216.0
Radiation	CuKα (λ = 1.54184)
2θ range for data collection/°	6.882 to 145.092
Index ranges	-18 ≤ h ≤ 18, -10 ≤ k ≤ 10, -26 ≤ l ≤ 21
Reflections collected	16224
Independent reflections	5522 [R _{int} = 0.0239, R _{sigma} = 0.0226]
Data/restraints/parameters	5522/0/399
Goodness-of-fit on F ²	1.023
Final R indexes [I ≥ 2σ (I)]	R ₁ = 0.0418, wR ₂ = 0.1078
Final R indexes [all data]	R ₁ = 0.0532, wR ₂ = 0.1186
Largest diff. peak/hole / e Å ⁻³	0.13/-0.18

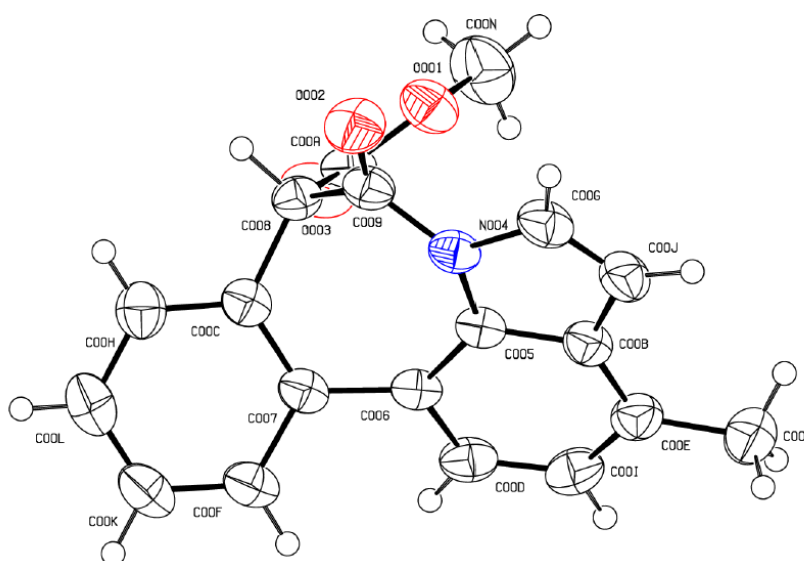


Table S6-3. 6-4b (CCDC 1939302)

Identification code	1
Empirical formula	C ₁₉ H ₁₅ NO ₃
Formula weight	305.32
Temperature/K	295.5(6)
Crystal system	triclinic
Space group	P-1
a/Å	7.9444(3)
b/Å	8.8275(4)
c/Å	10.9655(5)
α/°	78.813(4)
β/°	87.457(4)
γ/°	86.807(4)
Volume/Å ³	752.78(6)
Z	2
ρ _{calc} /cm ³	1.347
μ/mm ⁻¹	0.745
F(000)	320.0
Radiation	CuKα (λ = 1.54184)
2θ range for data collection/°	8.224 to 145.302
Index ranges	-8 ≤ h ≤ 9, -10 ≤ k ≤ 8, -13 ≤ l ≤ 11
Reflections collected	7649
Independent reflections	2903 [R _{int} = 0.0152, R _{sigma} = 0.0137]
Data/restraints/parameters	2903/0/210
Goodness-of-fit on F ²	1.081
Final R indexes [I >= 2σ (I)]	R ₁ = 0.0435, wR ₂ = 0.1150
Final R indexes [all data]	R ₁ = 0.0460, wR ₂ = 0.1191
Largest diff. peak/hole / e Å ⁻³	0.24/-0.26

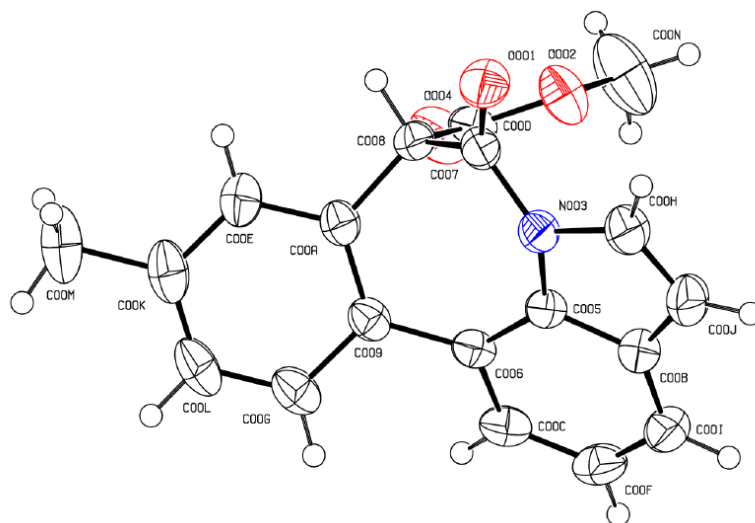


Table S6-4. 6-4c (CCDC 1939299)

Identification code	zh-yym-76
Empirical formula	C ₁₉ H ₁₃ NO ₃
Formula weight	303.30
Temperature/K	294.87(10)
Crystal system	monoclinic
Space group	P2 ₁ /n
a/Å	7.7040(2)
b/Å	13.0756(4)
c/Å	15.2485(4)
α/°	90
β/°	91.757(3)
γ/°	90
Volume/Å ³	1535.33(7)
Z	4
ρ _{calc} /cm ³	1.312
μ/mm ⁻¹	0.730
F(000)	632.0
Radiation	CuKα (λ = 1.54184)
2θ range for data collection/°	8.91 to 145.18
Index ranges	-7 ≤ h ≤ 9, -15 ≤ k ≤ 12, -18 ≤ l ≤ 17
Reflections collected	5689
Independent reflections	2963 [R _{int} = 0.0134, R _{sigma} = 0.0164]
Data/restraints/parameters	2963/0/210
Goodness-of-fit on F ²	1.094
Final R indexes [I ≥ 2σ (I)]	R ₁ = 0.0450, wR ₂ = 0.1156
Final R indexes [all data]	R ₁ = 0.0490, wR ₂ = 0.1199
Largest diff. peak/hole / e Å ⁻³	0.26/-0.36

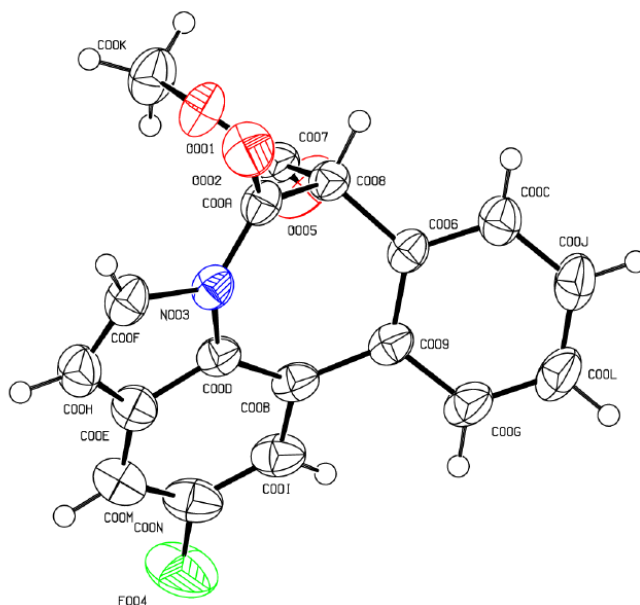


Table S6-5. 6-4e (CCDC 1939303)

Identification code	ZH-YYM116
Empirical formula	C ₁₈ H ₁₂ FNO ₃
Formula weight	309.29
Temperature/K	295.11(10)
Crystal system	triclinic
Space group	P-1
a/Å	7.5278(5)
b/Å	7.5377(5)
c/Å	13.1321(6)
α/°	98.873(4)
β/°	94.769(5)
γ/°	106.281(6)
Volume/Å ³	700.40(8)
Z	2
ρ _{calc} /cm ³	1.467
μ/mm ⁻¹	0.916
F(000)	320.0
Radiation	CuKα (λ = 1.54184)
2θ range for data collection/°	6.874 to 144.956
Index ranges	-9 ≤ h ≤ 8, -8 ≤ k ≤ 9, -16 ≤ l ≤ 14
Reflections collected	4401
Independent reflections	2638 [R _{int} = 0.0185, R _{sigma} = 0.0180]
Data/restraints/parameters	2638/0/209
Goodness-of-fit on F ²	1.042
Final R indexes [I ≥ 2σ (I)]	R ₁ = 0.0488, wR ₂ = 0.1280
Final R indexes [all data]	R ₁ = 0.0512, wR ₂ = 0.1314
Largest diff. peak/hole / e Å ⁻³	0.23/-0.25

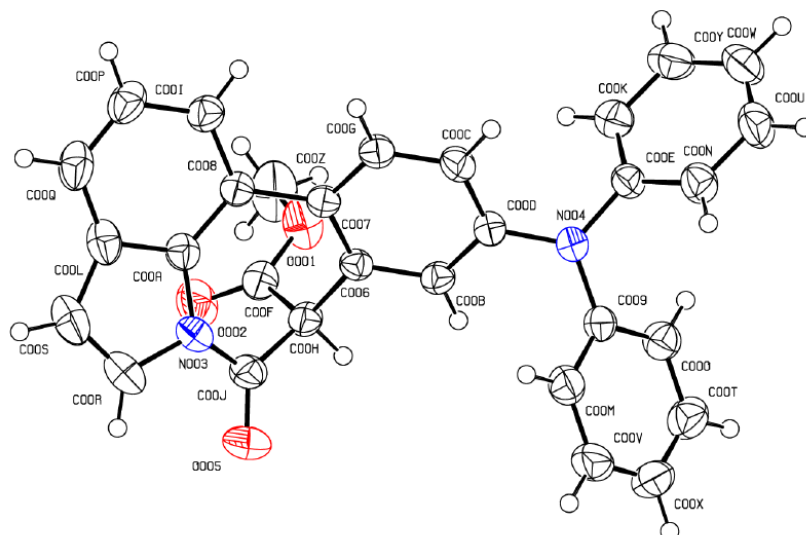


Table S6-6. 6-41 (CCDC 1940810)

Identification code	y-264
Empirical formula	C ₃₁ H ₂₂ NO ₃
Formula weight	456.49
Temperature/K	294.53(10)
Crystal system	monoclinic
Space group	P2 ₁ /c
a/Å	8.9419(3)
b/Å	28.4755(6)
c/Å	9.9467(3)
α/°	90
β/°	116.669(4)
γ/°	90
Volume/Å ³	2263.24(13)
Z	4
ρ _{calc} /cm ³	1.340
μ/mm ⁻¹	0.687
F(000)	956.0
Radiation	CuKα (λ = 1.54184)
2θ range for data collection/°	10.426 to 145.49
Index ranges	-11 ≤ h ≤ 9, -34 ≤ k ≤ 34, -12 ≤ l ≤ 11
Reflections collected	12668
Independent reflections	4383 [R _{int} = 0.0191, R _{sigma} = 0.0172]
Data/restraints/parameters	4383/0/317
Goodness-of-fit on F ²	1.049
Final R indexes [I ≥ 2σ (I)]	R ₁ = 0.0402, wR ₂ = 0.1020
Final R indexes [all data]	R ₁ = 0.0452, wR ₂ = 0.1075
Largest diff. peak/hole / e Å ⁻³	0.17/-0.23

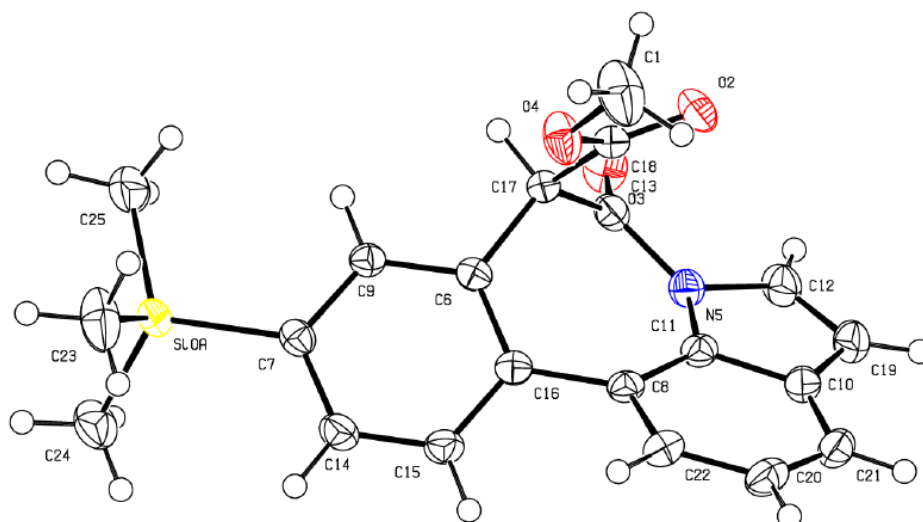


Table S6-7. 6-4m (CCDC 1940811)

Identification code	exp_6651
Empirical formula	C ₂₁ H ₂₁ NO ₃ Si
Formula weight	363.48
Temperature/K	150.00(10)
Crystal system	triclinic
Space group	P-1
a/Å	8.7270(7)
b/Å	9.2667(8)
c/Å	12.6797(12)
α/°	74.370(8)
β/°	72.940(8)
γ/°	84.241(7)
Volume/Å ³	943.79(15)
Z	2
ρ _{calc} /cm ³	1.279
μ/mm ⁻¹	1.262
F(000)	384.0
Radiation	CuKα (λ = 1.54184)
2θ range for data collection/°	7.536 to 145.832
Index ranges	-10 ≤ h ≤ 7, -11 ≤ k ≤ 11, -15 ≤ l ≤ 13
Reflections collected	10361
Independent reflections	3675 [R _{int} = 0.0260, R _{sigma} = 0.0274]
Data/restraints/parameters	3675/85/239
Goodness-of-fit on F ²	1.088
Final R indexes [I >= 2σ (I)]	R ₁ = 0.0654, wR ₂ = 0.1580
Final R indexes [all data]	R ₁ = 0.0739, wR ₂ = 0.1664
Largest diff. peak/hole / e Å ⁻³	0.96/-1.10

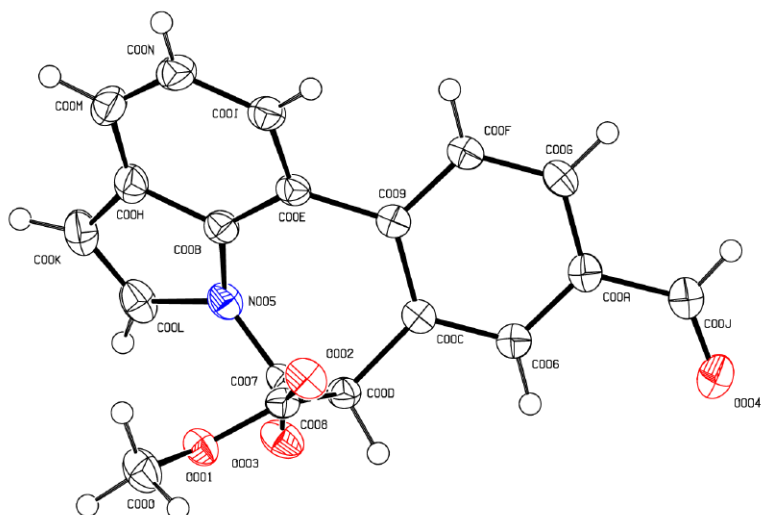


Table S6-8. 6-4p (CCDC 1939304)

Identification code	179
Empirical formula	C ₁₉ H ₁₃ NO ₄
Formula weight	319.30
Temperature/K	150.00(10)
Crystal system	triclinic
Space group	P-1
a/Å	7.8170(5)
b/Å	8.4933(6)
c/Å	12.0759(7)
α/°	76.529(5)
β/°	72.019(6)
γ/°	89.646(6)
Volume/Å ³	739.73(9)
Z	2
ρ _{calc} /cm ³	1.434
μ/mm ⁻¹	0.840
F(000)	320.0
Radiation	CuKα (λ = 1.54184)
2θ range for data collection/°	7.934 to 145.728
Index ranges	-9 ≤ h ≤ 8, -10 ≤ k ≤ 10, -14 ≤ l ≤ 14
Reflections collected	7371
Independent reflections	2876 [R _{int} = 0.0256, R _{sigma} = 0.0307]
Data/restraints/parameters	3018/0/218
Goodness-of-fit on F ²	1.035
Final R indexes [I ≥ 2σ (I)]	R ₁ = 0.0366, wR ₂ = 0.0913
Final R indexes [all data]	R ₁ = 0.0430, wR ₂ = 0.0974
Largest diff. peak/hole / e Å ⁻³	0.24/-0.23

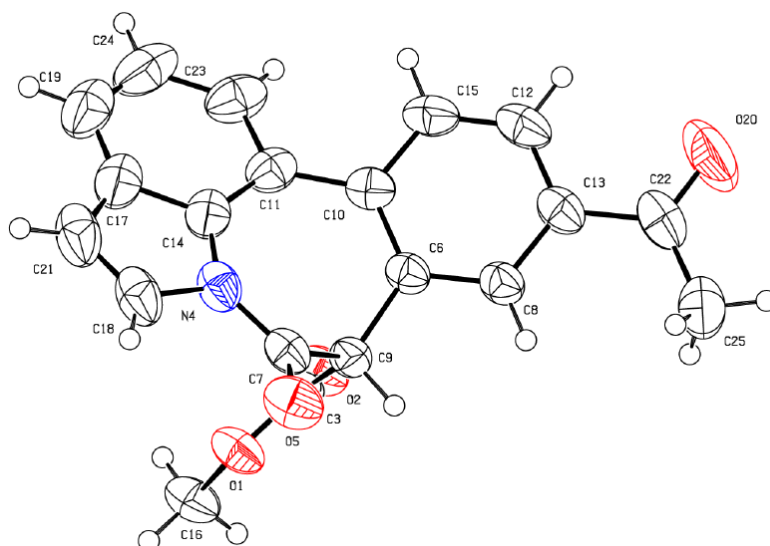


Table S6-9. 6-4q (CCDC 1940812)

Identification code	y-181
Empirical formula	C ₂₀ H ₁₅ NO ₄
Formula weight	333.33
Temperature/K	294.54(13)
Crystal system	monoclinic
Space group	P2 ₁ /c
a/Å	5.4768(15)
b/Å	12.5741(4)
c/Å	23.3420(6)
α/°	90
β/°	94.306(3)
γ/°	90
Volume/Å ³	1602.93(8)
Z	4
ρ _{calc} /cm ³	1.381
μ/mm ⁻¹	0.798
F(000)	696.0
Radiation	CuKα (λ = 1.54184)
2θ range for data collection/°	7.992 to 145.372
Index ranges	-6 ≤ h ≤ 6, -15 ≤ k ≤ 15, -28 ≤ l ≤ 28
Reflections collected	8554
Independent reflections	3114 [R _{int} = 0.0240, R _{sigma} = 0.0244]
Data/restraints/parameters	3114/0/228
Goodness-of-fit on F ²	1.036
Final R indexes [I ≥ 2σ (I)]	R ₁ = 0.0431, wR ₂ = 0.1099
Final R indexes [all data]	R ₁ = 0.0551, wR ₂ = 0.1213
Largest diff. peak/hole / e Å ⁻³	0.15/-0.19

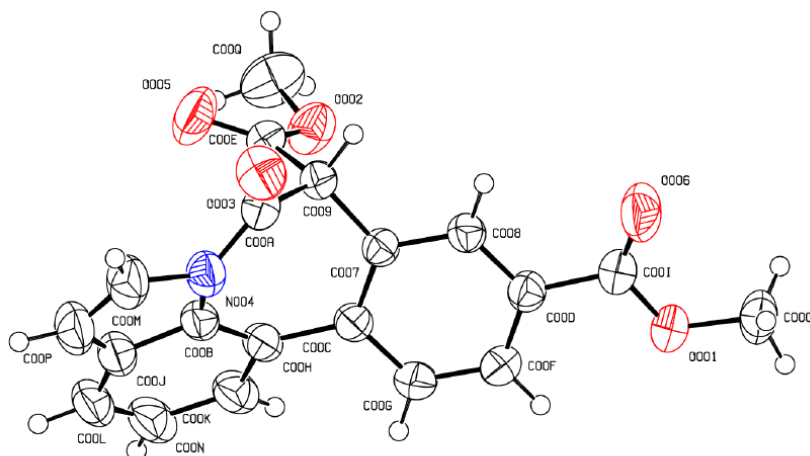


Table S6-10. 6-4r (CCDC 1939300)

Identification code	Y2-081
Empirical formula	C ₂₀ H ₁₄ NO ₅
Formula weight	348.32
Temperature/K	296.70(17)
Crystal system	triclinic
Space group	P-1
a/Å	7.7017(3)
b/Å	10.8099(5)
c/Å	11.7377(6)
α/°	115.040(5)
β/°	102.168(4)
γ/°	97.486(3)
Volume/Å ³	838.48(7)
Z	2
ρ _{calc} /cm ³	1.380
μ/mm ⁻¹	0.835
F(000)	362.0
Radiation	CuKα (λ = 1.54184)
2θ range for data collection/°	8.706 to 145.296
Index ranges	-9 ≤ h ≤ 7, -13 ≤ k ≤ 13, -14 ≤ l ≤ 14
Reflections collected	8898
Independent reflections	3206 [R _{int} = 0.0127, R _{sigma} = 0.0108]
Data/restraints/parameters	3206/0/245
Goodness-of-fit on F ²	1.046
Final R indexes [I >= 2σ (I)]	R ₁ = 0.0427, wR ₂ = 0.1148
Final R indexes [all data]	R ₁ = 0.0457, wR ₂ = 0.1190
Largest diff. peak/hole / e Å ⁻³	0.17/-0.26

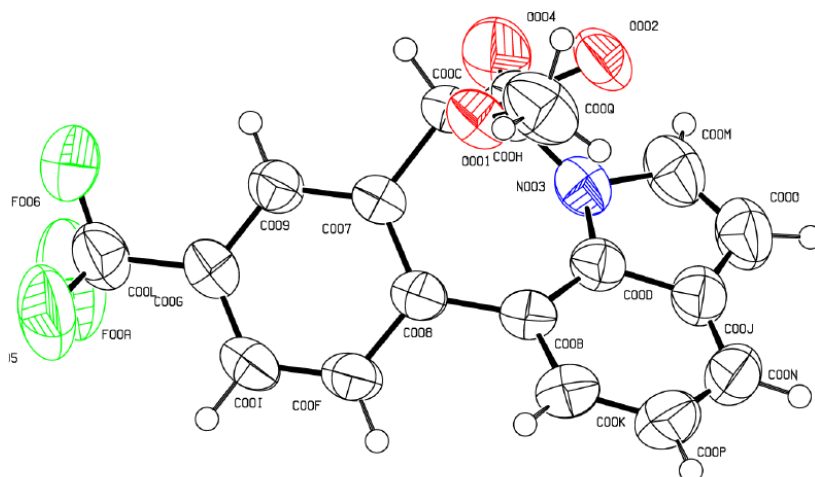


Table S6-11. 6-4s (CCDC 1940814)

Identification code	y2-261
Empirical formula	C ₁₉ H ₁₂ F ₃ NO ₃
Formula weight	359.30
Temperature/K	294.8(4)
Crystal system	monoclinic
Space group	C2/c
a/Å	18.5440(4)
b/Å	11.7459(4)
c/Å	14.8965(4)
α/°	90
β/°	93.306(2)
γ/°	90
Volume/Å ³	3239.30(16)
Z	8
ρ _{calc} /cm ³	1.473
μ/mm ⁻¹	1.061
F(000)	1472.0
Radiation	CuKα (λ = 1.54184)
2θ range for data collection/°	8.916 to 145.542
Index ranges	-22 ≤ h ≤ 22, -11 ≤ k ≤ 14, -16 ≤ l ≤ 18
Reflections collected	9109
Independent reflections	3156 [R _{int} = 0.0194, R _{sigma} = 0.0186]
Data/restraints/parameters	3156/0/236
Goodness-of-fit on F ²	1.081
Final R indexes [I >= 2σ (I)]	R ₁ = 0.0514, wR ₂ = 0.1482
Final R indexes [all data]	R ₁ = 0.0615, wR ₂ = 0.1588
Largest diff. peak/hole / e Å ⁻³	0.45/-0.38

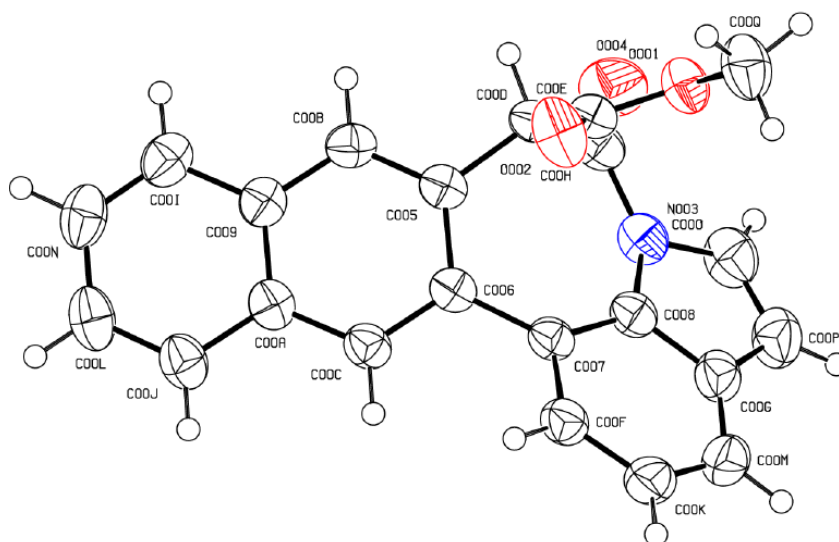


Table S6-12. 6-4u (CCDC 1940815)

Identification code	y2-262
Empirical formula	C ₂₂ H ₁₅ NO ₃
Formula weight	341.35(10)
Temperature/K	294.47(10)
Crystal system	monoclinic
Space group	P2 ₁ /c
a/Å	17.3010(4)
b/Å	7.8804(2)
c/Å	12.3166(3)
α/°	90
β/°	93.197(2)
γ/°	90
Volume/Å ³	1676.62(7)
Z	4
ρ _{calc} /cm ³	1.352
μ/mm ⁻¹	0.733
F(000)	712.0
Radiation	CuKα (λ = 1.54184)
2θ range for data collection/°	10.242 to 145.73
Index ranges	-16 ≤ h ≤ 21, -9 ≤ k ≤ 9, -15 ≤ l ≤ 14
Reflections collected	9776
Independent reflections	3295 [R _{int} = 0.0205, R _{sigma} = 0.0191]
Data/restraints/parameters	3295/0/236
Goodness-of-fit on F ²	1.049
Final R indexes [I >= 2σ (I)]	R ₁ = 0.0390, wR ₂ = 0.1024
Final R indexes [all data]	R ₁ = 0.0453, wR ₂ = 0.1089
Largest diff. peak/hole / e Å ⁻³	0.14/-0.20

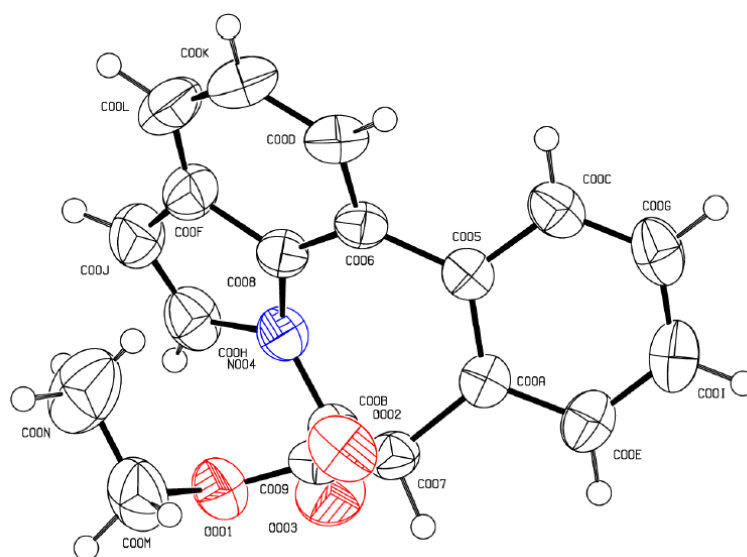


Table S6-13. 6-4x (CCDC 1939301)

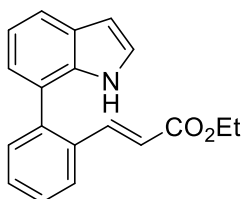
Identification code	y2-082
Empirical formula	$C_{19}H_{15}NO_3$
Formula weight	305.32
Temperature/K	296.2(4)
Crystal system	triclinic
Space group	P-1
a/Å	8.1949(5)
b/Å	8.5852(5)
c/Å	10.9177(7)
$\alpha/^\circ$	79.529(5)
$\beta/^\circ$	87.131(5)
$\gamma/^\circ$	85.915(5)
Volume/Å ³	752.86(8)
Z	2
$\rho_{\text{calc}}/\text{cm}^3$	1.347
μ/mm^{-1}	0.745
F(000)	320.0
Radiation	CuK α ($\lambda = 1.54184$)
2 θ range for data collection/ $^\circ$	8.242 to 145.616
Index ranges	$-9 \leq h \leq 9$, $-10 \leq k \leq 10$, $-12 \leq l \leq 13$
Reflections collected	8431
Independent reflections	2933 [$R_{\text{int}} = 0.0201$, $R_{\text{sigma}} = 0.0186$]
Data/restraints/parameters	2933/0/209
Goodness-of-fit on F^2	1.027
Final R indexes [$I \geq 2\sigma(I)$]	$R_1 = 0.0397$, $wR_2 = 0.1003$
Final R indexes [all data]	$R_1 = 0.0481$, $wR_2 = 0.1084$
Largest diff. peak/hole / e Å ⁻³	0.13/-0.20

9.3. Supporting information of Chapter 7

9.3.1. General Procedure for the *ortho* C-H olefination reaction (condition A)

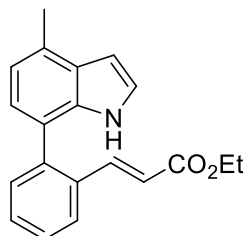
Under air atmosphere, 7-phenyl-1*H*-indoles **6-1** (0.3 mmol), alkenes **7-2** (0.75 mmol, 2.5 equiv.), [Cp**Rh*Cl₂]₂ (4.7 mg, 0.0075 mmol, 2.5 mol%), AgOAc (100.1 mg, 0.6 mmol, 2 equiv.) and acetone (2 mL) were placed in a 50 mL seal tube. The mixture was heated in oil bath at 80°C for 24h and then cooled to room temperature. The mixture was diluted with CH₂Cl₂ to 5 mL, filtered through a celite pad, and then washed with CH₂Cl₂. The volatiles were removed under reduced pressure, and the residue was subjected to silica gel column chromatography [eluting with petroleum ether/ethyl acetate] to afford the corresponding product **7-(3a-3w)**.

Ethyl (*E*)-3-(2-(1*H*-indol-7-yl)phenyl)acrylate **7-3a**



7-3a was obtained as colorless solid. (85 mg, 97%) M.P.: 123-124°C. ¹H NMR (400 MHz, CDCl₃) δ 7.98 (s, 1H), 7.82 – 7.78 (m, 1H), 7.68 (d, *J* = 7.9 Hz, 1H), 7.58 (d, *J* = 16.0, 1H), 7.53 – 7.42 (m, 3H), 7.23 – 7.15 (m, 2H), 7.04 (dd, *J* = 7.2, 1.0 Hz, 1H), 6.62 (dd, *J* = 3.2, 2.1 Hz, 1H), 6.40 (d, *J* = 16.0 Hz, 1H), 4.13 (q, *J* = 7.1 Hz, 2H), 1.21 (t, *J* = 7.1 Hz, 3H). ¹³C {¹H} NMR (100 MHz, CDCl₃) δ 166.6, 142.9, 139.6, 134.4, 133.3, 130.7, 130.1, 128.1, 127.0, 124.4, 123.7, 123.0, 120.6, 119.9, 119.4, 103.0, 60.3, 14.2. HRMS (ESI) calcd for C₁₉H₁₇NO₂ [M+Na]⁺ 314.1151, found 314.1151.

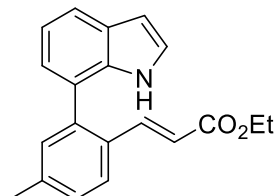
Ethyl (*E*)-3-(2-(4-methyl-1*H*-indol-7-yl)phenyl)acrylate **7-3b**



7-3b was obtained as yellow solid. (69 mg, 75%) M.P.: 126-127°C. ¹H NMR (400 MHz, CDCl₃) δ 8.07 (s, 1H), 7.79 (d, *J* = 7.3 Hz, 1H), 7.61 (d, *J* = 16.0 Hz, 1H), 7.54 – 7.38 (m, 3H), 7.13 (t, *J* = 2.7 Hz, 1H), 7.03 – 6.94 (m, 2H), 6.63 (t, *J* = 2.7 Hz, 1H), 6.41 (d, *J* = 16.0 Hz, 1H), 4.14 (q, *J* = 7.1 Hz, 2H), 2.64 (s, 3H), 1.23 (t,

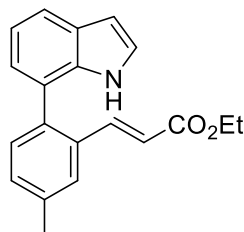
$J = 7.1$ Hz, 3H). $^{13}\text{C}\{^1\text{H}\}$ NMR (100 MHz, CDCl_3) δ 166.7, 143.1, 139.8, 133.9, 133.2, 130.7, 130.1, 130.0, 127.9, 127.8, 126.9, 123.9, 123.8, 120.6, 120.1, 119.0, 101.4, 60.3, 18.8, 14.2. HRMS (ESI) calcd for $\text{C}_{20}\text{H}_{19}\text{NO}_2$ $[\text{M}+\text{Na}]^+$ 328.1308, found 328.1308.

Ethyl (*E*)-3-(2-(1*H*-indol-7-yl)-4-methylphenyl)acrylate **7-3c**



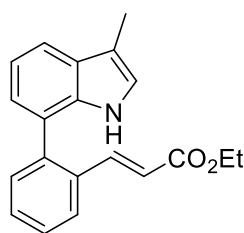
7-3c was obtained as colorless solid. (72 mg, 78%) M.P.: 189-190°C. ^1H NMR (400 MHz, CDCl_3) δ 7.98 (s, 1H), 7.70 (d, $J = 8.0$ Hz, 1H), 7.67 (dt, $J = 8.0, 1.0$ Hz, 1H), 7.55 (d, $J = 16.0$ Hz, 1H), 7.32 (s, 1H), 7.28 – 7.24 (m, 1H), 7.03 (dd, $J = 7.2, 1.0$ Hz, 1H), 6.61 (dd, $J = 3.2, 2.1$ Hz, 1H), 6.36 (d, $J = 16.0$ Hz, 1H), 4.12 (qd, $J = 7.1, 2.4$ Hz, 2H), 2.42 (s, 3H), 1.21 (t, $J = 7.1$ Hz, 3H). $^{13}\text{C}\{^1\text{H}\}$ NMR (100 MHz, CDCl_3) δ 166.8, 142.8, 140.5, 139.6, 134.4, 131.3, 130.4, 129.0, 128.0, 126.9, 124.4, 123.6, 123.1, 120.5, 120.0, 118.3, 102.9, 60.2, 21.4, 14.2. HRMS (ESI) calcd for $\text{C}_{20}\text{H}_{19}\text{NO}_2$ $[\text{M}+\text{Na}]^+$ 328.1308, found 328.1308.

Ethyl (*E*)-3-(2-(1*H*-indol-7-yl)-5-methylphenyl)acrylate **7-3d**



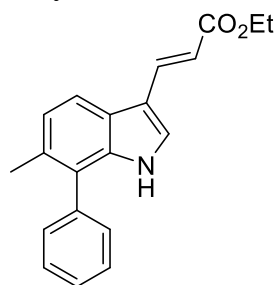
7-3d was obtained as colorless solid. (72 mg, 79%) M.P.: 148-149°C. ^1H NMR (400 MHz, CDCl_3) δ 7.97 (s, 1H), 7.67 (dt, $J = 7.8$ Hz, 1H), 7.62 – 7.53 (m, 2H), 7.40 (d, $J = 7.8$ Hz, 1H), 7.32 – 7.28 (m, 1H), 7.22 – 7.15 (m, 2H), 7.02 (dd, $J = 7.2, 1.0$ Hz, 1H), 6.61 (dd, $J = 3.2, 2.1$ Hz, 1H), 6.40 (d, $J = 16.0$ Hz, 1H), 4.13 (q, $J = 7.1$ Hz, 2H), 2.46 (s, 3H), 1.21 (t, $J = 7.1$ Hz, 3H). $^{13}\text{C}\{^1\text{H}\}$ NMR (100 MHz, CDCl_3) δ 166.7, 143.1, 137.8, 136.8, 134.5, 133.0, 131.1, 130.5, 128.0, 127.4, 124.4, 123.8, 123.0, 120.4, 119.9, 119.0, 102.9, 60.3, 21.2, 14.2. HRMS (ESI) calcd for $\text{C}_{20}\text{H}_{19}\text{NO}_2$ $[\text{M}+\text{Na}]^+$ 328.1308, found 328.1307.

Ethyl (*E*)-3-(2-(3-methyl-1*H*-indol-7-yl)phenyl)acrylate **7-3e**



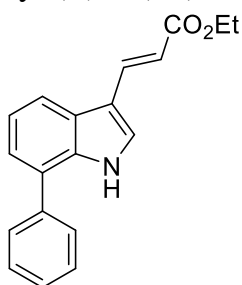
7-3e was obtained as yellow solid. (27 mg, 30%) M.P.: 133-134°C. ¹H NMR (400 MHz, CDCl₃) δ 7.81 – 7.77 (m, 1H), 7.71 (s, 1H), 7.64 – 7.56 (m, 2H), 7.52 – 7.41 (m, 3H), 7.21 (dd, *J* = 8.0, 7.2 Hz, 1H), 7.04 (dd, *J* = 7.2, 1.0 Hz, 1H), 6.94 (dd, *J* = 2.3, 1.2 Hz, 1H), 6.41 (d, *J* = 16.0 Hz, 1H), 4.13 (dd, *J* = 7.1 Hz, 2H), 2.37 (m, *J* = 1.1 Hz, 3H), 1.22 (t, *J* = 7.1 Hz, 3H). ¹³C{¹H} NMR (100 MHz, CDCl₃) δ 166.7, 143.1, 139.7, 134.8, 133.3, 130.7, 130.1, 128.5, 128.0, 126.9, 123.7, 122.9, 122.0, 119.3, 119.2, 118.7, 112.0, 60.4, 14.2, 9.8. HRMS (ESI) calcd for C₂₀H₁₉NO₂ [M+Na]⁺ 328.1308, found 328.1299.

Ethyl (*E*)-3-(6-methyl-7-phenyl-1*H*-indol-3-yl)acrylate **7-3g**



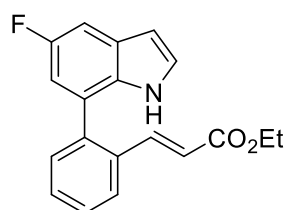
7-3g was obtained as yellow solid. (15 mg, 16%) M.P.: 119-120°C. ¹H NMR (400 MHz, CDCl₃) δ 7.87 (s, 1H), 7.61 (d, *J* = 16.0 Hz, 1H), 7.56 – 7.38 (m, 6H), 7.07 (dd, *J* = 8.1, 0.6 Hz, 1H), 6.81 (d, *J* = 2.1 Hz, 1H), 6.01 (d, *J* = 16.0 Hz, 1H), 4.23 (q, *J* = 7.1 Hz, 2H), 2.29 (s, 3H), 1.30 (t, *J* = 7.1 Hz, 3H). ¹³C{¹H} NMR (100 MHz, CDCl₃) δ 166.8, 137.3, 137.0, 134.2, 133.1, 131.8, 129.6, 129.1, 127.7, 126.4, 124.7, 123.8, 120.3, 114.9, 109.3, 60.5, 19.8, 14.3. HRMS (ESI) calcd for C₂₀H₁₉NO₂ [M+H]⁺ 306.1489, found 306.1488.

Ethyl (*E*)-3-(7-(*o*-tolyl)-1*H*-indol-3-yl)acrylate **7-3h**



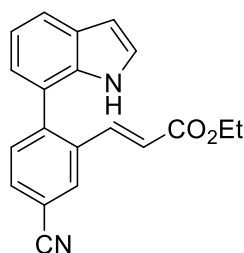
7-3h was obtained as yellow solid. (12 mg, 13%) M.P.: 101-102°C. ¹H NMR (400 MHz, CDCl₃) δ 7.94 (s, 1H), 7.66 – 7.60 (m, 2H), 7.39 – 7.31 (m, 4H), 7.21 – 7.17 (m, 1H), 7.13 (dd, *J* = 7.2, 1.2 Hz, 1H), 6.87 (d, *J* = 2.1 Hz, 1H), 6.09 (d, *J* = 16.0 Hz, 1H), 4.24 (q, *J* = 7.1 Hz, 2H), 2.18 (s, 3H), 1.31 (t, *J* = 7.1 Hz, 3H). ¹³C{¹H} NMR (100 MHz, CDCl₃) δ 166.7, 137.4, 136.5, 136.3, 134.1, 133.5, 130.7, 129.8, 128.3, 128.1, 126.2, 125.3, 125.1, 120.7, 120.5, 115.6, 109.1, 60.5, 20.0, 14.3. HRMS (ESI) calcd for C₂₀H₁₉NO₂ [M+H]⁺ 306.1489, found 306.1489.

Ethyl (*E*)-3-(2-(5-fluoro-1*H*-indol-7-yl)phenyl)acrylate **7-3i**



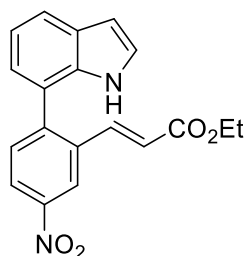
7-3i was obtained as colorless solid. (82 mg, 88%) M.P.: 153-154°C. ¹H NMR (400 MHz, CDCl₃) δ 7.91 (s, 1H), 7.79 (dd, *J* = 7.6, 2.0 Hz, 1H), 7.55 – 7.44 (m, 4H), 7.33 (dd, *J* = 9.3, 2.4 Hz, 1H), 7.21 (t, *J* = 2.9 Hz, 1H), 6.84 (dd, *J* = 9.7, 2.4 Hz, 1H), 6.58 (dd, *J* = 3.2, 2.1 Hz, 1H), 6.41 (d, *J* = 16.0 Hz, 1H), 4.14 (q, *J* = 7.1 Hz, 2H), 1.22 (t, *J* = 7.1 Hz, 3H). ¹³C{¹H} NMR (100 MHz, CDCl₃) δ 166.5, 157.6 (d, ¹J_{C-F} = 250.5 Hz), 142.3, 138.3, 133.2, 131.1, 130.6, 130.2, 128.5, 128.3 (d, ³J_{C-F} = 10.3 Hz), 126.9, 126.2, 123.8 (d, ³J_{C-F} = 9.5 Hz), 119.7, 111.8 (d, ²J_{C-F} = 26.6 Hz), 105.2 (d, ²J_{C-F} = 23.4 Hz), 103.1 (d, ³J_{C-F} = 4.8 Hz), 60.4, 14.1. ¹⁹F NMR (376 MHz, CDCl₃) δ -124.83 (t, *J* = 9.0 Hz). HRMS (ESI) calcd for C₁₉H₁₆FNO₂ [M+Na]⁺ 332.1057, found 332.1057.

Ethyl (*E*)-3-(5-cyano-2-(1*H*-indol-7-yl)phenyl)acrylate **7-3j**



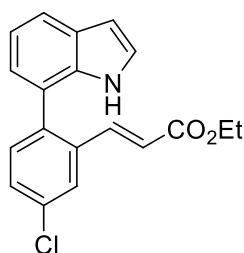
7-3j was obtained as yellow solid. (69 mg, 73%) M.P.: 152-153°C. ¹H NMR (400 MHz, CDCl₃) δ 8.05 (d, *J* = 1.6 Hz, 1H), 7.98 (s, 1H), 7.73 (dq, *J* = 7.9, 1.2 Hz, 2H), 7.64 (dd, *J* = 7.9, 0.5 Hz, 1H), 7.49 (d, *J* = 16.0 Hz, 1H), 7.24 – 7.19 (m, 2H), 7.02 (dd, *J* = 7.2, 1.0 Hz, 1H), 6.64 (dd, *J* = 3.2, 2.0 Hz, 1H), 6.44 (d, *J* = 16.0 Hz, 1H), 4.15 (q, *J* = 7.1 Hz, 2H), 1.23 (t, *J* = 7.1 Hz, 3H). ¹³C{¹H} NMR (100 MHz, CDCl₃) δ 165.9, 144.0, 140.6, 134.7, 133.7, 132.7, 131.6, 130.8, 128.5, 124.9, 123.6, 121.7, 121.1, 120.0, 118.2, 112.1, 103.3, 60.7, 14.1. HRMS (ESI) calcd for C₂₀H₁₆N₂O₂ [M+H]⁺ 317.1285, found 317.1285.

Ethyl (*E*)-3-(2-(1*H*-indol-7-yl)-5-nitrophenyl)acrylate **7-3k**



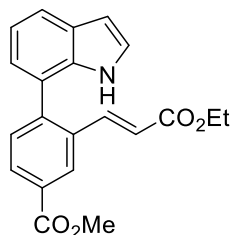
7-3k was obtained as yellow solid. (74 mg, 73%) M.P.: 153-154°C. ¹H NMR (400 MHz, CDCl₃) δ 8.65 (d, *J* = 2.3 Hz, 1H), 8.31 (dd, *J* = 8.5, 2.3 Hz, 1H), 7.94 (s, 1H), 7.75 (d, *J* = 8.1 Hz, 1H), 7.71 (d, *J* = 8.5 Hz, 1H), 7.54 (d, *J* = 16.0 Hz, 1H), 7.25 – 7.19 (m, 2H), 7.05 (dd, *J* = 7.2, 1.1 Hz, 1H), 6.66 (dd, *J* = 3.2, 2.0 Hz, 1H), 6.57 (d, *J* = 16.0 Hz, 1H), 4.17 (q, *J* = 7.1 Hz, 2H), 1.24 (t, *J* = 7.1 Hz, 3H). ¹³C{¹H} NMR (100 MHz, CDCl₃) δ 165.9, 147.5, 145.8, 140.6, 134.8, 133.7, 131.8, 128.5, 124.9, 124.2, 123.7, 122.1, 122.1, 121.9, 120.9, 120.1, 103.4, 60.8, 14.1. HRMS (ESI) calcd for C₁₉H₁₆N₂O₄ [M+H]⁺ 337.1183, found 337.1183.

Ethyl (*E*)-3-(5-chloro-2-(1*H*-indol-7-yl)phenyl)acrylate **7-3l**



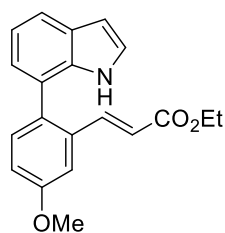
7-3l was obtained as colorless solid. (62 mg, 64%) M.P.: 180-181°C. ¹H NMR (400 MHz, CDCl₃) δ 7.94 (s, 1H), 7.77 (t, *J* = 1.0 Hz, 1H), 7.69 (dt, *J* = 7.9, 1.0 Hz, 1H), 7.51 – 7.43 (m, 3H), 7.22 – 7.16 (m, 2H), 7.00 (dd, *J* = 7.3, 1.1 Hz, 1H), 6.62 (dd, *J* = 3.2, 2.0 Hz, 1H), 6.40 (d, *J* = 16.0 Hz, 1H), 4.13 (q, *J* = 7.1 Hz, 2H), 1.22 (t, *J* = 7.1 Hz, 3H). ¹³C{¹H} NMR (100 MHz, CDCl₃) δ 166.2, 141.5, 137.9, 135.0, 134.3, 134.1, 132.0, 130.0, 128.2, 126.8, 124.6, 123.7, 121.8, 120.9, 120.6, 120.0, 103.1, 60.5, 14.2. HRMS (ESI) calcd for C₁₉H₁₆ClNO₂ [M+Na]⁺ 348.0762, found 348.0762.

Methyl (*E*)-3-(3-ethoxy-3-oxoprop-1-en-1-yl)-4-(1*H*-indol-7-yl)benzoate **7-3m**



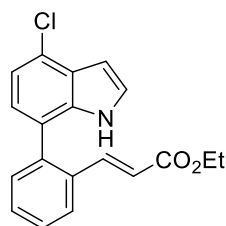
7-3m was obtained as yellow solid. (84 mg, 80%) M.P.: 128-129°C. ¹H NMR (400 MHz, CDCl₃) δ 8.46 (d, *J* = 1.7 Hz, 1H), 8.11 (dd, *J* = 8.0, 1.7 Hz, 1H), 8.04 (s, 1H), 7.71 (dt, *J* = 7.9, 0.8 Hz, 1H), 7.61 – 7.54 (m, 2H), 6.63 (dd, *J* = 3.2, 2.0 Hz, 1H), 6.52 (d, *J* = 16.0 Hz, 1H), 4.14 (q, *J* = 7.1 Hz, 2H), 3.98 (s, 3H), 1.23 (t, *J* = 7.1 Hz, 3H). ¹³C{¹H} NMR (100 MHz, CDCl₃) δ 166.4 (2C), 143.9, 141.9, 134.0, 133.6, 130.9, 130.7, 129.9, 128.3 (2C), 124.7, 123.6, 122.1, 121.2, 120.5, 120.0, 103.1, 60.5, 52.4, 14.2. HRMS (ESI) calcd for C₂₁H₁₉NO₄ [M+Na]⁺ 372.1206, found 372.1206.

Ethyl (*E*)-3-(2-(1*H*-indol-7-yl)-5-methoxyphenyl)acrylate **7-3n**



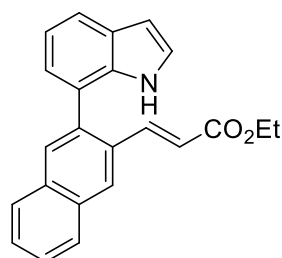
7-3n was obtained as yellow solid. 74 mg (77%) M.P.: 175-176°C. ¹H NMR (400 MHz, CDCl₃) δ 7.97 (s, 1H), 7.66 (dt, *J* = 8.0, 1.0 Hz, 1H), 7.55 (d, *J* = 16.0 Hz, 1H), 7.42 (d, *J* = 8.5 Hz, 1H), 7.28 (d, *J* = 2.7 Hz, 1H), 7.21 – 7.16 (m, 2H), 7.05 (dd, *J* = 8.5, 2.6 Hz, 1H), 7.01 (dd, *J* = 7.2, 1.1 Hz, 1H), 6.61 (dd, *J* = 3.2, 2.1 Hz, 1H), 6.39 (d, *J* = 16.0 Hz, 1H), 4.13 (q, *J* = 7.1 Hz, 2H), 3.90 (s, 3H), 1.21 (t, *J* = 7.1 Hz, 3H). ¹³C{¹H} NMR (100 MHz, CDCl₃) δ 166.6, 159.2, 143.0, 134.7, 134.3, 132.2, 131.8, 128.0, 124.4, 123.9, 122.8, 120.3, 119.9, 119.4, 116.6, 111.3, 103.0, 60.4, 55.5, 14.2. HRMS (ESI) calcd for C₂₀H₁₉NO₃ [M+Na]⁺ 344.1257, found 344.1257.

(*E*)-1-(2-(4-chloro-1*H*-indol-7-yl)phenyl)pent-1-en-3-one **7-3o**



7-3o was obtained as colorless solid. (77 mg, 79%) M.P.: 133-134°C. ¹H NMR (400 MHz, CDCl₃) δ 8.09 (s, 1H), 7.84 – 7.79 (m, 1H), 7.57 – 7.46 (m, 4H), 7.27 – 7.21 (m, 2H), 6.99 (d, *J* = 7.7 Hz, 1H), 6.75 (dd, *J* = 3.2, 2.2 Hz, 1H), 6.43 (d, *J* = 16.0 Hz, 1H), 4.17 (q, *J* = 7.1 Hz, 2H), 1.23 (t, *J* = 7.1 Hz, 3H). ¹³C{¹H} NMR (100 MHz, CDCl₃) δ 166.6, 142.5, 138.6, 135.0, 133.3, 130.6, 130.2, 128.4, 127.0, 126.8, 126.0, 125.1, 124.3, 121.8, 119.7, 119.6, 101.8, 60.5, 14.2. HRMS (ESI) calcd for C₁₉H₁₆ClNO₂ [M+H]⁺ 326.0942, found 326.0942.

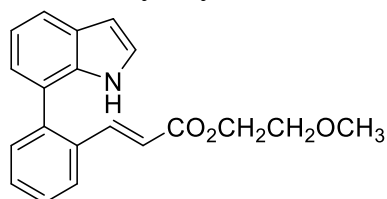
Ethyl (*E*)-3-(3-(1*H*-indol-7-yl)naphthalen-2-yl)acrylate **7-3p**



7-3p was obtained as colorless solid. (89 mg, 87%) M.P.: 120-121°C. ¹H NMR (400 MHz, CDCl₃) δ 8.28 (s, 1H), 8.04 (s, 1H), 7.97 (s, 1H), 7.94 (dd, *J* = 6.2, 3.4 Hz, 1H), 7.83 (dd, *J* = 6.2, 3.4 Hz, 1H), 7.71 (dt, *J* = 7.9, 0.9 Hz, 1H), 7.67 (d, *J* = 15.5 Hz, 1H), 7.58 – 7.53 (m, 2H), 7.24 (dd, *J* = 8.0, 7.2 Hz, 1H), 7.17 (dd, *J* =

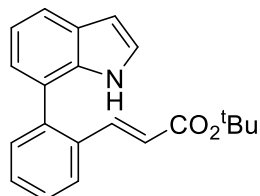
3.2, 2.5 Hz, 1H), 7.12 (dd, $J = 7.2, 1.1$ Hz, 1H), 6.64 (dd, $J = 3.2, 2.1$ Hz, 1H), 6.49 (d, $J = 16.0$ Hz, 1H), 4.13 (q, $J = 7.1$ Hz, 2H), 1.22 (t, $J = 7.1$ Hz, 3H). $^{13}\text{C}\{^1\text{H}\}$ NMR (100 MHz, CDCl_3) δ 166.6, 143.2, 136.5, 134.7, 133.9, 132.6, 131.8, 129.4, 128.3, 128.1, 127.6, 127.5, 127.1, 126.8, 124.5, 123.8, 123.0, 120.5, 120.0, 119.7, 103.0, 60.4, 14.2. HRMS (ESI) calcd for $\text{C}_{23}\text{H}_{19}\text{NO}_2$ $[\text{M}+\text{Na}]^+$ 364.1308, found 364.1314.

2-Methoxyethyl (*E*)-3-(2-(1*H*-indol-7-yl)phenyl)acrylate **7-3q**



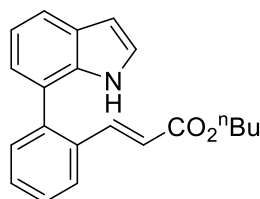
7-3q was obtained as colorless solid. (89 mg, 92%) M.P.: 85-86°C. ^1H NMR (400 MHz, CDCl_3) δ 8.01 (s, 1H), 7.84 – 7.80 (m, 1H), 7.70 (dt, $J = 8.0, 0.8$ Hz, 1H), 7.62 (d, $J = 16.0$ Hz, 1H), 7.55 – 7.45 (m, 3H), 7.24 – 7.17 (m, 2H), 7.06 (dd, $J = 7.2, 1.0$ Hz, 1H), 6.64 (dd, $J = 3.2, 2.1$ Hz, 1H), 6.49 (d, $J = 16.0$ Hz, 1H), 4.27 – 4.23 (m, 2H), 3.60 – 3.56 (m, 2H), 3.34 (s, 3H). $^{13}\text{C}\{^1\text{H}\}$ NMR (100 MHz, CDCl_3) δ 166.5, 143.4, 139.7, 134.4, 133.2, 130.7, 130.2, 128.1, 128.0, 126.9, 124.5, 123.7, 122.9, 120.6, 119.9, 118.8, 103.0, 70.4, 63.6, 59.0. HRMS (ESI) calcd for $\text{C}_{20}\text{H}_{19}\text{NO}_3$ $[\text{M}+\text{Na}]^+$ 344.1257, found 344.1257.

tert-Butyl (*E*)-3-(2-(1*H*-indol-7-yl)phenyl)acrylate **7-3r**



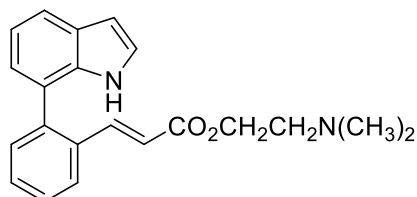
7-3r was obtained as colorless solid. (75 mg, 78%) M.P.: 132-133°C. ^1H NMR (400 MHz, CDCl_3) δ 7.97 (s, 1H), 7.80 (dd, $J = 7.4, 1.7$ Hz, 1H), 7.68 (dt, $J = 7.9, 0.9$ Hz, 1H), 7.52 – 7.41 (m, 4H), 7.21 (dd, $J = 7.9, 7.2$ Hz, 1H), 7.15 (dd, 1H), 7.06 (dd, $J = 7.2, 1.0$ Hz, 1H), 6.62 (dd, $J = 3.2, 2.1$ Hz, 1H), 6.35 (d, $J = 16.0$ Hz, 1H), 1.40 (s, 9H). $^{13}\text{C}\{^1\text{H}\}$ NMR (100 MHz, CDCl_3) δ 166.0, 141.8, 139.5, 134.4, 133.3, 130.6, 129.9, 128.0, 126.7, 124.4, 123.6, 123.0, 121.0, 120.5, 119.8, 102.9, 80.3, 28.0. HRMS (ESI) calcd for $\text{C}_{21}\text{H}_{21}\text{NO}_2$ $[\text{M}+\text{Na}]^+$ 342.1465, found 342.1465.

Butyl (*E*)-3-(2-(1*H*-indol-7-yl)phenyl)acrylate **7-3s**



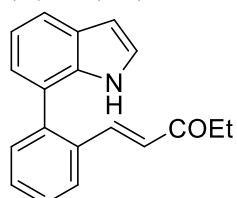
7-3s was obtained as colorless solid. (78 mg, 81%) M.P.: 94-95°C. ¹H NMR (400 MHz, CDCl₃) δ 8.02 (s, 1H), 7.83 – 7.77 (m, 1H), 7.69 (dt, *J* = 7.9, 1.0 Hz, 1H), 7.57 (d, *J* = 16.0 Hz, 1H), 7.52 – 7.42 (m, 3H), 7.20 (dd, *J* = 7.9, 7.2 Hz, 1H), 7.14 (dd, *J* = 3.2, 2.4 Hz, 1H), 7.05 (dd, *J* = 7.2, 1.0 Hz, 1H), 6.62 (dd, *J* = 3.2, 2.1 Hz, 1H), 6.40 (d, *J* = 16.0 Hz, 1H), 4.06 (t, *J* = 6.6 Hz, 2H), 1.59 – 1.51 (m, 2H), 1.34 – 1.24 (m, 2H), 0.90 (t, *J* = 7.4 Hz, 3H). ¹³C{¹H} NMR (100 MHz, CDCl₃) δ 166.7, 142.8, 139.6, 134.4, 133.2, 130.6 (2C), 130.1, 128.0, 126.8, 124.4, 123.6, 122.9, 120.5, 119.8, 119.2, 102.9, 64.2, 30.6, 19.1, 13.7. HRMS (ESI) calcd for C₂₁H₂₁NO₂ [M+H]⁺ 320.1645, found 320.1644.

2-(Dimethylamino)ethyl (*E*)-3-(2-(1*H*-indol-7-yl)phenyl)acrylate **7-3t**



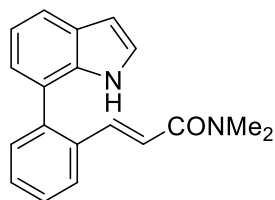
7-3t was obtained as colorless solid. (75 mg, 75%) M.P.: 95-96°C. ¹H NMR (400 MHz, CDCl₃) δ 7.98 (s, 1H), 7.79 (d, *J* = 7.2 Hz, 1H), 7.67 (d, *J* = 7.9 Hz, 1H), 7.56 (d, *J* = 16.0 Hz, 1H), 7.51 – 7.42 (m, 3H), 7.21 – 7.15 (m, 2H), 7.03 (d, *J* = 7.2 Hz, 1H), 6.61 (dd, *J* = 3.2, 2.1 Hz, 1H), 6.44 (d, *J* = 16.0 Hz, 1H), 4.17 (t, *J* = 5.6 Hz, 2H), 2.53 (t, *J* = 5.6 Hz, 2H), 2.21 (s, 6H). ¹³C{¹H} NMR (100 MHz, CDCl₃) δ 166.6, 143.2, 139.7, 134.5, 133.2, 130.7, 130.2, 128.2, 128.1, 126.9, 124.5, 123.7, 123.0, 120.6, 119.9, 119.0, 103.0, 62.2, 57.6, 45.5. HRMS (ESI) calcd for C₂₁H₂₂N₂O₂ [M+H]⁺ 335.1754, found 335.1754.

(*E*)-1-(2-(1*H*-indol-7-yl)phenyl)pent-1-en-3-one **7-3u**



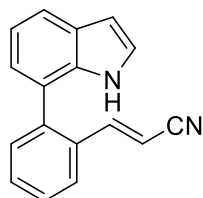
7-3u was obtained as yellow solid. (64 mg, 77%) M.P.: 125-126°C. ¹H NMR (400 MHz, CDCl₃) δ 8.02 (s, 1H), 7.80 (dd, *J* = 7.6, 1.7 Hz, 1H), 7.71 (dt, *J* = 7.9, 1.0 Hz, 1H), 7.54 – 7.44 (m, 3H), 7.39 (d, *J* = 16.5 Hz, 1H), 7.22 (dd, *J* = 7.9, 7.2 Hz, 1H), 7.19 – 7.15 (m, 1H), 7.06 (dd, *J* = 7.2, 1.0 Hz, 1H), 6.63 (dd, *J* = 3.2, 2.1 Hz, 1H), 6.64 (d, *J* = 16.5 Hz, 1H), 2.35 (s, 2H), 0.96 (t, *J* = 7.3 Hz, 3H). ¹³C{¹H} NMR (100 MHz, CDCl₃) δ 201.5, 141.1, 139.7, 134.4, 133.3, 130.7, 130.3, 128.2, 128.0, 127.7, 126.9, 124.5, 123.6, 123.0, 120.6, 119.9, 103.0, 32.5, 8.1. HRMS (ESI) calcd for C₁₉H₁₇NO [M+Na]⁺ 298.1202, found 298.1202.

(*E*)-3-(2-(1*H*-indol-7-yl)phenyl)-*N,N*-dimethylacrylamide **7-3v**



7-3v was obtained as colorless solid. (48 mg, 55%) M.P.: 183-184°C. ¹H NMR (400 MHz, CDCl₃) δ 8.12 (s, 1H), 7.70 – 7.66 (m, 1H), 7.64 (dt, *J* = 7.9, 1.0 Hz, 1H), 7.47 – 7.40 (m, 4H), 7.20 – 7.13 (m, 2H), 7.04 (dd, *J* = 7.2, 1.1 Hz, 1H), 6.58 (dd, *J* = 3.2, 2.1 Hz, 1H), 6.51 (d, *J* = 15.7 Hz, 1H), 2.89 (s, 3H), 2.80 (s, 3H). ¹³C{¹H} NMR (100 MHz, CDCl₃) δ 166.7, 140.0, 138.7, 134.2, 134.2, 131.0, 129.3, 128.2, 128.1, 127.9, 124.5, 123.9, 123.2, 120.3, 120.0, 119.7, 102.8, 37.1, 35.6. HRMS (ESI) calcd for C₁₉H₁₈N₂O [M+Na]⁺ 313.1311, found 313.1311.

(*E*)-3-(2-(1*H*-indol-7-yl)phenyl)acrylonitrile **7-3w**



7-3w was obtained as colorless solid. (47 mg, 64%) M.P.: 111-112°C. ¹H NMR (400 MHz, CDCl₃) δ 7.93 (s, 1H), 7.75 – 7.67 (m, 2H), 7.56 – 7.45 (m, 3H), 7.30 (d, *J* = 16.7 Hz, 1H), 7.25 – 7.17 (m, 2H), 7.01 (dd, *J* = 7.2, 0.9 Hz, 1H), 6.65 (dd, *J* = 3.2, 2.1 Hz, 1H), 5.83 (d, *J* = 16.7 Hz, 1H). ¹³C{¹H} NMR (100 MHz, CDCl₃) δ 149.0, 139.3, 134.3, 132.3, 131.1, 130.9, 128.3, 128.2, 126.0, 124.7, 123.6, 122.3, 120.9, 120.0, 118.1, 103.2, 96.9. HRMS (ESI) calcd for C₁₇H₁₂N₂ [M+Na]⁺ 267.0893, found 267.0891.

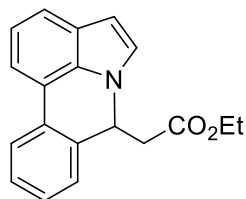
9.3.2. General Procedure for the aza-Michael reaction (condition B)

Under air atmosphere, compound **7-3** (0.2 mmol) and KO^tBu (0.06 mmol, 6.8 mg, 30 mol%) were dissolved in CH₂Cl₂ (2 mL), and the mixture was stirred at room temperature for 5 h. The mixture was diluted with 10 mL of CH₂Cl₂, filtered through a celite pad, and then washed with CH₂Cl₂. The organic phases were washed with saturated NH₄Cl solution (3×10 mL), dried over anhydrous Na₂SO₄. The organic solvent was removed under reduced pressure to furnish compounds which were identified as Pyrrolo[3,2,1-*de*]phenanthridines **7-(4a-4w)**.

9.3.3. General Procedure for the one pot synthesis of Pyrrolo[3,2,1-*de*]phenanthridines (condition C)

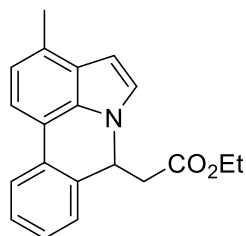
Under Ar atmosphere, 7-phenyl-1*H*-indoles **6-1** (0.3 mmol), alkenes **7-2** (0.75 mmol, 2.5 equiv.), [Cp**RhCl*₂]₂ (4.7 mg, 0.0075 mmol, 2.5 mol%), AgOAc (100.1 mg, 0.6 mmol, 2 equiv.), Me₄NOAc (3 mmol, 400 mg) and CH₃CN (2 mL) were placed in a 50 mL seal tube. The mixture was heated in oil bath at 80 °C for 24 h and then cooled to room temperature. The mixture was diluted with CH₂Cl₂ to 5 mL, filtered through a celite pad, and then washed with CH₂Cl₂. The volatiles were removed under reduced pressure, and the residue was subjected to silica gel column chromatography [eluting with petroleum ether/ethyl acetate] to afford the corresponding product **7-(4a-4w)**.

Ethyl 2-(7*H*-pyrrolo[3,2,1-*de*]phenanthridin-7-yl)acetate **7-4a**



7-4a was obtained as yellow solid. (58 mg, 100%) ¹H NMR (400 MHz, CDCl₃) δ 7.97 (dt, *J* = 7.7, 1.0 Hz, 1H), 7.58 (dd, *J* = 7.3, 0.8 Hz, 1H), 7.54 (dd, *J* = 7.9, 0.8 Hz, 1H), 7.42 – 7.37 (m, 1H), 7.33 – 7.28 (m, 2H), 7.25 (d, *J* = 3.1 Hz, 1H), 7.15 (dd, *J* = 7.9, 7.4 Hz, 1H), 6.55 (d, *J* = 3.1 Hz, 1H), 6.14 (dd, *J* = 7.3, 5.2 Hz, 1H), 4.10 (q, *J* = 7.1 Hz, 2H), 2.82 – 2.71 (m, 2H), 1.16 (t, *J* = 7.1 Hz, 3H). ¹³C{¹H} NMR (100 MHz, CDCl₃) δ 170.7, 133.6, 132.8, 129.9, 128.2, 127.83, 127.5, 126.7, 126.0, 122.8, 120.8, 120.6, 118.0, 113.7, 103.3, 60.9, 55.3, 46.4, 14.0. HRMS (ESI) calcd for C₁₉H₁₇NO₂ [M+H]⁺ 292.1332, found 292.1337.

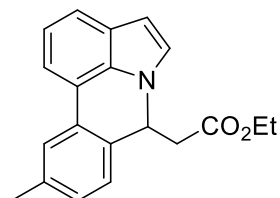
Ethyl 2-(3-methyl-7*H*-pyrrolo[3,2,1-*de*]phenanthridin-7-yl)acetate **7-4b**



7-4b was obtained as yellow oil. (57 mg, 93%) ¹H NMR (400 MHz, CDCl₃) δ 7.93 (d, *J* = 7.7 Hz, 1H), 7.50 (d, *J* = 7.4 Hz, 1H), 7.40 – 7.35 (m, 1H), 7.32 – 7.23 (m, 3H), 6.95 (d, *J* = 7.4 Hz, 1H), 6.57 (d, *J* = 3.1 Hz, 1H), 6.13 (dd, *J* = 7.4, 5.1 Hz, 1H), 4.18 – 4.06 (m, 2H), 2.82 – 2.71 (m, 2H), 2.57 (s, 3H), 1.18 (t, *J* = 7.1 Hz, 3H). ¹³C{¹H} NMR (100 MHz, CDCl₃) δ 170.7, 133.1, 132.5, 130.9, 130.1, 128.1,

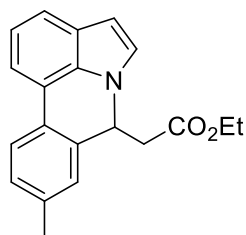
127.4, 126.6, 125.4, 122.5, 120.7, 115.8, 114.1, 104.9, 101.9, 60.9, 55.4, 46.3, 18.7, 14.0. HRMS (ESI) calcd for C₂₀H₁₉NO₂ [M+Na]⁺ 328.1308, found 328.1307.

Ethyl 2-(10-methyl-7*H*-pyrrolo[3,2,1-*de*]phenanthridin-7-yl)acetate **7-4c**



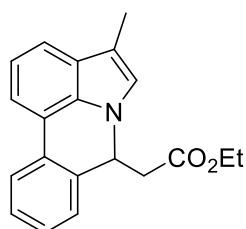
7-4c was obtained as yellow oil. (56 mg, 92%) ¹H NMR (400 MHz, CDCl₃) δ 7.77 (s, 1H), 7.57 (d, *J* = 7.3 Hz, 1H), 7.52 (d, *J* = 7.8 Hz, 1H), 7.23 (d, *J* = 3.2 Hz, 1H), 7.20 (d, *J* = 7.8 Hz, 1H), 7.16 – 7.09 (m, 2H), 6.54 (d, *J* = 3.2 Hz, 1H), 6.10 (dd, *J* = 7.1, 5.3 Hz, 1H), 4.16 – 4.04 (m, 2H), 2.80 – 2.69 (m, 2H), 2.43 (s, 3H), 1.16 (t, *J* = 7.1 Hz, 3H). ¹³C{¹H} NMR (100 MHz, CDCl₃) δ 170.7, 137.8, 132.9, 130.8, 129.6, 128.7, 127.3, 126.6, 126.0, 123.3, 120.6, 120.5, 118.1, 113.6, 103.2, 60.9, 55.1, 46.5, 21.3, 14.0. HRMS (ESI) calcd for C₂₀H₁₉NO₂ [M+Na]⁺ 328.1308, found 328.1307.

Ethyl 2-(9-methyl-7*H*-pyrrolo[3,2,1-*de*]phenanthridin-7-yl)acetate **7-4d**



7-4d was obtained as yellow solid. (55 mg, 90%) ¹H NMR (400 MHz, CDCl₃) δ 7.85 (d, *J* = 8.0 Hz, 1H), 7.54 (d, *J* = 7.3 Hz, 1H), 7.50 (dd, *J* = 8.0, 0.9 Hz, 1H), 7.23 (d, *J* = 3.1 Hz, 1H), 7.20 (dd, *J* = 8.0, 1.2 Hz, 1H), 7.15 – 7.11 (m, 2H), 6.53 (d, *J* = 3.1 Hz, 1H), 6.10 – 6.06 (m, 1H), 4.15 – 4.07 (m, 2H), 2.78 – 2.74 (m, 2H), 2.38 (s, 3H), 1.16 (t, *J* = 7.2 Hz, 3H). ¹³C{¹H} NMR (100 MHz, CDCl₃) δ 170.7, 137.7, 133.5, 132.6, 129.0, 127.9, 127.0, 126.5, 125.9, 122.6, 120.5, 120.2, 118.1, 113.3, 103.2, 60.8, 55.3, 46.4, 21.2, 13.9. HRMS (ESI) calcd for C₂₀H₁₉NO₂ [M+Na]⁺ 328.1308, found 328.1307.

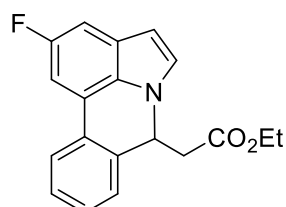
Ethyl 2-(4-methyl-7*H*-pyrrolo[3,2,1-*de*]phenanthridin-7-yl)acetate **7-4e**



7-4e was obtained as yellow oil. (53 mg, 87%) ¹H NMR (400 MHz, CDCl₃) δ 7.95 (d, *J* = 7.8 Hz, 1H), 7.56 (d, *J* = 7.3 Hz, 1H), 7.47 (dd, *J* = 7.9, 0.7 Hz, 1H), 7.40

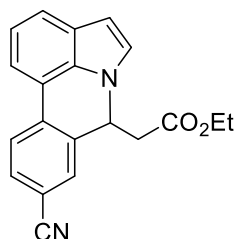
– 7.35 (m, 1H), 7.32 – 7.27 (m, 2H), 7.14 (dd, $J = 7.9, 7.3$ Hz, 1H), 7.01 – 6.95 (m, 1H), 6.05 (dd, $J = 7.2, 5.3$ Hz, 1H), 4.18 – 4.03 (m, 2H), 2.77 – 2.66 (m, 2H), 2.34 (s, 3H), 1.16 (t, $J = 7.1$ Hz, 3H). $^{13}\text{C}\{^1\text{H}\}$ NMR (100 MHz, CDCl_3) δ 170.8, 133.8, 133.3, 130.0, 128.1, 127.7, 127.5, 127.2, 123.6, 122.7, 119.9, 119.0, 117.8, 113.7, 113.1, 60.8, 55.2, 46.1, 14.0, 10.0. HRMS (ESI) calcd for $\text{C}_{20}\text{H}_{19}\text{NO}_2$ $[\text{M}+\text{Na}]^+$ 328.1308, found 328.1307.

Ethyl 2-(2-fluoro-7*H*-pyrrolo[3,2,1-*de*]phenanthridin-7-yl)acetate **7-4i**



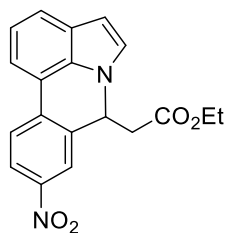
7-4i was obtained as yellow oil. (57 mg, 93%) ^1H NMR (400 MHz, CDCl_3) δ 7.87 (d, $J = 7.8$ Hz, 1H), 7.43 – 7.38 (m, 1H), 7.36 – 7.27 (m, 4H), 7.18 (dd, $J = 9.7, 2.1$ Hz, 1H), 6.50 (d, $J = 3.1$ Hz, 1H), 6.10 (d, $J = 6.3$ Hz, 1H), 4.14 – 4.05 (m, 2H), 2.78 – 2.73 (m, 2H), 1.16 (t, $J = 7.1$ Hz, 3H). $^{13}\text{C}\{^1\text{H}\}$ NMR (100 MHz, CDCl_3) δ 170.5, 157.2 (d, $^1\text{JC-F} = 233.5$ Hz), 134.0, 129.4, 129.1 (d, $^3\text{JC-F} = 2.0$ Hz), 128.4 (d, $^2\text{JC-F} = 11.9$ Hz), 127.4 (d, $^2\text{JC-F} = 9.0$ Hz), 126.6, 126.5, 123.1, 118.7, 118.6, 105.7, 105.4, 103.3 (d, $^3\text{JC-F} = 5.0$ Hz), 102.7, 102.4, 61.0, 55.3, 46.3, 14.0. ^{19}F NMR (376 MHz, CDCl_3) δ -123.46 (t, $J = 7.5$ Hz). HRMS (ESI) calcd for $\text{C}_{19}\text{H}_{16}\text{FNO}_2$ $[\text{M}+\text{Na}]^+$ 332.1057, found 332.1056.

Ethyl 2-(9-cyano-7*H*-pyrrolo[3,2,1-*de*]phenanthridin-7-yl)acetate **7-4j**



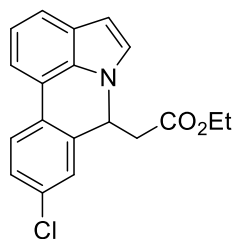
7-4j was obtained as yellow solid. (59 mg, 93%) ^1H NMR (400 MHz, CDCl_3) δ 8.00 (d, $J = 8.2$ Hz, 1H), 7.65 (dd, $J = 8.0, 1.7$ Hz, 1H), 7.63 – 7.58 (m, 3H), 7.25 (d, $J = 3.2$ Hz, 1H), 7.18 (dd, $J = 8.0, 7.4$ Hz, 1H), 6.59 (d, $J = 3.2$ Hz, 1H), 6.11 (dd, $J = 7.2, 5.1$ Hz, 1H), 4.10 (qd, $J = 7.1, 0.8$ Hz, 2H), 2.82 – 2.69 (m, 2H), 1.16 (t, $J = 7.1$ Hz, 3H). $^{13}\text{C}\{^1\text{H}\}$ NMR (100 MHz, CDCl_3) δ 169.9, 134.8, 134.3, 133.1, 131.8, 131.2, 127.0, 126.2, 123.3, 122.8, 120.9, 118.6, 116.1, 115.2, 110.9, 104.0, 61.2, 55.0, 46.0, 14.0. HRMS (ESI) calcd for $\text{C}_{20}\text{H}_{16}\text{N}_2\text{O}_2$ $[\text{M}+\text{H}]^+$ 317.1285, found 317.1285.

Ethyl 2-(9-nitro-7*H*-pyrrolo[3,2,1-*de*]phenanthridin-7-yl)acetate **7-4k**



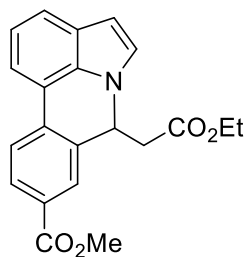
7-4k was obtained as yellow oil. (62 mg, 92%) ^1H NMR (400 MHz, CDCl_3) δ 8.18 (dd, $J = 8.6, 2.3$ Hz, 1H), 8.12 (dt, $J = 2.5, 0.5$ Hz, 1H), 7.98 (d, $J = 8.6$ Hz, 1H), 7.62 (dd, $J = 7.9, 0.8$ Hz, 1H), 7.58 (dd, $J = 7.5, 0.7$ Hz, 1H), 7.25 (d, $J = 3.2$ Hz, 1H), 7.17 (dd, $J = 7.9, 7.5$ Hz, 1H), 6.59 (d, $J = 3.2$ Hz, 1H), 6.10 (dd, $J = 7.2, 5.1$ Hz, 1H), 4.15 – 4.03 (m, 2H), 2.84 – 2.72 (m, 2H), 1.15 (t, $J = 7.2$ Hz, 3H). $^{13}\text{C}\{^1\text{H}\}$ NMR (100 MHz, CDCl_3) δ 169.8, 146.7, 136.6, 134.4, 133.2, 127.0, 126.3, 123.4, 123.2, 122.9, 120.9, 115.8, 115.6, 104.0, 61.2, 55.1, 46.0, 13.9. HRMS (ESI) calcd for $\text{C}_{19}\text{H}_{16}\text{N}_2\text{O}_4$ $[\text{M}+\text{H}]^+$ 337.1183, found 337.1183.

Ethyl 2-(9-chloro-7*H*-pyrrolo[3,2,1-*de*]phenanthridin-7-yl)acetate **7-4l**



7-4l was obtained as yellow oil. (59 mg, 91%) ^1H NMR (400 MHz, CDCl_3) δ 7.83 (d, $J = 8.4$ Hz, 1H), 7.55 (dd, $J = 7.9, 0.8$ Hz, 1H), 7.51 (d, $J = 7.3$ Hz, 1H), 7.33 (dd, $J = 8.4, 2.2$ Hz, 1H), 7.27 (d, $J = 2.2$ Hz, 1H), 7.22 (d, $J = 3.1$ Hz, 1H), 7.15 (dd, $J = 7.9, 7.3$ Hz, 1H), 6.57 (d, $J = 3.2$ Hz, 1H), 6.03 (dd, $J = 7.2, 5.3$ Hz, 1H), 4.11 (q, $J = 7.1$ Hz, 2H), 2.80 – 2.69 (m, 2H), 1.17 (t, $J = 7.2$ Hz, 3H). $^{13}\text{C}\{^1\text{H}\}$ NMR (100 MHz, CDCl_3) δ 170.3, 135.1, 133.2, 132.6, 128.6, 128.3, 127.4, 126.7, 126.0, 124.0, 121.1, 120.7, 117.0, 113.8, 103.5, 61.0, 55.0, 46.1, 14.0. HRMS (ESI) calcd for $\text{C}_{19}\text{H}_{16}\text{ClNO}_2$ $[\text{M}+\text{Na}]^+$ 348.0762, found 348.0761.

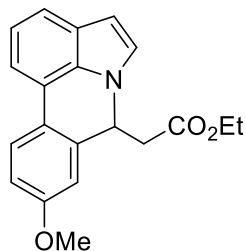
Methyl 7-(2-ethoxy-2-oxoethyl)-7*H*-pyrrolo[3,2,1-*de*]phenanthridine-9-carboxylate **7-4m**



7-4m was obtained as yellow oil. (47 mg, 72%) ^1H NMR (400 MHz, DMSO) δ 8.18 (d, $J = 8.2$ Hz, 1H), 8.02 (d, $J = 1.7$ Hz, 1H), 7.96 (dd, $J = 8.2, 1.7$ Hz, 1H), 7.72 (d, $J = 7.4$ Hz, 1H), 7.56 – 7.51 (m, 3H), 7.10 (t, $J = 7.6$ Hz, 1H), 6.56 (d, $J = 3.1$

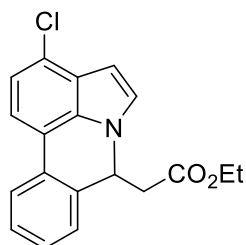
Hz, 1H), 6.23 (t, $J = 5.5$ Hz, 1H), 3.88 (s, 3H), 3.83 – 3.74 (m, 2H), 3.00 – 2.87 (m, 2H), 0.86 (t, $J = 7.1$ Hz, 3H). $^{13}\text{C}\{^1\text{H}\}$ NMR (100 MHz, DMSO) δ 170.3, 166.7, 135.2, 134.6, 133.8, 129.8, 129.5, 127.8, 127.1, 123.8, 122.7, 121.3, 117.5, 115.7, 103.8, 61.0, 55.3, 53.1, 46.1, 14.4. HRMS (ESI) calcd for $\text{C}_{21}\text{H}_{19}\text{NO}_4$ $[\text{M}+\text{Na}]^+$ 372.1206, found 372.1206.

Ethyl 2-(9-methoxy-7*H*-pyrrolo[3,2,1-*de*]phenanthridin-7-yl)acetate **7-4n**



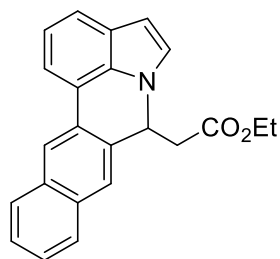
7-4n was obtained as yellow oil. (61 mg, 95%) ^1H NMR (400 MHz, DMSO) δ 7.96 (d, $J = 8.6$ Hz, 1H), 7.52 (d, $J = 7.3$ Hz, 1H), 7.42 (dd, $J = 3.1, 1.3$ Hz, 1H), 7.39 (dt, $J = 8.1, 1.0$ Hz, 1H), 7.07 – 6.96 (m, 3H), 6.50 (dd, $J = 3.2, 1.5$ Hz, 1H), 6.12 – 6.05 (m, 1H), 3.90 – 3.81 (m, 5H), 2.97 (ddd, $J = 15.6, 4.8, 1.3$ Hz, 1H), 2.83 (ddd, $J = 15.6, 6.6, 1.3$ Hz, 1H), 0.92 (td, $J = 7.0, 1.3$ Hz, 3H). $^{13}\text{C}\{^1\text{H}\}$ NMR (100 MHz, DMSO) δ 170.6, 160.0, 135.9, 132.9, 127.3, 126.7, 124.9, 123.0, 121.3, 120.2, 118.7, 115.0, 113.9, 113.6, 103.6, 61.0, 56.2, 55.5, 46.2, 14.6. HRMS (ESI) calcd for $\text{C}_{20}\text{H}_{19}\text{NO}_3$ $[\text{M}+\text{Na}]^+$ 344.1257, found 344.1256.

1-(3-chloro-7*H*-pyrrolo[3,2,1-*de*]phenanthridin-7-yl)butan-2-one **7-4o**



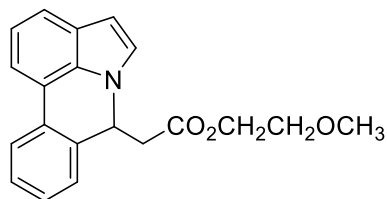
7-4o was obtained as yellow oil. (61 mg, 93%) ^1H NMR (400 MHz, CDCl_3) δ 7.91 (d, $J = 7.8$ Hz, 1H), 7.48 (d, $J = 7.8$ Hz, 1H), 7.41 – 7.37 (m, 1H), 7.33 – 7.29 (m, 2H), 7.28 (d, $J = 3.2$ Hz, 1H), 7.12 (d, $J = 7.8$ Hz, 1H), 6.62 (d, $J = 3.2$ Hz, 1H), 6.12 (t, $J = 6.2$ Hz, 1H), 4.14 – 4.06 (m, 2H), 2.76 (d, $J = 6.3$ Hz, 2H), 1.16 (t, $J = 7.2$ Hz, 3H). $^{13}\text{C}\{^1\text{H}\}$ NMR (100 MHz, CDCl_3) δ 170.5, 133.2, 129.2, 128.5, 128.4, 128.1, 127.5, 126.6, 125.8, 125.4, 122.8, 120.4, 116.9, 114.7, 102.0, 61.0, 55.5, 46.3, 14.0. HRMS (ESI) calcd for $\text{C}_{19}\text{H}_{16}\text{ClNO}_2$ $[\text{M}+\text{H}]^+$ 326.0942, found 326.0936.

Ethyl 2-(7*H*-benzo[*j*]pyrrolo[3,2,1-*de*]phenanthridin-7-yl)acetate **7-4p**



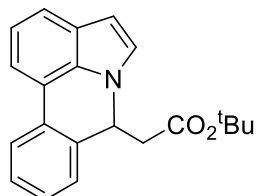
7-4p was obtained as yellow solid. (62 mg, 91%) ^1H NMR (400 MHz, CDCl_3) δ 8.41 (s, 1H), 7.90 (d, $J = 7.6$ Hz, 1H), 7.83 – 7.76 (m, 3H), 7.58 (d, $J = 7.7$ Hz, 1H), 7.52 – 7.44 (m, 2H), 7.31 – 7.19 (m, 2H), 6.59 (s, 1H), 6.27 (t, $J = 6.1$ Hz, 1H), 4.14 – 4.04 (m, 2H), 2.81 (d, $J = 5.5$ Hz, 2H), 1.13 (t, $J = 7.1$ Hz, 3H). $^{13}\text{C}\{^1\text{H}\}$ NMR (100 MHz, CDCl_3) δ 170.6, 133.2, 133.1, 132.8, 132.5, 128.0, 127.7, 127.6, 127.1, 126.6, 126.4, 126.2, 121.4, 120.8, 120.7, 118.0, 114.1, 103.4, 60.9, 55.4, 46.6, 14.0. HRMS (ESI) calcd for $\text{C}_{23}\text{H}_{19}\text{NO}_2$ $[\text{M}+\text{Na}]^+$ 364.1308, found 364.1310.

2-Methoxyethyl 2-(7*H*-pyrrolo[3,2,1-*de*]phenanthridin-7-yl)acetate **7-4q**



7-4q was obtained as yellow oil. (58 mg, 90%) ^1H NMR (400 MHz, CDCl_3) δ 7.99 (d, $J = 7.7$ Hz, 1H), 7.61 (d, $J = 7.3$ Hz, 1H), 7.57 (dd, $J = 7.9, 0.7$ Hz, 1H), 7.44 – 7.39 (m, 1H), 7.35 – 7.32 (m, 2H), 7.30 (d, $J = 3.1$ Hz, 1H), 7.18 (dd, $J = 7.9, 7.3$ Hz, 1H), 6.58 (d, $J = 3.1$ Hz, 1H), 6.17 (dd, $J = 7.2, 5.2$ Hz, 1H), 4.26 – 4.22 (m, 2H), 3.54 – 3.50 (m, 2H), 3.36 (s, 3H), 2.90 – 2.79 (m, 2H). $^{13}\text{C}\{^1\text{H}\}$ NMR (100 MHz, CDCl_3) δ 170.6, 133.4, 132.8, 129.9, 128.2, 127.8, 127.4, 126.7, 126.1, 122.7, 120.7, 120.6, 117.9, 113.7, 103.3, 70.1, 63.9, 58.9, 55.2, 46.2. HRMS (ESI) calcd for $\text{C}_{20}\text{H}_{19}\text{NO}_3$ $[\text{M}+\text{Na}]^+$ 344.1257, found 344.1257.

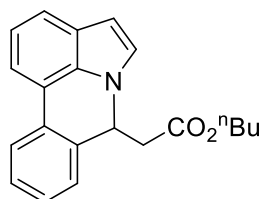
tert-Butyl 2-(7*H*-pyrrolo[3,2,1-*de*]phenanthridin-7-yl)acetate **7-4r**



7-4r was obtained as yellow oil. (56 mg, 88%) ^1H NMR (400 MHz, CDCl_3) δ 7.96 (dd, $J = 7.4, 1.0$ Hz, 1H), 7.58 (d, $J = 7.3$ Hz, 1H), 7.54 (dd, $J = 7.9, 1.0$ Hz, 1H), 7.41 – 7.36 (m, 1H), 7.33 – 7.28 (m, 3H), 7.15 (dd, $J = 7.9, 7.3$ Hz, 1H), 6.56 (d, $J = 3.2$ Hz, 1H), 6.11 (dd, $J = 6.7, 5.4$ Hz, 1H), 2.75 – 2.71 (m, 2H), 1.34 (s, 9H). $^{13}\text{C}\{^1\text{H}\}$ NMR (100 MHz, CDCl_3) δ 169.9, 133.7, 132.8, 129.9, 128.1, 127.8,

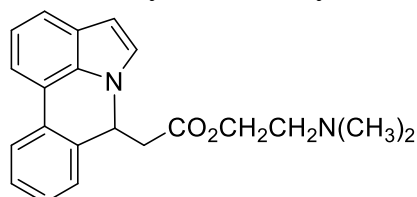
127.5, 126.6, 126.1, 122.6, 120.6, 120.5, 118.0, 113.6, 103.0, 81.2, 55.3, 47.5, 27.8. HRMS (ESI) calcd for C₂₁H₂₁NO₂ [M+Na]⁺ 342.1465, found 342.1465.

Butyl 2-(7*H*-pyrrolo[3,2,1-*de*]phenanthridin-7-yl)acetate **7-4s**



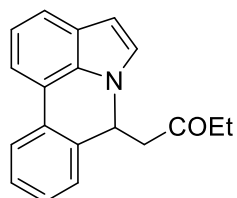
7-4s was obtained as yellow oil. (57mg, 89%) ¹H NMR (400 MHz, CDCl₃) δ 7.97 (d, *J* = 7.8 Hz, 1H), 7.59 (d, *J* = 7.3 Hz, 1H), 7.56 (dd, *J* = 7.8, 0.8 Hz, 1H), 7.42 – 7.36 (m, 1H), 7.33 – 7.25 (m, 3H), 7.20 – 7.15 (m, 1H), 6.57 (d, *J* = 3.1 Hz, 1H), 6.14 (dd, *J* = 7.3, 5.1 Hz, 1H), 4.12 – 4.01 (m, 2H), 2.84 – 2.73 (m, 2H), 1.55 – 1.47 (m, 2H), 1.33 – 1.23 (m, 2H), 0.90 (t, *J* = 7.4 Hz, 3H). ¹³C{¹H} NMR (100 MHz, CDCl₃) δ 170.8, 133.5, 132.7, 129.8, 128.1, 127.8, 127.4, 126.6, 126.0, 122.7, 120.7, 120.6, 117.9, 113.7, 103.3, 64.8, 55.3, 46.3, 30.4, 19.0, 13.6. HRMS (ESI) calcd for C₂₁H₂₁NO₂ [M+H]⁺ 320.1645, found 320.1645.

2-(Dimethylamino)ethyl 2-(7*H*-pyrrolo[3,2,1-*de*]phenanthridin-7-yl)acetate **7-4t**



7-4t was obtained as yellow oil. (60 mg, 90%) ¹H NMR (400 MHz, CDCl₃) δ 7.96 (d, *J* = 7.7 Hz, 1H), 7.58 (d, *J* = 7.3 Hz, 1H), 7.54 (dd, *J* = 7.9, 0.7 Hz, 1H), 7.41 – 7.36 (m, 1H), 7.33 – 7.27 (m, 3H), 7.15 (dd, *J* = 7.9, 7.3 Hz, 1H), 6.55 (d, *J* = 3.1 Hz, 1H), 6.13 (dd, *J* = 7.2, 5.3 Hz, 1H), 4.14 (t, *J* = 5.8 Hz, 2H), 2.86 – 2.75 (m, 2H), 2.47 – 2.42 (m, 2H), 2.22 (s, 6H). ¹³C{¹H} NMR (100 MHz, CDCl₃) δ 170.7, 133.5, 132.8, 129.9, 128.2, 127.8, 127.4, 126.7, 126.1, 122.7, 120.7, 120.6, 117.9, 113.7, 103.3, 62.6, 57.4, 55.3, 46.2, 45.6. HRMS (ESI) calcd for C₂₁H₂₂N₂O₂ [M+H]⁺ 335.1754, found 335.1754.

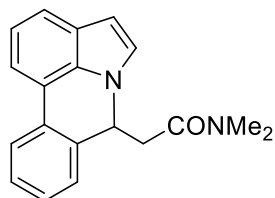
1-(7*H*-pyrrolo[3,2,1-*de*]phenanthridin-7-yl)butan-2-one **7-4u**



7-4u was obtained as yellow oil. (40 mg, 72%) ¹H NMR (400 MHz, CDCl₃) δ 7.95 (dd, *J* = 8.0, 1.1 Hz, 1H), 7.58 (d, *J* = 7.3 Hz, 1H), 7.53 (dd, *J* = 7.9, 0.8 Hz, 1H), 7.41 – 7.35 (m, 1H), 7.31 – 7.23 (m, 2H), 7.21 – 7.09 (m, 2H), 6.51 (d, *J* = 3.1 Hz, 1H), 6.23 (dd, *J* = 8.2, 4.0 Hz, 1H), 2.96 (dd, *J* = 17.0, 8.2 Hz, 1H), 2.75 (dd, *J* = 17.0, 4.0 Hz, 1H), 2.29 – 2.11 (m, 2H), 0.98 (t, *J* = 7.3 Hz, 3H). ¹³C{¹H} NMR

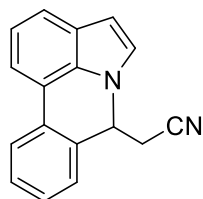
(100 MHz, CDCl₃) δ 208.9, 134.3, 132.7, 129.8, 128.0, 127.9, 127.4, 126.7, 126.5, 122.7, 120.7, 120.6, 118.1, 113.7, 103.1, 53.8, 37.2, 7.50. HRMS (ESI) calcd for C₁₉H₁₇NO [M+Na]⁺ 298.1202, found 298.1205.

N,N-dimethyl-2-(7*H*-pyrrolo[3,2,1-*de*]phenanthridin-7-yl)acetamide **7-4v**



7-4v was obtained as yellow oil. (51 mg, 87%) ¹H NMR (400 MHz, CDCl₃) δ 7.98 (dd, *J* = 7.7, 1.0 Hz, 1H), 7.60 (d, *J* = 7.3 Hz, 1H), 7.56 (dd, *J* = 7.9, 0.7 Hz, 1H), 7.43 – 7.36 (m, 2H), 7.35 – 7.29 (m, 2H), 7.17 (dd, 1H), 6.55 (d, *J* = 3.1 Hz, 1H), 6.27 (dd, *J* = 8.4, 4.4 Hz, 1H), 2.97 (s, 3H), 2.85 (dd, *J* = 15.1, 8.5 Hz, 1H), 2.65 (dd, *J* = 15.1, 4.4 Hz, 1H), 2.49 (s, 3H). ¹³C{¹H} NMR (100 MHz, CDCl₃) δ 169.6, 134.4, 132.6, 129.8, 128.0, 127.8, 127.7, 126.8, 126.7, 122.6, 120.7, 120.5, 118.1, 113.5, 102.7, 55.8, 44.8, 37.1, 35.6. HRMS (ESI) calcd for C₁₉H₁₈N₂O [M+Na]⁺ 313.1311, found 313.1311.

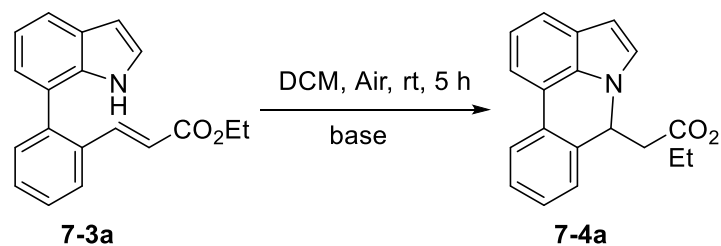
2-(7*H*-pyrrolo[3,2,1-*de*]phenanthridin-7-yl)acetonitrile **7-4w**



7-4w was obtained as white solid. (42 mg, 86%) ¹H NMR (400 MHz, CDCl₃) δ 8.00 (d, *J* = 7.8 Hz, 1H), 7.60 (dd, *J* = 15.7, 7.6 Hz, 2H), 7.48 – 7.43 (m, 1H), 7.37 (t, *J* = 2.9 Hz, 3H), 7.20 (t, *J* = 7.6 Hz, 1H), 6.66 (d, *J* = 3.1 Hz, 1H), 5.89 (t, *J* = 6.1 Hz, 1H), 2.74 (d, *J* = 5.7 Hz, 2H). ¹³C{¹H} NMR (100 MHz, CDCl₃) δ 132.5, 131.0, 129.8, 129.1, 128.1, 127.7, 126.9, 125.5, 123.1, 121.3, 121.2, 117.4, 116.7, 114.4, 104.6, 55.2, 29.2. HRMS (ESI) calcd for C₁₇H₁₂N₂ [M+Na]⁺ 267.0893, found 267.0894.

9.3.5. Optimization of the intramolecular aza-Michael addition of (*E*)-ethyl 3-(2-(1*H*-indol-7-yl)phenyl)acrylate **7-3a**

Table S7-2. Optimization results of the intramolecular aza-Michael addition ^a



entry	base (equiv.)	Yield 7-4a ^b (%)
1	KOH (0.3)	-
2	KO ^t Bu (0.3)	100
3	DMAP (0.3)	-
4	Et ₃ N (0.3)	-
5	Piperidine (0.3)	-
6	2,3-Dimethylquinoline (0.3)	-
7	ⁿ Bu ₄ NOAc (10)	-
8	Me ₄ NOAc (10)	-
9 ^c	Me ₄ NOAc (10)	-
10	ⁿ Bu ₄ NBF ₄ (10)	-
11	KPF ₆ (10)	-
12	KOAc (10)	-
13	NaOAc (10)	-
14	CsOAc (10)	-
15	LiOAc (10)	-

^aConditions: **7-3a** (0.2 mmol), base, DCM (1.5 mL), Air, 5 h.

^bIsolate yield.

^c1.5 mL MeCN

9.3.6. Single Crystal X-ray Structure Determination.

The detailed crystallographic data and structure refinement parameters for these compounds are summarized in **Tables S7-3** and **S7-4**. CCDC 1943455 and 1943456

contain the supplementary crystallographic data for this paper. These data can be obtained free of charge from The Cambridge Crystallographic Data Centre via www.ccdc.cam.ac.uk/data_request/cif.

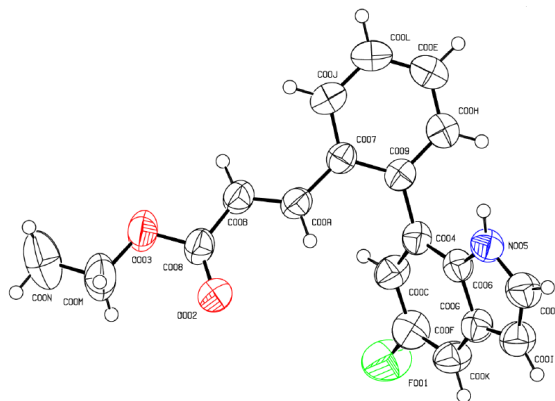


Table S7-3. 7-3i (CCDC 1943455)

Identification code	Y-117
Empirical formula	C ₁₉ H ₁₆ FNO ₂
Formula weight	309.33
Temperature/K	294.50(10)
Crystal system	orthorhombic
Space group	Fdd2
a/Å	9.0639(3)
b/Å	37.0554(13)
c/Å	19.0348(9)
α/°	90
β/°	90
γ/°	90
Volume/Å ³	6393.2(4)
Z	16
ρ _{calc} /cm ³	1.286
μ/mm ⁻¹	0.750
F(000)	2592.0
Radiation	CuKα (λ = 1.54184)
2θ range for data collection/°	9.548 to 145.422
Index ranges	-8 ≤ h ≤ 11, -45 ≤ k ≤ 34, -23 ≤ l ≤ 20
Reflections collected	8640
Independent reflections	2807 [R _{int} = 0.0226, R _{sigma} = 0.0182]
Data/restraints/parameters	2807/1/209
Goodness-of-fit on F ²	1.068
Final R indexes [I ≥ 2σ (I)]	R ₁ = 0.0482, wR ₂ = 0.1273
Final R indexes [all data]	R ₁ = 0.0540, wR ₂ = 0.1336
Largest diff. peak/hole / e Å ⁻³	0.23/-0.17

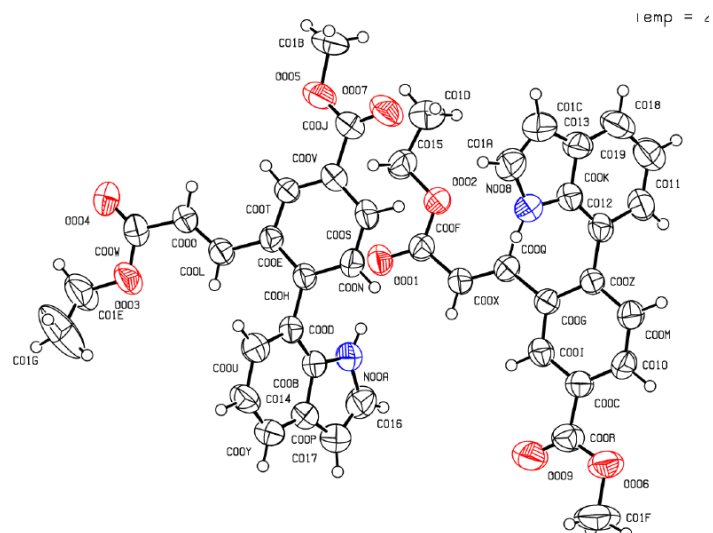


Table S7-4. 7-3m (CCDC 1943456)

Identification code	Y-I_164
Empirical formula	2(C ₂₁ H ₁₉ N ₄ O ₄)
Formula weight	698.74
Temperature/K	295.42(10)
Crystal system	monoclinic
Space group	P2 ₁ /n
a/Å	10.7100(8)
b/Å	13.5614(18)
c/Å	12.7131(8)
α/°	90
β/°	98.322(7)
γ/°	90
Volume/Å ³	1827.0(3)
Z	2
ρ _{calc} /cm ³	1.270
μ/mm ⁻¹	0.720
F(000)	736.0
Radiation	CuKα (λ = 1.54184)
2θ range for data collection/°	7.028 to 145.174
Index ranges	-8 ≤ h ≤ 13, -12 ≤ k ≤ 16, -15 ≤ l ≤ 14
Reflections collected	8673
Independent reflections	5544 [R _{int} = 0.0496, R _{sigma} = 0.0685]
Data/restraints/parameters	5544/1/473
Goodness-of-fit on F ²	1.017
Final R indexes [I >= 2σ (I)]	R ₁ = 0.0582, wR ₂ = 0.1264
Final R indexes [all data]	R ₁ = 0.1065, wR ₂ = 0.1598
Largest diff. peak/hole / e Å ⁻³	0.17/-0.21

9.4. Supporting information of Chapter 8

9.4.1. General Remarks

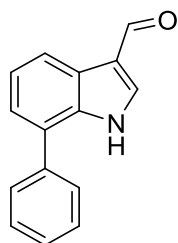
The alkynes **8-(2a-2n)** were prepared according to previously described methods ^[5], and **8-2o** was obtained from commercial source. The conventional reoxidation strategy ($[\text{Cp}^*\text{RhCl}_2]_2/\text{Ag}_2\text{CO}_3$) were carried out under Air using standard schlenk techniques. The electrooxidative rhodium-catalyzed C-H/N-H annulation reactions were performed in undivided electrochemical cells (10 mL), with Platinum electrodes (10 mm × 15 mm × 0.25 mm, 99.9%; obtained from ChemPur® Karlsruhe, Germany) as cathode and graphite felt (GF) electrodes (10 mm × 15 mm × 6 mm, SIGRACELL® GFA 6 EA, obtained from SGL Carbon, Wiesbaden, Germany) as anode, connected using stainless steel adapters. Electrocatalysis was conducted using an Bufan SS-L303SPD potentiostat in constant current mode. CV measurements were conducted with a Chenhua Autolab CHI660C potentiostat and CHI660E electrochemical software.

9.4.2. Procedure for synthesis of 7-phenyl-1*H*-indole-3-carbaldehydes **8-1**.

Under argon atmosphere, 7-phenyl-1*H*-indole (1 mmol, 1.0 equiv.) in dry DMF (15 mL) at 0 °C for 2 h, the mixture was added dropwise POCl₃ (1.5 mmol, 1.5 equiv.) in a ice bath. Then the ice bath was removed and the mixture was warmed up to 50 °C. The mixture continued to stir under argon at 50 °C for 2 h. Then cooled to room temperature and quenched by H₂O (1.0 mL), saturated NaHCO₃ solution (2.0 mL), and the crude reaction mixture was warmed up to 65 °C and stirred for 1 h. Then the mixture was filtered through a Celite pad, and then washed with 10 mL EtOAc. The volatiles were removed under reduced pressure, and the residue was subjected to silica gel column chromatography [eluting with petroleum ether/ethyl acetate] to afford the corresponding products **8-(1a-1r)**.

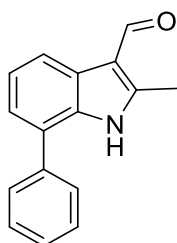
9.4.3. Characterization Data of materials 8-(1a-1r)

7-phenyl-1*H*-indole-3-carbaldehyde **8-1a**



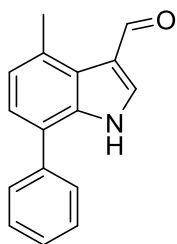
8-1a was obtained as white solid (201 mg, 91%), M.P.: 171 °C. Purification by column chromatography on silica gel (PE/EA = 3:1). ¹H NMR (400 MHz, CDCl₃) δ 10.03 (s, 1H), 9.22 (s, 1H), 8.30 (d, *J* = 7.7 Hz, 1H), 7.85 (d, *J* = 3.2 Hz, 1H), 7.61 – 7.57 (m, 2H), 7.55 – 7.50 (m, 2H), 7.45 – 7.38 (m, 2H), 7.34 (dd, *J* = 7.3, 1.3 Hz, 1H). ¹³C NMR (100 MHz, CDCl₃) δ 185.2, 138.0, 135.5, 134.6, 129.3, 128.3, 127.9, 126.3, 124.8, 124.2, 123.5, 121.1, 119.9. The NMR spectra data are in accordance with those reported in the literature. [6]

2-methyl-7-phenyl-1*H*-indole-3-carbaldehyde **8-1b**



8-1b was obtained as white solid (207 mg, 88%), M.P.: 180 °C. Purification by column chromatography on silica gel (PE/EA = 3:1). ¹H NMR (400 MHz, Acetone-*d*₆) δ 10.87 (s, 1H), 10.20 (s, 1H), 8.21 (d, *J* = 7.8 Hz, 1H), 7.63 – 7.59 (m, 2H), 7.52 – 7.47 (m, 2H), 7.44 – 7.39 (m, 1H), 7.29 (t, *J* = 7.8 Hz, 1H), 7.21 (dd, *J* = 7.4, 1.2 Hz, 1H), 2.75 (s, 3H). ¹³C NMR (100 MHz, Acetone) δ 184.5, 149.2, 139.3, 133.9, 129.7, 129.3, 128.2, 127.5, 126.5, 123.7, 123.2, 120.4, 115.4, 11.5. HR-MS (ESI) *m/z* calc. for C₁₆H₁₄NO [M+H]⁺ : 236.1070, found: 236.1072.

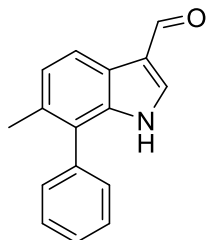
4-methyl-7-phenyl-1*H*-indole-3-carbaldehyde **8-1c**



8-1c was obtained as white solid (158 mg, 67%), M.P.: 191 °C. Purification by column chromatography on silica gel (PE/EA = 3:1). ¹H NMR (400 MHz, Acetone-*d*₆) δ 11.14

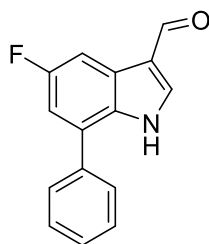
(s, 1H), 10.08 (s, 1H), 8.16 (d, $J = 3.4$ Hz, 1H), 7.63 – 7.59 (m, 2H), 7.53 – 7.48 (m, 2H), 7.43 – 7.38 (m, 1H), 7.19 (d, $J = 7.6$ Hz, 1H), 7.12 (dd, $J = 7.6, 0.8$ Hz, 1H), 2.89 (s, 3H). ^{13}C NMR (100 MHz, Acetone) δ 184.6, 139.1, 138.8, 136.2, 132.0, 129.8, 129.2, 128.2, 125.3, 125.1, 124.9, 124.4, 121.9, 22.6. HR-MS (ESI) m/z calc. for $\text{C}_{16}\text{H}_{14}\text{NO}$ $[\text{M}+\text{H}]^+$: 236.1070, found: 236.1076.

6-methyl-7-phenyl-1*H*-indole-3-carbaldehyde **8-1d**



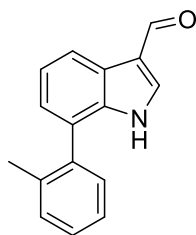
8-1d was obtained as white solid (188 mg, 80%), M.P.: 203 °C. Purification by column chromatography on silica gel (PE/EA = 3:1). ^1H NMR (400 MHz, Acetone- d_6) δ 10.60 (s, 1H), 10.01 (s, 1H), 8.11 (d, $J = 8.1$ Hz, 1H), 8.04 (d, $J = 3.2$ Hz, 1H), 7.54 – 7.48 (m, 2H), 7.46 – 7.40 (m, 1H), 7.40 – 7.36 (m, 2H), 7.21 (d, $J = 8.1$ Hz, 1H), 2.25 (s, 3H). $^{13}\text{C}\{^1\text{H}\}$ NMR (100 MHz, Acetone) δ 185.3, 137.7, 137.7, 137.2, 131.3, 130.4, 129.6, 128.3, 126.5, 125.7, 123.6, 121.0, 120.1, 19.7. HR-MS (ESI) m/z calc. for $\text{C}_{16}\text{H}_{14}\text{NO}$ $[\text{M}+\text{H}]^+$: 236.1070, found: 236.1076.

5-fluoro-7-phenyl-1*H*-indole-3-carbaldehyde **8-1e**



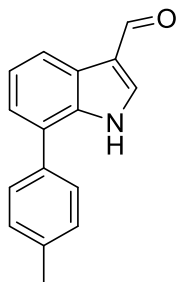
8-1e was obtained as white solid (122 mg, 51%), M.P.: 191 °C. Purification by column chromatography on silica gel (PE/EA = 2:1). ^1H NMR (400 MHz, Acetone- d_6) δ 11.22 (s, 1H), 10.05 (s, 1H), 8.27 (d, $J = 3.3$ Hz, 1H), 7.92 (dd, $J = 9.1, 2.5$ Hz, 1H), 7.70 – 7.67 (m, 1H), 7.67 – 7.66 (m, 1H), 7.57 – 7.52 (m, 2H), 7.50 – 7.44 (m, 1H), 7.14 (dd, $J = 10.1, 2.5$ Hz, 1H). $^{13}\text{C}\{^1\text{H}\}$ NMR (100 MHz, Acetone) δ 185.3, 161.5, 159.1, 139.4, 137.8, 132.0, 129.9, 129.2, 129.0, 128.8, 128.7, 126.7, 126.6, 120.1, 120.1, 112.4, 112.2, 106.3, 106.00. ^{19}F NMR (500 MHz, Acetone) δ -121.9. R-MS (ESI) m/z calc. for $\text{C}_{15}\text{H}_{11}\text{FNO}$ $[\text{M}+\text{H}]^+$: 240.0819, found: 240.0827.

7-(*o*-tolyl)-1*H*-indole-3-carbaldehyde **8-1f**



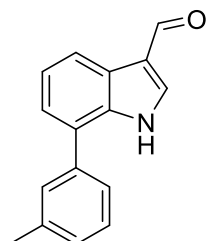
8-1f was obtained as white solid (167 mg, 71%), M.P.: 151 °C. Purification by column chromatography on silica gel (PE/EA = 3:1). ¹H NMR (400 MHz, CDCl₃) δ 9.80 (s, 1H), 9.46 (s, 1H), 8.27 (d, *J* = 7.9 Hz, 1H), 7.82 (d, *J* = 3.2 Hz, 1H), 7.37 (t, *J* = 7.6 Hz, 1H), 7.34 – 7.27 (m, 4H), 7.20 (dd, *J* = 7.3, 1.0 Hz, 1H), 2.16 (s, 3H). ¹³C{¹H} NMR (100 MHz, CDCl₃) δ 185.4, 136.9, 136.5, 136.3, 135.4, 130.6, 129.9, 128.1, 126.0, 124.8, 124.3, 122.9, 120.7, 119.4, 19.9. HR-MS (ESI) *m/z* calc. for C₁₆H₁₄NO [M+H]⁺: 236.1070, found: 236.1076.

7-(*p*-tolyl)-1*H*-indole-3-carbaldehyde **8-1g**



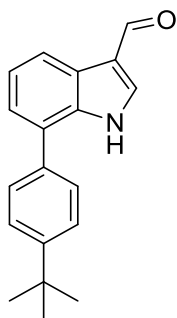
8-1g was obtained as white solid (172 mg, 73%), M.P.: 145 °C. Purification by column chromatography on silica gel (PE/EA = 2:1). ¹H NMR (400 MHz, CDCl₃) δ 10.00 (s, 1H), 9.89 (s, 1H), 8.29 (d, *J* = 7.2 Hz, 1H), 7.87 (s, 1H), 7.51 (d, *J* = 7.1 Hz, 2H), 7.43 – 7.26 (m, 4H), 2.40 (s, 3H). ¹³C{¹H} NMR (100 MHz, CDCl₃) δ 185.4, 137.5, 136.6, 134.9, 134.7, 129.8, 128.1, 126.4, 124.7, 124.0, 123.3, 120.5, 119.4, 21.1. HR-MS (ESI) *m/z* calc. for C₁₆H₁₄NO [M+H]⁺: 236.1070, found: 236.1072.

7-(*m*-tolyl)-1*H*-indole-3-carbaldehyde **8-1h**



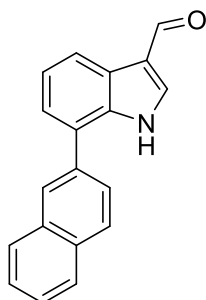
8-1h was obtained as white solid (160 mg, 68%), M.P.: 145 °C. ¹H NMR (400 MHz, DMSO-*d*₆) δ 11.97 (s, 1H), 9.99 (s, 1H), 8.26 (d, *J* = 3.2 Hz, 1H), 8.13 (dd, *J* = 7.6, 1.3 Hz, 1H), 7.45 – 7.38 (m, 3H), 7.31 (t, *J* = 7.2/7.6 Hz, 1H), 7.28 – 7.24 (m, 2H), 2.41 (s, 3H). ¹³C{¹H} NMR (100 MHz, DMSO) δ 185.4, 139.4, 138.4, 137.8, 134.4, 129.4, 129.1, 128.5, 126.7, 125.7, 125.2, 123.8, 122.9, 120.3, 118.6, 21.4. HR-MS (ESI) *m/z* calc. for C₁₆H₁₄NO [M+H]⁺: 236.1070, found: 236.1074.

7-(4-(*tert*-butyl)phenyl)-1*H*-indole-3-carbaldehyde **8-1i**



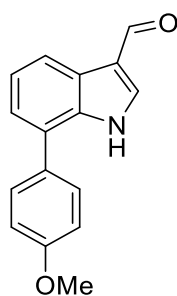
8-1i was obtained as white solid (188 mg, 68%), M.P.: 196 °C. ^1H NMR (400 MHz, Acetone- d_6) δ 11.22 (s, 1H), 10.07 (s, 1H), 8.27 (dd, $J = 7.5, 1.3$ Hz, 1H), 8.21 (d, $J = 2.9$ Hz, 1H), 7.59 – 7.56 (m, 2H), 7.56 – 7.52 (m, 2H), 7.37 – 7.29 (m, 2H), 1.36 (s, 9H). $^{13}\text{C}\{^1\text{H}\}$ NMR (100 MHz, Acetone) δ 185.3, 151.1, 138.3, 138.1, 136.0, 135.5, 128.8, 127.2, 126.6, 126.0, 124.3, 123.5, 121.2, 120.1, 34.9, 31.5. HR-MS (ESI) m/z calc. for $\text{C}_{19}\text{H}_{20}\text{NO}$ $[\text{M}+\text{H}]^+$: 278.1539, found: 278.1543.

7-(naphthalen-2-yl)-1*H*-indole-3-carbaldehyde **8-1j**



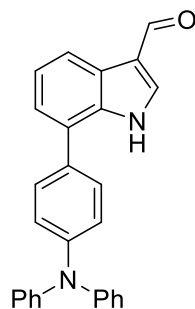
8-1j was obtained as white solid (247 mg, 91%), M.P.: 171 °C. Purification by column chromatography on silica gel (PE/EA = 2:1). ^1H NMR (400 MHz, Acetone- d_6) δ 11.30 (s, 1H), 10.09 (s, 1H), 8.30 (dd, $J = 7.8, 1.0$ Hz, 1H), 8.24 (d, $J = 3.0$ Hz, 1H), 8.18 (s, 1H), 8.06 (d, $J = 8.5$ Hz, 1H), 8.01 – 7.94 (m, 2H), 7.78 (dd, $J = 8.4, 1.7$ Hz, 1H), 7.61 – 7.53 (m, 2H), 7.45 (dd, $J = 7.3, 1.3$ Hz, 1H), 7.41 (t, $J = 7.5$ Hz, 1H). $^{13}\text{C}\{^1\text{H}\}$ NMR (100 MHz, Acetone) δ 185.3, 138.3, 136.4, 135.8, 134.5, 133.6, 129.5, 129.0, 128.4, 128.1, 127.5, 127.3, 127.2, 127.0, 126.2, 124.8, 123.6, 121.5, 120.3. HR-MS (ESI) m/z calc. for $\text{C}_{19}\text{H}_{14}\text{NO}$ $[\text{M}+\text{H}]^+$: 272.1070, found: 272.1074.

7-(4-methoxyphenyl)-1*H*-indole-3-carbaldehyde **8-1k**



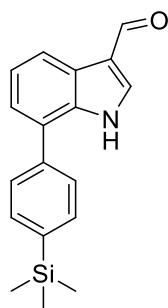
8-1k was obtained as yellow solid (198mg, 79%), M.P.: 158 °C. Purification by column chromatography on silica gel (PE/EA = 3:1). ¹H NMR (400 MHz, Acetone-*d*₆) δ 11.12 (s, 1H), 10.06 (s, 1H), 8.25 – 8.21 (m, 1H), 8.19 (d, *J* = 3.3 Hz, 1H), 7.59 – 7.55 (m, 2H), 7.33 (t, *J* = 7.6 Hz, 1H), 7.27 (dd, *J* = 7.3, 1.3 Hz, 1H), 7.09 – 7.05 (m, 2H), 3.86 (s, 3H). ¹³C {¹H} NMR (100 MHz, Acetone) δ 185.3, 160.2, 138.2, 135.6, 131.2, 130.3, 127.1, 126.0, 124.2, 123.5, 120.9, 120.2, 115.2, 55.5. HR-MS (ESI) *m/z* calc. for C₁₆H₁₄NO₂ [M+H]⁺: 252.1019, found: 252.1021.

7-(4-(diphenylamino)phenyl)-1*H*-indole-3-carbaldehyde **8-1l**



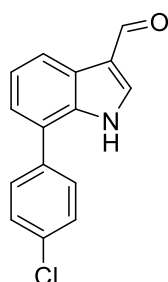
8-1l was obtained as white solid (307 mg, 79%), M.P.: 158 °C. Purification by column chromatography on silica gel (PE/EA = 1:1). ¹H NMR (400 MHz, Acetone-*d*₆) δ 11.09 (s, 1H), 10.06 (s, 1H), 8.43 – 7.97 (m, 2H), 7.62 – 7.55 (m, 2H), 7.39 – 7.28 (m, 6H), 7.18 – 7.07 (m, 8H). ¹³C {¹H} NMR (100 MHz, Acetone) δ 185.3, 148.4, 148.2, 138.1, 135.4, 134.4, 132.9, 130.2, 130.2, 130.0, 129.8, 126.9, 126.1, 125.2, 125.0, 124.6, 124.4, 124.2, 124.1, 123.8, 123.5, 121.1, 120.2, 120.2. HR-MS (ESI) *m/z* calc. for C₂₇H₂₁N₂O [M+H]⁺: 389.1648, found: 389.1653.

7-(4-(trimethylsilyl)phenyl)-1*H*-indole-3-carbaldehyde **8-1m**



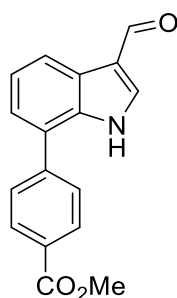
8-1m was obtained as white solid (240 mg, 82%), M.P.: 213 °C. Purification by column chromatography on silica gel (PE/EA = 3:1). ¹H NMR (400 MHz, DMSO-*d*₆) δ 12.04 (s, 1H), 9.98 (s, 1H), 8.25 (s, 1H), 8.14 (d, *J* = 7.5 Hz, 1H), 7.69 (d, *J* = 8.0 Hz, 2H), 7.62 (d, *J* = 7.7 Hz, 2H), 7.36-7.24 (m, 2H), 0.30 (s, 9H). ¹³C {¹H} NMR (100 MHz, DMSO) δ 185.4, 139.56, 139.2, 138.5, 134.5, 134.1, 128.1, 126.6, 125.3, 123.8, 123.0, 120.5, 118.6, -0.9. HR-MS (ESI) *m/z* calc. for C₁₈H₂₀NOSi [M+H]⁺: 294.1309, found: 294.1315.

7-(4-chlorophenyl)-1*H*-indole-3-carbaldehyde **8-1n**



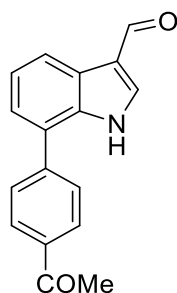
8-1n was obtained as white solid (189 mg, 74%), M.P.: 122 °C. Purification by column chromatography on silica gel (PE/EA = 3:1). ¹H NMR (400 MHz, Acetone-*d*₆) δ 11.21 (s, 1H), 10.07 (s, 1H), 8.27 (dd, *J* = 7.6, 1.4 Hz, 1H), 8.22 (s, 1H), 7.68 – 7.63 (m, 2H), 7.57 – 7.51 (m, 2H), 7.36 (t, *J* = 7.5 Hz, 1H), 7.31 (dd, *J* = 7.4, 1.4 Hz, 1H). ¹³C{¹H} NMR (100 MHz, Acetone) δ 185.4, 138.5, 138.3, 137.8, 135.4, 133.8, 130.9, 129.8, 126.1, 126.1, 124.5, 123.5, 121.9, 121.7, 120.2. HR-MS (ESI) *m/z* calc. for C₁₅H₁₁ClNO [M+H]⁺: 256.0524, found: 256.0530.

methyl 4-(3-formyl-1*H*-indol-7-yl)benzoate **8-1o**



8-1o was obtained as pale yellow solid (187 mg, 67%), M.P.: 225 °C. Purification by column chromatography on silica gel (PE/EA = 2:1). ¹H NMR (400 MHz, DMSO-*d*₆) δ 12.07 (s, 1H), 9.99 (s, 1H), 8.31 (s, 1H), 8.21 – 8.15 (m, 1H), 8.13 – 8.08 (m, 2H), 7.81 – 7.76 (m, 2H), 7.38 – 7.32 (m, 2H), 3.90 (s, 3H). ¹³C{¹H} NMR (100 MHz, DMSO) δ 185.5, 166.3, 142.7, 139.7, 134.4, 130.1, 129.1, 128.8, 125.5, 125.4, 124.1, 123.0, 121.3, 118.6, 52.5. HR-MS (ESI) *m/z* calc. for C₁₇H₁₄NO₃ [M+H]⁺: 280.0968, found: 280.0975.

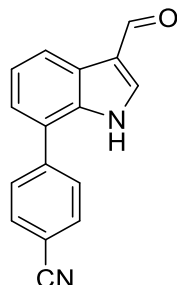
7-(4-acetylphenyl)-1*H*-indole-3-carbaldehyde **8-1p**



8-1p was obtained as yellow solid (184 mg, 70%), M.P.: 220 °C. Purification by column chromatography on silica gel (PE/EA = 3:1). ¹H NMR (400 MHz, DMSO-*d*₆) δ 12.11

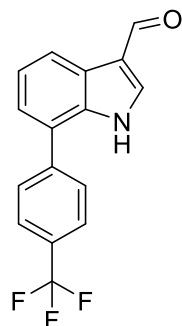
(s, 1H), 9.99 (s, 1H), 8.31 (s, 1H), 8.20 – 8.16 (m, 1H), 8.13 – 8.10 (m, 2H), 7.81 – 7.77 (m, 2H), 7.38 – 7.33 (m, 2H), 2.65 (s, 3H). $^{13}\text{C}\{^1\text{H}\}$ NMR (100 MHz, DMSO) δ 197.8, 185.5, 142.6, 139.6, 136.0, 134.3, 129.1, 129.0, 125.5, 125.4, 124.1, 123.0, 121.2, 118.6, 27.1. HR-MS (ESI) m/z calc. for $\text{C}_{17}\text{H}_{14}\text{NO}_2$ $[\text{M}+\text{H}]^+$: 264.1019, found: 264.1024.

4-(3-formyl-1*H*-indol-7-yl)benzonitrile **8-1q**



8-1q was obtained as a white solid. (145 mg, 55%) M.P.: 225 °C. Purification by column chromatography on silica gel (PE/EA = 1:1). ^1H NMR (400 MHz, Acetone- d_6) δ 11.33 (s, 1H), 10.08 (s, 1H), 8.34-8.30 (m, 1H), 8.27 – 8.24 (m, 1H), 7.95 – 7.92 (m, 2H), 7.90 – 7.87 (m, 2H), 7.41 – 7.38 (m, 2H). $^{13}\text{C}\{^1\text{H}\}$ NMR (100 MHz, Acetone) δ 185.4, 143.7, 138.5, 138.4, 133.6, 130.2, 126.3, 126.3, 125.6, 124.7, 123.6, 122.6, 119.1, 111.9. HR-MS (ESI) m/z calc. for $\text{C}_{16}\text{H}_{11}\text{N}_2\text{O}$ $[\text{M}+\text{H}]^+$: 264.1019, found: 264.1024.

7-(4-(trifluoromethyl)phenyl)-1*H*-indole-3-carbaldehyde **8-1r**

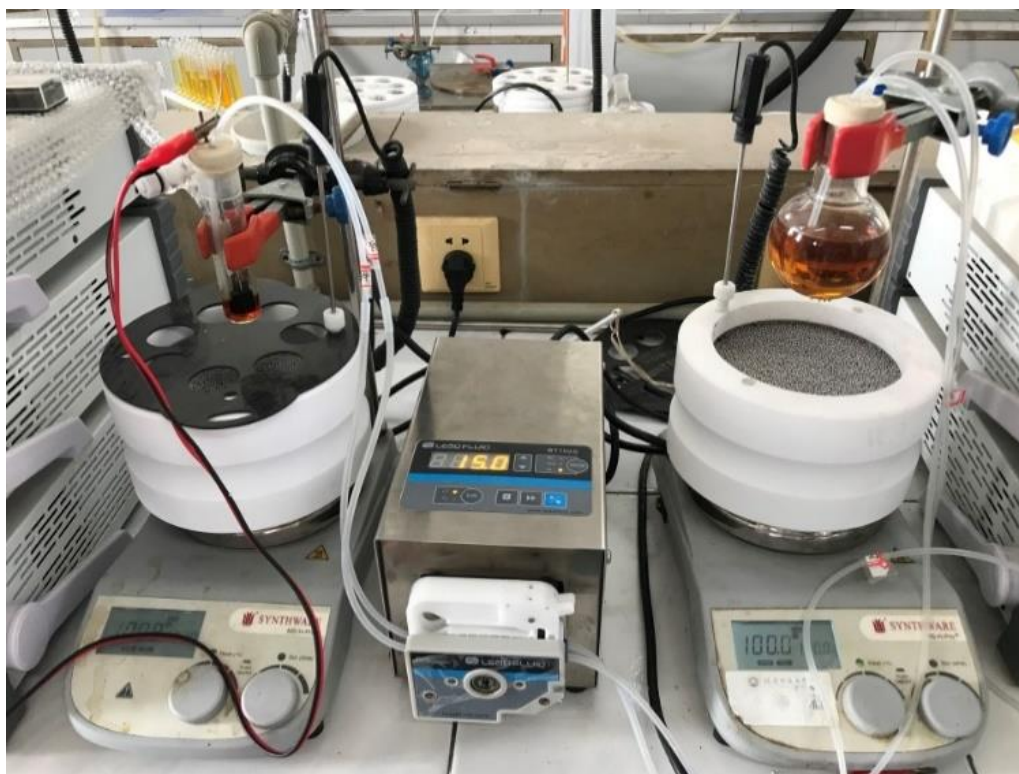


8-1r was obtained as a white solid. (223 mg, 77%) M.P.: 184 °C. Purification by column chromatography on silica gel (PE/EA = 3:1). ^1H NMR (400 MHz, Acetone- d_6) δ 11.27 (s, 1H), 10.08 (s, 1H), 8.36 – 8.28 (m, 1H), 8.24 (d, J = 3.1 Hz, 1H), 7.92 – 7.82 (m, 4H), 7.42 – 7.35 (m, 2H). $^{13}\text{C}\{^1\text{H}\}$ NMR (100 MHz, Acetone) δ 185.4, 143.1, 138.5, 135.4, 130.0, 129.9, 129.6, 126.6, 126.2, 125.8, 124.7, 123.9, 123.6, 122.3, 120.2. ^{19}F NMR (500 MHz, Acetone) δ -63.5. HR-MS (ESI) m/z calc. for $\text{C}_{16}\text{H}_{11}\text{F}_3\text{NO}$ $[\text{M}+\text{H}]^+$: 290.0787, found: 290.0795.

9.4.4. Procedure for synthesis of 4,5-diphenylbenzo[4,5]azepino[3,2,1-*hi*]indole-1-carbaldehydes **8-3**.



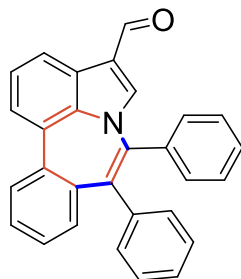
The electrooxidative rhodium-catalyzed C-H/N-H annulation reactions were performed in undivided electrochemical cells (10 mL), with Platinum electrodes as cathode and graphite felt (GF) electrodes as anode, connected using stainless steel adapters. Under air atmosphere, **8-1** (0.2 mmol), **8-2** (0.4 mmol), [Cp**RhCl*₂]₂ (2.5 mmol%), Li₂CO₃ (2.0 equiv) were dissolved in 1,4-Dioxane (3 mL) and H₂O (1 mL) at 100°C for 5-7 h. The conventional reoxidation strategy ([Cp**RhCl*₂]₂/Ag₂CO₃) was employing **8-1** (0.2 mmol), **8-2** (0.4 mmol), [Cp**RhCl*₂]₂ (2.5 mmol%), Ag₂CO₃ (3.0 equiv) in *t*-AmOH at 100°C for 12 h. After the reaction was cooled down to room temperature, the crude reaction mixture was then diluted with EtOAc to 5 mL, filtered through a Celite pad, and then washed with 10 mL of DCM. The volatiles were removed under reduced pressure, and the residue was subjected to silica gel column chromatography [eluting with petroleum ether (PE)/ethyl acetate (EA)] to afford the corresponding product **8-(3aa-3bn)**.



Gram-scale with a simple flow cell: The reaction unit consists of a flask (100 ml) and an undivided cell (15 ml) with two peristaltic pumps. The electrocatalysis was carried out in the undivided cell (15 mL) under air with a graphite felt (GF) anode (10mm × 15 mm × 6 mm) and a platinum cathode (10 mm × 15 mm × 0.25 mm). **8-1a** (1.0 g, 4.5 mmol), **8-2a** (1.6 g, 9.0 mmol), [Cp**Rh*Cl₂]₂ (70 mg, 2.5 mol%) and Li₂CO₃ (998 mg, 13.5 mmol) were first placed in the flask (100 mL) and then dissolved in 1,4-Dioxane (67 mL) and H₂O (22 mL). Using peristaltic pumps to circulate the solvent in the system at a rate of 0.15 ml/s, and keep 4 ml of solvent in the undivided cell. The electrocatalysis was performed at 100 °C with a constant current of 5.0 mA and maintained for 105 h. The electrodes were washed with CH₂Cl₂ (20 mL). The combined mixtures were extracted with CH₂Cl₂ and saturated brine (60 mL), dried over Na₂SO₄, filtered and concentrated under reduced pressure. The residue was purified by chromatography on silica gel to afford product **8-3aa** (1013 mg, 56%).

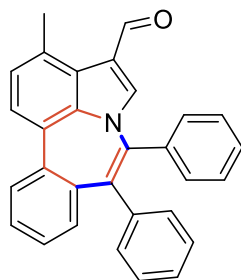
9.4.5. Characterization Data of products 8-(3aa-3bn)

4,5-diphenylbenzo[4,5]azepino[3,2,1-*hi*]indole-1-carbaldehyde **8-3aa**



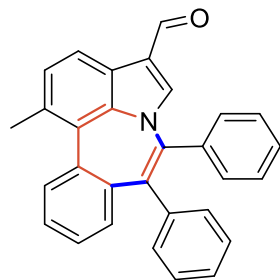
8-3aa was obtained as yellow solid. (64 mg, 80%) M.P.: 176 °C. Purification by column chromatography on silica gel (PE/EA = 10:1). ^1H NMR (400 MHz, CDCl_3) δ 9.71 (s, 1H), 8.10 (dd, $J = 7.8, 1.0$ Hz, 1H), 7.59 (d, $J = 7.4$ Hz, 1H), 7.42 – 7.35 (m, 2H), 7.29 – 7.17 (m, 4H), 7.13 – 7.00 (m, 9H), 6.82 (dd, $J = 8.0, 1.3$ Hz, 1H). $^{13}\text{C}\{^1\text{H}\}$ NMR (100 MHz, CDCl_3) δ 185.0, 145.6, 141.3, 140.4, 140.0, 138.3, 138.2, 137.3, 133.1, 131.1, 130.6, 129.8, 129.3, 128.9, 128.6, 128.2, 128.0, 127.7, 126.9, 126.3, 125.8, 123.1, 121.0, 119.6. HR-MS (ESI) m/z calc. for $\text{C}_{29}\text{H}_{20}\text{NO}$ $[\text{M}+\text{H}]^+$: 398.1539, found: 398.1544.

12-methyl-4,5-diphenylbenzo[4,5]azepino[3,2,1-*hi*]indole-1-carbaldehyde **8-3ac**



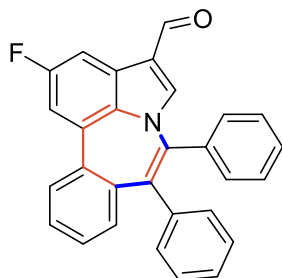
8-3ac was obtained as yellow solid. (58 mg, 71%) M.P.: 188 °C. Purification by column chromatography on silica gel (PE/EA = 10:1). ^1H NMR (400 MHz, CDCl_3) δ 9.85 (s, 1H), 7.48 (d, $J = 7.8$ Hz, 1H), 7.35 (d, $J = 7.8$ Hz, 1H), 7.30 – 7.00 (m, 14H), 6.88 – 6.83 (m, 1H), 2.77 (s, 3H). $^{13}\text{C}\{^1\text{H}\}$ NMR (100 MHz, CDCl_3) δ 184.7, 146.6, 141.2, 140.5, 139.9, 138.4, 137.8, 137.6, 132.8, 131.4, 131.0, 130.5, 129.8, 129.5, 129.3, 128.5, 128.1, 127.6, 127.3, 127.2, 126.4, 126.3, 125.7, 123.0, 121.3, 22.1. HR-MS (ESI) m/z calc. for $\text{C}_{30}\text{H}_{22}\text{NO}$ $[\text{M}+\text{H}]^+$: 412.1696, found: 412.1706.

10-methyl-4,5-diphenylbenzo[4,5]azepino[3,2,1-*hi*]indole-1-carbaldehyde **8-3ad**



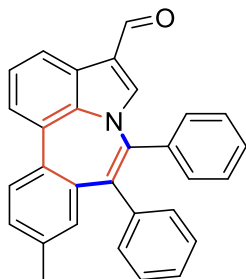
8-3ad was obtained as yellow solid. (7 mg, 8%) M.P.: 280 °C. Purification by column chromatography on silica gel (PE/EA = 10:1). ¹H NMR (400 MHz, CDCl₃) δ 9.71 (s, 1H), 7.94 (d, *J* = 7.9 Hz, 1H), 7.33 (d, *J* = 8.0 Hz, 1H), 7.28 – 7.23 (m, 2H), 7.22 – 7.03 (m, 12H), 6.96 (dd, *J* = 8.0, 1.3 Hz, 1H), 2.70 (s, 3H). ¹³C {¹H} NMR (100 MHz, CDCl₃) δ 185.2, 149.9, 141.2, 140.9, 140.8, 138.9, 138.5, 137.2, 132.9, 132.8, 132.00, 131.1, 129.8, 129.4, 128.3, 128.1, 127.7, 127.5, 127.1, 126.5, 124.2, 120.5, 119.8, 21.7. HR-MS (ESI) *m/z* calc. for C₃₀H₂₂NO [M+H]⁺: 412.1696, found: 412.1704.

11-fluoro-4,5-diphenylbenzo[4,5]azepino[3,2,1-*hi*]indole-1-carbaldehyde **8-3ae**



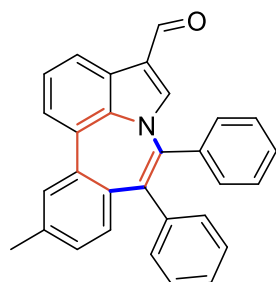
8-3ae was obtained as yellow solid. (55 mg, 66%) M.P.: 198 °C. Purification by column chromatography on silica gel (PE/EA = 10:1). ¹H NMR (400 MHz, CDCl₃) δ 9.69 (s, 1H), 7.77 (dd, *J* = 8.1, 2.4 Hz, 1H), 7.39 (d, *J* = 7.9 Hz, 1H), 7.33 – 7.28 (m, 2H), 7.24 – 7.18 (m, 3H), 7.16 – 6.98 (m, 9H), 6.83 (d, *J* = 7.6 Hz, 1H). ¹³C {¹H} NMR (100 MHz, CDCl₃) δ 184.7, 141.7, 141.2, 139.9, 138.2, 138.1, 136.0, 133.3, 131.1, 130.5, 129.8, 129.5, 128.7, 128.4, 127.8, 126.5, 111.0, 110.7, 106.4, 106.2. ¹⁹F NMR (500 MHz) δ -118.9. HR-MS (ESI) *m/z* calc. for C₂₉H₁₉FNO [M+H]⁺: 416.1445, found: 416.1454.

7-methyl-4,5-diphenylbenzo[4,5]azepino[3,2,1-*hi*]indole-1-carbaldehyde **8-3ag**



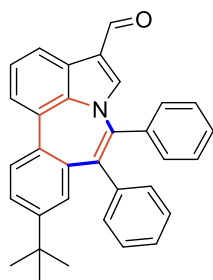
8-3ag was obtained as yellow solid. (67 mg, 81%) M.P.: 201 °C. Purification by column chromatography on silica gel (PE/EA = 10:1). ¹H NMR (400 MHz, CDCl₃) δ 9.71 (s, 1H), 8.07 (dd, *J* = 7.8, 0.9 Hz, 1H), 7.56 (d, *J* = 7.4 Hz, 1H), 7.36 (t, *J* = 7.7 Hz, 1H), 7.30 (d, *J* = 8.1 Hz, 1H), 7.23 – 7.16 (m, 3H), 7.11 – 7.01 (m, 9H), 6.62 (dd, *J* = 1.8, 0.8 Hz, 1H), 2.13 (s, 3H). ¹³C {¹H} NMR (100 MHz, CDCl₃) δ 185.0, 145.4, 141.3, 140.5, 139.9, 138.5, 137.9, 137.5, 134.4, 133.8, 131.1, 130.7, 130.2, 129.9, 128.9, 128.6, 128.2, 128.0, 127.7, 126.9, 126.3, 125.8, 122.7, 120.6, 119.6, 20.9. HR-MS (ESI) *m/z* calc. for C₃₀H₂₂NO [M+H]⁺: 412.1696, found: 412.1704.

8-methyl-4,5-diphenylbenzo[4,5]azepino[3,2,1-*hi*]indole-1-carbaldehyde **8-3ah**



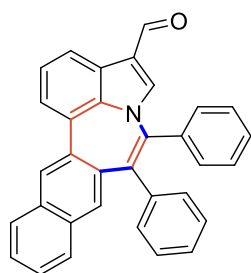
8-3ah was obtained as yellow solid. (62 mg, 76%). M.P.: 189 °C. Purification by column chromatography on silica gel (PE/EA = 10:1). ¹H NMR (400 MHz, CDCl₃) δ 9.71 (s, 1H), 8.10 (dd, *J* = 8.0, 0.8 Hz, 1H), 7.60 (d, *J* = 7.5 Hz, 1H), 7.37 (t, *J* = 7.7 Hz, 1H), 7.25 – 7.14 (m, 4H), 7.12 – 7.01 (m, 7H), 6.88 – 6.85 (m, 2H), 6.70 (d, *J* = 8.1 Hz, 1H), 2.33 (s, 3H). ¹³C {¹H} NMR (100 MHz, CDCl₃) δ 185.0, 145.5, 141.5, 140.4, 139.3, 139.2, 138.4, 137.0, 135.3, 133.2, 131.4, 131.2, 131.1, 129.9, 128.9, 128.6, 128.5, 128.1, 128.0, 127.7, 126.9, 126.5, 126.3, 125.7, 125.1, 122.9, 121.0, 119.5, 21.0. HR-MS (ESI) *m/z* calc. for C₃₀H₂₂NO [M+H]⁺: 412.1696, found: 412.1705.

7-(*tert*-butyl)-4,5-diphenylbenzo[4,5]azepino[3,2,1-*hi*]indole-1-carbaldehyde **8-3ai**



8-3ai was obtained as yellow solid. (74 mg, 82%) M.P.: 189 °C. Purification by column chromatography on silica gel (PE/EA = 10:1). ¹H NMR (400 MHz, CDCl₃) δ 9.71 (s, 1H), 8.07 (dd, *J* = 7.8, 1.0 Hz, 1H), 7.57 (d, *J* = 7.3 Hz, 1H), 7.38 – 7.33 (m, 2H), 7.28 (dd, *J* = 8.3, 2.1 Hz, 1H), 7.24 – 7.17 (m, 3H), 7.14 – 7.07 (m, 7H), 7.07 – 7.01 (m, 1H), 6.83 (d, *J* = 2.1 Hz, 1H), 1.08 (s, 9H). ¹³C {¹H} NMR (100 MHz, CDCl₃) δ 185.0, 150.4, 145.1, 141.5, 140.3, 139.5, 138.4, 137.5, 134.3, 131.1, 130.8, 130.2, 129.9, 129.2, 128.6, 128.2, 127.8, 127.6, 126.9, 126.4, 126.3, 125.7, 122.7, 120.7, 119.4, 34.3, 30.7. HR-MS (ESI) *m/z* calc. for C₃₃H₂₈NO [M+H]⁺: 454.2165, found: 454.2173.

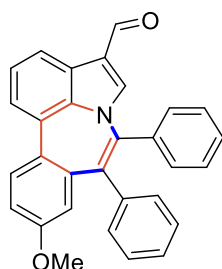
4,5-diphenylnaphtho[2',3':4,5]azepino[3,2,1-*hi*]indole-1-carbaldehyde **8-3aj**



8-3aj was obtained as yellow solid. (65 mg, 73%) M.P.: 248 °C. Purification by column chromatography on silica gel (PE/EA = 8:1). ¹H NMR (400 MHz, CDCl₃) δ 9.74 (s,

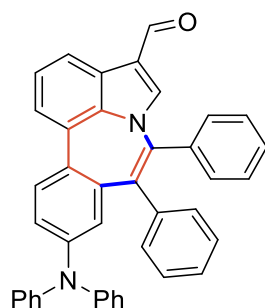
1H), 8.18 (dd, $J = 7.7, 0.9$ Hz, 1H), 7.87 (s, 1H), 7.81 (d, $J = 7.5$ Hz, 1H), 7.76 (d, $J = 8.1$ Hz, 1H), 7.47 – 7.42 (m, 2H), 7.42 – 7.37 (m, 1H), 7.34 – 7.30 (m, 1H), 7.25 – 7.18 (m, 4H), 7.17 – 7.03 (m, 8H). $^{13}\text{C}\{^1\text{H}\}$ NMR (100 MHz, CDCl_3) δ 185.0, 143.7, 141.6, 140.5, 139.1, 138.6, 136.0, 134.8, 133.8, 133.2, 132.5, 131.4, 130.2, 130.0, 128.6, 128.4, 128.2, 128.1, 127.8, 127.6, 127.5, 127.1, 126.7, 126.4, 125.8, 123.8, 121.3, 119.5. HR-MS (ESI) m/z calc. for $\text{C}_{33}\text{H}_{22}\text{NO}$ $[\text{M}+\text{H}]^+$: 448.1696, found: 448.1700.

7-methoxy-4,5-diphenylbenzo[4,5]azepino[3,2,1-*hi*]indole-1-carbaldehyde **8-3ak**



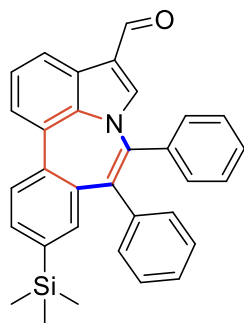
8-3ak was obtained as yellow solid. (53 mg, 62%) M.P.: 185 °C. Purification by column chromatography on silica gel (PE/EA = 5:1). ^1H NMR (400 MHz, CDCl_3) δ 9.70 (s, 1H), 8.04 (dd, $J = 7.8, 1.0$ Hz, 1H), 7.50 (d, $J = 7.3$ Hz, 1H), 7.36 – 7.32 (m, 2H), 7.23 – 7.16 (m, 3H), 7.10 – 7.00 (m, 8H), 6.82 (dd, $J = 8.8, 2.8$ Hz, 1H), 6.37 (d, $J = 2.8$ Hz, 1H), 3.61 (s, 3H). $^{13}\text{C}\{^1\text{H}\}$ NMR (100 MHz, CDCl_3) δ 185.0, 159.0, 144.8, 141.2, 140.4, 140.0, 139.4, 138.4, 132.0, 131.1, 129.8, 129.7, 128.6, 128.4, 128.2, 127.8, 127.7, 126.9, 126.4, 125.8, 122.4, 120.2, 119.6, 119.4, 114.1, 55.0. HR-MS (ESI) m/z calc. for $\text{C}_{30}\text{H}_{22}\text{NO}_2$ $[\text{M}+\text{H}]^+$: 428.1645, found: 428.1645.

7-(diphenylamino)-4,5-diphenylbenzo[4,5]azepino[3,2,1-*hi*]indole-1-carbaldehyde **8-3al**



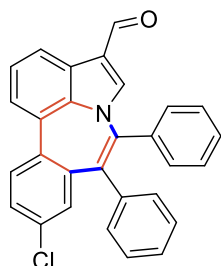
8-3al was obtained as yellow solid. (78 mg, 69%) M.P.: 283 °C. Purification by column chromatography on silica gel (PE/EA = 10:1). ^1H NMR (400 MHz, CDCl_3) δ 9.71 (s, 1H), 8.03 (d, $J = 7.5$ Hz, 1H), 7.50 (d, $J = 7.5$ Hz, 1H), 7.33 (t, $J = 7.7$ Hz, 1H), 7.24 (d, $J = 8.8$ Hz, 2H), 7.20 – 7.10 (m, 7H), 7.07 – 7.02 (m, 3H), 6.99 – 6.89 (m, 11H), 6.48 (d, $J = 2.5$ Hz, 1H). $^{13}\text{C}\{^1\text{H}\}$ NMR (100 MHz, CDCl_3) δ 185.0, 147.1, 146.5, 144.6, 141.1, 140.3, 139.5, 138.7, 138.4, 131.2, 130.7, 129.9, 129.8, 129.2, 128.7, 128.5, 128.2, 127.8, 127.5, 126.9, 126.6, 126.0, 125.8, 124.8, 123.4, 122.1, 122.0, 120.2, 119.5. HR-MS (ESI) m/z calc. for $\text{C}_{41}\text{H}_{29}\text{N}_2\text{O}$ $[\text{M}+\text{H}]^+$: 565.2274, found: 565.2276.

4,5-diphenyl-7-(trimethylsilyl)benzo[4,5]azepino[3,2,1-*hi*]indole-1-carbaldehyde **8-3am**



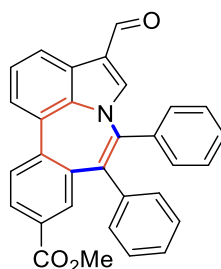
8-3am was obtained as yellow solid. (77 mg, 82%) M.P.: 195 °C. Purification by column chromatography on silica gel (PE/EA = 10:1). ^1H NMR (400 MHz, CDCl_3) δ 9.71 (s, 1H), 8.10 (dd, $J = 8.0, 0.8$ Hz, 1H), 7.59 (d, $J = 7.6$ Hz, 1H), 7.43 – 7.35 (m, 3H), 7.25 – 7.18 (m, 3H), 7.12 – 7.02 (m, 8H), 6.94 (s, 1H), 0.09 – 0.03 (m, 9H). $^{13}\text{C}\{^1\text{H}\}$ NMR (100 MHz, CDCl_3) δ 185.0, 145.5, 141.3, 140.4, 139.8, 139.7, 138.4, 137.6, 137.2, 134.2, 131.1, 129.9, 129.6, 129.1, 128.6, 128.2, 128.0, 127.6, 127.0, 126.3, 125.8, 123.0, 121.1, 119.4, -1.6. HR-MS (ESI) m/z calc. for $\text{C}_{32}\text{H}_{28}\text{NOSi}$ $[\text{M}+\text{H}]^+$: 470.1935, found: 470.1941.

7-chloro-4,5-diphenylbenzo[4,5]azepino[3,2,1-*hi*]indole-1-carbaldehyde **8-3an**



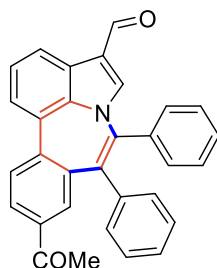
8-3an was obtained as yellow solid. (64 mg, 74%) M.P.: 192 °C. Purification by column chromatography on silica gel (PE/EA = 10:1). ^1H NMR (400 MHz, CDCl_3) δ 9.71 (s, 1H), 8.10 (dd, $J = 7.8, 0.8$ Hz, 1H), 7.51 (d, $J = 7.5$ Hz, 1H), 7.36 (t, $J = 7.7$ Hz, 1H), 7.29 (d, $J = 8.6$ Hz, 1H), 7.24 – 7.17 (m, 4H), 7.15 – 7.03 (m, 8H), 6.77 (d, $J = 2.2$ Hz, 1H). $^{13}\text{C}\{^1\text{H}\}$ NMR (100 MHz, CDCl_3) δ 185.0, 145.4, 141.0, 140.5, 139.9, 138.1, 135.9, 134.0, 132.7, 131.9, 131.0, 129.7, 129.2, 128.7, 128.4, 128.0, 127.6, 127.1, 127.0, 126.7, 125.9, 123.1, 121.3, 119.7, 104.9. HR-MS (ESI) m/z calc. for $\text{C}_{29}\text{H}_{19}\text{ClNO}$ $[\text{M}+\text{H}]^+$: 432.1150, found: 432.1156.

methyl 1-formyl-4,5-diphenylbenzo[4,5]azepino[3,2,1-*hi*]indole-7-carboxylate **8-3ao**



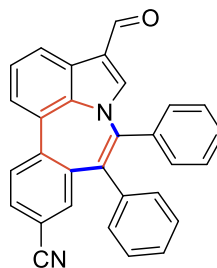
8-3ao was obtained as yellow solid. (34 mg, 37%) M.P.: 200 °C. Purification by column chromatography on silica gel (PE/EA = 7:1). ¹H NMR (400 MHz, CDCl₃) δ 9.72 (s, 1H), 8.14 (dd, *J* = 7.8, 1.0 Hz, 1H), 7.87 (dd, *J* = 8.3, 1.8 Hz, 1H), 7.62 (d, *J* = 7.5 Hz, 1H), 7.50 (d, *J* = 1.8 Hz, 1H), 7.44 (d, *J* = 8.4 Hz, 1H), 7.39 (t, *J* = 7.8 Hz, 1H), 7.24 – 7.18 (m, 3H), 7.14 – 7.08 (m, 5H), 7.08 – 7.03 (m, 3H), 3.79 (s, 3H). ¹³C{¹H} NMR (100 MHz, CDCl₃) δ 185.0, 166.3, 145.9, 141.9, 140.7, 140.7, 140.6, 138.5, 138.2, 134.2, 131.0, 130.7, 129.9, 129.7, 129.2, 128.7, 128.4, 128.3, 128.0, 127.1, 126.9, 126.7, 125.9, 123.7, 122.0, 119.7, 52.1. HR-MS (ESI) *m/z* calc. for C₃₁H₂₂NO₃ [M+H]⁺: 456.1594, found: 456.1600.

7-acetyl-4,5-diphenylbenzo[4,5]azepino[3,2,1-*hi*]indole-1-carbaldehyde **8-3ap**



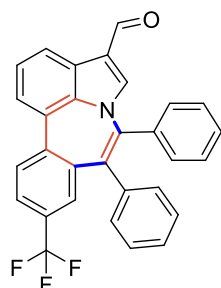
8-3ap was obtained as yellow solid. (49 mg, 56%) M.P.: 89 °C. Purification by column chromatography on silica gel (PE/EA = 8:1). ¹H NMR (400 MHz, CDCl₃) δ 9.73 (s, 1H), 8.14 (dd, *J* = 7.8, 0.8 Hz, 1H), 7.80 (dd, *J* = 8.3, 1.9 Hz, 1H), 7.61 (d, *J* = 7.6 Hz, 1H), 7.47 (d, *J* = 8.4 Hz, 1H), 7.41 – 7.36 (m, 2H), 7.24 – 7.17 (m, 3H), 7.15 – 7.05 (m, 8H), 2.31 (s, 3H). ¹³C{¹H} NMR (100 MHz, CDCl₃) δ 197.1, 184.9, 145.7, 142.1, 140.8, 140.7, 140.5, 138.6, 138.1, 135.9, 133.3, 131.0, 130.8, 129.7, 128.7, 128.5, 128.4, 128.2, 128.0, 127.2, 126.9, 126.8, 125.9, 123.8, 122.2, 119.7, 26.3. HR-MS (ESI) *m/z* calc. for C₃₁H₂₂NO₂ [M+H]⁺: 440.1645, found: 440.1646.

1-formyl-4,5-diphenylbenzo[4,5]azepino[3,2,1-*hi*]indole-7-carbonitrile **8-3aq**



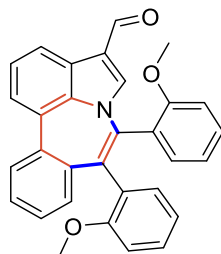
8-3aq was obtained as yellow solid. (38 mg, 45%) M.P.: 160 °C. Purification by column chromatography on silica gel (PE/EA = 4:1). ¹H NMR (400 MHz, CDCl₃) δ 9.73 (s, 1H), 8.16 (dd, *J* = 7.8, 1.0 Hz, 1H), 7.80 – 7.76 (m, 1H), 7.73 – 7.65 (m, 1H), 7.55 (d, *J* = 7.5 Hz, 1H), 7.50 (dd, *J* = 8.3, 1.7 Hz, 1H), 7.44 (d, *J* = 8.3 Hz, 1H), 7.39 (t, *J* = 7.8 Hz, 1H), 7.23 – 7.21 (m, 2H), 7.15 – 7.04 (m, 8H). ¹³C{¹H} NMR (100 MHz, CDCl₃) δ 184.9, 145.9, 142.3, 141.9, 140.5, 140.0, 139.8, 137.8, 136.3, 132.9, 132.1, 131.3, 131.0, 129.5, 128.8, 128.6, 128.3, 127.9, 127.4, 127.1, 127.1, 126.3, 126.1, 123.9, 122.7, 119.9, 118.4, 118.4, 111.5. HR-MS (ESI) *m/z* calc. for C₃₀H₁₉N₂O [M+H]⁺: 423.1492, found: 423.1498.

4,5-diphenyl-7-(trifluoromethyl)benzo[4,5]azepino[3,2,1-*hi*]indole-1-carbaldehyde **8-3ar**



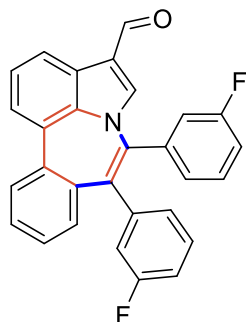
8-3ar was obtained as yellow solid. (38 mg, 41%) M.P.: 240 °C. Purification by column chromatography on silica gel (PE/EA = 8:1). ^1H NMR (400 MHz, CDCl_3) δ 9.72 (s, 1H), 8.14 (dd, $J = 7.8, 0.9$ Hz, 1H), 7.58 (dd, $J = 7.6, 0.8$ Hz, 1H), 7.50 – 7.45 (m, 2H), 7.39 (t, $J = 7.8$ Hz, 1H), 7.25 – 7.19 (m, 3H), 7.15 – 7.03 (m, 9H). $^{13}\text{C}\{^1\text{H}\}$ NMR (100 MHz, CDCl_3) δ 185.0, 145.9, 141.3, 141.0, 140.6, 140.4, 139.1, 138.0, 131.1, 131.0, 129.6, 128.7, 128.5, 128.1, 127.8, 127.2, 126.9, 126.7, 126.0, 125.7, 125.7, 123.7, 122.1, 119.8. ^{19}F NMR (500 MHz) δ -64.3. HR-MS (ESI) m/z calc. for $\text{C}_{30}\text{H}_{19}\text{F}_3\text{NO}$ $[\text{M}+\text{H}]^+$: 466.1413, found: 466.1417.

4,5-bis(2-methoxyphenyl)benzo[4,5]azepino[3,2,1-*hi*]indole-1-carbaldehyde **8-3ba**



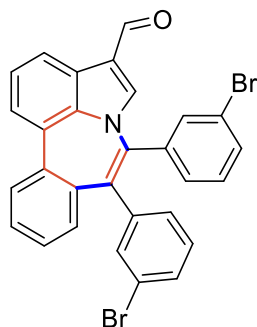
8-3ba was obtained as yellow solid. (44 mg, 48%) M.P.: 194 °C. Purification by column chromatography on silica gel (PE/EA = 10:1). ^1H NMR (400 MHz, CDCl_3) δ 9.73 (s, 1H), 8.06 (dd, $J = 7.8, 1.0$ Hz, 1H), 7.55 (d, $J = 7.6$ Hz, 1H), 7.41 (dd, $J = 8.0, 1.1$ Hz, 1H), 7.33 (t, $J = 7.7$ Hz, 1H), 7.25 – 7.21 (m, 1H), 7.20 – 7.12 (m, 2H), 7.10 – 7.00 (m, 4H), 6.82 (dd, $J = 8.0, 1.3$ Hz, 1H), 6.75 – 6.61 (m, 4H), 3.76 (s, 3H), 3.65 (s, 3H). $^{13}\text{C}\{^1\text{H}\}$ NMR (100 MHz, CDCl_3) δ 185.1, 156.4, 155.8, 145.2, 140.1, 137.4, 137.1, 136.4, 131.8, 130.9, 130.4, 130.3, 130.3, 129.3, 129.1, 128.6, 128.0, 127.8, 126.9, 125.5, 125.5, 122.9, 120.7, 120.1, 119.9, 119.5, 110.4, 110.1, 55.2, 55.1. HR-MS (ESI) m/z calc. for $\text{C}_{31}\text{H}_{24}\text{NO}_3$ $[\text{M}+\text{H}]^+$: 458.1751, found: 458.1758.

4,5-bis(3-fluorophenyl)benzo[4,5]azepino[3,2,1-*hi*]indole-1-carbaldehyde **8-3bb**



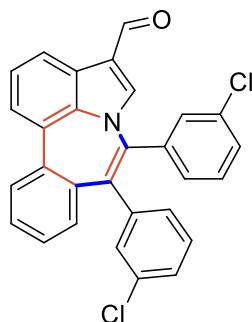
8-3bb was obtained as yellow solid. (61 mg, 70%) M.P.: 194 °C. Purification by column chromatography on silica gel (PE/EA = 10:1). ^1H NMR (400 MHz, CDCl_3) δ 9.74 (s, 1H), 8.13 – 8.06 (m, 1H), 7.58 (d, $J = 7.6$ Hz, 1H), 7.42 – 7.35 (m, 2H), 7.31 – 7.27 (m, 1H), 7.25 – 7.20 (m, 1H), 7.14 – 7.05 (m, 3H), 6.97 – 6.92 (m, 1H), 6.92 – 6.88 (m, 2H), 6.86 – 6.75 (m, 4H). $^{13}\text{C}\{^1\text{H}\}$ NMR (100 MHz, CDCl_3) δ 184.9, 163.8, 163.5, 161.3, 161.0, 145.7, 143.1, 143.0, 139.8, 139.7, 139.7, 138.8, 137.3, 137.3, 132.9, 130.8, 130.6, 130.5, 129.8, 129.5, 129.4, 128.1, 127.9, 127.7, 127.0, 126.9, 126.0, 125.7, 125.6, 123.4, 121.2, 120.0, 118.1, 117.9, 117.0, 116.8, 115.8, 115.6, 113.9, 113.7. ^{19}F NMR (500 MHz, CDCl_3) δ -112.0, -114.1. HR-MS (ESI) m/z calc. for $\text{C}_{29}\text{H}_{18}\text{F}_2\text{NO}$ $[\text{M}+\text{H}]^+$: 434.1351, found: 434.1357.

4,5-bis(3-bromophenyl)benzo[4,5]azepino[3,2,1-*hi*]indole-1-carbaldehyde **8-3bc**



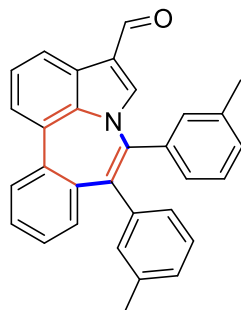
8-3bc was obtained as yellow solid. (72 mg, 65%) M.P.: 213 °C. Purification by column chromatography on silica gel (PE/EA = 10:1). ^1H NMR (400 MHz, CDCl_3) δ 9.77 (s, 1H), 8.09 (dd, $J = 7.8, 0.6$ Hz, 1H), 7.58 (d, $J = 8.0$ Hz, 1H), 7.42 – 7.35 (m, 3H), 7.33 – 7.27 (m, 3H), 7.24 – 7.21 (m, 1H), 7.15 – 7.02 (m, 5H), 7.01 – 6.98 (m, 1H), 6.77 (dd, $J = 8.0, 1.0$ Hz, 1H). $^{13}\text{C}\{^1\text{H}\}$ NMR (100 MHz, CDCl_3) δ 185.0, 145.6, 142.9, 139.8, 139.6, 138.9, 137.3, 137.2, 134.0, 133.0, 132.7, 131.7, 130.8, 130.3, 129.9, 129.8, 129.7, 129.4, 128.3, 128.2, 127.9, 127.7, 127.0, 126.1, 123.4, 122.7, 121.9, 121.2, 120.1. HR-MS (ESI) m/z calc. for $\text{C}_{29}\text{H}_{18}\text{Br}_2\text{NO}$ $[\text{M}+\text{H}]^+$: 553.9750, found: 553.9756.

4,5-bis(3-chlorophenyl)benzo[4,5]azepino[3,2,1-*hi*]indole-1-carbaldehyde **8-3bd**



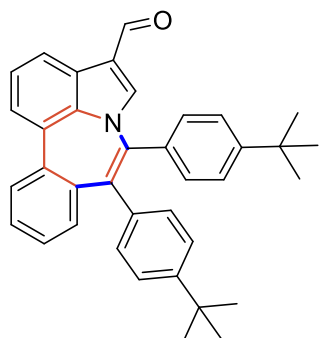
8-3bd was obtained as yellow solid. (60 mg, 65%) M.P.: 249 °C. Purification by column chromatography on silica gel (PE/EA = 10:1). ¹H NMR (400 MHz, CDCl₃) δ 9.74 (s, 1H), 8.10 (dd, *J* = 8.0, 0.4 Hz, 1H), 7.58 (d, *J* = 7.6 Hz, 1H), 7.42 – 7.35 (m, 2H), 7.31 – 7.26 (m, 1H), 7.22 – 7.16 (m, 2H), 7.13 – 7.04 (m, 6H), 7.02 – 6.93 (m, 2H), 6.76 (dd, *J* = 8.0, 0.8 Hz, 1H). ¹³C {¹H} NMR (100 MHz, CDCl₃) δ 184.9, 145.6, 142.6, 139.8, 139.4, 138.9, 137.3, 137.2, 134.6, 133.8, 133.0, 131.0, 130.8, 130.1, 129.8, 129.3, 129.1, 128.8, 128.1, 127.9, 127.7, 126.9, 126.1, 123.4, 121.2, 120.0. HR-MS (ESI) *m/z* calc. for C₂₉H₁₈Cl₂NO [M+H]⁺: 466.0760, found: 466.0760.

4,5-di-*m*-tolylbenzo[4,5]azepino[3,2,1-*hi*]indole-1-carbaldehyde **8-3be**



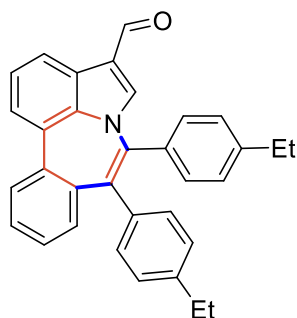
8-3be was obtained as yellow solid. (60 mg, 70%) M.P.: 189 °C. Purification by column chromatography on silica gel (PE/EA = 10:1). ¹H NMR (400 MHz, CDCl₃) δ 9.73 (s, 1H), 8.08 (dd, *J* = 7.8, 1.0 Hz, 1H), 7.57 (d, *J* = 7.3 Hz, 1H), 7.41 – 7.34 (m, 2H), 7.28 – 7.24 (m, 1H), 7.12 (s, 1H), 7.11 – 7.03 (m, 2H), 7.01 – 6.95 (m, 2H), 6.94 – 6.81 (m, 6H), 2.22 (s, 3H), 2.17 (s, 3H). ¹³C {¹H} NMR (100 MHz, CDCl₃) δ 185.0, 145.7, 141.2, 140.6, 140.0, 138.3, 138.2, 137.3, 137.1, 133.2, 131.8, 130.6, 130.4, 129.2, 128.9, 128.8, 128.3, 128.3, 128.0, 127.7, 127.4, 127.0, 127.0, 126.9, 125.8, 123.0, 121.0, 119.5, 21.3, 21.2. HR-MS (ESI) *m/z* calc. for C₃₁H₂₄NO [M+H]⁺: 426.1852, found: 426.1859.

4,5-bis(4-(*tert*-butyl)phenyl)benzo[4,5]azepino[3,2,1-*hi*]indole-1-carbaldehyde **8-3bf**



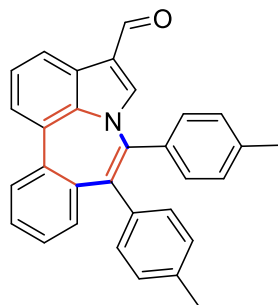
8-3bf was obtained as yellow solid. (90 mg, 88%) M.P.: 209 °C. Purification by column chromatography on silica gel (PE/EA = 10:1). ^1H NMR (400 MHz, CDCl_3) δ 9.74 (s, 1H), 8.09 (dd, $J = 7.8, 1.0$ Hz, 1H), 7.57 (d, $J = 7.4$ Hz, 1H), 7.40 (dd, $J = 8.0, 1.3$ Hz, 1H), 7.36 (t, $J = 7.7$ Hz, 1H), 7.27 – 7.23 (m, 2H), 7.18 – 7.13 (m, 2H), 7.07 – 7.03 (m, 3H), 6.97 – 6.87 (m, 5H), 1.21 (s, 9H), 1.18 (s, 9H). ^{13}C { ^1H } NMR (100 MHz, CDCl_3) δ 185.1, 150.9, 148.8, 145.3, 140.5, 140.0, 138.4, 138.3, 137.2, 135.5, 133.1, 130.7, 130.5, 129.6, 129.2, 128.9, 128.1, 127.7, 127.1, 125.7, 125.1, 124.3, 123.0, 120.9, 119.3, 34.5, 34.3, 31.2, 31.1. HR-MS (ESI) m/z calc. for $\text{C}_{37}\text{H}_{36}\text{NO}$ $[\text{M}+\text{H}]^+$: 510.2791, found: 510.2799.

4,5-bis(4-ethylphenyl)benzo[4,5]azepino[3,2,1-*hi*]indole-1-carbaldehyde **8-3bg**



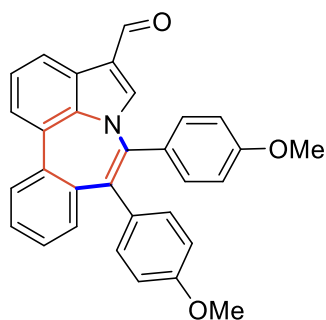
8-3bg was obtained as yellow solid. (49 mg, 54%) M.P.: 123 °C. Purification by column chromatography on silica gel (PE/EA = 10:1). ^1H NMR (400 MHz, CDCl_3) δ 9.71 (s, 1H), 8.10 (dd, $J = 8.0, 0.8$ Hz, 1H), 7.57 (d, $J = 7.6$ Hz, 1H), 7.40 – 7.34 (m, 2H), 7.27 – 7.22 (m, 1H), 7.14 (s, 1H), 7.07 – 6.90 (m, 9H), 6.85 (dd, $J = 8.0, 1.0$ Hz, 1H), 2.53 (dq, $J = 21.3, 7.6$ Hz, 4H), 1.14 (dt, $J = 15.2, 7.6$ Hz, 6H). ^{13}C { ^1H } NMR (100 MHz, CDCl_3) δ 185.0, 145.6, 144.1, 142.0, 140.7, 134.0, 138.7, 138.5, 137.2, 135.8, 133.2, 131.0, 130.5, 129.7, 129.1, 128.9, 128.0, 127.9, 127.6, 127.0, 126.9, 125.7, 122.9, 120.9, 119.4, 28.4, 28.3, 15.3, 15.2. HR-MS (ESI) m/z calc. for $\text{C}_{33}\text{H}_{28}\text{NO}$ $[\text{M}+\text{H}]^+$: 454.2165, found: 454.2170.

4,5-di-*p*-tolylbenzo[4,5]azepino[3,2,1-*hi*]indole-1-carbaldehyde **8-3bh**



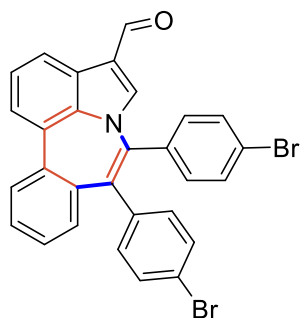
8-3bh was obtained as yellow solid. (43 mg, 51%) M.P.: 200°C. Purification by column chromatography on silica gel (PE/EA = 10:1). ^1H NMR (400 MHz, CDCl_3) δ 9.71 (s, 1H), 8.09 (dd, $J = 8.0, 0.8$ Hz, 1H), 7.57 (d, $J = 7.6$ Hz, 1H), 7.36 (t, $J = 7.7$ Hz, 2H), 7.28 – 7.22 (m, 1H), 7.09 (s, 1H), 7.06 – 6.89 (m, 9H), 6.82 (dd, $J = 8.0, 0.8$ Hz, 1H), 2.27 (s, 3H), 2.21 (s, 3H). $^{13}\text{C}\{^1\text{H}\}$ NMR (100 MHz, CDCl_3) δ 185.0, 145.7, 140.7, 139.9, 138.5, 137.9, 137.3, 135.7, 135.7, 133.1, 130.9, 130.5, 129.6, 129.2, 129.1, 128.8, 128.4, 128.0, 127.6, 126.9, 125.7, 122.9, 120.9, 119.4, 21.2, 21.1. HR-MS (ESI) m/z calc. for $\text{C}_{31}\text{H}_{24}\text{NO}$ $[\text{M}+\text{H}]^+$: 426.1852, found: 426.1853.

4,5-bis(4-methoxyphenyl)benzo[4,5]azepino[3,2,1-*hi*]indole-1-carbaldehyde **8-3bi**



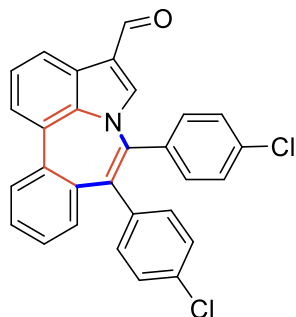
8-3bi was obtained as yellow solid. (64 mg, 70%) M.P.: 135 °C. Purification by column chromatography on silica gel (PE/EA = 8:1). ^1H NMR (400 MHz, CDCl_3) δ 9.73 (s, 1H), 8.08 (dd, $J = 7.8, 0.9$ Hz, 1H), 7.57 (d, $J = 7.4$ Hz, 1H), 7.39 – 7.33 (m, 2H), 7.28 – 7.22 (m, 1H), 7.11 (s, 1H), 7.07 – 7.02 (m, 1H), 7.02 – 6.94 (m, 4H), 6.82 (dd, $J = 8.0, 1.3$ Hz, 1H), 6.76 – 6.71 (m, 2H), 6.69 – 6.61 (m, 2H), 3.76 (s, 3H), 3.71 (s, 3H). $^{13}\text{C}\{^1\text{H}\}$ NMR (100 MHz, CDCl_3) δ 185.0, 158.9, 157.7, 145.7, 140.7, 139.9, 138.6, 137.3, 134.0, 133.1, 132.1, 131.2, 131.1, 130.5, 129.2, 128.8, 128.0, 127.6, 126.9, 125.7, 122.9, 120.9, 119.4, 113.9, 113.1, 55.0. HR-MS (ESI) m/z calc. for $\text{C}_{31}\text{H}_{24}\text{NO}_3$ $[\text{M}+\text{H}]^+$: 458.1751, found: 458.1755.

4,5-bis(4-bromophenyl)benzo[4,5]azepino[3,2,1-*hi*]indole-1-carbaldehyde **8-3bj**



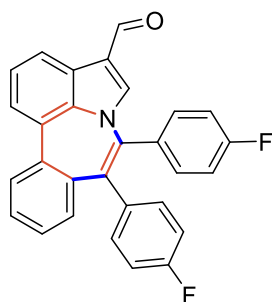
8-3bj was obtained as yellow solid. (77 mg, 70%) M.P.: 160 °C. Purification by column chromatography on silica gel (PE/EA = 10:1). ^1H NMR (400 MHz, CDCl_3) δ 9.75 (s, 1H), 8.09 (dd, $J = 8.0, 0.8$ Hz, 1H), 7.57 (d, $J = 7.5$ Hz, 1H), 7.43 – 7.35 (m, 4H), 7.31 – 7.25 (m, 3H), 7.09 – 7.02 (m, 2H), 7.01 – 6.91 (m, 4H), 6.72 (dd, $J = 8.0, 1.2$ Hz, 1H). $^{13}\text{C}\{^1\text{H}\}$ NMR (100 MHz, CDCl_3) δ 184.9, 145.8, 140.0, 139.9, 139.0, 137.5, 137.4, 136.9, 133.0, 132.7, 132.2, 131.4, 131.2, 130.8, 129.7, 128.3, 127.8, 127.8, 126.9, 126.0, 123.3, 122.9, 121.2, 120.9, 120.1. HR-MS (ESI) m/z calc. for $\text{C}_{29}\text{H}_{18}\text{Br}_2\text{NO}$ $[\text{M}+\text{H}]^+$: 553.9750, found: 553.9759.

4,5-bis(4-chlorophenyl)benzo[4,5]azepino[3,2,1-*hi*]indole-1-carbaldehyde **8-3bk**



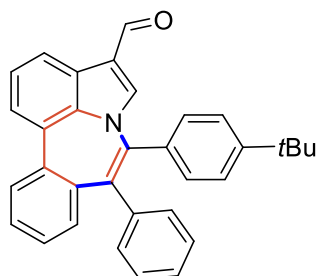
8-3bk was obtained as yellow solid. (62 mg, 67%) M.P.: 260 °C. Purification by column chromatography on silica gel (PE/EA = 10:1). ^1H NMR (400 MHz, CDCl_3) δ 9.75 (s, 1H), 8.09 (dd, $J = 7.8, 0.9$ Hz, 1H), 7.57 (d, $J = 7.5$ Hz, 1H), 7.41 – 7.35 (m, 2H), 7.31 – 7.25 (m, 1H), 7.25 – 7.20 (m, 2H), 7.14 – 7.10 (m, 2H), 7.09 – 7.05 (m, 1H), 7.05 – 6.99 (m, 5H), 6.73 (dd, $J = 8.0, 1.2$ Hz, 1H). $^{13}\text{C}\{^1\text{H}\}$ NMR (100 MHz, CDCl_3) δ 184.9, 145.8, 139.9, 139.6, 139.1, 137.5, 137.4, 136.5, 134.6, 133.0, 132.7, 132.4, 131.1, 130.8, 129.7, 129.2, 128.3, 128.3, 127.8, 127.8, 127.0, 126.0, 123.3, 121.2, 120.0. HR-MS (ESI) m/z calc. for $\text{C}_{29}\text{H}_{18}\text{Cl}_2\text{NO}$ $[\text{M}+\text{H}]^+$: 466.0760, found: 466.0762.

4,5-bis(4-fluorophenyl)benzo[4,5]azepino[3,2,1-*hi*]indole-1-carbaldehyde **8-3bl**



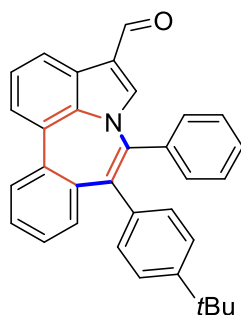
8-3bl was obtained as yellow solid. (69 mg, 80%) M.P.: 181 °C. Purification by column chromatography on silica gel (PE/EA = 10:1). ¹H NMR (400 MHz, CDCl₃) δ 9.74 (s, 1H), 8.09 (dd, *J* = 7.8, 1.0 Hz, 1H), 7.57 (d, *J* = 7.4 Hz, 1H), 7.42 – 7.33 (m, 2H), 7.31 – 7.26 (m, 1H), 7.14 – 6.98 (m, 6H), 6.97 – 6.89 (m, 2H), 6.87 – 6.79 (m, 2H), 6.77 (dd, *J* = 8.1, 1.2 Hz, 1H). ¹³C{¹H} NMR (100 MHz, CDCl₃) δ 184.9, 163.3, 162.4, 160.8, 160.0, 145.7, 140.0, 139.3, 137.8, 137.3, 137.2, 137.1, 134.4, 134.4, 133.0, 132.7, 132.6, 131.7, 131.7, 130.7, 129.6, 128.5, 127.8, 127.8, 127.0, 126.0, 123.3, 121.1, 119.9, 116.1, 115.9, 115.1, 114.9. ¹⁹F NMR (500 MHz, CDCl₃) δ -112.4, -116.0. HR-MS (ESI) *m/z* calc. for C₂₉H₁₈F₂NO [M+H]⁺: 434.1351, found: 434.1357.

4-(4-(*tert*-butyl)phenyl)-5-phenylbenzo[4,5]azepino[3,2,1-*hi*]indole-1-carbaldehyde **8-3bm**



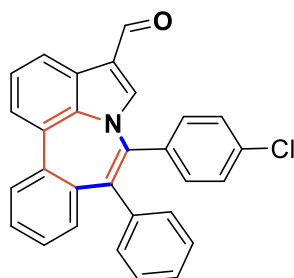
8-3bm was obtained as yellow solid. (40 mg, 44%) M.P.: 231 °C. Purification by column chromatography on silica gel (PE/EA = 9:1). ¹H NMR (400 MHz, CDCl₃) δ 9.71 (s, 1H), 8.08 (dd, *J* = 7.8, 1.0 Hz, 1H), 7.58 (d, *J* = 7.6 Hz, 1H), 7.39 (dd, *J* = 7.6, 1.4 Hz, 1H), 7.36 (d, *J* = 7.7 Hz, 1H), 7.28 – 7.23 (m, 1H), 7.21 – 7.15 (m, 3H), 7.11 (s, 1H), 7.09 – 7.03 (m, 5H), 6.99 – 6.96 (m, 2H), 6.86 (dd, *J* = 8.0, 1.2 Hz, 1H), 1.19 (s, 9H). ¹³C{¹H} NMR (100 MHz, CDCl₃) δ 185.0, 149.1, 145.7, 140.5, 139.9, 138.5, 138.4, 138.2, 137.3, 133.2, 131.1, 130.7, 130.6, 129.9, 129.3, 129.0, 128.5, 128.1, 128.0, 127.7, 127.6, 125.8, 124.5, 123.0, 121.0, 119.5, 34.3, 31.2. HR-MS (ESI) *m/z* calc. for C₃₃H₂₈NO [M+H]⁺: 454.2165, found: 454.2169.

5-(4-(*tert*-butyl)phenyl)-4-phenylbenzo[4,5]azepino[3,2,1-*hi*]indole-1-carbaldehyde
8-3bm'



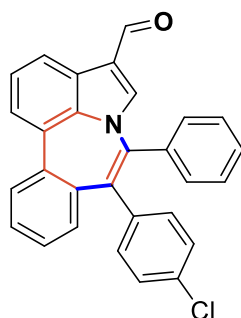
8-3bm' was obtained as yellow solid. (18 mg, 20%) M.P.: 234 °C. Purification by column chromatography on silica gel (PE/EA = 10:1). ^1H NMR (400 MHz, CDCl_3) δ 9.74 (s, 1H), 8.08 (d, $J = 7.7$ Hz, 1H), 7.57 (d, $J = 7.7$ Hz, 1H), 7.37 (q, $J = 7.4$ Hz, 2H), 7.28 – 7.23 (m, 1H), 7.22 – 7.16 (m, 3H), 7.09 – 7.00 (m, 6H), 6.97 (d, $J = 8.2$ Hz, 2H), 6.80 (d, $J = 8.0$ Hz, 1H), 1.23 (s, 9H). ^{13}C $\{^1\text{H}\}$ NMR (100 MHz, CDCl_3) δ 185.1, 151.2, 141.6, 140.6, 140.2, 137.3, 135.4, 133.2, 131.1, 130.6, 129.5, 129.3, 128.9, 128.1, 127.7, 127.6, 127.1, 126.1, 125.8, 125.4, 123.0, 121.0, 119.5, 34.6, 31.1. HR-MS (ESI) m/z calc. for $\text{C}_{33}\text{H}_{28}\text{NO}$ $[\text{M}+\text{H}]^+$: 454.2165, found: 454.2172.

4-(4-chlorophenyl)-5-phenylbenzo[4,5]azepino[3,2,1-*hi*]indole-1-carbaldehyde **8-3bn**



8-3bn was obtained as yellow solid. (28 mg, 33%) M.P.: 174°C. Purification by column chromatography on silica gel (PE/EA = 10:1). ^1H NMR (400 MHz, CDCl_3) δ 9.71 (s, 1H), 8.09 (dd, $J = 7.8, 1.0$ Hz, 1H), 7.58 (d, $J = 7.6$ Hz, 1H), 7.41 – 7.35 (m, 2H), 7.31 – 7.21 (m, 4H), 7.13 – 6.99 (m, 8H), 6.74 (d, $J = 7.9$ Hz, 1H). ^{13}C $\{^1\text{H}\}$ NMR (100 MHz, CDCl_3) δ 185.0, 145.7, 140.4, 140.4, 139.9, 138.1, 137.9, 137.4, 133.0, 132.5, 132.3, 130.7, 129.7, 129.5, 128.9, 128.5, 128.0, 127.9, 127.8, 127.7, 127.0, 125.9, 123.2, 121.1, 119.8. HR-MS (ESI) m/z calc. for $\text{C}_{29}\text{H}_{19}\text{ClNO}$ $[\text{M}+\text{H}]^+$: 432.1150, found: 432.1155.

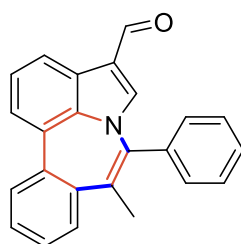
5-(4-chlorophenyl)-4-phenylbenzo[4,5]azepino[3,2,1-*hi*]indole-1-carbaldehyde **8-3bn'**



8-3bn' was obtained as yellow solid. (22 mg, 25%) M.P.: 171°C. Purification by column chromatography on silica gel (PE/EA = 11:1). ¹H NMR (400 MHz, CDCl₃) δ 9.74 (s, 1H), 8.09 (dd, *J* = 7.8, 1.1 Hz, 1H), 7.58 (d, *J* = 7.8 Hz, 1H), 7.43 – 7.34 (m, 2H), 7.29 – 7.24 (m, 1H), 7.20 – 6.99 (m, 11H), 6.81 (dd, *J* = 8.1, 1.3 Hz, 1H). ¹³C{¹H} NMR (100 MHz, CDCl₃) δ 184.9, 145.8, 141.0, 140.0, 138.7, 137.9, 137.3, 136.8, 134.3, 133.2, 131.3, 131.0, 130.7, 129.6, 129.0, 128.0, 127.8, 126.9, 126.7, 126.0, 123.2, 121.1, 119.9, 115.3. HR-MS (ESI) *m/z* calc. for C₂₉H₁₉ClNO [M+H]⁺: 432.1150, found: 432.1159.

9.4.6. Results of the synthesis of 8-3bo

5-methyl-4-phenylbenzo[4,5]azepino[3,2,1-*hi*]indole-1-carbaldehyde **8-3bo**



The electrooxidative rhodium-catalyzed C-H/N-H annulation reaction was followed using **8-1a** (0.2 mmol), **8-2a** (0.4 mmol), [Cp**RhCl*₂]₂ (2.5 mmol%), Li₂CO₃ (2.0 equiv) in 1,4-Dioxane (3 mL) and H₂O (1 mL) at 100°C for 6 h. However, the desired products were difficult to separate in pure form (Fig. 2-S1) from the unknown side-product because they have the same R_f value (Fig. 2-S2). *m/z* = 308.1053 was observed for unknown side product (Fig. 2-S3). The corresponding products were produced in 16% NMR yields, and the conventional reoxidation strategy ([Cp**RhCl*₂]₂/Ag₂CO₃) resulted a trace yield.

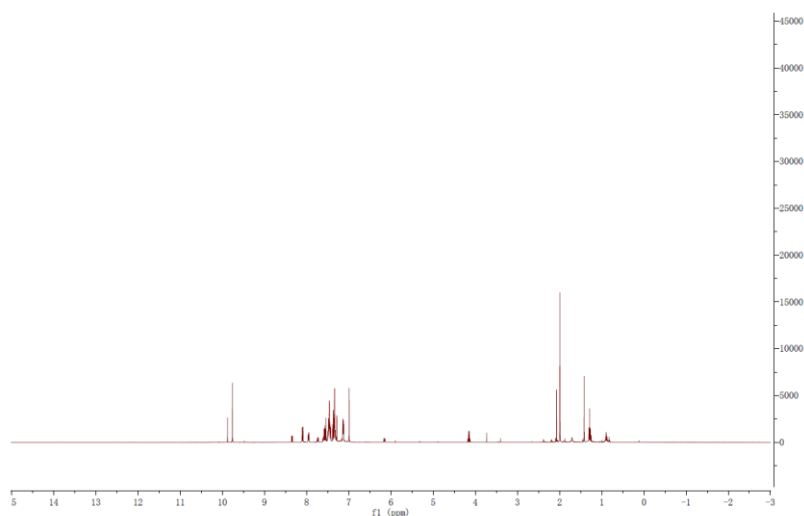
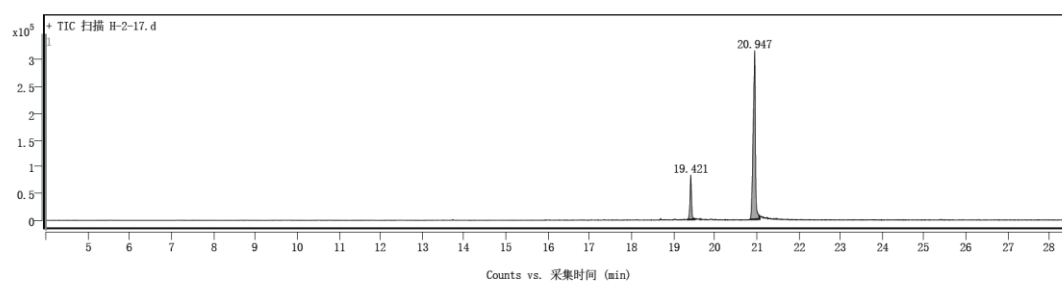


Figure S8-1. copy of ¹H NMR of the separated products



Figure S8-2. TLC result of the separated products



色谱峰	峰	起始	RT	终止	峰高	面积	面积 %	SNR
1	19.351	19.421	19.421	19.517	82905	209585	17.57	
2	20.832	20.947	20.947	21.063	314369	1192895	100.00	

样品谱图

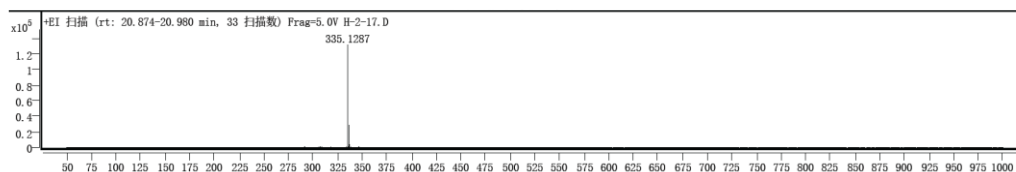
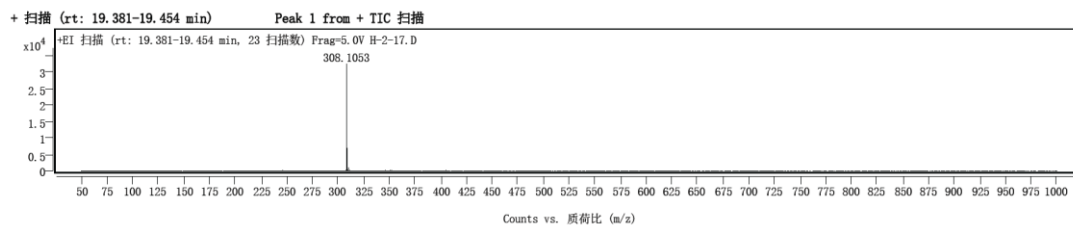
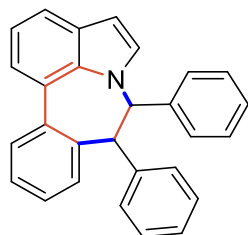


Figure S8-3. GC-HRMS analysis of the separated products

7.4.7. Characterization Data of synthetic transformation products 8-4aa

Under Ar atmosphere, and followed using the general procedure **8-3aa** (0.5mmol), Pd(OAc)₂ (8 mmol%), molecular sieves (4 Å) (150 mg) in cyclohexane (1.5 mL) at 130°C for 5 h. Purification by column chromatography on silica gel (PE/EA = 500:1).

4,5-diphenyl-4,5-dihydrobenzo[4,5]azepino[3,2,1-*hi*]indole **8-4aa**

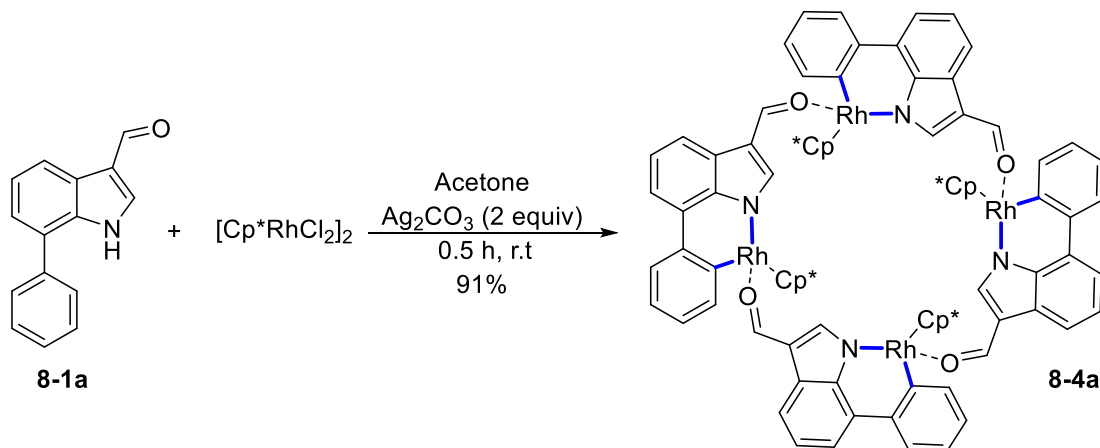


8-4aa was obtained as yellow solid. (61 mg, 82%) M.P.: 165 °C. ¹H NMR (400 MHz, CDCl₃) δ 7.41 (d, *J* = 7.5 Hz, 1H), 7.35 – 7.31 (m, 2H), 7.24 – 6.98 (m, 15H), 6.77 (d, *J* = 8.0 Hz, 1H), 6.47 (d, *J* = 3.5 Hz, 1H), 6.26 (d, *J* = 3.4 Hz, 1H). ¹³C {¹H} NMR (100 MHz, CDCl₃) δ 146.6, 142.0, 141.8, 139.6, 139.3, 138.6, 132.7, 131.6, 130.9, 130.8, 130.5, 129.8, 128.7, 128.4, 128.1, 127.5, 127.5, 127.3, 125.9, 125.3, 123.6, 121.1, 119.7, 104.7. HR-MS (ESI) *m/z* calc. for C₂₈H₂₂N [M+H]⁺: 372.1747, found: 372.1759.

9.4.8. Mechanistic Studies

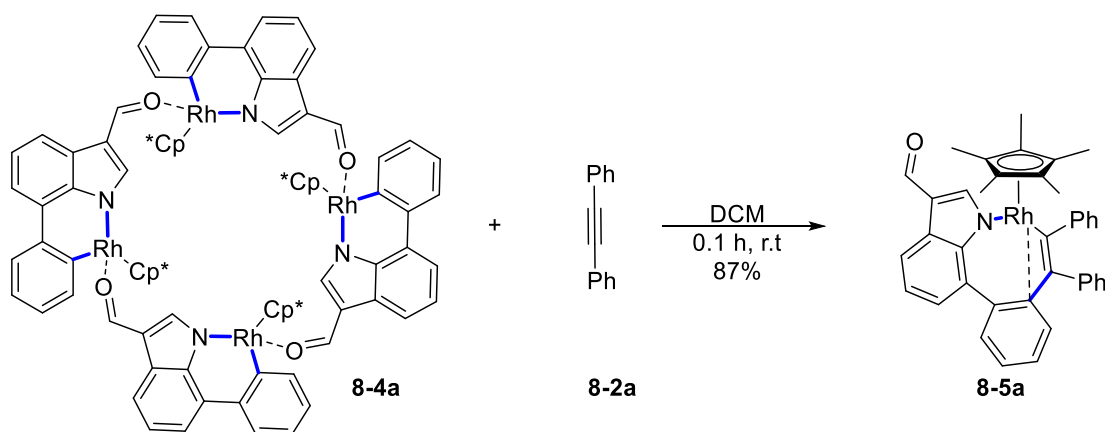
1) Synthesis of Rhodium Complexes **8-(4a, 5a)**

A 30 mL Schlenk tube was charged with **8-1a** (44 mg, 0.2 mmol), [Cp*₂RhCl₂]₂ (61 mg, 0.1 mmol) and Ag₂CO₃ (2.0 equiv) in Acetone (5 mL) at room temperature for 0.5 h. Red precipitate appears rapidly in the reaction, and washed with large amount of Acetone and Ether, the solid was dissolved in DCM and filtered to remove excess Ag₂CO₃.



The filtrate was concentrated under vacuo to yield **8-4a** (42 mg, 91%) as red solid. ^1H NMR (400 MHz, CDCl_3) δ 8.03 (d, $J = 7.2$ Hz, 4H), 7.93 (s, 4H), 7.80 (dd, $J = 8.0, 1.2$ Hz, 4H), 7.74 (d, $J = 7.4$ Hz, 4H), 7.64 (dd, $J = 7.5, 1.2$ Hz, 4H), 7.49 (s, 4H), 7.26 (d, $J = 15.2$ Hz, 4H), 7.06 – 7.00 (m, 4H), 6.91 – 6.85 (m, 4H), 1.24 (s, 60H). $^{13}\text{C}\{^1\text{H}\}$ NMR (101 MHz, CDCl_3) δ 185.5, 166.3, 166.0, 156.1, 142.3, 138.9, 136.8, 129.9, 127.2, 126.1, 124.2, 123.0, 122.4, 121.6, 119.8, 117.7, 94.8, 94.7, 8.9. HR-MS (ESI) m/z calc. for $\text{C}_{100}\text{H}_{96}\text{N}_4\text{O}_4\text{Rh}_4$ $[\text{M}+\text{H}]^+$: 1829.3725, found: 1829.3724.

A 30 mL Schlenk tube was charged with **8-4a** (91 mg, 0.2 mmol), **8-2a** (36 mg, 2.0 equiv) in DCM (5 mL) at room temperature for 0.1 h. After removal of the solvent in vacuum, purified by column chromatography on silica gel (PE/EtOAc = 1:1) yielded **8-5a** (111 mg, 87%) as deep red solid which was stable in air.



^1H NMR (400 MHz, CDCl_3) δ 10.02 (s, 1H), 8.17 (s, 1H), 7.91 (s, 1H), 7.81 (t, $J = 7.4$ Hz, 1H), 7.63 (t, $J = 7.2$ Hz, 1H), 7.48 (dd, $J = 16.1, 7.6$ Hz, 2H), 7.22 (t, $J = 7.5$ Hz, 2H), 7.13 (t, $J = 7.3$ Hz, 1H), 7.03 (t, $J = 7.5$ Hz, 1H), 6.83 – 6.72 (m, 6H), 6.25 – 6.16 (m, 2H), 1.16 (s, 15H). $^{13}\text{C}\{^1\text{H}\}$ NMR (101 MHz, CDCl_3) δ 182.3, 156.8, 156.6, 150.3, 150.3, 147.9, 144.0, 140.6, 138.5, 131.5, 129.9, 128.1, 127.2, 126.8, 126.7, 125.6, 125.5, 125.1, 121.8, 121.1, 107.0, 95.3, 95.2, 8.8. HR-MS (ESI) m/z calc. for $\text{C}_{39}\text{H}_{35}\text{NORh}$ $[\text{M}+\text{H}]^+$: 636.1768, found: 636.1772.

2) Reductive Elimination of **8-5a**

A standard NMR tube was charged with **8-5a** (45 mg, 0.1 mmol), the tube was evacuated and purged with N_2 for three times. Then fill the tube with $\text{DMSO}-d_6$ (0.7 mL) using a syringe. The NMR tube was then placed in a metal bath at 130°C for 0.5 h. Then cooled to temperature, and subjected to ^1H NMR spectroscopy. Compared with the ^1H NMR spectra before heating and found no change in **8-5a**.

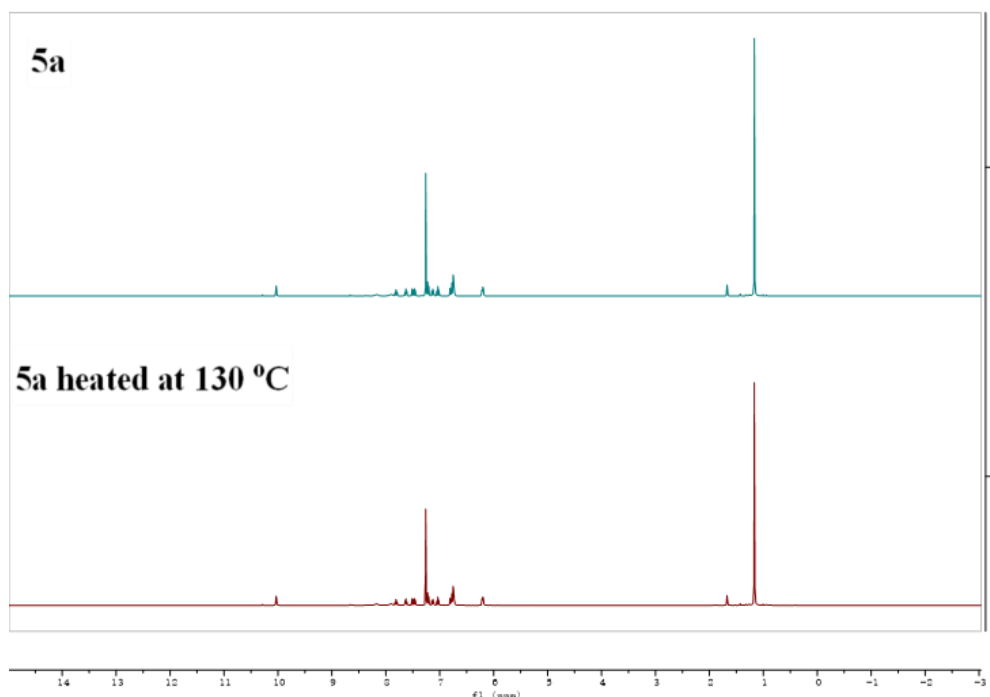
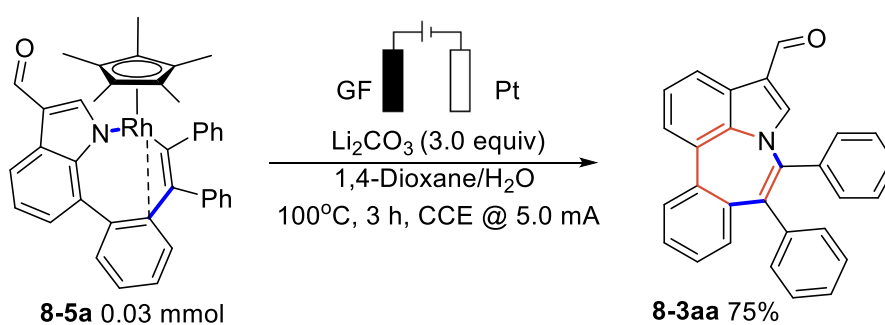
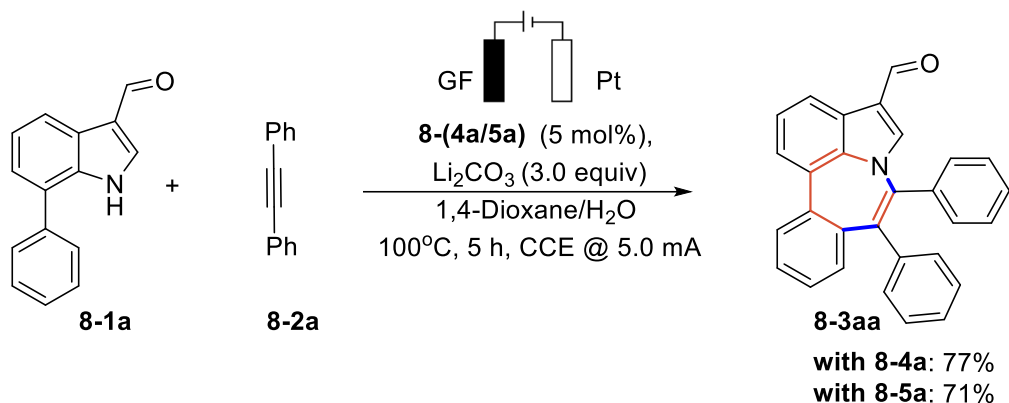


Figure S8-4



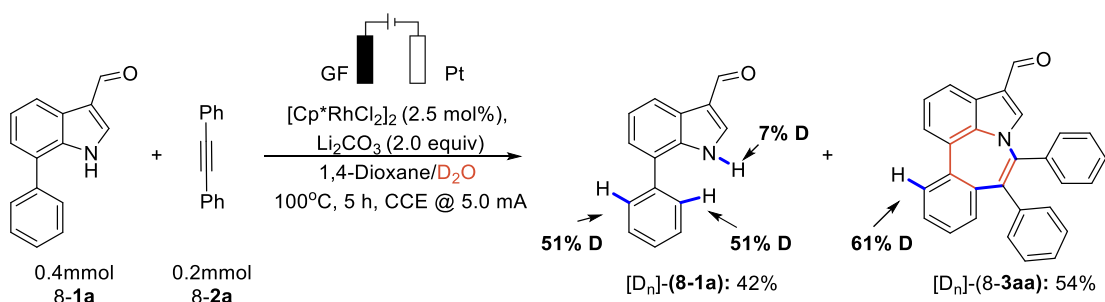
A 15 mL Schlenk tube was charged with **8-5a** (19 mg, 0.03 mmol) and Li_2CO_3 (15 mg, 0.2 mmol). The tube was evacuated and filled with N_2 three times. Then, 1,4-Dioxane/ H_2O =3/1 (4 mL) was added and the mixture was electrolyzed at a constant current of 5 mA for 3 h at ambient temperature 100°C. (GF anode, (10mm × 15 mm × 6 mm) and a platinum cathode (10 mm × 15 mm × 0.25 mm). The solvent was removed *in vacuo* and dibromomethane was added as standard. Then, the residue was dissolved in CDCl_3 (0.7 mL) and subjected to ^1H NMR spectroscopy.

3) Catalytic reactions with **8-(4a / 5a)**



A 15 mL Schlenk tube was charged with **8-1a** (44 mg, 0.2 mmol), **8-2a** (71 mg, 0.4 mmol) and Li_2CO_3 (3.0 equiv). **8-4a** (5 mol%) and **8-5a** (5 mol%) were added as the catalyst, respectively. The tube was evacuated and filled with N_2 three times. Then, 1,4-Dioxane/ H_2O =3/1 (4 mL) was added and the mixture was electrolyzed at a constant current of 5 mA at ambient temperature 100°C for 5 h. (GF anode, (10mm \times 15 mm \times 6 mm) and a platinum cathode (10 mm \times 15 mm \times 0.25 mm). The volatiles were removed under reduced pressure, and the residue was subjected to silica gel column chromatography [eluting with petroleum ether (PE)/ethyl acetate (EA)] to afford the corresponding product.

4) H/D Exchange Experiment



In an undivided cell equipped with a GF anode (10 mm \times 15 mm \times 6 mm) and a platinum cathode (10 mm \times 15 mm \times 0.25 mm), **8-1a** (44 mg, 0.2 mmol), **8-2a** (18 mg, 0.1 mmol), $[\text{Cp}^*\text{RhCl}_2]_2$ (2.5 mmol%), Li_2CO_3 (2.0 equiv) were all dissolved in 1,4-

Dioxane (3 mL) and D₂O (1 mL) at 100°C for 5 h. Electrocatalysis was performed with a constant current of 5.0 mA. Evaporation of the solvent and subsequent column chromatography (PE/EA = 10:1 → 2:1) yielded [D_n]- (**8-1a**) (19 mg, 42%) as a yellow solid and [D_n]- (**8-3aa**) (22 mg, 54%) as a white solid. The D-incorporation was estimated by ¹H NMR spectroscopy.

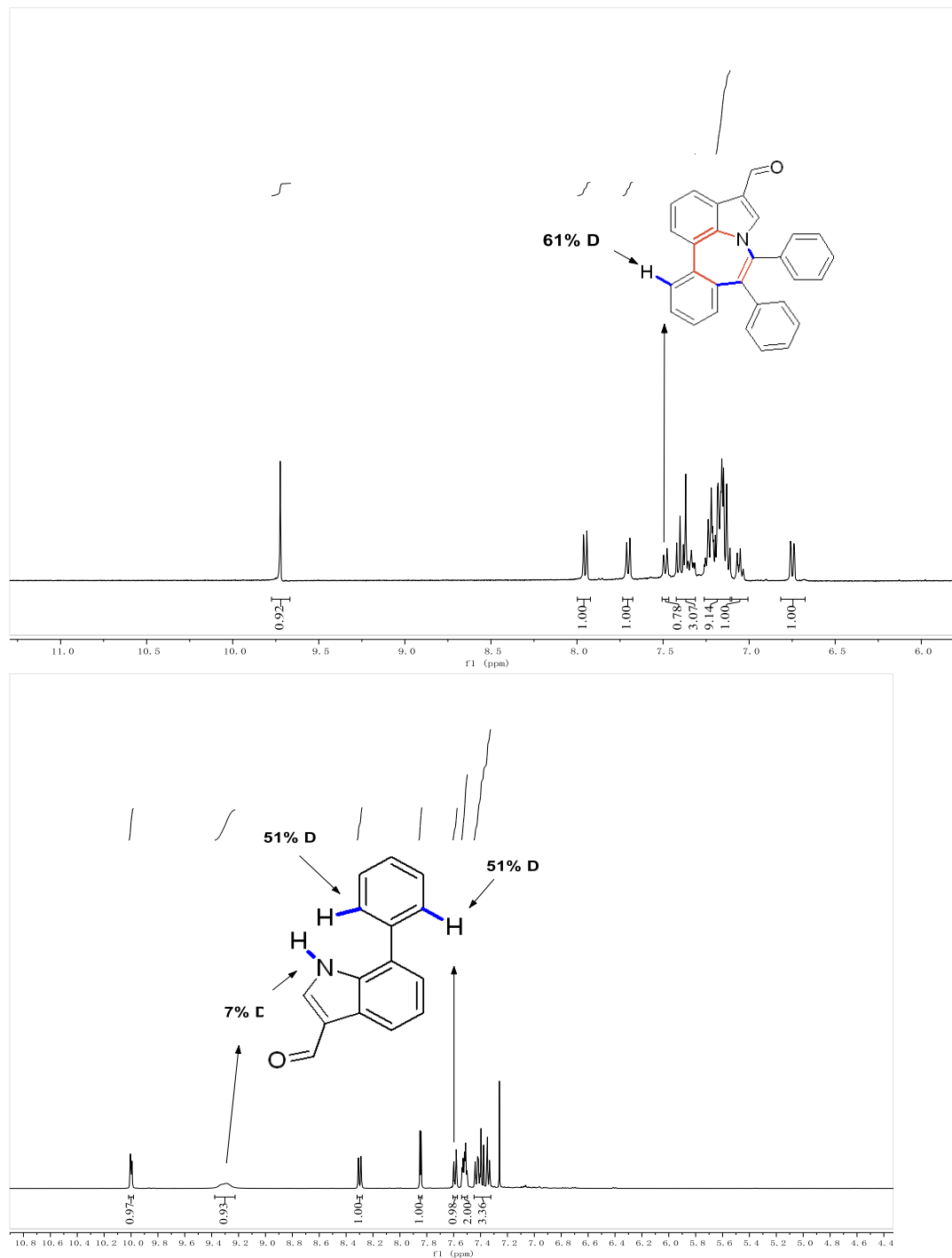
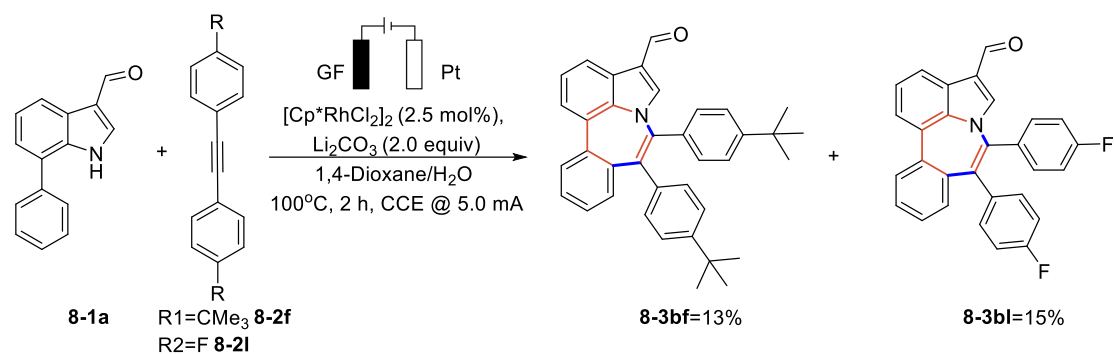
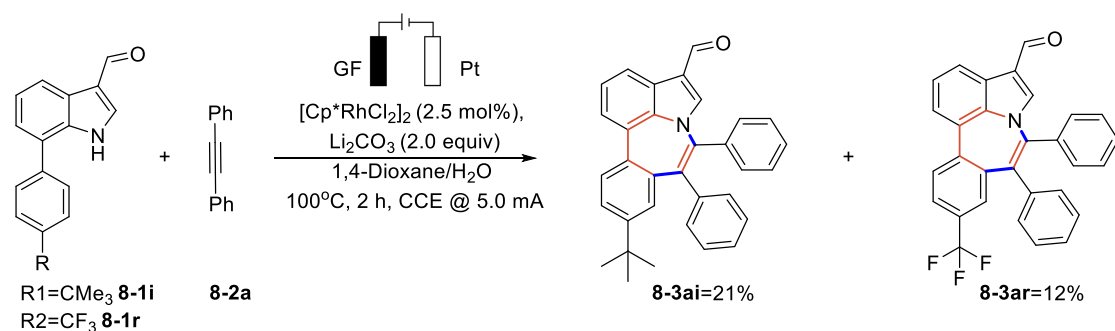


Figure S8-5

5) Competition Experiments



The general procedure was followed using **8-1a** (44 mg, 0.2 mmol), **8-2f** (58 mg, 0.2 mmol), **8-2l** (43 mg, 0.2 mmol), $[\text{Cp}^*\text{RhCl}_2]_2$ (2.5 mmol%), and Li_2CO_3 (2.0 equiv) all dissolved in 1,4-Dioxane (3 mL) and H_2O (1 mL) at 100°C for 2 h. Electrocatalysis was performed with a constant current of 5.0 mA. Evaporation of the solvent and subsequent column chromatography (PE/EA = 10:1), **8-3bf** (13 mg, 13%) and **8-3bl** (13 mg, 15%) were then isolated as yellow solids.



The general procedure was followed using **8-1i** (28 mg, 0.1 mmol), **8-1r** (29 mg, 0.1 mmol), **8-2a** (71 mg, 0.4 mmol), $[\text{Cp}^*\text{RhCl}_2]_2$ (2.5 mmol%), and Li_2CO_3 (2.0 equiv.) all dissolved in 1,4-Dioxane (3 mL) and H_2O (1 mL) at 100°C for 2 h. Electrocatalysis was performed with a constant current of 5.0 mA. Evaporation of the solvent and subsequent column chromatography (PE/EA = 10:1), **8-3ai** (19 mg, 21%) and **8-3ar** (11 mg, 12%) were then isolated, respectively.

6) Proposed mechanism

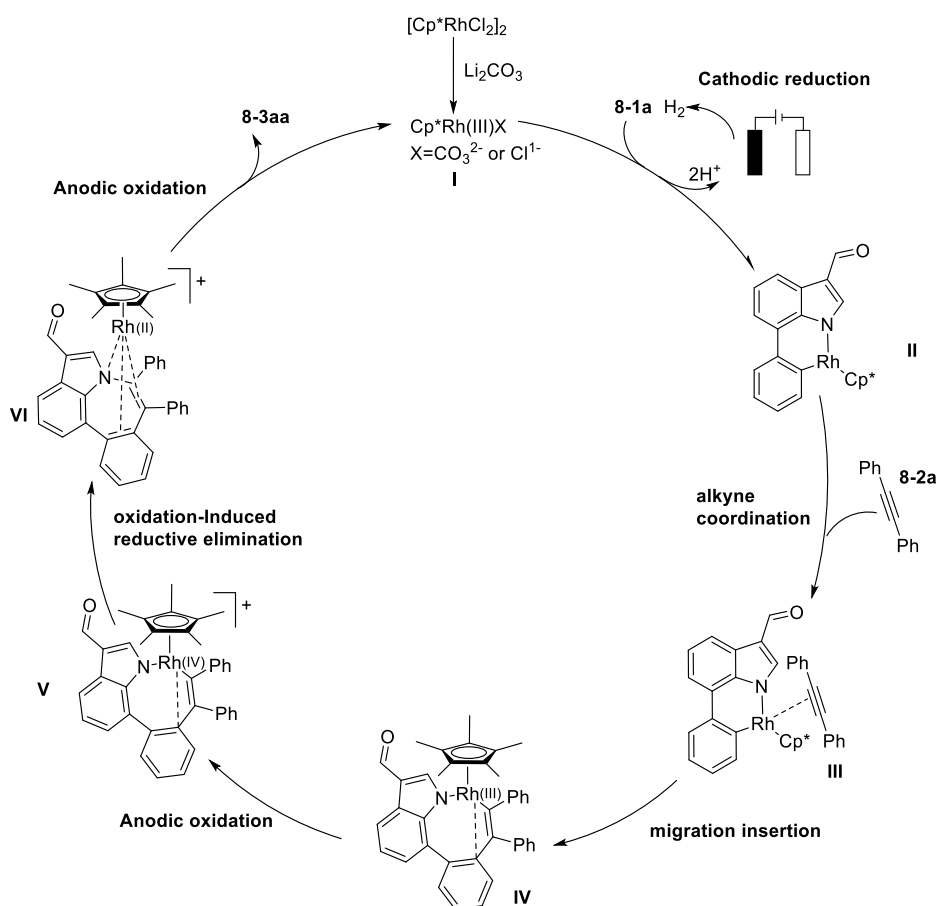


Figure S8-6: Proposed catalytic cycle

9.4.9. X-Ray Crystallographic Analysis

The detailed crystallographic data and structure refinement parameters for these compounds are summarized in **Table S1-S4**. CCDC 2045896, 2110757, 2110456 and 2110326 contain the supplementary crystallographic data for this paper. These data can be obtained free of charge from The Cambridge Crystallographic Data Centre via www.ccdc.cam.ac.uk/data_request/cif.

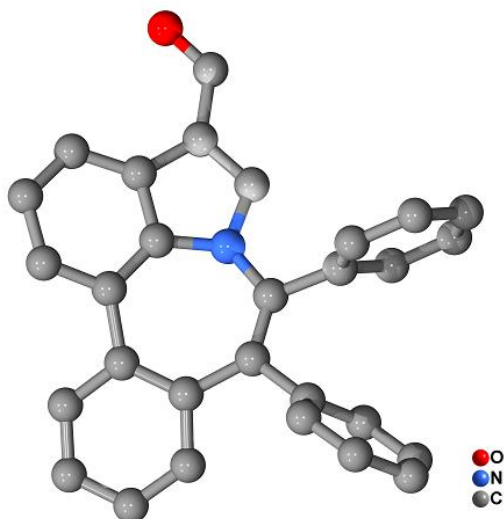


Table S8-1. 8-3aa CCDC 2045896

Identification code	yym-IV
Empirical formula	C ₂₉ H ₁₉ NO
Formula weight	397.45
Temperature/K	187(50)
Crystal system	monoclinic
Space group	P2 ₁ /n
a/Å	13.4735(3)
b/Å	9.2079(2)
c/Å	16.8922(4)
α/°	90
β/°	107.205(3)
γ/°	90
Volume/Å ³	2001.91(8)
Z	4
ρ _{calc} /cm ³	1.319
μ/mm ⁻¹	0.619
F(000)	832.0
Crystal size/mm ³	0.2 × 0.1 × 0.1

Radiation	CuK α ($\lambda = 1.54184$)
2 Θ range for data collection/ $^\circ$	7.412 to 145.604
Index ranges	$-16 \leq h \leq 14$, $-11 \leq k \leq 10$, $-20 \leq l \leq 20$
Reflections collected	11377
Independent reflections	3910 [$R_{\text{int}} = 0.0175$, $R_{\text{sigma}} = 0.0159$]
Data/restraints/parameters	3910/0/280
Goodness-of-fit on F^2	1.066
Final R indexes [$I \geq 2\sigma(I)$]	$R_1 = 0.0393$, $wR_2 = 0.1012$
Final R indexes [all data]	$R_1 = 0.0417$, $wR_2 = 0.1043$
Largest diff. peak/hole / $e \text{ \AA}^{-3}$	0.22/-0.26

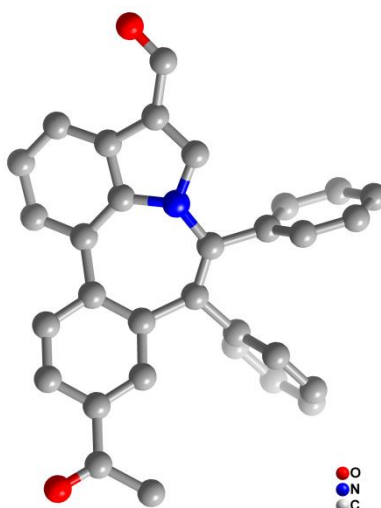


Table S8-2. 8-3ap CCDC 2110757

Identification code	exp_9954
Empirical formula	$C_{31}H_{21}NO_2$
Formula weight	439.49
Temperature/K	149.99(10)
Crystal system	monoclinic
Space group	$P2_1/c$

a/Å	11.4138(4)
b/Å	12.0291(4)
c/Å	20.3978(6)
α /°	90
β /°	105.727(3)
γ /°	90
Volume/Å ³	2695.73(16)
Z	4
ρ_{calc} /cm ³	1.083
μ /mm ⁻¹	0.531
F(000)	920.0
Crystal size/mm ³	0.2 × 0.2 × 0.15
Radiation	CuK α (λ = 1.54184)
2 Θ range for data collection/°	8.62 to 145.908
Index ranges	-14 ≤ h ≤ 11, -14 ≤ k ≤ 14, -21 ≤ l ≤ 25
Reflections collected	10369
Independent reflections	5206 [R_{int} = 0.0339, R_{sigma} = 0.0336]
Data/restraints/parameters	5206/0/308
Goodness-of-fit on F ²	1.073
Final R indexes [$I \geq 2\sigma(I)$]	R_1 = 0.0782, wR_2 = 0.2593
Final R indexes [all data]	R_1 = 0.0825, wR_2 = 0.2663
Largest diff. peak/hole / e Å ⁻³	0.50/-0.60

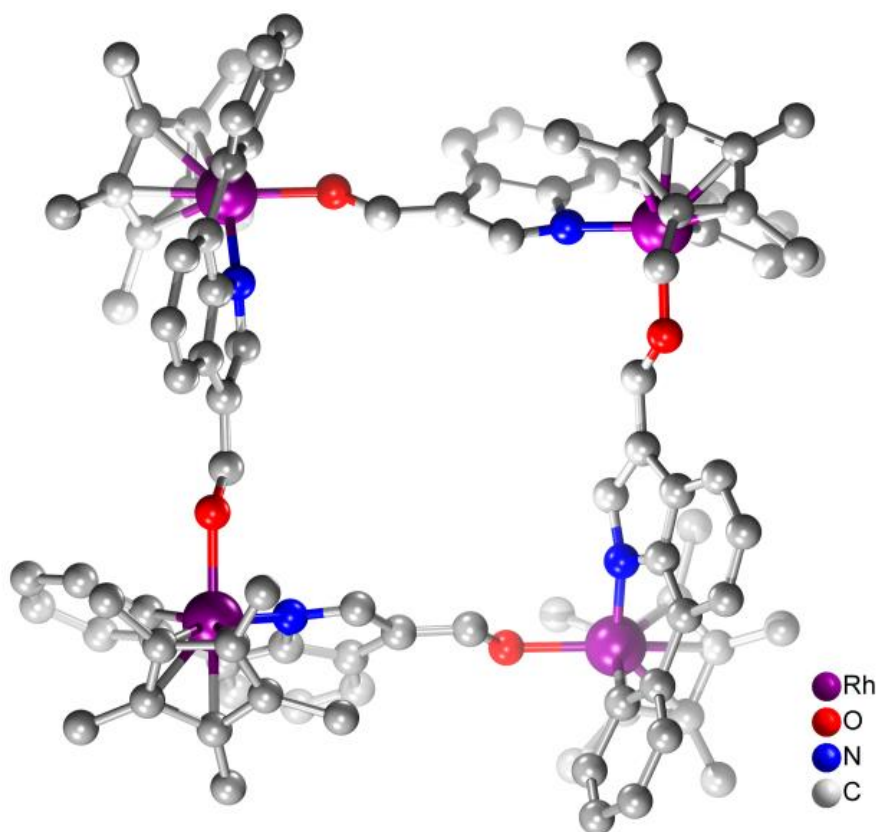


Table S8-3. 8-4a CCDC 2110456

Identification code	yz-73
Empirical formula	C ₂₄ H ₂₄ NO ₂ Rh
Formula weight	461.35
Temperature/K	181(40)
Crystal system	cubic
Space group	I-43d
a/Å	33.3930(4)
b/Å	33.3930(4)
c/Å	33.3930(4)
α /°	90
β /°	90
γ /°	90
Volume/Å ³	37236.3(13)

Z	48
$\rho_{\text{calc}}/\text{cm}^3$	0.988
μ/mm^{-1}	4.545
F(000)	11328.0
Crystal size/ mm^3	$0.03 \times 0.03 \times 0.03$
Radiation	CuK α ($\lambda = 1.54184$)
2 Θ range for data collection/ $^\circ$	6.484 to 146.014
Index ranges	$-24 \leq h \leq 39, -24 \leq k \leq 38, -41 \leq l \leq 29$
Reflections collected	40171
Independent reflections	6082 [$R_{\text{int}} = 0.0786, R_{\text{sigma}} = 0.0382$]
Data/restraints/parameters	6082/0/259
Goodness-of-fit on F^2	1.129
Final R indexes [$I \geq 2\sigma(I)$]	$R_1 = 0.0735, wR_2 = 0.2094$
Final R indexes [all data]	$R_1 = 0.0972, wR_2 = 0.2395$
Largest diff. peak/hole / $e \text{ \AA}^{-3}$	1.20/-0.78
Flack parameter	-0.007(12)

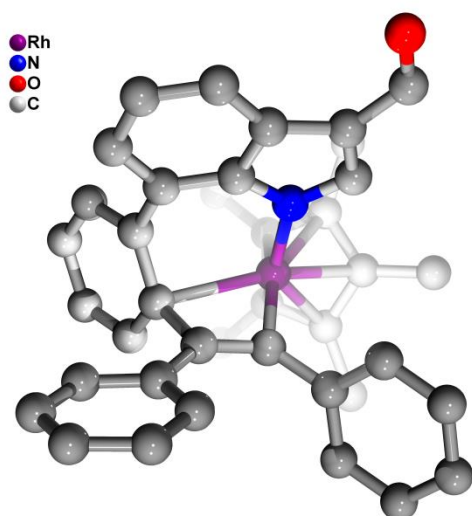


Table S8-4. 8-5a CCDC 2110326

Identification code	exp_9962
Empirical formula	C ₃₉ H ₃₄ NORh
Formula weight	635.58
Temperature/K	293.4(2)
Crystal system	triclinic
Space group	P-1
a/Å	10.4491(5)
b/Å	10.8753(6)
c/Å	16.4440(9)
α /°	96.115(4)
β /°	107.189(4)
γ /°	108.757(4)
Volume/Å ³	1647.88(16)
Z	2
$\rho_{\text{calc}}/\text{cm}^3$	1.281

μ/mm^{-1}	4.406
F(000)	656.0
Crystal size/ mm^3	$0.12 \times 0.12 \times 0.08$
Radiation	CuK α ($\lambda = 1.54184$)
2Θ range for data collection/ $^\circ$	8.808 to 145.444
Index ranges	$-12 \leq h \leq 9, -13 \leq k \leq 13, -20 \leq l \leq 20$
Reflections collected	11734
Independent reflections	6334 [$R_{\text{int}} = 0.0524, R_{\text{sigma}} = 0.0627$]
Data/restraints/parameters	6334/0/385
Goodness-of-fit on F^2	1.031
Final R indexes [$I \geq 2\sigma(I)$]	$R_1 = 0.0370, wR_2 = 0.0878$
Final R indexes [all data]	$R_1 = 0.0436, wR_2 = 0.0932$
Largest diff. peak/hole / $e \text{ \AA}^{-3}$	0.50/-0.42

9.4.10. Cyclic Voltammetry studies

CV measurements were conducted with a Chenhua Autolab CHI660C potentiostat and CHI660E electrochemical software. A glassy carbon working electrode (disk, diameter: 3mm), a platinum wire counter electrode and a non-aqueous Ag/AgNO₃ reference electrode were employed. The voltammograms were recorded at room temperature in dry MeCN at a substrate concentration of 2.5 mmol/L for **8-5a** with 100 mmol/L ⁿBu₄NPF₆ as supporting electrolyte. All solutions were degassed with N₂ prior to the measurement and an overpressure of protective gas was maintained throughout the experiment. The scan rate is 100 mV/s. Deviations from the general experimental conditions are indicated in the respective figures and descriptions.

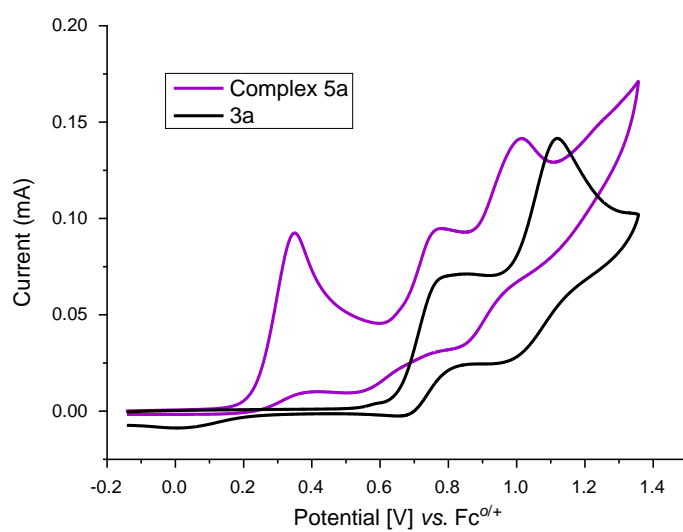


Figure S8-7. Cyclic voltammograms at 100 mV/s using **8-5a** (2.5 mmol/L), **8-3aa** (2.5 mmol/L) with ${}^n\text{Bu}_4\text{NPF}_6$ (100 mmol/L) in MeCN.

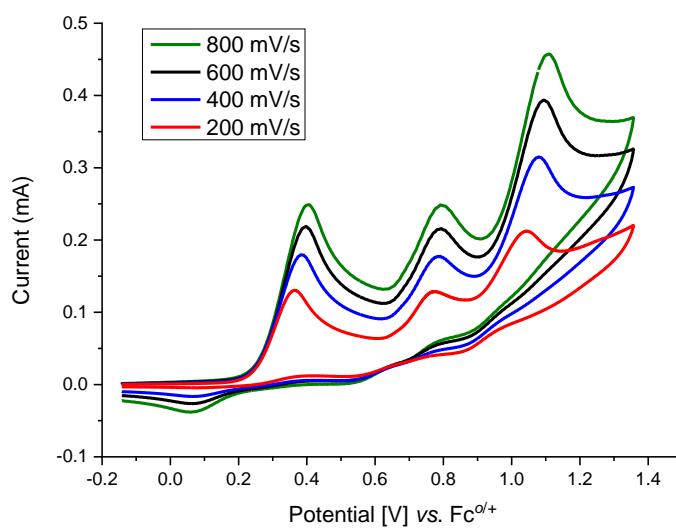


Figure S8-8. Full potential window CVs of **8-5a** at various scan rates.

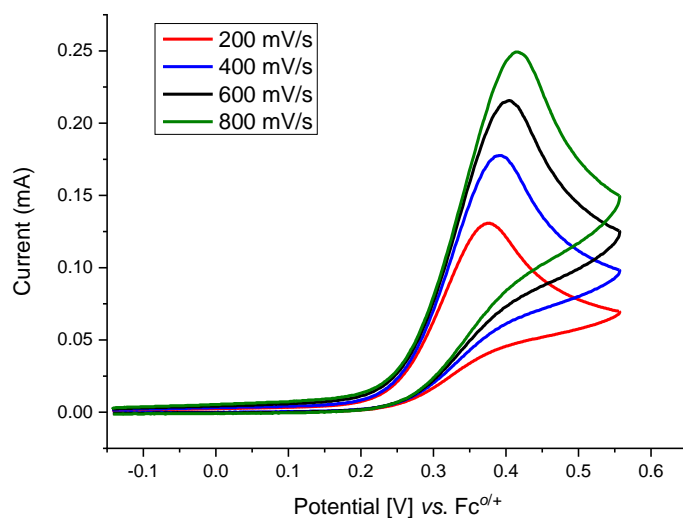


Figure S8-9. Narrow potential window CVs of **8-5a** at various scan rates.

7.4.11. XPS studies

The samples **8-5a** (20 mg, 0.03 mmol) was electrolysed at the current of 5 mA for 6 h, After 650 CV cycles across a potential range of 0 to 0.5 V of **8-5a** (20 mg, 0.03 mmol), Cp*RhCO₃ (29 mg 0.01 mmol) and [Cp*RhCl₂]₂ (20 mg, 0.03 mmol) of X-ray photoelectron spectroscopy (XPS, Escalab 250Xi) were measured at the excitation light source of Al K α . Then using OriginPro (2021) to analyze data.

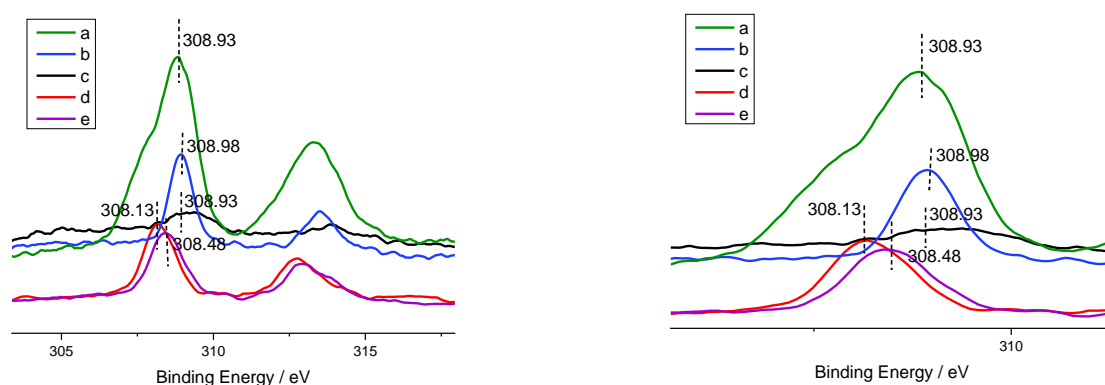


Figure S8-10. XPS Rh 3d spectra (left) and XPS Rh 3d_{5/2} (right) spectra showing: a) Cp*RhCO₃ (green line); b) [Cp*RhCl₂]₂ (blue line); c) **8-5a** was electrolysed at the current of 5 mA for 6 h (black line); d) After 650 CV cycles across a potential range of 0 to 0.5 V of **8-5a** (red line); e) **8-5a** (purple line).

The XPS experiments with Ag_2CO_3 have been investigated. Under the standard reaction condition: **8-5a** (1 equiv.), Ag_2CO_3 (2 equiv.), *t*-AmOH, 100 °C, 11 h. The peak of Rh 3d_{5/2} shifts toward higher binding energy (309.00 eV). Under the reaction condition: **8-5a** (1 equiv.), Ag_2CO_3 (1 equiv.), *t*-AmOH, 100 °C, 1 h. The peak of Rh 3d_{5/2} also shifts toward higher binding energy (308.95 eV). These results suggested that low valent state of rhodium is apparently difficult to obtain by chemical oxidant.

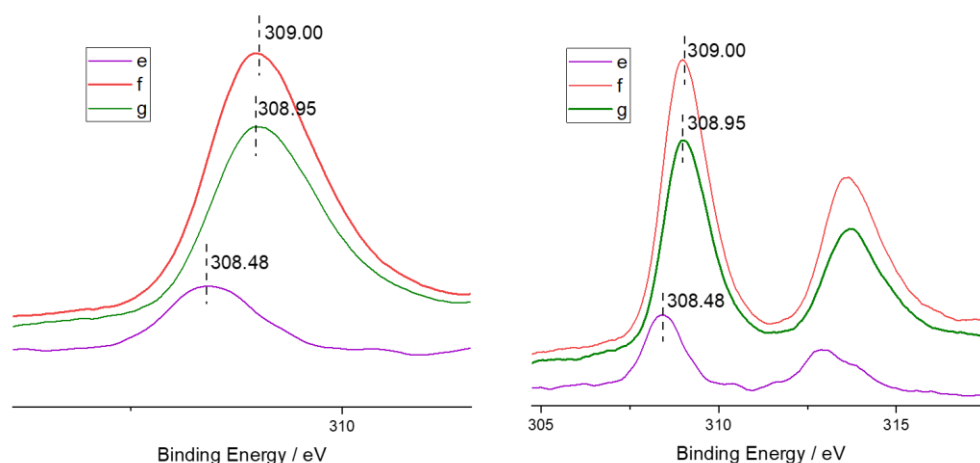


Figure S8-11. XPS Rh 3d spectra (left) and XPS Rh 3d_{5/2} (right) spectra showing: e) **8-5a** (purple line); f) **8-5a** (1 equiv.) and Ag_2CO_3 (2 equiv.) in *t*-AmOH at 100 °C for 11h (red line); g) **8-5a** (1 equiv.) and Ag_2CO_3 (1 equiv.) in *t*-AmOH at 100 °C for 1h (green line).

9.4.12. Computational Details

All calculations were performed using Gaussian 16, Revision A.03 package.^[7] All of the reactants, intermediates, transition states, products were optimized by the DFT with the ω B97X-D functional.^[8] For geometry optimizations and frequency calculations, BS-I basis set system was employed. In BSI, we employed LANL2DZ basis set for Rh with effective core potentials, 6-31G(d) basis sets for H, C, O, and N. All the stationary structures were characterized with no imaginary frequency and the transition state structures (TSs) were characterized with a single imaginary frequency. Intrinsic reaction coordinate (IRC) calculations were performed on all the TSs. The solvent effect of 1,4-dioxane was evaluated through the SMD method,^[9] in which a better basis system BS-II was used. In BS-II, we employed LANL2DZ basis sets for Rh, 6-311++G(d,p) basis sets for the other atoms. All reported energies are free energies at a

concentration of 1 M and a temperature of 298.15 K. All the 3D molecular structures of the species were generated by using the CYLview program. ^[10]

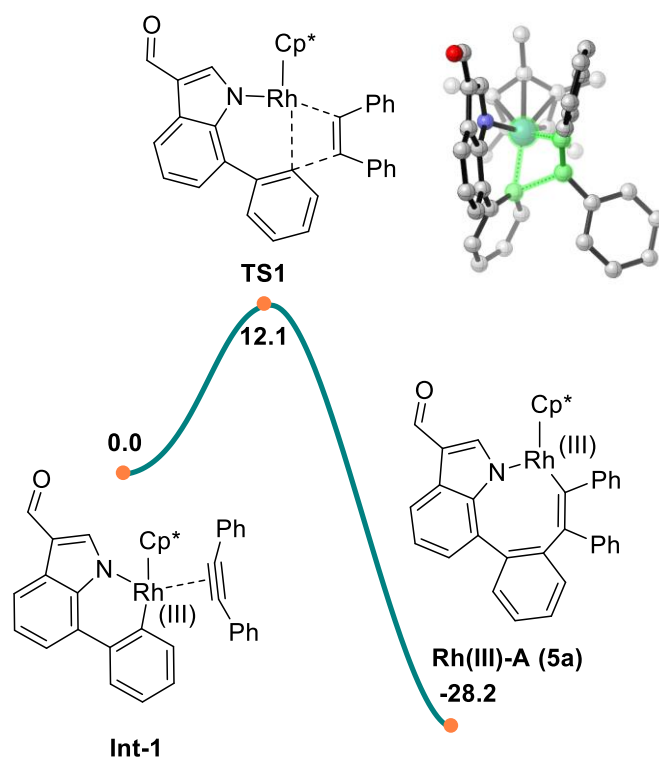


Figure S8-12. DFT calculated Gibbs free energy profile in kcal/mol for the migratory insertion process at the ω B97X-D/6-311++G(d,p), LANL2DZ(Rh)+SMD(1,4-dioxane)// ω B97X-D/6-31G(d), LANL2DZ(Rh) level of theory.

Cartesian coordinates of the optimized structures:

Int-1

E = -1745.562260 a.u.

Rh	-5.45926400	1.51298400	-0.76162400
O	-1.63556100	-2.59421900	-4.17995800
N	-3.87083200	0.74105400	-1.84966800
C	-2.69537900	2.49541800	0.29811800
C	-2.57553700	0.64812600	-1.39418700
C	-1.87211700	-0.33513500	-2.12967200
C	-4.09273800	2.68216000	0.24702500
C	-6.67664200	3.27993600	-1.50013000
C	-7.44089700	2.58091100	-0.51952400
C	-2.64163900	-1.91645000	-4.03650900
H	-3.54566400	-2.12693000	-4.65506700
C	-1.98955300	1.36166900	-0.34124900
C	-1.91704900	3.44778800	0.98510200
H	-0.83664100	3.35447500	0.96234000

C	-2.80343900	-0.83687200	-3.09779900
C	-7.73962400	1.26579500	-1.05812300
C	-2.47441200	4.51645700	1.66861400
H	-1.83459500	5.22567300	2.18558100
C	-3.98875300	-0.15827700	-2.85302500
H	-4.93406100	-0.32158600	-3.34803000
C	-3.85569500	4.65910900	1.67927700
H	-4.33093000	5.46596200	2.23046400
C	-6.40501800	2.36805500	-2.56654500
C	-8.58780200	0.24053700	-0.37365900
H	-8.88386200	-0.55216700	-1.06660900
H	-9.49812900	0.69459300	0.03266400
H	-8.04700600	-0.22569800	0.45749700
C	-0.70177500	0.96188000	0.01934800
H	-0.21220800	1.42590800	0.86969300
C	-7.36420200	0.02286700	-3.29903000
H	-6.87550400	0.23106900	-4.25435000
H	-8.43494500	-0.09306800	-3.50407100
H	-6.98989100	-0.93743600	-2.93177300
C	-6.26962300	4.72195400	-1.50959200
H	-5.18579400	4.83223000	-1.60123900
H	-6.57390400	5.23916000	-0.59802100
H	-6.74136200	5.23082500	-2.35817900
C	-7.14729300	1.14486100	-2.32601500
C	-4.63534000	3.74772100	0.97839800
H	-5.70892400	3.85787000	1.04214300
C	-0.56491200	-0.67839800	-1.77181700
H	-0.03538000	-1.44508600	-2.32661400
C	-0.00547000	-0.03965500	-0.67704300
H	0.99544700	-0.30576300	-0.34908100
C	-8.09821800	3.14926300	0.70278500
H	-7.79550700	2.62920700	1.61657100
H	-9.18865200	3.06835800	0.61713900
H	-7.86271800	4.20868000	0.83029900
C	-5.67113400	2.71951500	-3.82199700
H	-4.92483700	3.49398400	-3.63088500
H	-6.37248200	3.09453200	-4.57774600
H	-5.14510000	1.85733700	-4.23785700
C	-5.36568900	0.47879700	1.27412300
C	-5.17600300	-0.38655600	0.40595600
C	-5.60151800	1.03372500	2.58600200
C	-6.85956100	0.88111100	3.18459400
C	-4.57934500	1.68402700	3.28874800
C	-7.09606000	1.38485900	4.45875200

H	-7.64649800	0.35823600	2.64967700
C	-4.82295700	2.18166800	4.56275000
H	-3.60397300	1.80152900	2.82975200
C	-6.07882900	2.03963100	5.14863700
H	-8.07398600	1.26043500	4.91375900
H	-4.02518300	2.68776100	5.09721900
H	-6.26325800	2.43368100	6.14349800
C	-4.84263900	-1.64657100	-0.20981200
C	-5.81152700	-2.37478500	-0.91073500
C	-3.53400700	-2.13263300	-0.12293700
C	-5.46735200	-3.56348600	-1.54034600
H	-6.83025900	-2.00178300	-0.95251100
C	-3.19594100	-3.31920000	-0.76256100
H	-2.78179700	-1.55704800	0.40586100
C	-4.15504200	-4.03051000	-1.47722100
H	-6.22033500	-4.12336900	-2.08691500
H	-2.16933000	-3.66825100	-0.73013100
H	-3.87832600	-4.94529100	-1.99170400

Rh(III)-A (5a)

E = -1745.610095 a.u.

Rh	-5.47731000	1.74954000	-1.21920800
O	-0.28262400	-1.94107900	-3.15909400
N	-3.61876200	0.92837500	-1.65298300
C	-3.29072800	3.01115900	0.50694400
C	-2.46348900	1.12355100	-0.91873600
C	-1.44246100	0.25797100	-1.37213000
C	-4.51753000	2.55010400	1.03695000
C	-6.41015400	3.45240800	-2.47193200
C	-7.35400800	2.90350200	-1.48989400
C	-1.43075300	-1.53710100	-3.24900800
H	-2.11467800	-1.97308300	-4.01541700
C	-2.22962700	2.07011700	0.08905300
C	-3.07205700	4.39273300	0.40136800
H	-2.12966300	4.73595100	-0.01479800
C	-2.02952500	-0.51071800	-2.43342000
C	-7.58663100	1.54655100	-1.80041200
C	-4.02778000	5.30688200	0.82098100
H	-3.82835800	6.37179300	0.74227800
C	-3.33774300	-0.05211600	-2.54013400
H	-4.09738200	-0.41344800	-3.22168800
C	-5.24449200	4.85861100	1.34001800
H	-5.99475300	5.56914300	1.67470200
C	-6.02802100	2.42704500	-3.33503100

C	-8.59644600	0.63124400	-1.18765200
H	-8.26649000	-0.40962200	-1.22651700
H	-9.54734200	0.71066600	-1.72890000
H	-8.77909100	0.87804500	-0.13873900
C	-0.95179300	2.12026900	0.63410000
H	-0.74472800	2.83720100	1.42443800
C	-6.69946600	-0.10761600	-3.60043200
H	-5.88928500	-0.17129900	-4.33078100
H	-7.64487500	-0.21104500	-4.14706800
H	-6.61645100	-0.95212800	-2.90946400
C	-5.94463800	4.87325400	-2.45655000
H	-5.16005100	5.04911200	-3.19542600
H	-5.54153600	5.13777600	-1.47217500
H	-6.77687600	5.55452500	-2.67025400
C	-6.67967900	1.19796700	-2.86922300
C	-5.48249700	3.49641600	1.43336800
H	-6.41628700	3.12776200	1.84839200
C	-0.16682200	0.31905600	-0.79879300
H	0.61303900	-0.34704700	-1.15131500
C	0.06214900	1.24709100	0.20440200
H	1.04227800	1.30954900	0.66795700
C	-8.13051400	3.72900300	-0.51313400
H	-8.45496200	3.13492200	0.34525800
H	-9.02603600	4.13475000	-1.00014400
H	-7.53969600	4.56959500	-0.14317500
C	-5.07047900	2.48363700	-4.48242800
H	-4.62453200	3.47535600	-4.58370100
H	-5.58082100	2.24264500	-5.42222400
H	-4.25282700	1.76799500	-4.34629700
C	-4.77790800	1.09433500	1.32881000
C	-5.42035300	0.46274000	0.33960900
C	-4.30116300	0.53870800	2.61869000
C	-3.87075800	-0.79159400	2.70870400
C	-4.23351700	1.33982200	3.76459100
C	-3.41651400	-1.30988100	3.91497700
H	-3.87510800	-1.41463800	1.82083300
C	-3.77727600	0.82041700	4.97193200
H	-4.53952800	2.38120800	3.71335400
C	-3.37163500	-0.50832200	5.05368800
H	-3.08188200	-2.34207800	3.96153400
H	-3.73640500	1.45833100	5.85034400
H	-3.01140000	-0.91381800	5.99460100
C	-6.00222700	-0.88395700	0.34194000
C	-7.01351000	-1.19968700	1.25992200

C	-5.61020500	-1.86029800	-0.58340200
C	-7.62491700	-2.44847300	1.24397500
H	-7.31194800	-0.45121600	1.98852800
C	-6.21949100	-3.11133100	-0.59482100
H	-4.80395000	-1.63798900	-1.27525200
C	-7.23470900	-3.40799100	0.31235600
H	-8.40731000	-2.67404200	1.96298700
H	-5.89363200	-3.86022700	-1.31115400
H	-7.71171800	-4.38343000	0.29935600

Rh(I)-B

E = -1745.599286 a.u.

Rh	-6.02687600	1.44232600	-1.45337800
O	-1.63726800	-2.36360600	-4.59285700
N	-4.05944400	0.20229600	-1.58277300
C	-2.79522400	2.49292600	0.06718400
C	-2.67580500	0.46424600	-1.43214800
C	-1.96544500	-0.34585300	-2.33185000
C	-4.13628700	2.40465000	0.49627700
C	-6.97651000	3.36562200	-2.22961700
C	-7.80653900	2.72909200	-1.27266100
C	-2.73091500	-2.03540500	-4.17990600
H	-3.65591200	-2.46696200	-4.61932200
C	-2.05770100	1.39965700	-0.60166700
C	-2.12828500	3.72886400	0.18500000
H	-1.12194100	3.81672500	-0.21051300
C	-2.95439700	-1.08134900	-3.09967200
C	-8.23543900	1.43610900	-1.81024600
C	-2.71858800	4.84348500	0.74942500
H	-2.16808700	5.77638900	0.81979300
C	-4.17257100	-0.74566600	-2.60455000
H	-5.14977900	-1.13035400	-2.85998500
C	-4.03427500	4.75116700	1.20415100
H	-4.52916100	5.61011500	1.64823300
C	-6.76690600	2.40686700	-3.27804500
C	-9.31006800	0.57485600	-1.21879300
H	-9.09525700	-0.49236100	-1.33298500
H	-10.26797200	0.77383400	-1.71608700
H	-9.44964500	0.77887300	-0.15401200
C	-0.65661500	1.33880600	-0.59087400
H	-0.11030100	1.98871900	0.08506800
C	-7.84288700	0.12856500	-4.02610700
H	-6.93590500	-0.09671400	-4.59675700
H	-8.63412400	0.35671400	-4.75233000

H	-8.13618300	-0.78393200	-3.49624800
C	-6.36295800	4.72793900	-2.10880200
H	-5.97516000	4.90545500	-1.09975900
H	-7.09129300	5.51634600	-2.33754500
H	-5.52269200	4.84531400	-2.79865000
C	-7.62696500	1.26512400	-3.07361500
C	-4.71666800	3.55895100	1.06802600
H	-5.74462000	3.49313600	1.40891700
C	-0.57303900	-0.33494400	-2.34647100
H	-0.02905800	-0.96417800	-3.04088500
C	0.06754100	0.48835700	-1.42956000
H	1.15202800	0.49683800	-1.37829500
C	-8.31994700	3.33897300	-0.00483400
H	-8.28240200	2.63170400	0.82974000
H	-9.36147100	3.66235000	-0.12691300
H	-7.72875100	4.21593200	0.27237300
C	-5.88761600	2.60821000	-4.47620900
H	-5.02401600	3.23391500	-4.23482800
H	-6.44168900	3.09450100	-5.28829100
H	-5.50701000	1.65464900	-4.85426400
C	-5.03778700	1.21447600	0.44183400
C	-4.96800700	0.07246100	-0.44122700
C	-5.79013300	0.94514900	1.71840200
C	-7.08950000	0.43119700	1.71982100
C	-5.15951400	1.13063000	2.95512300
C	-7.74422900	0.12148200	2.90729000
H	-7.58060300	0.26072200	0.76913600
C	-5.80991400	0.82470300	4.14551200
H	-4.14638500	1.52110400	2.98283300
C	-7.10827000	0.32104000	4.12862500
H	-8.75426200	-0.27762900	2.87497300
H	-5.29686600	0.97696800	5.09084600
H	-7.61697600	0.08387800	5.05832500
C	-5.22232500	-1.33759800	-0.00886000
C	-6.32645400	-2.05200600	-0.47120000
C	-4.31373400	-1.96261600	0.84757600
C	-6.52521300	-3.37386200	-0.08535900
H	-7.03022500	-1.54931200	-1.13044700
C	-4.50877700	-3.28435100	1.23356300
H	-3.45832100	-1.40202700	1.21471600
C	-5.61507100	-3.99196800	0.76819300
H	-7.39184300	-3.92001900	-0.44657000
H	-3.79862000	-3.76223800	1.90169500
H	-5.76878900	-5.02278500	1.07341300

Rh(IV)-A'

E = -1745.377837 a.u.

Rh	-5.90752400	1.65742300	-1.61407800
O	-1.06701000	-2.72769400	-2.86090300
N	-4.19769000	0.54903500	-1.97339600
C	-3.83267600	2.75348100	0.06835100
C	-3.02468600	0.74639800	-1.21519900
C	-2.07355900	-0.24684700	-1.52595900
C	-5.03590300	2.39165400	0.72651800
C	-6.53944900	3.40724400	-2.94150000
C	-7.56102800	3.10652200	-1.93539200
C	-2.17608200	-2.30016000	-3.11248900
H	-2.84410500	-2.81614900	-3.82743400
C	-2.80548600	1.74221600	-0.29426900
C	-3.51154300	4.11352300	-0.08697300
H	-2.58688400	4.38031000	-0.59033600
C	-2.70664600	-1.08889700	-2.48897800
C	-8.05728300	1.80341400	-2.15802000
C	-4.33985300	5.10299300	0.41500500
H	-4.06751100	6.14728600	0.29850500
C	-4.01114600	-0.52932300	-2.70058300
H	-4.79272000	-0.92968200	-3.33320900
C	-5.50828900	4.75217000	1.09939700
H	-6.14318500	5.52321200	1.52479500
C	-6.36629100	2.26712500	-3.72999200
C	-9.26733200	1.21384100	-1.50376700
H	-9.45069700	0.19527800	-1.85053000
H	-10.14778200	1.81365500	-1.76112600
H	-9.17847900	1.20263200	-0.41395400
C	-1.52883400	1.74264700	0.31966300
H	-1.30895900	2.50999000	1.05620000
C	-7.47142400	-0.12869900	-3.81029500
H	-6.67816800	-0.38509500	-4.51736400
H	-8.41452000	-0.12622400	-4.36939000
H	-7.52912000	-0.91343300	-3.04899800
C	-5.84291700	4.72507800	-3.04669800
H	-5.48539900	5.05506100	-2.06553900
H	-6.53015400	5.49040000	-3.42533000
H	-4.98362500	4.67830600	-3.71878100
C	-7.24060500	1.21318700	-3.19084100
C	-5.84684000	3.41900800	1.24504700
H	-6.74165400	3.13622500	1.79134600
C	-0.82301200	-0.23699800	-0.90321800

H	-0.08507000	-0.99601800	-1.13504000
C	-0.56810800	0.78193400	0.02223800
H	0.39194600	0.81888400	0.52521900
C	-8.16730300	4.11148400	-1.01205100
H	-8.57104600	3.64031300	-0.11271800
H	-8.99222300	4.61819500	-1.52834400
H	-7.44467000	4.87110200	-0.70964500
C	-5.44574300	2.08429100	-4.89308100
H	-4.72211700	2.89830300	-4.96688400
H	-6.01972900	2.05237900	-5.82604900
H	-4.88525900	1.14715600	-4.81808100
C	-5.40889200	0.95928600	1.00464300
C	-5.94177600	0.32427700	-0.04896800
C	-5.15701600	0.43178700	2.36685200
C	-5.93352300	-0.59910300	2.91262900
C	-4.12044400	0.97065000	3.13973900
C	-5.66214300	-1.09089100	4.18322500
H	-6.75907700	-1.01202000	2.34300800
C	-3.84799400	0.47507200	4.41015900
H	-3.51700200	1.78403100	2.74571700
C	-4.61632200	-0.55982000	4.93521300
H	-6.27586200	-1.88776300	4.59167600
H	-3.03651100	0.90118800	4.99207000
H	-4.40815000	-0.94446000	5.92861600
C	-6.17922600	-1.11813400	-0.20073100
C	-7.43703400	-1.65986900	-0.48753600
C	-5.08577000	-1.99373900	-0.09428900
C	-7.59902900	-3.02996000	-0.67219000
H	-8.29878100	-1.00507800	-0.53388400
C	-5.24607200	-3.36145300	-0.28592000
H	-4.11095700	-1.59028000	0.16597000
C	-6.50276300	-3.88462800	-0.58222600
H	-8.58623300	-3.43216200	-0.87906400
H	-4.38882500	-4.02154700	-0.19217900
H	-6.62988800	-4.95254600	-0.72817600

Rh(II)-B'

E = -1745.410064 a.u.

Rh	-5.86498700	1.50367700	-1.39665700
O	-1.64440100	-2.37148000	-4.50351400
N	-4.13792300	0.13381300	-1.50429200
C	-3.00669100	2.60445400	-0.08498400
C	-2.76075700	0.52707000	-1.47902900
C	-2.04533800	-0.27825900	-2.36778500

C	-4.26207600	2.34943500	0.52446300
C	-6.75554700	3.38027200	-2.26652100
C	-7.64569200	2.76462900	-1.32349500
C	-2.74831700	-2.15703800	-4.05850500
H	-3.63498600	-2.71654400	-4.41822300
C	-2.19413800	1.57867800	-0.77048700
C	-2.51747700	3.92017000	-0.08024300
H	-1.58783600	4.13334100	-0.59624900
C	-3.01335800	-1.15577900	-3.01292200
C	-8.07680900	1.48793800	-1.86161500
C	-3.19030600	4.95804300	0.54316500
H	-2.77391100	5.95983300	0.52675000
C	-4.22241700	-0.90433700	-2.47156000
H	-5.17258900	-1.38554700	-2.64862600
C	-4.39966700	4.70162900	1.19104000
H	-4.93404700	5.49728300	1.70024800
C	-6.48226700	2.40473800	-3.27217700
C	-9.19254900	0.65870600	-1.31142300
H	-9.11230900	-0.39218800	-1.59985400
H	-10.14719200	1.03235800	-1.70174500
H	-9.24671400	0.71572400	-0.22160400
C	-0.79979000	1.68036100	-0.87841000
H	-0.28004200	2.43765900	-0.30082800
C	-7.48240800	0.08276500	-3.97147300
H	-6.53830900	-0.13720400	-4.47772700
H	-8.22905600	0.28772200	-4.74774500
H	-7.79979300	-0.81681900	-3.43590600
C	-6.15285000	4.74311100	-2.14960500
H	-5.92080000	4.98978300	-1.11023900
H	-6.84915000	5.50002000	-2.52987200
H	-5.22618500	4.82274800	-2.72264000
C	-7.34958600	1.25573600	-3.05271700
C	-4.91738400	3.42273300	1.17693700
H	-5.85625900	3.22242500	1.68000800
C	-0.66814000	-0.12208400	-2.50134400
H	-0.11008100	-0.74116200	-3.19315500
C	-0.05480200	0.84390200	-1.71191000
H	1.02119900	0.97329100	-1.76092100
C	-8.22209600	3.41219600	-0.10373000
H	-8.30522500	2.70340300	0.72575400
H	-9.22548600	3.79756800	-0.31985300
H	-7.60622100	4.25098300	0.22810600
C	-5.56683200	2.56607700	-4.44624200
H	-4.77913300	3.29507900	-4.24342000

H	-6.12873000	2.90883600	-5.32266400
H	-5.08452700	1.61969700	-4.70708000
C	-4.94347200	1.02847000	0.63688600
C	-4.87918400	-0.03662200	-0.26977200
C	-5.66554700	0.77004200	1.92183100
C	-7.01403500	0.41462100	1.95594500
C	-4.95579100	0.86975300	3.12196200
C	-7.64725800	0.15946700	3.16749200
H	-7.56081300	0.33008300	1.02297200
C	-5.58568200	0.60567300	4.33307400
H	-3.90738200	1.15460900	3.10543400
C	-6.93299600	0.25251100	4.35879500
H	-8.69759700	-0.11434300	3.18083200
H	-5.02370200	0.67836000	5.25864300
H	-7.42469200	0.05204900	5.30527600
C	-5.31116300	-1.42412900	0.06429100
C	-6.52070400	-1.95413500	-0.38302100
C	-4.44558700	-2.21409200	0.82286000
C	-6.86711100	-3.26476600	-0.07455200
H	-7.18938000	-1.32638500	-0.96506800
C	-4.79282800	-3.52558800	1.12998000
H	-3.50681600	-1.79780300	1.17712200
C	-6.00217100	-4.05158600	0.68243800
H	-7.81265700	-3.67101600	-0.41965200
H	-4.11925900	-4.13593100	1.72260900
H	-6.27210000	-5.07401700	0.92623500

TS1

E = -1745.546079 a.u.

Rh	-5.52481300	1.58497100	-0.94245500
O	-1.63639500	-2.71543900	-3.98073600
N	-3.85982600	0.84307000	-1.97632800
C	-2.79297500	2.51911900	0.27956800
C	-2.62912900	0.65797900	-1.38101700
C	-1.93120700	-0.40050700	-2.00736100
C	-4.20008900	2.59648500	0.38378900
C	-6.78154300	3.38248900	-1.62496400
C	-7.50593300	2.59725000	-0.65570700
C	-2.61462800	-1.98554400	-3.94316200
H	-3.46669900	-2.16202600	-4.64073200
C	-2.09080600	1.36022200	-0.29655300
C	-2.02453900	3.59547100	0.75674700
H	-0.94753700	3.55744400	0.62615200
C	-2.80251600	-0.87665700	-3.04303000

C	-7.78545800	1.31209500	-1.23822000
C	-2.60032900	4.70498700	1.35624100
H	-1.97388700	5.51909100	1.70829800
C	-3.94561400	-0.09549100	-2.94877400
H	-4.84191700	-0.19471800	-3.54398500
C	-3.98388700	4.75656900	1.50804500
H	-4.45795600	5.60139100	1.99925400
C	-6.49616200	2.53753000	-2.71951400
C	-8.63577300	0.25930000	-0.59815600
H	-8.78935300	-0.58982600	-1.26955500
H	-9.62148400	0.66409300	-0.34024900
H	-8.18152600	-0.11744900	0.32505200
C	-0.85210700	0.92730400	0.17757900
H	-0.41590500	1.41494200	1.04529000
C	-7.30968600	0.15918000	-3.51214700
H	-6.75075200	0.38413800	-4.42422600
H	-8.36468000	0.06395800	-3.79513400
H	-6.97270600	-0.81427400	-3.14289300
C	-6.37646100	4.82135800	-1.51324500
H	-5.30250300	4.94880100	-1.67822400
H	-6.60049300	5.22918500	-0.52559800
H	-6.91267200	5.42585700	-2.25384600
C	-7.14725200	1.24988900	-2.49443000
C	-4.75757400	3.70759800	1.03947900
H	-5.82362300	3.72773500	1.22176700
C	-0.68092500	-0.79900300	-1.52630700
H	-0.15702400	-1.62049500	-2.00249500
C	-0.16229800	-0.13729600	-0.42284700
H	0.79619800	-0.44167200	-0.01217300
C	-8.14306300	3.07069400	0.61841400
H	-7.83642900	2.46518200	1.47831300
H	-9.23490500	3.00352500	0.53854600
H	-7.89950200	4.11336600	0.83536800
C	-5.75614000	2.91801900	-3.96320200
H	-5.19814700	3.84593000	-3.81781000
H	-6.45309500	3.06424800	-4.79741600
H	-5.03664800	2.14472300	-4.24823000
C	-4.96445400	0.90016800	1.10026500
C	-5.09251400	-0.04601900	0.24639900
C	-5.19695400	1.12302100	2.53039500
C	-6.38360800	0.64001300	3.09411500
C	-4.25305000	1.74632800	3.35368300
C	-6.62961000	0.78702200	4.45566000
H	-7.10764200	0.14432300	2.45413600

C	-4.49670500	1.88050500	4.71455100
H	-3.32868500	2.11794100	2.92365500
C	-5.68604500	1.40867100	5.26805800
H	-7.55600300	0.41206300	4.88021300
H	-3.75418300	2.35741100	5.34702900
H	-5.87424600	1.52319000	6.33140500
C	-4.88889200	-1.42659600	-0.11784000
C	-5.83861900	-2.14222900	-0.85627600
C	-3.66511100	-2.03336900	0.19776200
C	-5.57240300	-3.43975300	-1.27257800
H	-6.78376300	-1.66995300	-1.09980800
C	-3.40001300	-3.32713100	-0.23250900
H	-2.91196600	-1.46409800	0.73326200
C	-4.34760500	-4.03186300	-0.97028100
H	-6.31562500	-3.98616300	-1.84579100
H	-2.43619700	-3.77497700	-0.01314800
H	-4.12771600	-5.03613600	-1.31871100

TS(A-B)

E = -1745.562268 a.u.

Rh	-6.10953600	1.47762000	-1.39248800
O	-2.14434500	-3.03512900	-4.06130700
N	-4.20854700	0.64041500	-2.09410600
C	-2.86720300	2.45990300	-0.01273500
C	-2.92233800	0.47331600	-1.56231700
C	-2.29553100	-0.63790600	-2.16595800
C	-4.18197400	2.51048000	0.48342600
C	-7.10206700	3.39773700	-2.15474400
C	-7.93339200	2.68426600	-1.23187600
C	-3.10937800	-2.29395900	-4.00424300
H	-3.99268600	-2.47466000	-4.65840600
C	-2.27345700	1.22959900	-0.57670000
C	-2.08004500	3.61870100	0.02211600
H	-1.07478300	3.56696400	-0.38636000
C	-3.23977600	-1.15372100	-3.12116500
C	-8.34091300	1.42937800	-1.84452500
C	-2.55259000	4.81240400	0.54774400
H	-1.91795900	5.69310600	0.56124800
C	-4.35601500	-0.35122300	-3.01822700
H	-5.29130800	-0.45904300	-3.55182600
C	-3.85096100	4.86318700	1.04917700
H	-4.24786500	5.78582500	1.46282900
C	-6.85001000	2.50772500	-3.23201700
C	-9.35466000	0.47235200	-1.29612700

H	-9.06586800	-0.56878500	-1.47330300
H	-10.33055900	0.63189000	-1.77184500
H	-9.49278900	0.60635600	-0.21975000
C	-0.99838300	0.81033800	-0.20297500
H	-0.47622000	1.36738800	0.57058500
C	-7.86517400	0.23586900	-4.09802100
H	-7.03479000	0.20355700	-4.80972300
H	-8.78027300	0.39843300	-4.68211300
H	-7.94677100	-0.75166900	-3.63019200
C	-6.54459200	4.77282800	-1.94697700
H	-6.10355400	4.88360100	-0.95041200
H	-7.32427600	5.53642100	-2.05998300
H	-5.75572300	4.99427400	-2.67029400
C	-7.67808400	1.31990400	-3.08090300
C	-4.64652900	3.72904100	1.01070300
H	-5.65849600	3.77028000	1.40304500
C	-1.00874700	-1.02958900	-1.78280500
H	-0.54308100	-1.88668800	-2.25582100
C	-0.37584700	-0.30259300	-0.78930500
H	0.61864100	-0.58779600	-0.45886100
C	-8.48364200	3.24891200	0.04230000
H	-8.56719700	2.49053100	0.82550400
H	-9.48055600	3.67488300	-0.12647600
H	-7.84022100	4.04685300	0.42301200
C	-5.96280400	2.76490000	-4.41255100
H	-5.23359900	3.54971700	-4.20014900
H	-6.55595600	3.07193500	-5.28228800
H	-5.39995200	1.86740200	-4.68691100
C	-5.13330100	1.36253600	0.53201200
C	-5.25278000	0.20239600	-0.28887000
C	-5.85794400	1.14702600	1.83425400
C	-7.11609000	0.53407900	1.87149400
C	-5.24405300	1.46612900	3.05365000
C	-7.74883800	0.26124800	3.08026700
H	-7.59790600	0.26551700	0.93653000
C	-5.87765900	1.19934800	4.26130600
H	-4.26170100	1.92778700	3.05234900
C	-7.13468300	0.59804300	4.28200400
H	-8.72587900	-0.21353800	3.07948500
H	-5.38284800	1.45796300	5.19298700
H	-7.62792000	0.39199000	5.22715300
C	-5.05562400	-1.20990000	-0.09459900
C	-5.80959800	-2.13151900	-0.83382400
C	-4.06186600	-1.66560600	0.78495500

C	-5.58707600	-3.49254800	-0.68366100
H	-6.56591800	-1.75366500	-1.51610800
C	-3.83530900	-3.02637600	0.92546400
H	-3.46651900	-0.93939500	1.32946200
C	-4.59807300	-3.93655500	0.19353200
H	-6.17146300	-4.20829300	-1.25299100
H	-3.05933800	-3.38109000	1.59580300
H	-4.41514800	-5.00144000	0.30253800

TS(A'-B')

E = -1745.367087 a.u.

Rh	-5.98500500	1.65324800	-1.49519500
O	-1.32824200	-2.64895800	-3.38684600
N	-4.33185200	0.38536200	-1.60523000
C	-3.59543900	2.73758700	0.08153600
C	-3.02591800	0.68341500	-1.19172700
C	-2.13123000	-0.24300800	-1.74638600
C	-4.82880100	2.30859200	0.63451600
C	-6.48844200	3.41440800	-2.80659600
C	-7.59538900	3.09476500	-1.90977300
C	-2.48693400	-2.29662000	-3.32111000
H	-3.28441200	-2.84937400	-3.85986100
C	-2.61130300	1.76136800	-0.41527800
C	-3.31118300	4.10815300	0.04510400
H	-2.37394700	4.43619700	-0.39340000
C	-2.93931800	-1.14579400	-2.54222700
C	-8.08400000	1.80020100	-2.22114000
C	-4.20286300	5.04073100	0.55720300
H	-3.95086900	6.09640700	0.53036300
C	-4.23636400	-0.72379900	-2.41971900
H	-5.12866600	-1.17787300	-2.82693300
C	-5.41824400	4.62609300	1.10544500
H	-6.11302200	5.35228600	1.51491900
C	-6.24350400	2.28420500	-3.60276700
C	-9.34087600	1.18898500	-1.68511200
H	-9.45394800	0.15235400	-2.00990000
H	-10.20799300	1.74539800	-2.05960200
H	-9.37613100	1.21707200	-0.59243400
C	-1.23906500	1.86614900	-0.17565800
H	-0.86938000	2.67723800	0.44522500
C	-7.38187000	-0.06960900	-3.90013300
H	-6.50270200	-0.33928300	-4.48939600
H	-8.23191000	-0.00140100	-4.58915100
H	-7.58635600	-0.87850100	-3.19218100

C	-5.76397100	4.72100000	-2.81500400
H	-4.83214400	4.66291600	-3.38094100
H	-5.51771600	5.03963900	-1.79725900
H	-6.38951200	5.49940200	-3.26697500
C	-7.19340700	1.24017100	-3.20315400
C	-5.72154200	3.27527300	1.14427200
H	-6.64464500	2.93387400	1.60356300
C	-0.76379400	-0.12152800	-1.49723500
H	-0.06633400	-0.83071000	-1.92743900
C	-0.33550100	0.93492400	-0.69988500
H	0.72176300	1.04803500	-0.48425100
C	-8.25387500	4.06331000	-0.98104800
H	-8.71358100	3.55520400	-0.12938200
H	-9.04456000	4.59983200	-1.51959000
H	-7.54597000	4.80257800	-0.60231800
C	-5.19443500	2.11109600	-4.65445900
H	-4.43597500	2.89401800	-4.59816100
H	-5.64995600	2.14808600	-5.65044700
H	-4.68501500	1.14810900	-4.55202300
C	-5.15531800	0.86485500	0.92529600
C	-5.63421100	0.14495600	-0.16544000
C	-5.12324800	0.44651100	2.32523800
C	-5.95213300	-0.56429900	2.84986000
C	-4.22427200	1.09506200	3.19613800
C	-5.86216900	-0.92443400	4.18641300
H	-6.68413400	-1.05180100	2.21772800
C	-4.12837800	0.71822800	4.52696400
H	-3.57857300	1.88043400	2.81531100
C	-4.94707900	-0.29293000	5.02753200
H	-6.51509900	-1.69842000	4.57666700
H	-3.41457100	1.21410200	5.17668200
H	-4.87801100	-0.58218200	6.07129700
C	-6.00324900	-1.27293300	-0.16888100
C	-7.29508200	-1.67196400	-0.52050700
C	-5.05133100	-2.24380000	0.17553900
C	-7.64142300	-3.01969000	-0.51271700
H	-8.02898600	-0.91456200	-0.77171300
C	-5.39362200	-3.58896600	0.16545800
H	-4.04617000	-1.93233800	0.44509100
C	-6.68908200	-3.97864400	-0.17566900
H	-8.65165000	-3.32176100	-0.77050100
H	-4.65135000	-4.33617600	0.42672300
H	-6.95542500	-5.03079700	-0.17722900

9.5. References

- [1] S. Cacchi, G. vFabrizi, A. Goggiamani, A. Lazzetti, R. Verdiglione, *Tetrahedron* **2015**, *71*, 9346.
- [2] V. Kanchupalli, D. Joseph, S. Katukojvala, *Org. Lett.* **2015**, *17*, 5878.
- [3] Y. Yu, C. Kuai, R. Chauvin, N. Tian, S. Ma, X. Cui, *J. Org. Chem.* **2017**, *82*, 8611.
- [4] (a) G. M. Sheldrick, *Acta Crystallogr., Sect. A: Found. Crystallogr.* **2008**, *64*, 112; (b) A. V. Dolomanov, L. J. Bourhis, R. J. Gildea, J. A. K. Howard, H. Puschman, *J. Appl. Crystallogr.* **2009**, *42*, 339.
- [5] A. Biswas, S. Bera, P. Poddar, D. Dhara, R. Samanta, *Chem. Commun.* **2020**, *56*, 1440.
- [6] Z. Nova'k, P. Nemes, A. Kotschy, *Org. Lett.* **2004**, *6*, 26, 4917.
- [7] Gaussian 16, Revision A.03, M. J. Frisch, G. W. Trucks, H. B. Schlegel, G. E. Scuseria, M. A. Robb, J. R. Cheeseman, G. Scalmani, V. Barone, G. A. Petersson, H. Nakatsuji, X. Li, M. Caricato, A. V. Marenich, J. Bloino, B. G. Janesko, R. Gomperts, B. Mennucci, H. P. Hratchian, J. V. Ortiz, A. F. Izmaylov, J. L. Sonnenberg, D. Williams-Young, F. Ding, F. Lipparini, F. Egidi, J. Goings, B. Peng, A. Petrone, T. Henderson, D. Ranasinghe, V. G. Zakrzewski, J. Gao, N. Rega, G. Zheng, W. Liang, M. Hada, M. Ehara, K. Toyota, R. Fukuda, J. Hasegawa, M. Ishida, T. Nakajima, Y. Honda, O. Kitao, H. Nakai, T. Vreven, K. Throssell, J. A. Montgomery, Jr., J. E. Peralta, F. Ogliaro, M. J. Bearpark, J. J. Heyd, E. N. Brothers, K. N. Kudin, V. N. Staroverov, T. A. Keith, R. Kobayashi, J. Normand, K. Raghavachari, A. P. Rendell, J. C. Burant, S. S. Iyengar, J. Tomasi, M. Cossi, J. M. Millam, M. Klene, C. Adamo, R. Cammi, J. W. Ochterski, R. L. Martin, K. Morokuma, O. Farkas, J. B. Foresman, and D. J. Fox, Gaussian, Inc., Wallingford CT, **2016**.
- [8] S. Grimme, Semiempirical GGA-type density functional constructed with a long-range dispersion correction. *J. Comp. Chem.* **2006**, *27*, 1787.
- [9] A. V. Marenich, C. J. Cramer, D. G. Truhlar, Universal Solvation Model Based on Solute Electron Density and on a Continuum Model of the Solvent Defined by the Bulk Dielectric Constant and Atomic Surface Tensions. *J. Phys. Chem. B* **2009**, *113*, 6378.
- [10] CYLview, 1.0b; Legault, C. Y., Université de Sherbrooke, 2009 (<http://www.cylview.org>)

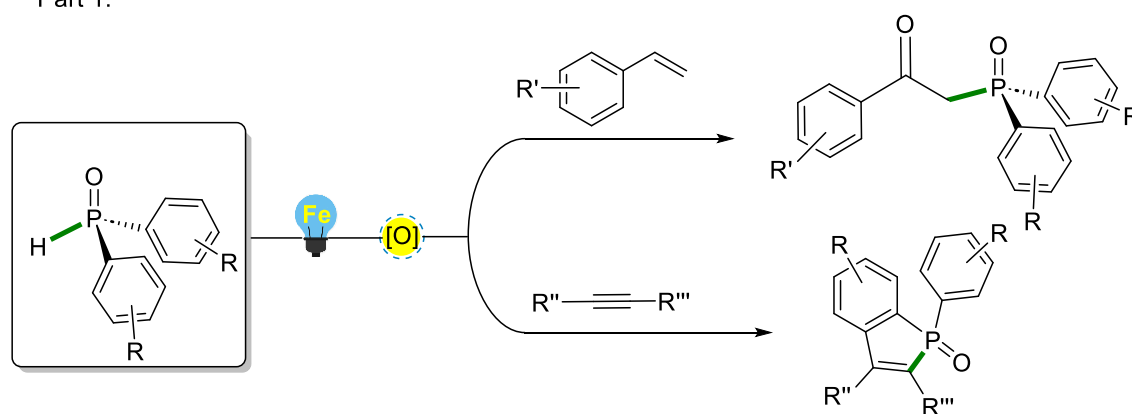
General conclusions and perspectives

General conclusions and perspectives

In this doctoral work, we described the development of homogeneous catalytic systems based on transition metals with high catalytic activity as rhodium and iron, respectively. Thus, these oxidative catalytic systems are able to perform C–H/C–P bonds functionalization, successfully constructed C–C, C–N, C–P bonds, obtained a variety of N- and P-containing heterocycles molecules and a class of β -ketophosphine oxides.

The strategies involved to form C–P bonds was described in the **first part** of this manuscript. Iron salts was first employed as catalysts under blue LED ($h\nu = 450\text{-}460\text{ nm}$) irradiation, for oxyphosphination of secondary phosphine oxides and activated alkenes. (Scheme 1) First of all, under aerobic condition, substituted styrenes was found to occur the intermolecular oxo-phosphinylation in the presence of 10 mol% $\text{Fe}(\text{OTf})_2$ in 1,4-dioxane at room temperature and the corresponding β -ketophosphine oxide products in moderate to good yields. However, while performing the reaction with 4-vinylpyridine and 4-trifluoromethylstyrene afforded only anti-Markonikov hydrophosphination products. Noticeably, the mechanism studies highlighted that this reaction proceeded in radical way, and that blue light in association with iron salt and air were responsible of the production of a phosphinoyl radical which then reacted with activated olefins.

Part 1.



Scheme 1. Organophosphorus derivatives prepared *via* C–P bonds formations.

Afterwards, we established the proof of concept of another light promoted iron catalyzed protocol for the constructing the framework of benzo[*b*]phosphole oxides *via*

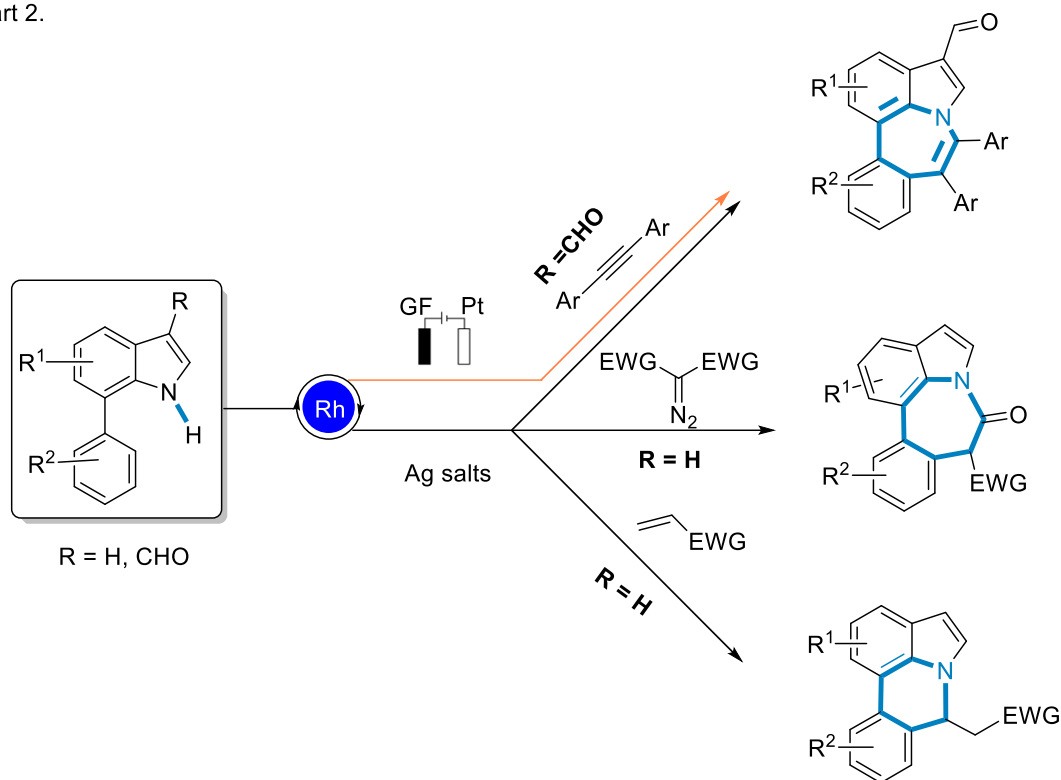
the H–P bond cleavage of diphenylphosphine oxides and formation of new C–P bonds with internal alkynes. This reaction was performed by using only iron salts as the catalysts, *tert*-butyl hydroperoxide (TBHP) as the oxidant at room temperature for 10 hours under blue light irradiation. Importantly, with a fine control of the nature of the iron salts and solvents, a tandem intermolecular-intramolecular C–P/C–C bond annulation product 9-phenyltribenzo[*b,e,g*]phosphindole 9-oxide was obtained in good yield. Even if these preliminary results opened exciting perspectives, future plans have to be done including the study of the substrate scope, and the mechanistic study.

On the other hand, in the **second part** of this work, we focused on rhodium-catalyzed formations of C–N bonds for the preparation of nitrogen containing heterocycles. We have successfully developed Rh(III)-catalyzed C–H/C–N annulations, in the presence of 2.5–5 mol% [Cp*RhCl₂]₂ as the catalyst and Ag salts as the oxidants for the efficient synthesis of six-membered and seven-membered 1,7 fused indoles. In these contributions, we have described the intramolecular amidation of 7-phenylindoles with diazomalonates, the olefination/aza-Michael addition of 7-phenyl-1*H*-indoles with alkenes and annulation of 7-phenylindoles with alkynes, respectively. The preparation of azepino[3,2,1-*hi*]indoles was performed by reaction of 7-phenyl-1*H*-indoles with diazomalonates using 2.5 mol% [Cp*RhCl₂]₂ associated to catalytic amounts of AgOAc (15 mol%) and DBU (30 mol%) at 60 °C. Additionally to obtain efficiently pyrrolo[3,2,1-*de*]phenanthridines from 7-phenyl-1*H*-indoles, an interesting one-pot reaction with activated alkenes was conducted with 5 mol% [Cp*RhCl₂]₂ associated to AgOAc (2 equiv.) and Me₄NOAc (10 equiv.) at 80 °C. (Scheme 2)

Besides the use of Ag salts in stoichiometric or catalytic amounts, the exogenous-oxidant-free rhodium version of these transformations can be a good alternative in terms of sustainability. Indeed, metal-electrocatalysis can be considered as a lower-cost, more environment friendly methodology. Thus, using platinum electrodes as the cathode and graphite felt (GF) electrodes as the anode, in the presence of [Cp*RhCl₂]₂ as the catalyst, and 2 equiv. of base (Li₂CO₃), seven-membered azepino[3,2,1-*hi*]indoles from 7-phenylindoles were obtained efficiently by reaction with alkynes. Two important intermediates including six-membered cyclometalated rhodium(III)

complex via *NH*-directed C-H activation and an eight-membered metallacyclic rhodium(III) species via alkyne insertion were successfully isolated. Additionally, experimental evidences obtained by cyclic voltammetric analysis and XPS studies associated to DFT calculations, suggested a rhodium(III-IV-II-III) manifold. (Scheme 2)

Part 2.



Scheme 2. Nitrogen containing heterocycles prepared via rhodium-catalyzed C-N formations.

The studies summarized in this manuscript clearly illustrated that transition metal catalysis system using rhodium or iron are efficient and promising for C-C, C-N, C-P bond formations, notably as they are able to promote the formation of annulated heterocycles which are often versatile scaffolds in medicinal chemistry. Additionally, such C-H/N-H or C-H/P-H activation/annulation approaches using simple catalyst systems are efficient and short pathways, and should be amenable to a broad range of further applications in heterocycle synthesis.

Of notable interest, some of the described synthesizes were promoted by promising more

sustainable activation technologies such as electrocatalysis avoiding to use extra oxidant salts, or blue light irradiation, permitting to work at ambient conditions.

The direct perspectives of this work is to generalize the iron-catalyzed preparation of benzo[*b*]phosphole oxides and 9-phenyltribenzo[*b,e,g*]phosphindole 9-oxide derivatives. Thus, extension of such methodologies for the preparation of diverse N- and P-containing heterocycles will be the medium term perspectives in both research groups.

Conclusions générales et perspectives

Conclusions générales et perspectives

Dans ce travail de doctorat, nous avons décrit le développement de systèmes catalytiques homogènes basés sur des métaux de transition à forte activité catalytique comme le rhodium et le fer, respectivement. Ainsi, ces systèmes catalytiques oxydatifs sont capables d'effectuer la fonctionnalisation des liaisons C-H/C-P, de construire avec succès des liaisons C-C, C-N, C-P, d'obtenir une variété de molécules hétérocycles contenant de l'azote et du phosphore et une classe d'oxydes de β -cétophosphine. Les stratégies impliquées pour former des liaisons C-P ont été décrites dans la première partie de ce manuscrit. Les sels de fer ont d'abord été utilisés comme catalyseurs sous irradiation LED bleue ($h\nu = 450-460$ nm), pour l'oxyphosphination des oxydes de phosphine secondaires et des alcènes activés. (Schéma 1) Tout d'abord, dans des conditions aérobies, on a constaté que des styrènes substitués se produisaient l'oxyphosphinylation intermoléculaire en présence de 10 % mol de $\text{Fe}(\text{OTf})_2$ dans le 1,4-dioxane à température ambiante et des produits d'oxyde de β -cétophosphine correspondants avec des rendements modérés à bons. Cependant, lors de l'exécution de la réaction avec la 4-vinylpyridine et le 4-trifluorométhylstyrène, on n'a obtenu que des produits d'hydrophosphination anti-Markonikov. Il est à noter que les études de mécanisme ont mis en évidence que cette réaction se déroulait de manière radicale, et que la lumière bleue associée au sel de fer et à l'air était responsable de la production d'un radical phosphinoyle qui réagissait ensuite avec les oléfines activées.

Part 1.

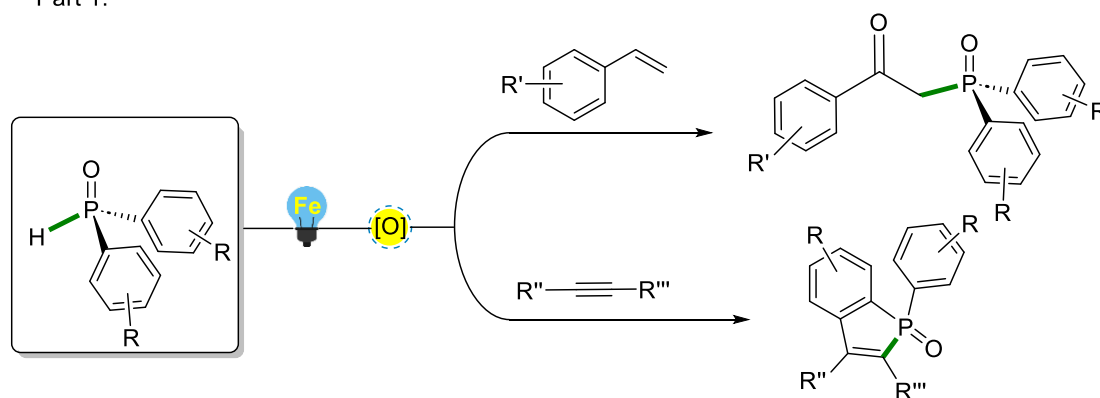


Schéma 1. Dérivés organophosphorés préparés via des formations de liaisons C-P.

Par la suite, nous avons établi la preuve de concept d'un autre protocole catalysé par le

fer promu par la lumière pour la construction de la structure des oxydes de benzo[*b*]phosphole via le clivage de la liaison H–P des oxydes de diphenylphosphine et la formation de nouvelles liaisons C–P avec les alcynes internes. Cette réaction a été réalisée en utilisant uniquement des sels de fer comme catalyseurs, de l'hydroperoxyde de *tert*-butyle (TBHP) comme oxydant à température ambiante pendant 10 heures sous irradiation à la lumière bleue. Il est important de noter qu'avec un contrôle fin de la nature des sels de fer et des solvants, un produit d'annulation de liaison C-P/C-C intermoléculaire-intramoléculaire en tandem a été obtenu avec un bon rendement. Même si ces résultats préliminaires ont ouvert des perspectives intéressantes, des plans futurs doivent être réalisés, y compris l'étude de l'étendue du substrat et l'étude mécanistique.

D'autre part, dans la deuxième partie de ce travail, nous nous sommes concentrés sur les formations de liaisons C-N catalysées par le rhodium pour la préparation d'hétérocycles contenant de l'azote. Nous avons développé avec succès des annulations C-H/C-N catalysées par Rh(III), en présence de 2,5-5 % mol [Cp*RhCl₂]₂ comme catalyseur et de sels d'Ag comme oxydants pour la synthèse efficace d'indoles fusionnés 1,7 à six et sept chaînons. Dans ces contributions, nous avons décrit l'amidation intramoléculaire des 7-phénylindoles avec les diazomalonates, l'oléfin/aza-Michael addition des 7-phényl-1*H*-indoles avec les alcènes et l'annulation des 7-phénylindoles avec les alcynes, respectivement. La préparation de l'azépino[3,2,1-*hi*]indoles a été réalisée par réaction du 7-phényl-1*H*-indoles avec des diazomalonates en utilisant 2,5 % molaire [Cp*RhCl₂]₂ associés à des quantités catalytiques d'AgOAc (15 mol%) et de DBU (30 mol) à 60 °C. Et pour obtenir efficacement des pyrrolo[3,2,1-*de*]phénanthridines à partir de 7-phényl-1*H*-indoles, une réaction intéressante en un pot avec des alcènes activés a été menée avec 5 % mol [Cp*RhCl₂]₂ associés à l'AgOAc (2 équivalents) et au Me₄NOAc (10 équivalents) à 80 °C. (Schéma 2)

Outre l'utilisation de sels agricoles en quantités stœchiométriques ou catalytiques, la version rhodium sans oxydant exogène de ces transformations peut être une bonne alternative en termes de durabilité. En effet, la métalla-électrocatalyse peut être

considérée comme une méthodologie moins coûteuse et plus respectueuse de l'environnement. Ainsi, en utilisant des électrodes de platine comme cathode et des électrodes en feutre de graphite (GF) comme anode, en présence de $[\text{Cp}^*\text{RhCl}_2]_2$ comme catalyseur, et de 2 équivalents de base (Li_2CO_3), des azépino[3,2,1-*hi*]indoles à sept chaîons ont été obtenus efficacement par réaction des 7-phénylindoles avec des alcynes. Deux intermédiaires importants, y compris le complexe de rhodium(III) cyclométallé à six chaîons par activation C-H dirigée par NH et une espèce de rhodium(III) métallacyclique à huit chaîons par insertion d'alcyne ont été isolés avec succès. De plus, les preuves expérimentales obtenues par l'analyse cyclovoltampmétrique et les études XPS associées aux calculs DFT, ont suggéré une variété de rhodium (III-IV-II-III). (Schéma 2)

Part 2.

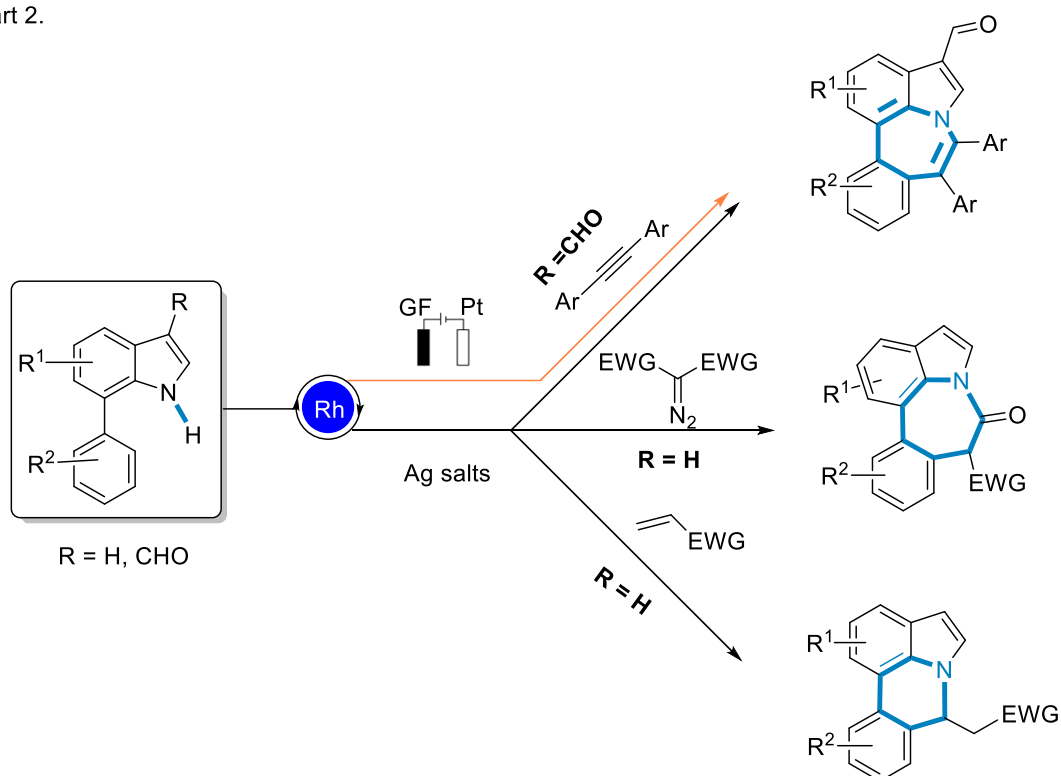


Schéma 2. Hétérocycles contenant de l'azote préparés par des formations C-N catalysées par le rhodium.

Les études résumées dans ce manuscrit ont clairement démontré que les systèmes de catalyse des métaux de transition utilisant le rhodium ou le fer sont efficaces et prometteurs pour la formation de liaisons C-C, C-N, C-P, notamment parce qu'ils sont

capables de favoriser la formation d'hétérocycles annulés qui sont souvent des échafaudages polyvalents en chimie médicinale. De plus, de telles approches d'activation/annulation C-H/N-H ou C-H/P-H utilisant des systèmes catalytiques simples sont efficaces et des voies courtes, et devraient se prêter à un large éventail d'applications ultérieures dans la synthèse d'hétérocycles.

Il est intéressant de noter que certaines des synthèses décrites ont été promues en promettant des technologies d'activation plus durables telles que l'électrocatalyse évitant d'utiliser des sels oxydants supplémentaires, ou l'irradiation à la lumière bleue, permettant de travailler dans des conditions ambiantes.

La perspective directe de ce travail est de généraliser la préparation catalysée par le fer d'oxydes de benzo[*b*]phosphole et de dérivés de 9-phényltribenzo[*b,e,g*]phosphindole 9-oxyde. Ainsi, l'extension de ces méthodologies pour la préparation de divers hétérocycles contenant de l'azote et du phosphore sera la perspective à moyen terme dans les deux groupes de recherche.

Titre : Transformations catalysées par le rhodium et le fer via des activations C-H, N-H et P-H.

Mots clés : Catalyse, rhodium, fer, activation C-H, activation N-H, activation P-H, hétérocycles

Résumé : L'objectif de ce travail de thèse a été de développer des catalyseurs de rhodium et de fer pour activer et fonctionnaliser des liaisons C-H/N-H et C-H/C-P afin de créer des liaisons C-C, C-N, C-P bonds, et ainsi obtenir notamment des N- et P-hétérocycles.

Dans une première partie de ce travail, des oxydes de β -cétophosphine ont été préparées à partir d'oxydes de phosphines secondaires et d'alcènes *via* une réaction d'oxophosphination catalysée par $\text{Fe}(\text{OTf})_2$ à 25 °C sous irradiation par une lumière bleue. En particulier, le caractère radicalaire du mécanisme de la réaction a été démontré. En utilisant la lumière bleue et la catalyse au fer, une preuve de concept pour la préparation d'oxydes benzo[*b*]phosphole et de 9-oxyde de 9-phenyltribenzo[*b,e,g*]-phosphindole à partir d'oxydes de diphenylphosphine et d'alcynes internes a été établie en utilisant un catalyseur de fer, un oxydant (TBHP) à 25 °C sous lumière bleue.

Dans une seconde partie, nous nous sommes focalisées sur la formation de liaisons C-N rhoda-catalysée pour la préparation d'hétérocy-

cles azotés. Ainsi, des annulations C-H/C-N catalysées par des espèces de Rh(III) ont été réalisées en utilisant le catalyseur $[\text{Cp}^*\text{RhCl}_2]_2$ et des sels d'argent comme oxydants et ont permis de préparer des dérivés indoles polycycliques à 6 ou 7 chaînons à partir de 7-phénylindoles. Par réaction avec des diazomalonates, avec de quantités catalytiques de $[\text{Cp}^*\text{RhCl}_2]_2$, AgOAc et DBU, les dérivés azépino[3,2,1-*h*]indoles ont été obtenus. Pour synthétiser les pyrrolo[3,2,1-*de*]phénanthridines à partir d'alcènes, l'asso-ciation du catalyseur $[\text{Cp}^*\text{RhCl}_2]_2$ et de AgOAc et Me_4NOAc a été utilisée. Une version alternative sans utilisation d'oxydants externes a été développée par électrocatalyse, avec une cathode de Pt et une anode de graphite, et $[\text{Cp}^*\text{RhCl}_2]_2$ et a permis de préparer des azépino[3,2,1-*h*]indoles à partir d'alcynes.

Il faut souligner que certaines réactions décrites sont promues par des technologies alternatives plus éco-compatibles telles que l'électrocatalyse, évitant l'utilisation d'oxydants ou par la lumière bleue permettant de travailler à température ambiante.

Title: Rhodium and iron catalyzed transformations via C-H, N-H and P-H activation

Keywords: Catalysis, Rhodium, Iron, C-H activation, P-H activation, N-H activation, heterocycles

Abstract: This research work described the development of homogeneous rhodium and iron catalytic systems able to perform C-H/N-H and C-H/C-P bond functionalization for building C-C, C-N, C-P bonds, thus notably obtaining a variety of N- and P-containing heterocycles.

First of all, β -ketophosphine oxides were prepared efficiently from secondary phosphine oxides and activated alkenes *via* the intermolecular oxophosphination catalyzed by $\text{Fe}(\text{OTf})_2$ at 25 °C under blue LED irradiation. Noticeably, the mechanism studies highlighted the radical nature of the reaction.

Still using iron catalyzed blue light promoted technology, a proof of concept for preparing benzo[*b*]phosphole oxides and 9-phenyltribenzo[*b,e,g*]-phosphindole 9-oxide from diphenylphosphine oxides and internal alkynes was established, using iron catalyst and TBHP oxidant at 25 °C under blue light irradiation.

In the other hand, the **second part** of this research focused on Rh-catalyzed formations of C-N bonds for the preparation of nitrogen

containing heterocycles. Rh(III)-catalyzed C-H/C-N annulations were successfully accomplished, using $[\text{Cp}^*\text{RhCl}_2]_2$ catalyst and Ag salt oxidants for the synthesis of six-membered and seven-membered 1,7 fused indoles, starting from 7-phenylindoles. By reaction with diazomalonates, and catalytic amounts of $[\text{Cp}^*\text{RhCl}_2]_2$, AgOAc and DBU, azepino[3,2,1-*h*]indoles were prepared. Additionally, pyrrolo[3,2,1-*de*]phenanthridines were obtained in a one-pot fashion by reaction with activated alkenes, and $[\text{Cp}^*\text{RhCl}_2]_2$ catalyst associated to AgOAc and Me_4NOAc . Alternatively, an exogenous-oxidant-free rhodium version of these reactions was conducted by Rh-electrocatalysis using Pt cathode and graphite felt anode, with $[\text{Cp}^*\text{RhCl}_2]_2$: Azepino[3,2,1-*h*]indoles were obtained by reaction with alkynes.

Of notable interest, some of the described syntheses were promoted by more sustainable activation technologies: electrocatalysis avoiding to use of oxidants, or blue light irradiation, permitting to work at ambient conditions.